Investigation of *Theileria annulata* as modulator of activation associated host cell gene expression

ZEESHAN DURRANI, M.Phil, DVM

UNIVERSITY
of
GLASGOW

Submitted in fulfilment of the requirements for the degree of

Doctor of Philosophy

College of Medical, Veterinary and Life Sciences
School of Veterinary Medicine
Division of Infection and Immunity
University of Glasgow
2012

Author's Declaration

I hereby declare that the work presented in this thesis is entirely my own original work and carried out with the help of those people mentioned in acknowledgements. Where other sources of information have been used, they have been acknowledged.The research work presented in this thesis has not been previously submitted to any other university for the award of a degree.

Zeeshan Durrani
December 2011

Abstract

Infection of bovine leukocytes by the intracellular protozoan parasites *Theileria annulata* and *Theileria parva* represents a unique model of reversible host cell transformation; characterised by uncontrolled proliferation and protection against apoptosis. Host cell transformation is known to involve parasite dependent manipulation of a number of signalling pathways that result in constitutive activation of pro-inflammatory transcription factors. Activation of these factors has been shown to confer protection against apoptosis or influence the metastatic potential of the infected cell, respectively. However, transcription factors have the potential to be detrimental as well as beneficial to the infected cell and the infected animal. This study investigated the potential of the parasite to manipulate the outcome of cellular activation by comparing the outcome of stimulating *Theileria*-infected and uninfected bovine cells with LPS. The results clearly indicate that prolonged stimulation of uninfected cells generated a phenotype associated with loss of proliferation, cell death and activation of NF-κB. In contrast, infected TBL20 cells were refractory to stimulation, despite displaying high levels of constitutively activated NF-κB.

Using a microarray approach, expression profiling of infected and uninfected cells established that *T. annulata* infection imposes a remarkable level of control over host cell pathways and gene expression networks that are targets of transcription factors, typically activated by inflammatory mediators such as LPS. Importantly, Ingenuity Pathway Analysis (IPA) of the modulated dataset showed enrichment of molecular function and disease categories associated with known phenotypic characteristics of the *Theileria*-transformed cell. Categories included inflammatory response, cancer and tissue morphology, allowing postulation that parasite manipulates the expression of genes that function in the inflammatory response and are associated with cancer to generate a phenotype that is beneficial to survival and dissemination of the infected leukocyte.

Various proteins secreted by the parasite are believed to contribute to regulation of the transformed host cell. The majority of parasite candidate proteins contain predicted signal peptides, suggesting secretion into the infected-host cell cytoplasm or location on the parasite surface. A prime

candidate for a *Theileria* encoded regulator of host cell gene expression is TashAT2, a protein bearing nuclear localisation/AT-hook DNA binding motifs, previously located to the host cell nucleus and shown to bind DNA. A transfected bovine macrophage cell line (BoMac) expressing TashAT2 was activated with PMA to provide RNA for microarray hybridisation and compared to RNA derived from vector alone control cells and non-stimulated transfected cells. Activation of NF-κB by PMA was demonstrated by reporter assay, with TashAT2-transfected cells displaying a marked resistance to PMA induced cell death and higher levels of NF-κB dependent reporter activity relative to PMA stimulated control cells.

Expression profiling of TashAT2-transfected BoMacs provided evidence for TashAT2 associated manipulation of both activated cell and non-activated gene expression networks. Furthermore, comparison of the TashAT2-modulated with infection-associated gene lists revealed a significant overlap in genes modulated by the macroschizont infected cell and TashAT2. IPA analysis of this common gene set highlighted biological functions and disease categories previously identified for the infection-modulated LPS dataset with some variation in the order of significance. Identified categories include cancer, inflammatory response and cell death. Comparative analysis of the TashAT2 associated profiles also identified a subset of genes that displayed significant modulation of gene expression changes in response to PMA stimulation, including reversal of the PMA response.

Taken together, these results of this study provide further evidence that TashAT2 proteins are candidate molecules involved in manipulating expression of host cell genes that could play an important role in determining establishment of infected-transformed cells. The ability of the parasite and potentially TashAT family proteins to significantly regulate gene networks that mediate inflammatory disease and cancer could provide a platform to investigate how these disease outcomes can be manipulated.

Table of Contents

List of Figure

List of Tables

Acknowledgements

I would like to express my sincere gratitude to my supervisor Professor Brian Shiels for the opportunity, support and valuable guidance he has given me to pursue this research degree as part of his group.

I would like to thank Higher Education Commission (HEC), Pakistan for funding my studies without which this study would have been impossible to complete. Thanks are also due to the University of Glasgow for accepting me into the Ph.D. programme and for providing some consumable funding for the project

I would like to thank the Post-doctoral research scientists of the *Theileria* group, in particular Dr. Jane Kinnaird and Dr. William Weir for their important roles as enthusiastic mentors to the world of molecular biology and bioinformatics. I appreciated their patience, support, encouragement and willingness to provide consultation and guidance during the course of my study. I am also grateful to Margaret Baird for her instruction for laboratory techniques when I joined the group. I feel myself very privileged to have had you all there, thank you.

A special thanks to my assessor Professor Eileen Devaney, Division of Infection Immunity and Inflammation Life Sciences, for her valuable suggestions and encouragement during my studies.

Thanks also to Margaret McFadyen for keeping the lab running and tolerating all the untidiness surprises generated over weekends. I also thank numerous members of the old Division of Infection and Immunity staff for their support and assistance, especially to Kerry O'Neill, Jasmine Moroney and Charlie Cameron for sorting out my many purchase orders and abundant paper work. I would like to thank Lesley Dinning (Graduate School Administrator, MVLS), Dr. Jane Robinson (Associate Academic, School of Veterinary Medicine) for their help in resolving problems in graduate school matters.

My past and present colleagues and friends in the Department, Dr. Martin Simuunza, Dr. Roz Laing, Dr. Garry Saunders, David Pertab, Stephanie Johnston, Dr. Joana Carvalho, Dr. Nik Him Irwin, Dr. Amy Joans, Dr. Hussein Beljik and

Selin Uner and Sreerekha Sreedharan Pillai all helped to make late nights in the lab less lonely.

Last but not least, I thank my well wishers and friends outside the lab in Glasgow especially Naseem Anwar, Dr. Azra Meadow (OBE), Professor Peter Meadows, Dr. Sameer Zeino, Hassan Mushfique, Dr. Newton Alex, and elsewhere for their support and encouragement throughout my stay here at Glasgow.

Most importantly, I would like to express deepest gratitude to my parents, brother, sisters, and other relatives for their everlasting love, support and encouragement during my studies.

Zeeshan Durrani

List of Abbreviations and Symbols

ACTβ	Actin beta
ATF-2	Activating transcription factor 2
AP-1	Activator protein 1
ATPase	adenosine triphosphatase
ATP	adenosine triphosphate
α	Alpha
ANOVA	Analysis of variance
p65	avian reticuloendotheliosis viral (v-rel) oncogene homolog A/ RELA
bp	Base pair
β	Beta
BSA	bovine serum albumin
BW720c	Buparvaquone
CO2	carbon dioxide
CK-II	casein kinase II
cm	centimeter
JNK	c-jun NH2-terminal kinase
CD14	cluster of differentiation 14
cDNA	complementary deoxyribonucleic acid
ºC	Degrees celsius
ΔΔCt	delta delta, cycle threshold
DNase	Deoxyribonuclease
DNA	Deoxyribonucleic acid
dNTP	Deoxyribonucleotidetriphosphate
DAPI	4',6-diamidino-2-phenylindole, dihydrochloride
DEPC	Diethylpyrocarbonate
DMSO	dimethyl sulfoxide
Na_2HPO_4	Disodium hydrogen phosphate anhydrous
dH2O	distilled water
ELISA	enzyme linked immunosorbent assay
EtBr	Ethidium bromide
EDTA	Ethylenediaminetetracetic acid
EFC	East Coast Fever

EST	expressed sequence tag
FDR	False Discovery Rate
FBS	foetal bovine serum
γ	Gama
GAPDH	Glyceraldehyde-3-phosphate dehydrogenase
g	Gram
HMG	high mobility group AT-hook proteins
HMGA2	High-mobility group protein (HMGI-C)
HMGA1	High-mobility group protein HMG-I/HMG-Y
h	hour
HCl	Hydrogen Chloride/ Hydrochloric acid
IFAT	immunofluorescent antibody test
iNOS	inducible Nitric oxide synthase
IKKγ	inhibitor of kappa light polypeptide gene enhancer in B-cells, kinase gamma
IFN	Interferon
IRF	Interferon regulatory factor
ISG15	interferon-stimulated protein, 15 kDa
K	Kilo (10^3)
kb	Kilobase or 1000bp
kDa	Kilodalton
LBD	Ligand binding domain
LPS	Lipopolysaccharide
l	litre
Tm	melting temperature
mRNA	messenger ribonucleic acid
μ	Micro (10^{-6})
μAMP	microampere
μg	microgram
μl	microlitre
μM	micromolar
mg	milligram
ml	millilitre (10^{-3})
mM	millimolar
min	minute

M	Molar
mAb	monoclonal antibody
MOPS	4-Morpholinepropanesulfonic acid
c-Myc	myelocytomatosis viral oncogene homolog (avian) transcription factor
ng	nanogram (10^{-9})
nm	nanometer
NF-κB	nuclear factor-kappa B
n	number of samples
Oligo	Oligodeoxyribonucleotide
ω	Omega
p	p value; statistical significance
PFA	Paraformaldehyde
PMA	Phorbol 12-myristate 13-acetate
PBS	Phosphate buffered saline
PI-3K	phosphatidylinositol 3-kinase
PAGE	Polyacrylamide gel electrophoresis
PCR	Polymerase chain reaction
KCl	Potassium chloride
KH_2PO_4	Potassium dihydrogen orthophosphate
qRT-PCR	Quantitative reverse transcription PCR
RFU	relative fluorescence units
RT	Reverse transcriptase
RT-PCR	Reverse transcription PCR
rpm	revolutions per minute
RNase	Ribonuclease
RNA	Ribonucleic acid
Sec	second
STAT3	Signal transducer and activator of transcription 3
NaCl	Sodium chloride
SDS	Sodium dodecyl sulphate
SDS-PAGE	sodium dodecyl sulphate polyacrylamide gel electrophoresis
NaOH	Sodium hydroxide
SD	Standard deviation
SE	Standard error of the mean

SVSP	sub-telomeric variable secreted protein
S	svedberg unit
Ta9	*T. annulata* hypothetical protein (TA15705)
Tams1	*T. annulata* merozoite piroplasm surface antigen (TA17050)
TpScope	*T. parva* schizont-derived cytoskeleton binding protein
SuAT1	*T. annulata* encoded host-nuclear protein (TA03135)
TashAT3	*T. annulata* schizont host-nuclear protein (TA20082)
TashAT1	*T. annulata* schizont host-nuclear protein (TA20085)
TashHN	*T. annulata* schizont host-nuclear protein (TA20090)
TashAT2	*T. annulata* schizont host-nuclear protein (TA20095)
TaSP	*T. annulata* surface protein (TA17315)
Taq	Thermus aquaticus polymerase
TLR	Toll-like receptor
TGF-β	Transforming growth factor β
Tris	Tris(hydroxymethyl) amino methane
TAE	Tris-Acetate EDTA
TBE	Tris-Borate EDTA
TBS	Tris-Buffered Saline
TNF-α	Tumor necrosis factor alpha
p53	Tumour protein 53
UV	Ultraviolet
U	Unit
V	Volt
v	Volume
w	Weight

Chapter 1

Introduction

1 Introduction

1.1 Introduction

Tropical or Mediterranean theileriosis is an economically important lymphoproliferative disorder of cattle that occurs throughout much of the old world. It is a tick-borne disease (TBD) of bovines and the prevalence reflects the geographical distribution of the tick vector, which is primarily tick species within the genus *Hyalomma*. The range of *Hyalomma* extends over a wide region of the old world including Southern Europe and North Africa through the Middle East and Southern Russia into India and Southern China (Uilenberg, 1981). The disease is caused by the protozoan parasite *Theileria annulata,* which for the *Theileria* genus can be considered to be the most important species based on its pathogenicity combined with a wide geographical range.

T. annulata is the predominant species of *Theileria* in Southeast Asia, Middle East, Europe and some parts of Africa. The parasite mainly affects domestic cattle (*Bos taurus* and *Bos indicus*), zebu (*Bos primigenius indicus*), Asian buffalo (*Bubalus bubalis*) and wild cattle (*Bos bison*) (Dumanli *et al.*, 2005;Robinson, 1982). Tropical theileriosis is an extremely debilitating and often fatal condition especially in exotic breeds of cattle imported to improve productivity (Preston *et al.*, 1999). It is estimated that over 250 million cattle in disease endemic regions are at risk from infection with *T. annulata* (Robinson, 1982). In several developing countries the parasite is a major constraint for improved livestock production due to the high morbidity and mortality rates. This is due, in particular, to the increased susceptibility of *Bos taurus* to the disease, limiting programmes that have aimed at higher production levels by introduction of European breeds. However there is also a marked loss of production in indigenous cattle kept in endemic regions (Irvin *et al.*, 1981), and the disease imposes a considerable economic drain on both large scale farming operations and, very often, small holder subsistence farmers.

Of the other the *Theileria* species of cattle, *T. parva* is the most important. *T. parva* shows a higher level of virulence than disease caused by *T. annulata* but has a more limited range, as the *Rhipicephalus appendiculatus* tick is found only

in sub-saharan Africa. *T. parva* causes a disease, commonly known as East Coast Fever (ECF) which is often fatal (Newson *et al.*, 1986;Norval *et al.*, 1992). Up to 50 million cattle are at risk and in years of high incidence up to 1 million deaths have been recorded. Cattle *Theileria* parasites described as more benign have also been associated with disease. Species include *T. mutans* and members of the *T. orientalis* group. Of the latter group *T. sergenti* has been most often associated with disease, primarily in Japan, Eastern Russia and Eastern China. Clinical episodes of disease attributed to *T. orientalis* were recently reported in South Australia (Islam *et al.*, 2011;Kamau *et al.*, 2011).

It has been reported that the greatest economic losses from tropical theileriosis are due to loss of productivity (beef and milk production), followed by the cost of disease control (vaccination and acaricides) and chemotherapy (Cicek *et al.*, 2009;Gharbi *et al.*, 2006;Inci *et al.*, 2007;Minjauw and McLeod, 2003). Economic losses for tropical theileriosis in India alone have been estimated at US $ 800 million per year (Wilkie *et al.*, 1998). A recent study performed in Tunisia estimated that up to half of the economic losses attributed to tropical theileriosis could be accounted for by the reduced productivity of sub clinically infected animals (Gharbi *et al.*, 2006).

T. annulata and *T. parva* are closely related parasites and considered to be among the most recently evolved *Theileria* species (Allsopp and Allsopp, 2006). Both species cause similar disease syndromes marked by a lymphoproliferative phase followed by metastasis (Irvin and Morrison, 1987). Following metastasis of infected cells, mortality in acute disease cases usually results from respiratory failure, due to pulmonary oedema or extensive destruction of lymphoid tissue (Irvin and Morrison, 1987). Therefore, much of the information described below for *T. annulata*, with respect to pathology and life cycle is also valid for *T. parva*. Moreover, study of the cellular and molecular biology associated with cellular transformation has been conducted on bovine cells infected with either species, and many of the mechanisms described are applicable to both. One major difference, however, is that *T. annulata* prefers to infect and transform cells of myeloid lineage, and also B cells, whereas *T. parva* is thought to preferentially infect T cells (Baldwin *et al.*, 1988;Glass *et al.*, 1989;Spooner *et al.*, 1989).

Theileria parasites are unique, as the schizont stage of certain species, including *T. annulata* and *T. parva*, can induce the host leukocyte to proliferate in an uncontrolled manner, causing immortalisation and transformation of infected cells (Adamson *et al.*, 2000;Baylis *et al.*, 1995;Hulliger, 1965;Irvin and Morrison, 1987). The importance of this event to generation of disease pathology underscores a requirement to understand how the parasite controls the infected host leukocyte. Furthermore, as well as being of inherent biological interest, this information has potential to be relevant to design of novel therapeutics.

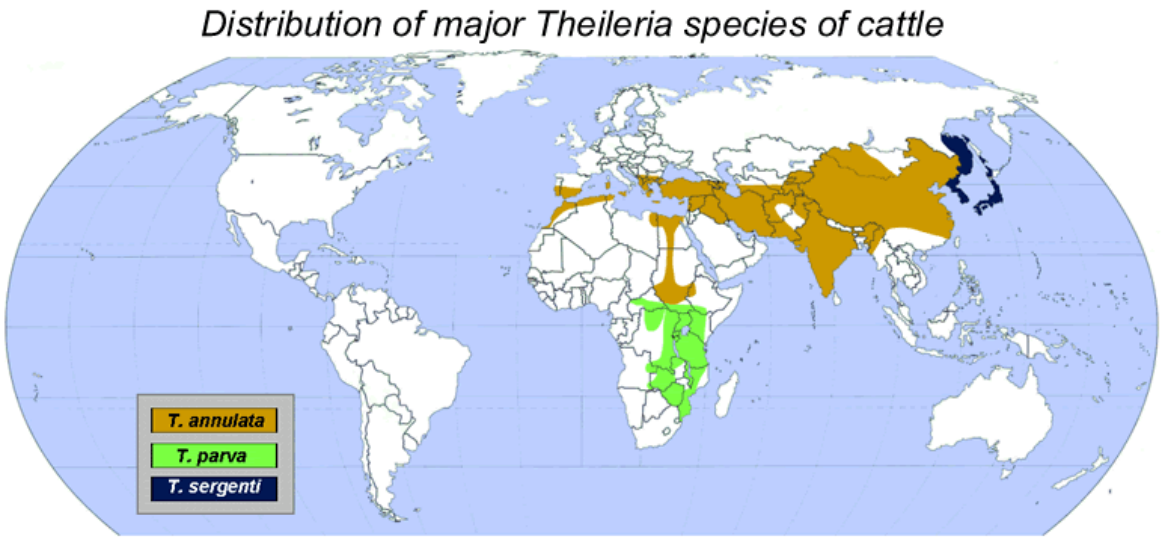

Figure 1.1: Geographical distribution of major *Theileria* species of cattle worldwide
Theileria annulata, responsible for Tropical Theileriosis and primarily found in Southern Europe and North Africa extending up to sub-Saharan Africa in Sudan and Eritrean. It also extends through the Middle East and Southern Russian into India and Southern China. *Theileria parva* is responsible for East Cost Fever and primarily found in the African countries highlighted. *Theileria sergentii,* responsible for a disease often termed as persistent Theileriosis, is found in Eastern Asia including Korea and Japan. (Source: http://www.Theileria.org/ahdw/background.htm)

1.2 *Theileria* and related Apicomplexan parasites

Theileria is an Apicomplexan hemoparasite of veterinary significance. Members of the phylum Apicomplexa comprise more than 5000 species of intracellular, protozoan parasites including those placed in the genera: *Plasmodium*, *Toxoplasma*, *Cryptosporodium* and *Babesia* (Noble *et al.*, 1989). All are unicellular eukaryotic microbes and, collectively, apicomplexans can be classified as one of the most significant groups of infectious pathogens that cause disease in humans and domesticated animals. Therefore, the cell and molecular biology of *Theileria* bears similarity to that of other eukaryotes, of which the phylogenetic relationship is obviously stronger among closely related

apicomplexan species. For *Theileria*, research conducted on *Babesia* and *Plasmodium* parasites is likely to be of greatest comparative value with respect to processes that allow evolution of their parasitic lifestyle. However *Theileria*-infected leukocytes provide a unique model of how one eukaryotic cell can transform another, and study of how the parasite transforms its host cell may have wider relevance and relationship to cancer biology [reviewed in (Luder *et al.*, 2009)]. Host-parasite interactions related to the cancer like pathology of tropical theileriosis can be addressed in three phases: the ability of the infected leukocyte to survive, proliferate and metastasise. Maintenance of the infected host cell in a constantly activated state is likely to be a key mechanism in these processes. Other apicomplexan parasites that may modulate the infected activated nucleated cell in a similar manner include *Toxoplasma gondii* and *Neospora caninum* [reviewed in (Hemphill, 1999;Hemphill and Gottstein, 2006;Melo *et al.*, 2011)]. Comparison of the mechanisms by which these different apicomplexan parasites have evolved is relevant to identify key modulatory events required for control of the nucleated host cell and survival within their mammalian hosts.

1.3 Life cycle of *Theileria annulata*

Theileria annulata has a complex life-cycle, involving both tick (*Hyalomma spp*) and bovine host. As expected, the life cycle of *Theileria* displays the principal stages of general apicomplexan differentiation events such as gametogony, sporogony and merogony. However, different apicomplexan life cycles show specific variation, two common differences being the host cell types invaded after entering the mammalian host and intracellular location of the parasite. For example, unlike *Plasmodium* and *Toxoplasma* parasites, the macroschizont of *Theileria* does not reside in a parasitophorous vacuole (PV) but lies free in the cytoplasm (like Babesia parasites) (Shaw, 1997). Differentiation from one stage to another is a vital process for the parasite biology that facilitates the transmission and propagation within and between vector and host. The basic life cycle of *T. annulata* is essentially the same for all *Theileria* species and is illustrated in Figure 1.2. *Theileria* parasites replicate asexually as three different stages, by sporogony in the tick vector, and by schizogony and merogony in bovine host cells. In *T. orientalis* proliferation (merogony) occurs

within the erythrocyte but this is limited or absent for *T. annulata* and *T. parva* (Conrad *et al.*, 1985). Sexual reproduction of the parasite occurs in the tick.

1.3.1 Bovine stages of *T. annulata*

Infected ticks inoculate sporozoites (bovine infective stage) into the host blood stream during feeding, and the sporozoites rapidly invade host target leukocytes. *Theileria annulata* mainly infects leukocytes of monocyte and B-lymphocyte lineage (Spooner *et al.*, 1989). Morphologically sporozoites are oval shaped bodies measuring approximately 1µm in length that are formed in the salivary gland of the infected tick. Upon contact between sporozoite and the target leukocyte cell surface, a point of connection is established via MHC class II receptors, that promotes the invasion of host cell by the parasite (Glass *et al.*, 1989). The surface coat of the sporozoite becomes closely associated with the host membrane and the parasite is internalised by a progressive circumferential 'zippering' process, during which the surface coat of the sporozoite is shed. Once internalised the *Theileria* parasite is able to disrupt the parasitophorous vacuole membrane by discharging the contents of the rhoptries and micronemes and lies free in the cytoplasm surrounded by host cell microtubules (Mehlhorn and Shein, 1984;Shaw and Tilney, 1995).

Following successful entry the parasite forms a trophozoite, which then differentiates into the multinucleated schizont (macroschizont) stage. The macroschizont maintains the association with the microtubule network and is normally located in the perinuclear region of the host cell. As the schizont develops the leukocyte is induced to divide and synchronisation of the parasite's own cell division is achieved by close interaction with the host mitotic and central spindles (Shaw, 1997). This interaction allows the successful dissemination of the growing macroschizont to each daughter leukocyte. Proliferating infected leukocytes rapidly produce a large population of infected cells due to clonal expansion. Initially the parasite infects and multiplies in cells of the lymph nodes draining the site of inoculation (Forsyth *et al.*, 1999;Glass, 2001) but subsequently infected cells may be found in the bloodstream or invade a variety of tissues and organs, giving the infection 'cancer-like' features of leukoproliferation and metastasis. Parasite dependent leukocyte transformation

generates various phenotypes including a loss of myeloid differentiation status (Jensen *et al.*, 2009;Sager *et al.*, 1997), resistance to apoptosis (Heussler *et al.*, 1999), proliferation to generate immortal cell line cultures in vitro (Baumgartner *et al.*, 2000) and the ability to transverse matrigel matrices (Lizundia *et al.*, 2006). Approximately 7 to 28 days post-infection, macroschizont infected cells may be detected in biopsy smears from superficial lymph nodes in live animals and impression smears of the lymph node, spleen and liver in dead animals (Radley *et al.*, 1974;Young *et al.*, 1977).

Following a set time period in vivo (between 7-10 days), the macroschizont undergoes differentiation to the next life cycle stage, the merozoites (Jarrett *et al.*, 1969). This process initially involves a slowing down of proliferation of the macroschizont-infected cell (Shiels *et al.*, 1992). The parasite enlarges and switches from production of macroschizont to merozoite stage proteins (Shiels *et al.*, 1992). Morphological changes to nuclei occur; rhoptry organelles are produced and become associated with the merozoite nuclei. Uni-nucleated merozoites are then formed by budding of the nuclei and rhoptry complex through the plasma membrane of the developing syncytium. Morphologically, merozoites of *T. annulata* contain a single nucleus, 1-2 mitochondria, microneme and 3-6 rhoptries and are covered in the major merozoite surface protein Tams1 (Mehlhorn and Shein, 1984;Shaw *et al.*, 1991;Shaw and Tilney, 1995). The mature merozoites are released into the bloodstream following cell membrane rupture of infected cells, and rapidly invade erythrocytes, subsequently forming intra-erythrocytic forms collectively known as piroplasms. Generally two forms of piroplasm may be seen inside erythrocytes a slender comma shaped form or spherical ovoid bodies surrounded by a single-layered plasma membrane (Mehlhorn and Shein, 1984). The infected erythrocytes are long lived and act as a carrier stage in the bovine host. It is likely some piroplasms within erythrocytes represent gametocytes and when ingested by the ticks during feeding are primed for the continuation of the life-cycle within *Hyalomma* ticks (see Figure 1.2).

1.3.2 Tick vector stages of *T. annulata*

Following ingestion of the infected mammalian red blood cells (infective piroplasm), the sexual stage of the life cycle occurs within the intestinal lumen of the tick. Initially the piroplasms develop into slender, spindle-shaped bodies called raybodies/microgamonts (Schein *et al.*, 1975). Up to four long flagellum-like appendages form, which then break off to generate uni-nucleated filiform microgametes. At the same time spherical bodies thought to represent the macrogamonts can be observed. It is presumed that syngamy occurs with the fusion of micro- and macro-gametes forming the zygote (Levine, 1985;Schein *et al.*, 1975). The immotile zygotes possess a vacuole-like centre and appear from five days post-repletion in the intestinal cells. After 12-15 days the zygote transforms into motile elongated shaped bodies, termed kinetes (Mehlhorn and Shein, 1984). The kinetes are then released into the haemolymph of ticks and following the moult of the tick, migrate to the salivary gland (Schein and Friedhoff, 1978).

During the act of feeding, sporogony is activated in the salivary glands, allowing amplification of parasite numbers and generation of the stage infective for the bovine host. Interestingly, a study pertaining to *Hyalomma anatolicum* has demonstrated that unfed ticks were incapable of inducing infection in experimental calves, sporozoites only appear in the salivary gland after the adult ticks had been fed for 2-3 days (Singh *et al.*, 1979). On the other hand it has been shown that environmental conditions, such as high temperature (37^{o}C) and humidity (95%) can potentially stimulate the production of sporozoites in infected *Hyalomma excavatum* ticks irrespective of blood meal (Singh *et al.*, 1979), however this usually takes longer and with a reduced output in sporozoite number. Sporogony solely occurs within the acini of the salivary glands and once initiated gives rise to massive sporozoite production. It is estimated that approximately 40,000 sporozoites may be formed from each infected acinus (Young *et al.*, 1992). Upon disintegration of the acinar cells sporozoites are liberated into the tick saliva, ready to be delivered into the bovine host during the blood meal (see Figure 1.2).

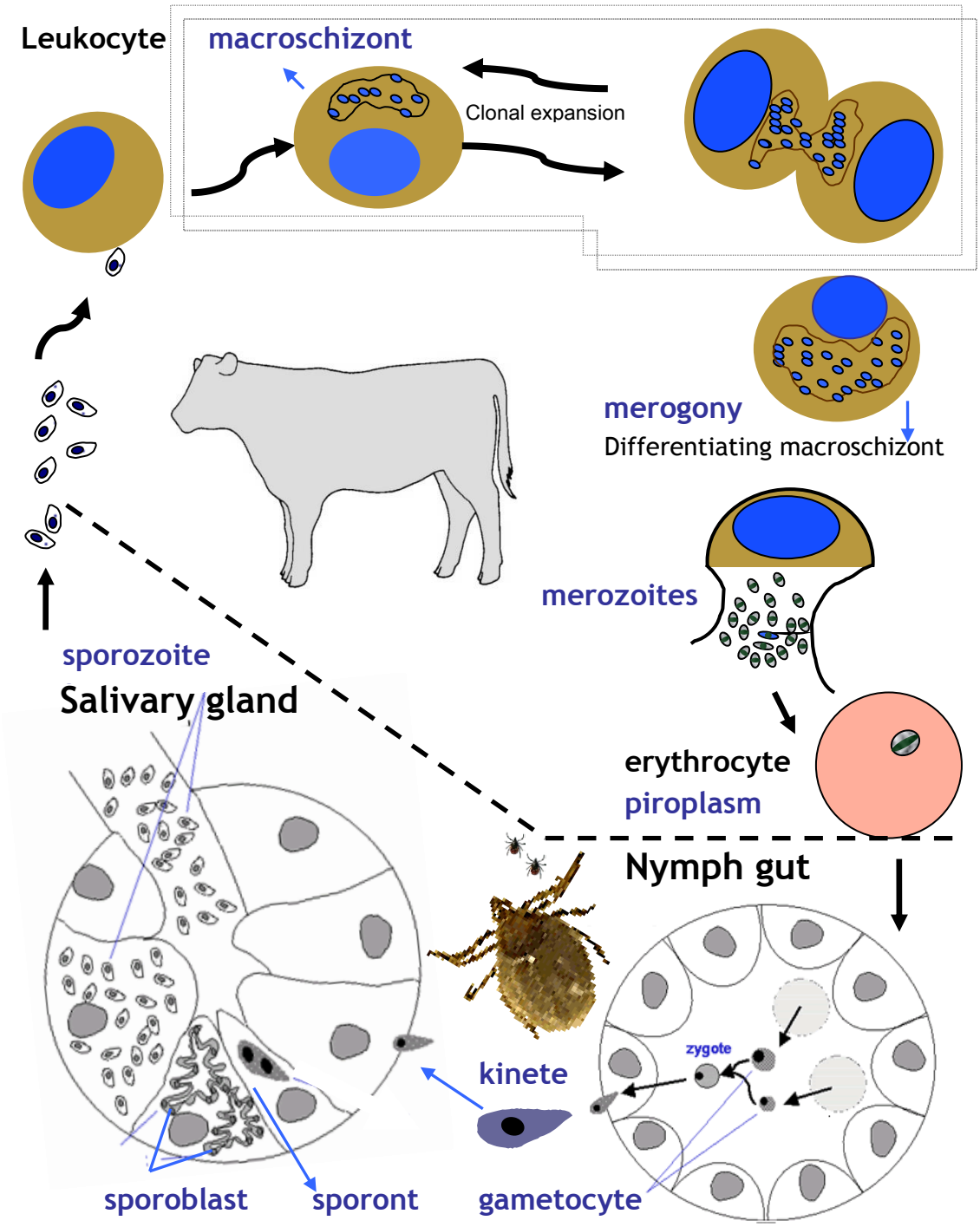

Figure 1.2: The life cycle of *Theileria annulata*
Bovine stage: *Theileria* parasite can be found in both erythrocytes and lymphocytes of infected bovine host. The infective stages of the life cycle, **sprozoites** are inoculated by tick during feeding that invade leukocytes to form **macroschizont** stage. Following a phase of uncontrol proliferation a proportion of macroschizonts differentiate into **merozoites.** Consequently, after the cell membrane rupture merozoites are liberated into the blood-stream, invading erythrocytes to form **piroplasm.**
Tick stage: During the infective stage, piroplasms are ultimately taken by a feeding tick during blood meal which develops into **gametocytes** in the tick gut. The gametocytes then fuse to form immotile **zygote**, which later on transform into motile **kinete.** Finally the kinetes migrate to the salivary gland of the vector where after several cycles of asexual replication, **sporozoites** are formed.
Adapted from: http://www.Theileria.org/ahdw/pictures/lifecyclelg.gif

1.4 Epidemiology of Theileriosis

T. annulata is transmitted trans-stadially by ticks of the genus *Hyalomma* and, thus, the geographic distribution of the disease is determined by climate (hot, dry or humid summer) suitable for tick survival and questing activity. Several important *Hyalomma* species have been reported to transmit *Theileria annulata* in various part of the world; for example *Hyaloma detritum* in north Africa; *H. detritum* and *H. excavatum* in the former Soviet States; *H. truncatum* in parts of Africa; *H. dromedarii* in central Asia; and *H. marginatum* and *H. anatolicum* in India; (Bouattour *et al.*, 1996;Flach and Ouhelli, 1992;Islam *et al.*, 2006;Taylor *et al.*, 2007). Beside factors that contribute to seasonal questing activity of tick populations, there are a number of reports suggesting that susceptibility to the disease observed in cattle populations is higher in exotic breeds relative to indigenous breeds in endemic areas (Minjauw and McLeod, 2003;Preston *et al.*, 1992). Recently, experimental studies have shown that exotic breeds particularly Holstein-Friesians, are associated with poor prognosis and detrimental outcome of the disease relative to indigenous breeds (Sahiwal; originating from Punjab, India and Kenana cattle; Sudan) (Bakheit and Latif, 2002;Glass *et al.*, 2005). A number of publications have provided evidence that different field strains, and presumably different genotypes, show variable levels of virulence (Askarov, 1975;Kamau *et al.*, 2011;Somerville *et al.*, 1998b;Tindih *et al.*, 2010). The mechanisms behind such differences are not understood but one possibility is that virulence relates to the cytokine profile of the macroschizont infected cell line (Brown *et al.*, 1995a). The ability of infection to generate a long lasting carrier phase contributes to epidemiology, as there is always a risk of disease introduction by importation of cattle that cannot be detected as infected using traditional diagnostic procedures (Bilgic *et al.*, 2010).

1.5 Pathogenesis, clinical signs and diagnosis of *Theileria infection*

The pathological progression of events in a typical acute, often fatal, infection occurs through three stages each spanning about one week. The severity of outcome is influenced by breed (see above), immune status and is dependent on the number of sporozoites inoculated by feeding ticks (Preston *et al.*,

1992;Samantaray *et al.*, 1980). The first stage comprises an incubation period of roughly around 7-8 days where neither parasite nor lesions can be detected. Following the incubation period, the second phase also of around a week is marked by lymphoid hyperplasia, initially in the region of lymph node draining the area and later the whole body (Irvin *et al.*, 1981). This phase of infection is manifested by the onset of clinical signs including enlarged lymph nodes, persistent fever (41^{o}C), anorexia, tachycardia and tachypnea (Beniwal *et al.*, 1998;Irvin *et al.*, 1981;Preston *et al.*, 1992). During the advanced third stage the animal may show severe signs of lymphoid depletion and disorganisation associated with massive lymphocytolysis and depressed leucopoiesis causing severe leukopenia (Forsyth *et al.*, 1999;Omer *et al.*, 2002;Preston *et al.*, 1992). Due to widespread destruction of the immune system encountered during the late stage of infection the animal may show clinical signs of severe dyspnoea, recumbency and finally death (Irvin and Morrison, 1987). Additionally, *T. annulata* infection is associated with profound changes in haematological and biochemical profiles and investigations of peripheral blood may reveal severe anaemia, leukopenia, lymphocytopenia, hypocalcaemia and hypoproteinemia (Hasanpour *et al.*, 2008;Omer *et al.*, 2002;Sandhu *et al.*, 1998;Singh *et al.*, 2001).

Diagnosis of the clinical *T. annulata* infection can be made based on combined clinical signs or pathological findings with confirmation by identification of parasitic stages in the blood or infected organs. Preliminary diagnosis of the disease is achieved on the basis of case history of a farm, non-specific clinical signs (pyrexia, anaemia, and lymphadenopathy) and post-mortem findings. Definitive differential diagnosis (Babesiosis, Anaplasmosis) is always based on the detection of macroschizonts in Giemsa stained lymph node biopsy smears in live animals and impression smears of lymph nodes and spleen in dead animals (Aktas *et al.*, 2002). In some cases, microscopic examination of a blood smear may reveal intra-erythrocytic piroplasms but this, particularly for ECF, will not distinguish between acute current infection and the carrier stage. On the other hand, detection of macroschizonts in infected leukocytes along with piroplasms in erythrocytes of peripheral blood smears will identify clinical disease and in such cases the prognosis is poor (Pipano and Shkap, 2006).

Serological based diagnostic tests employing indirect fluorescent antibody test (IFAT) has been used in several epidemiological investigations (Dumanli *et al.*, 2005;Salih *et al.*, 2007). Although utilisation of IFAT for early detection of infection has been shown to be more sensitive than examination of blood smears (Darghouth *et al.*, 1996;Dhar and Gautam, 1977), there is a potential risk of obtaining false positive and negative results due to non-specific reactivity or a weak cross reactive immune response. Enzyme-linked immunosorbent assay (ELISA) has been developed for serological identification of *Theileria* infection by detecting anti-*Theileria* antibodies that react against piroplasm antigens (Gray *et al.*, 1980). Recently, more robust ELISAs have been developed utilising recombinant antigen representing parasite surface proteins, *Theileria annulata* merozoite surface antigen 1 (Tams1) (Gubbels *et al.*, 2000) and macroschizont *Theileria annulata* surface protein (TASP) (Bakheit *et al.*, 2004;Salih *et al.*, 2005).

DNA-based identification of parasite infection using polymerase chain reaction (PCR) has been recommended as the most sensitive assay and is the method of choice for the diagnosis of tropical theileriosis in the carrier state (Bilgic *et al.*, 2010). Several epidemiological studies have favourably compared the specificity and sensitivity of PCR with other conventional methods such as serological or microscopic based techniques (Aktas *et al.*, 2002;Aktas *et al.*, 2006;Almeria *et al.*, 2001;d'Oliveira *et al.*, 1995;Dumanli *et al.*, 2005;Martin-Sanchez *et al.*, 1999) and since then this technique is widely in use. Although, DNA-based PCR methodology is relatively costly compared to serological and microscopic examination, it is highly sensitive and more efficient (Aktas *et al.*, 2002;d'Oliveira *et al.*, 1995). Thus, using gene specific primers and amplification of specific fragments representing the Tams-1 gene has allowed detection of *T. annulata* in blood samples of carrier animals or infected ticks (d'Oliveira *et al.*, 1995;d'Oliveira *et al.*, 1997). In addition species specific PCR-RFLP tests have been developed (d'Oliveira *et al.*, 1995;d'Oliveira *et al.*, 1997;Heidarpour *et al.*, 2009), as well as a highly sensitive species-specific PCR test using primers designed against the cytochrome b gene (Bilgic *et al.*, 2010).

1.6 Chemotherapy and available control strategies

Several chemotherapeutic agents have been used worldwide for the treatment of theileriosis including parvaquone, halofuginone lactate, long acting oxytetracyclines and buparvaquone. However, most of these drugs have their own limitations including a requirement for early administration, repeated doses, drug resistance and lack of effectiveness against a particular stage of the infection. Previously, halofuginone has been shown to be effective against the schizont stage but at the same time the difference between toxic and therapeutic doses is marginal (Mbwambo *et al.*, 1986;Schein and Voigt, 1979). In the past tetracycline has also been used in large doses but has limited action against the piroplasm stage, which can cause pathology in tropical theileriosis (Dhar *et al.*, 1990;Gill *et al.*, 1978;Mallick *et al.*, 1987;Singh *et al.*, 1993). Research trials conducted for comparing the efficacy of different drugs has shown that buparvaquone (BW720c), a second-generation hydroxynaphthaquinone, is the drug of choice (Dolan *et al.*, 1984;Hawa *et al.*, 1988;McHardy *et al.*, 1985;Mutugi *et al.*, 1988;Ngumi *et al.*, 1992;Singh *et al.*, 1993). However, early treatment of the disease with BW720c has been recommended to achieve a rapid and desirable outcome in eliminating the parasite from the blood and lymph nodes and improvement of the clinical state of the animal. It has been reported that treatment with BW720c in animals in the advanced stage of disease failed to improve the clinical condition of the animal (Morrison and McKeever, 2006;Osman and Al-Gaabary, 2007).

Vaccination has been a focus of research and has shown some success in the field. Vaccination either in combination with drug treatment and tick control or in isolation has been used in different parts of the world for both tropical theileriosis and East Coast Fever (ECF). Vaccines against *T. annulata* are generated by attenuation of parasite virulence by prolonged culture *in vitro*, while for *T. parva* virulence of infection is controlled by co-delivery of a dose of long acting tetracycline (Morrison and McKeever, 2006;Morzaria *et al.*, 1987;Musoke *et al.*, 1993;Radley *et al.*, 1975). A number of authors have reviewed various control strategies against theileriosis (Brown, 1990;Dolan, 1989;Tait and Hall, 1990). Effective control of theileriosis is best achieved through a combined strategy of tick vector control and vaccination, while in

clinical cases chemotherapy is the only option. However, based on the continuing prevalence of the disease in endemic countries there is a dire need for improved control strategies because drug resistance against BW720c has been reported *in vivo* (Mhadhbi *et al.*, 2010), acaracides are costly and resistance has developed and existing vaccines have production and delivery limitations (Boulter and Hall, 1999;Mbassa *et al.*, 1998;McKeever *et al.*, 1999;Tait and Hall, 1990).

1.7 Cellular and molecular interactions between the *Theileria* macroschizont and the infected host leukocyte

Bovine leukocytes infected with *Theileria* have been demonstrated to acquire a number of phenotypic changes that involve cellular events induced by the presence of the parasite. Upon successful entry into the leukocyte and development to the macroschizont stage, the parasite fascinatingly takes control over the infected-host cellular machinery resulting, *in vitro*, in the establishment of an immortalised transformed phenotype.

1.7.1 Host cell transformation

Theileria-infected leukocytes display characteristic signs of transformed mammalian cells. Infected cells can be readily cultured *in vitro* and display both metastatic properties (Heussler and Stanway, 2008;von *et al.*, 2010) and resistance to programmed, apoptotic, cell death [reviewed in (Dobbelaere and Heussler, 1999)]. However, unlike classical transformation events, parasite induced transformation is reversible, as infected cells stop proliferating and die upon elimination of the parasite with theilericidal drug BW720c (Dobbelaere and Rottenberg, 2003;Rintelen *et al.*, 1990), unless they are supported by the addition of exogenous growth factors. At the molecular level transformation is known to be associated with modulation of normal host cell signaling pathways [reviewed in (Dobbelaere and Kuenzi, 2004;Luder *et al.*, 2009)]. Several of these pathways have been shown to result in constitutive activation of bovine transcription factors. Moreover, a link between activation and cellular proliferation, or proliferation and protection against cell death has been made

primarily by using drugs to specifically inhibit steps in the activation pathways. Additionally, it has been demonstrated that macroschizont infected leukocytes exhibit invasive tumour like growth *in vivo* when inoculated into immuno-compromised mice (Fell *et al.*, 1990;Irvin *et al.*, 1975), causing a malignant neoplastic like condition similar to human B cell lymphomas.

Activation of transcription factors can have a detrimental outcome and may act as tumour suppressors (Perkins and Gilmore, 2006;Sharpless and Depinho, 2002). Evidence has recently been generated that for some of these factors the parasite must take action to prevent a manifestation of function, and the best example to date concerns the classical tumour suppressor, p53.

While much information has been gained on pathways associated with *Theileria* mediated transformation, one area where detailed information is lacking is identification of parasite genes and proteins that are responsible for initiating the transformation event.

1.7.2 Activation of host cell transcription factors

It is widely accepted that the alteration of host cell phenotype by a number intracellular pathogens (viruses, bacteria and parasites) involves both activation and modulation of mammalian transcriptional factors (Gyles *et al.*, 2007;Julkunen *et al.*, 2001;Luder *et al.*, 2009). As a survival and defence strategy it is likely that *Theileria*, like other pathogens, have attained sophisticated mechanisms to interfere with the host response to infection. These mechanisms include the unique ability of pathogens to directly and indirectly manipulate and evade inflammatory and innate cellular defence pathways [reviewed in (Finlay and McFadden, 2006;Leiriao *et al.*, 2004;Luder *et al.*, 2009;Mogensen, 2009)]. It is clear from a large number of studies that leukocyte signal transduction pathways are significantly altered by *Theileria* parasites. Thus, in *Theileria* transformed cells, activation of c-Jun NH2-terminal kinase (JNK), NF-κB, casein-kinase 2 (CK2), PI3K-PKB and JAK2/STAT3 pathways have been documented [reviewed in (Baumgartner *et al.*, 2000;Dessauge *et al.*, 2005a;Dessauge *et al.*, 2005b;Dobbelaere and Kuenzi, 2004;Shiels *et al.*, 2006)] (see Figure 1.3). These pathways and factors are known to contribute to stimulation and regulation of the inflammatory, innate immune and cellular

defence responses. A summary of key transcription factors activated in *Theileria*-infected cells studied to date, and the role they play in regulation of inflammatory and innate immunity is discussed below.

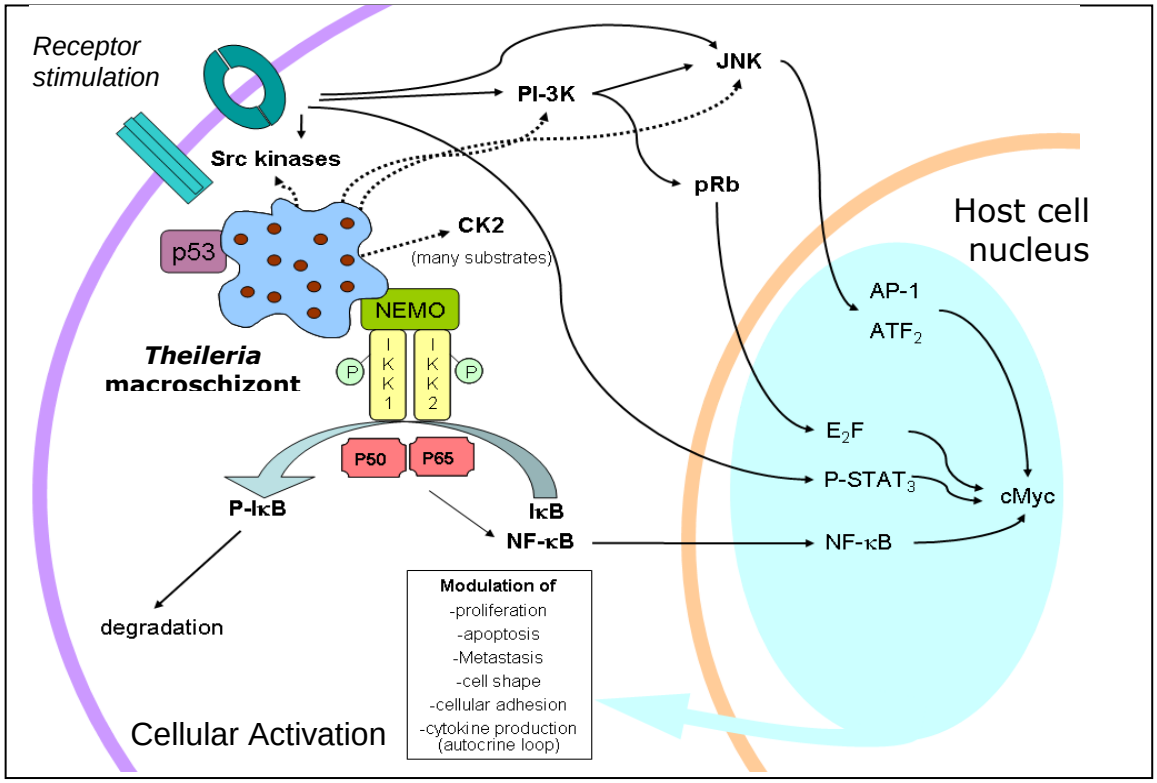

Figure 1.3: Pathways implicated in manipulation of *Theileria*-infected host cell phenotype
Theileria parasites invade bovine leukocytes and activate a number of signal transduction pathwys resulting in translocation of transcription factors to host nucleus. The transcription factors AP-1 and ATF-2 are constitutively activated via c-Jun NH2-terminal kinase (JNK) that is permanently activated in *Theileria* infected leukocytes. Constitutive cMyc expression is dependent on the JAK2/P-STAT3 pathways and is also influenced by AP1. Constitutive activation of NF-κB occurs via recruitment of IKK complexes (signalosomes) to the macroschizont surface. p53 apoptotic pathway of host cells is not induced by *Theileria* and it has been shown that parasite is involved in cytoplasmic sequestration of p53. Association of host-cell p53 with the parasite membrane has been postulated to either interact directly with p53, or mediate cytoplasmic sequestration of p53 by interacting with other host cell proteins regulating p53 localization. Apapted from (Shiels *et al.*, 2006)

1.7.2.1 Nuclear Factor kappa B (NF-κB)

NF-κB is a family of inducible, dimeric transcription factors that regulate the expression of genes involved in the inflammatory response, immune response, cell proliferation and apoptosis (Baldwin, Jr., 1996;Barkett and Gilmore, 1999;Barnes and Karin, 1997;Gilmore, 1999). NF-κB was first characterized as a transcription factor that constitutively binds to the κB motif in the enhancer element within the immunoglobulin κ light-chain gene (Sen and Baltimore, 1986). The family of NF-κB transcription factors consist of five subunits: RelA (also called p65), RelB, c-Rel, NF-κB1 (p50) and NF-κB2 (p52). The last two

proteins are synthesized as larger precursors of 105 (p105) and 100 kDa (p100), respectively, which are then proteolytically processed to their sub-unit forms. Activated hetero or homodimers of combinations of these subunits are then translocated into the nucleus to regulate the expression of a wide range of target genes (Hayden and Ghosh, 2004;Karin *et al.*, 2002). In unactivated cells, NF-κB/Rel dimers are sequestered in the cytoplasm in an inactive form as a result of their association with members of another family of proteins called Inhibitors of NF-κB (IκBs). IκBs form another evolutionary conserved multigenic family, composed of IκBα and IκBβ. In response to recognition of a wide variety of stimuli via Toll, IL1 and TNF receptors, a multi sub-unit kinase complex called IκB kinase (IKK), consisting of two catalytic subunits IKK1 (IKKα) and IKK2 (IKKβ), and a modulating subunit NEMO (IKKγ) is generated (see Figure 1.4).

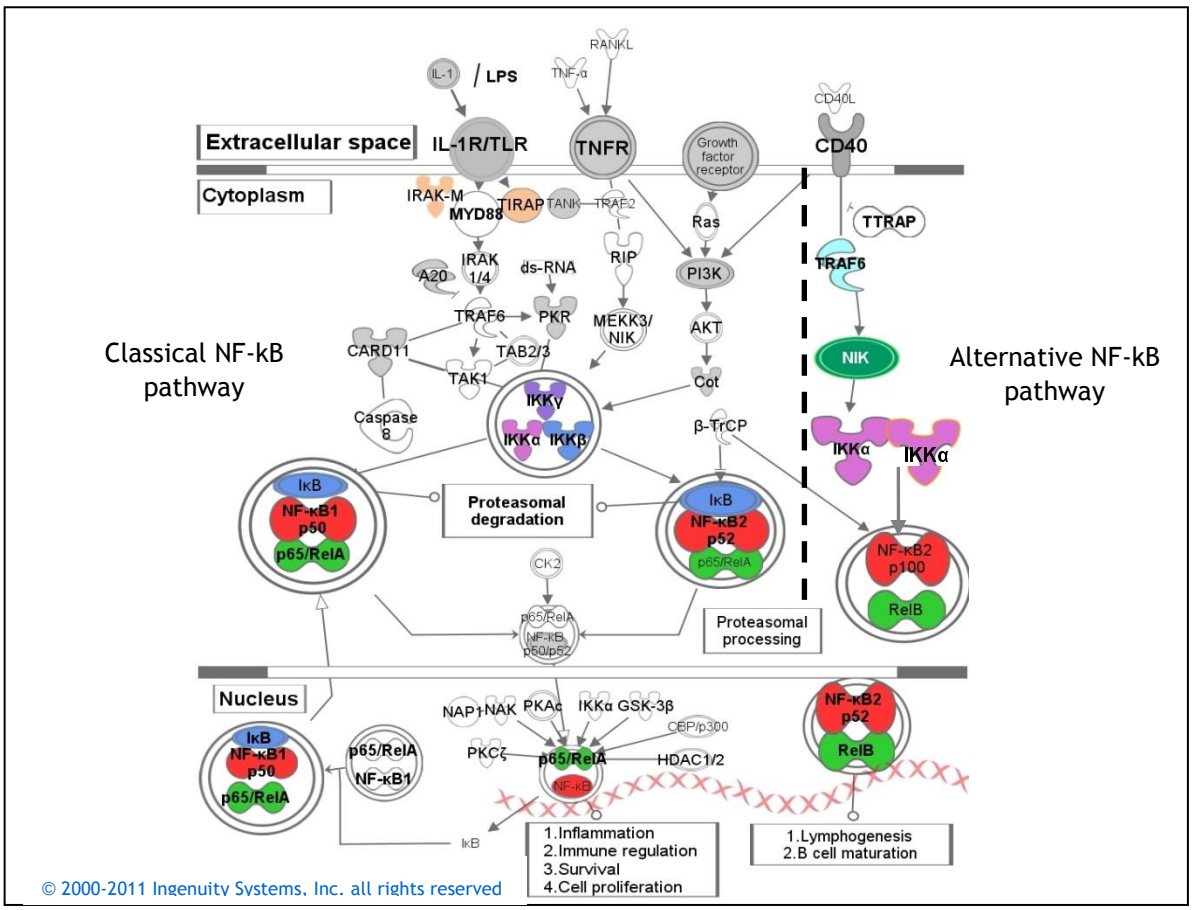

Figure 1.4: Schematic illustration of NF-κB **activation pathway in general**
Major signaling pathways that lead to NF-κB activation. NF-κB can be activated by a variety of receptors on the cell surface that transduce the signal via number of adaptor proteins (e.g TRAFs) and kinases (IRK and MEKK3/NIK). Classical activation of NF-κB occurs via recruitment of IKK complexes leading to phosphorylation and degradation of the IkB. Inputs for the classical pathway include TNFR1/2, TLR/IL-R. The alternative pathway involves NIK activation of IKKα and leads to phosphorylation and processing of p100, activating p52/RelB heterodimers.

The IKK complex phosphorylates specific serine residues within the IκBs, leading to their ubiquitination and degradation through the proteasome pathway. Ultimately free NF-κB dimers translocate to the nucleus to regulate the transcription of a large number of target genes (Weil *et al.*, 1997;Whiteside and Israel, 1997).

In uninfected cells the activation of NF-κB is usually triggered through a range of different surface receptors or intracellular events, including cellular stress [reviewed in (Oeckinghaus *et al.*, 2011;Perkins, 2012)]. The parasite factor(s) that induces NF-κB activation are still unknown but it has been postulated that parasite proteins either expressed on the surface of the schizont or secreted into the host cell cytoplasm may interfere with the signal-transduction pathway of the host cells. Heussler *et al.*, (2002) provided remarkable evidence that parasite associated factors almost certainly contribute to NF-κB activation, as it was shown by immunofluorescence imaging that the macroschizont stage of the parasite infected cell is decorated with active IKK Signalosome complexes. Due to the apparent proximity of the signalosome formation with the parasite it was logical to propose that parasite derived proteins located at the surface of the schizont act directly as a ligand for an IKK protein, leading to enforced oligomerisation of the signalosome complex and subsequent "proximity induced activation". However, after extensive research it has not yet been possible to establish a direct interaction between parasite protein and components of the signalosome (Dobbelaere and Kuenzi, 2004;Heussler *et al.*, 2002). One possibility is that additional host proteins that act as a scaffold for IKK oligomerisation are required, and evidence that the actin cytoskeleton promotes formation of parasite dependent IKK signalosomes has been found (Schmuckli-Maurer *et al.*, 2010).

A clear role for activated NF-κB in preventing apoptosis of *Theileria* infected leukocytes has been established (see below). However, activated NF-κB is unlikely to be restricted to this role, as NF-κB is known to regulate genes that are important for several other vital cellular processes such as proliferation, differentiation, and development. NF-κB is also a critical activator of genes involved in inflammation and immunity activated via Toll like receptors, IL1 and TNF receptors (Gerondakis *et al.*, 1998;Li and Verma, 2002) and it is well known that prolonged activation of NF-κB is associated with diseases that result from

chronic stimulation of the inflammatory response (Aggarwal *et al.*, 2006;Makarov *et al.*, 1997). Thus NF-κB is a transcription factor with a wide range of potential functions which includes regulation of genes encoding cytokines and growth factors, adhesion molecules, acute phase reactants and receptors and chemoattractants which influence the outcome of disease (Schwartz *et al.*, 1999). It has been predicted that NF-κB dependent regulation of inflammatory genes contributes to the pathogenesis of theileriosis (Heussler *et al.*, 2002).

1.7.2.2 Activator Protein 1 (AP-1)

AP-1 is a complex multi-protein transcription factor, composed of proteins from a number of families [members of Fos (c-Fos, FOSB, FRA1, FRA2), c-Jun (c-Jun, JUNB, JUND), ATF (ATF2, ATFa, ATF3, ATF4, B-ATF) and MAF (c-MAF, MAFA, MAFB)] that exists ubiquitously as either a homo- or heterodimeric complex. These complexes are formed via the basic leucine zipper, a domain that is important for dimerisation and DNA binding, and is represented in a large family of proteins that act as DNA binding proteins (Halazonetis *et al.*, 1988;Hess *et al.*, 2004a). In response to various inflammatory stimuli, activated AP-1 in turn regulates the expression of genes that control a number of critical cellular events including proliferation, differentiation and apoptosis (Ameyar *et al.*, 2003;Jacobs-Helber *et al.*, 1998). Furthermore, regulation of these cellular events is dependent on the relative abundance of AP-1, the composition of AP-1 dimers, and the types of stimuli and cellular context of the activation event (Kaminska *et al.*, 2000).

Ap-1 proteins have versatile functions in the regulation of cell proliferation, and several direct targets have been identified whose expression is directly linked to the cell cycle regulatory apparatus [reviewed in (Jochum *et al.*, 2001)]. Normally activation of AP-1 is dependent on activation of various signaling cascades including JNK, ErK and mitogen activating protein kinases (MAPKs). It has been shown that for *Theileria*-infected bovine leukocytes, AP-1 activity is exclusively dependent on JNK via its main substrate c-jun (Chaussepied and Langsley, 1996;Lizundia *et al.*, 2006). Supporting evidence has also been provided by Chaussepied *et al.*, (1996) who demonstrated that both JNK activity and elevated nuclear localisation of jun proteins occur in *T. parva*-transformed B cells compared to uninfected B cells. The elevated activity of JNK in an infected

cell causes constitutive phosphorylation of the N-terminus of c-jun, which in turn results in up-regulation of AP-1 driven transcription.

The constitutive activation of AP-1 is believed to contribute significantly to the metastatic potential of the infected cell line. In support of this conclusion, AP1 has been implicated in induction of host cell metalloprotease-9 (MMP9) gene expression (Adamson and Hall, 1997). In addition, attenuated vaccine cell lines exhibiting lower metastatic potential display reduced metalloprotease gene expression. The reduction was postulated to be associated with loss of a parasite induced AP-1 recognition factor, as indicated by an altered (EMSA) profile of proteins binding to the AP-1 site in the promoter region of the MMP9 gene (Adamson et al., 2000).

1.7.3 Induction of proliferation by *Theileria*

Several studies have shown that resting leukocytes have the ability to proliferate after stimulation; however most of the cells are sensitive to inflammatory stimuli and die via a special mechanism called activation induced cell death (AICD) (Arnold *et al.*, 2006;Donjerkovic and Scott, 2000). In contrast, macroschizont-infected cells of *T. annulata* and *T. parva* display continuous proliferation and are resistant to AICD. Uncontrolled proliferation is one of the most important features of *Theileria*-transformed cells. Previously it has been reported that *Theileria*-transformed leukocytes exhibit moderate but constitutive levels of PI3K (Baumgartner *et al.*, 2000). Moreover this study showed that this constitutive PI3-kinase activity is essential for proliferation of the infected cell using the specific inhibitors LY294002 and wortmannin. It was also shown that the granulocyte-monocyte stimulating factor (GM-CSF) is induced by PI3-Kinase, allowing postulation that a GM-CSF autocrine loop functions to maintain proliferation of the host leukocyte. A second study confirmed a role for constitutive PI3-K activity in contributing to proliferation of the infected cell (Heussler *et al.*, 2001). Furthermore both studies generated evidence through the use of inhibitors that PI-3K activity was not required to protect the cell from apoptosis. However discrepancies between the two studies were obtained in relation to activation of Akt/PKB and NF-κB. Heussler *et al.*, found no role for PI3-K in activation of NF-κB, while Baumgartner concluded PI3-

K did not act via PKB. How the PI3-K pathway is activated is not conclusively known but an indirect event via surface receptors or adhesion molecules upregulated in infected cells have been proposed (Heussler *et al.*, 2001). More recent studies proposed a role for the Src family kinase Hck (Baumgartner *et al.*, 2000), with constitutive activation of PI3-K postulated to result from a loss of negative regulation of Hck present in lipid rafts of *Theileria* infected leukocytes.

As discussed by Huessler *et al.*, (2001), Akt/PKB could feed into regulation of proliferation of *Theileria*-infected cells at different levels by stimulating expression genes that control cell cycle progression such as c-fos, c-myc and the G1 cyclins. Regulation of the cell cycle may also be achieved via negative regulation of tumour suppressors such as p53 and retinoblastoma protein and activation of the E2F transcription factor [reviewed by (Shiels *et al.*, 2006)]. PI3-K activation may also contribute to metastasis of the infected cell by increased expression of c-Fos and inhibition of PI3-K was found to reduce AP-1 transcriptional activity (Baumgartner *et al.*, 2000).

1.7.4 Inhibition of host cell apoptosis by *Theileria*

Many infections are strongly associated with activation of the NF-κB pathway and stimulation of the inflammatory response. Upon activation NF-κB translocates to the nucleus and is found in this location in *Theileria* infected cells. However, after elimination of the parasites by BW720c, NF-κB is no longer located in the nucleus indicating that a viable parasite is required for its constitutive activation (Heussler *et al.*, 1999;Ivanov *et al.*, 1989). Although studies have shown that NF-κB can be involved in promoting proliferation of transformed cells, for the *Theileria* infected cell, the proven role of NF-κB is in protecting cells from programmed cell death (apoptosis), with a potential to promote proliferation presumed but not substantiated (Dessauge *et al.*, 2005b;Guergnon *et al.*, 2003;Palmer *et al.*, 1997). Thus, inhibition of constitutive NF-κB activation by dominant negative inhibitors of NF-kB has been shown to induce rapid apoptosis of infected cells, supporting the key role of NF-κB in the survival of *Theileria* transformed cells (Heussler *et al.*, 1999). Since apoptosis and proliferation are two physiologically active phenomena closely linked and regulated (Ginaldi *et al.*, 2000), it was difficult to conclude what the effect on proliferation was

following inhibition of NF-kB. Constitutive activation of NF-κB has been shown to protect the *Theileria* infected cell from apoptosis probably via up-regulation of some well known antiapoptotic proteins such as c-FLIP, X-IAP, c-IAP (Dobbelaere and Kuenzi, 2004). Regulation of these proteins by NF-κB has also been demonstrated for other cell types, supporting their role as putative anti-apoptotic targets of NF-κB in *Theileria*-transformed cells. NF-κB mediated expression of anti-apoptotic proteins can provide protection against apoptosis at different levels. For instance, c-FLIP could block the processing of procaspase 8/10, triggered upon ligand-induced activation of death receptors (e.g. Fas). IAPs counter effector caspases, and pro-survival proteins of the Bcl-2 family prevent mitochondria-initiated apoptosis, by regulating cytochrome C release (Kataoka *et al.*, 2000;Peter, 2004;Schimmer and Dalili, 2005;Tschopp *et al.*, 1998;Yang *et al.*, 1997).

In addition to NF-κB, other factors and pathways have also been implicated in protecting the infected cell from cellular death. In the study of (Dessauge *et al.*, 2005a) constitutive expression of the oncogenic protein c-myc via Jak-Stat signal transduction was described. Inhibition of c-myc was shown to induce death of infected cells and it was postulated that the anti-apoptotic effect could be due to c-myc-dependent induction of Bcl-2 family member, Mcl-1. As predicted, expression of c-myc was shown to be dependent on the presence of a viable parasite (Dessauge *et al.*, 2005b). The transciption factor c-Myc is well established as an oncogneic protein with a broad range of cellular functions, including regulation of cell cycle progression, cell growth, differentiation, transformation, angiogenesis and apoptosis [reviewed in (Gonzalez and Hurley, 2010)]. C-Myc can act as an inducer and suppressor of its target genes and these include: Cyclin A, Cyclin D and Cdk4, p53, MHC class 1, C/EBPα, cdc42 (Dang, 1999;Dang *et al.*, 2006).

The tumour suppressor p53 is a key molecule involved in regulation of cell cycle progression and cell death and provides a major checkpoint in the prevention of cells becoming cancerous (Collins *et al.*, 1997). The function of p53 in normal cells is to arrest cell division and initiate apoptosis in response to cellular stress and DNA damage [reviewed in (Amaral *et al.*, 2010)]. Loss or block of p53 function is a common feature of transformed cells and it might be expected that *Theileria* infected leukocytes limit functional expression of this tumour

suppressor protein. This prediction was tested by Haller *et al.*, (2010), who investigated p53 apoptosis related events as a target of parasite modulation. This result indicated that *T.annulata* infected cells are able to inhibit the p53 apoptotic pathway, mainly by sequestration of the majority of p53 to the cytoplasm of the infected cell. Immunodetection revealed close association of p53 with the schizont membrane, and this sequestration was destabilized following elimination of the viable parasite with BW720c. This led to nuclear translocation of p53 and was associated with upregulation of proapototic proteins Bax and Apaf1 and downregulation of anti-apoptotic Bcl-2. It was proposed that modulation of p53 activity could occur via direct interaction with a parasite surface protein or via other host proteins that regulate localisation of p53 (Haller *et al.*, 2010).

Although, it has been shown that PI3K/PKB pathways in *Theileria annulata*-is primarily linked to the promotion of proliferation some evidence has been produced that residual PKB activity can contribute to protection against cell death in *Theileria*-infected BL3 cells. Thus in the study of (Guergnon *et al.*, 2006) apoptosis could only be inhibited by dual inhibition of PKB together with PKA. It was concluded however, that PKA was predominant in the infected cell, and functioned by inhibiting the pro-apoptotic molecule Bad (member of the BCL-2 family). Taken together these studies indicate the parasite must manipulate cellular pathways that promote programmed cell death in response to stress or induction of uncontrolled proliferation.

1.7.5 Manipulation of activated host cell gene expression

Constitutive activation of inflammatory transcription factors could result in events that are detrimental as well as beneficial to the infected cell. Thus, constitutive activation of factors primarily associated with anti-apoptotic activity may lead to the death of lymphocytes under certain circumstances (Dutta *et al.*, 2006). NF-κB, for example generally protects cells from apoptosis by inducing the expression of genes responsible for encoding anti-apoptotic proteins (Dobbelaere and Kuenzi, 2004). However, the role of NF-κB in apoptosis can vary markedly in different cell contexts and it can sensitize cells to a variety of death inducing stimuli like pro-inflammatory cytokines, Tumour Necrosis

Factor alpha (TNFα) and inducible Nitric Oxide Synthase (iNOS) (Dutta *et al.*, 2006). Consequently NF-κB was described as a Janus-like transcriptional factor (Youssef and Steinman, 2006). Moreover, constant activation of NF-κB can lead to chronic inflammatory conditions by promoting the expression of cytokine genes (Beinke and Ley, 2004) or contributing to pathogenesis associated with many tumors (Basseres and Baldwin, 2006). Therefore, parasite associated persistent activation of NF-κB and other Janus-like transcription factors, c-Jun (Chaussepied *et al.*, 1998) and c-Myc (Dessauge *et al.*, 2005a), have the potential to be detrimental to the transformed infected leukocyte and the infected host.

The first evidence that *Theileria* parasites may manipulate the outcome of infection was provided by Sager *et al.*, (1997) who demonstrated that lipopolysaccharide (LPS) induced expression of pro-inflammatory cytokines IL-1, TNFα and iNOS in the *Theileria annulata* transformed cells were impaired, as none of these activities were up regulated following LPS treatment relative to significant elevation in uninfected cells. Sager *et al.,* (1997) also provided evidence that infection of macrophages by *T. annulata* induces a reversible dedifferentiation event, that may occur as a consequence of, or is involved in establishing, cellular transformation. Further evidence for modulation of macrophage status has also been provided by the more recent study of Jensen *et al.,* (2009) which demonstrated a parasite dependent suppression of MAF transcription factors. MAFs are known to be involved in regulating the monocyte/macrophage differentiation step from myeloid precursor cells.

Oura *et al.,* (2006) also demonstrated the ability of parasite infection to down-regulate the expression of pro-inflammatory genes associated with cellular defence. Thus, while infection induced an increase in expression of genes involved in the interferon inducible ISGylation pathway, the level of expression was significantly lower than that obtained by stimulation of uninfected cells with LPS. Furthermore, killing the cell with BW720c led to a significant elevation in interferon stimulated gene 15 (ISG15) and ubiquitin like protease (UBP-3) gene expression, indicating full expression of these genes is repressed by a viable parasite. ISG15 has been shown to be a direct target of NF-κB (Li *et al.*, 2001) and NF-κB and AP-1 are strongly activated via LPS to induce expression of pro-inflammatory cytokines IL-1, TNFα and iNOS (Cho *et al.*, 2005). Since NF-κB and

AP-1 are constitutively activated in *Theileria* transformed cells, it can be hypothesised that the attenuated expression profile of genes such as TNFα, iNOS and ISG15 (Oura *et al.*, 2006;Sager *et al.*, 1997) is due to active modulation by the parasite-infected leukocyte.

1.7.6 Candidate parasite regulators of the transformation phenotype

Despite the wealth of information on modulation of host cell gene expression, parasite factors responsible for controlling these events have not been conclusively identified. However, three major points of parasite-host interaction (parasite surface, host cytoplasm, and nucleus) are under current investigation, with candidate proteins obtained both from experimental work and mining the available genome sequences of *T. annulata* and *T. parva* (Pain *et al.*, 2005;Shiels *et al.*, 2006).

One of the most obvious points of interaction is the interface between the membrane surface of the macroschizont and the host cell cytoplasm. This is a key area for the mechanism behind IKK signalosome formation, as it has been postulated that the primary event is likely to be an interaction between a signalosome component and a parasite-encoded surface ligand. In this context, it has recently been shown that the parasite surface protein known as TpSCOP (*T. parva* schizont-derived cytoskeleton binding protein) has the ability to interact with F-actin (Hayashida et al., 2010) and activate NF-κB in transfected mammalian cells. Furthermore, transient transfection of TpSCOP in *T. parva*-infected cells also showed enhanced activation of NF-κB. However, this protein is expressed by the piroplasm stages of *Theileria* species that are non-transforming, and it is known that altering actin structure can result in activation of host dependent NF-kB signalling. Furthermore, co-localisation of TpSCOP and parasite/signalosome complexes was not demonstrated.

Additional parasite proteins studied as candidates for interaction with the host cytoskeleton include TaSP, TaSE and gp34. *T. annulata* secretory protein (TaSE) is secreted into the host cell compartment and is speculated to have a functional role in host-parasite interaction (Schneider *et al.*, 2007). Confocal microscopic

examination revealed co-localisation of TaSE with host cell microtubules, especially apparent during mitosis. Evidence of specific interaction was provided by co-precipitation of TaSE and alpha-tubulin. However, co-localisation and co-immunoprecipitation experiments showed that only a fraction of the expressed TaSE associated with tubulin, suggesting that TaSE may interact via microtubule-associated proteins. Based on the patterns identified for TaSE during mitosis it was postulated that this protein might play a role in ensuring the uniform distribution of schizont into the host-daughter cells during cell division (Schneider *et al.*, 2007).

A similar role has been proposed for TaSP, an immunodominant *Theileria annulata* surface protein proposed to be involved in the attachment of the parasite to the host cell microtubule network (Seitzer *et al.*, 2010). TaSP was shown to co-localise with the mitotic spindle of dividing cells and co-immunoprecipitated with alpha-tubulin in transiently transfected Cos-7 cells. Moreover, results obtained from pull-down assay provided evidence of direct interaction between TaSP and polymerised microtubules. Immunofluorescence analysis located TaSP at various sites of mitotic cells including spindle poles, mitotic spindle apparatus and the mid-body (Seitzer *et al.*, 2010). Based on localisation to the microtubule organising centre, it was speculated that TaSP is involved in regulation of microtubule assembly in the host cell.

One further protein identified as potentially interacting with the host cell cytoskeleton is gp34, a GPI anchored protein specifically expressed at the macroschizont surface (Xue *et al.*, 2010). Tagged *T. parva*-gp34 but not *T. annulata-gp34* localised to the central spindle and mid body. Interestingly gp34 was associated with a disruption of cytokinesis, as over expression of transgene increased the number of bi-nucleate cells detected. It was proposed that this result could reflect a capacity of gp34 to interact with regulators of host cell cytokinesis

The *T. annulata* encoded antigen Ta9 is an immunodominant protein recognised by CD8 T cells, indicating presentation of peptides at the infected cell surface (MacHugh *et al.*, 2011). Sequence analysis of Ta9 genes from field isolates of *T. annulata* revealed extensive divergence, resulting in amino acid polymorphism within two distinct major histocompatibility restricted T cell epitopes.

Functional studies have confirmed that differences in sequence of this epitope correspond with differential recognition of infected cells by individual CD8 T cell clones. The Ta9 protein is predicted to have a cleaved signal peptide, indicating secretion by the parasite into the cytosolic compartment. Identification of Ta9 polypeptide in the cytoplasm of macroschizont-infected cells was reported (MacHugh *et al.*, 2011). It is unknown what role TA9 plays in the transformation process, if any. However, given it is a major antigen it seems reasonable to propose that it must bear some important function, since as a presented T cell antigen it would appear to generate a selective disadvantage to the survival of the infected cell. Conserved signal sequence and partially conserved motifs were described at the c-terminus of TA9 and a clear orthologue is present in *T. parva*.

Ta9 is a secretome protein and is encoded by a member of a small gene family (5 genes). Two additional larger secretome gene families have been described in some detail (Pain et al., 2005). The subtelomere-encoded variable secreted protein (SVSPs) family consists of 85 members in *T. parva* and 51 members in *T. annulata* (Pain *et al.*, 2005;Schmuckli-Maurer *et al.*, 2009;Shiels *et al.*, 2006;Weir *et al.*, 2010). Almost all SVSPs are expressed at the RNA level by the macroschizont stage. SVSPs consist of a short conserved N-terminal region, containing a putative signal peptide for secretion, followed by a highly variable QP-rich region which is predicted to be highly unstructured (Pain et al., 2005;Schmuckli-Maurer et al., 2009). Interestingly, a number of SVSPs also contain functional nuclear localisation signals (NLS), suggesting that proteins released from the parasite could contribute to phenotypic changes of the host cell (Schmuckli-Maurer *et al.*, 2009). This study also suggested that the transcript levels of single SVSP genes can vary considerably depending on the parasite genotype but no evidence was found for a possible influence of the host cell background on differential SVSP mRNA expression (Schmuckli-Maurer *et al.*, 2009). Despite the identification of conserved motifs, a potential biological function for the SVSPs has yet to be proposed. In the study performed by *Weir et al., 2010,* a large number of alleles were sequenced and assessed for evidence of selection of amino acid substitutions. None was found and it was proposed that SVSP's have evolved in a neutral manner and may act to subvert protective immunity.

The second secretome family that has been studied in some detail is the TashAT family. In *T. annulata* this family consists of 17 contiguous genes. The first member to be identified encodes the TashAT2 polypeptide that was shown to be located to the host cell nucleus of the transformed leukocyte. It has been postulated that these parasite polypeptides have the ability to modulate bovine gene expression since they contain AT hooks. AT hooks are motifs that primarily function in transportation of proteins to the nucleus and bind to AT-rich DNA. AT hook domain proteins are conserved in eukaryotes from yeast to humans and play critical roles in regulation of gene expression and determination of cell fate (Cleynen and Van de Ven, 2008;Reeves, 2010;Reeves and Beckerbauer, 2001). AT hook proteins are commonly associated with the generation of neoplasias (Fusco and Fedele, 2007). Five AT hook bearing TashAT proteins are encoded in the genome: TashAT2, TashAT1/3, TashHN, and SuAT1 (Shiels *et al.*, 2004;Swan *et al.*, 1999;Swan *et al.*, 2001;Swan *et al.*, 2003). Interestingly no AT hook motif has been identified in *T. parva*, although an orthologous cluster of 18 TpHN genes have been described. The reason for this is not known, but may be due to the different preferred lineage of leukocyte infected by either species (Shiels et al., 2006).

Functional data supporting a role of TashAT cluster proteins in manipulating bovine gene expression was reported by Shiels *et al.,* (2004) and Oura *et al.*, (2006). Thus TashAT 1/3, TashAT2 and SuAT1 have all been shown to bind to AT rich DNA. Stable transfections of both TashAT2 and SuAT1 into a bovine macrophage cell line was found to be associated with changes to cellular morphology, mRNA profile and the proteome of TashAT expressing cells (Shiels *et al.*, 2004;Swan *et al.*, 1999). Interestingly SuAT1 promotes changes to the level of intermediate proteins that function to control cell shape, and repression of these proteins (cytokeratins) was demonstrated to be under control of a viable parasite (Shiels *et al.*, 2004). Cytokeratins are a large family of proteins which form the intermediate filament (IF) of the cytoskeleton and have been found to modulate host-cell proliferation process (Paramio *et al.*, 1999). Furthermore it is known that mammalian AT hook genes function to modulate the expression of genes targeted by NF-κB in myeloid cells. TashAT factor proteins can therefore be considered as candidates for parasite-encoded factors that function to manipulate the profile of host gene expression resulting from

infection associated cellular activation events. Summary of candidate parasite proteins released into the host cell cytoplasm and their interactions with the transformed-host cell is shown in Table 1.1.

Table 1.1: List of *Theileria* proteins that are candidate manipulators of host cell phenotype

Parasite proteins	Location	SignalP	NLS	Relationship to host cell transformation
TaSP	-Parasite membrane	Yes	-	Interacts with host cell microtubule network. (Seitzer *et al.*, 2010)
TaSE	-Parasite membrane -Schizont -Host cell cytoplasm	Yes	-	Close association of TaSE with the host tubulin network and co-localization at distinct points with host microtubule (with centromere, mitotic spindle and mid body) has been demonstrated. (Schneider *et al.*, 2007)
gp-34	-Parasite membrane	Yes	-	gp-34 is a GPI-anchored protein that is expressed at the schizont surface and interacts with regulators of the host cell cytokines and localize to the central spindle and midbody. Predicted to have functional role during host cell division. (Xue *et al.*, 2010)
Ta9	-Parasite - Host cell cytoplasm	Yes	-	An immunodominent protein recognised by $CD8^+$ T cells. The presence of a signal peptide indicates that T9 is likely to be secreted by the parasite and hence be available for cytosolic antigen processing. (MacHugh *et al.*, 2011)
TashATs TashAT2 TashAT1/3 SuAT1 TasHN	Host cell cytoplasm Host cell nucleus	Yes	Yes	Members of TashAT family bearing AT-hook motifs are secreted by the parasite and translocated to the host cell nucleus. These proteins are predicted to function as accessory factors for regulators of gene expression. [reviewed in (Shiels *et al.*, 2006)] and (Weir *et al.*, 2010)
SVSPs	* Host cell cytoplasm * Host cell nucleus	Yes	Yes	SVSPs are sub-telomeric hypothetical proteins. A subset of these is predicted to be secreted suggesting their role in phenotypic changes of the infected host cell. (Schmuckli-Maurer *et al.*, 2009)
TPSCOP	Released into the cytoplasm of infected cells	Yes		TPSCOP is a schizont derived cytoskeleton binding protein and has the ability to interact with F-actin and can result in activation of host dependent NF-kB signaling. (Hayashida *et al.*, 2010)
Unknown	-	-	-	Parasite proteins involved in the formation of parasite-dependent IKK signalosome and interaction between its component
Unknown	-	-	-	Parasite proteins involved in sequestration of p53 in host cell cytoplasm

* Minority of the SVSP family members are secreted into the host cell cytoplasm and translocated to the nucleus. However, almost all are expressed at the RNA level by the macroschizont stage.

1.8 Aims and objectives

Theileria is a major pathogen, causing a significant economic burden to countries where this parasite is endemic. Research to understand the factors contributing to disease pathology is required and is of scientific interest. An aim of this thesis was to elucidate one of the primary molecular mechanisms implicated in *Theileria* pathology, the induction of host leukocyte proliferation and prevention of apoptosis by the macroschizont stage of the life cycle. Evidence from literature has indicated that this may be a two-step process involving parasite-induced activation of host transcription factors, particularly NF-κB and Ap-1, followed by modulation of the outcome of transcription factor activation in controlling host cell gene expression. Data supporting this postulation at a global level was required particularly with regard to whether the parasite is able to alter the outcome of activating inflammatory signal transduction pathways. The mechanisms utilised by the parasite in directing host cell gene expression have not been identified. However, parasite polypeptides (TashATs) that are translocated to the host cell nucleus of the infected leukocyte are candidates for this role.

The main objectives of the work presented in this thesis were as follows:

I. Establishment and characterisation of an experimental model for comparison of uninfected and *Theileria*-infected cells activated by stimulation with inflammatory mediators.

II. Identification of host cell gene expression changes representative of uninfected and infected cells following stimulation with inflammatory mediators and identification of profiles indicating modulation of inflammatory gene expression by parasite infection

III. Bioinformatic analysis of any infection modulated dataset to identify gene expression events that can be predicted to benefit the establishment of the infected leukocyte: with emphasis on transcription factors and pathways known to be associated with *Theileria* infection.

IV. To investigate a parasite protein (TashAT2) as a candidate factor for modulation of bovine gene expression profiles associated with infection and inflammatory stimulation.

It was anticipated that by addressing these aims and objectives further insight into the complex relationship between *Theileria* parasites and host cell regulatory pathways responsible for the establishment of the activated, transformed leukocytes would be gained. Furthermore, knowledge arising from this study could lead to the development of novel intervention strategies against theileriosis, inflammatory and neoplastic diseases.

Chapter 2

Materials and Methods

2 Materials and methods

2.1 Maintenance of cell culture

All types of cell lines used in this study were maintained in culture at 37ºC, with 5 % CO_2. Cells were cultured in tissue culture flasks (25cm^2 or 75cm^2) and the cell number of each culture was started at 2 x 10^5 cells/ml and maintained by feeding with fresh complete medium every two to three days at, usually, a 1 in 5 dilution. Details of specific cell lines used and their media requirements are given in relevant chapters.

2.1.1 Preparation of cell culture reagents and complete medium

Reagents used for making complete medium

1. RPMI-1640 with added L-Glutamine and 25mM HEPES (Gibco)
2. Heat-inactivated foetal bovine serum (FBS; Sigma)
3. Streptomycin 8 µg/ml,
4. Penicillin 8 units/ml
5. Amphotericin B 0.6 µg/ml
6. Sterile sodium bicarbonate 0.05%.

2.1.2 Cryopreservation and thawing of cell lines

Cell lines were preserved in liquid nitrogen for long term storage. Approximately 8 ml of cell culture was centrifuged at 750 ×g for 5 min at 4ºC and resuspened in 3 ml of appropriate complete medium containing 10 % dimethylsulphoxide (DMSO). The resuspended cells were split between two 2 ml cryotubes, wrapped in cotton wool and frozen in pre chilled polystyrene box at -80ºC freezer overnight before transfer to liquid nitrogen.

To recover cells from liquid nitrogen, cryopreserved tubes were quickly thawed at 37ºC and added immediately to 8 ml prewarmed complete medium (37ºC). The cells were pelleted by centrifugation at 750 ×g for 5 min at room temperature to wash off the traces of DMSO. Cells were washed twice in pre-

warmed medium with 5 ml of fresh medium to ensure complete removal of DMSO. Finally the cell pellet was resuspended in 5 ml fresh complete medium and transferred to 25cm^2 culture flasks and incubated at above mentioned culture conditions.

2.2 Reagents and Solutions

The buffers and solutions commonly used in the experimental protocols of this thesis are listed below:

2.2.1 Dual Luciferase Assay

Luciferase assays in cells transfected with firefly luciferase (NF-κB-LUC) and Renilla luciferase (phRG-TK renilla) plasmids were carried out using the Dual-Luciferase® reporter Assay kit (Promega: cat # E1910).

Dual luciferase® reporter (DLR) assay chemistry

The DLR assay system provides an efficient means of performing dual reporter assay which is based on the simultaneous use and sequential measurement of Firefly (*Photinus pyralis*) luciferase and Renilla (*Renilla reniformis*) luciferase activities in order to directly obtain normalised data. Each luciferase breaks down its distinct substrate allowing discrimination between the 2 different bioluminescent reactions (Figure 2.1). The Renilla luciferase provides a measurement of the amount of cells successfully co-transfected (i.e. that contain the firefly vector) and the ratio of Firefly/Renilla gives the actual luciferase value that corresponds to the gene of interest being studied (NF-κB). The Renilla control vector allows measurement of the baseline transcription levels and normalises the differences in cell viability, cell lysis efficiency, transfection efficiency etc. Thus, using phRG-TK, Renilla luciferase, allows efficient use of both the experimental and control vectors to be measured using the same apparatus and in the same units. These can then be compared directly without any separation of the samples or conversion of the units.

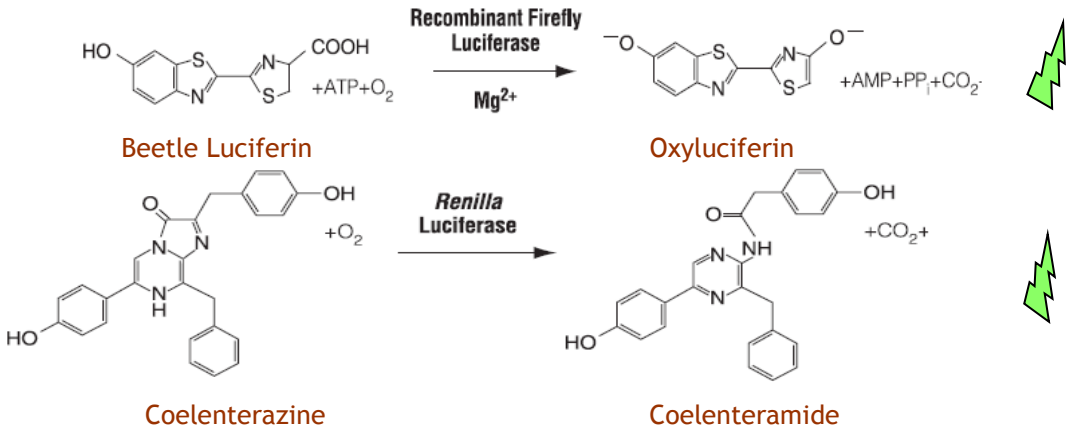

Figure 2.1: Bioluminescent reactions catalysed by firefly and *Renilla* luciferase
http://kirschner.med.harvard.edu/files/protocols/Promega_dualluciferase.pdf

Product Components and Storage Conditions

Reporter Assay System 100 assays E1910

Reporter Assays. Includes:

- 10ml Luciferase Assay Buffer II
- 1 vial Luciferase Assay Substrate (lyophilized Product)
- 10ml Stop & Glo®

Buffer

- 200µl Stop & Glo® Substrate, 50X
- 30ml Passive Lysis Buffer, 5X

Once the Luciferase Assay Substrate were reconstituted, working aliquots were stored at -20°C for up to 1 month or at -70°C for up to 1 year.

2.2.2 Indirect immunofluorescence analysis

2.2.2.1 Phosphate buffered saline (PBS x 1)

Dissolve 8g NaCl, 0.2g KCl, 1.15g Na_2HPO_4 and 0.2g KH_2PO_4 in dH_2O up to 1 L of total volume and adjust to pH 7.4.

2.2.2.2 Paraformaldehyde fixation solution (3.7 %)

Dissolve 3.7g paraformaldehyde in 100ml of 1 x PBS, Add 150µl of 1M NaOH, heat to 50ºC in microwave (do not boil), cool on ice and PH to 7.4 with HCl. Store at 4ºC (lasts for about 1 week).

2.2.2.3 Permeabilisation solution (Triton x 0.2)

Add 200 µl Triton X-100 in 100ml 1 x PBS, Stir contonously until dissolved properly and store at room temperature.

2.2.2.4 Mounting medium

For 1 ml solution, add 50 % glycerol in 1 x PBS (i.e. 0.5ml glycerol, 0.5ml 1X PBS), 10µl of anti-fade reagent (diphenylamine @ 100mg/ml) and 1µl of DAPI (4', 6-diamidino-2-phenylindole, dihydrochloride) for nuclear staining and store at -20^{o}C before use (lasts for about 1 month). The antifade working solution was stored at 4° C in the dark

2.2.2.5 0.1% (w/v) Evans blue stain

Dissolve 0.1g Evans blue in 90ml 1 x PBS and bring to 100 ml with 1 X PBS and store at room temperature.

2.2.3 Caspase 3/7-Glo assay

In order to measure apoptosis, an assay measuring caspase -3 and -7 activity was used. In the presence of these caspases, a substrate containing tetrapeptide DEVD sequence is cleaved and light is produced by luciferase (Figure 2.2). Thus, luminescence generated is directly proportional to caspase activity. Detailed protocol of caspase 3/7 assay is given in respective chapters where subsequent experiments were performed.

Caspase-3/7 reagent kit

Each system Contains
1% (v/v) Caspase-Glo® 3/7 substrate Z-DEVD-R110 (lyophilized)
Caspase-Glo® 3/7 Buffer
Both components were elements of the Apo-ONE®
The Caspase-3/7 reagent was prepared freshly before use.

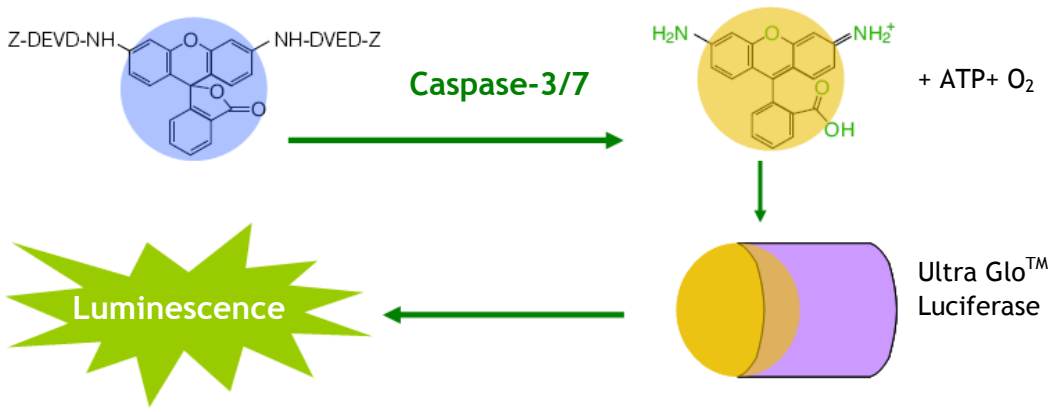

Figure 2.2: Bioluminescent reaction of caspase 3/7 Assay.
Caspase cleaves a substrate (containing tetrapeptide DEVD sequence) for luciferase (amino-luciferin) which is then consumed in luciferase reaction to produce luminescence. (http://www.promega.com/resources/protocols/technical-bulletins/0/apoone-homogeneous-caspase-3-7-assay-protocol/)

2.2.4 SDS Polyacrylamide Gel Electrophoresis (SDS-PAGE) and Western blotting

Total proteins extract were analysed by sodium dodecyl sulphate polyacrylamide gel electrophoresis (SDS-PAGE) using the Mini-Protean Cell System (Bio-Rad, UK). Separation of proteins was carried out either in 10% or 12% polyacrylamide gels. Approximately, equal amounts protein extracts dissoled in 1x PBS was mixed with SDS-PAGE sample buffer (Laemmli 2x concentrate (Sigma; S3401), briefly sonicated to shear DNA and boiled for 10 min prior to analysis by SDS-PAGE gel electrophoresis. For the assessment of equal loadings, gels were stained with Coomassie blue (Section 2.2.4.11) for 60 min and destained in the destaining solution (Section 2.2.2.13). Proteins separated by SDS-PAGE were transferred onto 0.45-µM nitrocellulose membranes (Protan BA 85, Whatman) using the Mini Trans-Blot Electrophoretic Transfer Cell System (Bio-Rad, UK). The transfer set up consisted of pre-wetting the nitocellulose membrane in transfer buffer (Section 2.2.4.9). The transfer sandwich was assembled with a fibre pad pre-soaked in transfer buffer. Then two pre-soaked filter papers were laid on top, followed by the equilibrated membrane. The SDS-PAGE gel, having been equilibrated in transfer buffer for 15 min, was then laid on the membrane. Another layer of pre-soaked filter papers was laid on the gel and finally, a pre-soaked fibre pad completing the transfer sandwich. The completed cassette was placed in the module and electroblotting was performed at a constant 280 milliamps current for 60 min. Following protein transfer, the membrane was

stained with Ponceau S (Section 2.2.4.14) for 5 min with slight agitation to confirm that the transfer of protein to the NCP membrane was achieved. The membrane then was incubated in blocking solution (Section 2.2.4.10) for 60 min at room temperature with gentle agitation. Recipe of various important buffers utilised for SDS-PAGE and western blotting are given in the following.

2.2.4.1 10% (w/v) SDS

Dissolve 10 g SDS in 90 ml dH_2O and bring to 100 ml with dH_2O and store at room temperature.

2.2.4.2 10x SDS-PAGE running buffer, pH 8.3 (makes 1 L)

Dissolve 30.3 g Tris-base, 144.0 g Glycine, and 10.0 g SDS with dH_2O up to 1 L of total volume and store at 4^oC before use. Dilute 50 ml of 10x stock with 450 ml dH_2O for each electrophoresis.

2.2.4.3 Western blotting buffer/Transfer buffer (makes 1 L)

Dissolve 3.0 g Tris-base, 14.0 g Glycine in 200 ml dH_2O, add 200 ml Methanol and dH_2O to make up to 1 L. Store buffer at 4^oC before use.

2.2.4.4 Separating gel buffer (1.5 M Tris-HCl, pH 8.8)

Dissolve 18.2 g Tris-base in 80 ml dH_2O. Adjust to pH 8.8 with HCl. Bring total volume to 100 ml with dH_2O and store at 4^oC.

2.2.4.5 0.25 M Tris-HCl, 0.2 % SDS, pH 6.8/ Stacking gel buffer

Dissolve 3 g Tris base, 2 ml of 10 % SDS in 60 ml dH_2O. Adjust to pH 6.8 with HCl. Bring total volume to 100 ml with dH_2O and store at 4^oC.

2.2.4.6 10% (w/v) APS

Dissolve 0.1 g ammonium persulfate (APS) in 1 ml dH_2O. Always prepare fresh as required.

2.2.4.7 Separating gel formulation (10 or 12 % SDS-PAGE gel)

For 12% resolving gel, add 3.35 ml dH_2O, 4 ml 30% Acrylamide/Bis, 2.5 ml 1.5 M Tris-HCl pH 8.8, 100 µl 10% (w/v) SDS, 50 µl 10% (w/v) APS and 5.0 µl TEMED.
For 10% resolving gel, add 4.05 ml dH_2O, 3.3 ml 30% Acrylamide/Bis, 2.5 ml 1.5 M Tris-HCl pH 8.8, 100 µl 10% (w/v) SDS, 50 µl 10% (w/v) APS and 5 µl TEMED.

2.2.4.8 5% Stacking gel formulation

Add 1.8 ml dH_2O, 0.63 ml 30% Acrylamide/Bis, 2.5 ml of stacking gel buffer, 50 µl 10% (w/v) SDS, 50 µl 10% (w/v) APS and 5.0 µl TEMED.

2.2.4.9 Transfer buffer

Dissolve 3.03 g Tris-base, 14.0 g Glycine in 200 ml dH_2O; add 200 ml Methanol and dH_2O to make uo to 1 L. Store buffer at 4^oC before use.

2.2.4.10 5% blocking buffer for Western blotting

Dissolve 5.0 g of dried milk to 50.0 ml 1 x PBS. Add 10ml of horse serum, 10 ml of 10 x Tris-saline, 100 µl of Tween-20, 100 µl of 10% Thimerosol. Add 1 x PBS to give total volume of 100.0 ml. Prepare fresh as required.

2.2.4.11 Washing buffer

Dissolve 1 ml of Tween-20 in 1 L 1 x Tris-saline. Store at 4^oC.

2.2.4.12 Coomassie blue staining R-250 (makes 500 ml)

Dissolve 1.25 g of Coomassie blue in 250 ml methanol, 50 ml acetic acid and 200 ml dH_2O and and keep at room temperature.

2.2.4.13 Destaining solution (makes 1.7 L, 10% acetic acid solution)

Add 175 ml of acetic acid and 500 ml methanol to 1.025 L of dH_2O and store at room temperature.

2.2.4.14 Ponceau stain

Add 3.0 g of TCA (Trichloroacetic acid) to 100 ml of dH_2O and add 0.2 g of Ponceau S. Store at room temperature.

2.2.4.15 Antibody detection

Detection of any bound antibody was achieved by using enhanced chemiluminescence Plus™ Western blot detection reagent (ECL; Amersham) and exposed to autoradiography.

2.2.5 Semiquantitative RT-PCR

2.2.5.1 One-Step Semiquantitative RT-PCR System

SuperScript™ One-Step RT-PCR with Platinum® *Taq*, cat no. 12574-026

Kit Components	100-rxn kit
RT/ Platinum® Taq Mix	100 µl
2X Reaction Mix (a buffer containing 0.4 mM of each dNTP, 2.4 mM MgSO4)	3 × 1 ml
5 mM Magnesium Sulfate	500 µl
5 mM Magnesium Sulfate	1 ml

Store all components at -20°C

Standard reaction mix used in the RT-PCR	Volume/ 50 µL	Volume/ 25 µL
2x Reaction Mix	25 µL	2.5 µl
Forward primer (10 µM)	1 µL	0.5 µl
Reverse primer (10 µM) 1 µL	1 µL	0.5 µl
Template RNA (12.5 ng)	2 µL	1 µl
RT/ Platinum® Taq Mix	1 µL	0.5 µl
Autoclaved double distilled water to	50 µL	25 µl

Note: Reactions master mix was made for multiple reactions and aliquots were dispensed in micro centrifuge PCR tubes

2.2.5.2 Tris-acetate-EDTA (TAE) buffer 50X (makes 1 L)

Dissolve 242 g Tris in 100 ml of 0.5 M EDTA pH 8.0 with glacial acetic acid, make uo to 1 L with sterile dH_2O and store at room temperature. Dilute to 1 x for working concentration.

2.2.5.3 DNA loading buffer

0.25% bromophenol blue, 0.25% xylene cyanol FF, 15% Ficoll (type 400; Pharmacia) in dH_2O and store at room temperature.

2.2.6 Two step quantitaive RT-PCR system

2.2.6.1 cDNA synthesis

AffinityScript QPCR cDNA Synthesis Kit, Cat no 600559, Stratagene.

Kit Components	100-rxn kit
cDNA synthesis Master mix (2x)	500 µl
AffinityScript RT/ RNasae Block Enzyme mixture	50 µl
Oligo(dT) primer (100ng/ µl)	15 µg
Random primers (100ng/ µl)	15 µg
RNase-free H_2O	1.2 ml

Store all components at -20°C

2.2.6.2 Brilliant SYBR® Green QPCR Master Mix, Cat no. 600548

Kit Components	100-rxn kit
2 x Brilliant SYBR Green QPCR master mix	2 x 2.5 ml
Reference dye, 1 mM	100 µl

Chapter 3

Development of an experimental model for study of infection-associated modulation of activation status in *Theileria annulata* infected cells

3 Development of an experimental model for study of infection-associated modulation of activation status in *Theileria annulata* infected cells

3.1 Introduction

An important and interesting feature of the *Theileria* parasite is the unique ability of the multinucleate intracellular macroschizont stage to induce transformation and proliferation of the infected host cell (Spooner *et al.*, 1989). However, the transformation state of parasite infected cells is reversible and requires the presence of a viable parasite, as treatment of infected cells with the theilericidal drug buparvaquone (BW720c) halts the process of proliferation and induces cell death (McHardy *et al.*, 1985).

Transformation of bovine leukocytes infected with *T. annulata* and the closely related species, *T. parva,* is known to be dependent upon constitutive activation of bovine transcription factors and associated signal transduction pathways. The mechanism underlying this transformation event has been extensively studied, but is not yet fully elucidated [reviewed in (Ahmed *et al.*, 1999;Dessauge *et al.*, 2005a;Dobbelaere and Heussler, 1999;Dobbelaere and Kuenzi, 2004)]. Previous work has demonstrated that an extremely complex network of interactions exists between the parasite and infected host cell, involving numerous cellular pathways and their associated host cell transcription factors such as; Activator protein 1 [AP-1] (Chaussepied *et al.*, 1998), Activating transcription factor 2 [ATF-2] (Botteron and Dobbelaere, 1998), Signal transducer and activator of transcription 3 [STAT3], c-Myc (Dessauge *et al.*, 2005a), Nuclear factor kB [NF-κB] (Heussler *et al.*, 2002;Ivanov *et al.*, 1989), c-jun NH2-terminal kinase [JNK] (Galley *et al.*, 1997) phosphoinositide-3 kinase [PI3-K] (Baumgartner *et al.*, 2000) and SRC-related tyrosine kinase (Eichhorn and Dobbelaere, 1994). Activation of these factors is likely to bring about a range of beneficial phenotypic alterations, only some of which have been defined at the cellular level.

Activation of NF-κB involves translocation from the cytosol to the nucleus, where it binds to its consensus sequences within the promoter region of target

genes, consequently promoting the transcription of a variety of proinflammatory genes (Baeuerle and Henkel, 1994). For example, NF-κB is known to regulate the transcription of a variety of cytokines [Interleukin (IL-1), IL2, IL-6, IL-8, tumor necrosis factor (TNF) as well as some adhesion molecules (e.g. intercellular adhesion molecules (ICAM-1), vascular adhesion molecule (VCAM-1)] and some specific enzymes such as inducible nitric oxide synthase [iNOS] (Baeuerle and Henkel, 1994;Collins *et al.*, 1995a;Read *et al.*, 1995;Xie *et al.*, 1994). Similarly constitutive activation of AP-1, a dimeric transcription factor composed of members of Jun and Fos proto-oncogene families (Curran and Franza, Jr., 1988), is also involved in regulating gene expression required for host cell proliferation and a transformation state (Kovary and Bravo, 1991) in fibroblast cells. Constitutive activation of c-Jun, a dominant component of AP-1, is thought to play an important role in metastasis of *Theileria* infected cells via regulation of metalloprotease gene expression (Adamson *et al.*, 2000;Baylis *et al.*, 1995) and activation of NF-κB confers protection against apoptosis probably by regulating anti-apoptotic genes (e.g. c-IAP-1/2, XIAP, TRAF2, Bcl-2 and Bcl-XL) and the cell-cycle regulator cyclin D1, which increase cellular survival and proliferation respectively (Dessauge *et al.*, 2005b;Heussler *et al.*, 1999;Karin and Lin, 2002).

Despite the strong evidence of NF-κB and c-Jun transcription factors as anti-apoptotic factors, there is increasing evidence indicating that they also have pro-apoptotic functions (Janus-like factors) and have the potential to compromise the survival of an infected host cell (Gagliardi *et al.*, 2003;Lindwall and Kanje, 2005;Youssef and Steinman, 2006). For example, Kasibhatla *et al.*, (1999) have provided evidence that NF-κB and Ap-1 induce pro-apoptotic Fas ligand protein in response to chemotherapeutic agents or T-cell activation that promotes apoptosis. Similarly there is evidence that NF-κB can regulate expression of the tumour suppressor p53, which is required to induce cell death (Dutta *et al.*, 2006;Shishodia and Aggarwal, 2004). Indeed the possibility that the transformation event may not be guaranteed was illustrated in a recent study which showed that only a proportion of *T. parva* infected leukocytes successfully progress to proliferation, while the rest undergo apoptosis (Rocchi *et al.*, 2006). Thus, events that are detrimental to the infected cell occur following sporozoite invasion and in order to establish transformation, potential detrimental processes may have to be overridden or blocked, suggesting that a delicate

balance exists between sending a *Theileria* infected cell towards sustained proliferation or death.

There have been few studies investigating the phenotypic and functional alterations imparted in macrophages (mφ) by *T. annulata*. Sager *et al.,* (1997) have reported that *T. annulata* infection is associated with modulation of the bovine mφ phenotype and impairment of its cellular defence function. In this particular study, transformation was associated with a progressive loss of mφ-specific properties (e.g phagocytosis, lipopolysaccharide (LPS) induced tumor necrosis factor-α (TNF-α) and nitric oxide production) and cell surface markers (e.g CD14, CD11b, CD11a/CD18). Furthermore elimination of parasite by treatment with BW720c resulted in re-acquisition of monocyte lineage properties.

More recently, a study was also performed by Jensen *et al.*, (2009) to investigate the possible role of *T. annulata* infection in regulation of mφ differentiation. This work has investigated the effect of *T. annulata* infection on the expression of the mφ differentiation markers. It was observed that mRNA levels of transcription factor such as Musculoaponeurotic fibrosarcoma oncogene (MAF) family, c-MAF associated with bovine monocytes differentiation to mφ, was suppressed by *T. annulata* infection. c-MAF has been implicated as a candidate marker for human mφ differentiation studies (Liu *et al.*, 2008). In addition to its role in differentiation, c-MAF was originally identified as an oncogene (Kataoka *et al.*, 1993). Similarly the down stream targets of c-MAF such as integrin B7 (ITGB7) and chemokine receptor 1(CCR1) suppressed by *T. annulata* were increased while Interleukin 12A (IL12A) was decreased upon elimination of parasite with buparvaquone treatment (Jensen *et al.*, 2009). This supported the hypothesis that the parasite may modulate the differentiation state of the host cell, which may be linked to and essential for establishment of the parasite-induced transformation event.

Further evidence for parasite mediated control of the infected host cell has recently been provided by evidence that parasite infected cells are able to modulate the expression of LPS and type I interferon inducible pro-inflammatory cytokine genes, genes associated with cellular defence, cell growth and differentiation. For example, parasite-mediated repression of high-level mRNA

expression has been shown to occur for ISGylation pathway genes (UBP43 and ISG15), which are co-ordinately induced by IFNs and LPS (Oura *et al.*, 2006). LPS is a known inducer of NF-κB and in a murine pre-B lymphoma cell line high level induction of *ISG15* expression was found to be a direct target of LPS induced NF-κB activation (Li *et al.*, 2001). High level expression of these genes has been reported to occur in response to infection of cell by various microorganisms such as viruses and bacteria (Kim and Zhang, 2003;Zhang *et al.*, 1999). It has been proposed that ISG15 conjugation plays a role in the stress response of cells and provides protection against infection. Thus negative control of *bISG15* induction may allow *Theileria*-infected cells to bypass a protective immune response (Oura *et al.*, 2006), despite constitutive activation of transcription factors (Ap-1 and NF-κB) associated with this event.

Taken together the above mentioned findings lead to the hypothesis that *Theileria* parasite may modulate gene expression networks associated with activation of host cell transcription factors, and that this manipulation promotes an outcome that favours establishment of the transformed cell. In order to test this hypothesis it was necessary to develop an experimental system allowing comparison of gene expression profiles of *Theileria*-infected and un-infected cells under conditions that induce cellular activation. The ultimate strategy was to obtain global expression profiles of activated uninfected cells relative to control cells and compare this to the expression profile of infected cells.

To establish methodology for investigation of the influence of *Theileria* infection on host cellular activation status by gene expression profiling, we utilised an available uninfected immortalised bovine lymphosarcoma (BL20) and its *in vitro T. annulata* infected (TBL20) counterpart. Several reasons exist behind selection of BL20 cell line as an experimental model in the current study: BL20 is a spontaneous B-cell lymphosarcoma exhibiting the uncontrolled proliferation characteristic of immortalized cell lines; it is amenable to sporozoite infection and as TBL20 cells possess a higher proliferation rate compared to uninfected BL20 (Figure 3.2; *unpublished* supporting data kindly provided by Dr. Jane Kinnaird), a homogeneous parasite infected population can be obtained following sporozoite infection and passage in culture; utilisation of BL20 therefore provides an identical host cell background for comparative gene expression studies (Firestein and Pisetsky, 2002). Importantly, BL20 leukocytes

acquire characteristics of naturally infected cells. For example, TBL20 cells exhibit significant changes to the shape of the host leukocyte; BL20 cells possess a smaller more uniform shape whereas TBL20 cells display a larger, uneven shape with cytoplasmic projections and blebs (see Figure 3.1). Morevover, *Theileria* infection of BL20 has been shown to result in activation of NF-κB (Heussler *et al.*, 2002;Schmuckli-Maurer *et al.*, 2010) and as in *in vivo* derived infected cells, NF-κB is also activated in TBL20 cells via IKK signalosome aggregation on the surface of macroschizont surface (Schmuckli-Maurer *et al.*, 2010; Figure 2A). In addition preliminary experiments showed that BW720c treatment of TBL20 results in arrest of host cell division, whereas BL20 cells treated in parallel show no phenotypic effects of the treatment (Figure 3.2) (Oura *et al.*, 2006). In addition, TBL20 can undergo differentiation of the macroschizont to generate extracellular merozoites on culture at 41ºC and during this event host cell proliferation subsides (Shiels and Kinnaird, unpublished data). Therefore, parasite infected BL20 cells have characteristics typical of naturally infected bovine cells and provide a useful tool to enable studies investigating the consequences of parasite infection on host cell activation.

To fully trigger a cellular activation response in uninfected cells in a manner resembling activation via parasite infection, bacterial lipopolysaccharide (LPS) was used. LPS, which belongs to a class of pathogen-associated molecular patterns (PAMPs), is a potent biological response modifier and is well known to activate the inflammatory responses in a wide variety of cell types. Activation of cells, mostly macrophages, monocytes and lymphocytes results in activation of transcription factors, production of cytokines and other inflammatory molecules (Wong *et al.*, 2007). Because of this, LPS has been used extensively by various *Theileria* research groups to stimulate monocytes/macrophages and un-infected BL20 cells for investigating expression of genes predicted to be under parasite control (Jensen *et al.*, 2006b;Oura *et al.*, 2006;Sager *et al.*, 1997).

Objectives of this study

A major aim of the work presented in this thesis was to investigate the possibility that changes to host gene expression profiles associated with parasite infection are functionally relevant for establishment of an activated,

transformed leukocyte. The starting point for study of such parasite mediated manipulation at a global level was development of an experimental model allowing comparison of uninfected and *Theileria* infected cells under cellular activation conditions. Described in this section are experiments performed to characterise the viability and proliferation responses of BL20 and TBL20 cells following LPS stimulation. In addition, assessment of NF-κB activation and the expression profiles of a panel of selected host genes were performed.

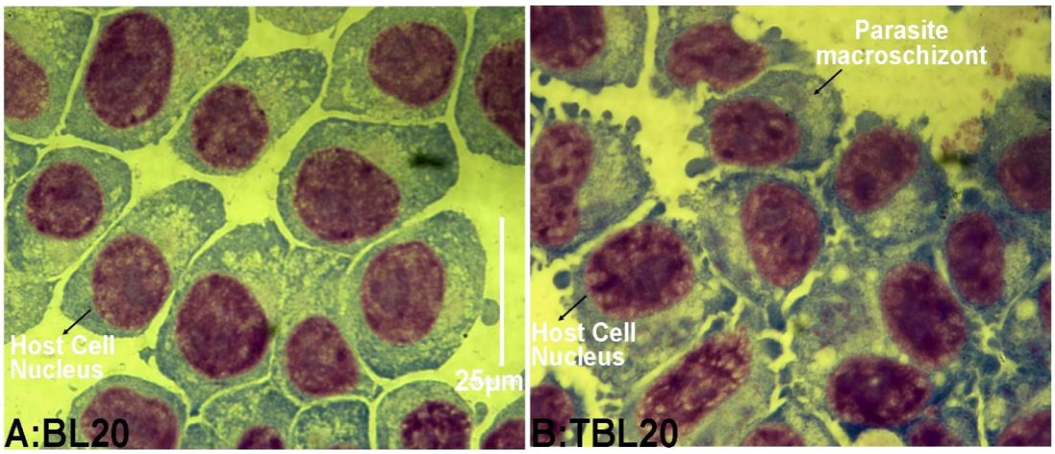

Figure 3.1: Morphological differences of *Theileria*-infected and uninfected BL20 cells
Panel A, BL20 cells stained with Giemsa showing uniform cell morphology
Panel B, TBL20 cells stained with Giemsa showing parasite macroschizont and significant morphological alterations to the host cell membrane and formation of membrane blebs. Bar =25µm

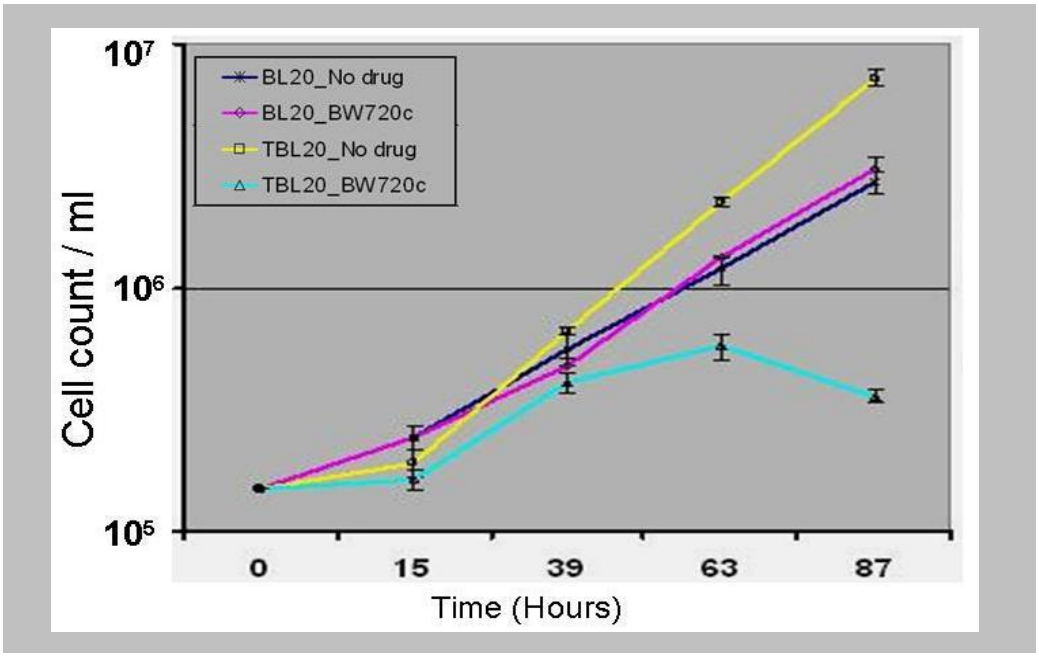

Figure 3.2: Comparative growth rate analysis of *Theileria*-infected TBL20 and uninfected BL20 cells following Buparvaquone treatment
For analysis of comparative growth rates cultures were set up in triplicate at 1.5 x 10^5 / ml using fresh starter cultures and buparvaquone (BW720c) added to 50ng /ml after overnight incubation (15 hours). Cell numbers were estimated each day by Trypan Blue exclusion. As required, cultures were fed by 2 fold dilution with fresh medium and drug to maintain growing cultures in exponential phase. Calculation of growth rate (cell number / ml) was determined by extrapolation using the dilution factors.

3.2 Methods

3.2.1 Cell lines and culture

BL20, an uninfected bovine lymphosarcoma cell line (Morzaria *et al.*, 1982;Olobo and Black, 1989) and TBL20, a *T. annulata* (Ankara strain) infected BL20 cell line previously derived from *in vitro* infection (Shiels *et al.*, 1986), were used in the experimental model. Cells were cultured in standard complete medium using RPMI-1640 with added L-Glutamine and 25mM HEPES (Gibco), supplemented with 20% heat-inactivated foetal bovine serum (FBS; Sigma), 8µg/ml streptomycin, 8 units/ml penicillin, 0.6µg/ml amphotericin B and 0.05% sterile sodium bicarbonate. Generally the cell number of each culture was started at $2x10^5$ /ml and maintained by feeding with fresh medium every two to three days at, usually, a 1 in 5 dilution.

3.2.2 Stimulation of cells with lipopolysaccharide (LPS)

Cells were cultured in tissue culture flasks ($25cm^2$ or $75cm^2$) and complete medium at 5% CO_2 and 37°C humidified atmosphere, until they reached a density of approximately 5×10^5 cells/ml (i.e. in the logarithmic phase of growth). Stimulation of cells was carried out in 6 well plates with the cell concentration adjusted to give 5×10^6 cells/well in a total of 5ml medium. Cells were then stimulated by adding 1µg/ml final concentration of LPS (Sigma: L 2630) and incubated at various time points ranging from 6h-48h depending on the individual experimental protocol. Preliminary LPS titration experiments were performed to measure the minimum concentration of drug required to stimulate cells (based on NF-κB reporter activity, see section 3.2.3) without causing rapid cellular cytotoxicity (data not shown). Thus, 1µg/ml of LPS was subsequently determined as an appropriate standard stimulation concentration. LPS was dissolved in dimethyl-sulfoxide (DMSO; Sigma D-8418) and non-stimulated control cells were incubated with the same volume of DMSO as vehicle contol.

3.2.3 NF-κB dependent reporter assay (Dual Luciferase Assay) and LPS stimulation

Estimation of NF-κB activity was performed by transient co-transfection of a reporter plasmid containing a promoter with an NF-κB$_3$ recognition sequence linked to Firefly luciferase (NF-κB-LUC) and a Renilla luciferase plasmid (phRG-TK renilla), followed by sequential measurement of Firefly and Renilla luciferase activity, essentially as described by Heussler *et al.*, (2001). 2.0µg of NF-κB$_3$-Luc and 0.5µg of phRG-TK Renilla plasmids were mixed in an electroporation gene pulser cuvette (0.4cm electrode gap) with 4×10^6 BL20 or TBL20 cells in 300µl of RPMI-1640-2% FBS without antibiotics. Electroporation was performed using a Gene pulser (Bio-Rad) set at 220V, 950µF. After electroporation cells were immediately added to 5ml of pre-warmed complete medium and incubated in six well plates.

After 24h recovery, LPS (1µg/ml) or equal volume of DMSO were added for 4h. Cells were then harvested from each well, centrifuged at 750 × g and 4°C, for 5 minutes. The cell pellet was then washed with 500µl of 1x PBS (phosphate buffer saline) and centrifuged at 925 × g for 2 min.

A commercially available luciferase assay reagent kit (Dual Luciferase® Reporter Assay System; Promega) was used to assay luciferase activity, using the manufacturer's protocol. Briefly, 100µl of Passive Lysis Buffer (PLB) was added to the cell pellet recovered from the previous step and mixed gently for 15min in the dark. Samples were briefly centrifuged (14000rpm) and kept on ice. 20µl cell extract was used per assay with 100µl of LAR (Luciferase Assay Reagent) and 100µl of Stop & Glo reagent. A TD-20/20 luminometer (Turner Designs) was used for detection of luminescence. NF-κB promoter activity was calculated by normalizing firefly luciferase activity relative to the activity of constitutive Renilla luciferase, the internal control for electroporation efficiency, for each sample. Each electroporation and luciferase assay was performed in quadruplicate.

3.2.4 Indirect immunofluorescence analysis

Indirect Immunofluorescence (IFA) analysis of uninfected and infected cells with or without LPS treatment was performed using the basic protocol described by Schmuckli-Maurer *et al*. (2010).125µl from cultures of approximately 2×10^6 cells/ml were cytospun on to glass slides at 1500rpm for 5min using a Shandon cytospin 2 centrifuge. Different fixation protocols were performed for the immunodetection by each primary antibody and are detailed in 3.2.4.1 and 3.2.4.2. Following fixation and incubation with antibodies slides were washed three times in 1×PBS for 3min each then incubated with secondary antibody (either goat anti-rabbit (Invitrogen; A-11034) or -mouse IgG (Invitrogen; A-11029) conjugated to Alexa 488) at 1 in 200 dilution for 1h at RT, followed by PBS washes as before. After the final wash, cells were counter-stained with 0.1% Evan's blue for 1min, rinsed in 1× PBS and allowed to dry. Slides were then mounted in 10µl of mounting medium containing 50% glycerol in PBS, 4, 6-diamindino-2-phenylindole (DAPI) at 1µg/ml and phenydiamine at 1mg/ml. Immunofluorescence images were examined using an Olympus BX60 microscope and acquired by SPOT camera and SPOTTM Advanced image software Version Mac: 4.6.1.26 (Diagnostic Instruments, Inc).

3.2.4.1 Fixation protocol for anti-mouse IKKγ /NEMO

For detection of IKKγ (NEMO) containing signalosomes, slides were dried for 5min, fixed in 3.7% Paraformaldehyde in 1x PBS, pH 7.4 at 4°C for 30min. Slides were washed three times briefly with 1x PBS then extracted in 0.2% Triton X-100 in 1x PBS for 10min at room temperature (RT) and washed three times with 1x PBS. Anti-IKKγ/NEMO (BD Biosciences 611306) antibody was used at a dilution of 1/50 in complete culture medium for 1h at RT.

3.2.4.2 Fixation protocol for anti-p65 (NF-κB sub-unit)

For detection of the p65 sub unit of NF-κB, slides were immediately fixed in ice cold 3.7% Paraformaldehyde-PBS, pH 7.4 for 30min. Slides were then washed three times briefly with 1×PBS and incubated in methanol pre-chilled to -20°C for 5min followed by washing three times with PBS. Anti- NF-κB p65 (sc-372;

Santa Cruz) antibody was used at a dilution of 1/50 in complete medium for 1h at room temperature.

3.2.5 Cell proliferation/viability assay

Assessment of viable cell counts on cultures following stimulation with LPS or DMSO was performed using Trypan Blue exclusion. Dead or damaged cells stain with trypan blue, while viable cells exclude the dye. Four replicate cultures of BL20 and TBL20 were seeded with 2.5×10^5 cells/ml and incubated at 37°C for 24 and 48h in the presence of LPS (1µg/ml) or DMSO (1µl/ml). An aliquot (50µl) of the cell culture was mixed with an equal volume of 0.4% (w/v) trypan blue solution (Gibco) and the numbers of non-viable and viable cells counted using a haemocytometer. Cell viability was expressed as the percentage of trypan blue negative cells compared to the total number of cells (Shiels *et al.*, 1992). Viable and dead cells were expressed as cell number/ml for each cell culture.

3.2.6 Cell apoptosis assay (caspase 3/7 assay)

To assess cellular apoptosis, Caspase-3/7 activities were measured using a commercial Caspase-3/7 Assay kit (Promega; Madison, WI) according to the manufacturer's protocol. Assays were performed for four replicate cultures per experimental condition at designated time points (24h and 48h). In cell culture experiments, cells were washed three times with phosphate-buffered saline (PBS). 50µl Caspase-Glo reagent was added to an equal volume of cell suspension containing $2.0\text{x}10^4$ cells and incubated for 1h at room temperature to lyse the cells. The assay utilizes a luminogenic caspase 3/7 substrate (Bayascas *et al.*, 2002). After caspase cleavage, a substrate (amino-luciferin) for added luciferase is released resulting in the generation of luminescence. In addition to an untreated DMSO control, a no-cell control was performed to account for baseline signal generated from fresh complete medium. The baseline signal was subtracted from the signal produced by LPS treated and untreated cells. Caspase 3/7 activity is reported as relative fluorescence unit (RFU) of cells compared to DMSO-treated uninfected BL20 cells.

3.2.7 Statistical analysis

Statistical analysis and generation of graphs presented were performed using GraphPad Prism Software version 5.0 (La Jolla, CA). Data were expressed as mean, ±standard error of the mean (SEM). Differences and significance between mean values of each experimental condition were calculated using a two-tailed Student's *t* test and p-values less than 0.05 were considered as statistically significant.

3.2.8 Total RNA isolation

Total RNA was isolated from infected and uninfected cells with TRI Reagent (Sigma; T9424), according to the manufacturer's instructions. Processing of RNA was carried out in RNase-free 14ml polypropylene tubes (Sarstedt). Cell pellets of approximately 6-9×10^6 cells were resuspended and homogenized in 3 ml of TRI Reagent by pipetting up and down ~15 times and left at room temperature for 5min. Insoluble debris was removed by centrifuging at 12080 ×g for 10min at 4ºC. The supernatant was transferred to a fresh tube and 0.2 ml chloroform per ml of TRI Reagent and mixed with the lysate by vigorous shaking for 15 sec and left at room temperature for 5min. Following centrifugation at 12080 ×g for 15min at 4^{o}C the top aqueous layer containing the RNA was removed to a fresh tube. RNA was precipitated by adding 500µl of isopropanol per ml of original TRI Reagent, mixed and incubated for 10min at RT. The RNA was pelleted by centrifugation at 12080 ×g for 10min at 4^{o}C. The supernatant was discarded and the RNA pellet washed with 1ml of 75 % ethanol per ml of initial TRI Reagent and centrifuged at 12080 ×g for 5min at 4^{o}C. Finally, the RNA pellet was briefly dried then dissolved in 80µl of DEPC treated RNase free water and stored at -80^{o}C for further purification and analysis.

3.2.9 RNA processing

3.2.9.1 Handling, storage and quantification

RNase contamination was minimised by use of DNase/RNase-free plasticware and pipette tips. Total RNA samples were stored at -80^{o}C and multiple aliquots made to minimise freeze/thawing. RNA samples were quantified and purity assessed by

UV-absorbance at 260nm and 280nm. A A260/A280 ratio of 2 or greater was indicative of good quality RNA. A260/A280 ratios for RNA samples obtained for Tri Reagent preparations ranged from 2.057 to 2.195. Quantification and assessment of RNA was repeated after the DNase I treatment and clean up protocol.

3.2.9.2 Clean up of total RNA and removal of genomic DNA by DNase I treatment

To eliminate possible contamination with genomic DNA, RNA samples to be used in RT-PCR analysis were treated with DNase I (Qiagen; 79254) either before column purification on a silica-gel membrane based RNeasy® column (Qiagen cat. 74104) or by an on-column DNase I treatment. DNase I treatment and column purification was carried on approximately 100µg RNA exactly according to manufacturer's protocol. For quantification after the column purification 2µl of purified RNA was diluted in TE buffer (1M Tris Cl, 0.5M EDTA, ph 8.0) and absorbance measured as above. A260/A280 ratios obtained for all samples fell in the acceptable range of 1.78-2.1. The highly purified RNA was stored in aliquots at -80^{o}C.

3.2.9.3 Assessment of RNA quality using gel electrophoresis

To analyse the quality and integrity of the total RNA preparations gel electrophoresis (1.2% agarose TBE gel, with ethidium bromide, 100V, 1h) was performed, using the standard protocol described by Applied Biosystems (http://www.ambion.com/techlib/append/supp/rna_gel.html). Agarose gels were visualised under UV light using a FluorChem 5500 transilluminator system and image capturing software (Alpha Innotec; San leandvo, CA USA). The integrity of total RNA samples (2.0µg each) was assessed on the basis of visualisation of 28S and 18S ribosomal RNA subunits from the gel image as bands at positions 4.8 kb and 1.8 kb, respectively, as shown in Figure 3.3. The RNA preps were considered to show no obvious pattern of degradation if the 28S: 18S band ratio was estimated to be approximately 2:1.

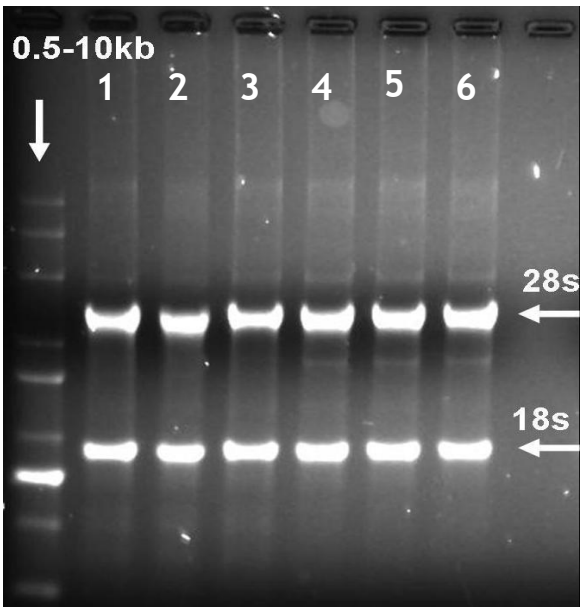

1. BL20 **2.** BL20-LPS 4h **3.** BL20-LPS 18h
4. TBL20 **5.** TBL20-LPS 4h **6.** TBL20-LPS 18h

Figure 3.3: Example of RNA quality assessment by gel electrophoresis
Gel image of total RNA samples extracted under different experimental conditions separated on denaturing formaldehyde agarose gel. 1µg of RNA was loaded in each well.

3.2.10 Semi-quantitative Reverse-Transcription PCR (RT-PCR)

Relative gene expression levels of the selected candidate genes of interest were analysed by semi-quantitative PCR using Superscript III-One Step RTPCR and standard protocols outlined by Invitrogen. http://tools.invitrogen.com/content/sfs/manuals/superscriptIII_onestepRTPCR_man.pdf).

3.2.10.1 Primers design and analysis

All primers for standard RT-PCR were designed and tested for specificity using NCBI's online program (http://www.ncbi.nlm.nih.gov/tools/primer-blast/index.cgi) and oligonucleotide properties calculator (http://www.basic.northwestern.edu/biotools/oligocalc.html).
Primer sequences, GenBank accession numbers, annealing temperatures and product lengths for all gene-specific primers used in this study are given in Table 3.1. Primers were synthesized and purchased from Eurofins MWG Operon (Ebersberg, Germany). Whenever possible, primers were designed to the following criteria: primers were between 18-27 bp long; the predicted product

of the PCR was between 159-321bp; the primer spanned an intron so that only cDNA could be amplified or the predicted product spanned at least one intron in the target gene to give differentially sized genomic and cDNA products; the melting temperatures of both primers of each primer pair were closely matched to achieve a similar annealing temperature. All Primers were diluted to a stock concentration of 100μM and the working concentration of all primers for PCR was 10μM.

3.2.10.2 RT-PCR reagents and cycling conditions

Initial PCR optimisation reactions were performed to ascertain the best annealing temperature (Tm), Magnesium Concentration and overall PCR efficiency. RT-PCR was performed in a final reaction volume of 25 μl containing: gene-specific primers, 12.5 ng of RNA template and 12.5μl of 2 × reaction mixes (SuperScript® III One-Step RT-PCR System with Platinum® Taq DNA polymerase; Invitrogen, Cat no. 12574-026). The thermal cycling conditions were: an initial cycle 50°C for 30 min, 94°C for 2 min: followed by 36 cycles of 94°C 15 sec, X°C for 30 sec (where X°C indicates the experimentally determined annealing temperature (generally Tm of primers minus 3°C) and 72°C for 1 min; a final extension step was performed at 72°C for 10 min. Tm of primers, product length and primer sequences are indicated in Table 3.1.

3.2.10.3 Gel electrophoresis and quantification of RT-PCR products

RT-PCR products were resolved relative to a 1kb DNA ladder molecular weight standard by electrophoresis through 1% (W/V) agarose gels prepared by dissolving powdered agarose (Sigma Aldrich) in 1 x TAE solution and ethidium bromide staining. Gels were cast and run in 1 x TAE buffer using horizontal electrophoretic tanks. Visualisation and quantitation of band intensity was performed using the image analysis software FluorChem 500 spot density method (Biosciences; Santa Clara, CA, USA). Values for each band were based on image pixel intensity and designated as an “integrated density value” (IDV). Image background values were automatically subtracted.

Table 3.1: Primers used in RT-PCR for candidate gene expression profiling

S.No	Gene symbol	Accession No		Primer sequences	Product size(bp)	Tm
1	**ZNF828**	AJ817183	F R	5'-AGCAGTGACCAAGAGCAGGT-3' 5'-TGGACCTGAGCTTTAACTACCTG-3'	205	60.0 59.0
2	**TLR4**	NM_174198	F R	5'-TTCCCGTCAGTATCAAGGTG-3' 5'-TTCCCGTCAGTATCAAGGTG-3'	159	59.8 58.5
3	**ISG15**	NM_174366	F R	5'-ATCGCCCAGAAGATCAATG-3' 5'-TTGTCGTTCCTCACCAGG-3'	167	58.6 58.0
4	**IL8**	NM_173925	F R	5'-CTGGCTGTTGCTCTCTTGG-3' 5'-CAGACCTCGTTTCCATTGG-3'	218	59.7 59.0
5	**IL10**	NM_174088	F R	5'-CAAGCCTTGTCGGAAATG-3' 5'-CTCTTCACCTTCTCCACCG-3'	191	57.7 58.3
6	**IFNß**	NM_174350	F R	5'-AGGACGAAGGACATTCACTCTG-3' 5'-CACTCTTTAAGGCTCTGACGTTG-3'	201	60.6 60.4
7	**IL2RA**	NM_174358	F R	5'-ACGGTTCATTACCAGTGCG-3' 5'-TGGTCCCTGCCATCCTG-3'	223	59.5 61.7
8	**TNF-α**	NM_173966	F R	5'-AAGTTGCTTGTGCCTCAGC-3' 5'-TACCGGCTTGTTACTTGAGG-3'	187	59.1 57.9
9	**iNOS**	NM_001076799	F R	5'-AAGACACGCTTCACCAGAAG-3' 5'-TTGTTACTGCTTCCACCCTG-3'	222	58.0 58.7
10	**CD14**	NM_174008	F R	5'-CAGTCTCCGTAACGTATCGTG-3' 5'-ACTTGTTCGGACAGAGAGCTG-3'	221	58.3 59.6
11	**IFN-α**	Z46508	F R	5'-ACAAGAGCCTCCTGGACAAG-3' 5'-AAGTATTTCCTCACAGCCAGG-3'	139	59.4 58.3
12	**IFN-ω**	XM_001250228	F R	5'-ACTTGTCTCCGAACCACG-3' 5'-AGGTTGAAGCTCTGCTGGAG-3'	169	57.0 59.7
13	**TLR3**	NM_001008664	F R	5'-GGTGTCCTTGAACTTGAAGC-3' 5'-GAATTTCTGGACCCAAGTGC-3'	320	57.3 59.5
14	**IL6**	NM_173923	F R	5'-AGCAAGGAGACACTGGCAG-3' 5'-TTGTGGCTGGAGTGGTTATTAG-3'	262	59.1 59.1

ZNF828, zinc finger protein 828 (control); **TLR4**, toll-like receptor 4; **ISG15**, ISG15 ubiquitin-like modifier; **IL8**, interleukin 8; **IL10**, interleukin 10; **IFNb,** interferon type b; **IL2RA**, IL-2 receptor subunit alpha; **TNF-α,** tumor necrosis factor a **; iNOS,** inducible nitric oxide synthase**; CD14,** CD14 molecule; **IFN-α,** Interferon alpha ; **IFN-ω,** Interferon omega-1**; TLR3,** toll-like receptor 3 ; **IL6,** interleukin 6.

For all semi-quantitative RT-PCR assays the expression levels of candidate genes were normalised to the levels obtained with primers for the gene encoding the zinc finger protein 828 (ZNF828), previously denoted as Chromosome 13 open reading frame 8. ZNF828 has been used as a normalizing gene for both microarray and qRT-PCR analysis, as it was assessed as a constitutively and moderately expressed gene in activated *T. annulata* infected and resting bovine monocytes (Jensen *et al.*, 2008).

3.2.11 Western Blotting

3.2.11.1 Sample preparation of whole cell extracts

Total cell extracts were prepared from approximately $5x10^6$ cells growing in logarithmic phase at a density of $1x10^6$ cells/ml in a six well plate. Cells were either incubated with LPS or equal volume of DMSO (LPS 1µg/ml or DMSO 1µl/ml) for 4 h or 18. Proteasomal inhibition was achieved by adding 4µg /ml of MG132 (Sigma-Aldrich; C2211) for 3 hours prior to harvesting the cells. Cells were harvested from each well and centrifuged at 4°C, 750 ×g, for 5 min. The cell pellet was washed twice with 3ml 1xPBS and the last traces of supernatant were carefully removed without disturbing the pellet. The cell pellet was resuspended in 100µl of 1xPBS and lysed with an equal volume of SDS sample buffer (Laemmli 2x concentrate (Sigma; S3401). Samples were sonicated briefly to shear the DNA, boiled for 10 min, prior to analysis by SDS-PAGE gel electrophoresis.

3.2.11.2 SDS gel electrophoresis and Immunoblotting

Total proteins extracts were separated by polyacrylamide gel electrophoresis (SDS-PAGE) using a 12% resolving gel with a 5% stacking gel (see Section 2.2.4.7). After 1h of electrophoresis at 120V, proteins were electroblotted onto 0.45-µM nitrocellulose membrane (Protan BA 85, Whatman®) in a standard Tris-Glycine-methanol transfer buffer (ref) for 1 h using a constant 280 milliamps current. Transfer of proteins to the nitrocellulose membrane and assessment of equal protein loading was confirmed using Ponceau S staining. Adjustments for equal protein loading between samples were previously estimated by SDS-PAGE and Coomassie Blue staining

3.2.11.3 Immunodetection

The membrane was washed briefly with a wash buffer (1xTris-saline with 0.1% Tween 20) to remove Ponceau stain and then pre-incubated with block buffer for 1h at room temperature with gentle agitation. Blots were incubated with polyclonal rabbit anti-TLR4 (sc-10741, 1:1000; Santa Cruz-Biotechnology) or monoclonal mouse anti-Tubulin (TUB-1A2; 1:5000; Sigma T9028) diluted in fresh block buffer (5% Marvel skimmed milk in Tris buffered saline plus 0.1% Tween 20)

over night at 4°C with constant gentle agitation. The membranes were washed twice briefly then twice for 15min each with wash buffer. The membranes were incubated with appropriate secondary antibodies; goat-anti-rabbit-HRP (1:10000, Sigma, A6154) or anti-mouse IgG peroxidase conjugate (1:10000, Sigma, A5906) diluted in block buffer for 1h at room temperature. The membranes were washed as above with a final brief wash with 1x Tris-saline without Tween 20. Detection was carried out using a SuperSignal® West Pico Chemiluminescent Substrate kit (Pierce, supplied by Thermo Scientific, Rockford, IL). The blots were immediately exposed to X-ray film to capture the chemiluminescent signal. Several exposures were made to achieve the optimal signal for each antibody. The molecular weight of proteins was determined by comparison with Precision Plus Protein™ Standard dual colour marker (Bio-Rad Laboratories; 161-0374). Complete details of reagents and buffers used in western blotting are described separately in chapter2.

3.3 Results

3.3.1 Response of uninfected (BL20) and *Theileria annulata* infected (TBL20) cells to stimulation with LPS.

3.3.1.1 NF-κB activation by *T. annulata* and LPS

Constitutive activation of NF-κB and other inflammatory associated transcription factors is known to be a critical component of *Theileria* dependent host cell transformation. However, the phenotypic response to activation and the mechanism of activation relative to uninfected cells has not been directly compared. To perform this type of analysis, initial experiments compared the cellular activation status of infected and uninfected cells following stimulation by bacterial lipopolysaccharide (LPS). LPS is known to be a strong inducer of NF-κB transcription factor complexes and persistent activation of NF-κB can be achieved by exposure to soluble agonists such as LPS (Hauf *et al.*, 1997;McKinsey *et al.*, 1996;Thompson *et al.*, 1995). Therefore, BL20 (uninfected) and TBL20 (infected) cells were stimulated with LPS and NF-κB dependent luciferase-reporter assays performed to assess the levels of NF-κB activation. The results represented in Figure 3.4 showed that stimulation of BL20 significantly elevated NF-κB ctivity ($P < 0.005$), as a 16 fold induction of NF-κB reporter activity was observed in LPS-stimulated BL20 cells relative to non-treated BL20 control cultures. In contrast, stimulation of TBL20 (infected cells) with LPS did not show significant induction of NF-κB activity relative to the TBL20-DMSO (control) cultures ($P > 0.05$). The data also indicated that constitutive NF-κB activity observed in TBL20 cells was significantly higher than LPS stimulated and un-stimulated BL20 cells($P < 0.001$) (Figure 3.4).

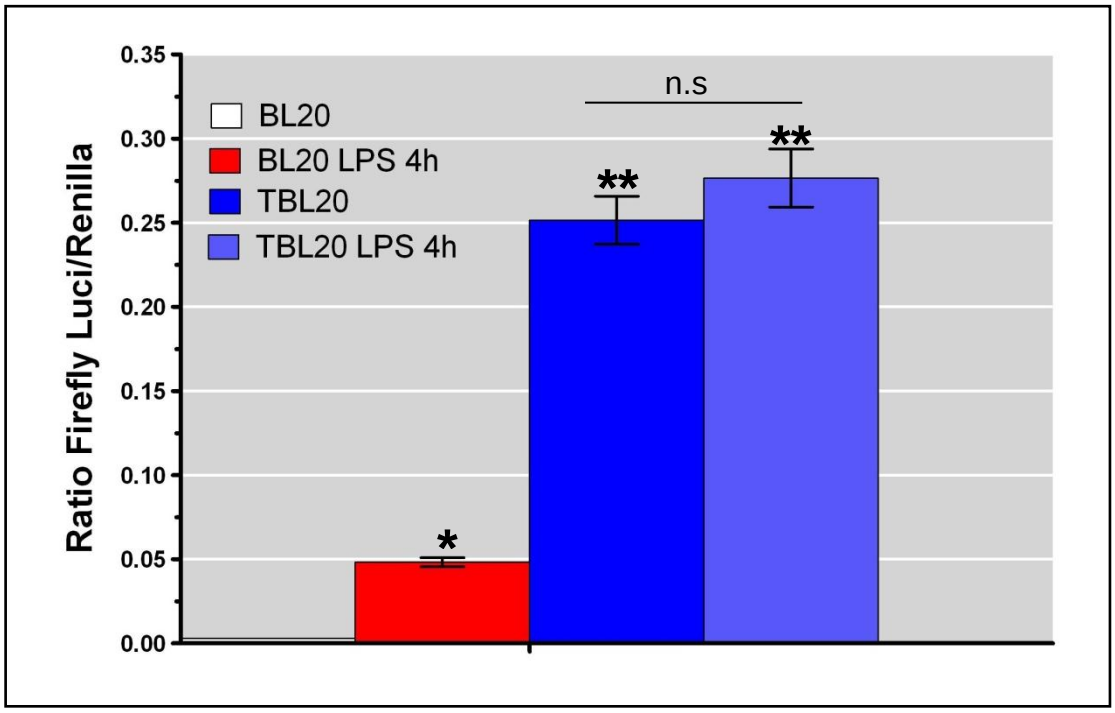

Figure 3.4: NF-κB dependent reporter activity in LPS stimulated BL20, TBL20 and control cells

Activated levels of NF-κB in *Theileria annulata* infected cell TBL20 & uninfected BL20 cells (control) following stimulation with or without LPS are shown. Cells were transiently co-transfected with luciferase reporter constructs. After 24h of co-transfections, cells were either stimulated with LPS (1µg/ml) or DMSO (1µl/ml) for 4h before luciferase assay. Cell extracts were prepared to measure NF-κB promoter activity, which is expressed as ratio of NF-κB Firefly luciferase/Renilla activity (mean ± S.E, n = 4). The asterisk (*) above the bars indicates the statistical significance of the results (Student's t-test, *P < 0.005, **P < 0.001). Whereas, (n.s) indicates non-statistical difference of TBL20 LPS results relative to TBL20 cells.

3.3.1.2 Activation of NF-κB by LPS and *Theileria* infection are both associated with nuclear translocation of p65

In an attempt to confirm that elevated reporter activity was associated with activation of NF-κB, assessment of the level of NF-κB in the nucleus of stimulated cells was carried out by immunofluorescence assay for the p65 sub-unit of NF-κB. The result shown in Figure 3.5 (panel 1 and 2) clearly indicated elevated host cell nuclear reactivity using the anti-p65 antibody in LPS stimulated BL20 cells relative to control cells. In addition, while the nuclear reactivity of p65 in TBL20 cells was greater than that detected for LPS stimulated BL20 cells, no significant difference in levels of p65 nuclear staining was detected in TBL20 when stimulated with LPS (Figure 3.5; panel 1-4) relative to the TBL20 DMSO control cells.

3.3.1.3 Activation of NF-κB by LPS and *Theileria* infection are both associated with IKK signalosome aggregation

Theileria dependent activation of NF-κB has been shown to involve aggregation of IKK signalosomes complexes close to or at the surface of the macroschizont. Aggregation of the kinase complex results in phosphorylation of NF-κB inhibitor, IKBα, which is then constitutively degraded, subsequently allowing the translocation of the previously sequestered cytoplasmic NF-κB to the nucleus (Heussler *et al.*, 2002). To test whether a similar mechanism operated following LPS stimulation in BL20 or whether LPS might alter signalosome levels in TBL20, IKK signalosome complexes were assessed by immunofluorescence (Figure 3.5), using a monoclonal antibody against IKKγ as described previously (Schmuckli-Maurer *et al.*, 2010). The results showed increased reactivity against IKKγ in the form of punctate bodies in the cytoplasm of LPS-stimulated BL20 cells relative to control (Figure 3.5; panel 5-6). It was concluded that these bodies were highly likely to represent aggregated signalosomes. Similar bodies were also detected in the proximity of the multinucleated schizont in parasite infected TBL20 cells and supporting results of previous studies (Heussler *et al.*, 2002;Schmuckli-Maurer *et al.*, 2010) have indicated aggregation of signalosomes at this location. However, no obvious difference in the level of anti-IKKγ reactivity was obtained in TBL20 cells when stimulated with LPS relative to unstimulated TBL20 cells (Figure 3.5; panel 7-8). These results together with the results obtained from the NF-κB reporter assay suggest LPS significantly activates NF-κB in uninfected BL20- cells but has no effect on the infected TBL20 counterpart.

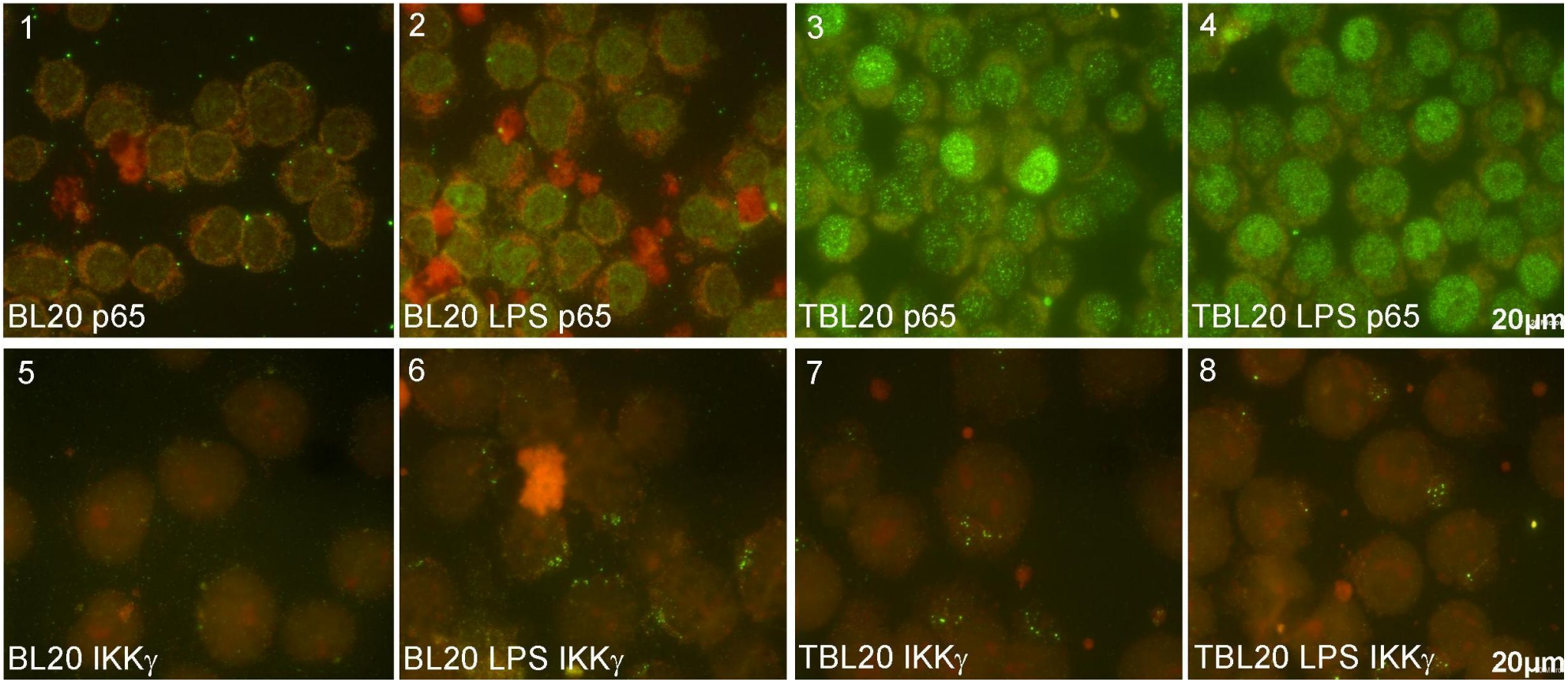

Figure 3.5: mmunofluorescence analysis of activated NF-κB levels in BL20 and TBL20 cells in response to LPS stimulation
Panels1-4: Immunofluorescence analysis of activated **NF-κB** levels using anti-p65 against BL20, LPS stimulated BL20, TBL20 and LPS stimulated TBL20 cells respectively. Expression and nuclear localization of anti-p65 in BL20 LPS, TBL20 and LPS stimulated TBL20 cells.
Panels 5-8: Immunofluorescence analysis of IKK signalosomes using a mouse monoclonal anti-IKKγ against BL20, LPS stimulated BL20, TBL20 and LPS stimulated TBL20 cells respectively. Immunodetection of IKK signalosomes (green dots) are detected by anti-IKKγ of BL20 LPS, TBL20 and LPS stimulated TBL20 cells. Bar = 20µm.

3.3.2 Differential growth response of BL20 and TBL20 cells to stimulation by LPS

Prolonged stimulation of cells with LPS and constitutive cellular activation of NF-κB have both been associated with a detrimental effect on cell viability (Garay-Malpartida *et al.*, 2011). To test whether the response of BL20 and TBL20 to LPS stimulation is associated with a potential detrimental outcome, cultures were treated with LPS and the numbers of viable and dead cells counted after 24 and 48 hours incubation. The results showed that the growth potential of uninfected BL20 cells stimulated with LPS at 48h was significantly reduced, with a 1.73-fold reduction in cell number relative to the un-stimulated control (see Figure. 3.6). In addition, this loss of growth was accompanied by a significant elevation in the percentage of non-viable cells in the BL20-LPS cultures (Figure 3.7) at both 24 and 48 hours. *Theileria* infected cells, in contrast, were found to be resistant to a loss of growth potential following stimulation with LPS and continued to proliferate at a rate comparable to untreated control cells (Figure 3.6). Furthermore, although an increase in the percentage of non-viable cells was obtained in LPS-stimulated TBL20 (2.55 fold) relative to control cells at 48 hr, this was significantly less than the increase in percentage cell death found for the LPS stimulated uninfected cells (22.5 fold).

To determine whether the increase in non-viable cells may be linked to activation of programmed cell death, caspase 3/7 activity was assayed using cell lysates generated from cultures at both the 24h and 48h time points. A 2.5 fold and 5.7 fold induction in caspase 3/7 activity was detected in lysates of BL20 cells stimulated with LPS at 24h and 48h respectively (Figure 3.8). In contrast, while *Theileria* infected TBL20 cells showed a higher baseline caspase 3/7 activity level relative to control uninfected BL20 cells, there was no detection of a significant elevation in activity following stimulation of TBL20 with LPS at either time point (see Figure 3.8). In addition, the level of caspase activity in LPS stimulated TBL20 at 48 hr was shown to be significantly lower (1.86 fold) than LPS stimulated uninfected BL20 cells at this time point.

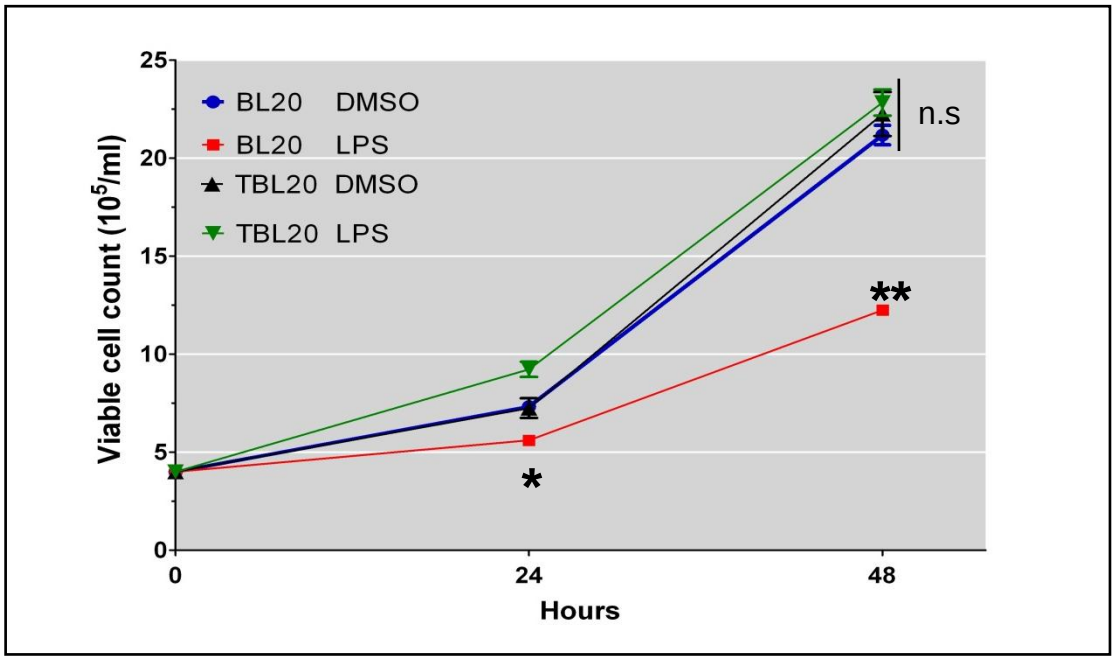

Figure 3.6: Proliferation assays of BL20 and TBL20 cells following LPS stimulation relative to control cells.
Cell viability of BL20 and TBL20 cells in cultures was assessed using Trypan blue exclusion in the presence of either LPS (1µg/ml) or the DMSO vehicle control (1µl/ml) at 24h and 48h post-treatment as described previously (section 3.2.5). Results are presented as Mean ± SE, n = 4 from one of several independent experiments. The asterisk (*****) above the data points indicates the statistical significance of the pair wise comparisons tested against the controls (Student's t-test, *P< 0.01, **P< 0. 001). Whereas, n.s indicates non-statistical differences of the data points relative to controls (BL20 cells) at given conditions.

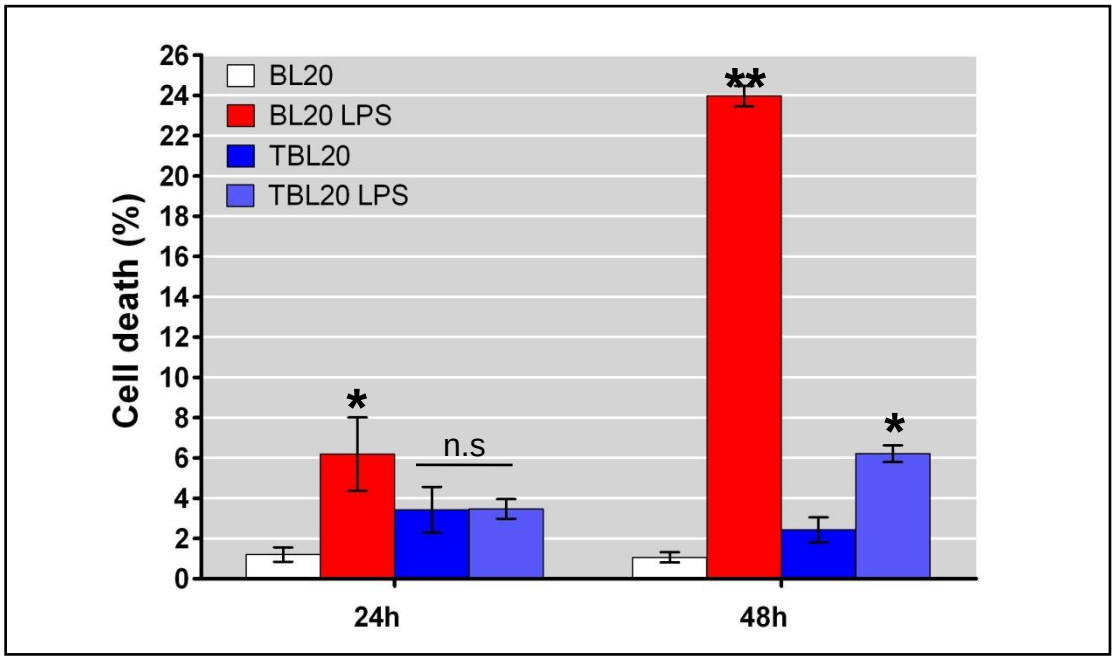

Figure 3.7: Assessment of cell death of BL20 and TBL20 cells following LPS stimulation.
Cells were cultured in the absence or presence of LPS (1µg/ml) for 24h and 48h. Cell death was measured using the trypan-blue exclusion assay and is expressed as percentage of cell. Values are presented as Mean ± SE of four replicate cell cultures from one of several independent experiments. The asterisk (*****) above the bars indicates the statistical significance of the pair wise comparisons tested against the controls (Student's t-test, *P< 0.05, **P< 0.001). Whereas, (n.s) indicates non-statistical difference of TBL20 LPS results relative to TBL20 cells and control cells.

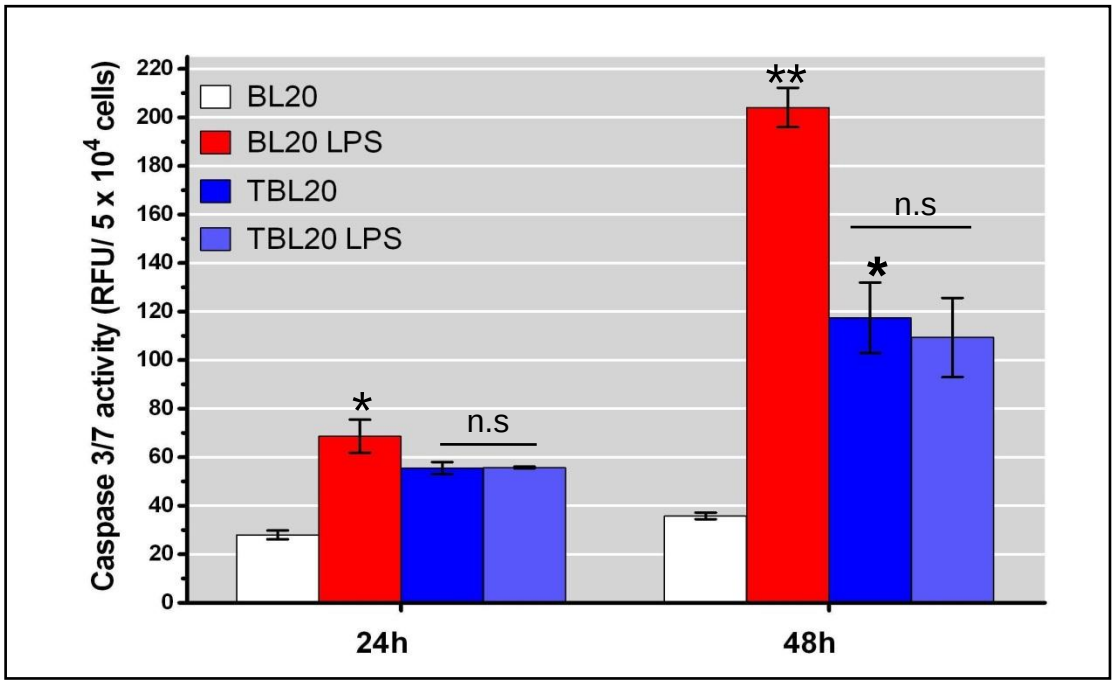

Figure 3.8: Caspase 3/7 activity assayed in TBL20 and BL20 cells following stimulation with LPS.
Caspase activation was determined using a modified caspase 7 or 3-like protease substrate where cleavage yields a product that activates a reaction and generates a measurable fluorescence. Caspase 3/7 activity was determined after incubation of cells in the presence of either LPS (1µg/ml) or the DMSO vehicle control (1µl/ml) for 24h and 48h. Results are expressed as relative fluorescence units (mean, ± SEM, n = 4). The asterisk (*****) above the bars indicates the statistical significance of the pair wise comparisons tested against the controls (Student's t-test, *P< 0.005, **P< 0.00001). Whereas, (n.s) indicates non-statistical difference of TBL20 LPS results relative to TBL20 cells at given conditions.

3.3.3 Comparison of candidate gene expression profiles of BL20 and TBL20 cells stimulated with LPS

From the results presented above, it can be concluded that the outcome of LPS stimulation and activation of uninfected BL20 cells relative to the infected TBL20 counterpart is different. A premise of this thesis was that such a difference would be manifest at the level of gene expression and that infection may manipulate the outcome of the gene expression profile associated with LPS stimulation. Prior to testing this hypothesis at a global level, it was decided to conduct a preliminary analysis using semi-quantitative RT-PCR on a panel of genes. This panel of genes was selected on the basis that their expression profile is manipulated by *Theileria* infection, or they were known LPS response gene and/or targets of activated NF-κB. The panel of genes and their predicted expression profile with respect to infection, LPS stimulation and NF-κB activation is shown in Table 3.2.

Table 3.2: Panel of genes and their predicted expression profile with respect to infection, LPS stimulation and NF-κB activation

S.No	Gene symbol	Stimulus/context	Predicted expression	References
1	TNF-α	*Theileria* infection	Induced	(Guergnon *et al.*, 2003;Preston *et al.*, 1993;Schnittger *et al.*, 2000)
		LPS stimulation	Induced	(Jones *et al.*, 2001)
		NF-κB stimulation	Induced	(Collart *et al.*, 1990)
2	iNOS	*Theileria* infection	Repressed	(Brown *et al.*, 1995b;Sager *et al.*, 1998)
		LPS or NF-κB stimulation	Induced	(Jungi *et al.*, 1996;Sager *et al.*, 1997;Xie *et al.*, 1994)
3	CD14	*Theileria* infection	Repressed	(Sager *et al.*, 1997)
		LPS stimulation	Induced	(Yang *et al.*, 1995)
4	IFN-α	*Theileria* infection	No expression	(Brown *et al.*, 1995b;Sager *et al.*, 1998)
		LPS stimulation	Induced	(Jungi *et al.*, 1996;Sager *et al.*, 1998)
5	IFN-β	*Theileria* infection	Induced	(Sager *et al.*, 1998)
		LPS or NF-κB stimulation	Induced	(Lenardo *et al.*, 1989;Sager *et al.*, 1998;Yamamoto *et al.*, 2003)
6	IFN-ω	*Theileria* infection	No expression	(Sager *et al.*, 1998)
		LPS stimulation	Induced	(Sager *et al.*, 1998)
7	ISG 15	*Theileria* infection	Repressed	(Oura *et al.*, 2006)
		LPS or NF-κB stimulation	Induced	(Kim *et al.*, 2005;Malakhova *et al.*, 2002;Oura *et al.*, 2006)
8	TLR4	*Theileria* infection	No literature	Not reported
		LPS	Induced	(Elner *et al.*, 2005;Jensen *et al.*, 2006b)
9	TLR3	LPS	Induced	(Hoebe *et al.*, 2003)
		NF-κB stimulation	Induced	(Alexopoulou *et al.*, 2001)
10	IL2R	*Theileria* infection	Induced	(Dobbelaere *et al.*, 1990;Herrmann *et al.*, 1989;Heussler *et al.*, 1992;McKeever *et al.*, 1997)
		NF-κB stimulation	Induced	(Cross *et al.*, 1989)
11	IL6	*Theileria* infection	Induced	(Campbel and Spooner, 1999)
		LPS or NF-κB stimulation		(Helfgott *et al.*, 1987;Sanceau *et al.*, 1989)
12	IL-10	*Theileria* infection	Induced	(Campbel and Spooner, 1999;McKeever *et al.*, 1997)
		LPS or NF-κB stimulation		(Barsig et al., 1995;Chanteux et al., 2007)
		Theileria infection	Induced	(Schnittger *et al.*, 2000)
13	IL8	LPS stimulation	Induced	(Jensen *et al.*, 2006b)
		NF-κB stimulation	Induced	(Kunsch and Rosen, 1993)

TNF-α, tumor necrosis factor a ; **iNOS,** inducible nitric oxide synthase; **CD14**, CD14 molecule; **IFN-α**, Interferon alpha; **IFNb**, interferon type b; **IFN-ω**, Interferon omega-1; **ISG15,** ISG15 ubiquitin-like modifier; **TLR4,** toll-like receptor 4; **TLR3,** toll-like receptor 3 **; IL2RA**, IL-2 receptor subunit alpha; **IL6,** interleukin 6; **IL10**, interleukin 10; **IL8,** interleukin 8;

Following RT-PCR the amplified cDNA reaction products were analysed by agarose gel electrophoresis. No product was obtained for primer pairs designed to amplify TNF-α, iNOS, CD14, IFN-α and IFN-ω. RT-PCR for these genes was repeated at a later date with different primer sets for each of these genes and validated a lack of PCR product for these genes. Products were obtained for the other 7 primer sets and the expression profile across the different cellular conditions tested for these genes, relative to the constitutive control (ZNF828). For one of these genes, TLR3, no observable difference in expression level across the range of conditions could be detected (data not shown).

The other six genes displayed a range of modulated expression profiles. Of these the profile obtained for IL8 and IL2RA (CD25) appeared to be of least interest because although they showed evidence of elevated expression associated with parasite infection of BL20; i.e. clearly higher in TBL20 vs BL20, there was no obvious difference in the levels of expression products amplified from RNA representing TBL20-LPS cells vs uninfected BL20-LPS cells. In a similar manner, the profile for IL10 indicated that while slightly elevated expression of this gene was associated with parasite infection of the host cell, an increase in product was not detected for LPS stimulated BL20 cells (Figure 3.9). Therefore a conclusion that infection can modulate the expression outcome of an LPS responsive gene could not be made on the basis of these profiles.

The final three genes all showed evidence for infection-associated modulation of an LPS stimulated response. Thus, the profiles obtained for both TLR4 (CD284) and IFNB1 indicated that the parasite repressed expression of these genes, despite evidence for induction of elevated expression following LPS stimulation of BL20 cells. The profile for ISG15 also showed evidence for infection associated repression relative to an LPS (4h) induced expression profile obtained in the BL20 line. In non-stimulated cells though, the level of expression was higher in TBL20 cells vs uninfected BL20 (Figure 3.9). This profile of ISG15 expression, indicative of infection associated activation but repression of higher-level expression, was observed previously by northern blotting (Oura *et al.*, 2006).

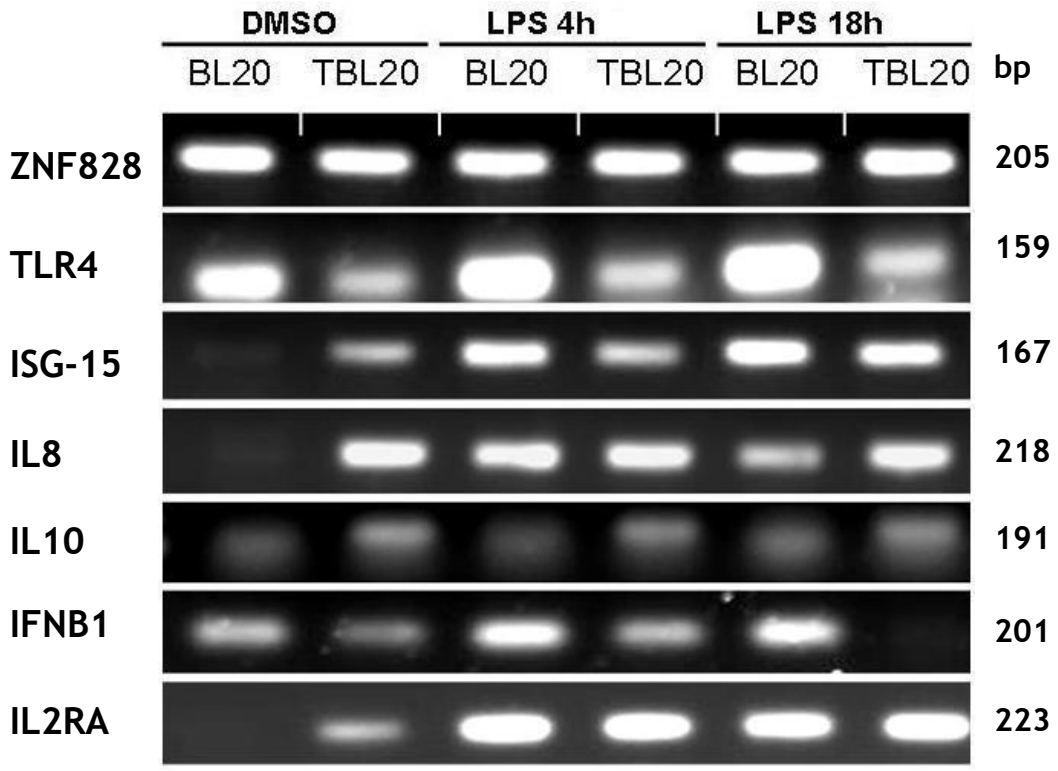

Figure 3.9: Semi quantitative RT-PCR expression analysis of candidate genes following stimulation (of BL20 and TBL20 cells) with LPS
Differential mRNA expression levels of six candidate genes. Gel electrophoresis analysis of all RT-PCR products showed the appropriate size on ethidium bromide stained agarose gels. The mRNA expressions of TLR4, ISG15, IL8, IL10, IFNB and IL2R genes normalized against ZNF828 are shown for TBL20 & BL20 cells (control) stimulated with LPS (1µg/ml).

3.3.4 *Theileria annulata* infection of BL20 cells is associated with repression of TLR4 expression

Following initial results obtained from the semi-quantitative PCR, it was of interest to further validate the infection associated repression profile of TLR4 expression at the protein level. Western blotting was performed to determine whether decreased TLR4 mRNA expression is manifest post-translationally in *Theileria* infected cells. The western blot results showed that the TLR4 protein profile reflected the trend obtained at the mRNA level. Thus, a marked decrease in TLR4 expression was observed in TBL20 cells compared to BL20 cells (Figure 3.10). However, unlike the RNA pattern no significant differences were noticed in the protein levels of TLR4 when stimulated BL20 cells were stimulated with LPS while infected cells continued to display evidence of repression relative to their uninfected counterpart. In general, the levels of Tubulin detected by western blotting (constitutive control) appeared to be slightly lower for the LPS stimulated extracts (see Figure 3.10).

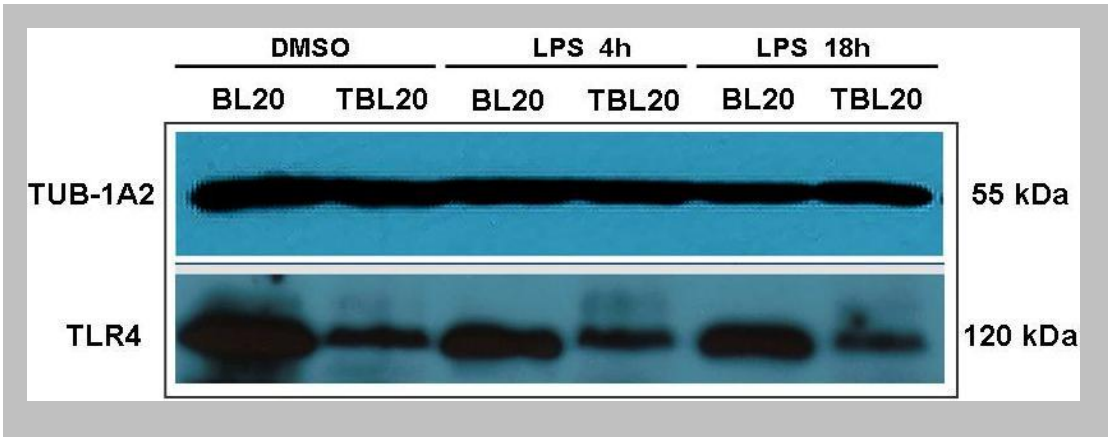

Figure 3.10: Imunoblot analysis of TLR4 protein expression following stimulation of BL20 and TBL20 cells with LPS

Expression of TLR4 was detected by western blot analysis of total cell extracts derived from uninfected and *Theileria* infected cell cultures either stimulated with LPS or unstimulated (DMSO). Tubulin expression was used as constitutive control.

3.4 Discussion

The aim of the work presented in this chapter was to establish a cellular model for comparing the gene expression profiles of uninfected and *Theileria* infected cells following induction of cellular activation by an inflammatory mediator. Therefore, experiments were performed to assess the influence of LPS on the activation state of NF-κB in uninfected and parasite infected host cells.

The reporter construct data (Figure 3.4) showed that LPS stimulation of uninfected BL20 cells significantly induces NF-κB activation. Further confirmatory evidence of NF-κB activation was obtained by immunofluorescence analysis, as LPS stimulation was associated with detection of IKK signalosome aggregation in the cytoplasm of the uninfected BL20 cells. Such IKK complexes, consisting of two kinases, IKKα, IKKβ and the regulatory unit NEMO (IKKγ), have been shown to serve as the focal point for signalling pathways that are activated by numerous stimuli such as TNFα, dsRNA and LPS, all of which lead to activation of NF-κB [reviewed in (Kanarek *et al.*, 2010)].

As in the case of LPS stimulated BL20 cells, parasite infected TBL20 cells provide strong evidence for NF-κB activation via aggregation of IKK signalosomes. In agreement with previous studies, TBL20 cells displayed a uniform pattern of parasite-associated signalosome complex over the surface of the macroschizont. This particular finding supports the previous model of proximity-induced IKK activation, where it is hypothesised that membrane parasite and/or complexed host proteins act as platform for the formation of parasite dependent IKK complex (Heussler *et al.*, 2002). No obvious increase in the number or intensity of detected signalosomes was observed following LPS stimulation of TBL20 cells and this is supported by data indicating high levels of constitutive NF-κB activation, which did not show significant change following stimulation by LPS (see Figures 3.4 and 3.5). Possible reasons for this finding may be that either *Theileria* infected cells are refractory to stimulation by LPS or activated NF-κB is maximal in the infected cell. The latter possibility appears to be unlikely as Schmuckli-Maurer *et al*. (2010) have shown that *T. annulata* infected cell lines can show increased levels of activated NF-κB following stimulation by cytochalasin D.

To investigate whether activation of the host cell by LPS is potentially associated with a detrimental outcome, the BL20 and TBL20 cell lines were stimulated with LPS and measurements made on cell viability and death. The results demonstrated that stimulation of uninfected BL20 cells with LPS proved to be detrimental and causes cell death. Similar responses have been reported in several studies indicating that prolonged activation with LPS induces apoptosis through various mechanisms such as modulation of TLR4 signalling, NF-κB activation, activation of caspases, prolonged or excessive production of cytokines, production of nitric oxide and induction of apoptotic signalling molecules (Akgul *et al.*, 2001;Alikhani *et al.*, 2003;Bannerman *et al.*, 2002;Garay-Malpartida *et al.*, 2011) . In contrast *Theileria* infected cells displayed no adverse effect following LPS treatment and continued to proliferate at the same rate as the untreated control.

Experimental evidence of LPS induced programmed cell death of BL20 cells was obtained by performing caspase 3/7 activation assays. In general the caspase results revealed a similar trend to the data obtained for cell proliferation and death, with stimulation of uninfected BL20 cells generating a significantly higher level of caspase activation relative to the unstimulated control and its infected TBL20 counterpart. No significant difference was observed between un-stimulated and control TBL20 cells (Figure 3.8), suggesting TBL20 cells are refractory to LPS stimulated caspase activation. Activation of caspases is considered to be a hallmark of apoptosis (Porter and Janicke, 1999;Saraste and Pulkki, 2000) and *in vitro* studies have shown that LPS can induce apoptosis through activation of caspase 3 and 7 (Bannerman and Goldblum, 2003;Deaciuc *et al.*, 1999). Thus, in the context of uninfected BL20 cells, LPS stimulation is associated with activation of NF-κB, elevated cell death and loss of proliferation potential; while infected TBL20 cells show constitutive activation of NF-κB that confers resistance to apoptosis (Heussler *et al.*, 1999;Schmuckli-Maurer *et al.*, 2010), and these cells are refractory to cell death or the loss in proliferation potential associated with LPS stimulation of BL20 cells. This apparent Janus-like response to LPS stimulation and NF-κB activation could be explained by the ability of infected cells to generate a modulated NF-κB target gene expression profile compared to that of LPS activated BL20 cells, although it should be borne in mind that additional activation pathways and transcription factors such as AP-

1 are likely to operate in establishing the distinct activation phenotypes associated with infection (TBL20) and inflammatory stimulation (LPS-BL20).

To investigate whether parasite dependent control of infected host cell phenotype could be associated with major modulation of leukocyte gene expression, RNA profiling was performed using RT-PCR. Initially, investigation was limited to a small subset of 13 genes with expression profiles obtained for LPS stimulated BL20 and TBL20 cells relative to non-stimulated controls. Primer sets representing seven of these genes gave clear specific PCR products. While it cannot be discounted that the failure to obtain a PCR product for the other six genes was due to incorrect primer design or function, the repeated failure with redesigned sets of primers for each of these genes (TNF-α, iNOS, CD14, IL6, IFN-α and IFN-ω) suggest this is unlikely. An alternative explanation is that these genes are expressed below the detection limit of the assay in the context of the tested cell types and conditions. For example as CD14 is considered to be primarily a monocyte and macrophage cell surface marker (Song *et al.*, 2001), that plays an important role in LPS binding (Anas *et al.*, 2010;Duchow *et al.*, 1993;Steinemann *et al.*, 1994;Ulevitch and Tobias, 1995), failure to detect mRNA expression of CD14 could be due to the fact that the BL20 cell model belongs to the lymphocyte lineage. A number of studies have postulated that *Theileria* transformed bovine macrophage cells actively repress LPS inducible TNF, iNOS and IFN induction by modulating CD14 repression (Sager *et al.*, 1997;Sager *et al.*, 1999). However, lack of CD14 in BL20 cells clearly does not remove LPS associated activation of NF-κB or induction of other LPS associated response genes tested by RT-PCR (see below). It is possible that a requirement for a CD14, LPS interaction can be supplied by the soluble form CD14 (sCD14) present in fetal calf serum (FCS), or LPS activation of BL20 cells operates in a CD14 independent manner (Cohen *et al.*, 1995;Lynn *et al.*, 1993;Sauter *et al.*, 2007). The lack of gene expression for the 6 genes in the context of BL20 is supported by the array analysis performed in Chapter 4 of this thesis.

TLR3 mRNA was shown to be constitutively expressed in both infected and uninfected cells and the levels did not change across the range of experimental conditions. This finding indicates that TLR3 mRNA is not regulated by LPS or parasite infection and is therefore not indicative of an infection associated modulation of inflammatory/ NF-κB induced gene expression.

Of the six differentially expressed genes, IL8 and IL2RA mRNA were expressed at similar levels in LPS stimulated uninfected BL20 cells and infected TBL20 cells. However, for both of these genes the level of PCR-product was higher in non-treated TBL20 compared to control BL20 cells. The elevated levels of IL8 and IL2 receptor (IL2RA) mRNA expression observed in response to LPS stimulation was consistent with an earlier study where bovine peripheral blood monocyte (PBMC) cells were shown to exhibit high levels of induction of these genes when stimulated with LPS (Jensen *et al.*, 2006b). It may not be surprising that the expression level of IL8 and IL2R were up-regulated in BL20 cells when stimulated with LPS or infected with *Theileria*, since both are known targets of NF-κB (Toshchakov *et al.*, 2002;Yoshida *et al.*, 1998). The results suggest that these genes are targets for transcription factors activated by LPS treatment (BL20) and parasite infection and that their elevated expression is either of benefit to infected cells or has limited (neutral) detrimental potential. There is no evidence, however, that the outcome of LPS associated induction is significantly manipulated by infection of BL20 cells by the parasite.

Regardless of whether TBL20 or BL20 cells were treated with LPS or left un-stimulated, a slight induction of IL10 mRNA expression was observed in TBL20 compared to BL20 cells. Previous studies have also shown that *in vitro* infection of bovine lymphocyte lineages with *T. parv*a and a macrophage derived cell line infected with *T. annulata* were associated with IL-10 expression (Brown *et al.*, 1995b;McKeever *et al.*, 1997). Indeed, it appears that IL-10 is universally expressed in *T.parva* and *T. annulata* transformed cell lines. Though NF-κB has been proposed to be involved in the up-regulation of IL-10 expression in *Theileria*-transformed cells (Dobbelaere and Heussler, 1999), it appears to be unlikely in the BL20 model as LPS stimulation of BL20 cells failed to generate any differences in IL-10 mRNA expression levels while clearly activating NF-κB. Interestingly phosphatidylinositol 3-kinase (PI-3K) has been reported to contribute toward IL-10 expression (Crawley *et al.*, 1996). PI-3K is continuously activated in *Theileria* transformed cells (Heussler *et al.*, 2001) and speculated to have an important role in cellular proliferation and survival of the parasitized cell via IL-10 expression (Dobbelaere and Heussler, 1999;Dobbelaere and Kuenzi, 2004). Moreover, IL-10 serum levels have been found to correlate with tumor progression in murine B16 melanoma cell line (Sredni *et al.*, 2004) and *in vitro*

studies have demonstrated that IL-10 can favour tumor growth by stimulating cell proliferation and inhibiting cell apoptosis (Mocellin *et al.*, 2005).

Stimulation of uninfected BL20 cells with LPS showed elevated expression of Interferon stimulated gene-15 (ISG15), IFN-beta (IFNβ) and Toll-like receptor-4 (TLR4) but the parasite-infected TBL20 cells were clearly refractory to induction of ISG15 at 4h and INFβ/TLR4 at both 4 and 18 hours LPS treatment. ISG15 was essentially a positive control for parasite-mediated manipulation of an LPS activation response. Previous northern blot analysis had shown that *Theileria* infection renders TBL20 cells refractory to a high level induction of ISG15 expression, 14h post LPS treatment. The marked elevation of ISG15 mRNA in BL20 LPS stimulated cells detected by both northern blotting (Oura *et al.*, 2006) and RT-PCR validated an expected LPS induction response for this cell line in the current study.

Like ISG15, the results presented in Figure 3.9 indicate that infection by the parasite modulates the LPS activation expression profile of the IFN-β1 gene, a member of the family of type I IFNs. Thus, upon stimulation with LPS, BL20 cells displayed higher levels of IFN-β relative to the untreated cells. Moreover, in the context of infected TBL20 the level of product remained lower than the BL20 counterpart whether stimulated with LPS or not. This profile indicates a requirement of infected TBL20 to repress expression of the IFN-β1 gene and maintain this repression in the face of stimulation with an inflammatory mediator. There have been numerous citations indicating the possibility of NF-κB involvement in IFN-β gene regulation (Lenardo *et al.*, 1989;Megyeri *et al.*, 1995). A Type I interferon (IFN-alpha/beta) response is one of the major host defence mechanisms against viruses and has been shown to exhibit diverse functions under inflammatory conditions; for instance it could act in an anti-proliferative and immunoregulatory manner (Dunn *et al.*, 2006). These functions are considered to be of prime importance in *Theileria* associated infection. Studies pertaining to regulation of different types of IFN in *Theileria*-infected cells have shown that only *T. annulata* but not *T. parva* transformed cell lines are restricted to IFN-β production (Sager *et al.*, 1998). However, *T. annulata* infected leukocytes were found to be resistant to this high level induction of IFNβ expression by LPS. In contrast, high level expression was induced by stimulation of several *T. annulata* infected cell lines with poly (I:C), indicating

subtle manipulation by parasite infection of the signal transduction pathways associated with regulation of IFNβ expression (Sager *et al.*, 1998). This finding is in agreement with the above mentioned study indicating similarity of the BL20 system infected with *T. annulata* used in the current study.

The TLR4 (CD284) receptor complex has been identified as the major receptor involved in recognition and transduction of the LPS stimulated activation event (Beutler, 2000;Beutler, 2002;Hoshino *et al.*, 1999;Kalis *et al.*, 2003). TLR4 belongs to a class of pathogen recognition receptors (PRRs) and has the ability to recognize a variety of microbial products bearing pathogen-associated molecular patterns (PAMPs) (Garay-Malpartida *et al.*, 2011;Takeda and Akira, 2005). Activation via this receptor is known to operate through activation of NF-κB and IRF3 (Kawai and Akira, 2007) and results in up-regulation of IFN-β and a range of inflammatory cytokines [reviewed in (Akira and Takeda, 2004;Honda *et al.*, 2005)] involved in triggering innate immune responses. In addition, infection of BL20 cells with *T. annulata* is associated with significant repression of TLR4 at both the mRNA (Figure 3.9) and protein level (Figure 3.10) relative to control and LPS stimulated cells. Therefore following initial results obtained from the semi-quantitative PCR, it was of interest to further validate the infection associated repression profile of TLR4 expression at the protein level. Western blotting was performed to determine whether decreased TLR4 mRNA expression is manifest post-translationally in *Theileria*-infected cells. The western blot results showed that the TLR4 protein profile reflected the trend obtained at the mRNA level. Thus, a marked decrease in TLR4 expression was observed in TBL20 cells compared to BL20 cells (Figure 3.10). However, unlike the RNA pattern no significant differences were noticed in the protein levels of TLR4 when uninfected BL20 cells were stimulated with LPS while infected cells continued to display evidence of repression relative to their uninfected counterpart. In general, the levels of Tubulin detected by western blotting (constitutive control) appeared to be slightly lower for the LPS stimulated extracts (see Figure 3.10).

Why should *Theileria* repress expression of TLR4? Simplistically this would appear not to be in the interest of the parasite infected cell, since it has been demonstrated that constitutive activation of NF-κB is required for its survival (Heussler *et al.*, 1999;Palmer *et al.*, 1997). However, Heussler *et al.*,(2002) demonstrated using dominant negative mutants that signal transduction events

upstream of IKK signalosome aggregation are not required for NF-κB activation in the *Theileria*-infected leukocyte. Thus, the parasite bypasses a requirement for transduction of the NF-κB activation signal from the cell membrane, potentially allowing down regulation of molecules involved in this event.

The outcome of reducing the influence of TLR4 activation pathways can only be speculated upon, but a number of potential benefits to the infected cell can be postulated. Reduction of a major route of extrinsic stimulation of NF-κB could allow the level of NF-κB activation to be determined primarily by parasite dependent IKK signalosome aggregation. Cellular activation via the TLR4 receptor can induce apoptosis (Haase *et al.*, 2003;Ruckdeschel *et al.*, 2004), hence repressing expression of TLR4 may therefore promote parasite establishment. In myeloid cells TLR4 can synergise with the TREM1 pathway leading to neutrophil degranulation, phagocytosis and the respiratory burst (TREM1 review SAB biosciences). The generation of pro-inflammatory cytokines via a host dependent pathway could abrogate parasite-mediated modulation of these effector molecules, leading to stimulation of the innate immune response by the infected cell. Several protozoan parasites such as *Entamoeba histolytica* (Maldonado et al., 2000), *Trypanosoma* spp (Ropert and Gazzinelli, 2004), *Leishmania* spp (Tuon *et al.*, 2008), *Toxoplasma gondii* (Kim *et al.*, 2004b) and *Plasmodium falciparum* (McCall *et al.*, 2007) have been shown to actively modulate the expression of various TLR receptors especially TLR4 and TLR2 and their associated immune responses. It can be postulated therefore that the infected cell may down-regulate TLR4 to prevent extraneous activation via this receptor, allowing the activated infected cell to be under control deployed by the *Theileria* parasite to provide protection against stimulation of the immune response.

Despite the evidence that *T. annulata* may suppress the ability of the host cell to respond to LPS signalling, infection of the cell generates a dichotomy, since transcription factors that operate in cellular activation and induce a pro-inflammatory cytokine response (NF-κB, AP1, STAT3 and ATF2) are constitutively activated by infection. If the outcome of parasite mediated activation is to be advantageous for the parasite then it can be postulated that expression of target genes that are beneficial would be promoted/allowed while those that are detrimental are suppressed. The preliminary data presented in this chapter and

data from previous studies (Jensen *et al.*, 2009;Oura *et al.*, 2006;Sager *et al.*, 1997) suggests that such modulation occurs. For example, IL2RA and IFNB are both NF-κB dependent genes but Figure 3.9 shows that IFNB is repressed while IL2RA is elevated relative to uninfected control cells. However, the extent and specificity to which the parasite manipulates the expression profile of the activated host cell is unknown. If detailed knowledge on the pathways that the parasite utilises to establish the infected cell phenotype is to be gained, a global analysis of the gene expression profile of TBL20 relative to uninfected activated BL20 cells is required.

In summary, use of the current cellular model generated data that was both biologically valid as well as consistent with the past studies associated with *Theileria* infection. These findings indicated that *in vitro* stimulation of bovine leukocytes with LPS shows similarity to a typical activation of NF-κB via IKK signalosome complex formation and represents a valuable model system for the study of the mechanisms of the host cellular activation state. Activation of the cell can be detrimental but evidence using only a limited number of genes indicated that *T. annulata* subverts the normal response of transcription factor activation. Apparently this may operate by blocking signal transduction pathways that responds to inflammatory mediator like TLR4. The results have indicated that the parasite manipulates the outcome of cellular events to promote the establishment of infected cells and prevent cell death.

Chapter 4

Modulation of activation associated host cell gene expression by *T. annulata*

4 Modulation of activation associated host cell gene expression by *T. annulata*

4.1 Introduction

Bioinformatics combined with high-throughput technologies such as microarray analysis and next generation sequencing have been of great use to studies investigating the molecular mechanisms that underlie normal and dysfunctional biological processes. Such methodologies provide the ability to measure the expression level of tens of thousands of genes simultaneously using a single RNA sample (Gobert *et al.*, 2005;Manger and Relman, 2000). This property clearly has advantage over conventional northern blot analysis or more recent real time-PCR-based techniques that are more applicable for expression profiling a smaller number of target genes. To date, several different types of microarray platforms have been developed to monitor the expression levels of thousands of genes, the basis for each methodology being essentially a glass slide or membrane spotted or "arrayed" with DNA fragments or oligonucleotides that represent specific gene regions predicted to encode mRNA and protein. Purified RNA or cDNA is then fluorescently labelled and hybridized to the slide/membrane. In some cases, hybridization is performed simultaneously with reference RNA to facilitate comparison of data across multiple experiments. After thorough washing, raw data is obtained by a laser scanning system. With the advancement of microarray technology, a new generation of terminology and acronyms has evolved and examples of these are included in Table 1.1, Appendix 1.

Gene expression profiling has emerged as a powerful tool to investigate host pathogen interactions and is increasingly being used in the field of parasitology in general. Thus, a number of large-scale array projects have been performed to expression profile RNA derived from different parasites and/or their respective infected host cells. These include several parasites of medical and veterinary importance such as *Trypanosma* spp*, Plasm*odium spp., *Toxoplasma*, *Leishmania spp.* and *Schistosoma spp.* (Bahl *et al.*, 2003;Blader *et al.*, 2001;Bozdech *et al.*, 2003;Leifso *et al.*, 2007;Minning *et al.*, 2003;Verjovski-Almeida *et al.*, 2003). Such studies include comparison of gene expression profiles obtained from, or

during transition of, different parasite life cycle stages. For example, Minning *et al*. (2003) utilised 4400 probes to monitor the transformation of *Trypanosoma cruzi* from the trypomastigote to the amastigote in an axenic system. Similarly, Le-Roch *et al*. (2003) also used high-density oligonucleotide array to identify expression profiles of both human and mosquito derived stages of the malaria parasite (*P. falciparum*) lifecycle. In this study nine different stages of the parasite lifecycle were examined using array of 367,226 probes.

Recent microarray studies in apicomplexan parasites have focused on specific biological/cellular events including regulation of host cell gene expression associated with parasite infection. Significantly, these studies have highlighted that parasite infection can dramatically alter host cell gene expression to overcome immune responses directed against the parasite. For example, Blader *et al.,* (2001) examined gene expression profiles generated from human foreskin fibroblasts (HFF) infected with *Toxoplasma gondii*, using a human cDNA microarray consisting of ~22,000 known genes and uncharacterized expressed sequence tags. The results revealed significant changes to expression of host genes encoding pro-inflammatory cytokines, MHC encoding genes involved in antigen presentation and genes encoding proteins that protect against apoptosis. Indeed, *T. gondii* has been shown to actively inhibit/ block IFN-gamma induced upregulation of MHC class II mRNA and proteins (Lang *et al.*, 2006). Investigation of the ability of *T. gondii* to block a host cell IFN-γ response was also performed by Kim *et al.,* (2007), using a microarray representing 23,228 putative human genes. The results demonstrated that parasite infection resulted in dysregulation of 65 of the 127 identified IFN-γ-inducible genes in human fibroblasts and that all 127 genes were refractory to IFN-γ stimulation in infected compared to uninfected fibroblast cells. Since 46 of the 127 IFN-gamma-responsive genes were already induced and 19 suppressed before infected cells were exposed to IFN-gamma, it was concluded that other stimuli produced during infection could regulate these genes.

To date, only a limited number of studies have used microarray methodology to characterise parasite or host gene expression profiles of *Theileria*-infected leukocytes. Recently, Schmuckli-Maurer *et al*. (2009) analysed *s*ubtelomeric *v*ariable *s*ecreted proteins (*SVSP*s) expression in five different *T.*

parva-transformed cell lines established *in vitro* by infection of T or B-lymphocytes. Macroschizont transcript levels were compared using a 70-mer oligonucleotide microarray representing 4060 *T. parva* genes and included 78 of the 85 *SVSP* genes. Transcripts for 56 genes were identified and, for the majority, expression was found to be simultaneous and stable, with only minor variation in the profiles established from the different infected cell lines that were tested. For the small percentage of genes displaying evidence of differential expression, it was concluded that this is likely to be largely defined by the parasite genotype and not host background or cell type.

To investigate the response of bovine macrophages to important activation stimuli and study early immune responses, Jensen *et al.*, (2006b) developed a 5K bovine macrophage specific (BoMP) cDNA microarray. The array was developed to investigate gene expression in bovine myeloid cells and was generated with clones derived from specially created normalised bovine macrophage library: representative of *Bos taurus* and *Bos indicus* derived monocytes and mφ subject to various stimuli, including infection with *T. annulata*. The established array was then used to investigate the response of bovine monocytes to stimulation with interferon-γ and LPS. In this study, 695 genes were identified as differentially expressed at 2 and 16 hours post stimulation and included a number of genes of immunological significance, such as interleukins, chemokine and TLR-4.

The validated BoMP array was also used by Jensen *et al.*,(2008) to compare the transcriptional response induced by *T. annulata* infection of bovine monocytes derived from disease resistant (Sahiwals, *Bos indicus*) and susceptible (Holstein-Friesians, *Bos taurus*) cattle breeds. 156 genes were identified exhibiting breed-specific differential expression during the course of infection. 25% of these genes had no functional annotation, whereas of the known genes a large proportion (30%) encode predicted proteins expressed on the plasma membrane or in the extracellular space, with cellular adhesion being one of the major biological processes identified. The study also allowed limited discrimination between the breed specific response of monocytes to infection and general activation, with several genes (TLR10, PRNP, ICAM1 and TNFRSF18) being highlighted.

As indicated above, previous studies demonstrate the suitability of microarray technology to investigate alteration of gene expression profiles following cellular activation or parasite infection. However, this has only been performed to a limited extent for *T. annulata* infection, as the published studies mainly focused on identification of breed specific differences in the response of macrophages to infection and activation. Moreover, the genome coverage of the BoMP array was limited by the available bovine genomic sequence and the number of annotated representative cDNA sequences derived from the constructed library. This lack of coverage has been resolved by completion of the bovine genome sequencing project and the design and generation of a new microarray platform by the Glasgow *Theileria* group. This array represents 34,315 putative or known RNA sequences, compiled from available transcriptomic databases of *Bos taurus* (Bt) version 4.0 (Btau_4.0) and T. *annulata (Ta)*, a format that allows simultaneous analysis of parasite and host gene expression profiles. Table 4.1 summarizes probe-based design features included on the Bt_Ta array.

Work in the previous chapter established that relative to uninfected BL20 cells, *Theileria* infected TBL20 showed resistance to a detrimental response induced by stimulation with LPS, a known major inflammatory mediator. In addition, while the identified down regulation of the TLR4 LPS receptor in TBL20 could generate the refractory behaviour of these cells to LPS, the results confirmed that TBL20 display high levels of constitutive activation of NF-κB. Since activation of NF-κB is a major event that transduces stimulation by LPS into a pro-inflammatory cellular response, it can be postulated that *Theileria* infection must modulate the outcome of cellular activation mediated by NF-κB. Moreover, such modulation could extend to other infection activated events that prevent establishment of the macroschizont-infected cell. To study these possibilities the primary aims of the work presented in this chapter were as follows:

1) To use the Bt_Ta microarray platform to generate differential gene expression profiles representative of LPS stimulated uninfected cells (BL20-LPS) and infected TBL20 cells.

2) Compare the expression profiles and perform bioinformatic analysis to screen for evidence of infection-associated modulation of LPS activated gene expression.

3) Focus on bioinformatics analysis of the NF-κB pathway and genes targeted by activated NF-κB to test postulation that *Theileria* infection modulates the outcome of this activation event.

4.2 Methods

4.2.1 Microarrays experiment

To access global expression differences among *Theileria* infected and LPS stimulated uninfected cells we utilized our previously studied model of uninfected bovine lymphosarcoma and *Theileria* infected bovine lymphosarcoma cell lines. The details of cell lines, cell culture protocol and stimulation of cells with LPS are described in section 3.2.1and 3.2.2 of Chapter 3

4.2.1.1 Total RNA Extraction, Clean-up and Quantification

Total RNA Extraction was performed using TRI reagent (Sigma; T9424-200ML) and RNeasy® Kit (Qiagen cat.74104) according to manufacture's instructions. The concentration and quality of the resultant RNA was determined using a NanoDrop spectrophotometer (ND-1000; NanoDrop Technologies). RNA integrity was verified by gel electrophoresis as described previously. For all samples the 260/280-nm ratio was >2.03 and the 260/230-nm ratio was >1.8. Detailed methodology of RNA extraction, DNase 1 treatment, Clean up and quantification is described in Chapter 3 (see Section 3.2.8 & 3.2.9).

4.2.1.2 Microarray pilot experiment

Total RNA Samples were prepared from three independent replicate cultures for each experimental condition according to the NimbelGen standards. All RNA Samples were submitted (30µg of total RNA per sample) to Roche NimbleGen Systems, Iceland for further processing. Figure 4.1 illustrates the design of the microarray experiment.

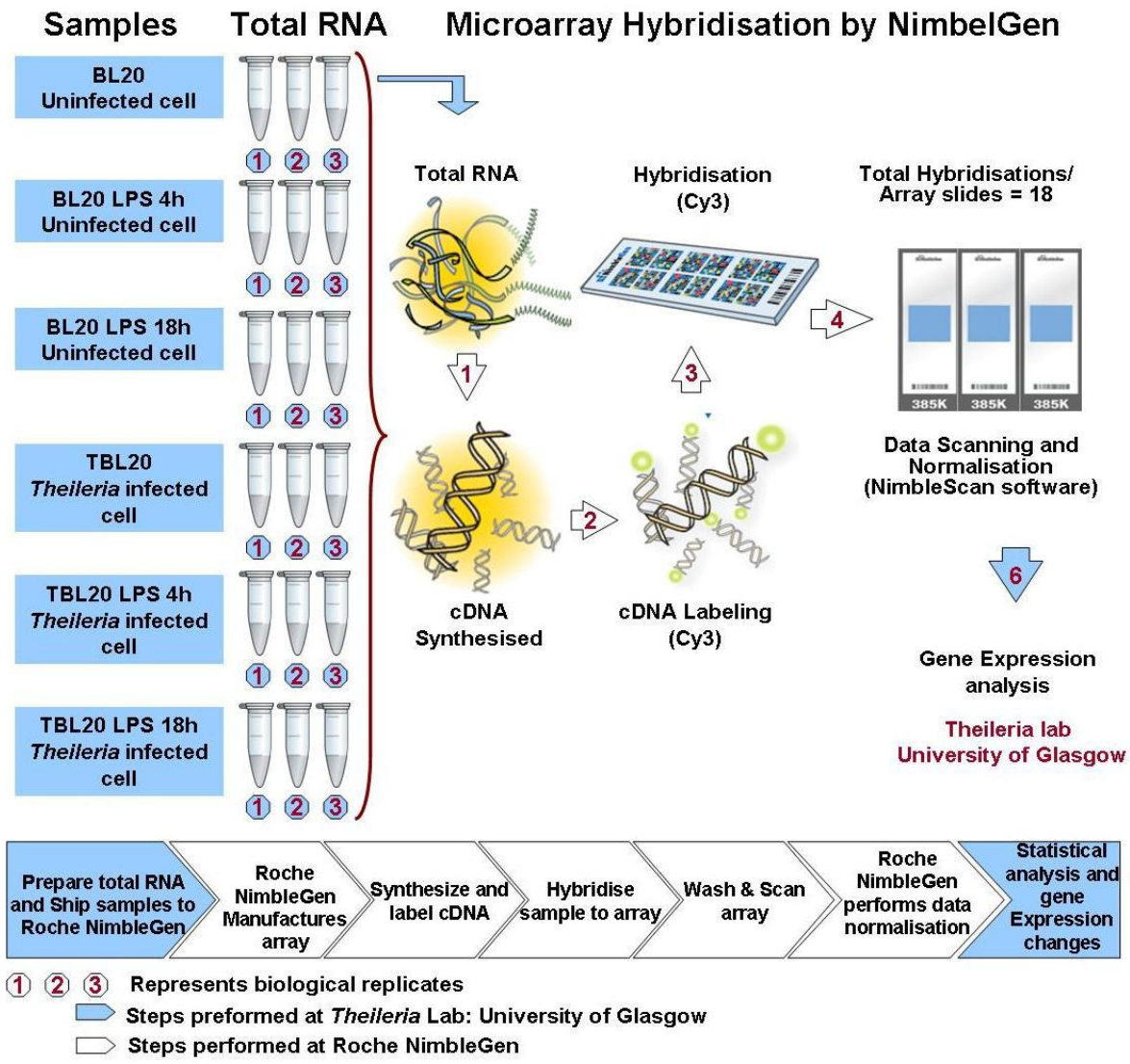

Figure 4.1: Schematic diagram illustrating microarray experimental design and the steps involved
Total RNA was isolated from uninfected and *Theileria* infected cells, the cells were either stimulated with LPS or unstimulated. Total RNA was shipped to Roche Nimblegen, Iceland for further processing and analysis to investigate the gene expression changes. Images courtesy of www.nimblegen.com

4.2.1.3 Design & specifications of array

The oligonucleotide microarray used in this study included all bovine RNA RefSeq DB available at NCBI (26751) obtained from latest Btau_4.0 (as of Oct. 4, 2007) assembly of the genome of Bos taurus, Hereford breed. (http://www.ncbi.nlm.nih.gov/RefSeq/) and a number of bovine putative RNA Sequences and ESTs (4730) (personal communication Kirsty Jensen, Roslin Institute, University of Edinburgh). This constituted of a total of 31481 bovine RNA sequences. In addition to these sequences the array contained oligonucleotide probes (3769) representing *Theileria annulata* genome obtained from GeneDB (http://www.genedb.org/Homepage/Tannulata). This array design

provides us an extensive platform that represents majority of the parasite and bovine transcriptome. Data from the *Theileria* probe set was not analysed during the course of this study. The final microarray design used in this study consisted of 34,315 features, making this the largest microarray available for the analysis of the *B.taurus* and *T. annulata* transcriptome simultaneously. The summary of the features present on the array is presented in Table 4.1.

Table 4.1: Summary of the microarray design and specifications used in the study

Array format	NimbleGen (similar to Affymetrix)					
Array design	Oligonucleotide tiling array (60mers) max 385,000 probes set per array					
Species coverage	Bovine (*Bos taurus*) Parasite (*Theileria annulata*)					
Array per slide	1					
Slide Size:	Slide Size: 1" x 3" (25 x 75mm)					
Array Size	17.4 x13mm					
Feature Size	16µm x 16µm					
Numbers of genes	Total of 35250 gene sequences were submitted to NimbleGen which included all **parasite ORFs** (3769), **Bovine** RNA RefSeq DB at NCBI (26751) and **Bovine Non-validated** RNA Seqs and ESTs (4730). The final probe coverage per gene on array obtained is summarised as follow.					
Probes per genes	**None**	**1**	**2**	**3**	**4**	**5**
Parasite (3769 genes)	18	6	13	2	2	3746
Bovine (31481genes)	351	24	10	15	10	30569
Hybridisation	Isothermal probes selected to have Tm within a set temperature range					

4.2.1.4 Microarray cDNA synthesis, fluorescent cDNA labelling, hybridisation and data scanning

The process of cDNA synthesis, labeling with Cy3, hybridization to array and data scanning were performed by Roche NimbleGen following their standard operating protocol. See www.nimblegen.com. The arrays were scanned to extract data using NimbelScan software. The array design files, raw gene expression data and RMA-normalised gene expression data was obtained and subjected to further subsequent analysis.

4.2.1.5 Raw data processing and Normalisation

The raw data (.pair file) was subjected to RMA (Robust Multi-Array Analysis) (Irizarry *et al.*, 2003), quantile normalization (Bolstad *et al.*, 2003), and background correction as implemented in the NimbleScan software package (Roche NimbleGen, Inc). Various types of data files were obtained from NimbelGen which contained information about the samples, arrays used, raw gene expression values and normalised gene expression files. Details of gene expression data and types of files obtained from Roche NimbleGen can be found in the Table 1.2, Appendix 1.

4.2.1.6 Annotation

An updated annotation database was assembled for the *Bos taurus* probesets (genes) present on the array. Data were sourced from *Bos taurus* RefSeq DB available at NCBI.

4.2.2 Microarray statistical analysis

4.2.2.1 Identification of differentially expressed genes by Rank Product analysis

Differentially expressed genes were identified by using Rank Product Analysis (RPA). RP score obtained by RPA sorts all the genes in a dataset according to their expression changes and assigns statistical confidence levels to each change in the form of false discovery rates (FDR) (Benjamini and Hochberg, 1995). This method is more robust than other techniques to find differentially expressed genes (such as Significance of microarray (SAM)) (Breitling *et al.*, 2004). All normalised hybridisation expression values were transformed to Log_2 expression values and subjected to further analysis by RPA. The output files generated from RPA of various pair wise comparisons were used in the subsequent analysis steps. Genes with FDR cut-off of 5% and ≥ 2 fold change were considered statistically significant, where a 5% FDR corresponds to a p-value of 0.05. Schematic illustration of overall methodology and steps involved in microarray analysis in the current study is described in Figure 4.2.

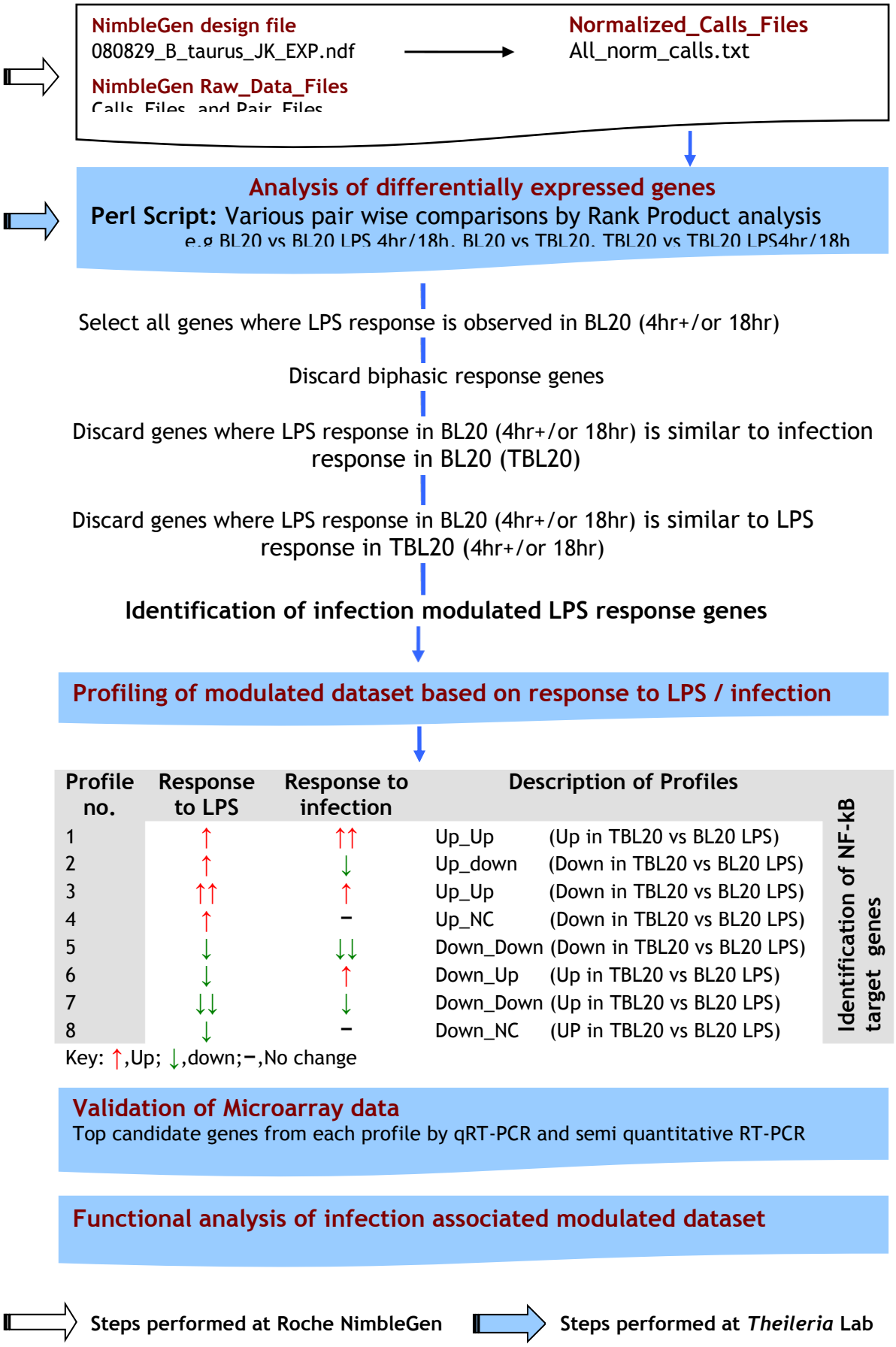

Figure 4.2: Flow chart of steps involved in the microarray data analysis
Schematic illustration of main steps in microarray data processing involving, statistical analysis, and filtering approach to identify differentially expressed genes, functional analysis and validation.

4.2.2.2 Monte Carlo simulation and Chi square test

In order to access the relationship and significance of the overlap between the differentially expressed genes identified by RPA in TBL20 and LPS stimulated BL20 datasets, Monte Carlo simulation was used to estimate the expected overlap likely to occur by chance between the results obtained from the two datasets (Kabakchiev *et al.*, 2010;METROPOLIS and ULAM, 1949). Only the most differentially expressed genes (FDR< 0.05, FC≥2) in each dataset were considered for this analysis and chi-quared test was used to compare the expected to the observed proportion of overlap as outlined below:

Number of genes expected to be common to lists A and B	Number of genes common to lists A and B
Number of genes not expected to be common to lists A and B	Total number of genes in list A and B, not common to both lists

4.2.3 Ingenuity Pathway Analysis

In order to identify gene expression networks which were enriched for genes highlighted in this study, Ingenuity Pathway Analysis V9 (Ingenuity® Systems, www.ingenuity.com) was utilised. Each bovine RNA sequence represented on the array was mapped to its corresponding gene in the Ingenuity Pathways Knowledge Base.

4.2.3.1 Canonical pathway analysis

The list of canonical pathways in the IPA system was augmented with a number of specific pathways, namely the NF-κB pathway, NF-κB response genes, the c-MYC pathway, validated targets of c-MYC transcriptional repression, validated targets of c-MYC transcriptional activation, AP1 target genes, ATF2 network genes and the WNT signalling pathway. The significance of the association between novel gene lists and each pathway was measured in two ways. Firstly, a ratio was calculated for the number of genes in a given list that map to the pathway divided by the total number of genes on the array that map to the same pathway. Secondly, Fisher's exact test was used to calculate a *p* value to

determine the probability that an association between gene list and the canonical pathway occur by chance alone.

4.2.3.2 Functional analysis

Gene lists identified from RPA that met FDR cut-off of 5% and 2-fold change (up- and downregulated) were uploaded in Ingenuity Pathway Analysis software (IPA 9.0; Ingenuity Systems;http://www.ingenuity.com). Fisher's exact test was used to calculate a p-value to determine the probability that each biological function assigned to that dataset can occurs by chance alone.

4.2.4 Comparison of Microarray data with other studies performed in Theileria Lab at University of Glasgow

Similar Microarray study has been conducted in *Theileria* Lab by Kinnaird *et al* (unpublished) to identify the gene set which are under direct control of a viable parasite showing reversion of TBL20 expression pattern upon treatment with theilericidal drug. In this experiment the parasite has been killed by buparvaquone (BW720c) (Datasets: BL20, TBL20 and buparvaquone treated BL20, TBL20). The gene set identified from BW20c experiment is of interest for comparison to my LPS dataset. Therefore, where necessary, this experimental dataset was superimposed and compared to my experimental datasets and is indicated in the subsequent analysis.

4.2.5 Reverse-transcriptase polymerase chain reaction (RT- PCR)

Microarrays evaluate thousands of genes in a single assay, but the data they produce may not always be reliable with respect to particular mRNAs expression, due to the diversity of experimental conditions and replicates involved in the hybridization process. Consequently an alternate methodology has to be used for validation of microarray results. Therefore, in this study semi-quantitative RT-PCR and quantitative real time RT-PCR techniques were used to confirm the results for those genes showing greatest fold change across the experimental conditions.

4.2.5.1 Primers design and analysis

The primers design software and methodology utilised in this study was same as described in chapter 3 (see section 3.2.10.1). Whenever possible, all primers were designed to the following criteria: Primers were all between 19-29bp long; the PCR product for all genes was between 159-346bp; for all genes the product spanned at least one intron to give differentially sized genomic and cDNA products. The melting temperature of the primer pairs were matched and were between 55 and 65ºC. Details of primer sequences, GenBank accession number, annealing temperature and product length for all gene-specific primers used in this study are listed in the Table 1.3, Appendix 1.

4.2.5.2 House keeping genes

In this study actin, beta (ACTβ) and glyceraldehyde-3-phosphate dehydrogenase (GAPDH) were used as normalising genes. These constitutively expressed genes did not show significant changes on our array analysis and have been extensively used as normalizing genes in differential gene expression studies in bovine (Anstaett *et al.*, 2010;Hruz *et al.*, 2011;Sager *et al.*, 1997). Amplification of ACTβ and GAPDH were used as positive controls for equal amounts of RNA across the samples.

4.2.5.3 Total RNA samples utilised in RT-PCR assay

Previously isolated and purified batch of total RNA samples used for the microarray experiment were utilised in subsequent RT-PCR assays for the validation of microarray results. Detailed methodology for RNA extraction and processing is described in chapter 3 (see section 3.2.8-9) whereas, reagents and kits used in the RNA extraction procedure are described separately in chapter2.

4.2.5.4 Semi-quantitative Reverse-Transcription PCR (RT-PCR)

Changes observed in the microarray results for differentially expressed top candidate genes were validated by semi-quantitative reverse-transcriptase polymerase chain reaction and gel electrophoresis analysis of the resultant PCR products. Semi-quantitative RT-PCR was conducted using Superscript III One-Step

RT-PCR kit from Invitrogen Corp (Cat no. 12574-026). Detailed methodology for semi-quantitative RT-PCR used in this study was same as outlined in chapter 3 (see section 3.2.10.2) whereas, all PCR reagents and kits used in this study are described in chapter2.

4.2.6 Quantitative Real-time Reverse-Transcription PCR (qRT-PCR)

With the advancement of PCR methodology, new technical developments refining its use have been developed. One of the powerful tools for analysing small scale gene expression is "real-time" PCR product quantification by fluorescence-kinetic detection methods. In this technique, PCR product is measured as it accumulates during sequential amplification cycles. The advantage of this method is that no post-PCR manipulation or product analysis is required since the quantitative measurement of the reaction product is known at the end of the cycling process. Therefore, in order to verify microarray results of differentially expressed genes in this study SYBR QRT-PCR methodology was utilized to quantify the mRNA expression of top candidate genes.

4.2.6.1 SYBR Green I chemistry

SYBR Green I is a fluorescent intercalating dye which binds to the double stranded DNA and generates a fluorescent signal upon binding. In qPCR, DNA product accumulates during amplification and fluorescent signal increases proportionally to the DNA concentration (Figure 4.3). When bound to double stranded DNA the dye absorbs light of 494nm and emits light wavelength 521nm, which makes it compatible with the use on any real-time thermo cycler.

The SYBR Green methodology has several advantages, such as the ability to add melting point analysis to the run. This allows comparison of the melting temperatures of the specific product and any suspected non-specific products. However, there is a limitation that it detects all double stranded products, including primer-dimers, which may result in an overestimation of the target concentration, and false positive results in cases where the melting curve does not clearly discriminate between primer-dimer and specific amplified product. Therefore, several important steps were taken to ensure accurate results. cDNA

synthesis and qPCR were performed on purified DNase I treated RNA samples, no template controls and no reverse transcriptase control were always included in the PCR reactions for all samples. In case of primers design special care was taken to avoid primer-dimers formation, and secondary structures. Wherever possible, primers were designed to span introns to minimise the risk of potential contamination of genomic DNA.

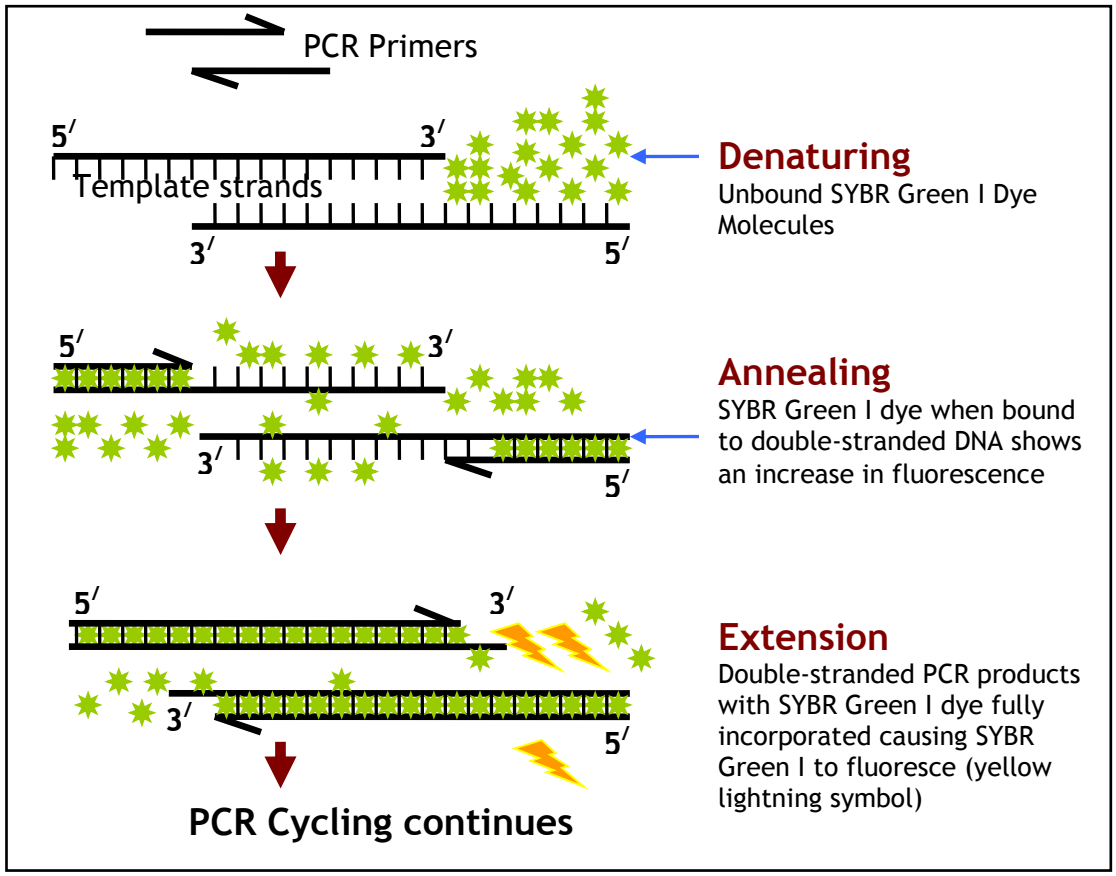

Figure 4.3: Schematic diagram illustrating SYBR Green I Chemistry during PCR amplification
SYBR Green I dye has a higher affinity for double-stranded DNA than single-stranded DNA or RNA. The SYBR Green I dye does not bind to the single-stranded RNA during denaturation and annealing stage and hence does not fluoresce. The cycle is repeated and the fluorescence is measured at the end of each extension reaction with the total amount of fluorescence being relative to the concentration of the amplified product.

4.2.6.2 Two-step qRT-PCR

In two-step qRT-PCR it is possible to store cDNA samples for later use in experiments at convenient conditions relative to the use of RNA for one step qRT-PCR. Although one-step qRT-PCR allows quantification in a single reaction which minimises the possibility of cross-contamination and provides a convenient system since less time and effort is involved. However, two-step qRT-PCR systems are generally considered to provide a somewhat higher sensitivity and

specificity than one-step QRT-PCR systems (Bustin, 2000). Therefore in this study two step methodology of qRT-PCR was used to validate the expression of genes. The details protocols and steps involved are described in the following.

4.2.6.2.1 Complementary DNA (cDNA) synthesis from total RNA

The first step in any RT-PCR methodology is to generate cDNA by reverse transcription of template RNA. First strand complementary DNA (cDNA) was reverse transcribed from 2.0µg of previously purified and DNase treated total RNA samples. cDNAs synthesis was carried out in a total volume of 20µl according to the manufacturer's instructions using oligo(dT) primers provided with the Affinityscript QPCR cDNA synthesis kit (Stratagene, USA; Cat no. 600559). cDNA synthesis was carried out for 25˚C for 5 min, 42˚C for 25 min and 25˚C for 5 min in a Techne thermocycler system (TC-512; Techne, UK).

4.2.6.2.2 qRT-PCR reaction parameters

Real-time fluorescence detection was achieved by using a Brilliant SYBR Green QPCR Master Mix buffer (Stratagene, 600548) which contains SYBR Green I dye, and Sure Start Taq DNA polymerase. The final concentration of primers was approximately 500nM in a total reaction volume of 25µl. Each 25µl of PCR reaction mix contained 10µl Nuclease-free PCR-grade water (including cDNA), 1µl of forward primer, 1µl of reverse primer and 13µl of 2 × qPCR master mix buffer. Real time fluorescence detection was performed in 96-Well Semi-Skirted Flat Deck PCR Plates (Thermo Fisher Scientific). A Stratagene Mx3005P Real-Time PCR System was used with the following thermal cycling parameters: 10 min at 95˚C (enzyme activation and initial denaturation); 40 cycles of 0.5min at 95˚C (denaturation), 0.5min of annealing at **X** ˚C and 0.5min at 72˚C (extension). Fluorescence was measured at the end of the elongation phase (72˚C) during each cycle of quantification. Where, X˚C indicates corresponding annealing temperatures (Tm of primers minus 3˚C) specific to different candidate genes tested. After 40 cycles of amplification, a melting curve analysis was carried out to verify the correct product by its specific melting temperature (Tm). The thermal profile for melting curve analysis consisted of an additional denaturation cycle for 1 min at 95˚C, lowered to 55˚C for 0.5min and

a gradient to 95°C with continuous fluorescence readings. All qPCR data was captured and analysed by Stratagene MxPro v4.10 software.

Additionally, standard curves for all primer set were run over 4-fold dilutions of the cDNA samples from 1:10-1:1000. Where necessary, the efficiency of the qPCR assay was determined by generating a set of standard curves for each primer pair. In most of the cases primer set generated a standard curve with an efficiency of 85-110 and an Rsq of 0.98-1.00, over the range of experimental sample dilutions. Rsq value is an indicator of the quality of the fit of all data to the standard curve plot, where 1 corresponds to perfect alignment and the closer the value is to 1, the better the fit of the line. In some cases despite several attempts being made to optimise the PCR this was not achievable. However, Standard curves were assessed for all qPCR reactions and their efficiencies applied to the quantitation algorithm for that experiment. Every plate for all experimental samples contained technical replicates of each cDNA sample, no-template controls with PCR grade water instead of cDNA templates and No RT control templates.

4.2.6.2.3 Statistical analysis

Real-time RT-PCR data were captured and analyzed using Stratagene MxPro v4.10 software (Strategene). The relative quantity values were normalized to the house keeping gene, which was either ß-actin or GAPDH and fold changes were calculated relative to the calibrator (DMSO-treated uninfected BL20 cells) using $-2^{-\Delta\Delta Ct}$ equation (Livak and Schmittgen, 2001). All normalised Ct values of the sample quantity relative to normaliser gene and $\log_2$ fold change of the samples relative to the calibrator calculated by MxPro software were exported as a text file for further analysis. Statistical analysis and generation of graphs presented were performed using a two-tailed Student's t-test with GraphPad Prism Software version 5.0 (La Jolla, CA). The difference was considered to be significant if the p-value was ≤ 0.05.

4.2.7 Indirect immunofluorescence analysis

Indirect immunofluorescence analysis of BL20 cells and TBL20 cells was performed essentially using the same protocol described in chapter 3 (see

section 3.2.4). Following cytospin preparations, fixation protocol was carried out immediately in pre-chilled methanol at -20^{o}C incubated for 10min. Slides were then washed briefly with 1x PBS and incubated with acetone in ice-cold (-20^{o}C) for 1min and washed three times with 1x PBS for 3min each. Immunodetection of LMO2 was acquired by incubation of fixed cells with monoclonal anti-LMO2 (1A9-3B11) (NB110-78626) (Novus Biologicals, USA) as primary antibody at a dilution of 1/100 in a complete medium for 1h at room temperature (RT). Cells were then washed three times with PBS for 3min each. Alexa Fluor 488 goat anti-mouse IgG (Invitrogen; A-11029) was used as secondary antibody at a dilution of 1/200 and incubated for 1h at RT. Following incubation of cells with antibodies slides were finally washed three times in 1× PBS for 3min each. After the final wash, cells were counter-stained with 0.1% Evan's blue for 1min, rinsed in 1×PBS three times and allowed to dry. Slides were then mounted in 10µl of mounting medium containing DABCO/glycerol, 4, 6-diamindino-2-phenylindole (DAPI) at 1mg/ml and phenydiamine at 1mg/ml and a cover slip. Immunofluorescence images were acquired using an Olympus BX60 microscope, a SPOT camera and SPOTTM Advanced image software Version Mac: 4.6.1.26 (Diagnostic Instruments, Inc).

4.2.8 Western Blotting

Sample preparation of whole extracts, SDS gel electrophoresis and immunoblotting was carried out as described previously in chapter 3 (see 3.2.11). Following electroblotting of the sample extracts onto membrane and Ponceau stain assessment, immunodetection was carried out by washing the membrane briefly with a wash buffer (1xTris-saline with 0.1% Tween 20) and then pre-incubated with block buffer for 1h at room temperature with gentle agitation. Blots were incubated with the following antibodies/reagent: monoclonal mouse anti-LMO2 (LMO2 Antibody; 1:2000; Novus NB110-78626; Novus Biologicals, Littleton, CO, USA), monoclonal mouse anti-Tubulin (TUB-1A2; 1:5000; Sigma T9028), polyclonal rabbit anti-VCAM1(sc- 8304, 1:1000; Santa Cruz-Biotechnology) were diluted in fresh block buffer (5% Marvel skimmed milk in Tris buffered saline plus 0.1% Tween 20) overnight at 4°C with constant gentle agitation. The membrane was washed twice briefly then twice for 15min each with wash buffer. The membranes were incubated with appropriate secondary antibodies; goat-anti-rabbit-HRP (1:10000, Sigma, A6154) or anti-mouse IgG

peroxidase conjugate (1:10000, Sigma, A5906) diluted in block buffer for 1h at room temperature. The membranes were washed as above with a final brief wash with 1x Tris-saline without Tween 20. Detection was carried out using a SuperSignal® West Pico Chemiluminescent Substrate kit (Pierce, supplied by Thermo Scientific, Rockford, IL). The blots were immediately exposed to X-ray film to capture the chemiluminescent signal. Several exposures were made to achieve the optimal signal for each antibody. The molecular weight of proteins was determined by comparison with Precision Plus Protein™ Standard dual colour marker (Bio-Rad Laboratories; 161-0374). Complete details of reagents and buffers used in western blotting are described separately in chapter 2.

4.3 Results

4.3.1 Microarray analysis of LPS stimulated BL20 and TBL20 cell lines

Gene expression profiling was performed by employment of a microarray representing the entire available bovine RNA REFSEQ database (26,751 sequences) and all *T. annulata* predicted mRNA open reading frames (3769 sequences). RNA was isolated from three replicate cultures of TBL20 and BL20 (DMSO) control cells and cultures treated with LPS for 4 hr and 18 hr.

4.3.2 Identification of differentially expressed genes

Following array hybridisation of each RNA sample in triplicate, differential gene expression on the normalised dataset provided by Roche/Nimblegen was initially assessed by pairwise comparisons using Ranked Product Analysis (RPA). This analysis allows a cut-off for significance of differential gene expression values to be set according to a false discovery rate (FDR) and fold change. In this study, differences in gene expression were taken to be statistically significant at ≥ 2 fold change with a FDR<0.05, a standard cut off for statistical significance commonly applied to microarray data (Benjamini and Hochberg, 1995;Jensen *et al.*, 2006b). Data analysis was also conducted using the Student's T-test (≥ 2 fold, F test Anova P-value <0.05) in the ArrayStar v2.1 software suite and the results of both analysis validated by cross comparison of the obtained datasets. The use of ArrayStar software also allowed enhanced visualisation of the data using scatter plot analysis, K-means clustering and heat maps with hierarchical clustering.

4.3.2.1 Rank product analysis of various microarray comparisons

Rank product analysis (see section 4.2.1.7.1) was used for the identification of genes that were up or down-regulated in *Theileria* infected and LPS stimulated uninfected cells. The descriptive statistics of this analysis is shown in Table 4.2. While the proportion of probe sets representing up or down-regulated genes is shown in Figure 4.4. Applying cut-off criteria of FC ≥ 2, FDR< 0.05, a total of 3643 genes were altered by LPS stimulation of BL20 cells (BL20-LPS dataset).

There were ~ 12.3% more up-regulated genes than down-regulated genes in LPS stimulated dataset. The highest fold change in hybridization value in the dataset of BL20-LPS up-regulated genes was recorded for myxovirus (influenza virus) resistance 2 (MX2) which was elevated 100 fold, while the most down-regulated gene was aquaporin 3 (AQP3) showing reduction of 39.3 fold.

Table 4.2: Descriptive statistics of microarray data analysis for all pair wise comparisons

Comparison	Largest Fold Change (Absolute)		No of Up-regulated genes	No of Down-regulated genes	Total No of gene
	Up	Down			
BL20 LPS 4h vs BL20	272.5	37.4	887	989	1876
BL20 LPS 18h vs BL20	100.5	39.2	1691	1082	2773
Composite BL20 LPS response vs BL20	100.5	39.2	**2045**	**1598**	**3643**
TBL20 vs BL20	**618**	**367.6**	**810**	**2145**	**2955**
TBL20 LPS 4h vs TBL20	6.16	6.4	153	70	223
TBL20 LPS 18h vs TBL20	45.9	3.1	293	31	324
Composite TBL20 LPS response vs TBL20	**45.9**	**6.4**	**369**	**98**	**467**

Genes that were altered at a fold change of ≥ 2 and FDR < 0.05 across all experimental conditions were considered as statistically significant and were selected for further analysis. Comparisons highlighted in grey represent the datasets that were subsequently used in further analysis. The composite datasets were generated from LPS stimulated datasets at to two different time points, where maximal fold change was taken in account at either time points.

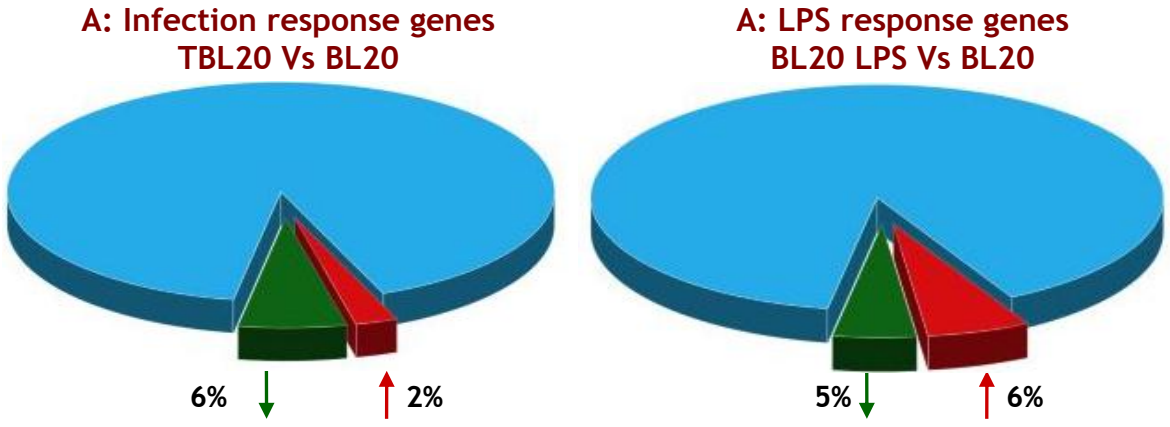

Figure 4.4: Pie chart showing the percentage of probe sets displaying evidence of altered expression values on pairwise comparison of TBL20 Vs BL20 and BL20-LPS Vs BL20 FDR<0.05 and FC ≥ 2.
The array contained 30656 probe sets, each representing a putative bovine gene. The percentage of probe sets displaying evidence of elevated expression in TBL20 and BL20-LPS are denoted by the red slice of the pie chart, while the green slice indicates probe sets with evidence of reduced expression.

A large number of bovine genes (2955) also showed significant alteration in expression levels associated with infection of BL20 cells by *T. annulata* (TBL20-infection associated dataset (TBL20 vs BL20). However, in contrast to the BL20-LPS dataset, 45% more genes were identified as down-regulated genes relative to those displaying evidence of up-regulation. In this dataset the highest fold change for an up-regulated gene was 618-fold, detected for a predicted gene similar to KIAA1598 protein (KIAA1598); while in the down-regulated dataset an unannotated Clone (CB467496), currently matching a bovine EST sequence exhibited 367.6 fold drop in expression value in TBL20 relative to uninfected BL20.

In a third pairwise comparison (TBL20 vs TBL20 LPS), the number of genes that showed evidence of significant alteration to expression following LPS stimulation of TBL20 cells (TBL20-LPS dataset) was obtained. Interestingly this dataset contained a significantly lower number of genes (467) relative to that obtained for uninfected BL20-LPS. This result indicates, as predicted from previous experiments (see Chapter 3) that infected TBL20 cells are significantly less responsive to stimulation by LPS, than the uninfected BL20 counterpart.

4.3.2.2 Comparative microarray analysis of the BL20-LPS and parasite infection associated (TBL20) datasets

In order to reveal the genes that are commonly regulated in parasite associated infection and LPS stimulated dataset, overlapping of the two datasets was performed by Excel based sorting and Venn diagram. A total of 2955 genes for parasite response genes set in TBL20 cells (dataset A) and 3,643 genes for LPS response genes set in BL20 (dataset B) were obtained from microarray analysis. Comparison of the BL20-LPS dataset and the TBL20 dataset generated an overlap of 1,296 genes (see Figure 4.5). To identify the statistical significance of the overlap, Monte Carlo (MC) simulation was used to measure the probability of the overlap of differentially expressed genes varying from the number expected by chance. In each simulation, the gene list for each condition was permutated and the random overlap between gene lists was recorded. From MC simulation, 369 genes were expected to be common between the two datasets and from observed analysis, 1296 genes were found to be common.

Finally after estimating the expected random overlap from MC, the empirical P-value was determined by Chi square analysis which estimated the probability that was significantly (P<0.001) greater than could have occurred by chance. The summary of the equation used to estimate the significance of the overlap is also described in Figure 4.5.

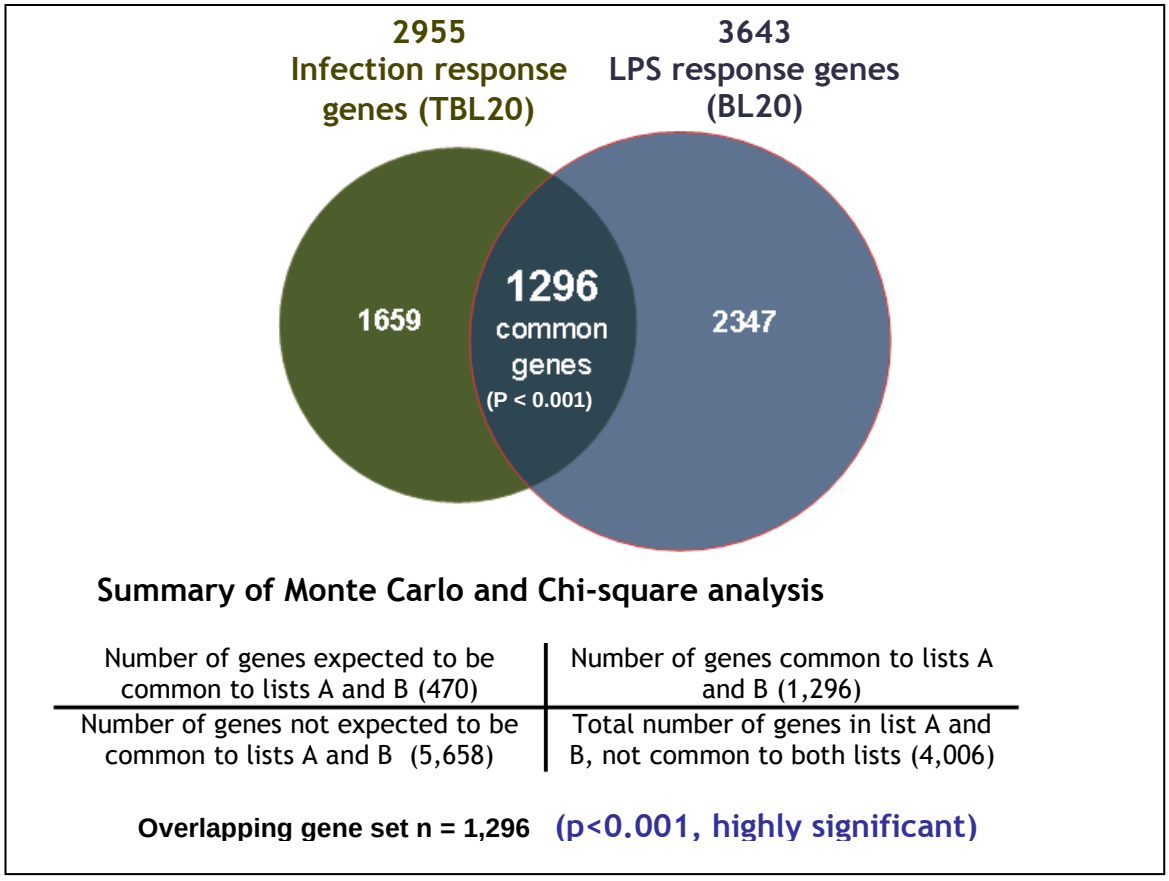

Figure 4.5: Comparison of differentially expressed gene sets using Venn diagram
The generated lists of significant genes (FDR<5%, FC ≥ 2) from each experimental condition contained a modulated set of 1,296 genes common to parasite infection and LPS treatment of uninfected cells. The identified overlap between two datasets was found to be highly significant (P<0.001). Whereas summary of observations obtained from Monte Carlo simulation and chi square analysis are also shown.

4.3.2.3 Identification of LPS stimulated gene expression profiles in BL20 cells with evidence of modulation in parasite infected TBL20.

To determine whether infection with *T. annulata* results in modulation of gene expression changes that occur in uninfected cells in response to LPS stimulation, the BL20-LPS and TBL20 datasets were compared. A subset of genes was identified representing BL20-LPS response genes that showed evidence of modulation by parasite infection. This subset was then reduced by removal of the relatively small number of genes that displayed an expression value in the

context of TBL20-LPS that was not significantly different from BL-20-LPS (146 genes). The final dataset (TBL20-M-LPS) representing infection associated modulation of BL20-LPS stimulated expression consisted of 1,959 genes (see Figure 4.6). Of the 1,959 genes, 269 were found to be elevated to a greater level in infected TBL20 cells relative to BL20-LPS cells, while for genes repressed in TBL20 cells relative to BL20-LPS the number was considerably higher (1,690).

A more detailed analysis of the modulated gene expression associated with infection relative to LPS stimulation was then conducted by expression profiling the 1,959 genes. This was achieved by sequential pairwise comparisons across all six cellular conditions and partitioning of genes with a similar kinetic profile (e.g. down in BL20-LPS Vs BL20; up in TBL20 Vs BL20-LPS and no change (NC) in TBL20 Vs TBL20-LPS) and representation of each profile in graphical form. In addition, information (obtained in an independent study; Kinnaird *et al*. unpublished) on the response of host cell gene expression following treatment of TBL20 with BW720c to kill the parasite was superimposed on to the profile datasets. This indicated whether target genes of interest were likely to be under direct control of parasite infection and operated in the predicted manner (i.e. reversed an infection-associated modulation). Eight gene clusters with distinct infection associated modulated BL20 LPS profiles were obtained; and for all eight profiles > 95% of the genes showed no significant change (NC) in expression in TBL20 cells stimulated with LPS.

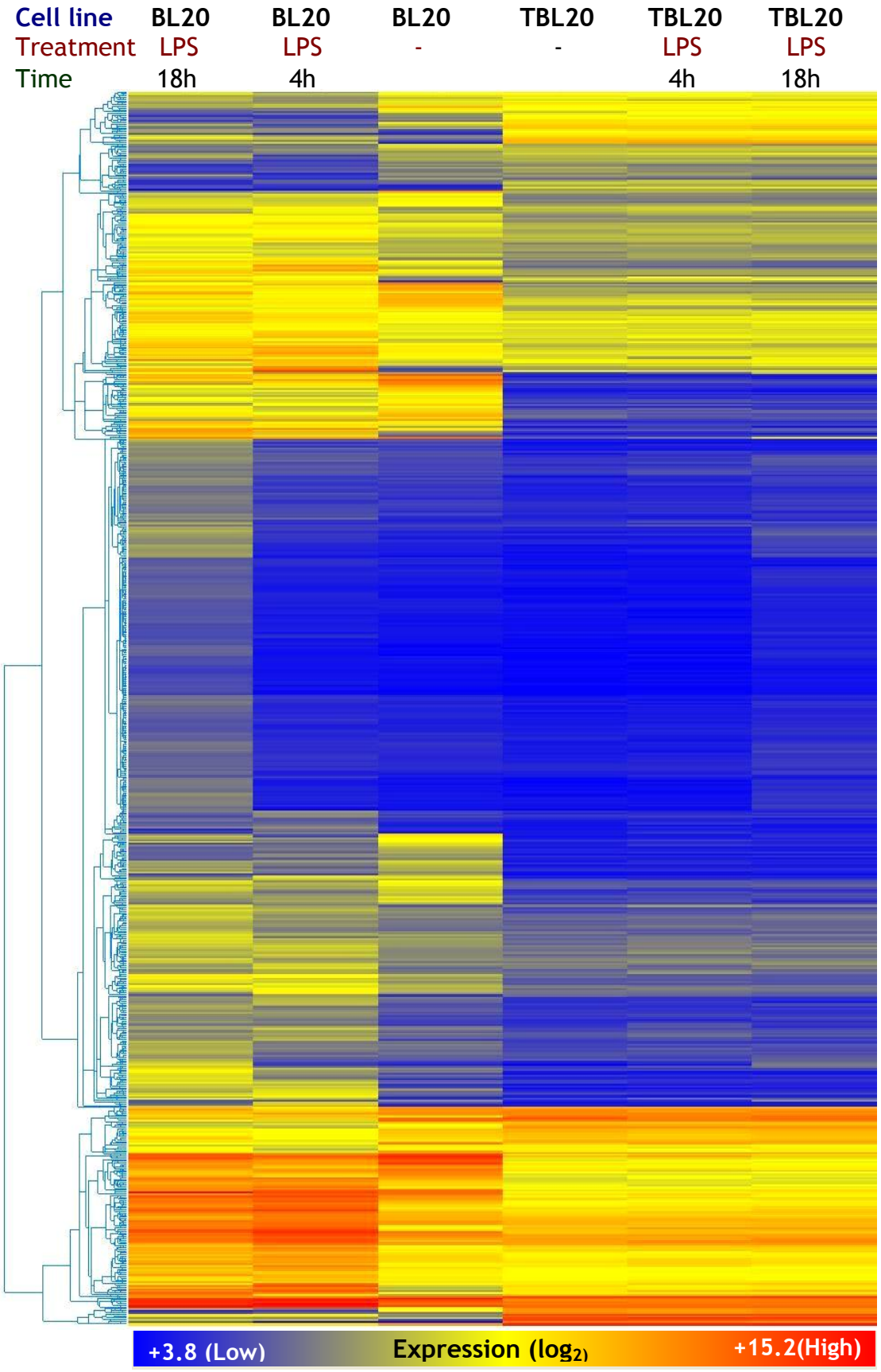

Figure 4.6: Hierarchical clustering of gene set modulated by *Theileria* infection
Visualization of changes in gene expression level of 1,959 genes identified by microarray analysis, showing modulated expression in *Theileria* infection. Hierarchical clustering was performed on modulated dataset and the results are shown as a heat-map. Each horizontal row represents an individual gene, where colour is used to represent arbitrary gene expression level based on log intensity values (see colour scale at the bottom): blue (low), yellow (intermediate), red (high).

4.3.2.4 Validation of house-keeping genes for quantitative real-time PCR expression analysis

To normalise qRT-PCR data it is important to select one or more reference genes with stable expression. Use of a valid normalising gene helps in correcting non-specific variation, such as differences in RNA or cDNA quantity and quantity which can affect the efficiency of the PCR reaction. Several reports have been published regarding variation in apparently stable reference genes (Schmittgen and Zakrajsek, 2000;Selvey *et al.*, 2001). In addition, it has been demonstrated that errors of up to 20-fold can be generated through normalization to a single house keeping gene (Vandesompele *et al.*, 2002). Consequently, normalisation to a single reference gene is thought to be insufficient and it is recommended that potential reference genes are validated for stability across the experimental conditions. In this study normalisation of RT-PCR data was carried out against actin, beta (ACTβ) or glyceraldehyde-3-phosphate dehydrogenase (GAPDH). These constitutively expressed genes did not show significant changes on my array analysis and have been extensively used as a normalizing gene in differential gene expression studies in the bovine (Anstaett *et al.*, 2010;Hruz *et al.*, 2011;Sager *et al.*, 1997). These genes were used to calculate a composite normalisation factor for analysis in qRT-PCR analysis. Figure 4.7 shows that mRNA expression of ACTβ was not changed when normalised against GAPDH and the same was true for vice versa.

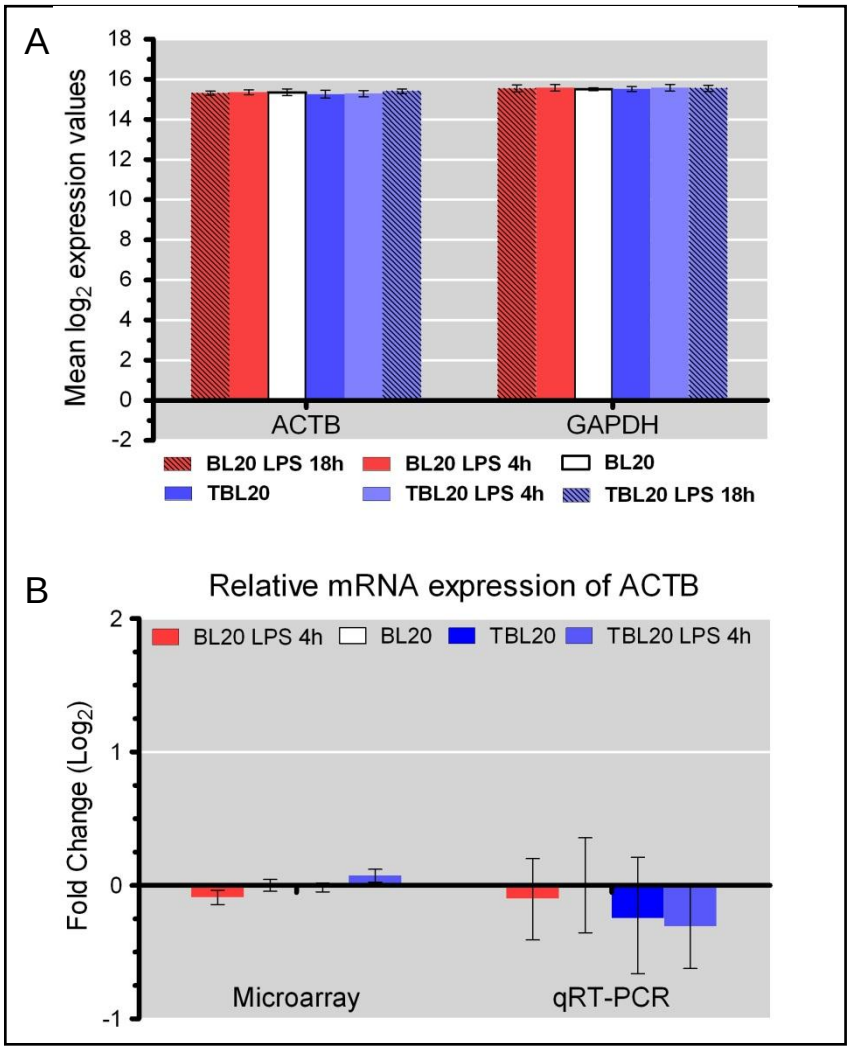

Figure 4.7: Microarray and qRT-PCR results of reference genes
Consistency of the average expression levels of house keeping genes across different experimental conditions is shown. (A) Microarray results of mRNA expression showing average hybridisation values (Log_2) of ACTB and GAPDH. Error bars indicate standard deviations obtained for six replicates from each cell lines. (B) qRT-PCR validation of changes in ACTB expression normalised against GAPDH. As predicted, these genes are constitutively expressed, and there was no significant gene expression difference between the groups for ACTB when normalised against GAPDH or vice versa. The lines for each bar on the graph represent the range in the relative expression and no statistical significance was obtained in the expression by using Student's t-test.

4.3.2.5 Expression profiles of genes modulated in parasite infected TBL20 Vs LPS stimulated uninfected BL20 (BL20-LPS)

Profile 1: Profile 1 is comprised of 44 genes whose expression was significantly enhanced (≥ 2 fold change, FDR < 5 %) in infected cells relative to an amplified uninfected BL20-LPS response (See Figure 4.8). The top 20 genes (based on highest fold expression difference between TBL20 Vs BL20 LPS) of the profile are listed in Table 4.3 and the full gene list for this profile is given in the Appendix 2.1.1).

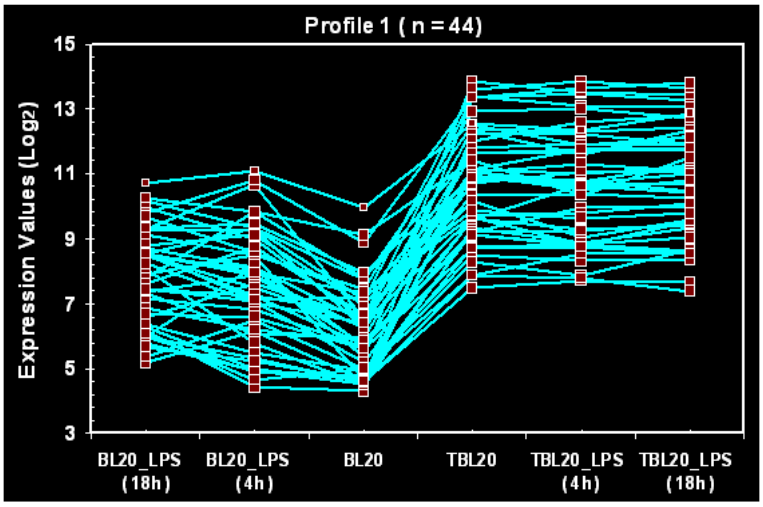

Figure 4.8: Graphical display of profile 1 showing the expression patterns of differentially expressed genes and modulated response in *Theileria* infection.
All candidate genes from profile 1 (n = 44) whose expression is elevated in both LPS stimulated BL20 and TBL20 cells, whereas TBL20 exhibit enhanced elevation relative to BL20-LPS. The x-axis corresponds to the experimental conditions, the y-axis to expression values (log_2) from array data. Each line represents an individual gene.

Table 4.3: Top 20 candidate genes of profile 1 showing pattern of modulated response in TBL20 cells relative LPS response in BL20 cells.

Gene Symbol	Annotation	BL20 LPS Vs BL20 FDR (4h/or18)	BL20 LPS Vs BL20 Abs: FC (4h/or18)	TBL20 Vs BL20	TBL20 Vs BL20 LPS Abs:FC (4h/or18)	BW720c Response 48h
			↑	↑↑	↑	
SLAMF7	Similar to 19A protein (CD319) (LOC790164)	0.000	2.8	415.38	148	–
LRRTM4	Similar to GFHL3075, transcript variant 3 (LOC521137)	0.000	3.6	242.65	67.93	–
-----	CO876689 BovGen_05014 normal cattle brain Bos taurus cDNA clone	0.007	2.0	114.17	55.85	–
MMP13	Matrix metallopeptidase 13 (collagenase 3)	0.001	3.1	168.24	54.2	↓
XCL1	Chemokine (C motif) ligand 1	0.000	8.5	356.63	42	↓
WC1	Similar to BoWC1.1 (LOC783109)	0.004	2.4	93.91	39.63	–
TP73	Similar to P73 alpha protein (LOC515105)	0.002	2.7	53.59	20.04	–
LOC788785	Similar to ATXN1 protein	0.001	2.9	42.99	15	–
SH3BGRL2	SH3 domain binding glutamic acid-rich protein like 2	0.000	3.2	44.97	14.01	–
IL2RB	Similar to IL2RB (LOC510185)	0.000	8.3	93.15	11.16	–
CD122	Similar to Interleukin-2 receptor subunit beta precursor (IL-2 receptor) (P70-75) (High affinity IL-2 receptor subunit beta) (CD122 antigen)	0.000	4.5	45.48	10.03	–
SELL	selectin L (lymphocyte adhesion molecule 1)	0.008	2.2	21.43	9.561	↑
LOC786204	Similar to chemokine CCL1/I-309	0.000	3.0	27.12	9.16	↓
MEIS3	Similar to Homeobox protein Meis3 (Meis1-related protein 2) (LOC617311)	0.000	8.3	71.00	8.521	↓
LOC785733	Similar to BoWC1.1 (LOC785733)	0.021	2.1	16.43	7.77	–
LOC786443	Hypothetical protein	0.000	14.4	92.29	6.403	–
ICAM1	Intercellular adhesion molecule 1(CD54)	0.000	3.8	22.81	6.029	–
LOC788239	Similar to regulator of G-protein signaling 16/-r	0.025	2.0	9.63	4.743	–
PGPEP1	Pyroglutamyl-peptidase I	0.000	4.8	22.43	4.709	–
LOC785427	Similar to epidermis-specific serine protease-like protein	0.000	4.7	22.10	4.662	↑

Summary of top 20 candidate genes whose expression was significantly altered (FDR<5%, FC≥ 2) in *Theileria* infected or LPS stimulated uninfected BL20 cells (maximal LPS response at 4h/or18) relative to control cells. Data is arranged in descending order of absolute fold difference between BL20-LPS and TBL20. Genes highlighted in light blue indicates Bw720c response previously identified in an independent microarray experiment (Kinnaird *et al*; unpublished). Gene symbols in bold indicate most recent annotation of the genes identified from NCBI.

For many of the genes in profile 1 the amplitude of enhanced expression associated with infection was considerable. Thus, mRNA expression levels of the SLAMF7 gene, a member of the immunoglobulin gene super family, is highly elevated in TBL20 cells with an absolute fold change of 148; followed by genes encoding MMP13, chemokine (C motif) ligand 1 and IL2RB which showed respective elevated responses of 54.2, 42 and 11.1 fold relative to the maximal BL20-LPS response (Table 4.3). A further 14 genes of this profile also displayed an elevation of greater than 5 fold. Of the 16 BW720c sensitive genes identified, 10 (62.5 %) responded in a predictive manner, i.e. expression was significantly reduced by treatment over 48 hours.

To determine any insight into potential biological relevance of the parasite associated modulation of LPS stimulated gene expression, the dataset for each profile was subjected to ingenuity pathway analysis software for enrichment of predicted molecular and cellular functions. Functional prediction (using data obtained from the bovine REFSEQ and NCBI databases) that may provide insight for the infection-associated modulation event was also utilised. For profile 1 the two most significant predicted functional groups were molecules involved in control of cellular movement and cell-to-cell signalling and an association with inflammation was identified. In addition, a number of genes in profile 1 show similarity with alterations that have been linked to the phenotype of *Theileria* transformed leukocytes. Thus, elevated expression of a matrix metallopeptidase gene (MMP13), the IL2 receptor B gene (IL2RB), genes encoding cellular adhesion molecules (ICAM1 and SELL) and genes that regulate the cytoskeleton (SDC4 and CTTN) were detected.

For profile validation, 3 to 9 genes were selected for semi-quantitative RT-PCR. Selection was based on amplitude of infection-associated modulation and/or bioinformatic functional prediction (using data obtained from the bovine REFSEQ and NCBI databases) that could provide possible insight for the infection-associated modulation event. Two validated genes with a predicted function of interest were then selected for each profile to compare the kinetics and amplitude of modulation obtained by micro-array analysis relative to the results of qRT-PCR. Semi-quantitative RT-PCR was performed for 8 genes of profile 1, all of which validated the microarray profile (see Figure 4.9); the gene encoding the Meis3 transcription factor, for example, showed a clear elevation in PCR

product in LPS-stimulated uninfected BL20 cells but was significantly enhanced in infected TBL20, with no obvious detectable alteration of product levels following LPS stimulation of TBL20. Furthermore, the RT-PCR profile for these genes following BW720c drug treatment of TBL20 validated the microarray expression profile obtained independently by Dr. Jane Kinnaird. Further validation of profile 1 was obtained by performing qRT-PCR for the Cortactin and Meis homeobox 3 genes. The results showed correlation between the microarray and qRT-PCR data, with qRT-PCR giving a 5.98 fold elevation (log_2) in expression level of MEIS3 in TBL20 relative to BL20-LPS compared to a difference of 3.1 fold (log_2) generated by the array data; while correlation of the profile was even stronger for Cortactin gene, as qRT-PCR calculated the difference to be 1.31 fold (log_2) relative to the 1.18 fold (log_2) computed from the array data.

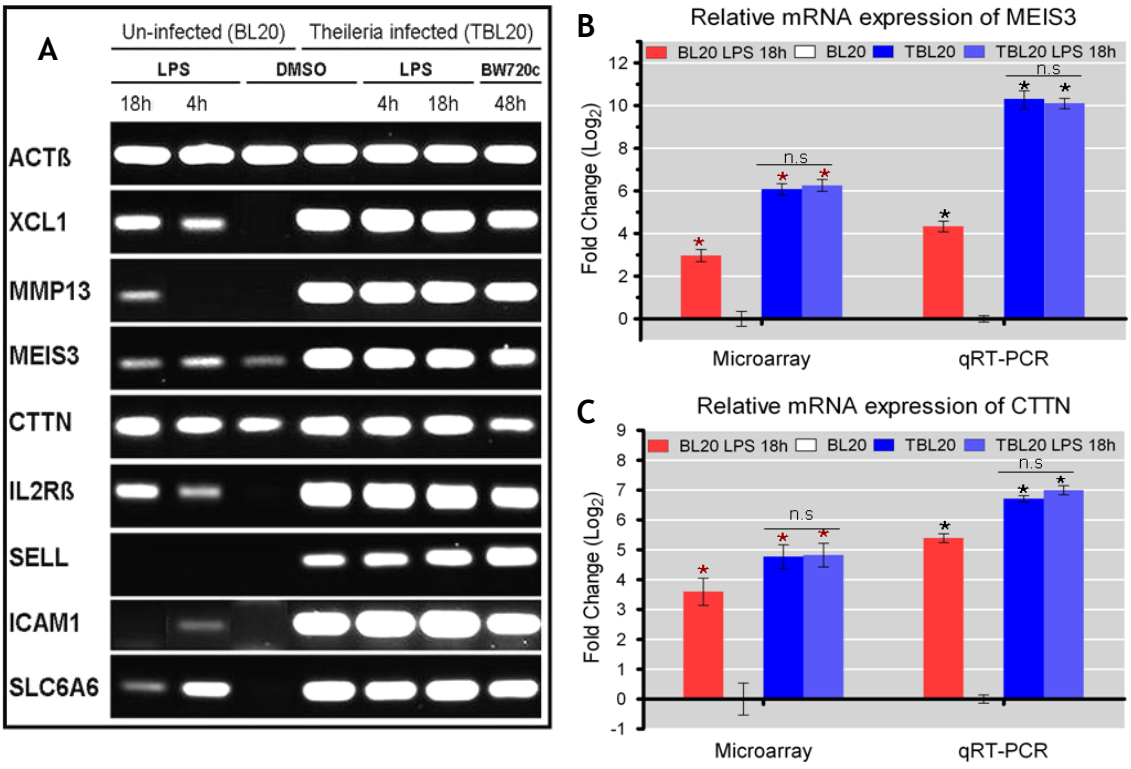

Figure 4.9: Validation of microarray results for profile 1
A. Semi-quantitative RT-PCR results showing mRNA expression of 8 candidate genes (XCL1, MMP13, MEIS3, CTTN, IL2RB, SELL, ICAM1 and SLC6A6) in BL20 cells and TBL20 cells either stimulated or un-stimulated with LPS. Semi-quantitative PCR products obtained using the gene specific primers were resolved on 1% agarose gel, whereas ACTB was used as an internal control.
B. Real-time qRT-PCR validation changes in MEIS3 mRNA expression.
C. Real-time qRT-PCR validation changes in CTTN mRNA expression.
For microarray results the asterisk (*) above the bars indicate the statistical significance of the relative log fold change compared to BL20 cells (*FDR< 0.05, ± S.E.M, n = 6). For qRT-PCR data the asterisk denotes the statistical significance of the relative log fold change compared to BL20 cells (Student's t-test, *P< 0.01).The lines for each bar on the graph represent the range in the relative expression. Whereas, n.s indicates statistically non-significant results in TBL20 LPS relative to TBL20 cells

Profile 2

Profile 2 represents genes elevated by LPS stimulation of uninfected cells that are significantly repressed in infected TBL20, with 98 % showing no significant change following stimulation of TBL20 with LPS. This profile generated one of the larger datasets and contained 254 genes (Figure 4.10). The top 20 genes of the profile, absolute fold change in expression, response to BW720c and functional prediction are presented in Table 4.4 whereas full list of gene is presented in Appendix 2.1.2.

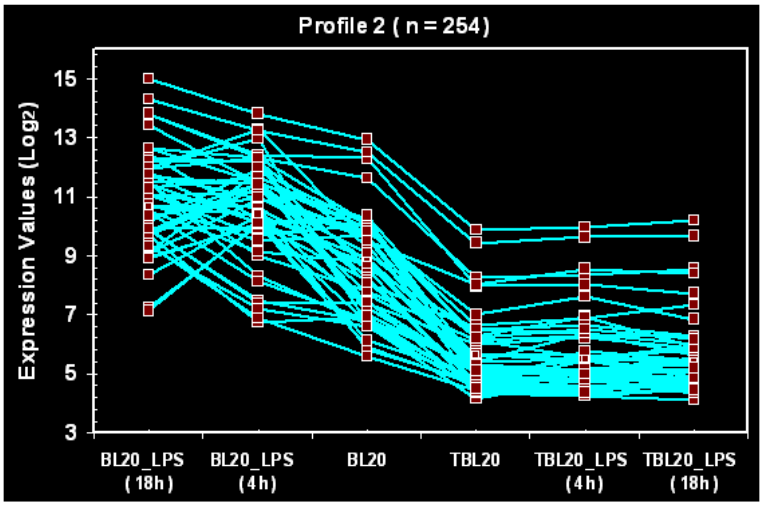

Figure 4.10: Graphical display of profile 2 showing the expression patterns of differentially expressed genes and modulated response in *Theileria* infection.
Top 50 candidate genes from profile 2 (n = 254) whose expression is elevated in BL20-LPS but significantly repressed in TBL20 cells; this repression was even greater in TBL20 when compared to BL20-LPS. The x-axis corresponds to the experimental conditions, the y-axis to expression values (log_2) from array data. Each line represents an individual gene.

Almost all of the 116 genes that were sensitive to BW720c treatment responded in the predicted manner (i.e. 98.2 % showed elevated expression with bpq treatment), indicating active repression by a viable parasite. Many genes showed a combined (up in BL20-LPS x down in TBL20-infection associated) absolute fold change >10 fold (128 genes). Genes of interest with major differences in expression values between TBL20 Vs BL20-LPS include MPEG1 (449.4 fold difference), CLU (280 fold), CD200 (132 fold), BOLA-DYA (132 fold), IL15 (107 fold), STAP1 (43 fold), and IJG (58 fold). IPA analysis showed enrichment for genes predicted to function in cell to cell signalling, cell morphology, cellular development and cellular growth and proliferation. A significant number of genes were associated with cancer and included molecules associated with apoptosis.

Table 4.4: Top 20 genes of profile 2 showing repression in TBL20 cells relative to an elevated LPS response in BL20 cells.

Gene Symbol	Annotation	BL20 LPS Vs BL20 FDR (4h/or18)	BL20 LPS Vs BL20 Abs: FC (4h/or18)	TBL20 Vs BL20	TBL20 Vs BL20 LPS Abs:FC (4h/or18)	BW720c Response 48h
			↑	↓	↓	
MPEG1	Macrophage expressed gene 1	0.000	79.8	-5.63	-449.4	↑
CLU	Clusterin	0.000	8.9	-31.71	-280.7	–
-------	CO882151 BovGen_10476 normal cattle brain cDNA clone RZPDp1056F0925Q 5', mRNA sequence	0.000	46.8	-3.98	-186.2	–
-------	Clone tghc9907 immunoglobulin gamma 1 heavy chain constant region mRNA	0.000	49.0	-3.62	-177.4	–
CD200R	CD200 Receptor(LOC529709)	0.000	5.2	-25.41	-132.8	↑
BOLA-DYA	Major histocompatibility complex, class II, DY alpha	0.000	27.4	-4.82	-132.1	↑
EPHA7	Eph receptor A7	0.000	4.6	-26.04	-120.1	–
LOC789139	Similar to IGLV3S1	0.000	7.4	-16.30	-119.8	↑
SMARCA1	Hypothetical (LOC535439)	0.000	3.4	-33.93	-115.3	↑
IL15	Interleukin 15	0.000	5.7	-18.88	-107.3	–
--------	N-acetylgalactosaminyltransferase A blood gro-like	0.000	2.8	-35.45	-99.96	–
-------	CO894237 BovGen_22562 normal cattle brain cDNA clone RZPDp1056O1038Q 5'	0.000	21.4	-4.61	-98.7	–
--------	CO874773 BovGen_03098 normal cattle brain cDNA clone RZPDp1056C1255Q 3'	0.000	8.2	-11.46	-94.19	–
--------	CO894397 BovGen_22722 normal cattle brain cDNA clone RZPDp1056H2051Q 5'	0.000	6.7	-12.71	-85.28	↑
BTN3A2	Butyrophilin, subfamily 3, member A2	0.000	6.5	-12.79	-82.84	↑
TNXB	Tenascin XB	0.000	6.6	-11.85	-78.05	–
LOC515679	Similar to putative protein product of HMFN0672	0.017	2.0	-32.39	-65.13	↑
THBS1	Thrombospondin 1	0.000	2.5	-25.72	-65.01	–
RGS18	Similar to regulator of G-protein signaling 13, transcript variant 2 (LOC613624)	0.000	29.2	-2.16	-63.29	–
IGJ	Immunoglobulin J chain	0.001	2.9	-20.28	-58.06	↑

20 genes from the profile whose expression was significantly altered (FDR<5%, FC ≥ 2) in *Theileria* infected or LPS stimulated uninfected BL20 cells (maximal LPS response at 4h/or18) relative to control cells. Data is arranged in descending order of absolute fold difference between BL20-LPS and TBL20. Genes highlighted in light blue shows Bw720c response previously identified in an independent microarray experiment (Kinnaird *et al*; unpublished). Gene symbols in bold indicate most recent annotation of the genes identified from NCBI.

The profile was validated for 7 genes by semi-quantitative RT-PCR (Figure 4.11A). The gene encoding MPEG1, for example, showed an elevation in PCR product in LPS-stimulated uninfected BL20 cells while the relative level of product was clearly repressed in infected TBL20, and this repression was reversed upon treatment of TBL20 with BW720c. Similar results were obtained for STAP-1, IGJ and BOLA-DYA. Additionally, qRT-PCR validation was performed for the BOLA-DYA and BIRC3 genes (Figure 4.11B and C). The qRT-PCR assay validated the micro-array profile, giving a 11.33 fold difference (log_2) in expression level of BOLA-DYA in TBL20 relative to BL20-LPS compared to a difference of 7.16 fold (log_2) generated by the array data; while qRT-PCR calculated the difference for BIRC3 to be 7.14 fold (log_2) relative to the 4.69 fold (log_2) computed from the array data.

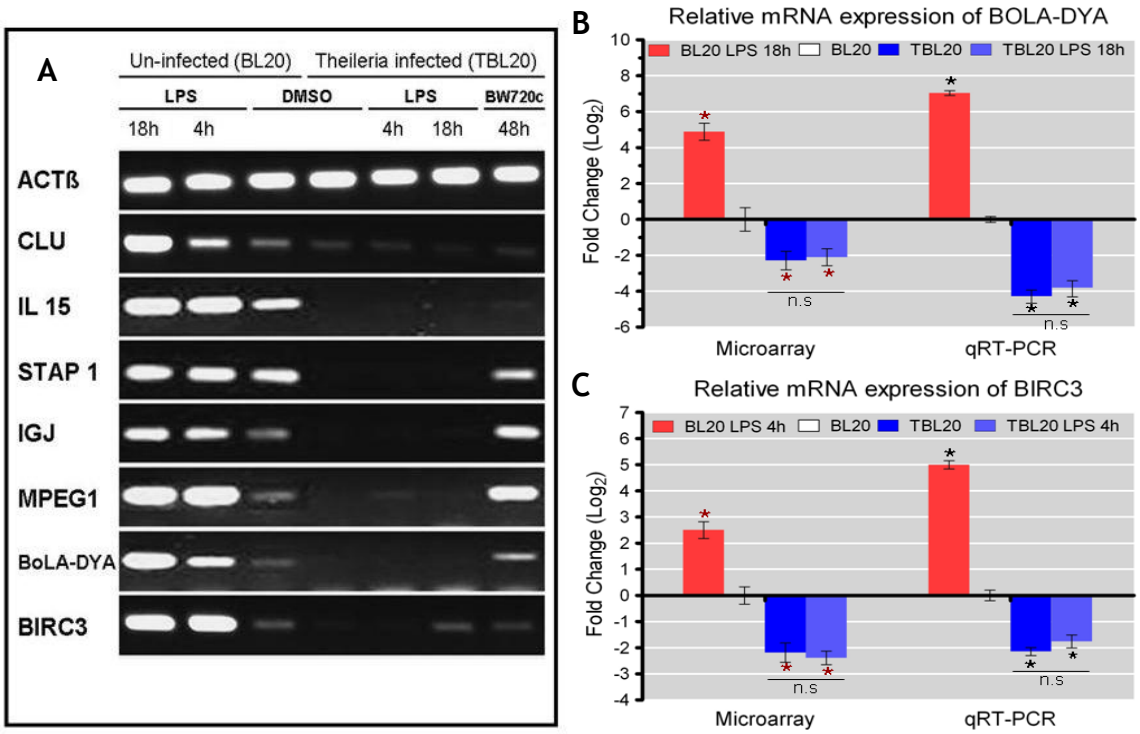

Figure 4.11: Validation of microarray results for profile 2
A. Semi-quantitative RT-PCR results showing mRNA expression of 7 candidate genes (CLU, IL15, STAP1, IGJ, MPEG1, BOLA-DYA, BIRC3) in BL20 cells and TBL20 cells either stimulated or un-stimulated with LPS. Semi-quantitative PCR products obtained using the gene specific primers were resolved on 1% agarose gel, whereas; ACTB was used as an internal control. **B.** Real-time qRT-PCR validation changes in BOLA-DYA mRNA expression. **C.** Real-time qRT-PCR validation changes in BIRC3 mRNA expression.
For microarray results the asterisk (*) above the bars indicate the statistical significance of the relative log fold change compared to BL20 cells (*FDR< 0.05, ± S.E.M, n = 6). For qRT-PCR data the asterisk denotes the statistical significance of the relative log fold change compared to BL20 cells (Student's t-test, * P< 0.01).The lines for each bar on the graph represent the range in the relative expression. Whereas, n.s indicates statistically non-significant results in TBL20 LPS relative to TBL20 cells

Profile 3

Profile 3 represents 55 genes that are elevated by LPS stimulation of BL20 and by *Theileria* infection relative to control BL20 cells, but for these genes elevation in TBL20 was significantly less than BL20-LPS (Figure 4.12). No significant alteration occurred in TBL20-LPS for 96% of the dataset. The top 20 candidate genes of this profile are represented in Table 4.5, while a full list of 55 genes is presented in Appendix 2.1.3. An example of this profile is the gene for interferon induced protein 15, ISG15: elevated 121 fold in BL20-LPS but only 26 fold by infection (TBL20-IA) and no change in TBL20-LPS. These kinetics match the profile of expression previously obtained by northern blotting (Oura *et al.*, 2006). Of the 25 bpq responsive genes in profile 320 (80 %) were elevated upon treatment, indicating repression by a viable parasite.

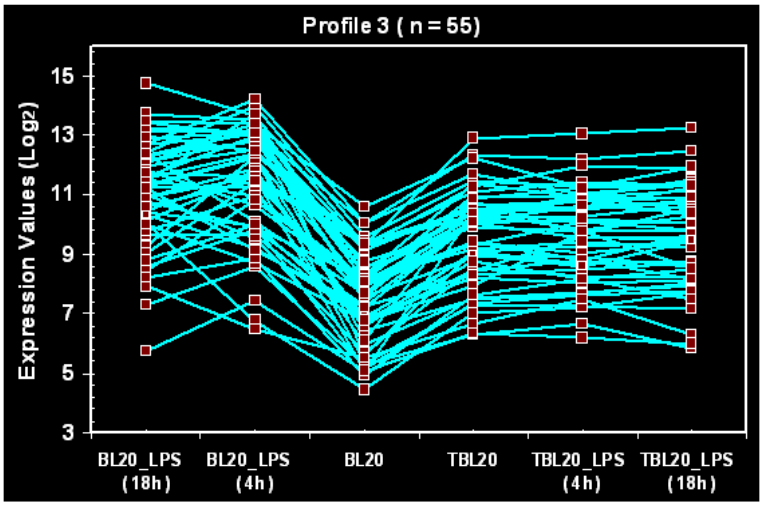

Figure 4.12: Graphical display of profile 3 showing the expression patterns of differentially expressed genes and modulated response in *Theileria* infection.
Top 50 candidate genes from profile 3 (n = 55) whose expression is elevated in both LPS stimulated BL20 and TBL20 cells, whereas there is significant repression in TBL20 when compared to BL20-LPS. The x-axis corresponds to the experimental conditions, the y-axis to expression values (log_2) from array data. Each line represents an individual gene.

Table 4.5: Top 20 genes of profile 3 showing repression in TBL20 cells relative to LPS response in BL20 cells.

Gene Symbol	Annotation	BL20 LPS Vs BL20 FDR (4h/or18)	BL20 LPS Vs BL20 Abs: FC (4h/or18)	TBL20 Vs BL20	TBL20 Vs BL20 LPS Abs:FC (4h/or18)	BW720c Response 48h
			↑↑	↑	↓	
OAS2	2'-5'-oligoadenylate synthetase 2, 69/71kDa	0.000	125.9	3.93	-32.07	↑
CD83	CD83 molecule	0.000	57.1	2.07	-27.51	–
CXCL10	Chemokine (C-X-C motif) ligand 10	0.000	272.5	11.23	-24.25	↓
LOC789736	Hypothetical protein LOC789736	0.000	38.2	2.88	-13.27	↑
-----	CB457261 714599 MARC 6BOV Bos taurus cDNA 5'	0.000	37.1	3.35	-11.08	↑
RELB	Similar to I-REL (LOC522670)	0.000	27.2	2.54	-10.74	–
LOC788393	Hypothetical protein LOC788393	0.000	36.9	3.68	-10.04	↑
TNFAIP3	Hypothetical LOC508105 (LOC508105)	0.000	57.1	6.60	-8.649	–
TGFBR3	Similar to transforming growth factor, beta receptor III (betaglycan, 300kDa)	0.000	37.0	4.48	-8.275	↑
CX3CR1	Chemokine (C-X3-C motif) receptor 1	0.000	48.5	5.93	-8.182	↑
LOC783896	Similar to TRAF-interacting protein with a forkhead-associated domain	0.000	31.9	4.09	-7.809	–
LOC789731	Hypothetical protein LOC789731	0.000	29.1	3.91	-7.428	↑
TIFA	Hypothetical protein LOC783855	0.000	34.8	4.96	-7.025	–
CD69	CD69 molecule	0.000	37.7	5.75	-6.56	↓
ZBP1	Z-DNA binding protein 1(LOC508333)	0.000	46.3	7.38	-6.273	↑
DDX58	Similar to DEAD/H (Asp-Glu-Ala-Asp/His) box polypeptide RIG-I, transcript variant 1 (LOC504760)	0.000	13.9	2.23	-6.243	–
USP18	Ubiquitin specific peptidase 18	0.000	21.5	3.74	-5.739	–
-----	AJ819856 AJ819856 KN206 Bos sp. cDNA clone C0006016I04	0.000	13.9	2.45	-5.664	–
----	DV934772 LB0308.CR_E16 GC_BGC-30 Bos taurus cDNA clone IMAGE:8135034 5'	0.000	39.3	7.13	-5.507	–
BCL2L11	BCL2-like 11 (apoptosis facilitator)	0.000	14.7	2.81	-5.224	↓

20 genes whose expression was significantly altered (FDR<5%, FC ≥ 2) in *Theileria* infected or LPS stimulated uninfected BL20 cells (maximal LPS response at 4h/or18) relative to control cells. Data is arranged in descending order of absolute fold difference between BL20-LPS and TBL20. Genes highlighted in light blue shows Bw720c response previously identified in an independent microarray experiment (Kinnaird *et al*; unpublished). Gene symbols in bold indicate most recent annotation of the genes identified from NCBI.

IPA analysis showed enrichment for genes predicted to function in protein modification, the antimicrobial response and the inflammatory response. Indeed, the top candidate gene in this profile is annotated as OAS2 (elevated 125.9 fold in BL20-LPS Vs BL20 but only 3.93 fold up in TBL20 Vs BL20) that encodes an essential protein involved in the innate immune response to viral infection. The dataset also contains additional genes predicted to function in cellular defence/innate immune response (e.g. ISG15, MX2, IRF5 and IL7) and genes associated with transcription factors activated by *Theileria* infection (NFκB2, NFκBIZ and Jun).

5 genes in the cluster were validated by semi quantitative RT-PCR (see (Figure 4.13A) and showed the expected profile of lower expression in TBL20 relative to the peak in BL20-LPS. Similarly Figure 4.13 B and 4.13 C show the qRT-PCR results for the CD69 and ISG15 genes respectively, validating the micro-array profile. A 3.37 fold (log_2) reduction in expression being computed for CD69 in TBL20 relative to BL20-LPS compared to a difference of 2.6 fold (log_2) generated by the array data; while qRT-PCR calculated the modulation for ISG15 to be 2.67 fold (log_2) for TBL20 Vs BL20-LPS, compared to 2.21 fold (log_2) from the array data.

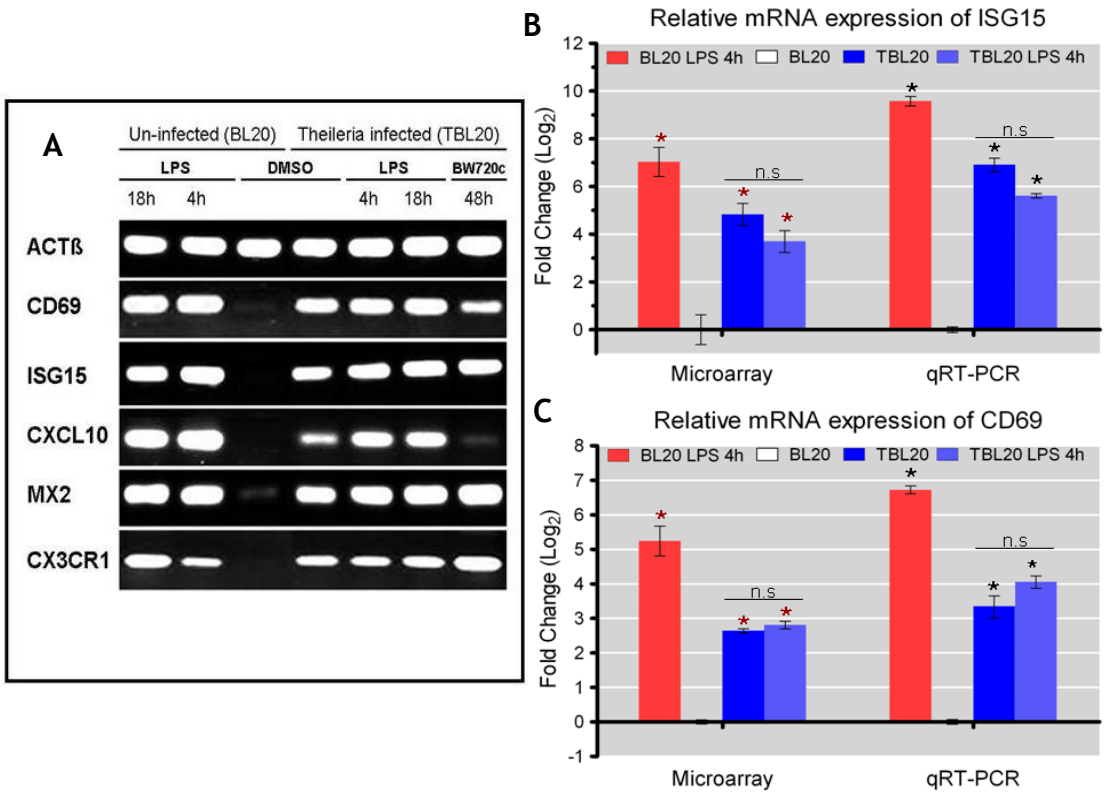

Figure 4.13: Validation of microarray results for profile 3
A. Semi-quantitative RT-PCR results showing mRNA expression of 5 candidate genes (**CD69**, ISG15, **CXCL10**, **MX2, CX3CR1**) in BL20 cells and TBL20 cells either stimulated or un-stimulated with LPS. Semi-quantitative PCR products obtained using the gene specific primers were resolved on 1% agarose gel. Whereas, ACTB was used as an internal control.
B. Real-time qRT-PCR validation changes in ISG15 mRNA expression.
C. Real-time qRT-PCR validation changes in CD69 mRNA expression.
For microarray results the asterisk (*) above the bars indicate the statistical significance of the relative log fold change compared to BL20 cells (*FDR< 0.05, ± S.E.M, n = 6). For qRT-PCR data the asterisk denotes the statistical significance of the relative log fold change compared to BL20 cells (Student's t-test, *P< 0.01). The lines for each bar on the graph represent the range in the relative expression. Whereas, n.s indicates statistically non-significant results in TBL20 LPS relative to TBL20 cells

Profile 4

Profile 4 represents genes elevated by LPS stimulation of BL20 but showed no change on comparison of BL20 with TBL20, and 95% of the dataset showed no significant change following stimulation of TBL20 with LPS (Figure 4.14). The dataset consisted of 1,093 genes and was the largest obtained by the study. The top 20 candidate genes of this profile are represented in Table 4.6, while a full list of 1,093 genes is presented in Appendix 2.1.4. Only a small number (16) of these genes were sensitive to BW720c and all of these were elevated upon treatment, indicating repression by the parasite. 248 genes displayed a > 5 fold difference between TBL20 and BL20-LPS.

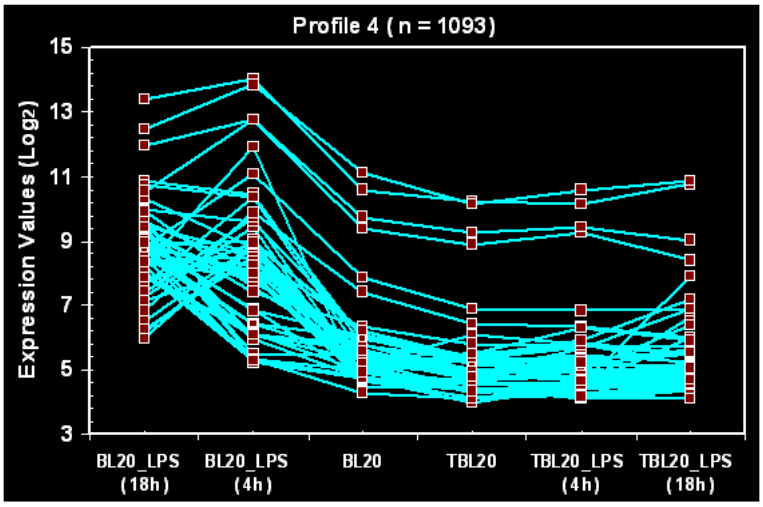

Figure 4.14: Graphical display of profile 4 showing the expression patterns of differentially expressed genes and modulated response in *Theileria* infection.
Top 50 candidate genes from profile 4 (n = 1093) whose expression is significantly elevated in BL20-LPS but not changed in TBL20 cells, Furthermore this condition was associated with repression in TBL20 when compared to BL20-LPS. The x-axis corresponds to the experimental conditions, the y-axis to expression values (log_2) from array data. Each line represents an individual gene.

Table 4.6: Top 20 genes of profile 4 showing elevated expression in LPS- BL20 cells, but no change in TBL20 Vs BL20 cells.

Gene Symbol	Annotation	BL20 LPS Vs BL20 FDR (4h/or18)	BL20 LPS Vs BL20 Abs: FC (4h/or18)	TBL20 Vs BL20	TBL20 Vs BL20 LPS Abs:FC (4h/or18)	BW720c Response 48h
			↑	No change (–)	↓	
VCAM1	Vascular cell adhesion molecule 1	0.000	183.1	-1.01	-184.6	–
TFEC	Transcription factor EC	0.000	34.2	-1.38	-47.09	–
LOC518403	Hypothetical LOC518403	0.000	30.5	-1.48	-45.13	–
LOC613624	Similar to regulator of G-protein signaling 13, transcript variant 1	0.000	27.5	-1.54	-42.28	–
LOC511753	Similar to seven transmembrane helix receptor	0.000	35.2	-1.13	-39.7	–
LOC786647	Hypothetical protein LOC786647	0.000	26.9	-1.25	-33.52	–
LOC784595	Similar to olfactory receptor Olfr1174	0.000	16.1	-1.67	-26.81	–
LOC616145	Similar to ADAMTS-like protein 5 precursor (ADAMTSL-5)	0.000	15.6	-1.71	-26.64	–
LOC783981	Similar to ribonuclease 12	0.000	14.4	-1.84	-26.51	–
LOC504861	Hypothetical LOC504861	0.000	13.5	-1.79	-24.22	–
ITK	IL2-inducible T-cell kinase	0.000	16.2	-1.39	-22.56	–
LOC509794	Similar to TESC protein, transcript variant 1	0.000	16.5	-1.36	-22.51	–
SYTK1	Serine/threonine/tyrosine kinase 1	0.000	23.1	1.08	-21.42	–
VCAM1	Vascular cell adhesion molecule 1	0.000	14.4	-1.45	-20.9	–
SRGAP1	SLIT-ROBO Rho GTPase activating protein 1 (LOC539452)	0.000	27.7	1.32	-20.88	–
-----	AJ814580 AJ814580 KN206 Bos sp. cDNA clone C0005204g20	0.000	10.4	-1.98	-20.59	↑
TP63	Tumor protein 63 (LOC615335)	0.000	36.2	1.90	-19.06	–
IRAK2	Interleukin-1 receptor-associated kinase 2	0.000	9.4	-1.97	-18.5	–
AICDA	Activation-induced cytidine deaminase	0.000	16.0	-1.14	-18.26	–
CCR8	Chemokine C-C motif receptor 8	0.000	18.2	1.03	-17.74	–

Summary of top 20 genes whose expression was significantly altered (FDR<5%, FC ≥ 2) in *Theileria* infected or LPS stimulated uninfected BL20 cells (maximal LPS response at 4h/or18) relative to control cells. Data is arranged in descending order of absolute fold difference between BL20-LPS and TBL20. Gene symbols in bold indicate most recent annotation of the genes identified from NCBI.

IPA analysis showed enrichment for genes predicted to function in cell death, cell function and maintenance, and cellular development. An association with the inflammatory response and inflammatory disease was indicated, and it was of interest that activation of IRF by cytosolic pattern recognition receptors and interferon signalling were significant top canonical pathways. In addition a number of these genes possess interesting predicted functions that could be associated with parasite infection including: VCAM1 (184.6 fold elevation in BL-20 LPS Vs TBL20), IFIT3 (14.7 fold), IF16 (9 fold), TP63 (34 fold) CFLAR (8.6 fold) and RUNX2 (5.3 fold). Semi-quantitative RT-PCR results of six candidate genes and qRT-PCR validation results of VCAM1 and RUNX2 are shown in Figure 4.15.

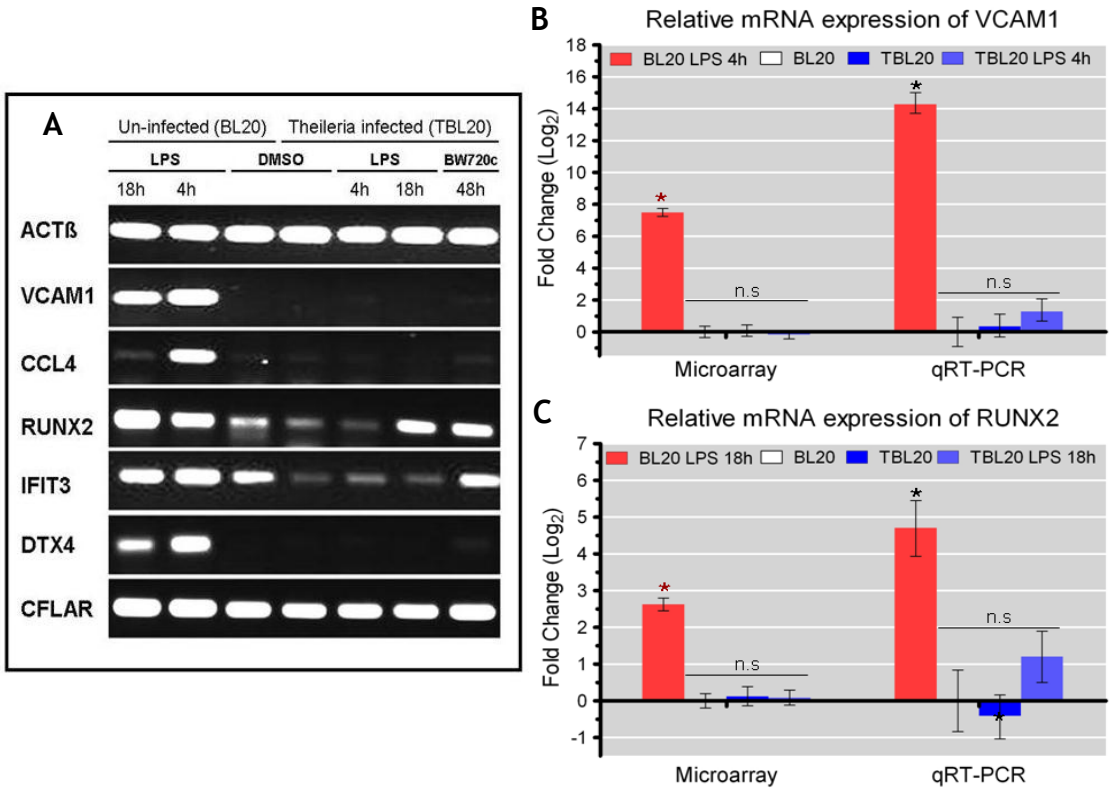

Figure 4.15: Validation of microarray results for profile 4
A. Semi-quantitative RT-PCR results showing mRNA expression of 6 candidate genes (VCAM1, CCL4, RUNX2, IFIT3, DTX4, CFLAR) in BL20 cells and TBL20 cells either stimulated or un-stimulated with LPS. Semi-quantitative PCR products obtained using the gene specific primers were resolved on 1% agarose gel. Whereas ACTB was used as an internal control.
B. Real-time qRT-PCR validation changes in VCAM1 mRNA expression.
C. Real-time qRT-PCR validation changes in RUNX2 mRNA expression.
For microarray results the asterisk (*) above the bars indicate the statistical significance of the relative log fold change compared to BL20 cells (*FDR< 0.05, ± S.E.M, n = 6). For qRT-PCR data the asterisk denotes the statistical significance of the relative log fold change compared to BL20 cells (Student's t-test, * P< 0.01).The lines for each bar on the graph represent the range in the relative expression. Whereas n.s indicates statistically non-significant results in TBL20 (+/- LPS) relative to BL20 cells.

Profile 5: Profile 5 is the reciprocal of profile 1 and represents 288 genes whose expression is repressed in BL20-LPS but super-repressed in TBL20 (see Figure 4.16).

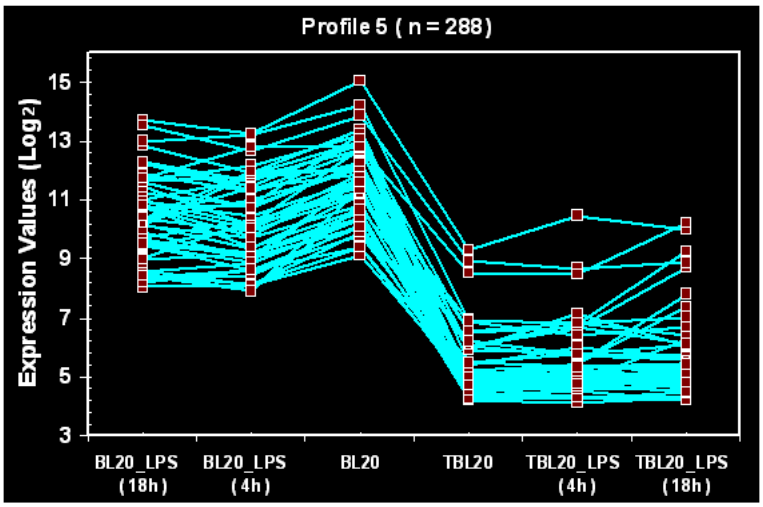

Figure 4.16: Graphical display of profile 5 showing the expression patterns of differentially expressed genes and modulated response in *Theileria* infection.
Top 50 candidate genes from profile 5 (n = 288) whose expression is repressed in both LPS stimulated BL20 and TBL20 cells, however TBL20 exhibit super-repression relative to BL20-LPS. The x-axis corresponds to the experimental conditions, the y-axis to expression values (log_2) from array data. Each line represents an individual gene.

No significant alteration occurred in > 95% of the genes in TBL20-LPS. 40 of these genes showed major repression (> 10 fold) in TBL20 Vs BL20 LPS. Of the 136 genes sensitive to BW720c 99.2% responded in the predicted manner (up), indicating active repression by a viable parasite. The top 20 candidate genes of this profile are represented in Table 4.7, while a full list of 288 genes is presented in Appendix 2.1.5. IPA showed enrichment of genes predicted to function in cell death, development, growth and proliferation and cellular function and maintenance. An association with infectious disease, cellular function and maintenance was identified. Interestingly genes encoding membrane proteins are prominent in the dataset (91) of which 34 are predicted to encode membrane receptors (26 G-protein coupled and 8 transmembrane receptor genes). Down-regulated receptor genes included those encoding the IGFR1 receptor (down 85 fold in TBL20 relative to BL20-LPS), the Toll-like receptor 4 (down 21.4 fold), the G-protein-coupled receptor CCR6 (down 23.18 fold), S1PR1 (down 5.8 fold) and the thrombospondin receptor (down 4.6 fold). A number of genes encoding transcription factors were also present in the dataset including LEF-1 (down 14.9 fold) and LMO2 (down 7.7 fold), both of which are strongly associated with leukaemia.

Table 4.7: Top 20 candidate genes of profile 5 showing evidence of super repression in TBL20 cells relative to BL20-LPS stimulated cells.

Gene Symbol	Annotation	BL20 LPS Vs BL20 FDR (4h/or18)	BL20 LPS Vs BL20 Abs: FC (4h/or18)	TBL20 Vs BL20	TBL20 Vs BL20 LPS Abs:FC (4h/or18)	BW720c Response 48h
			↓	↓↓	↓	
-----	CB467496 733248 MARC 6BOV Bos taurus cDNA 5'	0.000	-2.8	-367.58	-132.5	–
LOC786899	Hypothetical protein	0.010	-2.1	-220.93	-106.5	↑
LOC785289	Hypothetical protein	0.004	-2.2	-203.63	-93.3	↑
LOC404176	T-cell receptor delta chain	0.000	-2.7	-238.33	-88	↑
IGF1R	Insulin-like growth factor 1 receptor	0.012	-2.0	-171.47	-85.15	–
LOC507299	Hypothetical LOC507299	0.001	-2.7	-222.27	-83.31	–
F13A1	Similar to Coagulation factor XIII A chain precursor (Coagulation factor XIIIa) LOC617881	0.002	-2.3	-165.61	-71.17	–
SORCS3	Similar to Sortilin-related VPS10 domain containing receptor 3 (LOC531405)	0.000	-5.4	-364.83	-67.3	–
LOC513984	Similar to peptide transporter 3	0.002	-2.4	-158.80	-66.73	↑
LAIR1	Leukocyte-associated Ig-like receptor 1b (LOC615295)	0.000	-3.3	-174.72	-52.82	–
LOC786880	Hypothetical protein LOC786880	0.001	-2.4	-114.35	-47.42	↑
LOC786327	Hypothetical protein LOC786327	0.001	-2.5	-96.91	-39.12	↑
PPP1R14C	Protein phosphatase 1, regulatory (inhibitor) subunit 14C	0.000	-6.0	-218.98	-36.29	–
LOC789595	Hypothetical protein LOC789595	0.000	-4.2	-148.18	-35.48	↑
LOC512903	Similar to carboxypeptidase A3	0.000	-3.4	-119.24	-35.17	↑
CD22	B-cell receptor CD22-B (LOC514582)	0.001	-2.4	-82.08	-34.81	↑
LOC785058	Hypothetical protein LOC785058	0.000	-7.3	-243.50	-33.54	↑
-----	EG706640 nbm28c02.y1 Cow lens. Unnormalized (nbm) Bos taurus cDNA clone nbm28c02 5	0.000	-3.0	-90.80	-30.1	↑
-----	DT891920 1473102 MARC 7BOV Bos taurus cDNA 5	0.004	-2.2	-62.92	-28.27	–
FCRLA	Fc receptor-like A (LOC782871)	0.000	-2.8	-80.27	-28.2	↑

Summary of top 20 candidate genes whose expression was significantly altered (FDR<5%, FC ≥ 2) in *Theileria* infected or LPS stimulated uninfected BL20 cells (maximal LPS response at 4h/or18) relative to control cells. Data is arranged in descending order of absolute fold difference between BL20-LPS and TBL20. Genes highlighted in light blue shows Bw720c response previously identified in an independent microarray experiment (Kinnaird *et al*; unpublished). Gene symbols in bold indicate most recent annotation of the genes identified from NCBI.

Nine genes of this profile were validated by RT-PCR and agreed with the array profile (Figure 4.17A), although only a low level increase in the TLR4 gene PCR product was detected for the BW720c treated sample. qRT-PCR validation was performed for TLR4 and MYL4 and showed good correlation with the micro-array profile (see Figure 4.17 B & C), with strong evidence of super repression of gene expression associated with *Theileria* infection compared to LPS-stimulation of BL20. Thus for TLR4, qRT-PCR data showed that expression was repressed by 7.08 fold in TBL20 Vs BL20, while for BL20-LPS Vs BL20 expression was only repressed 1.34; the corresponding array values being 6.04 and 1.63 fold repression, respectively.

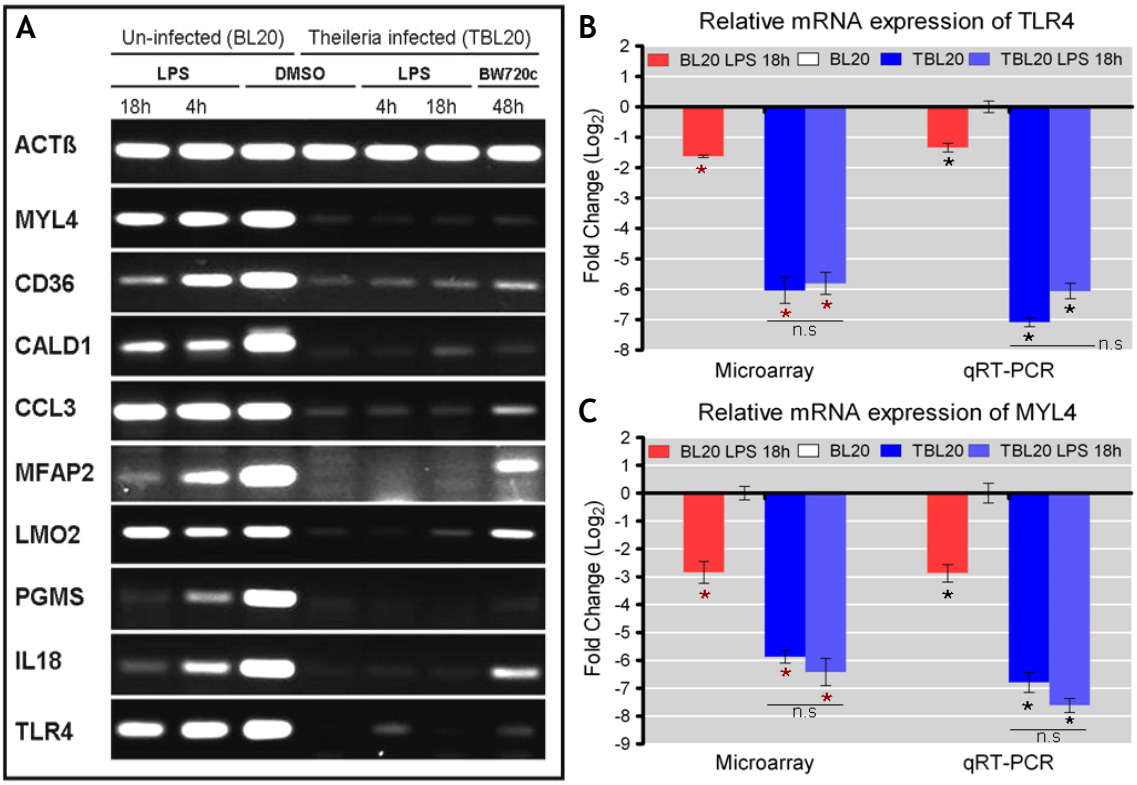

Figure 4.17: Validation of microarray results for profile 5

A. Semi-quantitative RT-PCR results showing mRNA expression of 9 candidate genes (MYL4, CD36, CALD1, CCL3, MFAP2, LMO2, PGM5, IL18, TLR4) in BL20 cells and TBL20 cells either stimulated or un-stimulated with LPS. Semi-quantitative PCR products obtained using the gene specific primers were resolved on 1% agarose gel, whereas; ACTB was used as an internal control. **B.** Real-time qRT-PCR validation changes in TLR4 mRNA expression.
C. Real-time qRT-PCR validation changes in MYL4 mRNA expression.
For microarray results the asterisk (*) above the bars indicate the statistical significance of the relative log fold change compared to BL20 cells (*FDR< 0.05, ± S.E.M, n = 6). For qRT-PCR data the asterisk denotes the statistical significance of the relative log fold change compared to BL20 cells (Student's t-test, * P< 0.01). The lines for each bar on the graph represent the range in the relative expression. Whereas, n.s indicates statistically non-significant results in TBL20 LPS relative to TBL20 cells

Profile 6: Profile 6 is the reciprocal of profile 2 and represents 71 genes that were repressed by LPS treatment of uninfected BL20 cells but were elevated in TBL20 vs BL20 cells (Figure 4.18). All 71 genes showed no significant difference following LPS treatment of TBL20. The combined (down in BL20-LPS, up in TBL20) change in expression of a number of genes in this profile was considerable. For example the genes encoding AHNAK, CMRF-35 and SLA were amplified, respectively 235.4 fold, 99 fold and 45.4 fold and a further 44 genes were elevated by more than 10 fold. The top 20 candidate genes of this profile are represented in Table 4.8, while a full list of 71 genes is presented in Appendix 2.1.6.

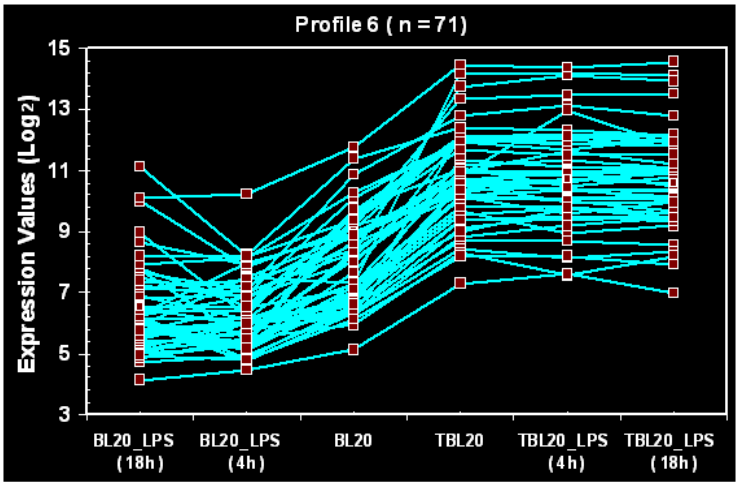

Figure 4.18: Graphical display of profile 6 showing the expression patterns of differentially expressed genes and modulated response in *Theileria* infection.
Top 50 candidate genes from profile 6 (n = 71) whose expression is significantly repressed in BL20-LPS but elevated in TBL20 cells, Furthermore this condition was associated with enhanced up-regulation in TBL20 when compared to BL20-LPS. The x-axis corresponds to the experimental conditions, the y-axis to expression values (log_2) from array data. Each line represents an individual gene.

Table 4.8: Top 20 candidate genes of profile 6 showing repression in BL20-LPS but elevated response in TBL20 relative to BL20 cells.

Gene Symbol	Annotation	BL20 LPS Vs BL20 FDR (4h/or18)	BL20 LPS Vs BL20 Abs: FC (4h/or18)	TBL20 Vs BL20	TBL20 Vs BL20 LPS Abs:FC (4h/or18)	BW720c Response
			↓	↑	↑	
AHNAK	Similar to AHNAK nucleoprotein, transcript variant 1 (LOC510341)	0.007	-2.1	112.38	235.4	–
LOC514557	Similar to OAF homolog (Drosophila)	0.000	-23.4	5.73	134.1	↓
CD99	CD99 molecule (LOC509230)	0.000	-5.1	22.26	113.1	–
LOC512831	Similar to Heterogeneous nuclear ribonucleoproteins A2/B1 (hnRNP A2 / B1)	0.001	-2.4	44.46	106.1	↓
THEM4	Thioesterase sUperfamily member 4	0.000	-19.4	5.38	104.2	–
CD300C	CD 300c molecule (LOC526163)	0.010	-2.1	47.40	99.01	–
TMEM62	Transmembrane protein 62, transcript variant 2 (LOC515078)	0.000	-3.3	22.75	75.4	–
RNASEL	Ribonuclease L (2',5'-oligoisoadenylate synthetase-dependent)	0.000	-3.3	18.55	60.56	–
-----	AJ677254 KN224 cDNA clone KN224-023_E12, mRNA sequence	0.000	-7.6	7.68	58.62	–
SPARC	Secreted protein, acidic, cysteine-rich	0.000	-14.0	3.82	53.38	–
SLA	SRC-like-adaptor	0.001	-2.5	18.37	45.47	–
NDRG1	N-myc downstream regulated gene 1	0.000	-7.9	5.52	43.42	–
PDE4C	Similar to phosphodiesterase 4C	0.001	-2.4	17.13	41.51	↑
ANGPT4	Angiopoietin 4	0.000	-7.5	4.88	36.45	↓
LOC789368	Similar to Solute carrier family 38, member 5	0.000	-9.8	3.72	36.38	–
GALNT6	UDP-N-acetyl-alpha-D-galactosamine:polypeptide N-acetylgalactosaminyltransferase 6	0.000	-2.6	12.41	32.77	–
LRRC6	Leucine rich repeat containing 6	0.000	-6.0	5.30	31.87	–
RNASEL	Similar to 2-5A-dependent RNase	0.002	-2.4	12.94	31.21	–
GCET2	Germinal centre expressed transcript 2	0.000	-8.1	3.70	30.13	↑
LOC790449	Similar to Pcdh19 protein	0.000	-5.2	5.64	29.36	↓

Summary of top 20 candidate genes whose expression was significantly altered (FDR<5%, FC ≥ 2) in *Theileria* infected or LPS stimulated uninfected BL20 cells (maximal LPS response at 4h/or18) relative to control cells. Data is arranged in descending order of absolute fold difference between BL20-LPS and TBL20. Genes highlighted in light blue shows Bw720c response previously identified in an independent microarray experiment (Kinnaird *et al*; unpublished). Gene symbols in bold indicate most recent annotation of the genes identified from NCBI.

Interestingly, a greater proportion (60%) of the 15 BW720c sensitive genes responded in a non-reciprocal manner (i.e. were up regulated by BW720c). IPA showed enrichment of genes predicted to function in cell death, development, growth and proliferation and cellular function and maintenance. An association with infectious disease, cellular function and maintenance was identified. Of the 51 genes that could be mapped by IPA, 21 showed association with cancer. Significant IPA predicted molecular functions included cell movement, cell death and cell growth and proliferation. Gene ontology predicted that a number of genes operate in signal transduction events and are associated with cancer. The microarray expression profile of the cluster was validated by RT-PCR for six genes (see Figure 4.19A).

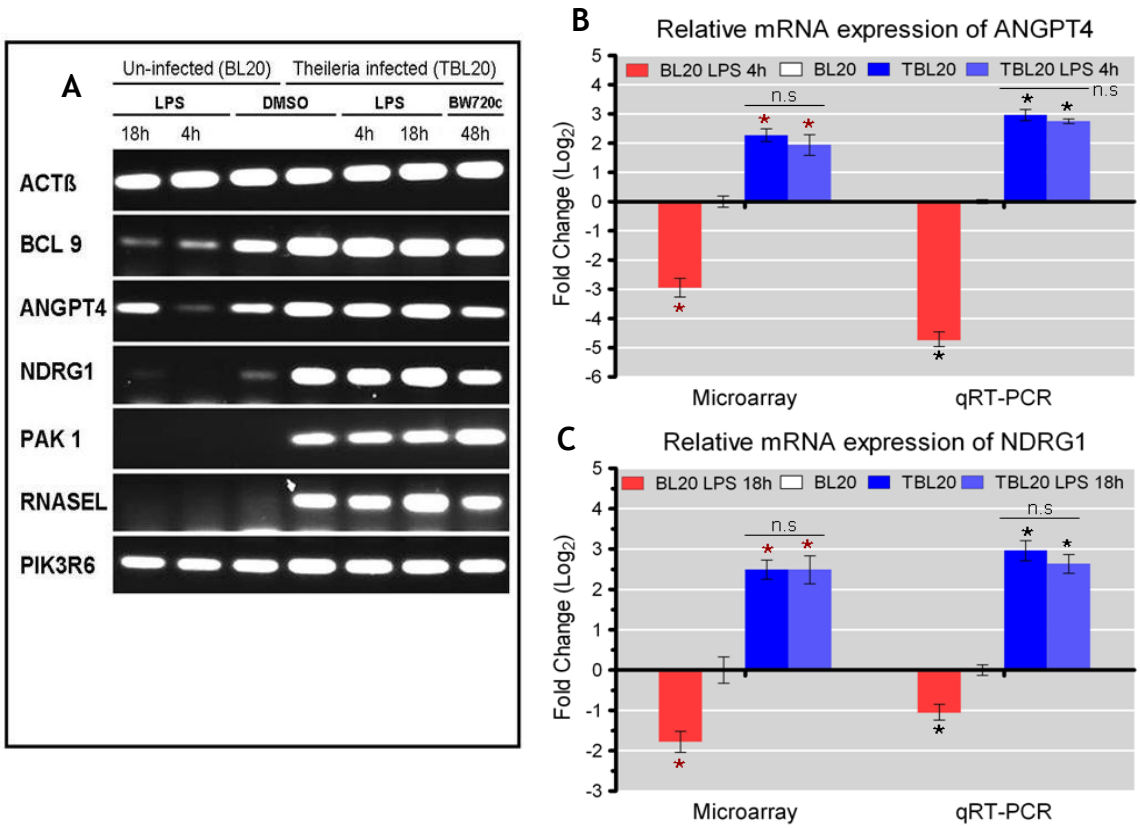

Figure 4.19: Validation of microarray results for profile 6

A. Semi-quantitative RT-PCR results showing mRNA expression of 6 candidate genes (BCL9, ANGPT4, NDRG1, PAK1, RNASEL, PIK3R6) in BL20 cells and TBL20 cells either stimulated or un-stimulated with LPS. Semi-quantitative PCR products obtained using the gene specific primers were resolved on 1% agarose gel. Whereas, ACTB was used as an internal control.

B. Real-time qRT-PCR validation changes in ANGPT4 mRNA expression.

C. Real-time qRT-PCR validation changes in NDRG1 mRNA expression.

For microarray results the asterisk (*) above the bars indicate the statistical significance of the relative log fold change compared to BL20 cells (*FDR< 0.05, ± S.E.M, n = 6). For qRT-PCR data the asterisk denotes the statistical significance of the relative log fold change compared to BL20 cells (Student's t-test, *P< 0.01).The lines for each bar on the graph represent the range in the relative expression. Whereas, n.s indicates statistically non-significant results in TBL20 LPS relative to TBL20 cells

qRT-PCR validation was performed for ANGPT4 and NDRG1 and showed good correlation with the micro-array profile (see Figure 4.19 B & C). For example, qRT-PCR estimated that NDRG1 was down regulated 1.06 fold (log_2) in BL20-LPS Vs BL20 but up regulated 2.96 fold (log2) in TBL20 Vs BL20, while the array data indicated a 1.78 fold (log2) repression in BL20-LPS and a 2.49 fold (log2) up – regulation in TBL20.

Profile 7: Profile 7 was the reciprocal of profile 3 and represented genes that were repressed more significantly in BL20-LPS relative to TBL20-LPS (see Figure 4.20).

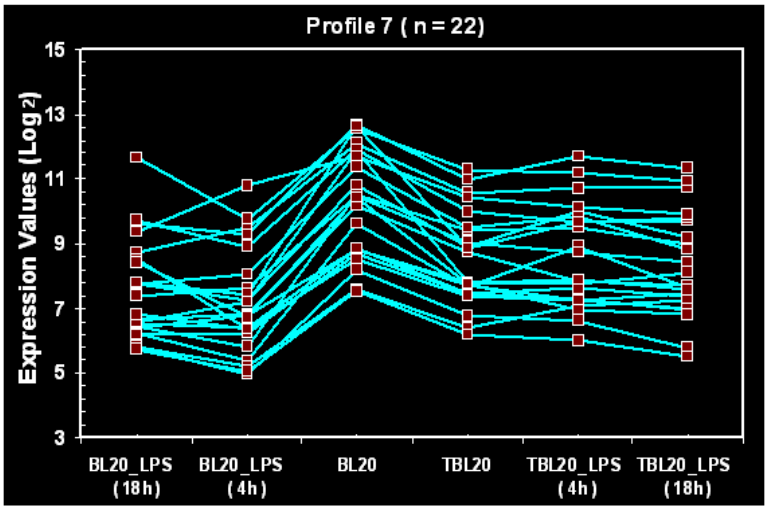

Figure 4.20: Graphical display of profile 7 showing the expression patterns of differentially expressed genes and modulated response in *Theileria* infection.
Candidate genes from profile 7 (n = 22) whose expression is repressed in both LPS stimulated BL20 and TBL20 cells, however TBL20 exhibit up-regulated response relative to BL20-LPS. The x-axis corresponds to the experimental conditions, the y-axis to expression values (log_2) from array data. Each line represents individual gene.

This profile represented the smallest number of genes (22), and 6 out of the 7 (85.7%) BW720c sensitive genes were elevated upon treatment. A full list of the 22 genes of this profile is presented in Table 4.9. An enrichment of genes with predicted functions that could be associated with the infected cell phenotype was not observed, although several receptors were present in the dataset. The microarray expression profile of the cluster was validated by RT-PCR for 3 genes (see Figure 4.21).

Table 4.9: Top 20 candidate genes of profile 7 showing evidence of an attenuated repression response in TBL20 cells relative BL20-LPS stimulated cells.

Gene Symbol	Annotation	BL20 LPS Vs BL20 FDR (4h/or18)	BL20 LPS Vs BL20 Abs: FC (4h/or18)	TBL20 Vs BL20	TBL20 Vs BL20 LPS Abs:FC (4h/or18)	BW720c Response
			↓↓	↓	↑	
-----	EH149305 LB01342.CR_C18 GC_BGC-13 Bos taurus cDNA clone	0.000	-25.8	-2.15	11.99	–
NLRP1	NLR family, pyrin domain containing 1 (LOC790698)	0.000	-19.4	-3.97	4.891	↑
LOC781353	Similar to receptor-like tyrosine kinase	0.000	-11.3	-2.69	4.196	–
CYP3A4	Cytochrome P450, subfamily IIIA, polypeptide 4	0.000	-9.4	-2.65	3.535	–
STXBP6	Syntaxin binding protein 6 (amisyn)	0.000	-10.3	-2.92	3.517	↑
CYP4F3	Cytochrome P450, family 4, subfamily F, polypeptide 3	0.000	-12.4	-3.63	3.402	–
GALNT4	UDP-N-acetyl-alpha-D-galactosamine:polypeptide N-acetylgalactosaminyltransferase 4	0.000	-10.5	-3.21	3.279	↑
LOC528166	Similar to NAC-beta splice	0.000	-11.5	-3.63	3.176	↑
PGLYRP1	Peptidoglycan recognition protein 1	0.000	-8.4	-2.70	3.121	–
TRAF3IP3	TRAF3 interacting protein 3	0.000	-6.8	-2.39	2.859	–
-----	DN641773 UMC-bof_0A02-012-f10 Ovarian follicle pre-ovulatory	0.000	-37.4	-13.58	2.751	↑
LOC537817	Similar to KIAA0882 protein	0.000	-5.4	-2.09	2.596	–
LOC782612	Hypothetical protein LOC782612	0.000	-5.6	-2.27	2.469	–
LOC789663	Similar to KIAA0882 protein	0.000	-5.3	-2.18	2.425	–
LOC503620	VEGF-receptor	0.000	-5.1	-2.21	2.314	–
AQP3	Aquaporin 3 (Gill blood groUp)	0.000	-39.2	-17.16	2.287	↑
DNTT	Deoxynucleotidyltransferase, terminal	0.000	-5.7	-2.67	2.151	↓
-----	CO893215 BovGen_21540 normal cattle brain Bos taurus cDNA clone RZPDp1056D0646Q 5'	0.000	-8.2	-3.81	2.144	–
CYP3A4	Cytochrome P450, family 3, subfamily A, polypeptide 5(LOC785314)	0.000	-5.4	-2.56	2.13	–
TSPAN7	Tetraspanin 7	0.000	-5.0	-2.38	2.106	–
LOC614782	Riken cDNA 4930503b20 gene	0.00	-5.0	-2.2	2.1	---
---	Ee895542 a98111a FFB cDNA clonea9811 3'	0.00	-4.6	-6.5	2.0	---

Summary of top 20 candidate genes whose expression was significantly altered (FDR<5%, FC ≥ 2) in *Theileria* infected or LPS stimulated uninfected BL20 cells (maximal LPS response at 4h/or18) relative to control cells. Data is arranged in descending order of absolute fold difference between BL20-LPS and TBL20. Genes highlighted in light blue shows Bw720c response previously identified in an independent microarray experiment (Kinnaird *et al*; unpublished). Gene symbols in bold indicate most recent annotation of the genes identified from NCBI.

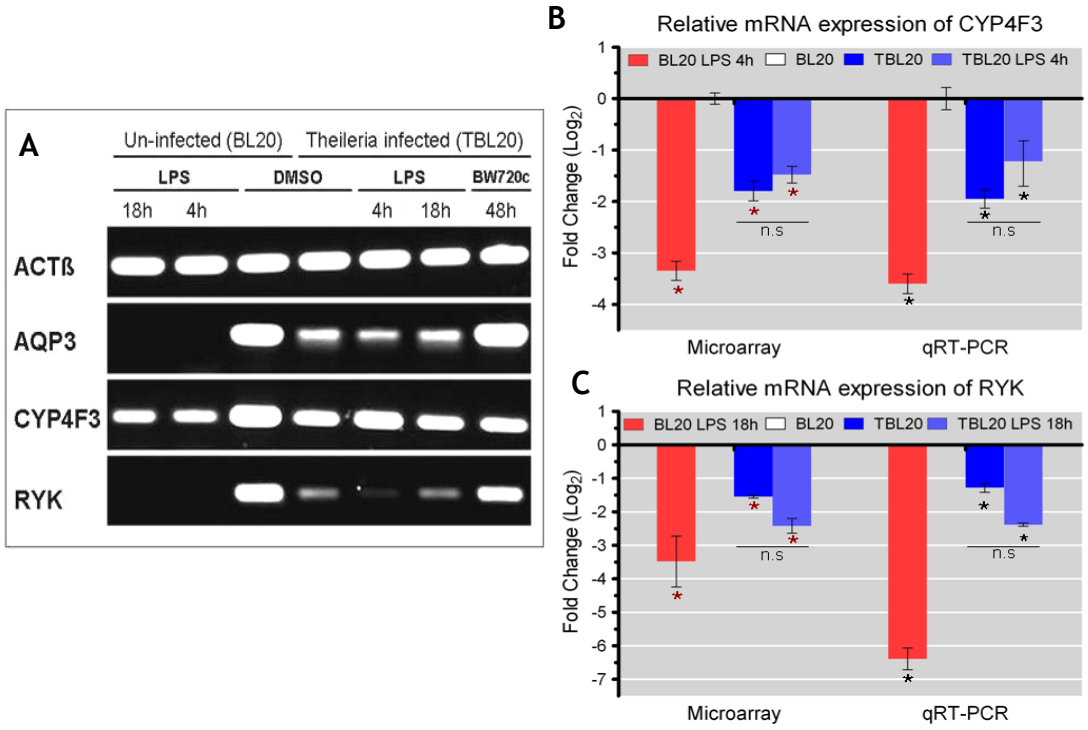

Figure 4.21: Validation of microarray results for profile 7
A. Semi-quantitative RT-PCR results showing mRNA expression of 3 candidate genes (AQP3, CYP4F3, RYK) in BL20 cells and TBL20 cells either stimulated or un-stimulated with LPS. Semi-quantitative PCR products obtained using the gene specific primers were resolved on 1% agarose gel, whereas; ACTB was used as an internal control.
B. Real-time qRT-PCR validation changes in CYP4F3 mRNA expression.
C. Real-time qRT-PCR validation changes in RYK mRNA expression.
For microarray results the asterisk (*) above the bars indicate the statistical significance of the relative log fold change compared to BL20 cells (*FDR< 0.05, ± S.E.M, n = 6). For qRT-PCR data the asterisk denotes the statistical significance of the relative log fold change compared to BL20 cells (Student's t-test, *P< 0.01).The lines for each bar on the graph represent the range in the relative expression. Whereas, n.s indicates statistically non-significant results in TBL20 LPS relative to TBL20 cells

Profile 8: Profile 8 was the reciprocal of 4 and represented 132 genes that were down regulated in BL20-LPS but showed no change associated with infection (BL20 vs TBL20) (see Figure 4.22). 99% of the dataset also showed no significant change in TBL20-LPS. Genes sensitive to BW720c treatment were under represented, and of the 2 present in the dataset, one was elevated and one repressed. The top 20 candidate genes of this profile are represented in Table 4.10, while the full list of 132 genes is presented in Appendix 2.1.7.

IPA showed enrichment for genes predicted to function in cell signalling, small molecule biochemistry and metabolism. Genes that could be putatively associated with the infected cell phenotype included toll like receptor 3 (TLR3), a Myeloid-associated differentiation marker, a janus kinase and microtubule interacting protein (JAKMIP1) and NFKB activating protein-like (NKAPL).

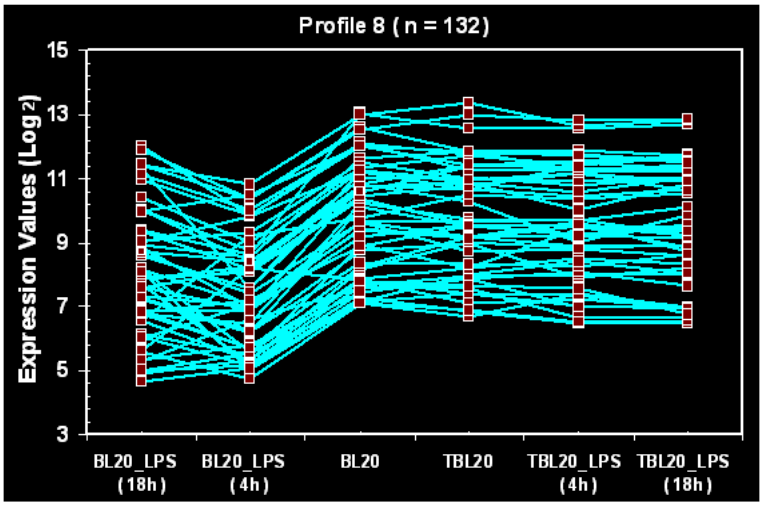

Figure 4.22: Graphical display of profile 8 showing the expression patterns of differentially expressed genes and modulated response in *Theileria* infection.
Top 50 candidate genes from profile 8 (n= 132) whose expression in repressed in LPS stimulated BL20 but not changed in TBL20 cells, whereas there is significant elevation in TBL20 when compared to BL20-LPS.The x-axis corresponds to the experimental conditions, the y-axis to expression values (log_2) from array data. Each line represents individual gene.

Table 4.10: 20 candidate genes of profile 8 showing evidence of repression of expression in BL20-LPS but no change in TBL20 Vs control BL20 cells.

Gene Symbol	Annotation	BL20 LPS Vs BL20 FDR (4h/or18)	BL20 LPS Vs BL20 Abs: FC (4h/or18)	TBL20 Vs BL20	TBL20 Vs BL20 LPS Abs:FC (4h/or18)	BW720c Response
			↓	No change (–)	↑	
M6PRBP1	Mannose-6-phosphate receptor binding protein 1	0.000	-9.5	1.82	17.24	–
BCOR	BCL-6 corepressor (LOC784529)	0.000	-21.0	-1.38	15.25	–
SERPINE2	Serpin peptidase inhibitor, clade E 2	0.000	-9.2	1.63	15.05	–
LOC505234	Similar to FYVE, RhoGEF and PH domain-containing protein 4 (Actin filament-binding protein frabin)	0.000	-9.4	1.58	14.87	–
C10orf132	Hypothetical protein C10orf132	0.000	-5.7	1.88	10.79	–
CAMKV	CaM kinase-like vesicle-associated	0.000	-15.7	-1.47	10.63	–
ARMCX6	Armadillo repeat containing, X-linked 6	0.000	-15.5	-1.52	10.2	–
LOC616063	Similar to Myeloid-associated differentiation marker	0.000	-8.3	1.17	9.737	–
-----	CO891936 BovGen_20261 normal cattle brain	0.000	-13.1	-1.37	9.61	–
NID2	Nidogen 2 (osteonidogen)	0.000	-8.7	1.03	8.98	–
LOC524078	Similar to cystine/glutamate exchanger	0.000	-9.3	-1.06	8.805	–
PLCL1	Phospholipase C-like 1(LOC537873)	0.000	-12.5	-1.42	8.802	–
LOC787162	Similar to Armadillo repeat containing, X-linked 6	0.000	-12.3	-1.46	8.47	–
LOC540831	Similar to FLJ20273 protein, transcript variant 1	0.000	-4.5	1.80	8.052	–
IGFBP4	Insulin-like growth factor binding protein 4	0.000	-4.4	1.78	7.918	–
-----	CO871894 BovGen_00219 normal cattle brain Bos taurus cDNA clone RZPDp1056I1952Q 3'e	0.000	-5.4	1.24	6.759	–
TNS1	Tensin 1	0.000	-10.8	-1.65	6.559	–
RGS1	Regulator of G-protein signalling 1, transcript variant 1 (LOC540836)	0.000	-5.6	1.16	6.553	–
SLC1A5	Solute carrier family 1 (neutral amino acid transporter), member 5	0.000	-3.6	1.83	6.527	–
PLVAP	Plasmalemma vesicle associated protein	0.000	-4.3	1.53	6.517	–

Summary of top 20 candidate genes whose expression was significantly altered (FDR<5%, FC ≥ 2) in *Theileria* infected or LPS stimulated uninfected BL20 cells (maximal LPS response at 4h/or18) relative to control cells. Data is arranged in descending order of absolute fold difference between BL20-LPS and TBL20. Gene symbols in bold indicate most recent annotation of the genes identified from NCBI.

The microarray data was validated by RT-PCR for three genes (see Figure 4.23A). qRT-PCR data for BCOR and RGS1 was also in agreement with the microarray data(Figure 4.23B-C). Thus, based on qRT-PCR, BCOR was repressed by 5.98 fold (log_2) in BL20-LPS compared to no significant alteration in TBL20 Vs BL20, while the array data computed a repression of 4.36 fold (log_2) for BL20-LPS and no change for TBL20 Vs BL20.

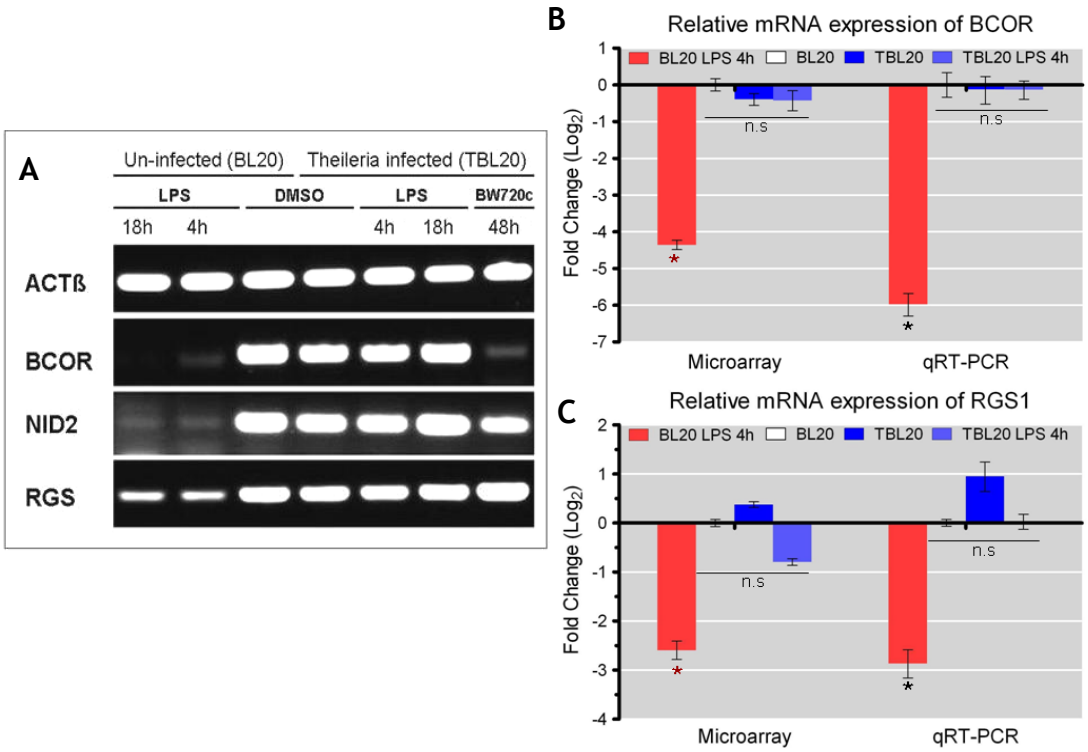

Figure 4.23: Semi-quantitative RT-PCR confirmation of microarray results for profile 8

A. Semi-quantitative RT-PCR results showing mRNA expression of 3 candidate genes (BCOR, NID2, RGS) in BL20 cells and TBL20 cells either stimulated or un-stimulated with LPS. Semi-quantitative PCR products obtained using the gene specific primers were resolved on 1% agarose gel, whereas; ACTB was used as an internal control.
B. Real-time qRT-PCR validation changes in BCOR mRNA expression.
C. Real-time qRT-PCR validation changes in RGS1 mRNA expression.
For microarray results the asterisk (*) above the bars indicate the statistical significance of the relative log fold change compared to BL20 cells (*FDR< 0.05, ± S.E.M, n = 6). For qRT-PCR data the asterisk denotes the statistical significance of the relative log fold change compared to BL20 cells (Student's t-test, *P< 0.01). The lines for each bar on the graph represent the range in the relative expression. Whereas, n.s indicates statistically non-significant results in TBL20 (+/- LPS) relative to BL20 cells.

4.3.3 Analysis of the infection associated modulated dataset by Ingenuity Pathway Analysis

Following identification of genes exhibiting modulated expression in *Theileria* infected cells relative to LPS stimulation of uninfected cells, Ingenuity pathway analysis (IPA) was used to investigate whether the modulation event could be associated with important biological functions. All genes previously identified as modulated by infection (5% FDR and ≥ 2 fold change) were uploaded to the IPA programme. The analysis was conducted in two different ways: firstly, global analysis was performed on the entire dataset of 1052 modulated genes that could be mapped by IPA; secondly, analysis was performed after dividing the dataset into two major subsets, genes showing evidence of repression or elevation of expression in parasite infected cells relative to BL20-LPS. In addition to the functional classification, canonical pathways analysis was also performed to identify most relevant and significant known biological pathways manipulated by the parasite for a given set of genes.

4.3.3.1 The infection modulated dataset is enriched for genes in important functional categories

Analysis of the global dataset of 1052 genes provided evidence that parasite infection extensively modulates a wide range of biological functions and/or diseases. Right-tailed Fisher's exact test was used to calculate a P-value determining the probability that each biological function and/or disease assigned to sets of genes enriched in the dataset could be due to chance alone. Genes placed in a number of important categories showed significant enrichment within the dataset were obtained. Thus, key categories identified included; Inflammatory response, Tissue morphology, Cellular movement, Cancer, Cell-to-Cell Signaling and Interaction, Cell Death, Cell-mediated Immune Response, Antimicrobial Response, Cellular Assembly and Organization (See Figure 4.24). A full list of functional categories identified is presented in Appendix 2.2.

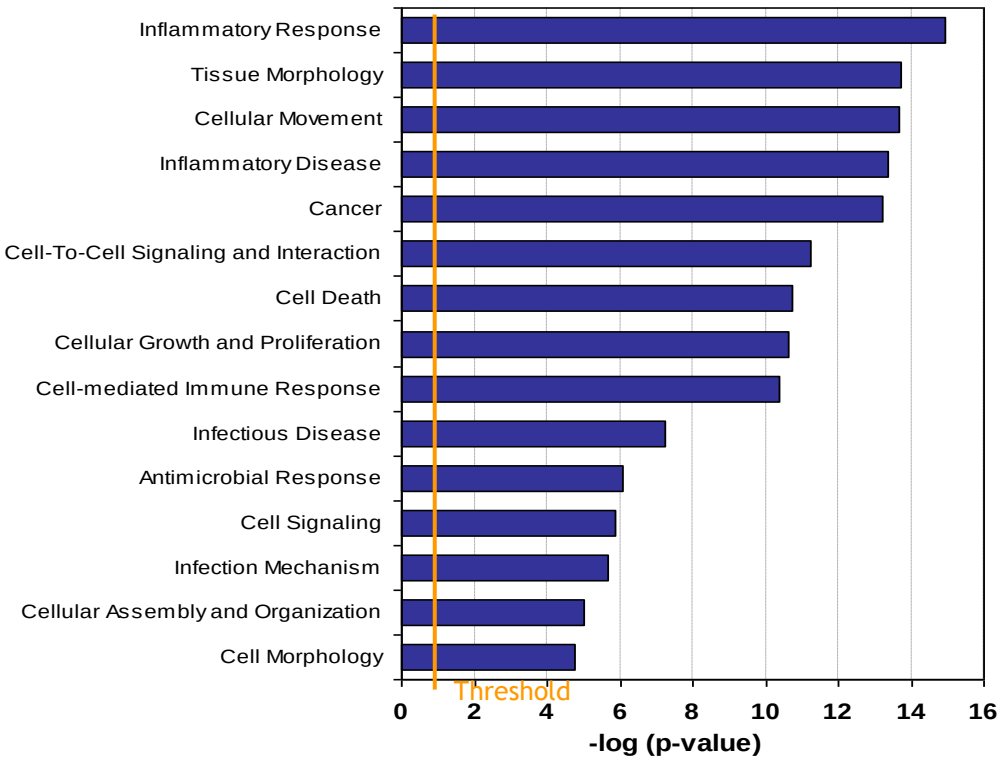

Figure 4.24: Important biological functions and diseases associated with genes significantly modulated by parasite infection relative to LPS response
Biological functions associated with genes enriched in the infection-modulated dataset of 1052 genes are shown along the y-axis with the significance of the enrichment (–log) denoted along the y-axis. Each bar represents –log (p-value) for the enrichment of genes in selected category. The orange vertical line represents the threshold for significance (p-value < 0.05).

While enrichment for a molecular function in the infection-modulated gene list is informative, prediction of how altered gene expression influences the outcome of the function would provide greater insight into the modulation event. To attempt this, further enrichment analysis was undertaken. Thus, IPA analysis was conducted for two subsets of genes, those displaying repressed expression in TBL20 Vs BL20-LPS (down-regulated dataset) and those that showed evidence of elevated expression (up-regulated dataset). These two datasets obtained were then compared on the basis of genes that were enriched and associated with different biological process and molecular functional categories (P-value < 0.05), combined with the IPA prediction of whether the gene promoted (pro) or inhibited (anti) the designated function. The proportion of genes designated as pro- or anti- for each functional category was then directly compared for the up- and down-regulated datasets. Selection of a category as informative was made on the basis that the observed ratio in the number of pro- or anti-genes for one dataset (e.g. down) was either absent (no genes present) or altered in the other dataset. A number of informative

categories of molecular function were identified, where the ratio of the number of pro- and anti-effect genes for one gene-set contrasted with that of the other (see Appendix 2.4 for full list of comparisons). Moreover, functional categories highlighted by this analysis predominantly show an association with a phenotype that is known or could be reasonably predicted for the infected cell. Thus, genes placed in the metastasis of cells sub-category showed a pattern indicative of anti-metastasis genes being repressed by parasite infection, while those that promote this function were favoured in the gene set associated with elevated expression. Moreover, there appeared to be a bias for elevation in expression of genes classified as pro-cancer and pro-tumourigenesis, but repression of genes predicted to be anti-disease of tumor and anti-growth of tumor. In a similar fashion parasite infection is known to be associated with changes to cell shape and manipulation of the actin cytoskeleton (Schmuckli-Maurer *et al.*, 2010). Enrichment of genes in categories (Cellular assembly and organisation and Cell morphology) associated with these alterations was obtained, with a bias towards pro-function for the up but not the down dataset. Additional categories highlighted by the analysis include the inflammatory response, cellular movement, cellular assembly and organisation, cellular growth and proliferation and cell death. A summary of the results and denotation of important genes within selected categories identified as modulated by infection is given below.

While this analysis was informative it should be noted that many genes were simultaneously placed in multiple categories by the IPA software. This could indicate a diverse functional role of these genes in determining the infected cell phenotype but could also hinder identification of the primary role that the gene plays in this process.

Table 4.11: Important biological functions identified by Ingenuity associated with genes modulated by Theileria infection relative to BL20-LPS

	Important functions	Repressed by infection no. Genes (Pro/anti)	*p*-value	Enhanced by infection no. Genes (Pro/anti)	*p*-value
1	**Inflammatory Response**	**111**		**34**	
	Immune response	100 (43,27)	2.12E-09	27 (15,7)	4.51E-04
	Activation of leukocyte	46 (27,9)	2.67E-06	13 (9,1)	3.76E-03
	Antimicrobial response	19 (3,1)	4.88E-05	_	_
	Activation of lymphocyte	31 (19,7)	9.48E-05	9 (5,1)	1.20E-02
	Antiviral response	13 (3,1)	9.60E-05	2 (0,0)	1.17E-02
	Inflammation	30 (12,3)	7.22E-04	12 (3,2)	6.49E-04
	Inflamatory response	41 (17,10)	3.34E-04	16 (7,3)	2.30E-04
2	**Cancer**	**189**		**60**	
	Metastasis of cells	10 (2,6)	3.23E-03	13 (3,1)	2.29E-03
	Tumourigenesis	179 (26,25)	1.73E-03	60 (6,2)	1.74E-05
	Cancer	173 (16,13)	7.55E-05	56 (3,1)	1.58E-05
	Disease of tumor	18 (2,4)	7.29E-04	_	_
	Growth of tumor	20 (2,9)	1.18E-03	_	_
	Tumor	_	_	43 (4,2)	1.11E-04
3	**Cellular Movement**	**100**		**46**	
	Movement of cells	82 (42,29)	1.67E-04	38 (19,12)	4.47E-09
	Migration of leukocytes	36 (22,9)	1.75E-03	17(6,3)	2.49E-05
	Invasion of eukaryotic cells	_	_	14(10,3)	5.92E-04
	Infiltration of leukocytes	25 (8,6)	3.30E-04	14 (2,3)	1.41E-06
	Migration of antigen presenting cells	14 (7,1)	1.65E-04	_	_
	Influx of leukocytes	7 (4,1)	2.02E-03	_	_
	Chemoattraction of leukocytes	6 (6,0)	4.19E-03	_	_
4	**Cellular Assembly and Organization**	**21**		**19**	
	Formation of actin filaments	_	_	8 (3,1)	1.30E-03
	Formation of cellular protrusions	_	_	10 (4,0)	2.71E-03
	Formation of actin cytoskeleton	4 (0,0)	1.01E-03	4 (2,0)	1.10E-02
	Formation of filaments	_	_	9 (5,1)	4.06E-03
	Formation of cytoskeleton	5 (0,0)	2.11E-04	_	_
	Elongation of plasma membrane projection	7 (4,0)	3.95E-03	_	_
5	**Cellular Growth and Proliferation**	**140**		**45**	
	Proliferation of normal cells	87 (43,29)	4.07E-05	29 (13,6)	1.48E-04
	Proliferation of eukaryotic cells	111 (56,47)	7.55E-05	35 (15,9)	3.51E-04
	Proliferation of cells	124 (72,51	3.13E-03	40 (18,13)	8.48E-04
	Proliferation of leukocyte	50 (25,17)	1.75E-06	6 (4,0)	7.66E-03
	Induction of leukocyte	9 (7,3)	2.23E-04	_	_
	Stimulation of leukocytes	11 (9,3)	2.87E-03	_	_
6	**Cell Death**	**170**		**52**	
	Cell death of cancer cells	20 (6,4)	1.15E-05	_	_
	Apoptosis of tumor cell line	72 (34,22)	2.34E-06	20 (12,7)	3.07E-03
	Apoptosis	134 (70,53)	2.10E-05	42 (24,19)	1.13E-04
	Cell death of tumor cell line	78 (38,28)	2.10E-05	24 (13,9)	9.39E-04
	Cell death	151 (75,62)	6.59E-05	49 (26,22)	3.22E-05
	Cytotoxicity of lymphocytes	15 (8,6)	1.65E-04	_	_
	Cell death of normal cell	_	_	23 (8,9)	6.77E-03

The criteria applied for the selection of major biological function categories were maximum number of genes and the P-value of significance. P-values in the range of 2.12E-09 to 1.10E-02 indicated statistical significance.

4.3.3.1.1 Modulation of inflammatory response genes

Modulation of the inflammatory response was highlighted by IPA software and several subcategories showed a bias for the infection associated repressed or elevated gene sets. Thus genes associated with a pro antimicrobial/viral response are predicted to be repressed by infection. On the other hand genes associated with cellular activation show evidence of elevation in infected cells (see Table 4.11). Many of the genes in this category have been documented to be involved in pro-inflammatory cascades. For example, several trans-membrane receptors genes (IGF1R, LAIR1, CCR6, TLR4 and CD40) predicted to be pro-inflammatory were down regulated in infected cells. Indeed, within the inflammation subcategory the bias was towards parasite-associated repression of pro inflammation genes. Interestingly a majority of the genes (CX3CR1, CXCL10, IL15, IRAK2, IRF8, CLU and VCAM1) enriched in the pro-inflammatory response category were related to TLR and NF-κB signalling pathway (see Table 4.12). In contrast anti-inflammatory genes upregulated (e.g. TNFRSF1B^{TNFR2}) by parasite infection relative to BL20-LPS could also be identified. It should be noted however that a clear bias toward repression of pro-inflammatory or elevation of anti-inflammatory gene expression was not detected for the dataset, in general.

4.3.3.1.2 Modulation of cancer associated genes

Perhaps not surprisingly, a highly significant category for enrichment of genes in the dataset was 'cancer'. Interestingly the percentage of genes placed in this functional category was higher (24%) for the up regulated relative to the down regulated subsets of genes (11.5%). Moreover, clear differences in the ratios for pro and anti function were observed when comparing the up and down datasets for several of the cancer related sub categories. For example, the down-regulated dataset was enriched for anti-cancer (metastasis of cells, tumourigenesis and cancer) molecules relative to the up-regulated dataset, which was enriched for pro-cancer genes (see Table 4.11). Important genes identified in the down-regulated dataset included anti-cancer CD40, HTATIP2 and IRF8, whereas the up-regulated pro-cancer genes included IL2RB, CCR7, TP73, ANGPT4, FOXA3, PAK1 and CTTN. Representative genes together with their relative fold change in gene expression and indication of a pro- or anti-

cancer effect are shown in Table 4.12 (up regulated dataset) and 4.13 (down regulated dataset) respectively.

4.3.3.1.3 Modulation of cellular movement associated genes

IPA analysis highlighted a group of genes linked to cellular movement function, revealing an impact of altered gene expression on cell motility and invasiveness. Within the up-regulated dataset for this category, several genes were predicted to promote cell migration, infiltration and invasion of cells. Of particular note, is that significant enrichment of genes in the 'invasion of eukaryotic cells' category was only obtained for the up-regulated dataset (see Table 4.11). Furthermore, 10 out of 14 genes (e.g. CCL1, CTTN, MMP13, ENPP2, F2R, HBEGF, PODXL, SLC2A1, SPARC and SPP1) in this sub category were predicted to have positive influence on this process.

Genes predicted to promote 'infiltration of leukocytes' and 'migration of leukocytes' were also identified and included ICAM1, IL2RB, XCL2, SELL, TP73 and NDRG1. However, as shown in Table 4.11 when the up and down datasets were compared for the ratio of pro and anti genes in 'infiltration of leukocytes' the indicated trend was repression of this function (elevation of anti combined with repression of pro). This result could be of significance as enrichment of genes in categories 'migration of antigen presenting cells', 'influx of leukocytes' and chemo-attraction of leukocytes was identified only for the down regulated dataset and suggested repression of pro function genes.

4.3.3.1.4 Modulation of cellular assembly and organisation associated genes

An interesting category distinctly altered by parasite infection was 'cellular assembly and organisation', which includes processes such as formation of actin filaments, formation of actin cytoskeleton and elongation of plasma membrane projections (podosomes, lamellipodia and filopodia). Several of these processes can be related to alterations in morphology and phenotype of the *Theileria* infected cell (Baumgartner, 2011b;Shiels *et al.*, 1989;Shiels *et al.*, 2004). Enrichment of genes in the majority of the associated sub-categories was predicted to promote these functions: i.e bias of pro-function in the parasite associated up-regulated dataset (see Table 4.11). Important pro-function genes

identified within the elevated dataset included ICAM1, F2R, PAK1, ELN and CTTN (see Table 4.13). In contrast, gene enrichment or information relating to pro- or anti effect on function was absent for most of the sub-categories in down-regulated dataset (see Table 4.11).

4.3.3.1.5 Modulation of cellular growth and proliferation

Based on the comparison of up and down datasets, no clear difference was observed in the pro/ anti ratio of genes placed in the first three sub categories of 'cellular growth and proliferation', although the trend was to a bias in the pro function for up regulated genes relative to down. This bias was more pronounced for the sub-category 'proliferation of leukocyte' with 4 out of 6 genes in the up-regulated dataset designated as pro-proliferation. In contrast, the last two sub-categories showed evidence, relative to all other sub-categories, of a bias towards repression of genes that promote 'induction of leukocytes' and 'stimulation of leukocytes'. Thus, in general, genes with an anti-proliferative effect (e.g CD40, CD80, LAIR1 and TP53INP1) were more likely to be present in the repressed by parasite infection dataset (Table 4.12); while genes predicted to have a positive effect on proliferation were proportionally more abundant in the parasite associated up-regulated dataset and included: ICAM1, IL2RB, ELN and TP73 (Table 4.13).

4.3.3.1.6 Modulation of cell death associated genes

Enrichment of genes in the category 'cell death associated' genes which are known to be involved in apoptosis and pro-inflammatory processes was identified for both the up and down datasets, with no obvious difference in the ratio of pro- or anti function genes. Indeed for most sub-categories the ratio between the number pro-and anti was approximately the same (all <2), the only exception to this being the 'cell death of normal cell' category where there was an increase in the number of anti cell death genes relative to pro. Selected genes identified in this category, repressed by the parasite included CFLAR, CD40, CD80, CD69, TP53INP1, EPHA7, TP63, THBS1 and CASP4 (Table 4.12). All of these genes have been implicated in promoting the process of cellular death. Thus differential regulation of these could potentially be related to the observed phenotype of LPS stimulated BL20 cells. Similarly, selected genes up regulated

by parasite infection relative to LPS stimulation and predicted to be anti-cell death include CCR7, TP73, RNASEL, CD5 and ARNT2 (see Table 4.13).

Table 4.12: Modulated genes present in the function categories significantly down-regulated by *Theileria* infection relative to BL20-LPS

Category	Molecules with fold change
Inflammatory Response (pro)	(Immune response, Antimicrobial response)
Transmembrane Receptor	LAIR1 (52.8), IGF1R (85.15), CCR6 (23.18), CD69 (6.56), CD40 (13.8), TLR4 (44.15), CD80 (37.8)
G-protein couple receptor	CCR8 (17.7), CX3CR1 (8.18), CASR (13.15)
Transcription Regulator	ATF3 (7.27), IRF8 (8.7), EPAS1 (39.8)
Cytokine	CXCL10 (24.2), CCL4 (17.3), IL15 (107.3)
Kinase	IRAK2 (18.49)
Other	CD207 (42.8), CD200R1 (132.8), CLU (280.7), CD83 (27.5), VCAM1 (184.5), CD48 (10.32)
Cancer (anti)	(Tumor, transformation of cells, growth of tumor)
Transmembrane Receptor	CD40 (13.8)
Transcription Regulator	HTATIP2 (27.86), IRF8 (8.77)
Other	COL18A1 (19.5), NFKB1A (13.01), THBSI (65.01)
Cellular Movement (Pro)	Migration of antigen presenting cells, Influx of leukocytes, Chemoattraction of leukocytes
Transmembrane Receptor	CD40 (13.8), TLR4 (44.15), IL6R (4.82)
Transcription Regulator	IRF4 (3.36)
Cytokine	CCL4 (17.3), IL15 (107.3), CSF1 (5.13), IL12B (2.69), IL18 (2.43), SPP1 (9.74), C5 (3.15)
Cell Death (pro)	(Apoptosis, apoptosis of cancer cells, apoptosis of leukocyte)
Transmembrane Receptor	CD40 (13.8), CD69 (6.56), CD80 (37.8), IGF1R (85.15), ITGB3 (6.29), LAIR1 (52.8), TLR4 (44.15)
G-protein couple receptor	CASR (13.15)
Transcription Regulator	ATF3 (7.27), HTATIP2 (27.86),IRF8 (8.77), LEF1 (14.9), TP63 (19.06)
Enzyme	IFIH1 (7.27), OAS1 (6.9)
Cytokine	CCL4 (17.3), IL15 (107.3)
Kinase	CDK5R1 (11.75), EPHA7 (120.1), IKBKE (6.47), MAP3K8 (5.2), SGK1 (9.92), TGFBR3 (8.2)
Growth Factor	BMP4 (12.38)
Other	CD48 (10.32), CFLAR (8.57), CLU (280.74), COL18A1 (19.5), KNG1 (8.43), THBS1 (65.01), TP53INP1 (18.93), TRAF4 (8.07), UBD (22.80)
Cellular assembly and organisation (anti)	(Organization of cytoskeleton, formation of actin cytoskeleton)
----------	----------
Cellular growth and proliferation (anti)	(Proliferation of leukocyte, growth of leukocyte)
Transmembrane Receptor	CD40 (13.8), CD80 (37.8), LAIR1 (52.8), TLR4 (21.37),
G-protein couple receptor	CASR (13.15)
Transcription Regulator	IRF8 (8.77),
Cytokine	CCL4 (17.3), IL15 (107.3), CXCL10 (24.2),
Growth Factor	BMP4 (12.38)
Other	CD83 (27.5), COL18A1 (19.5), TP53INP1 (18.93), CLU (280.74), NFKB1A (13.01)

The given table represents the most relevant biological process categories and key molecules from each category that can be linked to parasite infection and LPS stimulation of BL20 cells. Similarly, the prediction of whether the molecules promoted (pro) or inhibited (anti) the designated functional category by IPA is also indicated. The absolute fold change for each molecule is given in brackets.

Table 4.13: Modulated genes present in the function categories significantly up-regulated by *Theileria* infection relative to BL20-LPS

Category	Molecules with fold change
Inflammatory Response (anti)	(Immune response, Antimicrobial response)
Transmembrane Receptor	TNFRSF1B (5.85)
Other	RGS1 (6.55),
Cancer (pro)	(Tumor, transformation of cells, growth of tumor)
Transmembrane Receptor	IL2RB (11.15),
G-protein couple receptor	F2R (5.97), CCR7 (17.9)
Transcription Regulator	TP73 (20.04), FOXA3 (10.84),
Enzyme	ENPP2 (10.02), PDE4C (41.5)
Kinase	PAK1 (22.33), NDRG1 (43.4)
Peptidase	MMP13 (54.20), EPHX1 (10.25), GZMA (24.8),
Growth Factor	ANGPT4 (36.45),
Transporter	AP3M2 (10.35)
Other	CTTN (4.47), FGD4 (14.8), PLIN3 (17.23)
Cellular Movement (pro)	Infiltration, Invasion of cells, Migration of cells
Transmembrane Receptor	ICAM1 (12.02), IL2RB (11.15)
G-protein couple receptor	CCR7 (17.94)
Transcription Regulator	TP73 (20.04), ETV5 (6.22)
Enzyme	ENPP2 (10.02)
Cytokine	CCL1 (9.16), XCL2 (42)
Kinase	PAK1 (22.33), NDRG1 (43.4)
Peptidase	MMP13 (54.20)
Other	CTTN (4.47), ELN (3.216), SELL (9.50), SEMAF3 (5.09), SPARC (53.3), TNS1 (6.55)
Cell Death (anti)	(Apoptosis, apoptosis of cancer cells, apoptosis of leukocyte)
Transmembrane Receptor	CD5 (4.8)
G-protein couple receptor	CCR7 (17.94)
Transcription Regulator	TP73 (20.04), ARNT2 (4.26),
Enzyme	RNASEL (60.5)
Kinase	HCK (6.3), MLLT3 (13.94), PAK1 (22.33), SEMAF3 (5.09), SERPINE2 (15.05)
Transporter	SLC7A11 (8.80)
Other	ANTXR2 (5.39), NLRP1 (4.89), SPARC (53.3),
Cellular assembly and organisation (pro)	(Organization of cytoskeleton, formation of actin cytoskeleton)
Transmembrane Receptor	ICAM1 (12.02,
G-protein couple receptor	F2R (5.97),
Kinase	PAK1 (22.33),
Other	SDC4 (2.6), ELN (3.2), CTTN (4.47),
Cellular growth and proliferation (pro)	(Proliferation of leukocyte, growth of leukocyte)
Transmembrane Receptor	ICAM1 (12.02), IL2RB (11.15), FCGR2B (5.4), TNFSRSF1B (5.85)
G-protein couple receptor	F2R (5.97),
Transcription Regulator	TP73 (20.04)
Kinase	HCK (6.3)
Other	ELN (3.2), MLLT3 (13.9), LAMC1 (4.2), SUMO3 (6.03),

The given table represents the most relevant biological process categories and key molecules from each category that can be linked to the phenotype of parasite infection and LPS stimulation of BL20 cells. Similarly, prediction of whether the molecules promoted (pro) or inhibited (anti) the designated functional category identified by IPA is also indicated. The absolute fold change for each molecule is given in brackets.

4.3.3.2 Canonical pathway analysis

IPA analysis of the infection modulated date set identified several important canonical pathways as being manipulated by the parasite infection relative to LPS stimulation of BL20 cells. Significant pathways were identified by screening for enrichment of genes placed within canonical pathways available in the IPA library. The most significant canonical pathways identified are shown in Figure 4.25, while the full list of pathways can be view in Appendix 2.3. Not surprisingly, identified pathways included signalling pathways associated with the inflammatory and anti-microbial response including NF-κB and PI3K signalling pathways known to be manipulated by parasite infection. In addition, other pathways relevant to stimulation of the inflammatory response that showed evidence of modulation by parasite infection were 'activation of IRF by cytosolic pattern recognition receptor', 'TNFR2 signalling', 'role of pattern recognition receptors in recognition of bacteria and viruses', 'CD40 signalling', 'LPS-stimulated MAPK signalling', 'G-protein coupled receptor signalling', 'Toll-like receptor signalling' and interferon (IFN) signalling. Enrichment of genes that operate in pathways associated with induction of cell death/apoptosis ('death receptor signalling', 'p53 signalling') were also identified by IPA.

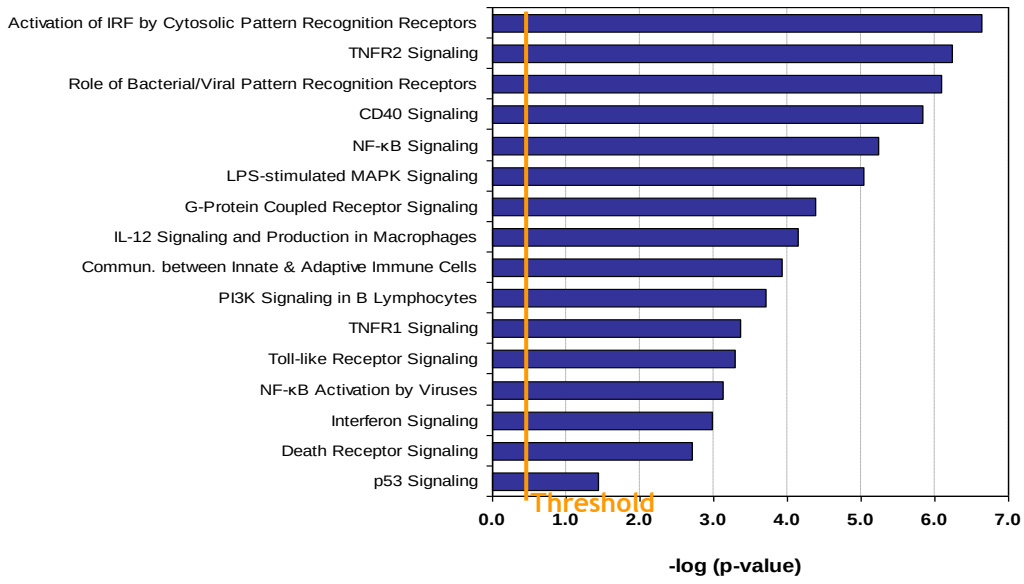

Figure 4.25: Identification of top canonical pathways in infection associated modulation dataset
Bar chart shows important canonical pathways enriched for genes significantly modulated by Theileria infection compared to LPS stimulation of BL20 cells. Each bar represents –log (p-value) for over representation of genes in the selected pathway. Threshold (orange line) denotes P = 0.05.

Detailed exploration of the canonical NF-κB signalling pathway showed a number of interesting infection associated modulations relative to the LPS stimulated response. These can be divided into two general categories: repression of genes encoding receptors that perceive a signal that activates NF-κB, and partial up-regulation of components of the pathway downstream of the IKK signalosome (p100/p52, RelB). Two additional modulations of note were found: (a) levels of the IkB inhibitors (NFKBIA, NFKBIE and NFKBIZ) were repressed in TBL20 relative to LPS-stimulated BL20 and (b) two PI3K regulatory subunits (PIK3R5 and PIK3R6) were predicted to be elevated in TBL20 but repressed in BL20-LPS. Similarly, several molecules upstream of the IKK signalosomes (TRAF2, PKR and TNFAIP3 $^{A20/MAD6}$) were also predicted to be repressed in TBL20 but elevated in BL20-LPS (see Figure 4.26).

4.3.3.3 Custom pathway analysis

Infection of bovine leukocytes with *T. annulata* or *T. parva* is known to result in constitutive activation of transcription factors associated with the inflammatory response. To investigate whether the outcomes of transcription factor/signalling pathway activation were being effectively modulated, sets of known target genes were uploaded to IPA using the custom pathways feature and screened for evidence of significant enrichment of genes within infection-modulated dataset. Pathways were selected on the basis of a known association with the *Theileria* transformed cells and generated using available lists of known and predicted NF-κB (http://www.bu.edu/nf-kb/gene-resources/target-genes/), C-myc (http://www.ncbi.nlm.nih.gov/biosystems/169353) and TGFb (http://www.netpath.org) response/target genes. As shown in Figure 4.27, significant enrichment in targets of NF-κB and cMYC repression targets was observed, together with a particular enrichment of genes known to be regulated in response to TGFb signalling.

Interestingly, 75 percent (46) of the 61 NF-κB target genes identified as modulated by infection showed a down-regulated response relative to LPS stimulated BL20 cells. Whereas a lower number of the NF-κB target genes (15) were up-regulated in TBL20 relative to BL20 LPS. For the 46 genes in the repressed dataset, enrichment was found in several IPA categories that could influence establishment of the parasite infected leukocyte and included:

activation of leukocytes (with a strong bias in genes designated as pro-function), differentiation of leukocytes (pro); apoptosis (pro and anti); immune response (pro) and inflammatory response (pro). Genes belonging to several members of NF-κB activation cascade and regulatory subunits were also present in the repressed dataset.

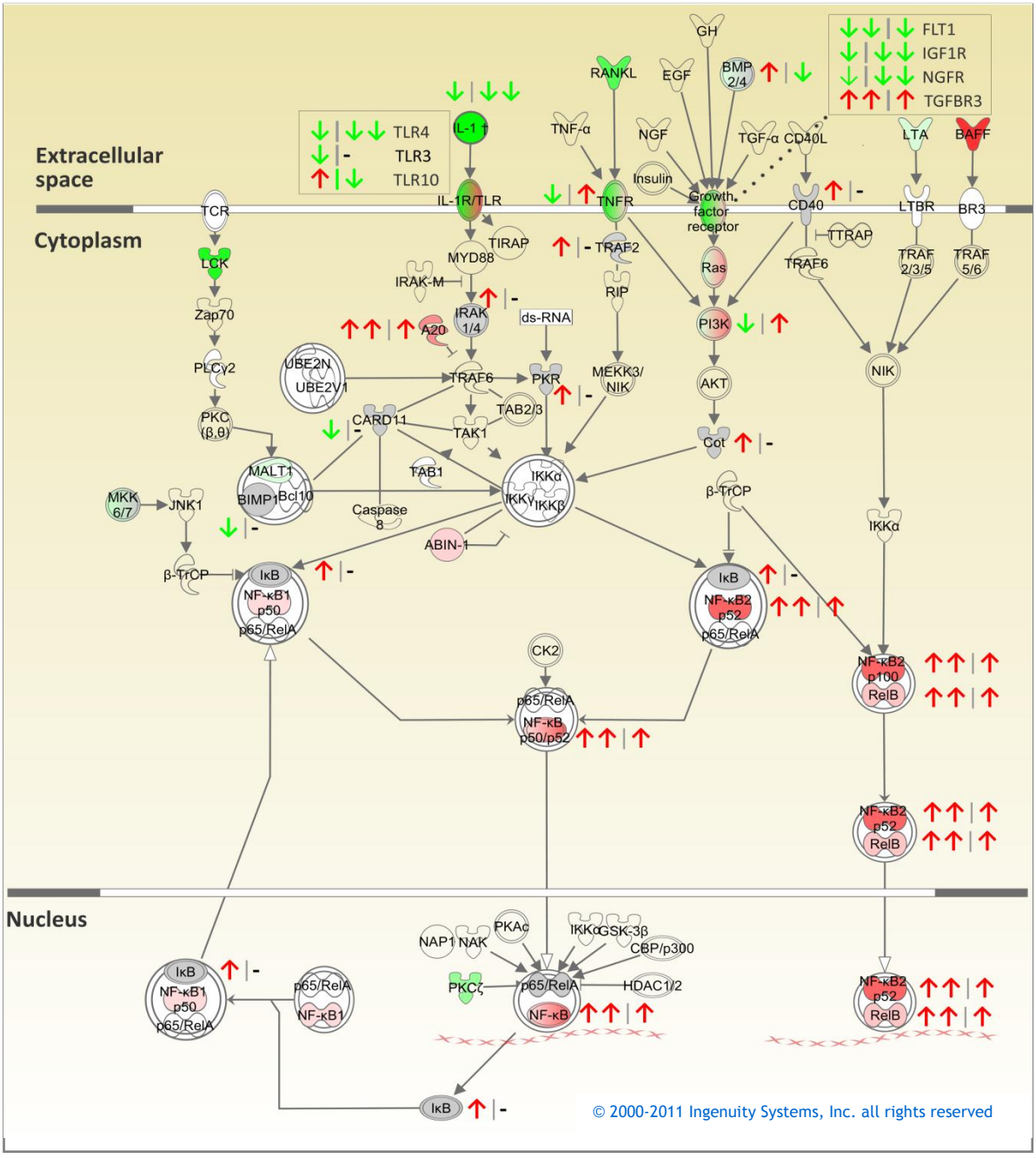

Figure 4.26: Modulation of NF-κB pathway in infection associated modulated dataset
NF-κB signaling pathway was the most significant (P< 0.001) canonical pathway modulated by parasite infection relative to LPS response. Modulated dataset was clustered into canonical pathway using IPA. The genes which are coloured are differentially expressed in TBL Vs BL (red = up in TBL, green = down in TBL). The arrows are beside those genes which are on the LPS modulated list (1,053/1,959). Green and red arrows indicate down and up-regulation response respectively. Whereas arrow signs before vertical bar (|) indicates LPS response and after bar indicates parasite response. For example ↑↑ | ↑ = super-up, up and ↑- means up, no change. The data for IL-1R/TLR and growth factor receptor are exploded in two boxes.

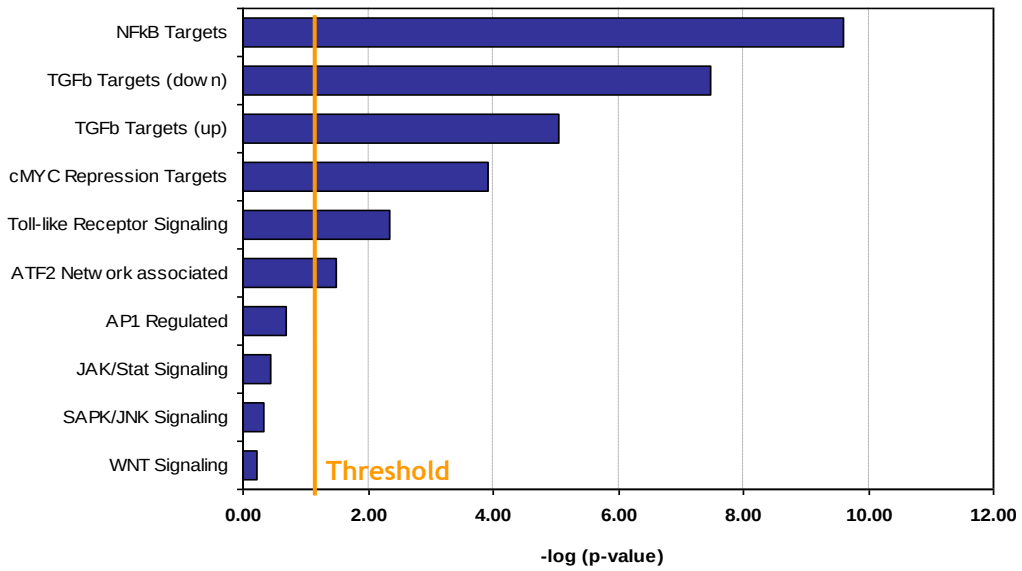

Figure 4.27: Custom pathway analysis of infection associated modulated dataset
Bar chart shows customised pathway analysis, performed by enrichment of modulated gene set against literature based compiled gene lists of selected pathways. Each bar represents –log (p-value) for over representation of the modulated genes in the selected pathway. Threshold (orange line) denotes the P= 0.05 level.

Thus, genes encoding NF-κB inhibitor proteins (NFKBIA/IkBα, NFKBE/IkBε and NFKBIZ), responsible for the sequestration of NF-κB in the cytoplasm, and 2 NF-κB subunits (REL-B and NFKB2/p52) were identified (see Figure 4.28). The number of target genes up-regulated by parasite infection was too small to screen for enrichment but up-regulation of several of these NF-κB targets (e.g. ICAM-1 and SPARC) could be predicted to strongly influence the phenotype of the infected cell. Secreted Protein Acid and Rich in Cystein (SPARC), for example, has been implicated in apoptosis, differentiation, metastasis and regulation of immune cell response. Moreover recent studies have indicated that SPARC can be pro-tumorigenic via inactivation of the p53 tumour suppressor (Fenouille *et al.*, 2011a).

Modulated NF-κB target genes included several chemokines and cytokines predicted to be involved in pro- or anti-inflammatory response: IL15, CXCL10, CCL4, and IL12B were significantly suppressed by the parasite infection; whereas CCL1, CCR7 and XCL2 were significantly up-regulated in infected cells. Additional molecular function categories designated to modulated NF-κB target genes belonged to transcription regulation (down regulated), protein binding activity (predominantly down), cell adhesion (up and down regulated), immunoreceptors (down regulated) and regulators of apoptosis (down regulated, Table 4.12).

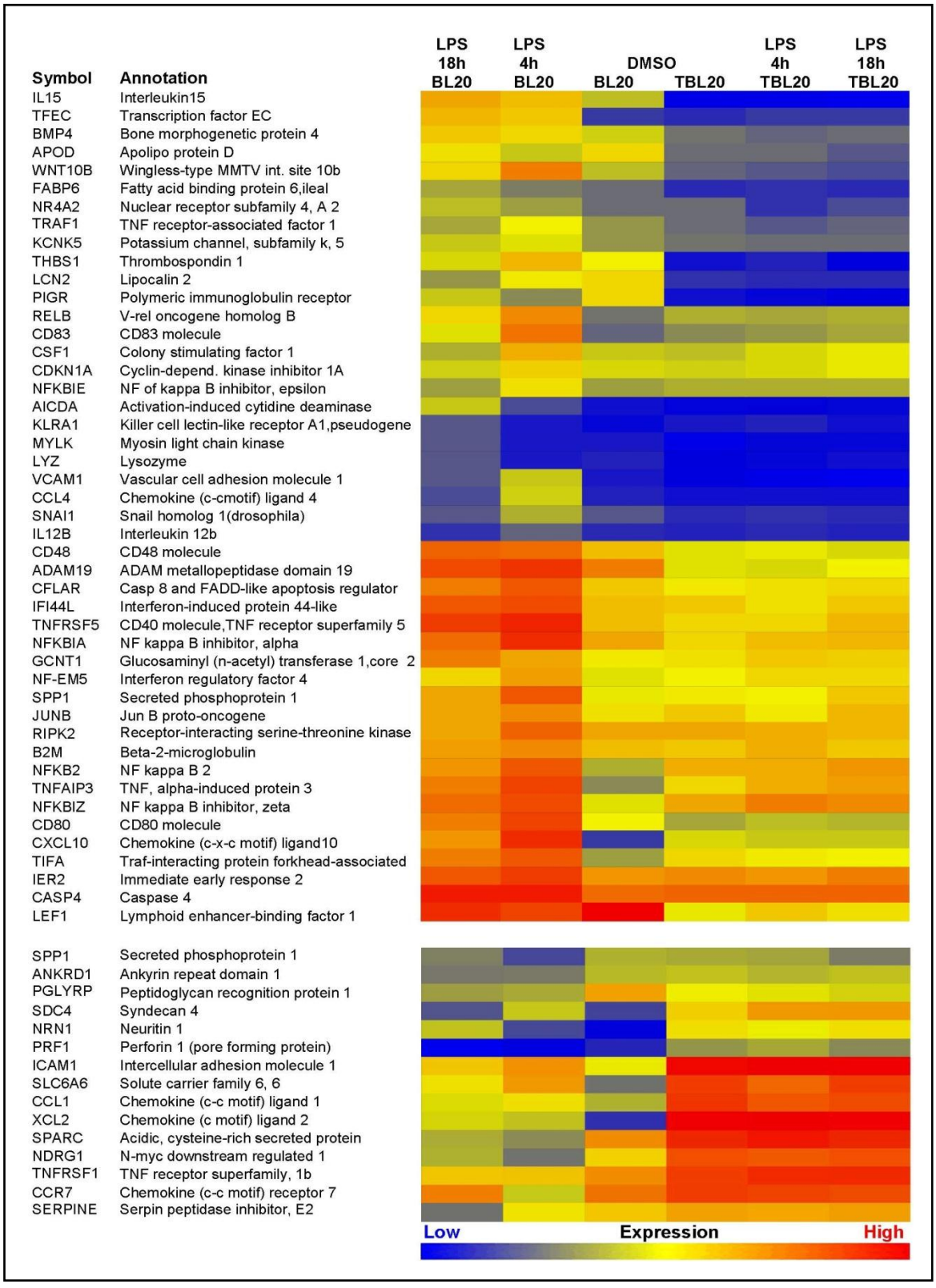

Figure 4.28: Expression profile of NF-κB response genes identified in infection associated modulated dataset

Data are presented in visualized expression of hybridization values as a heat map. The rows represent individual genes and columns represent each experimental condition. The red and blue colours reflect high and low expression (log_2-transformed scale) levels, respectively, as indicated in the scale bar.

Table 4.14: Molecular function or biological process categories of NF-κB target genes modulated by *Theileria* infection relative to BL20-LPS

Gene Symbol	Modulation (Fold change)	Gene Symbol	Modulation (Fold change)	Gene Symbol	Modulation (Fold change)
Cytokines/ Chemokines		**Immunoreceptors**		**Enzymes**	
CCL1	15.60	PGLYRP1	3.12	APOD	−8.69
CCR7	17.94	CD80	−37.89	ADAM19	−19.78
XCL2	54.23	CD83	−27.51	BMP4	−12.38
IL15	−107.32	PIGR	−16.02	CSF1	−5.14
CXCL10	−24.25	TNFRSF5	−13.83	KCNK5	−4.77
CCL4	−17.31	CD48	−10.33	GCNT1	−4.44
IL12B	−2.69			LYZ	−3.83
Regulators of apoptosis		**Transcription regulation**		**Protein binding activity**	
WNT10B	−42.63	TFEC	−47.09	SLC6A6	8.48
CFLAR	−8.58	LEF1	−21.21	SERPINE2	15.05
TRAF1	−7.23	NFKBIA	−13.01	NDRG1	43.42
CASP4	−2.74	RELB	−10.74	SPARC	53.38
Others		SNAI1	−7.28	THBS1	−65.01
SDC4	12.29	NFKB2	−4.0	LCN2	−18.46
NRN1	11.84	NFKBIE	−3.38	AICDA	−18.26
PRF1	8.94	NFKBIZ	−3.59	TNFAIP3	−8.65
TNFRSF1B	5.86	NR4A2	−3.51	TIFA	−7.02
SPP1	−9.74	NF-EM5	−3.37	FABP6	−6.41
IER2	−3.07	ANKRD1	2.72	MYLK	−4.21
IFI44L	−5.62	JUNB	−2.72	B2M	−2.48
KLRA1	−2.7	**Cell adhesion molecules**		RIPK2	−2.91
		ICAM1	12.03	CDKN1A	−2.64
		VCAM1	−20.9		

Modulated **NF-κB** response genes are described as those whose expression was altered in TBL20 relative to BL20-LPS cells, making a simple designation of either up- or down-regulated response. Fold change of individual gene is shown, and minus indicates down-regulated expression in parasite infection.

Investigation of genes classified as cMyc validated repression genes indicated that the majority, 7 out of 10, have an expression profile consistent with maintenance of repression associated with infection. The NDRG1 gene, however, showed a contrasting pattern from the rest of the dataset, as the RNA level for this gene was found to be elevated in infected TBL20 cells but repressed in LPS stimulated BL20 cells. 7 of the 10 genes in this pathway were designated as located to the nucleus with a predicted function as a regulator of transcription or a kinase.

Evidence for modulation of TGFβ target genes was also obtained, as the predicted response to stimulation could not be identified: roughly equivalent numbers of target genes that are up- or down-regulated by TGFß were identified within the 'parasite-repressed' gene list, with a similar finding for the 'parasite-enhanced' gene list. TGFß targets modulated by the parasite were categorised in

cancer, cell death, cellular growth and development. Of particular note was that inflammatory response TGFß target genes were generally associated with repression of expression by parasite infection. These results may be explained, in part, by the observation that expression of genes encoding TGFB2, TGFB3 and the TGFBR3 are slightly elevated in parasite infection of BL20 cells, while TGFB1 is slightly reduced. The TGFβ signalling pathway has been implicated as a determinant of pathogenicity and metastatic activity in tropical theileriosis. Reduced TGFβ2 expression and lower virulence was measured for infected cells derived from an attenuated vaccine line and disease resistant Sahiwal (*Bos indicus*) cattle (Chaussepied *et al.*, 2010). Differential expression of TGFβ target genes was also identified for the attenuated vaccine cell line, with elevated as well as repressed expression detected. Thus, modulation of TGFB signalling and the respective target genes appears to be a common event associated with *T. annulata* infected leukocytes.

4.3.4 Proteomic validation of microarray results

In addition to validation of modulation of Toll-like receptor 4 at the protein level (see Chapter 3) a further two proteins were validated for differential expression in *Theileria* infected and uninfected cells before and following LPS stimulation. These proteins were selected on the basis of high fold-change, interesting biological functions and availability of commercial antibodies suitable for western blot or immunofluorescence analysis.

The first gene of interest investigated was LIM domain only 2 (LMO2), which encodes a cysteine-rich, two LIM-domain protein that has a central and crucial role in hematopoietic development. Immunoblot analysis of LMO2 detected a ~24 kDa protein that was expressed in BL20 cells at a high level, with repression in LPS stimulated BL20, but associated with significant repression in *Theileria* infected control and LPS stimulated TBL20 cells (see Figure 4.29A). Thus, the protein data agreed with the RNA data indicating super repression associated with infection (profile 6). The expression pattern of LMO2 was also assessed by immunofluorescence analysis (IFA) of LPS stimulated and un-stimulated BL20 and TBL20 cells (see Figure. 4.29B). The results clearly showed high-level reactivity against LMO2 in BL20 relative to a virtually complete lack of staining in TBL20 cells (see Figure. 4.29B: panel 1 Vs panel 2). Moreover, as predicted from its

function as a regulator of gene expression, the IFA clearly demonstrated that the protein was located to the nucleus of BL20 cells. A significant reduction in staining by IFAT was not evident for LPS-stimulated BL20 cells. (Figure 4.29B: panel 1 Vs panel 3).

The second gene tested encoded Vascular cell adhesion molecule 1 (VCAM1), a member of the Ig superfamily which encodes a cell surface sialoglycoprotein and mediates leukocyte cell adhesion and signal transduction. As predicted VCAM1 protein was detected at 110 kDa, and was only detected in extracts derived from LPS stimulated BL20 cells (see Figure 4.29A). Consistent with the microarray and RT-PCR results, No band of predicted size (110 kDa) was observed in un-stimulated BL20, TBL20 and LPS stimulated TBL20 cells. Furthermore with respect to LPS stimulation of BL20 cells, VCAM1 was detected at a higher level at 18h relative to 4h post LPS stimulation. It was concluded that the strong band detected just below 110 kDa was due, most likely, to non-specific recognition of a protein by the poly-specific anti-VCAM1 serum.

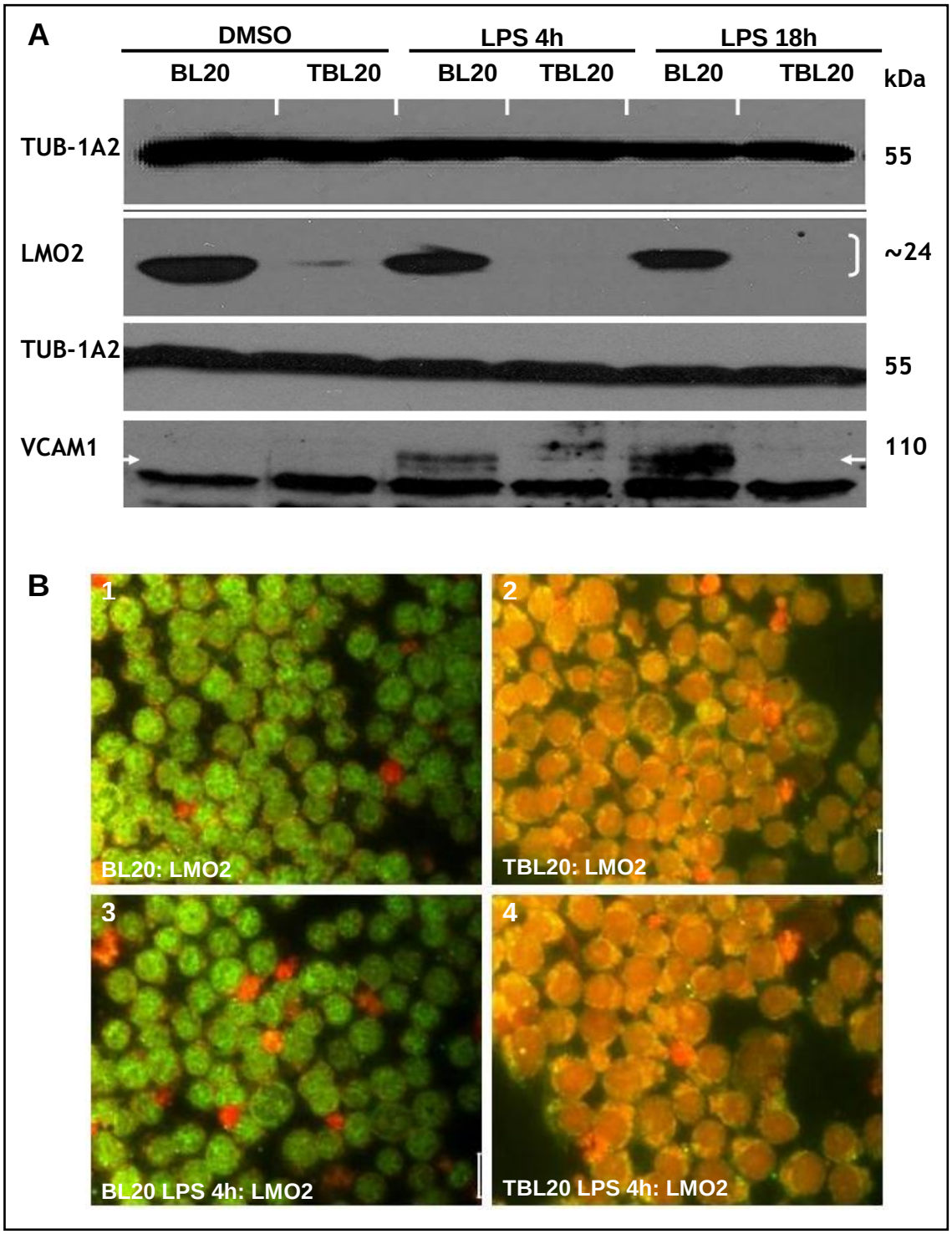

Figure 4.29: Validation of proteomic expression profile of candidate genes
A. Shows validation of the protein expression of 3 candidate genes by Immunoblotting. Expression of LMO2 and VCAM1 was detected by western blot analysis of total cell extracts derived from uninfected and *Theileria* infected cell cultures either stimulated with LPS (4h/18h) or unstimulated (DMSO). Equal protein loading was assessed by immunodetection of the Tubulin expression using a monoclonal anti-actin antibody (TUB-1A2).
B. Immunofluorescence analysis of LMO2 expression in un-infected BL20 and *Theileria* infected TBL20 cells. **Panel 1 and 2**, anti-LMO2 reactivity in BL20 and TBL20 cells respectively. Bar = 20µm. **Panel 3 and 4,** anti-LMO2 reactivity in LPS stimulated BL20 and TBL20 cells respectively.

4.4 Discussion

The aim of the work presented in this chapter was to investigate the postulation that infection of the bovine cell modulates the outcome of a cellular activation event at the global level. This was performed using an oligonucleotide microarray platform designed by the Glasgow *Theileria* group that represented the largest number of genes, at the time, for putative or known bovine RNA features (31,481). The Glasgow microarray therefore provided a considerable increase in the number of represented bovine genes compared to the cDNA (BoMP) array generated by Jensen *et al.*, 2006 and 2008, and limited gene expression studies performed by other co-workers (Jensen *et al.*, 2009;Oura *et al.*, 2006;Sager *et al.*, 1997). Moreover, studies using the BoMP array were aimed, primarily, at comparing the response of cells from different cattle breeds infected with *T. annulata* or stimulated with LPS. Therefore, the results described are the most comprehensive analysis to date of gene expression changes that occur following activation of uninfected cells compared to changes in gene expression associated with infection.

4.4.1 Interpretation of microarray data

It is clear form the results that both infection and LPS stimulation result in alteration in expression to a large number of bovine genes (approximately 3000 genes, 10% of array features). These numbers, although high, are supported by the earlier study of Jensen *et al.*, 2008 that reported 695 altered genes associated with LPS & IFN stimulated macrophages and 1000 differentially expressed genes associated with parasite infection (unpublished data in Jensen et al., 2008) using the smaller BoMP array. Of the 3634 BL20 LPS response genes 12.3% more showed evidence of elevated expression, while in contrast, 45% more of the infection altered genes showed evidence of repression. While this result may indicate that parasite infection is more associated with repression than elevation of host cell gene expression, it is possible that the large excess in repressed genes is caused by an unknown skew in the normalised dataset that increases the probability of a down regulated gene being scored as significant. However such a skew, if present, is unlikely to influence generation of the infection modulated dataset (1959 genes) as this represents genes scored as

significant by ranked product analysis (FDR < 0.05, fold change ≥ 2) in the BL20 dataset and a ≥ 2 fold difference between the expression value in TBL20 and LPS stimulated BL20.

Rank product analysis (Breitling *et al.*, 2004) has now been widely adopted to study differential gene expression due to its robust nature and has been utilised by several recent studies performed to identify differentially expressed genes (Leifso *et al.*, 2007;Morrison *et al.*, 2010;Veitch *et al.*, 2010). Gene expression analysis was also performed using a Student's T test (≥2 fold, F test Anova P-value <0.05) in the ArrayStar software suite and the results of both analyses were validated by cross comparison of the obtained datasets.

Comparison of the infection (TBL20) Vs the LPS (BL20) response datasets and Chi-square analysis demonstrated that a significant number of genes (1296) showed an altered expression response associated with both parasite infection and LPS stimulation of BL20 cells (see Figure 4.5). This result is important as it clearly demonstrates that the gene expression profile of the parasite-infected cell is related to an activated state induced by a classical inflammatory mediator. Indeed IPA analysis of the LPS BL20 dataset showed that enrichment for inflammatory response genes was of greatest significance (Figure 4.24). Thus, as indicated from previous studies it is likely that the parasite infection results in constitutive activation of transcription factors that are also activated by inflammatory mediators such as LPS. What is not clear from this analysis, however, is the degree of variability in the outcome of the activation event in these two cellular states and whether a difference in outcome could be predicted to influence the establishment of the parasite infected cell.

Initial analysis of the array results also showed that TBL20 cells were refractory to major LPS-induced global expression changes, as only a small subset of genes (1.5%) showed altered expression following stimulation of TBL20 with LPS. These results clearly indicated that parasite is a dominant suppressor of lipopolysaccharide (LPS) inducible gene expression. One way in which the parasite infected TBL20 cell may be able to achieve this relative non-responsiveness is via down regulation of the major LPS receptor TLR4 (see chapter 3). Consistent with the results obtained in the previous chapter, microarray and real time RT-PCR confirmed repression of 21-fold in TBL20 cells

relative to BL20-LPS. Furthermore, analysis of the TBL20 VS BL20 array data (Kinnaird et al., un-published) indicated that other genes encoding LPS receptors (integrin, alpha L (CD11a) and platelet-activating factor receptor (PTAFR)) are also down regulated by infection. Therefore the mechanism that leads to altered expression of the 1.5% genes of TBL20 that were stimulated by LPS may involve alternative surface molecules able to bind to LPS. For example, low-affinity lipopolysaccharide receptors P and L-selectin, which are exclusively expressed in parasite infection or HSP90/70 and class B scavenger receptor molecules (SCARB1 and SCARB2) are expressed at equal levels in BL20/TBL20 cells (non-LPS response genes identified in microarray analysis of Kinnaird *et al*; unpublished), each of which have been reported to bind LPS in various cell types (Bocharov *et al.*, 2004;Malhotra *et al.*, 1998;Malhotra and Bird, 1997a;Malhotra and Bird, 1997b;Pearson, 1996;Triantafilou and Triantafilou, 2004). Therefore, it is likely that the minor subset of LPS-inducible response genes associated with parasite infection is mediated via TLR-4 independent signalling.

The BL20 Vs TBL20 model was chosen for this study because it provided a cell culture system that would provide a reproducible response to simulation and infection. Moreover, TBL cells have been used in a number of previous studies to investigate infection-associated phenotypes (Baylis *et al.*, 1995;Dando and Shiels, 1997;Oura *et al.*, 2006) and it has been demonstrated that TBL cells are dependent on a viable parasite and undergo apoptosis when the schizont is killed by BW720c (see chapter 3). The results of the array data in general support the use of the TBL20 model to investigate parasite control of the infected cell phenotype. Thus, differential expression of a number of genes (for example, CCR1, ICAM1, TLR 10, ITGB7, ISG15) previously reported as altered in the context of infection was found (Jensen *et al.*, 2008;Jensen *et al.*, 2009;Oura *et al.*, 2006) . In addition, a significant number of genes show a change in expression pattern when TBL20 was treated with BW720C over a short time period (48h). Some of these changes are non-reciprocal and indicate that on removal of the parasite the cell does not simply revert to the uninfected BL20 state but instead progresses towards cell death. It has been concluded from the parallel study of Kinnaird *et al.,* that infection of the cell promotes a major alteration to the profile of host transcription factors resulting in a reconfiguration of gene expression networks that is not reversible following

removal of the parasite encoded signal(s) that control the infected cell phenotype. Irreversible reconfiguration of gene networks associated with cellular differentiation is increasingly proposed for stem cell systems (Chickarmane *et al.*, 2006;Wang *et al.*, 2010).

4.4.2 Interpretation of modulated expression profiles

The results presented in this chapter provide strong evidence that infection of BL20 cells with *T. annulata* is associated with modulation of gene expression changes induced by LPS. 8 profiles of modulated expression were obtained by comparison of expression data across all 6 cellular conditions. Two of these profiles (profile 1 and 5) represented an enhancement of the expression change induced by LPS (e.g. elevated expression of an LPS stimulated up regulated gene; repression of an LPS repressed gene) and it could be argued that these patterns of expression are caused by a greater activation status in the infected BL20 cell relative to the LPS stimulated counterpart. For example, the level of NF-κB reporter activity is significantly higher in TBL20 compared to LPS stimulated BL20 (see Figure. 3.4, Chapter 3). Therefore, if expression levels of the target genes were directly linked to quantitative changes in the level of an activated regulator, these enhanced expression profiles would be generated. This postulation is probably over simplistic and is also unlikely to account for the other 6 modulation profiles where infection is associated with either: a reversal of the change induced by LPS (profile 2 and 6); an attenuated response of the LPS induced alteration (profile 3 and 7); and no infection associated change in expression, compared to an LPS induced response (profile 4 and 8). This last modulation event (profile 4 and 8) could be explained in part by proposing that the infected cell simply does not respond to LPS stimulation. As stated above, infection down regulates receptors required for transduction of the LPS signal. For this mechanism to operate factors that control target gene expression in response to LPS stimulation of BL20 would not be activated by parasite infection. The observation that the largest number of genes were recorded for profile 4, and that the vast majority showed no response to BW720c, supports a lack of response mechanism, although in some cases this model may not be appropriate. VCAM1 for example is a classical NF-κB dependent gene but shows no change in expression associated with infection, and it is conceivable that

infection is modulating expression (repressing) of this gene in a more direct manner.

Direct modulation of host gene expression can be postulated where expression is reversed or attenuated by infection (and may also operate for enhanced expression e.g. profile 1). Where expression is reversed (profile 2 and 6), it can be postulated that the infected cell requires the gene to be strongly repressed or elevated and interestingly IPA analysis of the genes in profile 6 (elevated by infection) showed an associated with cancer, while IPA analysis of profile 2 (repressed by infection) showed an enrichment for genes in a range of categories, including cancer and apoptosis. Relative to LPS stimulation, repression of genes placed in profile 2 can be high (over 50 fold). These include repression of genes encoding the macrophage expressed MPEG1, the inflammatory cytokine IL15, and the major histocompatibility complex class II DY alpha. Repression of these genes could be predicted to be advantageous to the parasite infected cell by manipulating the immune response and promoting macrophage dedifferentiation.

A significant number of genes in these two profiles were sensitive to BW720c, also indicating direct modulation by infection. How this operates requires further investigation but could involve parasite-encoded molecules or a qualitative change in bovine regulators of gene expression induced by an infection dependent alteration of host cell status. Previous studies have concluded that the differentiation state of the host cell is under control of the *T. annulata* parasite (Sager *et al.*, 1997) and that this involves changes in expression regulators that regulate myeloid development (Jensen *et al.*, 2009). Microarray data generated in my study and the parallel study of Kinnaird *et al* showed significant changes to the expression levels of genes encoding regulators of developmental gene expression.

Like profiles 2 and 6 it can be proposed that infection promotes high level expression of genes in profile 1 and repression of genes in profile 5 because they are likely to be advantageous or detrimental to the infected cell, respectively. This supposition is supported by identification of gene classes in profile 1, in particular, previously identified as being markers for the macroschizont infected cell phenotype (e.g. IL2R, MMP13, ICAM1). Other potentially significant genes in

this profile include the lymphocyte adhesion molecule selectin L gene, the homeobox protein Meis 3 gene and the gene encoding cortactin. Profile 5 represents super repressed genes and indicates a requirement for the parasite-infected cell to down-regulate their expression. Genes encoding membrane proteins, including a number of important receptors are prominent in this profile. The data from this profile and others strongly suggests that the parasite significantly modulates the infected cell surface to influence interaction of the infected cell with a range of ligands, inflammatory mediators and cells of the bovine immune system.

A prediction that the modulations represented by profiles 3 and 7 are beneficial by repressing or elevating target gene expression is more difficult, since they represent attenuation of the LPS response. Thus, elevation of a target gene (profile 3) could be beneficial but does not occur at the same level as BL20 cells stimulated by LPS (e.g. the Jun proto oncogene). On the other hand it is possible, as postulated previously, that high-level expression of cellular defence genes, such as ISG15, that occur via activation of the cell are repressed by the parasite infection, as they are potentially detrimental. The enrichment of important genes (OAS2, ISG15, MX2, IRF5 and IL7) was associated with the interferon/innate immune/cellular defence response (Gessner *et al.*, 1993;Hovanessian and Justesen, 2007;Jin *et al.*, 1999;Lu *et al.*, 2006;Pitha-Rowe and Pitha, 2007;Sieling *et al.*, 1995). Furthermore, expression of 80% of the BW720c sensitive genes in profile 3 was elevated upon treatment, indicating a requirement for active repression by the parasite. IPA analysis for profile 7 showed enrichment for genes predicted to have a function in cellular metabolism. Metabolism genes were also enriched in profile 8 and since these two profiles could be taken as evidence for elevation in gene expression relative to the LPS response, it is possible they reflect a requirement for maintenance of cellular metabolism pathways in the infected cell.

4.4.3 Interpretation of qRT-PCR data

In addition to validation of genes representing each of the 8 profiles by semi-quantitative PCR analysis, sixteen genes candidate genes were also validated by real-time RT-PCR using relative quantification (ΔΔCt) methodology. Real time

PCR has advantages over semi-quantitative methodology, being quicker to perform and relatively more sensitive, allowing quantification of lesser fold changes in RNA levels (Ponchel *et al.*, 2003;Wong and Medrano, 2005). In the current study, the use of ACTβ or GAPDH as reference genes proved to be a good choice: they were validated as being equally expressed across all experimental conditions in both the microarray and RT-PCR experiments. These genes have previously been used as reference genes in several studies using RT-PCR (Habibi *et al.*, 2009;Lizundia *et al.*, 2006;Sager *et al.*, 1997) as they allow normalisation of candidate genes expression against potential variation in the amount of cDNA used in the reaction. In addition they allowed demonstration that PCR efficiencies of the target genes were in the acceptable range for comparative analysis. This is an essential standard for ΔΔCt equation, where the efficiencies of the control and target genes need to be approximately equal (Livak and Schmittgen, 2001). The results obtained from qRT-PCR were consistent with the microarray analysis and the trends in the expression pattern obtained were similar for all genes tested across the different expression profiles. However, qRT-PCR showed higher magnitudes of expression level alteration, presumably because qRT-PCR is a more sensitive technique than microarray (Bruder *et al.*, 2007).

4.4.4 Interpretation of IPA analysis of the infection modulated LPS dataset

In addition to performing analysis for predicted gene function on genes placed within the 8 profiles, IPA was performed on the 1052 genes of the complete infection modulated LPS dataset that could be mapped. This was carried out to give a more global assessment of the most important molecular functions, diseases and pathways manipulated by infection. Reassuringly, the most significant category mapped for the dataset was the inflammatory response, with many other categories that could be linked to the infected cell phenotype highlighted e.g. tissue morphology, cancer, cell death, antimicrobial response and cell signalling. Furthermore, enrichment of genes in the dataset that mapped to biological pathways highlighted modulation of signalling pathways associated with the inflammatory response and included the NF-κB, TNFR2 and interferon signalling pathways. Thus, it can be concluded that the infected cell

is significantly modulating pathways and a large number of target genes that regulate and execute the inflammatory response and cellular transformation. Also, the dataset is rich for mining infection associated candidate genes that operate in these processes.

Attempts were made using IPA to make the output of the analysis more predictive. This was performed utilising the designated pro or anti function of a given molecule and screening two lists representing genes displaying infection associated elevated or repressed expression for a change in the pro/anti bias across different functional categories. The power of the prediction is based on the number of genes enriched for each category, confidence of the IPA designation (accurate and unequivocal) and, preferably, an equal number of designated pro and anti genes. Unfortunately the gene number was often small, the designation equivocal and throughout the dataset a bias in pro-function was observed. These characteristics may, for example, have made it difficult to observe for the apoptosis category any obvious bias in upregulation of anti- together with down regulation of pro-apoptotic genes. Moreover genes functioning in apoptosis commonly switch from a pro to anti function depending on cellular context (Fannjiang *et al.*, 2003;Hess *et al.*, 2004b) and without knowledge of the context, a prediction of overall outcome would be impossible. Despite these caveats a number of interesting predicted outcomes were obtained that fit with known phenotypes displayed by *Theileria* infected cells (pro-metastasis and pro alteration of cell shape, for example). Mining functional categories highlighted by this analysis should provide candidate novel pathways and genes that operate in establishment of the infected cell. Two example categories are given below.

Cancer: This category showed significant enrichment for genes in the infection modulated LPS-dataset. Using the IPA knowledgebase, 60 genes (24%) were placed in the cancer category with high statistical significance (p-value, 1.56E-05 –1.57E-02). These include, for example, pro cancer genes MMP13, SPARC, NDRG1, PAK1, ICAM1, ANGPT4, IL2RB, RGS1, SELL, SERPINE2, CCR7, CTTN, LTB4R, SLC2A1 and TP73 which are expressed at significantly higher levels in parasite infection relative to BL20-LPS and are known to be involved in carcinoma, metastasis, tumourigenesis and malignant tumor conditions [reviewed in (Dummler *et al.*, 2009;Rosette *et al.*, 2005;Tai and Tang,

2008;Yamaguchi and Condeelis, 2007) and (Balbin *et al.*, 1999;Buchholz *et al.*, 2003;Elnemr *et al.*, 2003;Jiang *et al.*, 2010;Mannori *et al.*, 1995;Stiewe and Putzer, 2002)]. Interestingly the majority of these pro cancer genes and a significant proportion of cancer genes identified (21) were grouped in a distinct expression profile (profile 6; see Figure 4.18). Since this profile shows significant elevation of expression associated with infection but repression of expression associated with LPS stimulation of BL20, it can be postulated that they are likely to be involved in establishing the transformed infected TBL20 cell phenotype and possibly the loss of proliferation potential displayed by LPS stimulated BL20.

An example of an identified pro cancer gene is MMP13, which was found to be robustly up-regulated (54-fold) in TBL20 cells relative to BL20 LPS. MMP13 is a member of the matrix metalloproteinases (MMPs), a large group of secreted proteinases. MMPs have been reported to be involved in a variety of physiological and pathological processes including tissue remodelling, angiogenesis, cell proliferation and regulation of tumor progression, tumor cell invasion and metastasis (Deryugina and Quigley, 2006;Folgueras *et al.*, 2004;Sounni and Noel, 2005). Furthermore, altered expression of MMPs at the protein and mRNA levels has been strongly correlated to poor disease prognosis in various human cancer studies (Kondratiev *et al.*, 2008).

Previous studies have reported induction of other types of MMPs (MMP9 and MMP2) as important mediators of the metastatic phenotype of *Theileria* infected leukocytes via *in vitro* or *in vivo* model systems (Adamson and Hall, 1997;Adamson and Hall, 1996;Baylis *et al.*, 1992;Somerville *et al.*, 1998a). Evidence of involvement of MMPs in the metastatic potential of *Theileria annulata* infected has also been provided in initial studies where *T. annulata* infected attenuated vaccine cell lines were found to exhibit reduced MMP9 with a concomitant reduction in metastatic potential (Adamson *et al.*, 2000;Hall *et al.*, 1999). An association of high MMP13 production in low passage *Theileria* infected cell lines has been recently reported (Habibi *et al.*, 2009).

Intercellular adhesion molecule-1 (ICAM-1/CD54) is another gene whose expression is elevated at higher levels (12-fold) in TBL20 cells relative to BL20-LPS. ICAM-1 is a transmembrane glycoprotein and a member of the immunoglobulin supergene family. Although ICAM1 is known to play an important

role in the immune response (Yockell-Lelievre *et al.*, 2009), it has also been implicated to play a role in cancer metastasis and can illustrate tumor prognosis and progression in several types of cancer (Huang *et al.*, 2004;Li *et al.*, 1997;Lin *et al.*, 2006). It has been known for some time that infection and transformation of bovine cells with *T. annulata* generates alteration at the infected cell surface including the appearance and loss of specific polypeptides (Shiels *et al.*, 1989). A study on altered surface marker expression in *T. annulata* was performed where attempts were made to characterise a novel surface glycoprotein of 125 kDa. Peptide sequencing results indicated sequence homology with human ICAM-1(Dando, 1997).

Recently Jensen *et al.*, (2008) have also shown that mRNA expression level of ICAM-1 is up-regulated following infection of monocytes with *T. annulata* infected cells. In addition it was shown that while the level of ICAM1 mRNA was similar in infected monocytes derived from disease susceptible (Holstein) and disease resistant (Sahiwal) breeds at 2 h post infection the level of mRNA was significantly reduced in Sahiwal-derived monocytes at 72 h post infection.

Expression of the ICAM-1 gene is regulated by NF-κB (Chen *et al.*, 2001;Voraberger *et al.*, 1991), and IPA canonical and custom pathway analysis identified ICAM1 as an infection modulated NF-κB signaling response genes. Therefore it is possible that modulated ICAM-1 in different breeds could be due to differences in the level of NF-κB activation or a qualitative difference in a parasite dependent mechanism that modulates the expression of NF-κB target genes. Interestingly NF-κB regulated expression of ICAM-1 has also been shown in other apicomplexan parasite system, *Plasmodium falciparum*; elevated expression of ICAM1 occurring in human brain microvascular endothelial cells in response to exposure to *Plasmodium falciparum*-infected erythrocytes (Tripathi *et al.*, 2006).

Expression of ICAM-1 is known to have crucial role in cell–cell contact and cell–matrix adhesion and is associated with contact-mediated immune responses (Boyd *et al.*, 1988). The significance of ICAM-1 expression in the pathogenesis of *Theileria* infection is not clear. However, studies on *T. parva* have shown that continuous proliferation requires surface stimulation mediated via cell-cell contact (Dobbelaere *et al.*, 1991a) and it is possible that ICAM-1 plays a role in

this process (Boyd *et al.*, 1988) as well as recruitment of and interaction with cells of the immune response. Further investigations are required to characterise the role ICAM-1 expression in determining establishment and virulence of the *T. annulata* infected cell.

Secreted protein acidic and rich in cysteine (SPARC/Osteonectin/BM-40) is another interesting gene found to be up-regulated by 53-fold in *Theileria* infected cells relative to BL20-LPS (placed in profile 6). SPARC is a matricellular protein that influences cell-matrix interactions and has been reported to have multiple functions playing a role in immune evasion, inflammatory processes cell morphology, Inhibition of cell cycle progression and synthesis of the extracellular matrix (Bradshaw and Sage, 2001;Rempel *et al.*, 2001;Rittling and Chambers, 2004). In addition to its normal physiological role, SPARC has been correlated with cancer progression, as many cancer types exhibit increased SPARC levels upon invasion or metastasis (Massi *et al.*, 1999;Podhajcer *et al.*, 2008;Yamashita *et al.*, 2003). Furthermore, SPARC is well established to have pro-invasive activity and is known to alter the process of transformation related to tumor-host interaction (Fenouille *et al.*, 2011c).

Recent studies have implicated an interesting connection between expression of SPARC and the tumour suppressor p53 in melanoma cells (Fenouille *et al.*, 2011b). Essentially these studies showed that SPARC can act as an anti-stress factor by inactivating p53 through Akt-mediated MDM2 phosphorylation to promote melanoma cell survival. SPARC, PI3K/AKT has also been shown to be a potent pro-survival pathway that contributes to the malignancy of gliomas and in this system SPARC may mediate survival through increased AKT and decreased caspase 3/7 activity (Shi *et al.*, 2004). Whether SPARC could play a related role in *Theileria* infected cells is unclear, but worthy of consideration. The acquisition of a survival pathway promoting resistance to apoptosis is a characteristic feature of *Theileria* infected cells and has been linked to constitutive activation of both NF-κB and PI3-K/AKT pathways (Baumgartner *et al.*, 2000;Heussler *et al.*, 2001). The prediction from the findings of Fenouille *et al.* would be that if SPARC operated in a similar manner in *Theileria* infected cells, p53 protein levels would be reduced due to elevated degradation promoted by MDM2. Interestingly findings by the Glasgow group indicate that while levels of p53 mRNA are high, protein levels are virtually undetectable in *T.*

annulata infected cells (Shiels and McKellar unpublished) and similar results implicating a role for MDM2 and constitutive degradation of p53 have been obtained by Yashida et al (personal communication). p53 has been implicated in repression of SPARC expression via tumor protein 53 induced nuclear protein 1, TP53INP1 (Seux *et al.*, 2011). TP53INP1 expression is down regulated in *Theileria* infected cells relative to LPS stimulated BL20 (profile 2). Moreover SPARC is identified in my study as an elevated NF-κB response gene (see Figure 4.28) and has previously described as a c-Jun-responsive target gene (Briggs *et al.*, 2002). Thus, it would appear that the infected cell promotes expression of SPARC and further investigation of the role of this oncogenic protein in establishment of the transformed phenotype is warranted.

Additional genes that could promote a cancer phenotype of the *T. annulata* infected cell include NDRG1, ANGPT4, CCR7, XCL2 and CCL1. These genes have not been previously associated with the infected cell but were expressed at significantly higher fold differences relative to uninfected BL20-LPS. Overexpression of NDRG1 has been reported in different human prostate, breast and colon cancers and renal cell carcinomas (Cangul, 2004;Caruso *et al.*, 2004;Nishie *et al.*, 2001). Similarly, ANGPT4 has been implicated in promoting tumor cell progression by enhancing viability and angiogenesis in human glioblastoma (Brunckhorst et al., 2010). In summary, the microarray results strongly suggest an association of parasite infection in acquiring a cancer like cell phenotype. Identification of novel candidate genes and potential pathways will help to provide more detailed understanding of how the parasite manipulates the infected cell to achieve this state.

Cellular assembly and organisation: IPA significantly identified 17 genes in the infection-modulated dataset categorised as involved in cellular assembly and organisation. Genes belonging to this functional category were found to be distinctly up-regulated by parasite infection. Interesting genes include CTTN, SDC4, ICAM1, PAK1, ELN, SPARC, SORBS1, TNS1 and F2R that encode proteins involved in the formation of actin filaments and cellular protrusions, reorganisation of cytoskeleton, assembly of focal adhesion, size of lamellipodia and formation of podosomes (Barker *et al.*, 2005;Cosen-Binker and Kapus, 2006;Illes *et al.*, 2006;Longley *et al.*, 1999;Papakonstanti and Stournaras, 2002;Robinet *et al.*, 2005;Webb *et al.*, 2005;Webb *et al.*, 2006;Yang *et al.*,

2006). *Theileria* infection is known to alter the morphology of the infected host cell (Baumgartner, 2011b;Schneider *et al.*, 2007;Shiels *et al.*, 2004) and it has been postulated that changes to the cytoskeleton impact on parasite dependent host cell activation and transformation status (Schmuckli-Maurer *et al.*, 2010). However the mechanisms and molecules underlying these changes are not understood completely.

Recent elegant studies performed by Baumgartner (2011b) have shown that parasite dependent polarisation of actin based structures are critical for both attachment to substrates and motility [reviewed by (Baumgartner, 2011a)]. Thus Baumgartner (2011b) showed that *T. annulata* infection promotes alterations to the actin cytoskeleton of macrophage to regulate adherence and cell motility via enhanced podosomes and lamellipodia formation. Cell movement involves a sequential process that requires cell protrusions at the leading edge and retraction at the trailing edge of the cell, and the actin cytoskeleton plays a critical role in both processes. Furthermore polarised infected cell morphology is characterised by the formation of actin-rich single lamellipodium and cortactin-rich podosome type-adhesions (PTAs). Modulation of host cell actin dynamics has also been linked to the virulent host cell phenotype (Chaussepied *et al.*, 2010) by demonstration of a difference in the TGF-b2 dependent invasive potential of *Theileria*-transformed cells derived from disease resistant and susceptible cattle, and a cell line with an attenuated virulence profile. Thus, *Theileria* infected disease susceptible macrophages were found to exhibit increased actin dynamics in their lamellipodia and podosomal adhesion structures and develop more membrane blebs. Molecules thought to function in regulation of these structures include the Src kinase, Hck; the Rho kinase, ROCK, cortactin and ERM proteins [Reviewed by Baumgartner, 2011a).

The finding that expression of the cortactin (CTTN, also known as EMS1) and Hck genes are up-regulated at higher levels (4.4-fold and 6.3 fold, respectively) in TBL20 cells relative to BL20-LPS (profile 1) is, based on the above studies, likely to be of importance to regulation of cell shape. This difference for cortactin was even higher (25-fold) in TBL20 when compared to BL20 cells. CTTN has been shown to enhance lamellipodial persistence and the rate of adhesion formation in lamellipodia, consistent with an important function in regulation of directed cell motility (Bryce *et al.*, 2005). Modulation of cell motility and cell adhesion is

also believed to be an essential phenomenon for metastasis and arises as a result of changes in the cytoskeletal architecture (Yamaguchi *et al.*, 2005). Over expression of cortactin has been reported to promote contact and communication between the cell and the extracellular environment by modulating the clustering of ICAM1 and selectin receptors on endothelial cells in order to promote adherence of leukocytes at the site of inflammation (Barreiro and Sanchez-Madrid, 2009;Tilghman and Hoover, 2002). All of these molecules (CTTN, ICAM1 and SELL) were expressed at an elevated level in infected cells in my study (all profiled 1, enhanced elevation), and RT-PCR results successfully validated the microarray data (see Figure 4.9). Interestingly in line with previous findings in other cellular models (Barker *et al.*, 2005;Longley *et al.*, 1999;Robinet *et al.*, 2005), the array data identified additional up-regulated genes SDC4, PAK1, ELN and SAPRC that have potential roles in altering host cell cytoskeletal dynamics in the *Theileria* infected cell.

The gene "PAK1" encoding the p21 protein (Cdc42/Rac)-activated kinase 1 (family member of serine/threonine p21-activating kinases) was significantly up-regulated (>22 fold) in *Theileria* infection compared to BL20-LPS (profile 6) the elevation profile being confirmed by semi-quantitative RT-PCR (see Figure 4.19). Pak1 has been reported to have a number of functions including cell survival and motility, proliferation, and has been implicated in cell transformation and tumor progression (Huynh *et al.*, 2010). Furthermore, the role of Pak1 in coordinating the dynamics of the actin and microtubule cytoskeletons during directional motility of cells, cell-cell contact [reviewed by (Bokoch, 2003)] and formation of lamellipodias and filopodias (Crespin *et al.*, 2009) has been reported. It is also well known that cell-cell contact of *Theileria* infected T cells increases their proliferation (Chaussepied *et al.*, 2006;Dobbelaere *et al.*, 1991b) and the formation of actin-rich single lamellipodium and cortactin-rich podosome type-adhesions has been reported recently (Baumgartner, 2011b). Due to the function of Pak1 as a key molecule in the regulation of actin dynamics further studies are required to investigate the consequence of up-regulating this gene on the transformed phenotype of the *Theileria* infected cell. For example PAK plays a crucial role in formation of podosomes and membrane ruffles and can phosphorylate cortactin to regulate the dynamics of branched actin filaments (Webb *et al.*, 2006). More intriguingly, PAKs have been reported to activate

transcription factors associated with the *Theileria* infected cell: ATF2, c-Jun and NF-κB (Neumann *et al.*, 2006). Furthermore PAK1 also mediates signals through PI3K and Akt to sustain cell transformation.

Cellular defence and inflammatory response genes: A number genes associated with host cell defence responses against invading pathogens and the immune responses were identified in analysis of the microarray data. Many of the genes identified within this category are regulated by NF-κB, encoding proteins involved in signaling and regulation of transcription, as well as immune responses and defence mechanism pathways. Among these genes several cytokine and chemokine receptor genes were differentially expressed in TBL20 and BL20-LPS cells. These included genes encoding anti-inflammatory proteins (CCR7, CCL1 and XCL2) whose expression was associated with 15- to -54-fold enhancement in parasite infection versus LPS stimulated BL20. Modulated expression of the chemokine receptor CCR7 and other chemokines has also been reported during the early stage of infection with *Leishmania major* parasite in human dendritic cells *in vitro* (Steigerwald and Moll, 2005). Expression of CCL1 and XCL2 has been implicated as key players in cancer (Arya *et al.*, 2003). Genes encoding pro-inflammatory cytokines and chemokines whose expression was significantly down regulated by infection compared to LPS included CXCL10, CCL4 and IL15. CXCL10/IP-10 for example is a member of the chemokine family of cytokines and is induced in a variety of cell types in response to interferon gamma and lipopolysaccharide administration (Ohmori and Hamilton, 1990;Ohmori and Hamilton, 1995). Elevated expression of CXCL10 has been reported to inhibit the process of angiogenesis (Angiolillo et al., 1995) and reduced tumour angiogenesis (Sgadari *et al.*, 1996). Additionally, it has been reported that over expression of CXCL10 is involved in inhibition of proliferation process in variety of cell types including endothelial and melanoma cells (Feldman *et al.*, 2002;Luster *et al.*, 1995;Nagpal *et al.*, 2004;Romagnani *et al.*, 1999). Manipulation of chemokines/chemokine receptor expression is certainly an exciting area of research in the field of host-parasite interaction as expression of these factors can be used to either enhance or limit various cellular responses to infection. It is clear that the parasite interacts with and manipulates the immune and innate cellular defence responses. Further

investigation of the genes identified will provide greater insight into how the parasite avoids host defence mechanisms and stimulates them to cause disease.

4.4.5 Interpretation of pathways analysis and modulation of pathway response genes

The most significant pathways modulated by parasite infection were TNFR2, pattern recognition receptors, CD40, NF-κB, PI3K, LPS stimulated MAPK and interferon signaling pathways. Detailed exploration of individual pathways revealed that many of the transcripts identified were commonly associated with other pathways. Moreover, an event that is common to many of these pathways is the activation of NF-κB and the general implication is that the parasite infection of BL20 modulates signalling pathways associated with the inflammatory response relative to LPS stimulated BL20. Indeed the results of the study demonstrate that the *Theileria* parasite modulates the NF-κB at multiple levels. Firstly the parasite constitutively activates NF-κB by sequestration and activation of the IKK signalosome to its surface (Heussler *et al.*, 2002). This event may be aided by manipulation of the host actin cytoskelelton (Schmuckli-Maurer *et al.*, 2010) and involve elevation of PAK1 pathway genes (see above). Interestingly the microarray data generated little evidence for repression of the signalling pathway below the level of the activated signalosome: the repression of the IkB inhibitor (relative to LPS) would promote NF-κB activation. Secondly the parasite infected cell clearly represses expression of the gene encoding the TLR4, a major receptor that recognises extrinsic signals that activate NF-κB, (see chapter 3). Thirdly results from the custom pathway analysis indicate that infection relative to LPS stimulation modulates the response of NF-κB activation by either repression or elevating target gene expression. Thus a major premise of this study that the parasite infection modulates the outcome of activation is supported by the pathway analysis. The postulation that this modulation event is likely to be beneficial to the establishment of the infected cell is also indicated. For example, NF-κB response genes repressed in parasite infected cells showed enrichment by IPA for pro inflammatory response genes and pro differentiation of leukocytes.

Two genes included in the modulated dataset of NF-κB target encode molecules (ICAM-1 and VCAM-1) that have important functional roles in cellular adhesion and immune responses (Van and Mallard, 2001). Both genes were up regulated by LPS in uninfected BL20 and are known be regulated by immunomodulators, such as LPS and PMA and cytokines, including TNF-α (Bevilacqua, 1993;Carluccio *et al.*, 2007;Fakler *et al.*, 2000). Additionally, these molecules are known to contain sequences consistent with NF-κB and AP-1 binding sites (Dhawan *et al.*, 1997;Iademarco *et al.*, 1992;Lindner and Collins, 1996;Roebuck and Finnegan, 1999). Despite NF-κB being activated in both systems (TBL20/BL20-LPS), parasite infection was found to be associated with down-regulation VCAM-1(184-fold) but up-regulation of ICAM-1 (12-fold) when compared to BL20-LPS. At present it is not clear why parasite infection selectively modulates the expression of these two molecules. However, it is possible that activation of NF-κB alone is not responsible for the expression of these adhesion molecules. In fact, NF-κB-independent induction of VCAM-1 has also been reported in endothelial cells (Wolle *et al.*, 1996). Similarly differential expression of other host cell or parasite associated factor(s) could influence selective expression of these genes.

Repressed NF-κB target genes also included regulators of apoptosis. Several of these genes, CFLAR, CASP4, TRAF1 and WnT10B, up-regulated in BL20-LPS (repressed by parasite) are known to be involved in multiple biological effects on cells such as cell proliferation, cytokine production and cellular death response (Chang *et al.*, 2002;Henkler *et al.*, 2003;Mao *et al.*, 2010;Speiser *et al.*, 1997;Yoshikawa *et al.*, 2007;Zaitseva *et al.*, 2011) and include caspase gene family members CASP4 and CFLAR that are regulators of apoptosis (see table 4.12). The number of up regulated NF-κB response genes was too small for enrichment analysis, but did provide some interesting candidate genes e.g. SPARC (see above), ICAM1 and NDRG1.

NDRG1 was also mapped by the custom pathway analysis as a repression target of c-MYC. Constitutive activation of cMYC is known to occur in *Theileria* infected leukocytes and the data obtained in the present studies indicate a requirement for the parasite to maintain repression of these target genes. These include CFLAR, interferon regulatory factor 8(IRF8) and two inhibitors of the cell cycle (CDKN1A and CDKN2B) (Cazzalini *et al.*, 2010;Fournier *et al.*, 2004;Park and Lee, 2003;Satyanarayana *et al.*, 2008). In marked contrast to these genes, the N-myc

downstream regulated 1 (NDRG1) gene shows a significant elevation associated with parasite infection (profile 6), indicating a requirement for elevation of this cMYC repressed target. While NDRG1 has been associated with carcinogenesis (see above) elevation by the parasite infected cell is potentially counterintuitive. Thus NDRG1 has been proposed to be a suppressor of metastasis (Liu *et al.*, 2011) and has been found to operate as an attenuator of NF-κB activation (Hosoi *et al.*, 2009). However the function of NDRG1 can be strongly influenced by cellular context and has been linked to p53 dependent apotosis by some studies, while others have attributed pro-survival and anti-apototic functions [reviewed by (Kitowska and Pawelczyk, 2010)]. Interestingly, a role for NDRG1 at the spindle check-point of mitosis has been shown and it is thought to be important for maintaining correct microtubule functioning (Kim *et al.*, 2004a) and spindle formation. Recent work by the group of Dobbelare have shown an intricate relationship between the *Theileria* schizont and host cell mitotic and central spindles, dependent on recruitment and catalytic activity of host cell Polo-like kinase (von *et al.*, 2010). Further work investigating the role of NDRG1 in the relationship between parasite and host cell spindle would be of interest.

A further relevant pathway identified within the modulated dataset was PI3K/AKT. Of particular note, two cytosolic effectors or regulatory subunit (PIK3R5, and PIK3R6) of PI3K were identified to be up-regulated in parasite infection. PI3K/AKT is implicated in the process of proliferation and cell survival [reviewed in (Fresno Vara *et al.*, 2004;Hennessy *et al.*, 2005;Osaki *et al.*, 2004)]. Acquisition of survival pathways in promoting resistance to apoptosis is a characteristic feature of *Theileria* infected cells and has been linked to constitutive activation of the PI3-K/AKTpathway (Baumgartner *et al.*, 2000;Heussler *et al.*, 2001).

In summary, analysis of the microarray data presented in this chapter demonstrate that although the gene expression profiles of LPS stimulated uninfected BL20 and infected TBL20 cells significantly overlap, parasite infection promotes a major reorganisation of gene expression associated with cellular activation. Moreover, the findings indicate that parasite infection can modulate the outcome of a host cellular activation state in a manner that is predicted to

be beneficial for establishment and survival of the proliferating transformed cell.

Further work is needed to examine alteration of host gene expression at the proteomic level as well as test for predicted functional implication of altered expression. Investigations are also required to identify the mechanisms that the parasite utilises to manipulate the outcome of cellular activation. This is likely to involve a major reorganisation of host factors and chromatin states that regulate gene expression, as identified in a parallel microarray study conducted by Kinnaird *et al.,* (unpublished). However the export of polypeptides from the parasite that have the potential to manipulate gene expression could also be involved (Shiels *et al.*, 2004). Parasite encoded AT-hook DNA-binding proteins of the TashAT family have been implicated in altering gene expression in transfected uninfected bovine macrophage cells (Oura *et al.*, 2006). In addition, *Theileria* AT hook DNA binding protein SuAT1 (Shiels *et al.*, 2004) and secreted *Theileria* protein (TaSE) (Schneider *et al.*, 2007) has been identified as possible parasite regulators of host cell morphology. The work in the next chapter set out to investigate whether a TashAT2 gene could alter bovine gene expression in a related manner to parasite infection and manipulate the outcome of stimulation with inflammatory mediators.

Chapter 5

Global identification of modulated gene expression in a bovine macrophage (BoMac) cell line stably transfected with the *T. annulata* TashAT2 gene

5 Global identification of modulated gene expression in a bovine macrophage (BoMac) cell line stably transfected with the *T. annulata* TashAT2 gene

5.1 Introduction

In the previous chapter, it was established using a comparative microarray analysis approach that *T. annulata* infection imposes a remarkable level of control over host cell gene expression by modulating the outcome of a classical cellular activation response that is typically stimulated by inflammatory mediators such as LPS. An important question is how might the *Theileria* macroschizont stage achieve this degree of control over host cell gene expression? Increasingly, evidence points to multiple mechanisms that converge to promote a modulated activation status required for establishment, proliferation and dissemination of the parasite infected cell.

It is highly probable that significant modulation of host gene expression by apicomplexan parasites occurs via secretion of regulatory molecules into the host cell compartment. Within the Apicomplexa, predominantly in *Toxoplasma*, *Plasmodium* and *Theileria*, a number of proteins synthesised by the parasite have been located in the host cell (Luder *et al.*, 2009;Plattner and Soldati-Favre, 2008;Ravindran and Boothroyd, 2008;Saeij *et al.*, 2007) and data indicates that some interfere with the host cell signal transduction pathways. *Theileria* parasites are unique in that, unlike *Plasmodium* and *Toxoplasma*, they do not develop within a parasitophorous vacuole following invasion and the macroschizont membrane is in direct contact with the host cell cytoplasm (Shaw, 2003). It has been proposed that because of this fundamental difference in transport, control mechanisms engendered by apicomplexan secreted molecules are unlikely to be highly conserved (Ravindran and Boothroyd, 2008). In *T. gondii* infection it has been shown that parasite actively subverts host defence responses and co-opts various host cell processes. These processes have been shown to involve various

candidate parasite proteins secreted via the surface or from secretory organelles such as rhoptries, micronemes and dense granules into the host cell compartment during invasion process. Secreted molecules include protein phosphatase 2C (PP2C-hn) and rhoptry protein 16 (ROP16) both of which have been located to the host nucleus (Gilbert *et al.*, 2007;Ong *et al.*, 2010). Additionally, ROP16 has been reported to influence the activation of host signal transducer and activator of transcription (STAT) signalling pathways and expression of STAT target genes such as interleukin (IL)-12 (Saeij *et al.*, 2007). Since *Theileria* macroschizonts do not possess rhoptries, an orthologue of ROP16 could be considered unlikely to play role in maintaining the transformed host leukocyte.

Activation of NF-κB is central to the establishment of the *Theileria* transformed leukocyte and has been implicated in modulation of the host cell apoptosis and survival pathways in both *Toxoplasma gondii* and *Plasmodium* [reviewed in (Leiriao *et al.*, 2004) and (Nash *et al.*, 1998;Payne *et al.*, 2003)]. In *Theileria*, NF-κB is activated via aggregation of IKK complexes on the surface of the macroschizont (Heussler *et al.*, 1999;Heussler *et al.*, 2002) but evidence for this event was not obtained for *Toxoplasma* (Molestina *et al.*, 2003;Molestina and Sinai, 2005). Recently, a parasite derived protein; TpSCOP has been shown to be involved in the activation of NF-κB in *T. parva*-infected lymphocytes (Hayashida *et al.*, 2010), but the parasite molecule responsible for aggregation of the IKK signalosome at the parasite membrane is still unknown (Schmuckli-Maurer *et al.*, 2010).

Results obtained from chapter 4 showed a range of NF-κB target genes associated with cellular activation were differentially regulated in parasite infected cells. In *T.annulata* there is evidence that modulation of gene expression in the infected cell occurs by secretion of parasite encoded regulatory molecules that have the ability to localise to the host cell nucleus. *T. annulata* genome sequence data has identified a number of parasite genes that could function to manipulate the phenotype of infected cells (Pain *et al.*, 2005). Parasite polypeptides have been identified that are likely to be expressed on the surface of parasite or secreted into the host cell compartment. Some of these polypeptides have been described as potential

candidates for manipulators of gene expression and are known to possess signal peptides, nuclear localisation signals and DNA binding motifs. These are encoded by members of the TashAT and SuAT gene families (Shiels *et al.*, 2004;Swan *et al.*, 1999;Swan *et al.*, 2001;Swan *et al.*, 2003). Transfection of a construct expressing the *T. annulata* TashAT2 protein in uninfected bovine macrophages resulted in identification of a number of differentially expressed host genes by proteomic and RNA display analysis (Oura *et al.*, 2006). Although relatively small-scale, this analysis served to underpin the potential importance of parasite encoded TashAT proteins in manipulation of host cell gene expression.

The TashAT cluster of *T. annulata* contains seventeen contiguous genes, twelve of which encode proteins that are predicted to localise to the host nucleus (Pain *et al.*, 2005). Recent studies using comparative genomic analysis have also revealed that the TashAT and related *T. parva* TpHN gene clusters are probably specific to *Theileria* species that transform the leukocytes (Shiels *et al.*, 2006;Weir *et al.*, 2009). Experimental data obtained to date confirms that five TashAT parasite proteins are detected in the nucleus of infected leukocyte. In addition to localising to the host nucleus, members of TashAT family (TashAT1/3, TashAT2, and SuAT1) possess domains containing AT hook motifs that suggest the ability to bind DNA (Shiels *et al.*, 2004;Swan *et al.*, 1999) and TashAT1 and 2 have been experimentally shown to bind to AT-rich DNA sequences (Shiels *et al.*, 2004;Swan *et al.*, 1999;Swan *et al.*, 2001).

AT hooks are DNA binding motifs that show conservation in arrangement and sequence across multiple alleles of SuAT1, TashAT2 and TashAT3, implying they confer functional and target specificity (Swan *et al.*, 2001;Weir *et al.*, 2010). Interestingly AT hook motifs are also found in a range of DNA binding proteins including the mammalian High Mobility Group A (HMGA) family (Reeves, 2010). HMG proteins act as architectural elements by modulating chromatin structure and, therefore, regulating expression of large numbers of genes that control cell fate (Cleynen and Van de Ven, 2008;Reeves, 2001;Reeves, 2010). The majority of the HMG proteins are highly mobile, bind transiently to chromatin and compete with histone H1 for nucleosome binding

sites, thus loosening the nucleosomal structure to enable access of transcriptional regulators (Catez *et al.*, 2004;Garcia-Heras *et al.*, 2009). Furthermore, HMGA proteins can physically interact with a large number of proteins, including transcription factors such as NF-κB (p50/65), AP-1, ATF-2, IRF1, c-Jun, Oct-1, Oct-2A, PU.1 and NF-AT (Lewis *et al.*, 2001;Reeves, 2001;Thomas and Travers, 2001). Recently, other important molecular partners have also been discovered that suggest involvement of HMGA proteins in a variety of functions such as DNA replication and processing of RNA, as well as structural organisation and re-modelling of chromatin (Sgarra *et al.*, 2005). Over-expression of HMGA1 proteins has also been associated with certain types of malignant neoplasia and benign tumours (Catez *et al.*, 2004;Fedele *et al.*, 2001;Flohr *et al.*, 2003;Sarhadi *et al.*, 2006;Wood *et al.*, 2000;Wunderlich and Bottger, 1997) and may be a central event in oncogenesis (Resar, 2010;Wood *et al.*, 2000).

HMGA1/2 potentially controls expression of a wide range of target genes, including those encoding inflammatory mediators and cytokines (John *et al.*, 1995;Lin, 2006;Martinez *et al.*, 2004). Interestingly, TashAT2 bears three AT hook DNA binding motifs whose arrangement shows significant similarity to that in HMGA1 (Weir *et al.*, 2010), which is known as a co-regulator of inflammatory response genes including those targeted by NF-κB (Amiri *et al.*, 2006;Collins *et al.*, 1995a;Takamiya *et al.*, 2008;Yie *et al.*, 1997). The majority of these genes are positively regulated and their promoter regions contain multiple stretches of AT-rich sequence. Transcriptional activation may involve formation of 'enhancesosomes' which are multi-protein complexes containing HMGA/transcription factors. Likewise negative regulation of gene transcription by AT hook proteins may occur via inhibition of enhancesosome formation, possibly by preventing functional binding of critical transcription factors to their recognition sites in gene promoters (Reeves, 2001).

To date, functional analysis has shown that parasite polypeptides TashAT2 and SuAT1 can alter the morphology of transfected bovine cells. A small number of candidate response genes whose RNA and protein expression may altered in a similar way to that observed in parasite infected leukocytes have

been identified (Oura *et al.*, 2006;Shiels *et al.*, 2004). This small-scale analysis confirmed that members of the TashAT family should be considered prime candidates as modulators of infected host cell phenotype.

In summary, taking together the conclusive evidence of extensive modulation of inflammatory response gene expression, including targets of NF-κB in parasite infected cells presented in Chapter 4, and the evidence from previous studies where the functional role of TashAT2 protein was partly characterised, it was highly relevant to undertake a global analysis to identify the potential of TashAT proteins to alter bovine gene expression. Given the structural similarity to HMGA proteins, it was of particular interest to determine whether any of the differentially expressed genes might also be targeted by NF-κB or other transcription factors. The primary aims of the work presented in this chapter were as follows.

Objectives of this study

1. To use the available bovine microarray platform to perform a second microarray experiment to test the ability of a single member of the TashAT family, TashAT2, to function as a modulator of bovine gene expression, using a bovine cell line stably transfected with the TashAT2 plasmid.

2. To compare any TashAT2-altered dataset with the infection-modulated datasets (TBL/LPS-BL20 datasets) obtained in the previous chapter, to reveal host genes that may be manipulated by TashAT2 in the context of *T. annulata* infection.

3. To test the ability of TashAT2 to modulate altered gene expression induced by stimulation with an inflammatory mediator and compare any obtained dataset with the dataset representing infection-associated modulation of LPS induced gene expression obtained in the previous chapter.

4. To identify transcription factor (s) target genes, in particular NF-κB that may exhibit altered expression levels associated with to TashAT2

expression, and compare with the NF-κB target genes identified in infection associated datasets.

5. To perform Ingenuity Pathway Analysis of the TashAT2 manipulated dataset and compare with the results derived from the infection-associated datasets.

5.2 Methods

5.2.1 Cell lines and culture

Cell lines, BoMac-TashAT2 and BoMac-pCAGGS, used in this study were previously derived (Oura *et al.*, 2006) by transfection of an SV40 transformed bovine macrophage (BoMac) cell line (Stabel and Stabel, 1995). BoMac-pCAGGS contains a control plasmid (pCAGGS) and BoMac-TashAT2, the same pCAGGS plasmid expressing the TashAT2 gene.

Also used in this study were stably transfected BL20_TashAT2, BL20_pCAGGS, D7-TashAT2 and D7-pCAGGS, cell lines which were previously generated in this laboratory (Shiels et al., unpublished) using the plasmids as described above. BL20 is the previously described uninfected bovine lymphosarcoma (BL20) cell line (Chapters 2 and 3), and D7 is a *T. annulata* (Ankara) infected cloned cell line (Swan *et al.*, 2003). Transfected BL20 and D7 cell lines were cultured as described in Chapter 2, except that the medium was supplemented with 250 µg/ml of Geneticin (Gibco; 1013-019). Transfected BoMac cells were cultured under similar conditions, except that 10% heat-inactivated foetal calf serum was used with 500 µg/ml of Geneticin. BoMac cell lines were maintained by trypsinisation followed by dilution into fresh medium twice per week.

5.2.1.1 pCAGGS-TashAT2 construct

Generation of the pCAGGS-TashAT2 construct, transfection protocol and selection of lines was carried out previously and fully described (Oura *et al.*, 2006) Briefly, the TashAT2 coding sequence with a V5 epitope tag was cloned into the vector pCAGGS-Bstx1 IRES Bgeo (pCAGGS), which contains an internal ribosomal entry site (IRES) immediately downstream of the gene of interest, followed by the neomycin resistance gene. Thus the TashAT2 gene and the neomycin gene are transcribed as one long mRNA from a single chicken ß-actin promoter with a human cytomegalovirus (CMV) immediate early enhancer. This construct was called pCAGGS-TashAT2 and guarantees

expression of the TashAT2 transgene following successful selection of a stably transfected cell line.

5.2.2 Stimulation of cells with inflammatory mediators

Cells in logarithmic phase (approximately 5×10^5 cells/ml) were stimulated either by adding LPS (Sigma; L2630) to a final concentration of 1µg/ml for 4h or phorbol myristate acid (PMA) (Sigma; P8139) at 10ng/ml for 6h. Following stimulation, cells were harvested for luciferase assays, immunofluorescence assay or total RNA isolation. Prolonged stimulation (24-72h) was also performed where necessary for cell viability and caspase assays.

5.2.3 Treatment of pCAGGS-TashAT2 transfected Theileria infected (D7) cells with BW720c

Buparvaquone treatment of D7-TashAT2 cells was carried out as described (Oura *et al.*, 2006). Cells at 1×10^5 /ml were incubated in the presence of 50 ng/ml of BW720c for either 48 or 72h, followed by immunofluorescence assays or isolation of RNA for RT PCR.

5.2.4 NF-κB dependent reporter assay (Dual Luciferase Assay) and PMA stimulation

The NF-κB dependent reporter assay was essentially performed as described previously in Chapter 3, section 3.2.3 except that following transfection of the reporter constructs, BoMac cells were cultured in $75cm^2$ flasks and stimulated with PMA for 6h.

5.2.5 Indirect immunofluorescence analysis

Cytospin preparation of cells and indirect immunofluorescence analysis (IFA) of TashAT2-transfected BoMac or BL20 cells was performed using the basic protocol described by Oura *et al* (2006). Approximately 2-3 x 10^5 cells were used per cytospin preparation and centrifuged at 1500rpm for 5 minutes (Shandon cytospin 2).

For detection of the anti-V5 tag, cytospin slides were immediately fixed in pre-chilled methanol at -20°C for 10 min followed by acetone for 1 min. Detection was achieved using monoclonal anti-V5 (Sigma; V8012) primary antibody at 1/500 dilution in complete medium for 1h at room temperature (RT). The Lim Domain Only 2 (LMO2) protein was detected by IFAT using fixed cells as above and monoclonal anti-LMO2 (1A9-3B11) (NB110-78626) (Novus Biologicals, USA) at a 1/100 dilution. Slides were then washed three times with PBS for 3min each. Alexa Fluor 488 goat anti-mouse IgG (Invitrogen; A-11029) was used as secondary antibody at 1/200 dilution and incubated for 1h at RT followed by washing in 1× PBS. After the final wash, cells were counter-stained with 0.1% Evan's blue for 1min, rinsed in 1× PBS and allowed to dry. Slides were then mounted in 10µl of mounting medium containing 50% glycerol in PBS, 4, 6-diamindino-2-phenylindole (DAPI) at 1µg/ml and phenylenediamine at 1mg/ml.

5.2.6 Giemsa stain analysis

Morphological assessment of TashAT2 transfected BoMac cells following PMA stimulation was carried out on Giemsa stained samples. Cells were grown in standard culture conditions on a sterile slide in a Petri dish. 24 or 48h post-PMA incubation, slides were air dried at room temperature for 10 min, fixed in absolute methanol for 20 min, dried at room temperature for 20min and stained in 4% Giemsa solution for 30 min. Finally the slides were rinsed in tap water for 5 min; air dried and examined using an Olympus BX60 microscope. Images were acquired by a SPOT camera and SPOT™ Advanced image software Version Mac: 4.6.1.26 (Diagnostic Instruments, Inc).

5.2.7 Cell proliferation, viability and caspase 3/7 assay

Estimation of cell numbers and viability following stimulation with PMA or DMSO was performed using Trypan Blue exclusion as described previously in chapter 3 (see section3.2.5). Each experimental condition: 24, 48 and 72h incubation with PMA (10 ng/ml) or DMSO (1µl/ml) as unstimulated control, was carried out in quadruplicate. Cell viability and caspase 3/7 activity were then measured as described previously in section 3.2.6 of chapter 3. Caspase

3/7 was measured as relative fluorescence unit (RFU) of PMA stimulated cells compared to DMSO-treated control cells in either pCAGGS-TashAT2 or pCAGGS transfected BoMacs.

5.2.8 Comparative microarray analysis of Gene expression in BoMac-TashAT2 and BoMac-pCAGGS cell lines

5.2.8.1 Total RNA Extraction, Clean-up and Quantification

Detailed methodology of RNA extraction, DNase 1 treatment, clean up and quantification is described in Chapter 3 (see Section 3.2.8 & 3.2.9).

5.2.8.2 Hybridisation and Analysis of Data

In order to globally identify expression changes in host genes due to the influence of TashAT2, RNA was prepared from BoMac-TashAT2 and BoMac-pCAGGS with and without PMA stimulation, as described in section 5.2.1-2. Total RNA Samples were prepared from three independent replicate cultures for each experimental condition. 30µg from each RNA preparation was submitted to Roche NimbleGen Systems for cDNA synthesis and hybridisation. Figure 5.1 illustrates the design of the microarray experiment and steps involved in the analysis of microarray data. Details of the microarray, hybridisation, processing of raw data, statistical analysis, Ingenuity Pathway Analysis and Monte Carlo simulation are described in section 4.2.

5.2.9 Validation by semi-quantitative Reverse-Transcription PCR (RT-PCR)

Gene expression changes observed in the microarray analysis were validated for selected genes by semi-quantitative RT-PCR followed by gel electrophoresis analysis of the PCR products. RT-PCR validation was performed using the same RNA samples prepared for microarray analysis. Methodology for semi-quantitative RT-PCR used was similar to that outlined in chapter 3. Details of gene specific primer sequences, GenBank accession

numbers, annealing temperature and length of predicted product are listed in Table 1.3, Appendix 1.

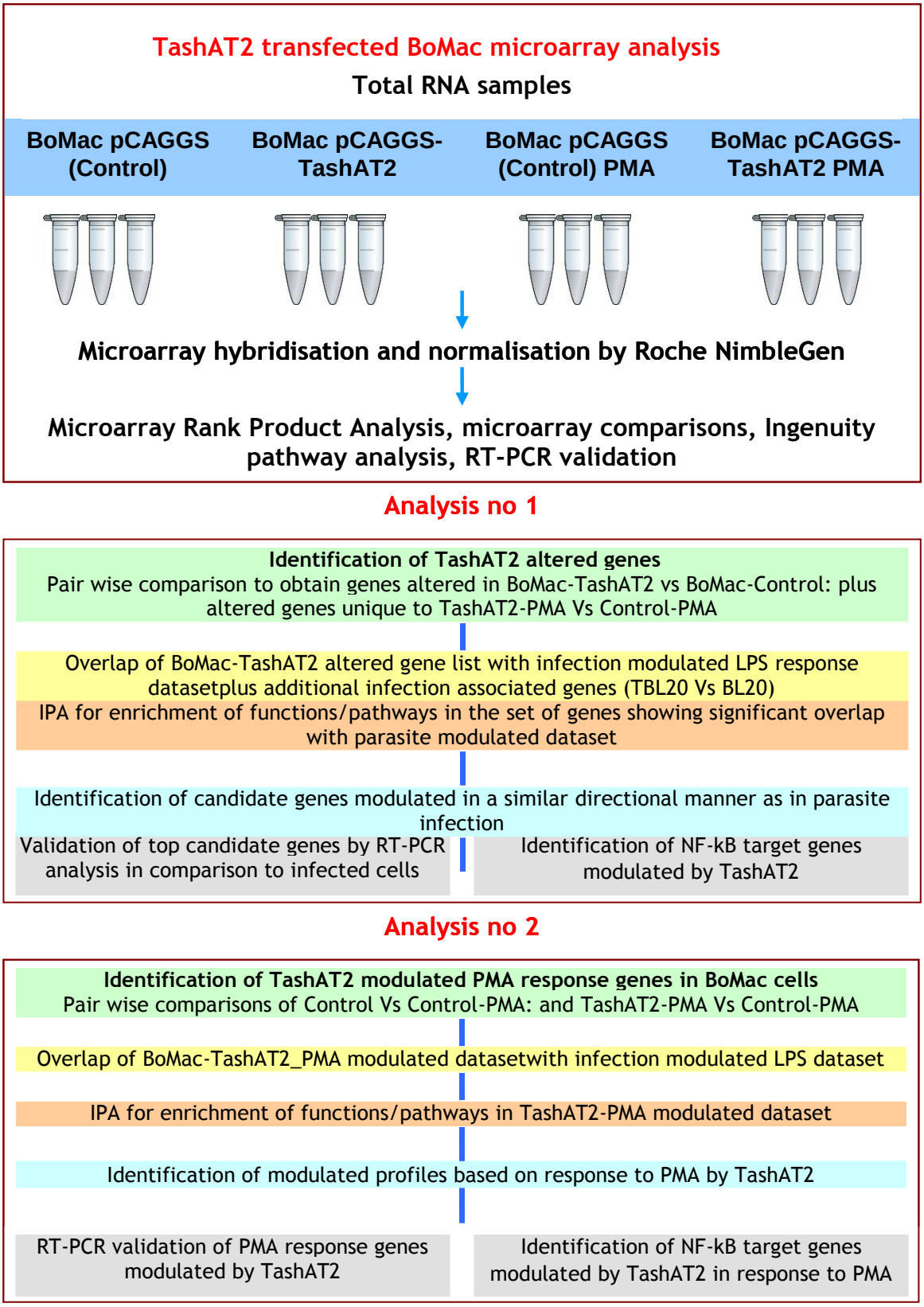

Figure 5.1: Schematic diagram illustrating microarray experimental design and the steps involved in data analysis
Total RNA was isolated from BoMac cells transfected with control (pCAGGS) or pCAGGS-TashAT2 construct; the cells were either stimulated with PMA or unstimulated.

5.3 Results

5.3.1 Validation of TashAT2 expression in BL20 and BoMac transfected cell lines

The gene expression analysis by microarray presented in the previous chapter was based on a comparison between the bovine lymphoid cell line BL20, with its *T. annulata* infected counterpart TBL20, under conditions of LPS stimulation. Experimental evidence has shown that TashAT2, a member of a parasite encoded family of DNA-binding proteins exported to the host cell, is involved in modulation of host cell gene expression. A BL20 cell line (BL20-TashAT2) stably transfected with the plasmid pCAGGS –V5_TashAT2 was available in the laboratory and was tested as to its suitability for use in a global microarray analysis. Unfortunately, immunofluorescence analysis using a monoclonal antibody to the V5 tag showed extremely weak fluorescence in the nucleus of the TashAT2-transfected BL20 cells (Figure 5.1 panels A & B).

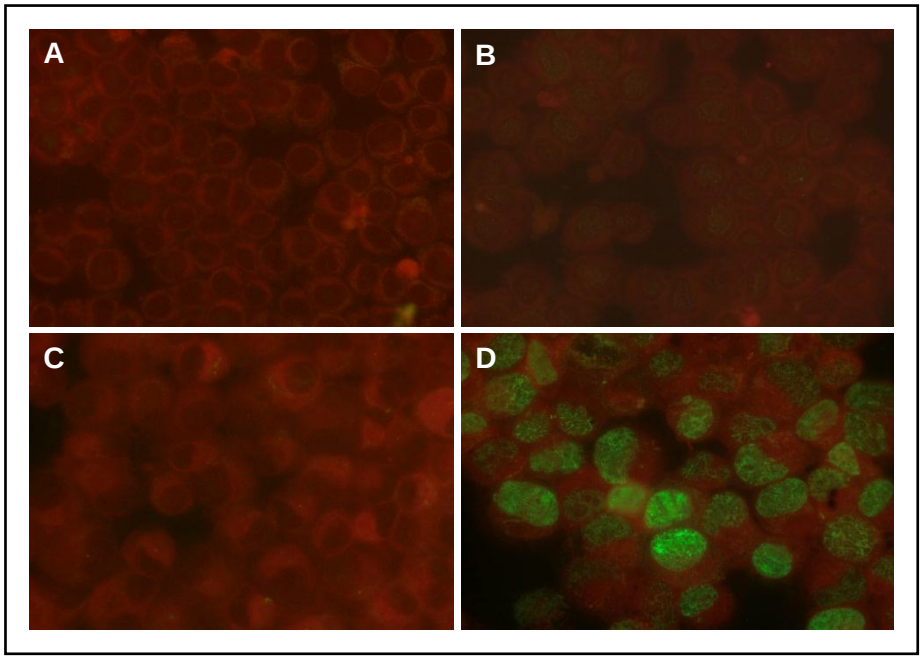

Figure 5.2: Expression levels of V5 tagged TashAT2 in the stable cell lines, BL20-TashAT2 and BoMac-TashAT2
TashAT2 expression was detected by immunofluorescence analysis using an anti-V5 monoclonal antibody. (A) BL20 transfected with pCAGGS (control) (B) BL20 transfected with pCAGGS-V5_TashAT2 construct. (C). pCAGGS transfected BoMacs (control) (D) pCAGGS-V5_TashAT2 transfected BoMacs

In contrast the previously reported (Oura *et al.*, 2006) transfected bovine macrophage cell line (BoMac-TashAT2) exhibited evidence of strong expression of V5 tagged TashAT2 in the nucleus (Figure 5.1 panels C and D) compared to a control cell line transfected with plasmid vector and was used for the remainder of the experimental work presented in this chapter.

5.3.2 Response of pCAGGS-TashAT2 transfected BoMac cells to cellular activation

In chapter three of the current study I compared the response of uninfected (BL20) cells and *Theileria*-infected (TBL20) cells under activated cellular conditions. The results clearly demonstrated that stimulation of uninfected cells with LPS was detrimental, resulting in cell death whereas *Theileria*-infected cells were refractory to LPS stimulation and continued to proliferate at the same rate as the unstimulated control. As an aim of the work performed in this chapter was to characterise the response of BoMac-TashAT2 cell line to cellular activation by microarray analysis, preliminary experiments were performed to assess the influence of inflammatory mediators (LPS and PMA) on TashAT2 transfected and control BoMac cell lines.

5.3.2.1 Influence of TashAT2 expression on NF-κB reporter activity in response to LPS and PMA stimulation

Activation of the transcription factor NF-κB is a central event in *Theileria*-infection of lymphoid cells. It was of major interest, therefore, to investigate the ability of TashAT2 to influence NF-κB activity. NF-κB dependent luciferase-reporter assays were performed to compare the levels of NF-κB activity between BoMac-pCAGGS (control) and BoMac-TashAT2 cell lines and following activation with either LPS or PMA. No difference in NF-κB reporter activity was found in non-stimulated BoMac cells expressing TashAT2 compared to the control (Figure. 5.3). In addition, when exposed to LPS, both control and TashAT2-transfected BoMac cell lines exhibited no significant increase in NF-κB reporter activity indicating that both cell lines were insensitive to stimulation by LPS. In contrast, significant elevation in NF-κB reporter activity was obtained for both control and TashAT2-expressing BoMac

cells when Phorbol myristate acid (PMA) was used for stimulation. Furthermore, PMA stimulation of BoMac-TashAT2 cells resulted in a much greater increase in NF-κB reporter activity compared to the control line. Therefore PMA stimulation was used to induce a cellular (NF-κB) activation state in all further experiments.

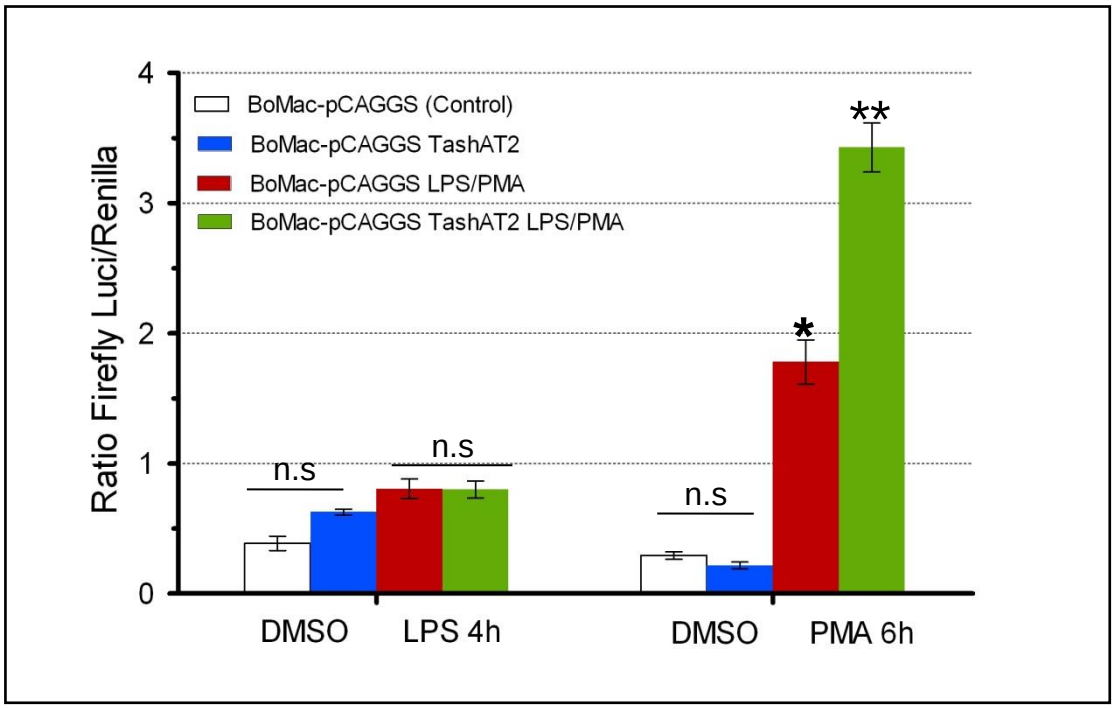

Figure 5.3: NF-κB-dependent reporter assays on BoMac cells expressing TashAT2 and control cells without treatment and following LPS or PMA stimulation.
Cells were either non-stimulated (DMSO) or stimulated with LPS (4h) or PMA (6h). **NF-κB** promoter activity was measured as the ratio of **NF-κB** Firefly luciferase/renilla activity (Mean ± S.E, n = 4). The asterisk (*) above the bars indicates the statistical significance of the results (Student's t-test, *P< 0.05, **P< 0.01) relative to control cells, whereas (n.s) indicates non-statistical difference of TashAT2 relative to pCAGGS controls in stimulated or non-stimulated conditions.

5.3.2.2 Differential growth response in pCAGGS and pCAGGS-TashAT2 transfected BoMac cells following PMA stimulation

Data presented in Chapter 3 demonstrated that stimulation of uninfected BL20 cells with LPS and constitutive activation of NF-κB, led to a loss in viability. *Theileria*-infected (TBL20) cells, despite having high NF-κB activity, were refractory to LPS induced cell death. To test whether expression of TashAT2 could influence the cellular activation response, the viability and proliferation of BoMac-TashAT2 cells compared to control cells was studied following PMA exposure for 24, 48, 72 hours. The results showed that growth potential of control cells stimulated with PMA at 24h was significantly

reduced, by 1.32-fold, relative to the unstimulated control (see Figure 5.4). This reduction in growth rate was even more pronounced (1.9-fold) by 72h of PMA stimulation. In contrast, TashAT2 transfected BoMac cells displayed no adverse effect when stimulated with PMA and continued to proliferate at the same rate as the untreated control (see Figure 5.4).

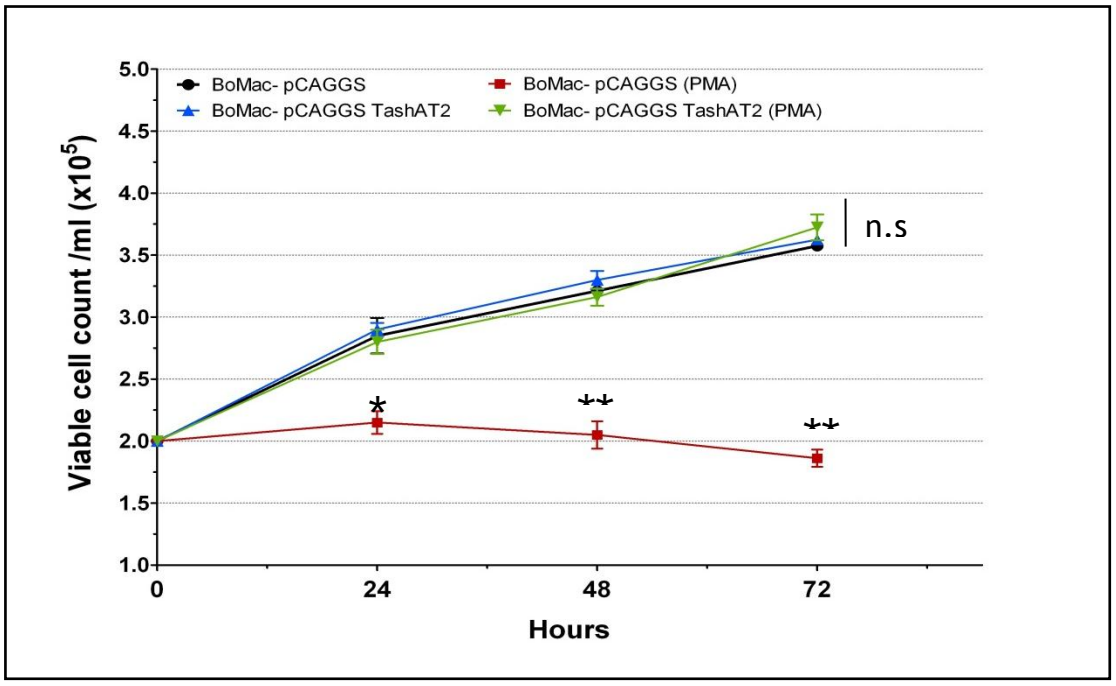

Figure 5.4: Proliferation assays of pCAGGS and pCAGGS-TashAT2 transfected BoMac cells following PMA stimulation relative to control cells.
Numbers of viable cells in control and BoMac-TashAT2 cultures growing in the presence of either PMA (10ng/ml) or the DMSO vehicle control (1µl/ml) were assessed using Trypan Blue exclusion at 24h, 48h and 72h exposure as described previously (3.2.5). Values are presented as Mean ± SE of four replicate cell cultures. The asterisk (*) sign associated with the data points indicate the statistical significance of the results (Student's t-test, *P< 0.05, **P< 0.01) of the data points relative to controls at given conditions.

In addition, this loss of growth was accompanied by a significant elevation in percentage of dead cells in the PMA stimulated control cells (see Figure 5.5) at 24h, 48 and 72 hours which was not seen in PMA- treated BoMAc-TashAT2 cells. A slight increase in the percentage of dead cells at 48 and 72 h was obtained in all cell lines but differences between controls and BoMac-TashAT2 PMA-treated cultures were not statistically significant and were considerably less than the level of cell death found for the PMA stimulated pCAGGS-transfected BoMac cells.

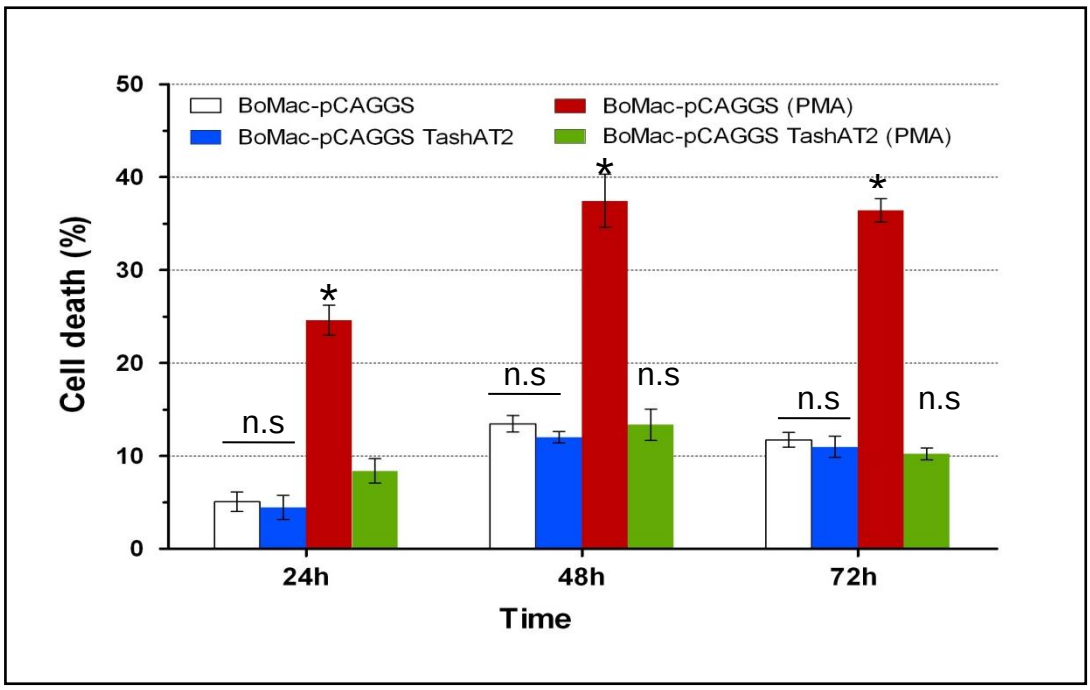

Figure 5.5: Estimation of cell death in pCAGGS and pCAGGS-TashAT2 transfected BoMac cells following PMA stimulation relative to untreated control cells.
Cells were cultured in the absence (DMSO) or presence of PMA (10ng/ml) for 24h, 48h and 72h. Cell death was measured using the Trypan Blue exclusion assay and is expressed as percentage of the total cell number for each culture. Values are presented as Mean ± SE of four replicate cell cultures. The asterisk (*****) above the bars indicates the statistical significance of the pair wise comparisons tested against the controls (Student's t-test, *P< 0.01) cells at given conditions. Whereas, n.s indicates statistically non-significant results in BoMac-pCAGGS TashAT2 (+/- PMA) relative to BoMac-pCAGGS (control) cells.

To confirm that TashAT2 expressing cells were resistant to cell death caspase 3/7 activity, a marker of apoptosis, was assayed using cell lysates obtained from the same cultures at 24, 48 and 72 hours. Significantly higher levels of caspase 3/7 activity was observed at all time points in BoMac-pCAGGS cells treated with PMA than in any of the other cultures (5.2, 3.8 and 2.4-fold increase compared to the untreated control at 24,48 and 72h respectively) (see Figure 5.6). This confirmed activation of the caspase cascade and initiation of apoptosis on stimulation with PMA in BoMac-pCAGGS cells and also that BoMac cells expressing TashAT2 were resistant to induction of apoptosis following exposure to PMA.

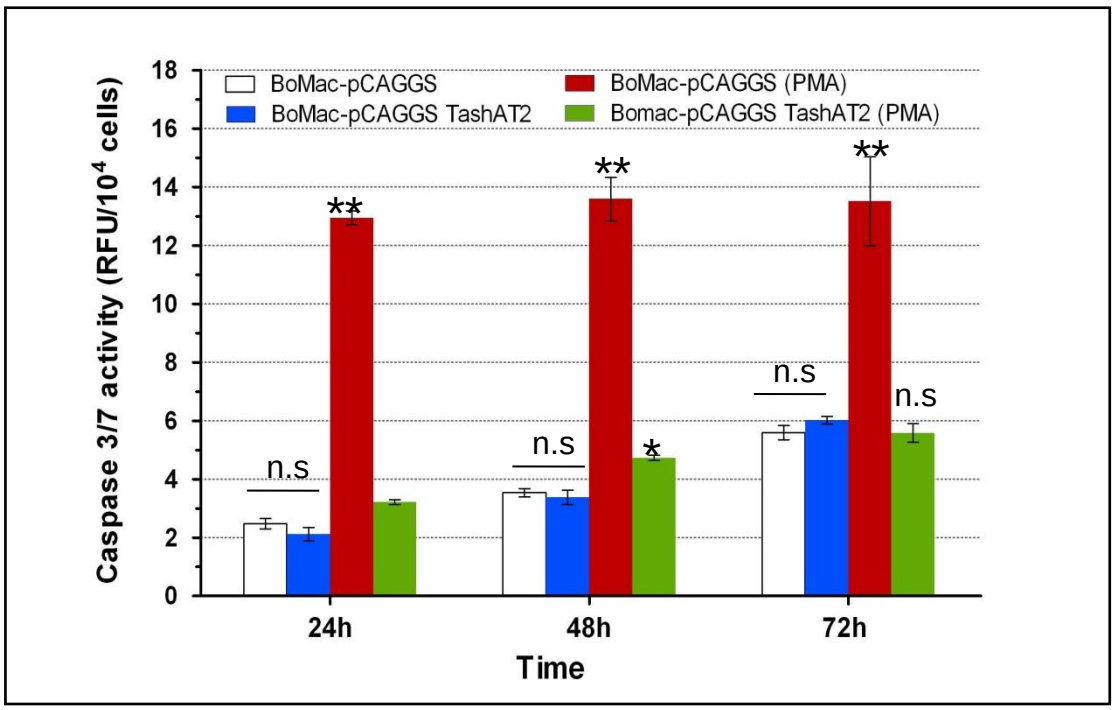

Figure 5.6: Caspase 3/7 activity assayed in BoMac-pCAGGS and BoMac-pCAGGSTashAT2 cells following PMA stimulation relative to unstimulated control cells. Caspase 3/7 activity was determined after incubation of cells in the presence of either PMA (10ng/ml) or the DMSO vehicle control (1µl/ml) for 24h, 48h and 72h. Results are expressed as relative fluorescence units (Mean ± SE, n = 4). The asterisk (*****) above the bars indicates the statistical significance of the pair wise comparisons (treated and untreated) tested against the controls (Student's t-test, *P< 0.05, **P< 0.01) cells at given conditions. Whereas, n.s indicates statistically non-significant results in BoMac-pCAGGS TashAT2 (+/- PMA) relative to BoMac-pCAGGS (control) cells.

5.3.2.3 Morphological assessment of BoMac-TashAT2 cells compared to BoMac-pCAGGS control cells following PMA stimulation

It was observed by Oura *et al.*, (2006) that the overall morphology of the BoMac-TashAT2 cell line was different from the control cell line; TashAT2 expressing cells tended to be slightly larger and more uniformly spread out with fewer cytoplasmic processes relative to pCAGGS control cells (see Figure.5.7, C and D). In this study, changes in the morphology were examined following exposure to PMA. Interestingly, Giemsa stain analysis of BoMac-pCAGGS cells when stimulated with PMA had typical morphological changes associated with apoptosis. These included cell shrinkage, reduction in cell volume, formation of cytoplasmic blebs and change from a rounded cell shape to a more elongated shape with extended cytoplasmic processes (see Figure 5.7, E) (Benjamin *et al.*, 1984;Hsu *et al.*, 1998;Malide *et al.*, 1998). In contrast, as shown in Figure 5.7, F TashAT2 expressing cells displayed little change in morphology when treated with PMA. Additionally, these results

suggest that the PMA-induced morphological alterations in the pCAGGS control cell line are associated with the detrimental outcome of cellular activation i.e. cell death.

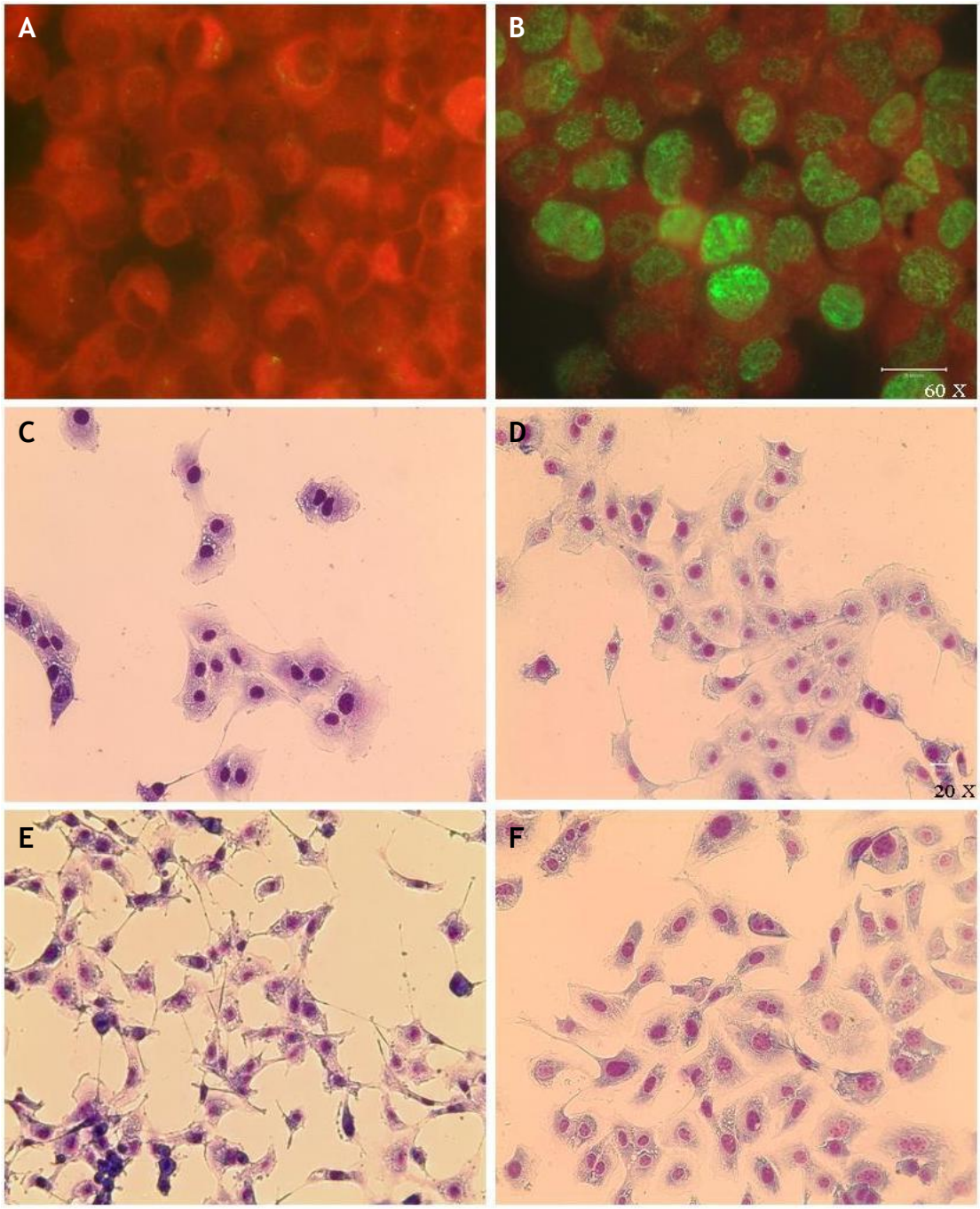

Figure 5.7: Morphological analysis of BoMac-pCAGGS (control) and BoMac-TashAT2 following PMA stimulation.
Immunofluorescence analysis with anti-V5 monoclonal antibody of pCAGGS-transfected BoMacs (A) and pCAGGS-TashAT2-transfected BoMacs (B) confirming expression of TashAT2: Bar = 25 µm; Giemsa stain of BoMac-pCAGGS (control) cells (C), BoMac-TashAT2-cells (D) growing under normal culture conditions; Bar = 25 µm. Giemsa staining of control cells stimulated with PMA (E) and the TashAT2 expressing BoMac cell line stimulated with PMA (F): panel A-B, 60x and panel C-F 20x.

5.3.3 Microarray analysis to identify the influence of TashAT2 on BoMac gene expression

Microarray analysis was performed in order to test the ability of TashAT2 to function as modulator of bovine gene expression. RNA was prepared in triplicate from cultures of unstimulated BoMac-pCAGGS and BoMac-TashAT2 cell lines and also following PMA stimulation for six hours. Array hybridisation and normalisation of the dataset was performed by Roche-NimbleGen as described in Chapter 4 and similar statistical analysis approaches were adopted as described in chapter four (see section 4.2.1.7.1). A number of pair-wise comparisons were undertaken: BoMac-pCAGGS Vs BoMac-TashAT2; BoMac-pCAGGS_PMA vs BoMac-TashAT2_PMA; BoMac-pCAGGS Vs BoMac-pCAGGS_PMA. Differentially expressed genes were identified using Rank Product analysis applying the criteria of a fold change $\geq$ 2, and FDR < 0.05.

5.3.3.1 Differentially expressed genes identified from pair-wise comparisons

The summary data from the various pairwise comparisons obtained from this Rank Product analysis are shown in Table 5.1. In the first pair wise comparison, BoMac-pCAGGS (control) vs pCAGGS-TashAT2, a total of 3,734 genes were differentially expressed and similar numbers of up-regulated and down-regulated genes were identified. The highest fold changes observed amongst the up-regulated genes was for cadherin 2 (CDH2) which showed a fold change of 598 and for down-regulated genes, matrix metallopeptidase 14 (MMP14) showed a -366 fold change.

Similarly a large number of genes (3,927) were altered in the BoMac- TashAT2 line relative to the control when both cell lines were treated with PMA. As in the non-PMA treated dataset, the highest up-regulated fold change observed in TashAT2 PMA-treated dataset was also that of cadherin 2 (CDH2) showing 785-fold difference. In the gene set that was down-regulated in PMA-treated TashAT2 cells, the greatest fold change was observed for the transcription factor ERG; v-ets erythroblastosis virus E26 oncogene homolog (avian) which exhibited a massive -511 fold change in expression level.

In the third pairwise comparison, PMA response genes were identified in BoMac cells by comparing unstimulated BoMac-pCAGGS cells with the same cells under PMA stimulation. A total of 1,177 PMA response genes were identified in BoMac cells and of these 690 genes were up-regulated and 487 genes were down-regulated (see Table 5.1). Here, the gene showing the greatest down-regulation (-19 fold) was chemokine (C-X3-C motif) ligand 1 (CX3CL1) while the gene showing the greatest up-regulation (109 fold) was an un-annotated bovine clone (CO884224) representing an identified bovine EST (Jensen *et al.*, 2006a) sequence.

Table 5.1: Summary statistics for all the pair wise comparisons undertaken in this microarray analysis

Comparison	Largest Fold Change (Absolute)		No of Up-regulated genes	No of Down-regulated genes	Total no of gene
	Up	Down			
1. BoMacs pCAGGS-TashAT2 vs BoMacs pCAGGS	598	-366	1884	1850	3734
2. BoMacs pCAGGS-TashAT2 PMA vs BoMacs pCAGGS PMA	785	-511	2001	1926	3927
3. BoMacs pCAGGS PMA vs BoMacs pCAGGS	108.8	-19	690	487	1177

Differentially expressed genes identified using Rank Product Analysis (≥ 2 fold change and FDR < 0.05) and selected for further analysis.

The pCAGGS (control) vs pCAGGS-TashAT2 dataset was compared with the dataset of the same cell lines stimulated with PMA revealing a large number of commonly altered genes (n = 2,804) (Figure 5.8). These results indicate that a large proportion of genes (40 %) altered in BoMac-TashAT2 cells were also differentially regulated in the pCAGGS control BoMac response to PMA. In contrast, 60 % of the genes differentially expressed in BoMac-TashAT2 cells were also altered in TashAT2 expressing BoMac cells treated with PMA vs the PMA treated control. Overall, this suggests that while BoMac-TashAT2 cells have the ability to respond to PMA, many genes are already altered by expression of TashAT2. In addition, over 800 genes exhibited altered expression in BoMac-TashAT2 cells in response to PMA that are not normally sensitive to PMA stimulation. Although the majority of these were close to the threshold for statistical significance (755 genes), the remaining 128 showed large differences in fold change of expression in TashAT-PMA stimulated cells relative to all other cellular conditions.

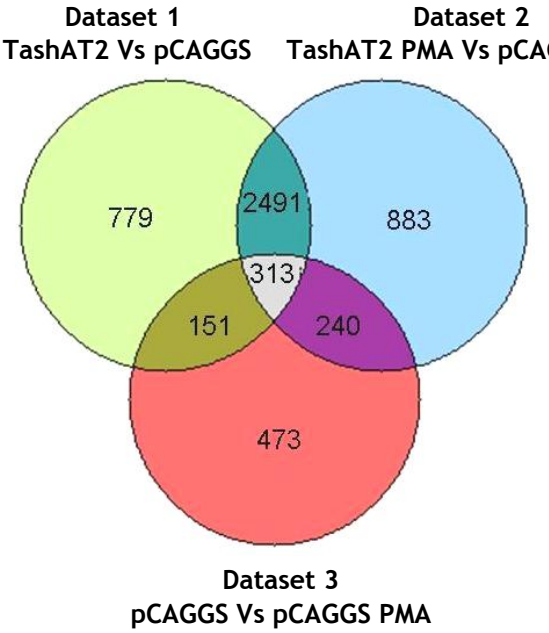

Analysis key

Datasets	Number of differentially expressed genes
1	3734
2	3927
3	1177
1 only	779
2 only	883
3 only	473
1 & 2	2804
2 & 3	553
1 & 3	464
1 & 2 & 3	313
1 & 2 only	2491
2 & 3 only	240
1 & 3 only	151

Figure 5.8: Commonly altered genes across experimental conditions
Total number of genes showing altered expression levels identified by pair-wise comparisons is shown by Venn diagram illustration. Numbers of genes for individual and intersecting datasets are shown in the table.

5.3.3.2 Identification of TashAT2 as manipulator of bovine gene expression

In order to identify putative TashAT2 target genes that are also modulated by infection, the gene set altered by TashAT2 expression in BoMac cells was compared with a combined TBL20-LPS modulated and TBL20 altered gene list (individual lists identified previously, see Chapter 3) to generate a global list of 4,280 parasite infection-LPS modulated candidate genes. In an attempt to identify TashAT2 modulated genes, all genes obtained for dataset 1 (see Figure 5.8) plus a further 1,123 (883 + 240) TashAT2 modulated genes unique to dataset 2 (Figure 5.8) were combined for a global list of 4,857 genes putatively altered by TashAT2 in the absence or presence of PMA. Comparison of the two datasets identified an overlapping subset of 1,206 genes (Figure 5.9). Using Monte Carlo simulation and Chi square analysis, it was determined that the size of the overlap was significantly greater than would be expected by chance ($p < 0.001$). A summary of the analysis used to estimate the significance of the overlap is shown in Figure 5.9.

Additional filtration was performed on the overlapping dataset of 1,206 genes to identify those that were altered by TashAT2 expression and by infection in a predictable manner (i.e. up in TashAT2 and up in parasite infection or vice versa). This process identified a subset of 466 genes which are listed in Appendix 3.1.

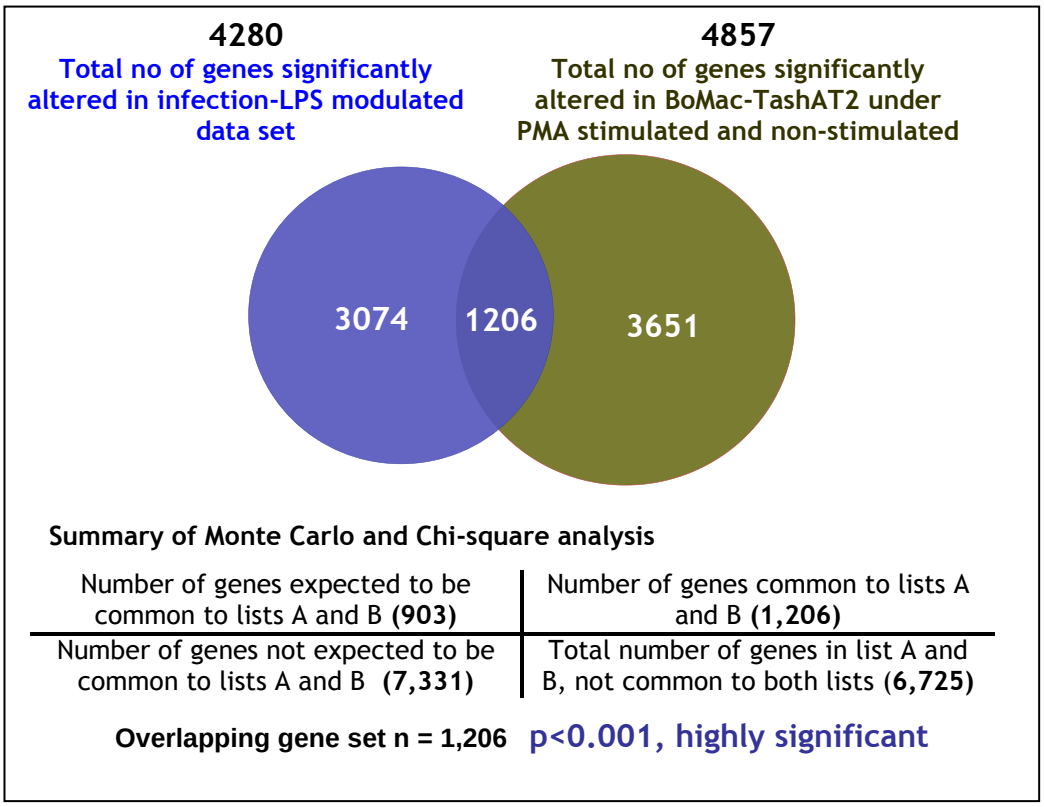

Figure 5.9: Comparison of differentially expressed gene sets
The lists of differentially expressed genes from the two global experimental datasets contained a set of 1,206 genes common to parasite infection and TashAT2-expressing BoMac cells. This overlap was found to be significantly larger than expected by chance alone ($p < 0.001$). A summary of the observations obtained from Monte Carlo simulation and Chi square analysis are also shown.

5.3.3.3 TashAT2 modulates gene expression profiles associated with *Theileria* infection

In the filtered dataset of 466 genes, expression of 353 genes was significantly repressed and 113 significantly elevated both by TashAT2 and parasite infection and are listed in Appendix 3.1.1 and 3.1.2, respectively. In the repressed gene set, 41 showed greater than ten-fold down-regulation in BoMac-TashAT2 when compared to pCAGGS control and also exhibited repression in infected (TBL20) compared to the uninfected (BL20) control. The 15 most down-regulated genes, ranked on expression difference between

BoMac-TashAT2 and BoMac-pCAGGS are listed in Table 5.2. For example, expression of the Microfibrillar-associated protein 2 (MFAP2) gene is highly repressed in BoMac-TashAT2 cells (fold change, -52.9); and also repressed by -22.5 fold in TBL20 cells relative to BL20 controls.

Table 5.2: Top 15 genes showing repression in BoMac-TashAT2 cells together with repression in TBL20 cells relative to BL20 cells or to the BL20 LPS response.

		TashAT2 transfected BoMac array results		Infection associated TBL20 array results		
Gene Symbol	Annotation	TashAT2 vs PCAGGS control Abs: FC	TashAT2 PMA vs Control PMA Abs: FC	TBL20 vs BL20	TBL20 LPS vs BL20 LPS Abs:FC (4h/or18)	BW720c Response
		↓	↓	↓	↓	
MFAP2	Microfibrillar-associated protein 2	-52.9	-68.4	-22.5	-8.6	↑
FAM20A	family with sequence similarity 20, member A	-31.3	-18.1	-21.3	-18.3	–
RAB15	RAB15, member RAS onocogene family	-17.5	-7.6	1.7	-5.0	–
KIF1A	Kinesin family member 1A	-11.9	-14.2	-23.7	-18.0	↑
RUNX2	PREDICTED: runt-related transcription factor 2	-11.6	-2.9	1.2	-5.7	–
TP63	tumor protein p63	-11.4	-3.6	1.9	-36.7	–
ANK1	Ankyrin 1, erythrocytic (ANK1), mRNA	-11.3	-10.1	-93.6	-82.9	↑
ANGPTL1	Angiopoietin-like 1	-9.6	-3.8	-8.7	-10.4	↑
MYOM1	Myomesin 1, 185kDa	-9.3	-2.9	-9.7	-8.3	↑
C1QTNF1	C1q and tumor necrosis factor related protein 1	-7.4	-8.5	-150.3	-69.5	↑
LOC520070	PREDICTED: Tumor endothelial marker 1,	-6.9	-6.0	-22.0	-13.9	–
IL18	interleukin 18 (interferon-gamma-inducing factor)	-6.7	-3.7	-10.4	-4.3	↑
LOC515697	Apolipoprotein L, 3-like (LOC515697), mRNA	-6.2	-9.4	-15.0	-11.8	↑
RASGEF1A	RasGEF domain family, member 1A	-5.5	-5.4	-6.2	-11.7	↑
BOLA-DOB	Major histocompatibility complex, class II, DO beta	-4.4	-3.7	-11.6	-27.6	↑

15 genes from the filtered overlap gene set of 353 that showed the greatest level of repression in BoMac-TashAT2 cells where the *Theileria*-infected BL20 cellular model showed a parallel profile. Data is arranged in descending order of absolute fold difference between BoMac-TashAT2 compared to BoMac pCAGGS. Bw720c indicates the direction of a buparvaquone response where present. Where expression was validated by semi-quantitative RT-PCR genes are highlighted in light blue.

Two other genes of note were identified in this group. Runt-related transcription factor 2 (RUNX2) and tumour protein p63 (TP63) were significantly repressed by 11.6 and 11.4 fold respectively in Bomac-TashAT2 relative to the control. Both also exhibited a significant degree of repression in parasite infection compared to control when stimulated by LPS.

The expression profiles of six genes MFAP2, RAB15, RUNX2, TP63, C1QTNF1 and IL18, from this group were validated by semi-quantitative RT-PCR. Thus,

for example, the gene encoding MFAP2 showed positive correlation of the RT-PCR results with the microarray profile, showing strong repression both in TashAT2 expressing cells and in *Theileria* infection relative to their corresponding controls. Similar supporting results were obtained for RUNX2 and TP63 mRNA where the RT-PCR analysis showed repression in Bomac-TashAT2 cells and in *Theileria* infected cells relative to their corresponding control cell lines (BL20_LPS for TP63) (see Figure 5.10).

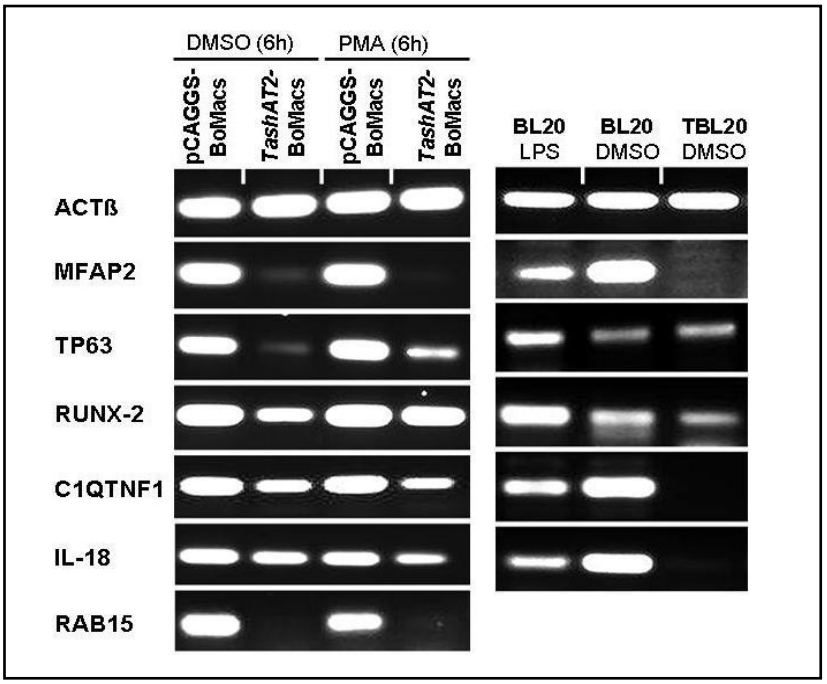

Figure 5.10: Semi-quantitative RT-PCR validation of microarray results for selected repressed genes in BoMac-TashAT2 cells compared to their profiles in the BL20-TBL20_LPS model

The RT-PCR expression pattern of MFAP2, TP63, RUNX2, C1QTNF1, IL-18 and RAB15 genes in BoMac-TashAT2 cells is shown in the left panel. The panel on the right represents RT-PCR results for the corresponding genes in TBL20 and BL20 cells (LPS +/-). ACTB was used as a constitutive standard.

113 genes had significantly elevated expression in BoMac-TashAT2 relative to the pCAGGS control and also showed elevated expression in *Theileria* infected cells when compared to BL20 cells either without or in the presence of LPS (LPS +/-) (see Appendix 3.1.2). 19 genes in this group showed an elevation greater than 10 fold and the top 15 are shown in Table 5.3. These included Von willebrand factor a domain containing 5a (VWA5A) elevated by 116 fold, Melanoma associated antigen (mutated) 1-like 1 (MUM1L1), 91 fold, Collagen type viii, alpha 1 (COL8A1), 74 fold, Thymocyte selection-associated high mobility group box (TOX), 64 fold and RasGEF domain family, member 1B

(RASGEF1B) by 5.8 fold. Furthermore, these genes also showed elevated expression in TBL20 relative to BL20 (LPS+/-) cells (Table 5.3).

Table 5.3: Top 15 genes showing elevation in BoMac-TashAT2 cells together with elevation in TBL20 cells relative to BL20 cells or to the BL20 LPS response.

		TashAT2 transfected BoMac array results		Infection associated TBL20 array results		
Gene Symbol	Annotation	TashAT2 vs PCAGGS control abs: FC	TahAT2 PMA vs control PMA abs: FC	TBL20 vs BL20 abs: FC	TBL20LPS vs BL20 LPS abs:FC (4h/or18)	BW720c Response
		↑	↑	↑	↑	
VWA5A	Von willebrand factor a domain containing 5a	116.3	199.8	31.5	33.2	–
MUM1L1	Melanoma associated antigen (mutated) 1-like 1	91.4	85.2	28.8	25.8	–
COL8A1	Collagen, type viii, alpha 1	74.9	100.6	5.0	3.2	↓
TOX	Thymocyte selection-associated high mobility group box	64.2	32.8	8.1	3.5	–
TMEM62	Transmembrane protein 62	61.8	50.9	22.8	65.5	–
PRSS23	protease, serine, 23	16.7	31.2	23.3	30.6	–
INPP4B	Inositol polyphosphate-4-phosphatase, type II, 105kDa	14.8	23.2	4.0	2.1	↑
ALDH1A1	Aldehyde dehydrogenase 1 family, member A1	10.5	112.8	14.0	64.4	↓
PDE3B	Phosphodiesterase 3B, cGMP-inhibited	9.1	11.7	3.0	2.3	–
SORL1	Sortilin-related receptor, L(DLR class) A repeats containing	8.9	6.5	4.1	18.5	↑
ZBTB20	Zinc finger and BTB domain containing 20	7.0	5.7	6.7	16.1	–
RASGEF1B	RasGEF domain family, member 1B	5.8	9.4	32.9	2.14	–
SERPINE1	Serpin peptidase inhibitor, clade E (nexin, plasminogen activator Inhibitor type 1), member 1	4.3	3.2	67.6	43.6	↓
RNASEL	Ribonuclease L (2',5'-oligoisoadenylate synthetase-dependent)	2.6	3.1	18.6	72.8	–
SLC6A6	Solute carrier family 6, member 6	2.4	2.3	55.6	8.3	↓

The top 15 genes whose expression is significantly elevated in BoMac-TashAT2 and in the *Theileria*-infected BL20 cellular model are shown. Data is arranged in descending order of absolute fold difference between BoMac-TashAT compared to the BoMac-pCAGGS (control). Bw720c indicates the direction of a buparvaquone response where present. Where expression was validated by semi-quantitative RT-PCR genes are highlighted in light blue.

Six members from this elevated group were validated by RT-PCR, and the results gave good correlation with the profile obtained by microarray. For example, genes encoding VWA5A, COL8A1, MUML and ALDH1A1 showed a clear elevation in the amount of PCR product in BoMac-TashAT2 cells relative to BoMac-pCAGGS control cells. A pattern of elevated expression was also observed for these genes in TBL20 cells when compared to BL20 (LPS+/-) cells (see Figure 5.11).

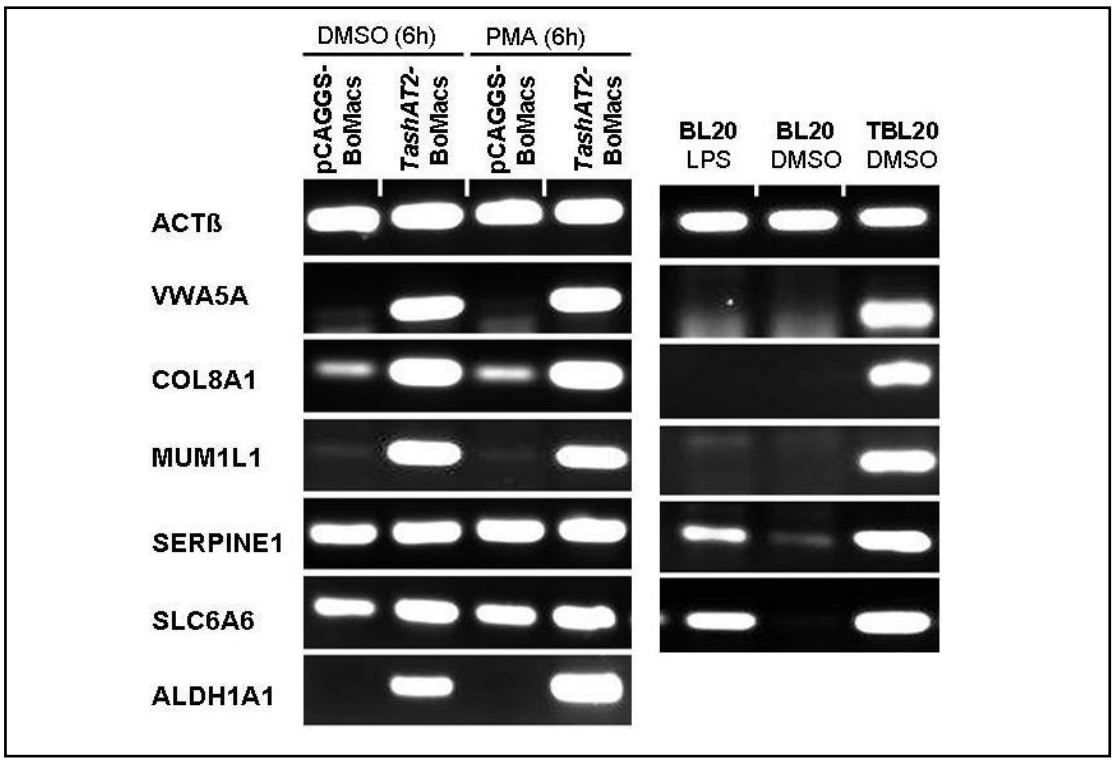

Figure 5.11: Validation of microarray results for selected up-regulated genes in BoMac-TashAT2 cells compared to their profiles in the BL20-TBL20_LPS model.
Semi-quantitative RT-PCR results showing the expression pattern of genes elevated in TashAT2-BoMacs and in *Theileria* infected TBL20 cells, relative to their respective controls. Panel on the left shows RT-PCR results of mRNA expression pattern of vWA5A, COL8A1, MUM1L1, SERPINE1, SLC6A6 and ALDH1A1 in BoMac-TashAT2 and BoMac-pCAGGS cell lines. Panel on the right shows RT-PCR results for the corresponding genes for TBL20 and BL20 (LPS +/-) cells. ACTB was used as a constitutive standard.

5.3.3.4 Ingenuity Pathway Analysis of the overlapping gene set identified for TashAT2 transfected BoMacs and *Theileria* infection.

Following identification of the common set of differentially expressed genes between the TashAT2 and infection-modulated global datasets, Ingenuity Pathway Analysis (IPA) was performed to identify potentially important biological functions and disease categories that could be associated with modulation of host gene expression by TashAT2/parasite infection. Thus, the dataset of 1,206 genes was uploaded to IPA software suite and analysis was performed to identify significant biological functions and disease categories, canonical and custom pathways, and target genes of selected known infection-associated transcription factors.

5.3.3.5 TashAT2 modulates set of genes enriched for important functional categories associated with *Theileria* infection.

Functional analysis of the dataset identified significant enrichment of genes for important biological function and disease categories. The statistical analysis used by IPA for determining the p-value for each functional category is discussed previously in Section 4.3.3.1. Important categories identified include; Cancer, Cell Death, Inflammatory Disease, Cellular movement, immunological disease, Cellular Growth and Proliferation, Cell-Cell-Signaling and Interaction, and Cell morphology (See Figure 5.12). The complete list of molecular functions and disease categories identified in TashAT2/infection modulated dataset is presented in Appendix 3.4.

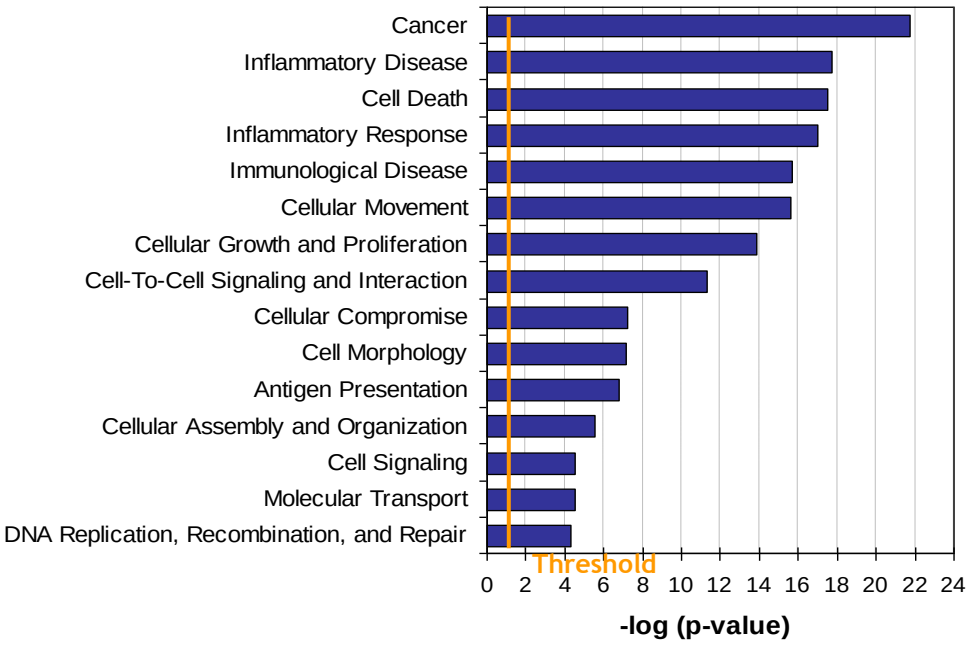

Figure 5.12: Selected key biological functions and diseases categories identified as significantly enriched by IPA in the TashAT2-modulated dataset
Biological functions associated with genes in the TashAT2-altered overlapping dataset of 1,206 genes are shown along the y-axis with the significance of the enrichment (–log transformed) denoted along the x-axis. Each bar represents –log (p-value) for the enrichment of genes in a category. The orange vertical line represents the threshold for significance (p-value = 0.05).

Interestingly most of the functional categories highlighted were also indentified in the IPA performed in Chapter 4 on the parasite modulated LPS dataset (TBL20-M-LPS). However, the significance of the enrichment for different categories differed between the two analysis with Cancer highlighted as most significantly enriched followed by inflammatory disease and Cell death for the TashAT2 IPA, while for the infection modulated LPS

dataset IPA order of significance was ‘Inflammatory Response’, ‘Tissue Morphology’, ‘Celular Development’, ‘Cellular Movement’, ‘Cell Death’, ‘Inflammatory Diseases’, ‘Cancer’ and so on (see Appendix 2.2 for the sequence of full analysis).

IPA was also performed on the subset of 466 TashAT2-modulated genes that show the same directional change of expression in response to parasite infection of BL20. The functional categories obtained by IPA for this subset was then compared to the analysis performed on the complete TashAT2/infection overlapping dataset of 1,206 genes, with the proportion of genes altered in each category being computed. Thus, it appeared that a greater percentage of genes were altered for the categories of Cancer (26.6%), Immune response (12%) and Cell morphology (12.2%) in the subset of genes relative to complete dataset (20.8%, 7.6% and 6.9% genes altered in these categories, respectively). A summary of the results is presented in Appendix 3.4. Many of the genes identified were placed in multiple categories within the IPA knowledge database. While this indicates a possible diverse functional role of these genes, it may hinder identification of the primary role that they may play in determining the phenotype of the TashAT2-transfected BoMac or parasite-infected TBL20 cell.

As highlighted above, the number of genes enriched in the category ‘Cancer’ was highly significant for the TashAT2-modulated and infection-modulated datasets. Important genes in this category included Aldehyde dehydrogenase 1 family, member A1 (ALDH1A1), Angiopoietin-like 1 (ANGPTL1), Apolipoprotein D (APOD), Bone marrow stromal cell antigen 2 (BST2), CD3g molecule, gamma (CD3G), Insulin-like growth factor binding protein 6 (IGFBP6), LIM domain only 2 (LMO2), Melanoma associated antigen (mutated) 1-like 1 (MUM1L1), Ribonuclease L (2',5'-oligoisoadenylate synthetase-dependent) (RNASEL), sphingosine-1-phosphate receptor 1 (S1PR1), Serpin peptidase inhibitor, clade E, member 1 (SERPINE1), Tumour protein 63 (TP63) and von Willebrand factor A domain containing 5A (VWA5A) (see Appendix 3.6).

Another interesting category modulated by TashAT2 and infection was 'Inflammatory response' which included genes placed in relevant sub-categories such as 'immune response','inflammation', 'phagocytosis of cell', and 'adhesion of phagocytes'. Important genes identified within this category included Interleukin 18 (IL18), Interferon regulatory factor 8 (IRF8), Inhibitor of kappa light polypeptide gene enhancer in B-cells, kinase epsilon (IKBKE), Interferon (alpha, beta and omega) receptor 2 (IFNAR2), Immediate early response 3 (IER3), Sphingosine-1-phosphate receptor 1 (S1PR1), Vascular cell adhesion molecule 1 (VCAM1) and Serpin peptidase inhibitor, clade E, member 1 (SERPINE1).

Enrichment of genes in the category 'Cell morphology' was also identified for TashAT2/infection-modulated dataset with a marked increase in enrichment for the subset of 446, where TashAT2-induced and infection-associated expression agree. Sub-categories identified were 'shape changes', 'morphology of cells', 'reorganisation of cytoskeleton' and 'ruffling'. Genes of particular interest are presented in Appendix 3.6 and included Cdc42 guanine nucleotide exchange factor (ARHGEF9), BAI1-associated protein 2 (BAIAP2), CD3g molecule, gamma (CD3G), chimerin 1(CHN1), LIM domain only 2 (LMO2), Nerve growth factor receptor (NGFR), Phosphodiesterase 3B, cGMP-inhibited (PDE3B) and Serpin peptidase inhibitor, clade E, member 1 (SERPINE1).

5.3.3.6 TashAT2 and *Theileria* infection modulate expression of genes in important canonical and custom pathways.

IPA analysis of the TashAT2/infection modulated common dataset also indicated enrichment of genes in important canonical and custom pathways. Important top ranking canonical pathways identified by IPA are shown in Figure 5.13; the full list of pathways along their –log (p-value) is presented in Appendix 3.5. Interestingly, identified pathways included 'Production of nitric oxide and reactive oxygen species in macrophages', 'Role of tissue factor in Cancer', 'G-Protein Coupled Receptor Signaling', 'TNFR2/1 Signaling', 'NF-κB Signaling', 'CD40 Signaling', 'NF-κB Activation by Viruses', 'PI3K Signaling in B Lymphocytes', 'LPS-stimulated MAPK Signaling' and 'apoptosis signalling'.

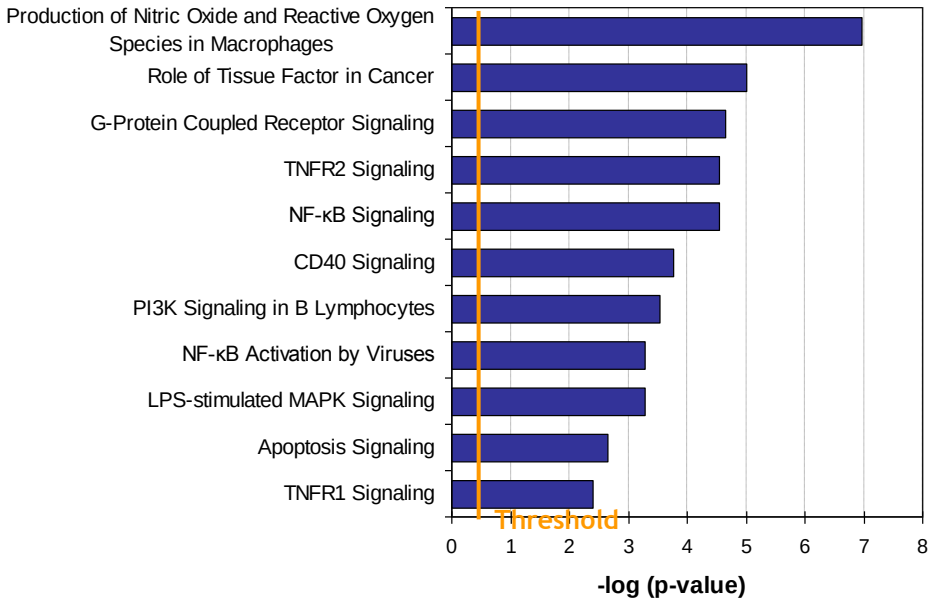

Figure 5.13: **Identification of top canonical pathways in TashAT2 modulated / infection-associated dataset**
Bar chart shows **selected** important canonical pathways enriched for genes modulated both by TashAT2 transfection and *Theileria* infection compared to LPS stimulation of BL20 cells. Each bar represents –log (p-value) for the enrichment of genes in a category. The orange vertical line represents the threshold for significance (p-value = 0.05).

To investigate whether TashAT2 could modulate the expression of genes that are targets of transcription factors known to be associated with *Theileria* infection, IPA was performed using a custom pathway library of known transcription factors targets. Interestingly, significant enrichment of gene targets of NF-κB (33 genes), AP-1 (06 genes), ATF-2 (05genes) and cMYC (03 genes) was obtained. Expression levels of 12 of the 33 NF-κB target genes were modulated by TashAT2 in a similar manner to the alteration associated with parasite infection (see Table 5.4). Functional categories associated with these NF-κB targets genes included chemokines (CCL5 and IL-8) predicted to be prime mediators of the inflammatory response; enzymes (TNFAIP3 and TGM2); growth factors (BMP and HGF); peptidases (MMP9 and ADAM19), transcription regulators (FOS and JUNB) and transmembrane receptors (CD3G, IL2R and TNFRSF1B).

Table 5.4: NF-κB target genes set commonly altered/ modulated in TashAT2 transfected BoMacs and *Theileria* infection

	Gene Symbol	Annotation	TashAT2 altered/ modulated response	Infection altered/ modulated response
		Cytokines/ Chemokines		
1	CCL5	Chemokine (C-C motif) ligand 5	↓	↑
2	IL8	Interleukin 8	↓	↑
		Enzyme		
3	GBP1	Guanylate binding protein 1, interferon-inducible	↑	↓
4	TGM2	Transglutaminase 2	↓	↑
5	TNFAIP3	Tumor necrosis factor, alpha-induced protein 3	↓	↑
		G-protein coupled receptor		
6	CCR7	Chemokine (C-C motif) receptor 7	↓	↑
		Growth Factor		
7	BMP4	Bone morphogenetic protein 4	↑	↓
8	HGF	Hepatocyte growth factor	↑	↓
9	MDK	Midkine (neurite growth-promoting factor 2)	↓	↓
		Ligand-dependent nuclear receptor		
10	NR4A2	Nuclear receptor subfamily 4, group A, member 2	↑	↑
		Peptidase		
11	ADAM19	ADAM metallopeptidase domain 19	↑	↓
12	MMP9	matrix metallopeptidase 9	↓	↑
13	PLAU	plasminogen activator, urokinase	↓	↓
		Phosphatase		
14	PTPN13	protein tyrosine phosphatase, non-receptor type 13	↓	↑
		Transcription regulator		
15	FOS	FBJ murine osteosarcoma viral oncogene homolog	↑	↑
16	JUNB	Jun B proto-oncogene	↑	↓
		Transmembrane receptor		
17	CD3G	CD3g molecule, gamma (CD3-TCR complex)	↓	↓
18	FAS	Fas (TNF receptor superfamily, member 6)	↑	↑
19	IL2RA	Interleukin 2 receptor, alpha	↓	↑
20	TLR2	Toll-like receptor 2	↓	↑
21	TNFRSF1B	Tumor necrosis factor receptor superfamily, member 1B	↓	↑
		Transporter		
22	ABCB1	ATP-binding cassette, sub-family B, member 1	↓	↑
23	APOD	Apolipoprotein D	↓	↓
24	SLC6A6	Solute carrier family 6, member 6	↑	↑
		Other		
25	BCL2A1	Bcl2-related protein A1	↓	↑
26	CD274	CD274 molecule	↓	↑
27	FCER2	Fc fragment of IgE, low affinity II (CD23)	↓	↓
28	IER3	Immediate early response 3	↑	↑
29	TIFA	TRAF-interacting protein with forkhead-associated domain	↑	↑
30	TNFAIP2	Tumor necrosis factor, alpha-induced protein 2	↓	↑
31	TRAF1	TNF receptor-associated factor 1	↓	↓
32	VCAM1	Vascular cell adhesion molecule 1	↓	↓
33	WNT10B	Wingless-type MMTV integration site family, member 10B	↑	↓

NF-κB response genes are shown whose expression was modulated in BoMac-TashAT2 and in *Theileria*-infected cells relative to control or uninfected counterparts. Gene expression patterns are indicated by either red (up-regulated) or green (down-regulated) arrows. Genes highlighted in grey are modulated in a similar direction.

Genes classified in the 'other' category by IPA includes those encoding products predicted to be involved in protein binding (FCER2, IER3, TIFA and TRAF1) and cell adhesion molecule binding (VCAM1), and the expression profile of all five of these genes showed a similar alteration associated with TashAT2 and infection (see Table 5.4).

Other transcription factor target genes identified in TashAT2/infection modulated dataset included AP-1 and ATF2. Detailed exploration of the AP-1 target gene list identified six genes in the common dataset (IL8, JUNB, MMP9, PLAU, NFATC1 and PLAUR) and several of these genes (IL8, JUNB, MMP, and PLAU) are also known to be targets of NF-κB (see Table 5.4). Similarly, five ATF2 target genes were identified (IL8, JUNB, PLAU, HES1 and CSRP2) with IL8, JUNB and PLAU also identified as NF-κB and AP-1 targets.

5.3.4 TashAT2 modulates the expression profile of genes stimulated by PMA

To investigate whether transfecting BoMac cells with TashAT2 would result in modulation of gene expression changes associated with PMA stimulation of BoMac-pCAGGS (control) cells, the BoMac pCAGGS-PMA and pCAGGS-TashAT2 PMA datasets were compared and a subset of 553 genes identified representing a PMA response in pCAGGS with evidence of modulated expression in pCAGGS-TashAT2-PMA. Further analysis revealed 342 genes whose expression was up-regulated by PMA stimulation of BoMac control cells. From the pair-wise comparisons, three distinct patterns of expression could be obtained and these are graphically represented in Figure 5.14 while the full list of 342 genes is presented in Appendix 3.2. The first profile consisted of subset of 52 genes whose elevated expression in pCAGGS-PMA was amplified in pCAGGS-TashAT2-PMA. Based on fold change, the top 15 genes from this profile are listed in tabulated form (see Figure 5.14, profile1). Many of these genes showed a considerable level of amplified expression in TashAT2-PMA relative to pCAGGS (control)-PMA. Important genes identified include a kinase (TRIB2, 13.3 f.c.), peptidases (AQPEP, 9.5 f.c. and MMP1, 3.4 f.c.), transcription regulators (SMAD7, 3.4 f.c.; TGIF1, 2.8 f.c. and JUNB, 2.1 f.c.) and chemokines such as IL24 with a fold change of 2.4.

Profile 1: n=52

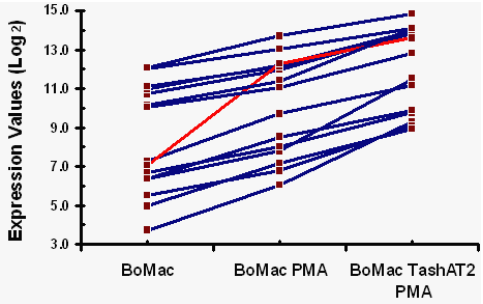

Gene Symbol	Annotation	BoMac PMA vs BoMac ↑	TahAT2 PMA vs BoMac PMA ↑↑
TRIB2	Tribbles homolog 2	2.7	13.3
AQPEP	Laeverin	5.0	9.5
PECAM1	platelet/endothelial cell adhesion molecule (CD31 antigen)	2.4	5.0
VASN	Vasorin	2.4	4.0
SMAD7	SMAD-family member 7	2.5	3.4
MMP1	Preprocollagenase	2.4	3.4
MT2A	Metallothionein-2	4.5	3.3
PLCXD2	Phosphatidylinositol-specific phospholipase C, X domain containing 2	2.1	3.2
TGIF1	TG-interacting factor	5.3	2.8
JHDM1D	KIAA1718 protein	4.3	2.6
IL24	Interleukin 24	37.6	2.4
JUNB	Jun B proto-oncogene	2.1	2.1
SEMA3C	Sema domain, immunoglobulin domain (Ig), short basic domain, secreted,	2.4	6.3
FAM117B	Family with sequence similarity 117, member B	2.0	3.4
INHBA	Inhibin, beta A	3.1	2.2

Profile 2: n=220

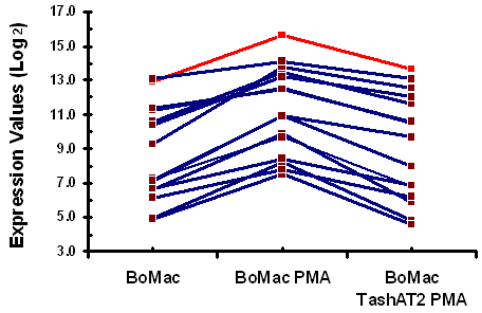

		↑	↓
TNFRSF11B	TNFR superfamily, member 11b	9.96	-16.3
PGLYRP2	Peptidoglycan recognition protein2	9.73	-10.8
SELP	Selectin P	5.51	-7.92
SELE	Selectin E	6.92	-3.85
CCL5	Chemokine (C-C motif) ligand 5	5.49	-7.53
LY6G6E	Lymphocyte antigen 6 complex, locus G6E	2.43	-3.99
PLAU	Plasminogen activator, urokinase	6.38	-3.87
LYST	Lysosomal trafficking regulator	2.09	-3.76
Bik1	BCL2-interacting killer	7.37	-3.49
FGF21	Fibroblast growth factor 21	3.11	-3.05
NFATC1	Nuclear factor of activated T-cells, cytoplasmic, calcineurin-dependent 1	3.45	-2.99
CYP3A4	Cytochrome P450, family 3, subfamily A, polypeptide 4	14.16	-2.37
TNFAIP3	TNF, alpha-induced protein 3	22.30	-2.36
ADAMTS6	ADAM metallopeptidase with thrombospondin type 1 motif, 6	7.27	-2.32
PTK2B	Protein tyrosine kinase 2 beta	2.07	-2.03

Profile 3: n=70

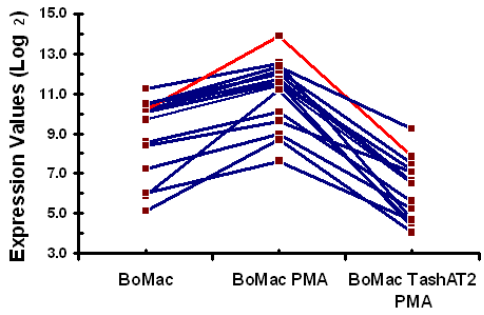

		↑	↓↓
OAF	OAF homolog (Drosophila)	2.46	-223
LGALS9	Lectin, galactoside-binding, soluble, 9	2.03	-146
CEACAM8	Carcinoembryonic antigen-related cell adhesion molecule 8	2.72	-39.6
CLMP	Cxadr-like membrane protein	2.76	-33.8
LMO2	LIM domain only 2	3.25	-30.1
CEACAM5	Carcinoembryonic antigen-related cell adhesion molecule 1	2.75	-21.3
ASGR2	asialoglycoprotein receptor 2	2.76	-20.2
LAMA3	Alpha3a chain laminin-like	4.02	-25.5
S1PR1	sphingosine-1-phosphate receptor1	12.56	-64.5
GPR110	**G protein-coupled receptor 110**	3.32	-13.5
CCL2	**Chemokine (C-C motif) ligand 2**	40.23	-105
SLC6A3	**Solute carrier family 6 (neurotransmitter transporter, dopamine), member 3**	3.08	-7.81
TRAF1	**TNF receptor-associated factor1**	2.38	-5.87
MERTK	**C-mer proto-oncogene tyrosine kinase**	3.75	-8.57
VCAM1	Vascular cell adhesion molecule 1	11.81	-24.7

Figure 5.14: Expression profiles of PMA responsive up-regulated genes showing modulated expression in TashAT2-PMA BoMac cells.
A summary of the absolute fold difference in BoMac pCAGGS-PMA and TashAT2-PMA relative to pCAGGS (control) cells is shown for top 15 representative genes of each profile. Trend of the profile is highlighted in red. Expression of genes highlighted in blue has been validated by semi-quantitative RT-PCR.

The second profile consisted of 220 genes, whose expression was elevated in BoMac-pCAGGS control cells when stimulated with PMA but showed slightly repressed expression in pCAGGS-TashAT2-PMA compared to pCAGGS-PMA (i.e. repression level was less than or equal to pCAGGS-PMA elevation, see Figure 5.14). Genes identified in this profile included those genes encoding BCL2-interacting killer (BIK1), Selectin P (SELP), Selectin E (SELE) and TNF, alpha-induced protein 3 (TNFAIP3) whose fold changes are given in Figure 5.14, Profile 2.

The third profile consisted of genes whose expression was elevated in BoMac-pCAGGS-PMA but highly repressed in pCAGGS-TashAT-PMA compared to pCAGGS-PMA (i.e. elevation associated with PMA significantly reversed in BoMac-TashAT2 cells, see Figure 5.14). The profile consisted of 70 genes; interesting genes with evidence of major repression of a PMA response associated with TashAT expression include OAF homolog (-223-fold), CEACAM8 (-39.6), LMO2 (-30.1), VCAM1 (-24.7), S1PR1 (-64.5) and TRAF1 (-5.9). IPA exploration of the profile gene list showed enrichment for genes in the categories of ‘immune response’, ‘cell death’, ‘cancer’, ‘gene expression’ and ‘cell signalling’. The microarray expression pattern of four genes from profile 3 was validated using semi-quantitative RT-PCR (see Figure 5.15). For example, VCAM1 and LMO2 showed clear elevation of PCR product in pCAGGS compared to pCAGGS-PMA BoMacs, while the relative level of product was clearly lower in TashAT2 and TashAT2-PMA. Additionally, the expression level of these genes in *Theileria* infected cells was also determined and showed a related profile of repression associated with infection (Figure 5.15). Similar results were obtained for CEACAM8 and TRAF1 whose expression was reduced in TashAT2-PMA cells.

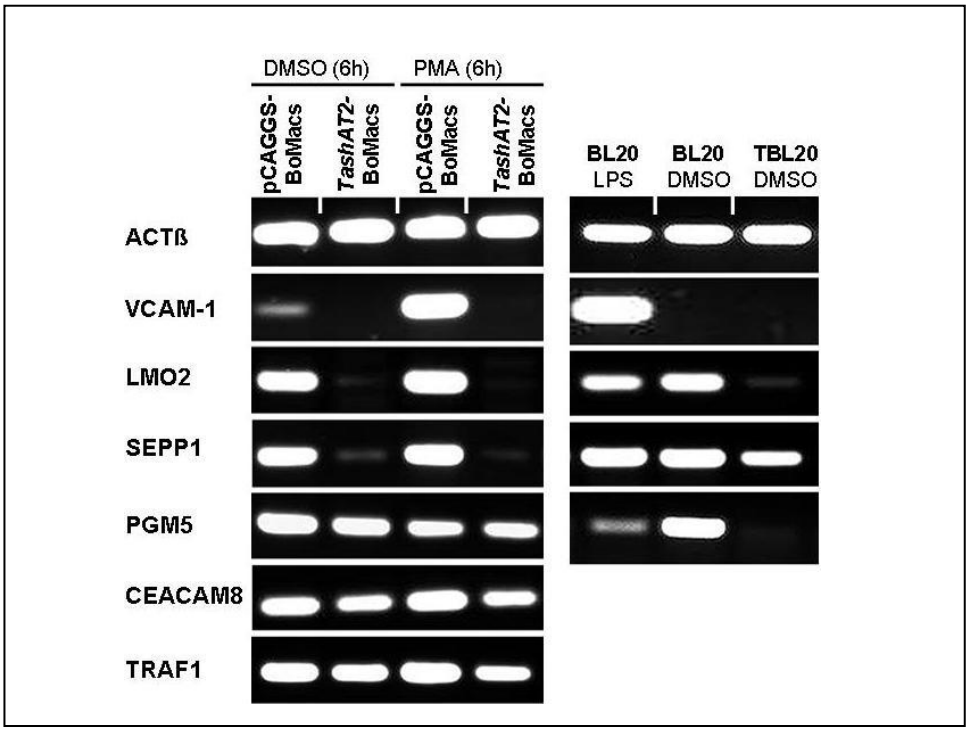

Figure 5.15: Semi-quantitative RT-PCR validation of microarray results of TashAT2 modulated PMA response genes
Panel on the left represents the mRNA expression of 6 genes (VCAM1, LMO2, SEPP1, PGM5, CEACAM8 and TRAF1) in BoMac cells. The panel on the right represents RT-PCR results of the corresponding genes set in TBL20 and BL20 (LPS +/-) cells. ACTB was used as a constitutive standard.

Profiling of a second subset of 211 down-regulated PMA responsive genes also revealed three distinct patterns of modulated expression associated with TashAT2-PMA cells that were the reciprocal of the three profiles described above. Thus, profile 4 represented 91 genes whose expression is repressed by PMA stimulation in BoMac-pCAGGS but highly-repressed in BoMac-TashAT2 cells when stimulated with PMA (see Figure 5.16, profile 4). 14 of these genes showed a major repression (> 10-fold), see table in Appendix 3.3 for a full list of genes in the profile). IPA showed enrichment for genes predicted to function in cell death, cellular development, cellular growth and proliferation and cancer. Interestingly, genes encoding enzymes (PGM5 and PTER), transcription regulators (HES1, HLF and TRERF1) and transporters such as AQP1, SLC23A1 and TRAF5 were included in this profile. Two of the genes in this profile (SEPP1 and PGM5) were validated by RT-PCR. The RT-PCR results were in agreement with the expression profile generated from microarray expression values and demonstrated super-repression associated with TashAT and TBL20 (see Figure 5.15).

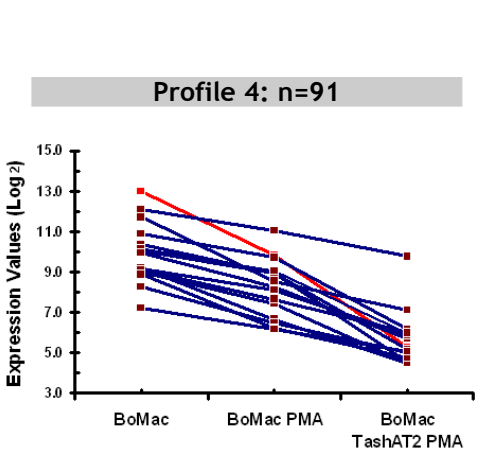

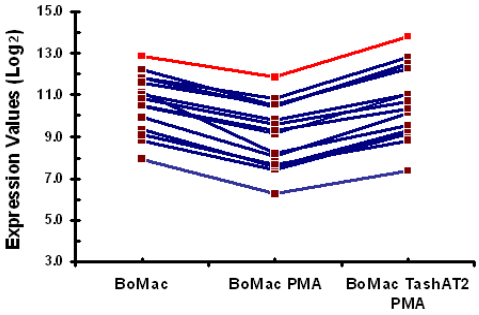

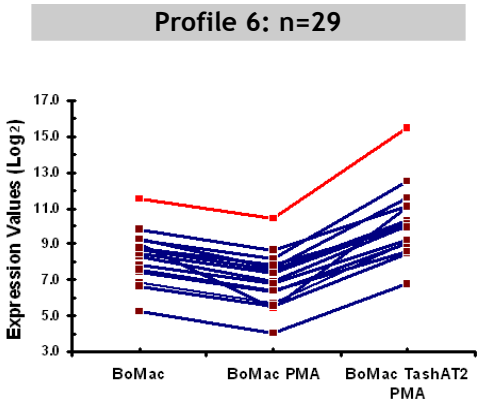

Gene Symbol	Annotation	BoMac PMA vs BoMac	TahAT2 PMA vs BoMac PMA
		↓	↓ ↓
KBTBD6	Kelch repeat and BTB (POZ) domain containing 6	-9.03	-23.7
SEPP1	Selenoprotein P, plasma, 1	-2.11	-20.7
PTER	Phosphotriesterase related	-2.80	-13.8
HLF	Hepatic leukemia factor	-2.18	-12.1
HVCN1	Hydrogen voltage-gated channel 1	-2.09	-8.6
PKNOX2	PBX/knotted 1 homeobox 2	-2.87	-7.6
JAKMIP3	Janus kinase and microtubule interacting protein 3	-3.21	-5.9
PNPLA3	Patatin-like phospholipase domain containing 3	-2.04	-4.8
LMOD1	Leiomodin 1	-5.94	-4.5
TRERF1	Transcriptional regulating factor 1	-2.72	-3.3
MYOM1	Myomesin 1, 185kDa	-3.37	-2.9
ZFP3	Zinc finger protein 3 homolog	-9.04	-2.7
PDE7B	Phosphodiesterase 7B	-6.29	-2.7
PGM5	Phosphoglucomutase 5	-2.12	-2.4
PTPN6	Protein tyrosine phosphatase, non-receptor type 6	-2.05	-2.2
		↓	↑
GADD45B	Growth arrest and DNA-damage-inducible, beta	-2.54	4.3
INSIG1	Insulin induced gene 1	-3.78	4.3
DNAJB5	DnaJ, subfamily B, member 5	-2.02	3.9
CRISPLD2	Cysteine-rich secretory protein LCCL domain containing 2	-2.02	3.9
PIK3R3	Phosphoinositide-3-kinase, regulatory subunit 3 (gamma)	-2.48	3.7
RNF150	Ring finger protein 150	-3.29	3.7
BST2	Bone marrow stromal cell antigen2	-2.72	3.4
ENPP5	Ectonucleotide pyrophosphatase/ phosphodiesterase 5	-2.09	3.3
OAS1	2',5'-oligoadenylate synthetase 1, 40/46kDa	-3.44	3.2
RASL11B	RAS-like, family 11, member B	-7.62	2.5
ARMCX6	Armadillo repeat containing, X-linked 6	-2.27	2.3
DDIT4L	DNA-damage-inducible transcript 4-like	-2.68	2.2
GPR137C	G protein-coupled receptor 137C	-3.20	2.2
TCEAL1	Transcription elongation factor A (SII)-like 1	-2.30	2.1
FBXL4	F-box and leucine-rich repeat protein 4	-2.28	2.0
		↓	↑ ↑
LRRTM4	Leucine rich repeat transmembrane neuronal 4	-11.59	47.50
EFEMP1	EGF containing fibulin-like extracellular matrix protein 1	-2.18	32.81
PDE4B	Phosphodiesterase 4B, cAMP-specific	-2.06	20.13
AMIGO2	Adhesion molecule with Ig-like domain 2	-2.94	14.81
JAKMIP2	Janus kinase and microtubule interacting protein 2	-2.17	10.61
VEPH1	Ventricular zone expressed PH domain homolog 1 (zebrafish)	-2.67	8.66
DAAM2	**Dishevelled associated activator of morphogenesis 2**	-2.11	7.59
PPAP2B	**phosphatidic acid phosphatase type 2B**	-2.24	6.73
ITGB8	**Integrin, beta 8**	-2.17	6.66
PCDHGA2	Protocadherin γ subfamily A, 2	-2.15	6.58
C5orf13	Chromosome 5 open reading frame 13	-2.28	6.52
MBNL3	Muscleblind-like 3 (Drosophila)	-2.24	5.49
TANC2	Tetratricopeptide repeat, ankyrin repeat and coiled-coil containing 2	-2.09	5.41
PLCH1	Phospholipase C, eta 1	-2.22	4.52
NTRK2	Neurotrophic tyrosine kinase, receptor, type 2	-2.02	4.41

Figure 5.16: Expression profiles of PMA responsive down-regulated genes showing modulated expression in TashAT2-PMA BoMac cells.
A summary of the absolute fold difference in BoMac pCAGGS-PMA and TashAT2-PMA relative to pCAGGS (control)cells is shown for top 15 representative genes of each profile. Trend of the profile is highlighted in red. Expression of genes highlighted in blue has been validated by semi-quantitative RT-PCR.

Profile 5 is the reciprocal of profile 2 and represents 91 genes that are repressed by PMA treatment in BoMac-pCAGGS cells but showed slight elevation in TashAT2-PMA compared to pCAGGS-PMA. The top 15 genes of this profile are listed in Figure 5.16 profile 5, while the full list of 91 genes is presented in Appendix 3.3. IPA showed enrichment for genes predicted to function in cell cycle, cell morphology, cellular growth, proliferation and cancer.

Profile 6 consisted of 29 genes whose expression was repressed slightly in pCAGGS upon PMA stimulation but significantly-elevated in TashAT2 under PMA stimulation (i.e. PMA response significantly reversed in BoMac-TashAT2 cells). A full list of the 29 genes of this profile is presented in Appendix 3.3, and the top ranking 15 genes are listed in Figure 5.16, profile 6. Important genes identified in this profile included genes encoding Leucine rich repeat (LRRTM4), EGF containing fibulin-like extracellular matrix protein 1 (EFBMP1) and Janus kinase and microtubule interacting protein 2 (JAKMIP2), which are predicted to have a functional role in protein binding.

5.3.5 Comparison of the TashAT2-modulated PMA and infection-modulated LPS datasets

To identify genes that are commonly altered in the TashAT2-modulated PMA response (552 genes) and the infection-modulated LPS response (1,995 genes), the two datasets were compared to identify common genes and the results are illustrated in a Venn diagram (Figure 5.17). The comparison revealed 86 common genes, which was a significantly larger number ($p < 0.001$) than expected to occur by chance, as MC simulation suggested only 48 genes would be expected to be common between the two datasets. The summary of the calculation used to estimate the significance of the overlap is described in Figure 5.17.

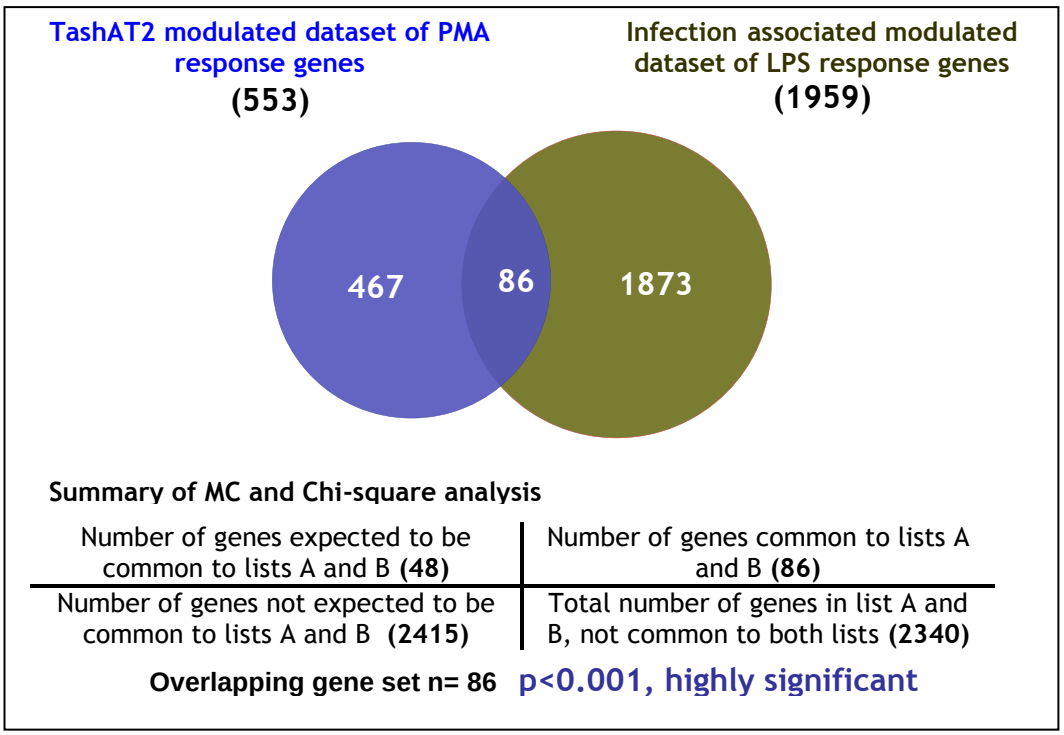

Figure 5.17: Comparison of TashAT2 modulated PMA response genes and Infection modulated LPS response genes sets
Comparison of the two lists of differentially expressed genes identified 86 common genes. This overlap was found to be significantly larger than expected by chance alone ($p < 0.001$). A summary of the observations obtained from Monte Carlo simulation and Chi square analysis are also shown.

Pathway analysis of the dataset of 86 common genes identified five NF-κB target genes. These included vascular cell adhesion molecule (VCAM1), chemokine (c-c motif) receptor 7 (CCR7), Jun B proto-oncogene (JUNB), TNF alpha-induced protein 3 (TNFAIP3) and TNF receptor-associated factor 1 (TRAF1). These genes were predicted to function in 'Cell-To-Cell Signaling and infection', 'Inflammatory Response', 'Cancer' and 'Cell death'. IPA analysis also identified enrichment for non NF-κB target genes in molecular function and disease categories of 'Cell-to Cell Signaling' (e.g. IRF8, BIRC3 and NFATC1), 'Inflammatory response' (IL24, IL2RB, LTB4R, S1PR1, IRF8, OAS1 and VCAM1), 'Cancer' (CCR7, LMO2, IL2RB and CYP3A4) and 'Cell death' (IRF8, TNFAIP3, CYP34A4 and IL24). These categories could be reasonably predicted to be associated with the known phenotype of the parasite-infected cell.

5.3.6 RT-PCR analysis of candidate gene expression in a TashAT2 transfected T. annulata infected D7 cell lines.

The results above indicate expression of TashAT2 can modulate the outcome of bovine genes whose expression is altered in the context of *Theileria* infection of the host cell. To investigate this further, *Theileria* infected D7 cell lines stably transfected with pCAGGS-TashAT2 or pCAGGS (control) constructs were utilised. D7-pCAGGS-TashAT2 were capable of expressing both endogenous TashAT2 produced by the parasite and experimentally induced exogenous TashAT2, with expression of exogenous TashAT2 validated by immunofluorescence analysis using an anti-V5 monoclonal antibody (see Figure 5.18, panel 1). Endogenous TashAT2 expression was confirmed with DE39 antisera (capable of reacting with both forms of TashAT2) but as expected the cell line transfected with the pCAGSS-TashAT2 construct generated a higher level of reactivity in the host cell nucleus but not the parasite (see Figure 5.18, panel 3 and 6). pCAGGS-TashAT2, D7-transfected cells were treated with buparvaquone (BW720c) for 48 and 72 hours in order to kill the parasite. Following BW720c treatment expression of endogenous and exogenous TashAT2 was tested using anti-V5 and DE39 antisera. The results showed reduced but persistent expression of TashAT2 (see Figure 5.18, panels 7 and 9) in the drug treated cells.

Semi-quantitative RT-PCR analysis was performed on the RNA samples isolated from TashAT2-transfectd and pCAGGS-transfected D7 cells (BW720c +/-). Of the previously PCR validated genes (see Figures 5.10-11 and 5.15) two, VWA5A and LMO2, showed a similar pattern of modulation in TashAT2-transfected D7 cells as that obtained for TashAT2 transfected BoMac. Thus for VWA5A, the level of PCR product was clearly higher in cells over expressing exogenous TashAT2 and this elevated expression was maintained in the presence of drug (BW720c) (see Figure 5.19). This result may not be surprising, because although a small increase in product was observed in the pCAGGS control cells treated with drug, an independent analysis (Kinnaird *et al*; unpublished) did not show any significant difference in the level of VWA5A RNA in TBL20 cells following buparvaquone treatment.

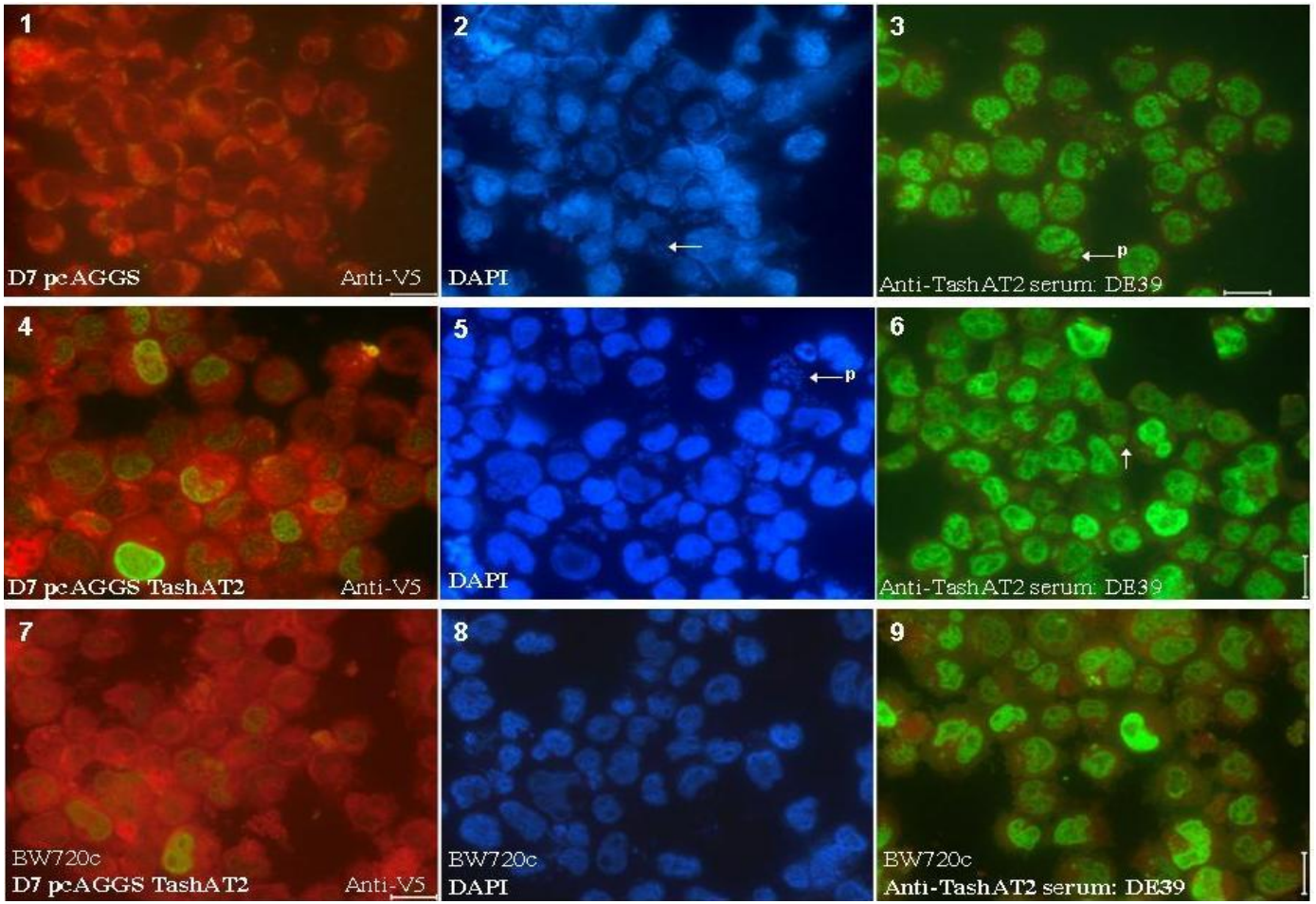

Figure 5.18: Immunofluorescence analysis of D7 cells transfected with pCAGGS and pCAGGS-TashAT2 using anti-V5 antibody and DE39 antisera **Panels 1-3:** pCAGGS (control) transfected D7 cells. **Panels 4-6:** pCAGGS-TashAT2 transfected D7 cells. **Panels 7-9:** pCAGGS-TashAT2 transfected D7 cells incubated with 50ng/ml buparvaquone (BW720c) for 48h. Panels 1, 4 and 7 were analysed using anti-V5 antibody and their respective DAPI-stained images are shown in panels 2, 5 and 8. Cells shown in panels 3, 6 and 9 were analysed using rabbit antisera DE39 raised against recombinant TashAT2 (Swan *et al*., 1999). P/white arrows denote the schizont/parasite nuclei: Bar = 20µm.

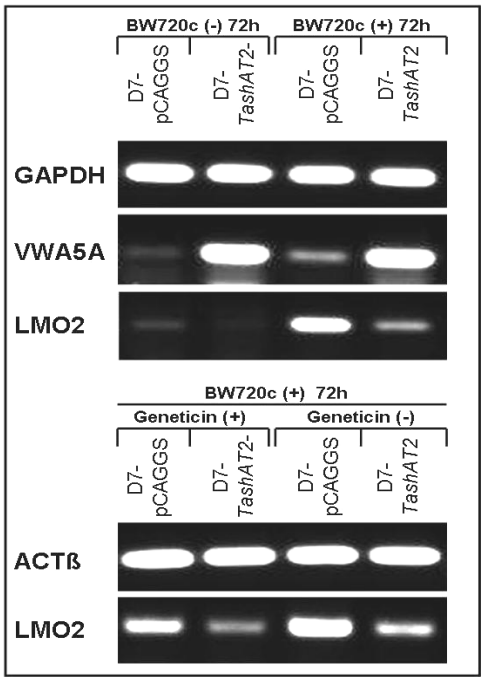

Figure 5.19: Semi-quantitative RT-PCR analysis of TashAT2 modulated genes in TashAT2 transfected and *T. annulata* infected D7 cell line.
RT-PCR results showing the modulated expression pattern of genes in TashAT2 transfected D7 cells relative to their controls. ACTβ and GAPDH were used as an internal control. Panel on the top represents the mRNA expression of VWA5A and LMO2 in D7-pcaggs and D7-TashAT2 cells following buparvaquone treatment for 72h.

The LMO2 expression pattern in D7-transfected cells was in agreement with previous array and RT-PCR expression profiles, as the data indicated that a viable parasite was required to maintain repression of this gene in the D7 cell line, because the PCR product was clearly elevated following treatment with BW720c to kill the parasite (see Figure 5.15 for evidence of repression by TashAT2 in BoMac and in TBL20 compared to BL20). Moreover, over-expression of TashAT2 in D7 appeared to be associated with maintenance of partial repression in the presence of BW720C (see Figure 5.19 top panel lane 3 vs 4 for LMO2 product). A further experiment was conducted to test if the level of maintained repression of the LMO2 gene might be sensitive to the level of exogenous TashAT2.To attempt this TashAT2 transfected cells were grown in the absence of the drug used for selection of stable transfectants (Geneticin), as it had been shown previously that this procedure resulted in a reduction of transgene expression (Shiels *et al.*, 2004). The RT-PCR results from RNA derived from these samples are shown in the bottom panel of Figure 5.19. The mRNA product obtained was significantly lower in D7-TashAT2 relative to D7-pCAGGS in both conditions (with or without Geneticin) but with an increase in the level of product in TashAT2 transfected cells cultured in the absence of Geneticin

compared to cells grown in the drug (compare lane 2 and 4). However, the LMO2 expression level was also relatively higher in RNA derived from the PCAGGS control transfected cell line grown in the absence of Geneticin. A definitive conclusion on the effect of altering the level of TashAT2 production (with or without geneticin) on LIMO2 levels could, therefore, not be made.

5.4 Discussion

Work presented in the previous chapter of this thesis provided conclusive evidence that the parasite extensively modulates the host cell gene expression profile to influence the outcome of cellular activation. The aim of the work presented in the current chapter was to investigate the ability of a candidate parasite protein, TashAT2 (TashAT family member), to function as a modulator of bovine gene expression at a global level.

Use of experimental model and modulation of phenotypic responses

To establish the suitability of TashAT transfected uninfected cell lines for further study IFAT was performed using a monoclonal anti-V5-tag. The result indicated that BL20-TashAT2 cells displayed an extremely low level reactivity in the nucleus. In contrast bovine macrophage cell line (BoMac-TashAT2) showed evidence of strong expression of V5-tagged TashAT2 in the nucleus compared to a control cell line transfected with plasmid vector alone (Figure 5.2). The reason for low expression in the BL20 line is unclear and was unfortunate as it prevented a direct comparison against the same host cell background used in the previous study. As, BoMac cells provided expression levels of TashAT2 comparable to the level detected in *Theileria* infected cells, it was decided to utilise this cell line. While utilisation of this model may make comparison with changes associated with infection more difficult, it could be argue that any overlap in modulation of genes between TashAT2 transfected BoMacs and infected cells may be less expected and therefore considered more significant.

NF-κB, reporter assays were performed on TashAT2 transfected BoMac and control cell lines following stimulation with either LPS or PMA. No difference in NF-κB reporter activity was found comparing non-stimulated cell lines or cell lines stimulated with LPS, confirming previous studies indicating that BoMacs are refractory to LPS stimulation (Oura *et al.*, 2006). However, TashAT2 transfected BoMacs showed a significantly greater increase in NF-κB reporter activity compared to the control line when stimulated with phorbol-12-myristate-13-acetate, PMA (see Figure 5.3). To test if this may be due to elevated activation of NF-κB IFAT was undertaken. Unfortunately, a firm difference between the

p65 nuclear reactivity of pCAGGS-PMA and TashAT2-PMA (data not shown) was not observed and the level of p65 nuclear reactivity appeared to be same. However, given the fact that no difference in reporter activity level was detected in non-stimulated TashAT2 and control cells, the most likely explanation is that elevated reporter values in TashAT2-PMA cells are due to an enhancement in NF-κB transcriptional activity rather than an increase in the amount of activated NF-κB. Further investigations are required to confirm these findings by performing more sensitive experimental methodology such as electrophoretic mobility shift analysis (EMSA) and gel-shift western blotting. Chromatin immunoprecipitation (ChIP) PCR using primers against the NF-κB reporter would also be of interest.

Experiments performed to assess whether prolonged activation of BoMac cells by PMA is potentially associated with detrimental outcome provided evidence that TashAT2 protects BoMac cells against a PMA induced activation response and cell death. Prolonged treatment of cells with the phorbol ester (PMA) has been reported to trigger apoptosis in several cellular models, via distinct mechanisms including NF-κB activation, activation of caspases, activation of protein kinase C (PKC) and associated pro-apoptotic genes (Chung and Kim, 1988;Day *et al.*, 1994;Gunji *et al.*, 1992;Hida *et al.*, 2000;Lai *et al.*, 2003). BoMac-TashAT2 cells were refractory to detrimental outcome of cellular death and continued to proliferate at the same rate as the untreated control. Giemsa staining and microscopic examination of PMA stimulated BoMac cells showed they displayed profound morphological alterations characteristically related to programmed cell death. This included obvious cytoplasmic blebbing, elongated cell shape, cell shrinkage and darkly stained apoptotic cells (see Figure 5.7). Conversely, BoMac-TashAT2 cells were refractory to these morphological changes when stimulated with PMA. Numerous studies have shown that PMA can induce such morphological changes that are typically related to apoptosis (Benjamin *et al.*, 1984;Hsu *et al.*, 1998;Malide *et al.*, 1998).

Confirmation of PMA induced cellular apoptosis of BoMac-pCAGGS cells was obtained by performing caspase 3/7 activation assays; higher caspase activation levels were obtained in PMA stimulated pCAGGS cells relative to unstimulated control confirming activation of the caspase cascade and initiation of apoptosis. In contrast, the activity of caspase 3/7 remained unchanged for PMA stimulated

TashAT2 transfected cell line. Numerous studies have shown that PMA can induce caspase 3/7 activity in a variety of cellular models (Busuttil *et al.*, 2002;Hida *et al.*, 2000;Varghese *et al.*, 2003). It can be concluded from these results that a BoMac cell line expressing TashAT2 showed greater levels of NF-κB activity but reduced levels of alterations associated with apoptosis when stimulated by PMA.

Interpretation of microarray analysis and gene expression profiles modulated by TashAT2 in BoMacs cells

Comparison of global datasets obtained from microarray analysis (BoMac: control/TashAT2/TashAT2_PMA vs TBL20/TBL20_LPS) demonstrated a large number of modulated genes (1,206) that were common to both TashAT2-transfected BoMac and parasite-infected cells. This overlap was significantly greater than expected to occur by chance ($P < 0.01$). IPA of this common gene set ascribed important biological functions and diseases categories identified for the infection-modulated LPS dataset, although the order of significance observed was different. While these results are not surprising they indicate TashAT2 transfected cells show similar modulations to infected cells and support TashAT2 as a potential modulator of gene expression in a parasite infected cell. Differences in the order of significance and the direction and size of any modulation may be explained by differences in the additional factor(s) that are highly likely to be present in parasite infected cells compared to BoMac cells. In addition to host cell factors the detected differences could also be influenced by presence of other parasite molecules that are candidate modulators of the host phenotype, including a number of other proteins encoded by the TashAT cluster (Shiels *et al.*, 2006).

Interestingly, the most significant enrichment in TashAT2-modulated dataset was found for genes placed in the categories of ‘Cancer’, followed by ‘Inflammatory disease’ and ‘Cell death’. One postulation from this result is that TashAT2 may operate together with NF-κB and be a key manipulator of cancer cell phenotype in the context of the infected cell. DNA binding AT hook motifs with a similar arrangement to that of TashAT2 are also found in mammalian HMGA family proteins that have been found to play major roles in Cancer [reviewed in (Fusco and Fedele, 2007;Pierantoni *et al.*, 2003)]. Enrichment of genes in ‘Cancer’ by

IPA was also found in the complete dataset of genes altered in TashAT2 transfected BoMac cells (data not shown). Further investigation of TashAT2 in disregulation of genes associated with cancer is required.

Excel based sorting of the common modulated dataset (1,206) generated a sub set of 466 genes that displayed the same directional change in expression level associated with TashAT2 and infection of BL20 cells with *T. annulata*. IPA mining of the down-regulated genes (353), revealed enrichment of genes biased towards anti-cancer and anti-tumor (i.e. IL18, IFR8, NGFR, PLAU and TP63), pro-cell death genes (i.e. CDKN2C, IL18, Il24, KIF1A, MAP3K1, IKBKE, IRF8, and TP63), and pro-inflammatory immune response genes (CD3G, FCER2, IL18, IRF8, S1PR1 and VCAM1). IPA exploration of up-regulated genes set (113) indicated enrichment of genes biased towards elevation of pro-tumourigenesis (FOS, IER3, NAUPR1, PLAUR) and cellular growth and proliferation (SMAD7, SERPINE1, IER3 and PLAUR). Six representative genes from each profile were analysed by semi-quantitative RT-PCR and the results obtained were consistent with the microarray analysis (see Figures 5.10-11). These results provide further evidence that expression of TashAT2 may be involved in manipulating expression of host cell genes that could play an important role in determining establishment of infected-transformed cells.

IPA also highlighted important canonical pathways: production of Nitric Oxide and Reactive Oxygen species in macrophages (NO & ROS), G-Protein Coupled Receptor Signaling, TNFR2, NF-κB and CD40 Signaling as being altered in TashAT2 BoMac cells. Activation of the ROS pathway is generally associated with strong inflammatory conditions (Bulua *et al.*, 2011;Hakim, 1993;Johar *et al.*, 2004) and implicated in the induction of apoptosis and antimicrobial defence mechanisms via activation of NADPH oxidase, also known as oxidative respiratory burst (Bjorkman *et al.*, 2008;Smith, 1994). Increasingly, it is proposed that activation of ROS plays a key role in human cancer development by causing structural damage to DNA (Feig *et al.*, 1994;Jackson and Loeb, 2001;Routledge *et al.*, 1994;Waris and Ahsan, 2006). Of the 20 genes identified in this pathway, fifteen were found to be down-regulated in the TashAT2-modulated dataset and included Cytochrome-b245, alpha polypeptide (CYBA), inhibitor of kappa light polypeptide gene enhancer in B-cells, kinase epsilon (IKBKE), protein phosphatase 1, regulatory (inhibitor) subunit 14A (PPP1R14A) and Tumor necrosis

factor receptor superfamily, member 11b (TNFRSF11b). These results are of interest and are indicative of involvement of TashAT2 in protecting the cell from stress induced DNA damage. Of the other important pathways, NF-κB was of particular interest with 17 genes identified, whereas Custom pathway indicated 33 NF-κB target genes modulated in TashAT2 BoMac and infected TBL20 cells (Table 5.4). The majority of the mapped NF-κB target genes showed enrichment for the pro-inflammatory response, and genes related to cancer. It would appear, therefore, that the majority of genes altered in TashAT2-BoMacs are not recognised targets of activated NF-κB. Such a result is potentially possible as AT hook mammalian genes have a wide range of gene targets, in addition to known NF-κB targets (Hommura *et al.*, 2004;Ogram and Reeves, 1995;Reeves and Beckerbauer, 2001).

Interpretation of TashAT2-modulated gene expression profiles and genes associated with inflammatory inducers

A second set of analysis of the TashAT2 dataset was performed to identify a subset of genes that showed a PMA response that is significantly modulated in TashAT2 expressing BoMac cells. Six profiles of modulated expression were obtained. These profiles clearly demonstrated distinct prototypes of manipulation of gene expression in TashAT2-PMA when compared to pCAGGS-PMA.

Profile 1 represented a subset of genes that showed super elevated expression in TashAT2-PMA relative to pCAGGS-PMA (see Figure 5.14). It is possible that such a profile is related to greater NF-κB reporter activity detected in TashAT2 BoMacs. In addition, since it is likely that genes that are not NF-κB targets are being up regulated in the context of PMA it is plausible to propose that TashAT2 generates enhancement of transcriptional activity for a number of factors activated by this phorbol ester. HMGA proteins bearing DNA binding AT hook motifs identical to TashAT2 have been shown to promote formation of the enhanceosome that results from combinatorial binding of transcription factors at target gene promoters resulting in efficient recruitment of core complexes that initiate efficient transcription (Mantovani *et al.*, 1998;Thanos *et al.*, 1993;Thanos and Maniatis, 1995). Interestingly these HMGA proteins operate together with several transcription factors (p50/p65 NF-κB heterodimer, ATF2 and c-Jun) that are

activated in *Theileria* infected cells to induce synergistic transcription from target promoters (Du *et al.*, 1993;Du and Maniatis, 1994;Mantovani *et al.*, 1998;Thanos *et al.*, 1993;Thanos and Maniatis, 1995). It is not unreasonable to propose that similar events are occurring in PMA stimulated BoMac cells and that TashAT2 acts as an analogue of HMGA architectural proteins to promote enhanceosome formation at promoters of genes represented by profile 1.

Genes indentified in profile 1 that show the same type of modulation in infected cells include SMAD7, MT2A, JHDM1D and JUNB, which are predicted to have a functional role in protein binding. SMAD7 and JHDM1D and JUNB are also predicted to have roles in transcription regulatory region DNA binding or chromatin modification. Metallothionein-2A (MT2A) belongs to the metallothionein gene family that encodes proteins involved in protein binding, cell proliferation, essential metal homeostasis and protection against several types of cell damage (Lazo and Pitt, 1995;Reinecke *et al.*, 2006;Yamasaki *et al.*, 2007). Over expression of MT2A is frequently observed in invasive human breast tumours and promotes cell invasion by up-regulating MMP-9 via AP-1 and NF-κB activation (Kim *et al.*, 2011). Elevated MMP-9 expression is known to be induced by infection of the leukocyte by *T. annulata* (Adamson and Hall, 1996).

JunB, is a member of Jun protein family and together with Fos proteins give rise to a large variety of either homodimers or heterodimers constituting the AP-1 transcription factor complex (Foletta *et al.*, 1998). A protective role for JunB against stress-mediated apoptosis (Gurzov *et al.*, 2008;Son *et al.*, 2010) has been proposed. However, the exact role of JunB in stress response signaling is still not clear. Moreover JUN family proteins have janus like properties and can be pro- and anti-apoptotic depending on the context of cell type and stress conditions (Shaulian and Karin, 2002). Increased AP-1 activity occurs in HMGA-expressing fully transformed rat thyroid cells and was found to be fully dependent on HMGA over expression (Vallone *et al.*, 1997). Vallone *et al.*, (1997) also demonstrated that cell lines expressing HMGA1 and HMGA2 display remarkable induction levels of JUNB and the FRA1 gene (FOSL1) proteins. FRA1 is required for mitotic progression at G1/G2 phase transition, (Casalino *et al.*, 2007;Jochum *et al.*, 2001), and is recruited to the promoter of cyclin A. *Theileria* transformed lymphocytes have been shown to express activated AP-1 components at varying levels that are dependent on viable parasite (Chaussepied

et al., 1998). The possibility that TashAT2 acts like HMGA to elevate expression of components of the AP1 complex in transfected BoMac cells and in parasite-infected cells requires further investigation.

Evidence of modulation of the BoMac PMA response in TashAT2 BoMac is also indicated by profile 2 and 3. Genes were either slightly or highly repressed in BoMac-TashAT2-PMA relative to the response identified for PMA stimulated BoMac-pCAGGS control cells (see Figure 5.14 profile 2-3). IPA analysis of these two profiles showed enrichment for genes in various categories: including Cellular Movement, Cellular Growth and Proliferation, Cancer, Tissue Morphology and Inflammatory Response and Cell Death. Repression of genes indentified in profile 3 showed high fold differences (maximum -511-fold) with 42 genes repressed (over 10 fold) in TashAT2-PMA. Genes encoding cell adhesion molecules VCAM1, P-selectin (SELP) and E-selectin (SELE), carcinoembryonic antigen-related cell adhesion molecules (CEACAM8/5) that are predicted to play critical role in inflammatory and immune responses were prominent. Expression of candidate genes in profile3 was validated by RT-PCR, confirming repression in TashAT2-BoMac.

VCAM1 has been implicated in a variety of inflammatory processes and immune cell interactions (Huo *et al.*, 2000;Neish *et al.*, 1995;Ou *et al.*, 2008;Ren *et al.*, 2010). Although resting cells do not express VCAM-1 message, exposure to pro-inflammatory mediators or cytokines (PMA, LPS and TNF-α) cause a rapid induction (Kawai *et al.*, 2001;Lee *et al.*, 2006;Marui *et al.*, 1993;Valentin *et al.*, 1997). Transcription of VCAM1 is regulated by several inflammatory transcription factors including NF-κB and Ap-1 (Ahmad *et al.*, 1998;Collins *et al.*, 1995b;Neish *et al.*, 1995;Shu *et al.*, 1993). VCAM1 regulation at the promoter level is a complex process and involves interaction of various transcription factors including NF-κB, IRF-1, Sp1, and DNA binding factors such as HMGA1 (Harris *et al.*, 2008;Neish *et al.*, 1995).

An increasing number of studies over the past few years have shown a major role for the HMGA proteins in controlling gene transcription of a large number of genes including IFN-β, IL2, IL-2Rα.. In addition to binding to DNA, HMGA proteins physically interact with large number of proteins, most of which are transcription factors, including NF-κB, c-Jun, Oct-2, ATF2, NFAT, and Elf-1

(Arlotta *et al.*, 1997;Boise *et al.*, 1993;Jain *et al.*, 1992;Jain *et al.*, 1995;Panne *et al.*, 2004;Rao *et al.*, 1997). Several models of interaction(s) between HMGAs, transcription factors and promoter elements have been proposed that influence positive or negative transcription of genes (Chuvpilo *et al.*, 1993;Shannon *et al.*, 1998). These include direct interaction of HMGA alone at the promoter; modification of DNA structure to influence binding of TFs and direct interactions with TFs that may or may not require the presence of DNA. Importantly, a high concentration of HMGA protein has been shown to inhibit the binding of certain transcription factors to promoter targets. For example, inhibition of AP-1 binding to NFIL-2A, NFAT binding to CD28RR and the IL-4 promoter has been proposed to operate (Bustin and Reeves, 1996;Chuvpilo *et al.*, 1993;Shang *et al.*, 1999). Based on the known ability of HMGA proteins to repress the expression of genes that are targeted by transcription factors activated by LPS, PMA and *Theileria*-infection, it is tempting to speculate that TashAT2 and other members of the TashAT cluster perform a similar role. The finding that TashAT2 expressing BoMac cells markedly repress VCAM1 induction by PMA supports this possibility. However it is also possible that a more indirect mechanism of repression is in operation. Further experiments are required to confirm the structural interactions of parasite secreted TashAT2 proteins (bearing AT hook motifs) and transcription factor bindings in the regulation of VCAM1.

LIM domain only 2 (*LMO2)*, a member of the LIM-only class proteins and formerly termed as rhombotin-2 (*rbtn-2* or *Ttg-2*) has been reported to play a critical role in normal hematopoietic stem cell development and differentiation (Boehm *et al.*, 1991;Hansson *et al.*, 2007;McGuire *et al.*, 1989;Yamada *et al.*, 1998). TashAT2-transfected BoMac cells hardly express LMO2 relative to control cells. Furthermore, marked repression was observed for *Theileria*-infected cells and elevated expression of LMO2 was observed following buparvaquone (BW720c) treatment (Figure 4.17). A role for TashAT2 as a repressor of LMO2 expression was supported by the result showing that in D7 transfected cells over expressing TashAT2 the increase of LMO2 PCR product in response to BW720 treatment was inhibited. Two explanations are possible: either LMO2 expression is sensitive to stress responses induced by drug treatment and cells over-expressing TashAT2 are protected against this event, or TashAT2 directly/indirectly alters the transcription factor complexes required for LM02 transcription.

Proximal and distal promoters have been described for LMO2 gene (Hammond *et al.*, 2005;Royer-Pokora *et al.*, 1995). The proximal promoter region of LMO2 has been shown to contain positive regulatory elements (3 conserved Ets factor binding sites) that mainly facilitate binding of the Ets transcription family. While the distal promoter of LMO2 has been demonstrated to repress transcriptional activity via the presence of tissue specific upstream negative regulatory elements, predicted to have functional role in leukaemia (Hammond *et al.*, 2005). Furthermore, Hammond *et al.,* (2005) have suggested the tissue-specific repressor activity could occur via a specific factor binding to negative promoter elements, or to a ubiquitous factor working in combination with tissue-restricted proteins interacting at the LMO2 promoter. Interestingly Tsunoda *et al.*, (2010) reported that the ZFAT factor is important for transcriptional regulation of LM02 and binds to the proximal promoter. ZFAT contains an AT hook as well as a zinc finger and conserved nucleotides within the proximal promoter region of LMO2 bear similarity to AT hook DNA binding motifs (Landry *et al.*, 2005).

PMA stimulation of TashAT2-transfected BoMac also provided reciprocal profiles to those described above. Thus, profile 4 represented 91 genes whose expression was down-regulated in BoMac-PMA and associated with greater repression in TashAT2-PMA. Candidate genes indentified in this profile included genes like SEPP1 and PGM5 whose expression is reported to be down-regulated in variety of cancers (Gresner *et al.*, 2009;Magee *et al.*, 2001). RT-PCR analysis validated the repression of these genes in BoMac and *Theileria*-infected cells (see Figure 5.15). IPA exploration of genes in this profile showed enrichment in Cell Death (SFRP2, PDE7B, PTPN6 and HLF), inflammatory response (PTPN6) and Cancer (SFRP2, LMOD1, HLF, PGM5 and SEPP1) categories. Repression of some genes was found to be high and included secreted frizzled-related protein 2 (SFRP2; over 159), kelch repeat and BTB (POZ) domain containing 6 (KBTBD6; 23 fold) and hydrogen voltage-gated channel 1 (HVCN; over 8 fold). Like SEPP1, HVCN 1 was also repressed in parasite-infected cells and these proteins are predicted to play a role in protein binding and the oxidative stress response (Burk and Hill, 2009;Capasso *et al.*, 2010;Gonzalez-Moreno *et al.*, 2011).

An extreme pattern of modulation was observed in profile 6 with a similar trend in profile 5: genes down-regulated in BoMacs in PMA response to PMA were up regulated in TashAT2-BoMac in BoMac cells. These profiles contained a smaller

number of genes relative to their reciprocal profiles (2 and 3). In general a lower number of PMA responsive genes were elevated than repressed in TashAT2-BoMacs, indicating TashAT2 is more likely to act as a repressor of PMA stimulated gene expression. Combined IPA analysis of profile 5 and 6 highlighted genes in the categories of cancer (ITGB8, PPAP2B, PDE4B, EFEMp1 and BST2) and cell cycle (GADD45B).

In addition to these results, analysis of the TashAT2-modulated_PMA dataset also identified 24 NF-κB target genes, with 14 NF-κB target genes not highlighted in my previous analysis. The implication is that TashAT2 can manipulate the outcome of expression of genes targeted by NF-κB, which is perhaps not surprising given the result showing enhanced NF-κB reporter activity in TashAT2 expressing BoMacs stimulated with PMA. However, given the large number of NF-κB transcription factor sites identified in whole genome ChIP analysis, it is probable that the NF-κB target gene list utilised in my study is not fully representative and the number of putative TashAT2/NF-κB targets are underestimated.

Interpretation of Common genes altered in 'TashAT2 modulated PMA' and infection modulated LPS datasets

A global comparison of the TashAT2 and *Theileria*-modulated datasets generated by stimulation with by LPS or PMA was performed to assess if there was a significant degree of overlap in gene expression changes representing these cellular states. Thus, results obtained showed significant association by Monte Carlo simulation, providing a dataset of 86 common genes that was greater than the number of common genes expected to occur by chance. This dataset included genes encoding VCAM1, LMO2, TRAF1, IRF8 and PGM5. It can be concluded that both TashAT2 and infection manipulate the outcome of cellular activation induced by two distinct inflammatory mediators in a related but distinct cellular context. This was unlikely to have occurred by chance and provides evidence that a parasite-encoded gene is able to promote a cellular outcome related to that displayed by *Theileria*-infected leukocytes. These results and the recent findings that TashAT/TpHN gene families are expanded and highly conserved in transforming *Theileria* species (Hyashida *et al.*, unpublished; *Weir et al.,* 2009) add further support to the hypothesis that,

together with activation of key host transcription factors, TashATs are likely to play a role in the regulatory circuits that define the gene expression networks of *T. annulata* infected leukocytes.

Conclusions and future directions

Results presented in the previous chapter provided evidence of a parasite dependent global reprogramming of gene expression networks in *Theileria* infected leukocytes. This is likely to occur via activation of host transcription factors, induction of a dedifferentiation event and transportation of parasite factors into the host cell compartment. Consistent with these models, results presented in this chapter provide further evidence that TashAT2 gene family proteins are involved in this process. Based on the available bioinformatic and experimental data it is likely that TashAT2 proteins bind to the promoter regions of host genes or influence the formation of complexes that operate as co-repressors or activators of transcription. TashAT2 expressing cells have demonstrated modulation of a number of functional activities that are also modulated by infection (resistance to apoptosis, control of cell shape, and repression of cellular defence genes). However it is also possible that TashATs mediate their effects in an indirect manner or operate in a regulatory cascade, and so genes identified by the microarray analysis may not be direct targets of TashAT2. Therefore it is important to validate the ability of TashAT2 to bind to the promoters of identified genes. Demonstration that TashATs are directly responsible for altered phenotypes following their expression is also required. Work that could be conducted to confirm these roles is outlined below.

1. **Global bioinformatic screening of putative target genes: Based on the datasets identified in my study** screening for known DNA binding motifs of TashAT2 and activated host transcription factors could be performed. Bioinformatic tools such as Multiple EM for Motif Elicitation (MEME), weight matrix-based tool (Match™) and TRANSFAC® for searching putative transcription factor binding sites in DNA sequences are available (Bailey *et al.*, 2006;Kel *et al.*, 2003;Matys *et al.*, 2006).

2. **Validation of TashAT2 targets for binding to host cell promoters:** Confirmation of physical interaction or binding of TashAT2 should be performed by ChIP-sequencing (ChIP-seq) methodology. This methodology involves chromatin immunoprecipitation (ChIP) followed by massively parallel sequence analysis to identify putative DNA targets sites at more global scale (Robertson *et al.*, 2007). Identification of mammalian DNA sequences bound by transcription factor(s) and/or TashAT2 across the host genome should be possible, including observations of changes to binding patterns associated with infection, inflammatory activation and expression of TashAT factors. My data indicates there is good probability that NF-κB and TashAT2 recognise common gene promoters. Affinity purified antibody specific to TashAT2 or Antibody specific to tagged versions of TashAT2 and commercial antibodies against NF-κB subunits are available for use in standard Chip-Seq protocols (http://www.illumina.com/Documents/products/datasheets/datasheet_chip_sequence.pdf). More precise investigations could then be undertaken by electrophoretic mobility shift analysis (EMSA), gel-shift western blotting, and DNA site mutated reporter constructs.

3. **Reversal of TashAT2 dependent altered phenotype:** attempts to reverse the phenotypes attributed to could be attempted by employing siRNA to knock out expression in BoMac cells. Alternatively cell lines expressing mutant generating TashAT2-truncated cell line (minus AT hook motifs) could be used. Experiments using a novel class of DNA minor groove binding (MGB) drugs such as Distamycin A that compete with HMGA proteins for binding in the minor groove of AT-rich DNA sequences (Baron *et al.*, 2010;Chiang *et al.*, 1994;Ghersa *et al.*, 1997;Smith and Buchmueller, 2011) may also be informative if performed on TashAT2 transfected or parasite infected cells. It is possible however that TashAT expression promotes an irreversible change in regulatory networks and if so knock out experiments would prove un-rewarding.

4. **Characterisation of TashAT2 as modulators of the attenuated cell phenotype:** It is of additional interest to investigate whether TashAT proteins are involved in generation of the attenuated cell phenotype that occurs during prolonged culture/cloning *in vitro*. *Theileria* lab (Glasgow)

has already established a cellular model system of two cloned infected cell lines (D7 and D7B12) that encounter marked differences in cell phenotype: attenuation of parasite differentiation, resistance to cell death, cell shape and expression of TashAT family genes (TashAT2 and TashHN) and a significant difference in activated levels of NF-κB (Schmuckli-Maurer *et al.*, 2010). An independent microarray analysis has been performed to study profile changes to host and parasite gene expression associated with altered phenotype (D7 vs D7B12). Preliminary results obtained from this analysis have already highlighted differential modulation in expression of NF-κB target genes and cytoskeleton signalling (*unpublished data*). Comparison of this dataset with my dataset may provide further information regarding the role of TashATs to modulate host cell gene expression and influence the phenotype and virulence of different *T. annulata* infected cell lines.

The results of this study provide evidence that the *T. annulata* infected cell controls and modulates the outcome of constitutive activation of NF-κB. Evidence is also provided that members of the TAshAT family are involved in this modulation event. In general, IPA indicates that these changes are beneficial to establishment of the infected cell. Additional pathways/transcription factors that operate in the inflammatory response and are associated with carcinogenesis are also manipulated e.g. TNF, TGFβ and cMYC, supporting previous findings (Chaussepied *et al.*, 2010;Dessauge *et al.*, 2005a;Guergnon *et al.*, 2003).It can be postulated that a major reorganisation of networks that regulate signal transduction pathways and gene expression occur following infection of the host leukocyte by *T. annulata*. Studies on *Toxoplama gondii* have identified parasite rhoptry and dense granular proteins that modulate inflammatory gene networks by activating transcription factors, including NF-κB (Rosowski *et al.*, 2011;Saeij *et al.*, 2007). Parasite dependent modification of histone H3 can also prevent transcription factors binding to host cell inflammatory gene promoters (Leng and Denkers, 2009) and it has been proposed that this mechanism accounts for the large-scale down-regulation of pro-inflammatory genes by *T. gondii (*Leng *et al., 2009)*. It is possible that *Theileria* parasites deploy similar mechanisms to manipulate gene expression on a wide scale and evidence of an alteration in the gene encoding a host histone deacetylase has been generated (Kinnaird *et al.*, unpublished data). However,

my results suggest additional alterations are involved. This is indicated by the pairs of reciprocal modulated expression profiles (Figures 5.14 and 5.16) associated with infection and TashAT2 expression; the indication that infection and TashAT2 can reverse gene expression changes induced by LPS and PMA and the non-reversible and non-reciprocal nature of a large number of host gene expression changes when the parasite is killed by drug (Kinnaird *et al.*, unpublished). Such changes could be generated by an irreversible reconfiguration of transcription factor networks associated with differentiation events, as increasingly proposed for stem cell systems (Chickarmane *et al.*, 2006;Chickarmane *et al.*, 2009;Wang *et al.*, 2010). Whether this reorganisation can be brought about by activation of one or several host factors in combination with deployment of TashAT family proteins to the host nucleus is not clear. Other studies have found evidence for additional events such as activation of host polo like kinase (von *et al.*, 2010) and other parasite proteins secreted into the host cell compartment (MacHugh *et al.*, 2011;Schmuckli-Maurer *et al.*, 2009). Given the propensity of *Theileria* parasites to control gene expression networks associated with inflammatory disease and cancer, further study of the mechanisms deployed and the outcomes they promote is warranted.

References

Adamson, R. and Hall, R. (1997) A role for matrix metalloproteinases in the pathology and attenuation of *Theileria annulata* infections. *Parasitol Today* **13:** 390-393.

Adamson, R., Logan, M., Kinnaird, J., Langsley, G., and Hall, R. (2000) Loss of matrix metalloproteinase 9 activity in *Theileria annulata*-attenuated cells is at the transcriptional level and is associated with differentially expressed AP-1 species. *Mol Biochem Parasitol* **106:** 51-61.

Adamson, R. E. and Hall, F. R. (1996) Matrix metalloproteinases mediate the metastatic phenotype of *Theileria annulata*-transformed cells. *Parasitology* **113 (Pt 5):** 449-455.

Aggarwal, B. B., Shishodia, S., Sandur, S. K., Pandey, M. K., and Sethi, G. (2006) Inflammation and cancer: how hot is the link? *Biochem Pharmacol* **72:** 1605-1621.

Ahmad, M., Theofanidis, P., and Medford, R. M. (1998) Role of activating protein-1 in the regulation of the vascular cell adhesion molecule-1 gene expression by tumor necrosis factor-alpha. *J Biol Chem* **273:** 4616-4621.

Ahmed, J. S., Schnittger, L., and Mehlhorn, H. (1999) Review: Theileria schizonts induce fundamental alterations in their host cells. *Parasitol Res* **85:** 527-538.

Akgul, C., Moulding, D. A., and Edwards, S. W. (2001) Molecular control of neutrophil apoptosis. *FEBS Lett* **487:** 318-322.

Akira, S. and Takeda, K. (2004) Toll-like receptor signalling. *Nat Rev Immunol* **4:** 499-511.

Aktas, M., Altay, K., and Dumanli, N. (2006) A molecular survey of bovine *Theileria* parasites among apparently healthy cattle and with a note on the distribution of ticks in eastern Turkey. *Vet Parasitol* **138:** 179-185.

Aktas, M., Dumanli, N., Cetinkaya, B., and Cakmak, A. (2002) Field evaluation of PCR in detecting *Theileria annulata* infection in cattle in eastern Turkey. *Vet Rec* **150:** 548-549.

Alexopoulou, L., Holt, A. C., Medzhitov, R., and Flavell, R. A. (2001) Recognition of double-stranded RNA and activation of NF-kappaB by Toll-like receptor 3. *Nature* **413:** 732-738.

Alikhani, M., Alikhani, Z., He, H., Liu, R., Popek, B. I., and Graves, D. T. (2003) Lipopolysaccharides indirectly stimulate apoptosis and global induction of apoptotic genes in fibroblasts. *J Biol Chem* **278:** 52901-52908.

Allsopp, M. T. and Allsopp, B. A. (2006) Molecular sequence evidence for the reclassification of some Babesia species. *Ann N Y Acad Sci* **1081:** 509-517.

Almeria, S., Castella, J., Ferrer, D., Ortuno, A., Estrada-Pena, A., and Gutierrez, J. F. (2001) Bovine piroplasms in Minorca (Balearic Islands, Spain): a comparison of PCR-based and light microscopy detection. *Vet Parasitol* **99:** 249-259.

Amaral, J. D., Xavier, J. M., Steer, C. J., and Rodrigues, C. M. (2010) The role of p53 in apoptosis. *Discov Med* **9:** 145-152.

Ameyar, M., Wisniewska, M., and Weitzman, J. B. (2003) A role for AP-1 in apoptosis: the case for and against. *Biochimie* **85:** 747-752.

Amiri, K. I., Ha, H. C., Smulson, M. E., and Richmond, A. (2006) Differential regulation of CXC ligand 1 transcription in melanoma cell lines by poly(ADP-ribose) polymerase-1. *Oncogene* **25:** 7714-7722.

Anas, A., van der Poll, T., and de Vos, A. F. (2010) Role of CD14 in lung inflammation and infection. *Crit Care* **14:** 209.

Angiolillo, A. L., Sgadari, C., Taub, D. D., Liao, F., Farber, J. M., Maheshwari, S. *et al.* (1995) Human interferon-inducible protein 10 is a potent inhibitor of angiogenesis in vivo. *J Exp Med* **182:** 155-162.

Anstaett, O. L., Brownlie, J., Collins, M. E., and Thomas, C. J. (2010) Validation of endogenous reference genes for RT-qPCR normalisation in bovine lymphoid cells (BL-3) infected with Bovine Viral Diarrhoea Virus (BVDV). *Vet Immunol Immunopathol* **137:** 201-207.

Arlotta, P., Rustighi, A., Mantovani, F., Manfioletti, G., Giancotti, V., Tell, G. *et al.* (1997) High mobility group I proteins interfere with the homeodomains binding to DNA. *J Biol Chem* **272:** 29904-29910.

Arnold, R., Brenner, D., Becker, M., Frey, C. R., and Krammer, P. H. (2006) How T lymphocytes switch between life and death. *Eur J Immunol* **36:** 1654-1658.

Arya, M., Patel, H. R., and Williamson, M. (2003) Chemokines: key players in cancer. *Curr Med Res Opin* **19:** 557-564.

Askarov, E. M. (1975) Virulence and immunogenic properties in strains of *Theileria annulata*. *Veterinariia* 76-78.

Baeuerle, P. A. and Henkel, T. (1994) Function and activation of NF-kappa B in the immune system. *Annu Rev Immunol* **12:** 141-179.

Bahl, A., Brunk, B., Crabtree, J., Fraunholz, M. J., Gajria, B., Grant, G. R. *et al.* (2003) PlasmoDB: the Plasmodium genome resource. A database integrating experimental and computational data. *Nucleic Acids Res* **31:** 212-215.

Bailey, T. L., Williams, N., Misleh, C., and Li, W. W. (2006) MEME: discovering and analyzing DNA and protein sequence motifs. *Nucleic Acids Res* **34:** W369-W373.

Bakheit, M. A. and Latif, A. A. (2002) The innate resistance of Kenana cattle to tropical theileriosis (*Theileria annulata* infection) in the Sudan. *Ann N Y Acad Sci* **969:** 159-163.

Bakheit, M. A., Schnittger, L., Salih, D. A., Boguslawski, K., Beyer, D., Fadl, M. *et al*. (2004) Application of the recombinant *Theileria annulata* surface protein in an indirect ELISA for the diagnosis of tropical theileriosis. *Parasitol Res* **92:** 299-302.

Balbin, M., Pendas, A. M., Uria, J. A., Jimenez, M. G., Freije, J. P., and Lopez-Otin, C. (1999) Expression and regulation of collagenase-3 (MMP-13) in human malignant tumors. *APMIS* **107:** 45-53.

Baldwin, A. S., Jr. (1996) The NF-kappa B and I kappa B proteins: new discoveries and insights. *Annu Rev Immunol* **14:** 649-683.

Baldwin, C. L., Black, S. J., Brown, W. C., Conrad, P. A., Goddeeris, B. M., Kinuthia, S. W. *et al*. (1988) Bovine T cells, B cells, and null cells are transformed by the protozoan parasite Theileria parva. *Infect Immun* **56:** 462-467.

Bannerman, D. D., Erwert, R. D., Winn, R. K., and Harlan, J. M. (2002) TIRAP mediates endotoxin-induced NF-kappaB activation and apoptosis in endothelial cells. *Biochem Biophys Res Commun* **295:** 157-162.

Bannerman, D. D. and Goldblum, S. E. (2003) Mechanisms of bacterial lipopolysaccharide-induced endothelial apoptosis. *Am J Physiol Lung Cell Mol Physiol* **284:** L899-L914.

Barker, T. H., Baneyx, G., Cardo-Vila, M., Workman, G. A., Weaver, M., Menon, P. M. *et al*. (2005) SPARC regulates extracellular matrix organization through its modulation of integrin-linked kinase activity. *J Biol Chem* **280:** 36483-36493.

Barkett, M. and Gilmore, T. D. (1999) Control of apoptosis by Rel/NF-kappaB transcription factors. *Oncogene* **18:** 6910-6924.

Barnes, P. J. and Karin, M. (1997) Nuclear factor-kappaB: a pivotal transcription factor in chronic inflammatory diseases. *N Engl J Med* **336:** 1066-1071.

Baron, R. M., Lopez-Guzman, S., Riascos, D. F., Macias, A. A., Layne, M. D., Cheng, G. *et al*. (2010) Distamycin A inhibits HMGA1-binding to the P-selectin promoter and attenuates lung and liver inflammation during murine endotoxemia. *PLoS One* **5:** e10656.

Barreiro, O. and Sanchez-Madrid, F. (2009) Molecular basis of leukocyte-endothelium interactions during the inflammatory response. *Rev Esp Cardiol* **62:** 552-562.

Barsig, J., Kusters, S., Vogt, K., Volk, H. D., Tiegs, G., and Wendel, A. (1995) Lipopolysaccharide-induced interleukin-10 in mice: role of endogenous tumor necrosis factor-alpha. *Eur J Immunol* **25:** 2888-2893.

Basseres, D. S. and Baldwin, A. S. (2006) Nuclear factor-kappaB and inhibitor of kappaB kinase pathways in oncogenic initiation and progression. *Oncogene* **25:** 6817-6830.

Baumgartner, M. (2011a) Enforcing host cell polarity: an apicomplexan parasite strategy towards dissemination. *Curr Opin Microbiol* **14:** 436-444.

Baumgartner, M. (2011b) *Theileria annulata* promotes Src kinase-dependent host cell polarization by manipulating actin dynamics in podosomes and lamellipodia. *Cell Microbiol* **13:** 538-553.

Baumgartner, M., Chaussepied, M., Moreau, M. F., Werling, D., Davis, W. C., Garcia, A. *et al.* (2000) Constitutive PI3-K activity is essential for proliferation, but not survival, of *Theileria parva*-transformed B cells. *Cell Microbiol* **2:** 329-339.

Bayascas, J. R., Yuste, V. J., Benito, E., Garcia-Fernandez, J., and Comella, J. X. (2002) Isolation of AmphiCASP-3/7, an ancestral caspase from amphioxus (Branchiostoma floridae). Evolutionary considerations for vertebrate caspases. *Cell Death Differ* **9:** 1078-1089.

Baylis, H. A., Megson, A., Brown, C. G., Wilkie, G. F., and Hall, R. (1992) Theileria annulata-infected cells produce abundant proteases whose activity is reduced by long-term cell culture. *Parasitology* **105 (Pt 3):** 417-423.

Baylis, H. A., Megson, A., and Hall, R. (1995) Infection with *Theileria annulata* induces expression of matrix metalloproteinase 9 and transcription factor AP-1 in bovine leucocytes. *Mol Biochem Parasitol* **69:** 211-222.

Beinke, S. and Ley, S. C. (2004) Functions of NF-kappaB1 and NF-kappaB2 in immune cell biology. *Biochem J* **382:** 393-409.

Beniwal, R. K., Sharma, R. D., and Nichani, A. K. (1998) Susceptibility to tropical theileriosis of calves born to dams immunized with Theileria annulata (Hisar) cell culture vaccine. *Trop Anim Health Prod* **30:** 341-349.

Benjamin, D., Magrath, I. T., Triche, T. J., Schroff, R. W., Jensen, J. P., and Korsmeyer, S. J. (1984) Induction of plasmacytoid differentiation by phorbol ester in B-cell lymphoma cell lines bearing 8;14 translocations. *Proc Natl Acad Sci U S A* **81:** 3547-3551.

Benjamini, Y. and Hochberg, Y. (1995) Controlling the False Discovery Rate: A Practical and Powerful Approach to Multiple Testing. *Journal of the Royal Statistical Society Series B (Methodological)* **57:** 289-300.

Beutler, B. (2000) Tlr4: central component of the sole mammalian LPS sensor. *Curr Opin Immunol* **12:** 20-26.

Beutler, B. (2002) LPS in microbial pathogenesis: promise and fulfilment. *J Endotoxin Res* **8:** 329-335.

Bevilacqua, M. P. (1993) Endothelial-leukocyte adhesion molecules. *Annu Rev Immunol* **11:** 767-804.

Bilgic, H. B., Karagenc, T., Shiels, B., Tait, A., Eren, H., and Weir, W. (2010) Evaluation of cytochrome b as a sensitive target for PCR based detection of *T. annulata* carrier animals. *Vet Parasitol* **174:** 341-347.

Bjorkman, L., Dahlgren, C., Karlsson, A., Brown, K. L., and Bylund, J. (2008) Phagocyte-derived reactive oxygen species as suppressors of inflammatory disease. *Arthritis Rheum* **58:** 2931-2935.

Blader, I. J., Manger, I. D., and Boothroyd, J. C. (2001) Microarray analysis reveals previously unknown changes in *Toxoplasma gondii*-infected human cells. *J Biol Chem* **276:** 24223-24231.

Bocharov, A. V., Baranova, I. N., Vishnyakova, T. G., Remaley, A. T., Csako, G., Thomas, F. *et al.* (2004) Targeting of scavenger receptor class B type I by synthetic amphipathic alpha-helical-containing peptides blocks lipopolysaccharide (LPS) uptake and LPS-induced pro-inflammatory cytokine responses in THP-1 monocyte cells. *J Biol Chem* **279:** 36072-36082.

Boehm, T., Foroni, L., Kaneko, Y., Perutz, M. F., and Rabbitts, T. H. (1991) The rhombotin family of cysteine-rich LIM-domain oncogenes: distinct members are involved in T-cell translocations to human chromosomes 11p15 and 11p13. *Proc Natl Acad Sci U S A* **88:** 4367-4371.

Boise, L. H., Petryniak, B., Mao, X., June, C. H., Wang, C. Y., Lindsten, T. *et al.* (1993) The NFAT-1 DNA binding complex in activated T cells contains Fra-1 and JunB. *Mol Cell Biol* **13:** 1911-1919.

Bokoch, G. M. (2003) Biology of the p21-activated kinases. *Annu Rev Biochem* **72:** 743-781.

Bolstad, B. M., Irizarry, R. A., Astrand, M., and Speed, T. P. (2003) A comparison of normalization methods for high density oligonucleotide array data based on variance and bias. *Bioinformatics* **19:** 185-193.

Botteron, C. and Dobbelaere, D. (1998) AP-1 and ATF-2 are constitutively activated via the JNK pathway in Theileria parva-transformed T-cells. *Biochem Biophys Res Commun* **246:** 418-421.

Bouattour, A., Darghouth, M. A., and Ben, M. L. (1996) Cattle infestation by Hyalomma ticks and prevalence of Theileria in *H. detritum* species in Tunisia. *Vet Parasitol* **65:** 233-245.

Boulter, N. and Hall, R. (1999) Immunity and vaccine development in the bovine theilerioses. *Adv Parasitol* **44:** 41-97.

Boyd, A. W., Wawryk, S. O., Burns, G. F., and Fecondo, J. V. (1988) Intercellular adhesion molecule 1 (ICAM-1) has a central role in cell-cell contact-mediated immune mechanisms. *Proc Natl Acad Sci U S A* **85:** 3095-3099.

Bozdech, Z., Zhu, J., Joachimiak, M. P., Cohen, F. E., Pulliam, B., and DeRisi, J. L. (2003) Expression profiling of the schizont and trophozoite stages of *Plasmodium falciparum* with a long-oligonucleotide microarray. *Genome Biol* **4:** R9.

Bradshaw, A. D. and Sage, E. H. (2001) SPARC, a matricellular protein that functions in cellular differentiation and tissue response to injury. *J Clin Invest* **107:** 1049-1054.

Breitling, R., Armengaud, P., Amtmann, A., and Herzyk, P. (2004) Rank products: a simple, yet powerful, new method to detect differentially regulated genes in replicated microarray experiments. *FEBS Lett* **573:** 83-92.

Briggs, J., Chamboredon, S., Castellazzi, M., Kerry, J. A., and Bos, T. J. (2002) Transcriptional upregulation of SPARC, in response to c-Jun overexpression, contributes to increased motility and invasion of MCF7 breast cancer cells. *Oncogene* **21:** 7077-7091.

Brown, C. G. (1990) Control of tropical theileriosis (*Theileria annulata* infection) of cattle. *Parassitologia* **32:** 23-31.

Brown, D. J., Campbell, J. D., Russell, G. C., Hopkins, J., and Glass, E. J. (1995a) T cell activation by Theileria annulata-infected macrophages correlates with cytokine production. *Clin Exp Immunol* **102:** 507-514.

Brown, D. J., Campbell, J. D., Russell, G. C., Hopkins, J., and Glass, E. J. (1995b) T cell activation by *Theileria annulata*-infected macrophages correlates with cytokine production. *Clin Exp Immunol* **102:** 507-514.

Bruder, E. D., Lee, J. J., Widmaier, E. P., and Raff, H. (2007) Microarray and real-time PCR analysis of adrenal gland gene expression in the 7-day-old rat: effects of hypoxia from birth. *Physiol Genomics* **29:** 193-200.

Brunckhorst, M. K., Wang, H., Lu, R., and Yu, Q. (2010) Angiopoietin-4 promotes glioblastoma progression by enhancing tumor cell viability and angiogenesis. *Cancer Res* **70:** 7283-7293.

Bryce, N. S., Clark, E. S., Leysath, J. L., Currie, J. D., Webb, D. J., and Weaver, A. M. (2005) Cortactin promotes cell motility by enhancing lamellipodial persistence. *Curr Biol* **15:** 1276-1285.

Buchholz, M., Biebl, A., Neesse, A., Wagner, M., Iwamura, T., Leder, G. *et al.* (2003) SERPINE2 (protease nexin I) promotes extracellular matrix production and local invasion of pancreatic tumors in vivo. *Cancer Res* **63:** 4945-4951.

Bulua, A. C., Simon, A., Maddipati, R., Pelletier, M., Park, H., Kim, K. Y. *et al.* (2011) Mitochondrial reactive oxygen species promote production of proinflammatory cytokines and are elevated in TNFR1-associated periodic syndrome (TRAPS). *J Exp Med* **208:** 519-533.

Burk, R. F. and Hill, K. E. (2009) Selenoprotein P-expression, functions, and roles in mammals. *Biochim Biophys Acta* **1790:** 1441-1447.

Bustin, M. and Reeves, R. (1996) High-mobility-group chromosomal proteins: architectural components that facilitate chromatin function. *Prog Nucleic Acid Res Mol Biol* **54:** 35-100.

Bustin, S. A. (2000) Absolute quantification of mRNA using real-time reverse transcription polymerase chain reaction assays
6. *J Mol Endocrinol* **25:** 169-193.

Busuttil, V., Bottero, V., Frelin, C., Imbert, V., Ricci, J. E., Auberger, P. *et al.* (2002) Blocking NF-kappaB activation in Jurkat leukemic T cells converts the survival agent and tumor promoter PMA into an apoptotic effector. *Oncogene* **21:** 3213-3224.

Campbel, J. D. and Spooner, R. L. (1999) Macrophages behaving badly: infected cells and subversion of immune responses to *Theileria annulata*. *Parasitol Today* **15:** 10-16.

Cangul, H. (2004) Hypoxia upregulates the expression of the NDRG1 gene leading to its overexpression in various human cancers. *BMC Genet* **5:** 27.

Capasso, M., Bhamrah, M. K., Henley, T., Boyd, R. S., Langlais, C., Cain, K. *et al*. (2010) HVCN1 modulates BCR signal strength via regulation of BCR-dependent generation of reactive oxygen species. *Nat Immunol* **11:** 265-272.

Carluccio, M. A., Ancora, M. A., Massaro, M., Carluccio, M., Scoditti, E., Distante, A. *et al*. (2007) Homocysteine induces VCAM-1 gene expression through NF-kappaB and NAD(P)H oxidase activation: protective role of Mediterranean diet polyphenolic antioxidants. *Am J Physiol Heart Circ Physiol* **293:** H2344-H2354.

Caruso, R. P., Levinson, B., Melamed, J., Wieczorek, R., Taneja, S., Polsky, D. *et al*. (2004) Altered N-myc downstream-regulated gene 1 protein expression in African-American compared with caucasian prostate cancer patients. *Clin Cancer Res* **10:** 222-227.

Casalino, L., Bakiri, L., Talotta, F., Weitzman, J. B., Fusco, A., Yaniv, M. *et al*. (2007) Fra-1 promotes growth and survival in RAS-transformed thyroid cells by controlling cyclin A transcription. *EMBO J* **26:** 1878-1890.

Catez, F., Yang, H., Tracey, K. J., Reeves, R., Misteli, T., and Bustin, M. (2004) Network of dynamic interactions between histone H1 and high-mobility-group proteins in chromatin. *Mol Cell Biol* **24:** 4321-4328.

Cazzalini, O., Scovassi, A. I., Savio, M., Stivala, L. A., and Prosperi, E. (2010) Multiple roles of the cell cycle inhibitor p21(CDKN1A) in the DNA damage response. *Mutat Res* **704:** 12-20.

Chang, D. W., Xing, Z., Pan, Y., Algeciras-Schimnich, A., Barnhart, B. C., Yaish-Ohad, S. *et al*. (2002) c-FLIP(L) is a dual function regulator for caspase-8 activation and CD95-mediated apoptosis. *EMBO J* **21:** 3704-3714.

Chanteux, H., Guisset, A. C., Pilette, C., and Sibille, Y. (2007) LPS induces IL-10 production by human alveolar macrophages via MAPKinases- and Sp1-dependent mechanisms. *Respir Res* **8:** 71.

Chaussepied, M., Janski, N., Baumgartner, M., Lizundia, R., Jensen, K., Weir, W. *et al*. (2010) TGF-b2 induction regulates invasiveness of Theileria-transformed leukocytes and disease susceptibility. *PLoS Pathog* **6:** e1001197.

Chaussepied, M., Lallemand, D., Moreau, M. F., Adamson, R., Hall, R., and Langsley, G. (1998) Upregulation of Jun and Fos family members and permanent JNK activity lead to constitutive AP-1 activation in *Theileria*-transformed leukocytes. *Mol Biochem Parasitol* **94:** 215-226.

Chaussepied, M. and Langsley, G. (1996) *Theileria* transformation of bovine leukocytes: a parasite model for the study of lymphoproliferation. *Res Immunol* **147:** 127-138.

Chaussepied, M., Michie, A. M., Moreau, M. F., Harnett, M. M., Harnett, W., and Langsley, G. (2006) Notch is constitutively active in Theileria-transformed B cells and can be further stimulated by the filarial nematode-secreted product, ES-62. *Microbes Infect* **8:** 1189-1191.

Chen, C., Chou, C., Sun, Y., and Huang, W. (2001) Tumor necrosis factor alpha-induced activation of downstream NF-kappaB site of the promoter mediates epithelial ICAM-1 expression and monocyte adhesion. Involvement of PKCalpha, tyrosine kinase, and IKK2, but not MAPKs, pathway. *Cell Signal* **13:** 543-553.

Chiang, S. Y., Welch, J., Rauscher, F. J., III, and Beerman, T. A. (1994) Effects of minor groove binding drugs on the interaction of TATA box binding protein and TFIIA with DNA. *Biochemistry* **33:** 7033-7040.

Chickarmane, V., Enver, T., and Peterson, C. (2009) Computational modeling of the hematopoietic erythroid-myeloid switch reveals insights into cooperativity, priming, and irreversibility. *PLoS Comput Biol* **5:** e1000268.

Chickarmane, V., Troein, C., Nuber, U. A., Sauro, H. M., and Peterson, C. (2006) Transcriptional dynamics of the embryonic stem cell switch. *PLoS Comput Biol* **2:** e123.

Cho, I. J., Lee, A. K., Lee, S. J., Lee, M. G., and Kim, S. G. (2005) Repression by oxidative stress of iNOS and cytokine gene induction in macrophages results from AP-1 and NF-kappaB inhibition mediated by B cell translocation gene-1 activation. *Free Radic Biol Med* **39:** 1523-1536.

Chung, T. and Kim, Y. B. (1988) Two distinct cytolytic mechanisms of macrophages and monocytes activated by phorbol myristate acetate. *J Leukoc Biol* **44:** 329-336.

Chuvpilo, S., Schomberg, C., Gerwig, R., Heinfling, A., Reeves, R., Grummt, F. *et al.* (1993) Multiple closely-linked NFAT/octamer and HMG I(Y) binding sites are part of the interleukin-4 promoter. *Nucleic Acids Res* **21:** 5694-5704.

Cicek, H., Cicek, H., Eser, M., and Tandogan, M. (2009) Current status of ruminant theileriosis and its economical impact in Turkey. *Turkiye Parazitol Derg* **33:** 273-279.

Cleynen, I. and Van de Ven, W. J. (2008) The HMGA proteins: a myriad of functions (Review). *Int J Oncol* **32:** 289-305.

Cohen, L., Haziot, A., Shen, D. R., Lin, X. Y., Sia, C., Harper, R. *et al.* (1995) CD14-independent responses to LPS require a serum factor that is absent from neonates. *J Immunol* **155:** 5337-5342.

Collart, M. A., Baeuerle, P., and Vassalli, P. (1990) Regulation of tumor necrosis factor alpha transcription in macrophages: involvement of four kappa B-like motifs and of constitutive and inducible forms of NF-kappa B. *Mol Cell Biol* **10:** 1498-1506.

Collins, K., Jacks, T., and Pavletich, N. P. (1997) The cell cycle and cancer. *Proc Natl Acad Sci U S A* **94:** 2776-2778.

Collins, T., Read, M. A., Neish, A. S., Whitley, M. Z., Thanos, D., and Maniatis, T. (1995a) Transcriptional regulation of endothelial cell adhesion molecules: NF-kappa B and cytokine-inducible enhancers. *FASEB J* **9:** 899-909.

Collins, T., Read, M. A., Neish, A. S., Whitley, M. Z., Thanos, D., and Maniatis, T. (1995b) Transcriptional regulation of endothelial cell adhesion molecules: NF-kappa B and cytokine-inducible enhancers. *FASEB J* **9:** 899-909.

Conrad, P. A., Kelly, B. G., and Brown, C. G. (1985) Intraerythrocytic schizogony of *Theileria annulata*. *Parasitology* **91 (Pt 1):** 67-82.

Cosen-Binker, L. I. and Kapus, A. (2006) Cortactin: the gray eminence of the cytoskeleton. *Physiology (Bethesda)* **21:** 352-361.

Crawley, J. B., Williams, L. M., Mander, T., Brennan, F. M., and Foxwell, B. M. (1996) Interleukin-10 stimulation of phosphatidylinositol 3-kinase and p70 S6 kinase is required for the proliferative but not the antiinflammatory effects of the cytokine. *J Biol Chem* **271:** 16357-16362.

Crespin, M., Vidal, C., Picard, F., Lacombe, C., and Fontenay, M. (2009) Activation of PAK1/2 during the shedding of platelet microvesicles. *Blood Coagul Fibrinolysis* **20:** 63-70.

Cross, S. L., Halden, N. F., Lenardo, M. J., and Leonard, W. J. (1989) Functionally distinct NF-kappa B binding sites in the immunoglobulin kappa and IL-2 receptor alpha chain genes. *Science* **244:** 466-469.

Curran, T. and Franza, B. R., Jr. (1988) Fos and Jun: the AP-1 connection. *Cell* **55:** 395-397.

d'Oliveira, C., van der Weide, M., Habela, M. A., Jacquiet, P., and Jongejan, F. (1995) Detection of *Theileria annulata* in blood samples of carrier cattle by PCR. *J Clin Microbiol* **33:** 2665-2669.

d'Oliveira, C., van der Weide, M., Jacquiet, P., and Jongejan, F. (1997) Detection of *Theileria annulata* by the PCR in ticks (Acari:Ixodidae) collected from cattle in Mauritania. *Exp Appl Acarol* **21:** 279-291.

Dando, C. (1997) Studies on altered gene expression in *Theileria annulata* infected cells and uninfected cells of a related lineage. *Ph D thesis University of Glasgow, Glasgow, UK*.

Dando, C. and Shiels, B. (1997) Modulation of growth relative to division regulates expression of a *Theileria annulata* infection associated antigen in HL-60 cells differentiating towards granulocytes. *Int J Oncol* **11:** 971-982.

Dang, C. V. (1999) c-Myc target genes involved in cell growth, apoptosis, and metabolism. *Mol Cell Biol* **19:** 1-11.

Dang, C. V., O'Donnell, K. A., Zeller, K. I., Nguyen, T., Osthus, R. C., and Li, F. (2006) The c-Myc target gene network. *Semin Cancer Biol* **16:** 253-264.

Darghouth, M. E., Bouattour, A., Ben, M. L., and Sassi, L. (1996) Diagnosis of *Theileria annulata* infection of cattle in Tunisia: comparison of serology and blood smears. *Vet Res* **27:** 613-621.

Day, M. L., Zhao, X., Wu, S., Swanson, P. E., and Humphrey, P. A. (1994) Phorbol ester-induced apoptosis is accompanied by NGFI-A and c-fos activation in androgen-sensitive prostate cancer cells
1. *Cell Growth Differ* **5:** 735-741.

Deaciuc, I. V., Fortunato, F., D'Souza, N. B., Hill, D. B., Schmidt, J., Lee, E. Y. *et al.* (1999) Modulation of caspase-3 activity and Fas ligand mRNA expression in rat liver cells in vivo by alcohol and lipopolysaccharide. *Alcohol Clin Exp Res* **23:** 349-356.

Deryugina, E. I. and Quigley, J. P. (2006) Matrix metalloproteinases and tumor metastasis. *Cancer Metastasis Rev* **25:** 9-34.

Dessauge, F., Hilaly, S., Baumgartner, M., Blumen, B., Werling, D., and Langsley, G. (2005a) c-Myc activation by *Theileria* parasites promotes survival of infected B-lymphocytes. *Oncogene* **24:** 1075-1083.

Dessauge, F., Lizundia, R., and Langsley, G. (2005b) Constitutively activated CK2 potentially plays a pivotal role in Theileria-induced lymphocyte transformation. *Parasitology* **130 Suppl:** S37-S44.

Dhar, S. and Gautam, O. P. (1977) Indirect fluorenscent antibody test for serodiagnosis in cattle infected with *Theileria annulata*. *Indian J Anim Sci* **47:** 720-723.

Dhar, S., Malhotra, D. V., Bhushan, C., and Gautam, O. P. (1990) Chemoimmunoprophylaxis against bovine tropical theileriosis in young calves: a comparison between buparvaquone and long-acting oxytetracycline. *Res Vet Sci* **49:** 110-112.

Dhawan, S., Singh, S., and Aggarwal, B. B. (1997) Induction of endothelial cell surface adhesion molecules by tumor necrosis factor is blocked by protein tyrosine phosphatase inhibitors: role of the nuclear transcription factor NF-kappa B. *Eur J Immunol* **27:** 2172-2179.

Dobbelaere, D. and Heussler, V. (1999) Transformation of leukocytes by *Theileria parva* and *T. annulata*. *Annu Rev Microbiol* **53:** 1-42.

Dobbelaere, D. A. and Kuenzi, P. (2004) The strategies of the Theileria parasite: a new twist in host-pathogen interactions. *Curr Opin Immunol* **16:** 524-530.

Dobbelaere, D. A., Prospero, T. D., Roditi, I. J., Kelke, C., Baumann, I., Eichhorn, M. *et al.* (1990) Expression of Tac antigen component of bovine interleukin-2 receptor in different leukocyte populations infected with *Theileria parva* or *Theileria annulata*. *Infect Immun* **58:** 3847-3855.

Dobbelaere, D. A., Roditi, I. J., Coquerelle, T. M., Kelke, C., Eichhorn, M., and Williams, R. O. (1991a) Lymphocytes infected with Theileria parva require both cell-cell contact and growth factor to proliferate. *Eur J Immunol* **21:** 89-95.

Dobbelaere, D. A., Roditi, I. J., Coquerelle, T. M., Kelke, C., Eichhorn, M., and Williams, R. O. (1991b) Lymphocytes infected with Theileria parva require both cell-cell contact and growth factor to proliferate. *Eur J Immunol* **21:** 89-95.

Dobbelaere, D. A. and Rottenberg, S. (2003) Theileria-induced leukocyte transformation. *Curr Opin Microbiol* **6:** 377-382.

Dolan, T. T. (1989) Theileriasis: a comprehensive review. *Rev sci tech Off int Epiz* **8:** 11-36.

Dolan, T. T., Young, A. S., Leitch, B. L., and Stagg, D. A. (1984) Chemotherapy of East Coast fever: parvaquone treatment of clinical disease induced by isolates of *Theileria parva*. *Vet Parasitol* **15:** 103-116.

Donjerkovic, D. and Scott, D. W. (2000) Activation-induced cell death in B lymphocytes. *Cell Res* **10:** 179-192.

Du, W. and Maniatis, T. (1994) The high mobility group protein HMG I(Y) can stimulate or inhibit DNA binding of distinct transcription factor ATF-2 isoforms. *Proc Natl Acad Sci U S A* **91:** 11318-11322.

Du, W., Thanos, D., and Maniatis, T. (1993) Mechanisms of transcriptional synergism between distinct virus-inducible enhancer elements. *Cell* **74:** 887-898.

Duchow, J., Marchant, A., Crusiaux, A., Husson, C., Alonso-Vega, C., De, G. D. *et al.* (1993) Impaired phagocyte responses to lipopolysaccharide in paroxysmal nocturnal hemoglobinuria. *Infect Immun* **61:** 4280-4285.

Dumanli, N., Aktas, M., Cetinkaya, B., Cakmak, A., Koroglu, E., Saki, C. E. *et al.* (2005) Prevalence and distribution of tropical theileriosis in eastern Turkey. *Vet Parasitol* **127:** 9-15.

Dummler, B., Ohshiro, K., Kumar, R., and Field, J. (2009) Pak protein kinases and their role in cancer. *Cancer Metastasis Rev* **28:** 51-63.

Dunn, G. P., Koebel, C. M., and Schreiber, R. D. (2006) Interferons, immunity and cancer immunoediting. *Nat Rev Immunol* **6:** 836-848.

Dutta, J., Fan, Y., Gupta, N., Fan, G., and Gelinas, C. (2006) Current insights into the regulation of programmed cell death by NF-kappaB. *Oncogene* **25:** 6800-6816.

Eichhorn, M. and Dobbelaere, D. A. (1994) Induction of signal transduction pathways in lymphocytes infected by *Theileria parva*. *Parasitol Today* **10:** 469-472.

Elnemr, A., Yonemura, Y., Bandou, E., Kinoshita, K., Kawamura, T., Takahashi, S. *et al.* (2003) Expression of collagenase-3 (matrix metalloproteinase-13) in human gastric cancer. *Gastric Cancer* **6:** 30-38.

Elner, S. G., Petty, H. R., Elner, V. M., Yoshida, A., Bian, Z. M., Yang, D. *et al.* (2005) TLR4 mediates human retinal pigment epithelial endotoxin binding and cytokine expression. *Trans Am Ophthalmol Soc* **103:** 126-135.

Fakler, C. R., Wu, B., McMicken, H. W., Geske, R. S., and Welty, S. E. (2000) Molecular mechanisms of lipopolysaccharide induced ICAM-1 expression in A549 cells. *Inflamm Res* **49:** 63-72.

Fannjiang, Y., Kim, C. H., Huganir, R. L., Zou, S., Lindsten, T., Thompson, C. B. *et al.* (2003) BAK alters neuronal excitability and can switch from anti- to pro-death function during postnatal development. *Dev Cell* **4:** 575-585.

Fedele, M., Battista, S., Manfioletti, G., Croce, C. M., Giancotti, V., and Fusco, A. (2001) Role of the high mobility group A proteins in human lipomas. *Carcinogenesis* **22:** 1583-1591.

Feig, D. I., Reid, T. M., and Loeb, L. A. (1994) Reactive oxygen species in tumorigenesis. *Cancer Res* **54:** 1890s-1894s.

Feldman, A. L., Friedl, J., Lans, T. E., Libutti, S. K., Lorang, D., Miller, M. S. *et al.* (2002) Retroviral gene transfer of interferon-inducible protein 10 inhibits growth of human melanoma xenografts. *Int J Cancer* **99:** 149-153.

Fell, A. H., Preston, P. M., and Ansell, J. D. (1990) Establishment of Theileria-infected bovine cell lines in scid mice. *Parasite Immunol* **12:** 335-339.

Fenouille, N., Puissant, A., Tichet, M., Zimniak, G., Abbe, P., Mallavialle, A. *et al.* (2011a) SPARC functions as an anti-stress factor by inactivating p53 through Akt-mediated MDM2 phosphorylation to promote melanoma cell survival. *Oncogene*.

Fenouille, N., Puissant, A., Tichet, M., Zimniak, G., Abbe, P., Mallavialle, A. *et al.* (2011b) SPARC functions as an anti-stress factor by inactivating p53 through Akt-mediated MDM2 phosphorylation to promote melanoma cell survival. *Oncogene*.

Fenouille, N., Robert, G., Tichet, M., Puissant, A., Dufies, M., Rocchi, S. *et al.* (2011c) The p53/p21Cip1/ Waf1 pathway mediates the effects of SPARC on melanoma cell cycle progression
1. *Pigment Cell Melanoma Res* **24:** 219-232.

Finlay, B. B. and McFadden, G. (2006) Anti-immunology: evasion of the host immune system by bacterial and viral pathogens. *Cell* **124:** 767-782.

Firestein, G. S. and Pisetsky, D. S. (2002) DNA microarrays: boundless technology or bound by technology? Guidelines for studies using microarray technology. *Arthritis Rheum* **46:** 859-861.

Flach, E. J. and Ouhelli, H. (1992) The epidemiology of tropical theileriosis (*Theileria annulata* infection in cattle) in an endemic area of Morocco. *Vet Parasitol* **44:** 51-65.

Flohr, A. M., Rogalla, P., Bonk, U., Puettmann, B., Buerger, H., Gohla, G. *et al.* (2003) High mobility group protein HMGA1 expression in breast cancer reveals a positive correlation with tumour grade. *Histol Histopathol* **18:** 999-1004.

Foletta, V. C., Segal, D. H., and Cohen, D. R. (1998) Transcriptional regulation in the immune system: all roads lead to AP-1. *J Leukoc Biol* **63:** 139-152.

Folgueras, A. R., Pendas, A. M., Sanchez, L. M., and Lopez-Otin, C. (2004) Matrix metalloproteinases in cancer: from new functions to improved inhibition strategies. *Int J Dev Biol* **48:** 411-424.

Forsyth, L. M., Minns, F. C., Kirvar, E., Adamson, R. E., Hall, F. R., McOrist, S. *et al.* (1999) Tissue damage in cattle infected with *Theileria annulata* accompanied by metastasis of cytokine-producing, schizont-infected mononuclear phagocytes. *J Comp Pathol* **120:** 39-57.

Fournier, C., Wiese, C., and Taucher-Scholz, G. (2004) Accumulation of the cell cycle regulators TP53 and CDKN1A (p21) in human fibroblasts after exposure to low- and high-LET radiation. *Radiat Res* **161:** 675-684.

Fresno Vara, J. A., Casado, E., de, C. J., Cejas, P., Belda-Iniesta, C., and Gonzalez-Baron, M. (2004) PI3K/Akt signalling pathway and cancer. *Cancer Treat Rev* **30:** 193-204.

Fusco, A. and Fedele, M. (2007) Roles of HMGA proteins in cancer. *Nat Rev Cancer* **7:** 899-910.

Gagliardi, M., Maynard, S., Miyake, T., Rodrigues, N., Tjew, S. L., Cabannes, E. *et al.* (2003) Opposing roles of C/EBPbeta and AP-1 in the control of fibroblast proliferation and growth arrest-specific gene expression. *J Biol Chem* **278:** 43846-43854.

Galley, Y., Hagens, G., Glaser, I., Davis, W., Eichhorn, M., and Dobbelaere, D. (1997) Jun NH2-terminal kinase is constitutively activated in T cells transformed by the intracellular parasite *Theileria parva*. *Proc Natl Acad Sci U S A* **94:** 5119-5124.

Garay-Malpartida, H. M., Mourao, R. F., Mantovani, M., Santos, I. A., Sogayar, M. C., and Goldberg, A. C. (2011) Toll-like receptor 4 (TLR4) expression in human and murine pancreatic beta-cells affects cell viability and insulin homeostasis. *BMC Immunol* **12:** 18.

Garcia-Heras, F., Padmanabhan, S., Murillo, F. J., and Elias-Arnanz, M. (2009) Functional equivalence of HMGA- and histone H1-like domains in a bacterial transcriptional factor. *Proc Natl Acad Sci U S A* **106:** 13546-13551.

Gerondakis, S., Grumont, R., Rourke, I., and Grossmann, M. (1998) The regulation and roles of Rel/NF-kappa B transcription factors during lymphocyte activation. *Curr Opin Immunol* **10:** 353-359.

Gessner, A., Vieth, M., Will, A., Schroppel, K., and Rollinghoff, M. (1993) Interleukin-7 enhances antimicrobial activity against Leishmania major in murine macrophages
3. *Infect Immun* **61:** 4008-4012.

Gharbi, M., Sassi, L., Dorchies, P., and Darghouth, M. A. (2006) Infection of calves with *Theileria annulata* in Tunisia: Economic analysis and evaluation of the potential benefit of vaccination. *Vet Parasitol* **137:** 231-241.

Ghersa, P., Whelan, J., Cambet, Y., DeLamarter, J. F., and Hooft van, H. R. (1997) Distamycin prolongs E-selectin expression by interacting with a specific NF-kappaB-HMG-I(Y) binding site in the promoter. *Nucleic Acids Res* **25:** 339-346.

Gilbert, L. A., Ravindran, S., Turetzky, J. M., Boothroyd, J. C., and Bradley, P. J. (2007) *Toxoplasma gondii* targets a protein phosphatase 2C to the nuclei of infected host cells. *Eukaryot Cell* **6:** 73-83.

Gill, B. S., Bhattacharyulu, Y., Kaur, D., and Singh, A. (1978) Chemoprophylaxis with tetracycline drugs in the immunisation of cattle against *Theileria annulata* infection. *Int J Parasitol* **8:** 467-469.

Gilmore, T. D. (1999) The Rel/NF-kappaB signal transduction pathway: introduction. *Oncogene* **18:** 6842-6844.

Ginaldi, L., De, M. M., D'Ostilio, A., Marini, L., Loreto, M. F., Corsi, M. P. *et al.* (2000) Cell proliferation and apoptosis in the immune system in the elderly. *Immunol Res* **21:** 31-38.

Glass, E. J. (2001) The balance between protective immunity and pathogenesis in tropical theileriosis: what we need to know to design effective vaccines for the future. *Res Vet Sci* **70:** 71-75.

Glass, E. J., Innes, E. A., Spooner, R. L., and Brown, C. G. (1989) Infection of bovine monocyte/macrophage populations with *Theileria annulata* and *Theileria parva*. *Vet Immunol Immunopathol* **22:** 355-368.

Glass, E. J., Preston, P. M., Springbett, A., Craigmile, S., Kirvar, E., Wilkie, G. *et al.* (2005) *Bos taurus* and *Bos indicus* (Sahiwal) calves respond differently to infection with *Theileria annulata* and produce markedly different levels of acute phase proteins. *Int J Parasitol* **35:** 337-347.

Gobert, G. N., Moertel, L. P., and McManus, D. P. (2005) Microarrays: new tools to unravel parasite transcriptomes. *Parasitology* **131:** 439-448.

Gonzalez, V. and Hurley, L. H. (2010) The c-MYC NHE III(1): function and regulation. *Annu Rev Pharmacol Toxicol* **50:** 111-129.

Gonzalez-Moreno, O., Boque, N., Redrado, M., Milagro, F., Campion, J., Endermann, T. *et al.* (2011) Selenoprotein-P is down-regulated in prostate cancer, which results in lack of protection against oxidative damage. *Prostate* **71:** 824-834.

Gray, M. A., Luckins, A. G., Rae, P. F., and Brown, C. G. (1980) Evaluation of an enzyme immunoassay for serodiagnosis of infections with *Theileria parva* and *T annulata*. *Res Vet Sci* **29:** 360-366.

Gresner, P., Gromadzinska, J., Jablonska, E., Kaczmarski, J., and Wasowicz, W. (2009) Expression of selenoprotein-coding genes SEPP1, SEP15 and hGPX1 in non-small cell lung cancer. *Lung Cancer* **65:** 34-40.

Gubbels, M. J., d'Oliveira, C., and Jongejan, F. (2000) Development of an indirect Tams1 enzyme-linked immunosorbent assay for diagnosis of *Theileria annulata* infection in cattle. *Clin Diagn Lab Immunol* **7:** 404-411.

Guergnon, J., Chaussepied, M., Sopp, P., Lizundia, R., Moreau, M. F., Blumen, B. *et al.* (2003) A tumour necrosis factor alpha autocrine loop contributes to

proliferation and nuclear factor-kappaB activation of *Theileria parva*-transformed B cells. *Cell Microbiol* **5:** 709-716.

Guergnon, J., Dessauge, F., Traincard, F., Cayla, X., Rebollo, A., Bost, P. E. *et al.* (2006) A PKA survival pathway inhibited by DPT-PKI, a new specific cell permeable PKA inhibitor, is induced by *T. annulata* in parasitized B-lymphocytes. *Apoptosis* **11:** 1263-1273.

Gunji, H., Hass, R., and Kufe, D. (1992) Internucleosomal DNA fragmentation during phorbol ester-induced monocytic differentiation and G0/G1 arrest. *J Clin Invest* **89:** 954-960.

Gurzov, E. N., Ortis, F., Bakiri, L., Wagner, E. F., and Eizirik, D. L. (2008) JunB Inhibits ER Stress and Apoptosis in Pancreatic Beta Cells. *PLoS One* **3:** e3030.

Gyles, C. L., Prescott, J. F., Songer, J. G., and Thoen, C. O. (2007) Themes in Bacterial Pathogenic Mechanisms.(in Pathogenesis of Bacterial Infections in Animals)
1. *Ames, IA: Blackwell Publishing,* p 9.

Haase, R., Kirschning, C. J., Sing, A., Schrottner, P., Fukase, K., Kusumoto, S. *et al.* (2003) A dominant role of Toll-like receptor 4 in the signaling of apoptosis in bacteria-faced macrophages. *J Immunol* **171:** 4294-4303.

Habibi, G., Esmaeil Nia, K., Hashemi-Fesharki, R., and Bordbar, N. (2009) Semi-quantitative Analysis of Expression of Various Genes in relation to Possible Markers for *Theileria annulata* Attenuation. *Archives of Razi Institute* **64:** 9-17.

Hakim, J. (1993) [Reactive oxygen species and inflammation]
2. *C R Seances Soc Biol Fil* **187:** 286-295.

Halazonetis, T. D., Georgopoulos, K., Greenberg, M. E., and Leder, P. (1988) c-Jun dimerizes with itself and with c-Fos, forming complexes of different DNA binding affinities. *Cell* **55:** 917-924.

Hall, R., Ilhan, T., Kirvar, E., Wilkie, G., Preston, P. M., Darghouth, M. *et al.* (1999) Mechanism(s) of attenuation of *Theileria annulata* vaccine cell lines. *Trop Med Int Health* **4:** A78-A84.

Haller, D., Mackiewicz, M., Gerber, S., Beyer, D., Kullmann, B., Schneider, I. *et al.* (2010) Cytoplasmic sequestration of p53 promotes survival in leukocytes transformed by Theileria. *Oncogene* **29:** 3079-3086.

Hammond, S. M., Crable, S. C., and Anderson, K. P. (2005) Negative regulatory elements are present in the human LMO2 oncogene and may contribute to its expression in leukemia
2. *Leuk Res* **29:** 89-97.

Hansson, A., Zetterblad, J., van, D. C., Axelson, H., and Jonsson, J. I. (2007) The Lim-only protein LMO2 acts as a positive regulator of erythroid differentiation. *Biochem Biophys Res Commun* **364:** 675-681.

Harris, T. A., Yamakuchi, M., Ferlito, M., Mendell, J. T., and Lowenstein, C. J. (2008) MicroRNA-126 regulates endothelial expression of vascular cell adhesion molecule 1. *Proc Natl Acad Sci U S A* **105:** 1516-1521.

Hasanpour, A., Moghaddam, G. A., and Nematollahi, A. (2008) Biochemical, hematological, and electrocardiographic changes in buffaloes naturally infected with *Theileria annulata*. *Korean J Parasitol* **46:** 223-227.

Hauf, N., Goebel, W., Fiedler, F., Sokolovic, Z., and Kuhn, M. (1997) Listeria monocytogenes infection of P388D1 macrophages results in a biphasic NF-kappaB (RelA/p50) activation induced by lipoteichoic acid and bacterial phospholipases and mediated by IkappaBalpha and IkappaBbeta degradation. *Proc Natl Acad Sci U S A* **94:** 9394-9399.

Hawa, N., Rae, D. G., Younis, S., Mahadi, W., Ibrahim, R., and al-Wahab, W. (1988) Efficacy of parvaquone in the treatment of naturally occurring theileriosis in cattle in Iraq. *Trop Anim Health Prod* **20:** 130-136.

Hayashida, K., Hattori, M., Nakao, R., Tanaka, Y., Kim, J. Y., Inoue, N. *et al.* (2010) A schizont-derived protein, TpSCOP, is involved in the activation of NF-kappaB in *Theileria parva*-infected lymphocytes. *Mol Biochem Parasitol* **174:** 8-17.

Hayden, M. S. and Ghosh, S. (2004) Signaling to NF-kappaB. *Genes Dev* **18:** 2195-2224.

Heidarpour, B. M., Haddadzadeh, H. R., Kazemi, B., Khazraiinia, P., Bandehpour, M., and Aktas, M. (2009) Molecular identification of ovine *Theileria* species by a new PCR-RFLP method. *Vet Parasitol* **161:** 171-177.

Helfgott, D. C., May, L. T., Sthoeger, Z., Tamm, I., and Sehgal, P. B. (1987) Bacterial lipopolysaccharide (endotoxin) enhances expression and secretion of beta 2 interferon by human fibroblasts. *J Exp Med* **166:** 1300-1309.

Hemphill, A. (1999) The host-parasite relationship in neosporosis. *Adv Parasitol* **43:** 47-104.

Hemphill, A. and Gottstein, B. (2006) *Neospora caninum* and neosporosis - recent achievements in host and parasite cell biology and treatment. *ACTA PARASITOLOGICA* **51:** 15-25.

Henkler, F., Baumann, B., Fotin-Mleczek, M., Weingartner, M., Schwenzer, R., Peters, N. *et al.* (2003) Caspase-mediated cleavage converts the tumor necrosis factor (TNF) receptor-associated factor (TRAF)-1 from a selective modulator of TNF receptor signaling to a general inhibitor of NF-kappaB activation. *J Biol Chem* **278:** 29216-29230.

Hennessy, B. T., Smith, D. L., Ram, P. T., Lu, Y., and Mills, G. B. (2005) Exploiting the PI3K/AKT pathway for cancer drug discovery. *Nat Rev Drug Discov* **4:** 988-1004.

Herrmann, T., Ahmed, J. S., and Diamantstein, T. (1989) The intermediate-affinity interleukin (IL)2 receptor expressed on Theileria annulata-infected cells

comprises a single IL 2-binding protein. Partial characterization of bovine IL2 receptors. *Eur J Immunol* **19:** 1339-1342.

Hess, J., Angel, P., and Schorpp-Kistner, M. (2004a) AP-1 subunits: quarrel and harmony among siblings. *J Cell Sci* **117:** 5965-5973.

Hess, J., Angel, P., and Schorpp-Kistner, M. (2004b) AP-1 subunits: quarrel and harmony among siblings. *J Cell Sci* **117:** 5965-5973.

Heussler, V. T., Eichhorn, M., Reeves, R., Magnuson, N. S., Williams, R. O., and Dobbelaere, D. A. (1992) Constitutive IL-2 mRNA expression in lymphocytes, infected with the intracellular parasite *Theileria parva*. *J Immunol* **149:** 562-567.

Heussler, V. T., Kuenzi, P., Fraga, F., Schwab, R. A., Hemmings, B. A., and Dobbelaere, D. A. (2001) The Akt/PKB pathway is constitutively activated in *Theileria*-transformed leucocytes, but does not directly control constitutive NF-kappaB activation. *Cell Microbiol* **3:** 537-550.

Heussler, V. T., Machado, J., Jr., Fernandez, P. C., Botteron, C., Chen, C. G., Pearse, M. J. *et al.* (1999) The intracellular parasite *Theileria parva* protects infected T cells from apoptosis. *Proc Natl Acad Sci U S A* **96:** 7312-7317.

Heussler, V. T., Rottenberg, S., Schwab, R., Kuenzi, P., Fernandez, P. C., McKellar, S. *et al.* (2002) Hijacking of host cell IKK signalosomes by the transforming parasite *Theileria*. *Science* **298:** 1033-1036.

Heussler, V. T. and Stanway, R. R. (2008) Cellular and molecular interactions between the apicomplexan parasites *Plasmodium* and *Theileria* and their host cells. *Parasite* **15:** 211-218.

Hida, A., Kawakami, A., Nakashima, T., Yamasaki, S., Sakai, H., Urayama, S. *et al.* (2000) Nuclear factor-kappaB and caspases co-operatively regulate the activation and apoptosis of human macrophages. *Immunology* **99:** 553-560.

Hoebe, K., Janssen, E. M., Kim, S. O., Alexopoulou, L., Flavell, R. A., Han, J. *et al.* (2003) Upregulation of costimulatory molecules induced by lipopolysaccharide and double-stranded RNA occurs by Trif-dependent and Trif-independent pathways. *Nat Immunol* **4:** 1223-1229.

Hommura, F., Katabami, M., Leaner, V. D., Donninger, H., Sumter, T. F., Resar, L. M. *et al.* (2004) HMG-I/Y is a c-Jun/activator protein-1 target gene and is necessary for c-Jun-induced anchorage-independent growth in Rat1a cells. *Mol Cancer Res* **2:** 305-314.

Honda, K., Yanai, H., Takaoka, A., and Taniguchi, T. (2005) Regulation of the type I IFN induction: a current view. *Int Immunol* **17:** 1367-1378.

Hoshino, K., Takeuchi, O., Kawai, T., Sanjo, H., Ogawa, T., Takeda, Y. *et al.* (1999) Cutting edge: Toll-like receptor 4 (TLR4)-deficient mice are hyporesponsive to lipopolysaccharide: evidence for TLR4 as the Lps gene product. *J Immunol* **162:** 3749-3752.

Hosoi, F., Izumi, H., Kawahara, A., Murakami, Y., Kinoshita, H., Kage, M. *et al.* (2009) N-myc downstream regulated gene 1/Cap43 suppresses tumor growth and angiogenesis of pancreatic cancer through attenuation of inhibitor of kappaB kinase beta expression. *Cancer Res* **69:** 4983-4991.

Hovanessian, A. G. and Justesen, J. (2007) The human 2'-5'oligoadenylate synthetase family: unique interferon-inducible enzymes catalyzing 2'-5' instead of 3'-5' phosphodiester bond formation. *Biochimie* **89:** 779-788.

Hruz, T., Wyss, M., Docquier, M., Pfaffl, M. W., Masanetz, S., Borghi, L. *et al.* (2011) RefGenes: identification of reliable and condition specific reference genes for RT-qPCR data normalization. *BMC Genomics* **12:** 156.

Hsu, S. L., Chou, Y. H., Yin, S. C., and Liu, J. Y. (1998) Differential effects of phorbol ester on growth and protein kinase C isoenzyme regulation in human hepatoma Hep3B cells. *Biochem J* **333 (Pt 1):** 57-64.

Huang, W. C., Chan, S. T., Yang, T. L., Tzeng, C. C., and Chen, C. C. (2004) Inhibition of ICAM-1 gene expression, monocyte adhesion and cancer cell invasion by targeting IKK complex: molecular and functional study of novel alpha-methylene-gamma-butyrolactone derivatives. *Carcinogenesis* **25:** 1925-1934.

Hulliger, L. (1965) Cultivation of three species of Theileria in lymphoid cells in vitro. *J Protozool* **12:** 649-655.

Huo, Y., Hafezi-Moghadam, A., and Ley, K. (2000) Role of vascular cell adhesion molecule-1 and fibronectin connecting segment-1 in monocyte rolling and adhesion on early atherosclerotic lesions. *Circ Res* **87:** 153-159.

Huynh, N., Liu, K. H., Baldwin, G. S., and He, H. (2010) P21-activated kinase 1 stimulates colon cancer cell growth and migration/invasion via ERK- and AKT-dependent pathways. *Biochim Biophys Acta* **1803:** 1106-1113.

Iademarco, M. F., McQuillan, J. J., Rosen, G. D., and Dean, D. C. (1992) Characterization of the promoter for vascular cell adhesion molecule-1 (VCAM-1). *J Biol Chem* **267:** 16323-16329.

Illes, A., Enyedi, B., Tamas, P., Balazs, A., Bogel, G., Melinda *et al.* (2006) Cortactin is required for integrin-mediated cell spreading. *Immunol Lett* **104:** 124-130.

Inci, A., Ica, A., Yildirim, A., Vatansever, Z., Cakmak, A., Albasan, H. *et al.* (2007) Economical impact of tropical theileriosis in the Cappadocia region of Turkey. *Parasitol Res* **101 Suppl 2:** S171-S174.

Irizarry, R. A., Hobbs, B., Collin, F., Beazer-Barclay, Y. D., Antonellis, K. J., Scherf, U. *et al.* (2003) Exploration, normalization, and summaries of high density oligonucleotide array probe level data. *Biostatistics* **4:** 249-264.

Irvin, A. D., Cunningham, A. P., and Young, A. S. (1981) Advances in the Control of Theileriosis: International Conference Proceedings (Current Topics in Veterinary Medicine). *Mertinus Nijhoff Publishers, The Hague* 73-175.

Irvin, A. D., Brown, C. G., Kanhai, G. K., and Stagg, D. A. (1975) Comparative growth of bovine lymphosarcoma cells and lymphoid cells infected with *Theileria parva* in athymic (nude) mice. *Nature* **255:** 713-714.

Irvin, A. D. and Morrison, W. (1987) Immunopathology, immunology, and immonoprophylaxis of *Theileria* infections, in Immune responses in parasitic infections:Immunology, Immunopathology, and immunoprophylaxis of *Theileria* infections. *E J L Soulsby, CRC Press Inc, Baton Rouge, Florida* 223-274.

Islam, M. K., Alim, M. A., Tsuji, N., and Mondal, M. M. (2006) An investigation into the distribution, host-preference and population density of ixodid ticks affecting domestic animals in Bangladesh. *Trop Anim Health Prod* **38:** 485-490.

Islam, M. K., Jabbar, A., Campbell, B. E., Cantacessi, C., and Gasser, R. B. (2011) Bovine theileriosis - An emerging problem in south-eastern Australia? *Infect Genet Evol*.

Ivanov, V., Stein, B., Baumann, I., Dobbelaere, D. A., Herrlich, P., and Williams, R. O. (1989) Infection with the intracellular protozoan parasite Theileria parva induces constitutively high levels of NF-kappa B in bovine T lymphocytes. *Mol Cell Biol* **9:** 4677-4686.

Jackson, A. L. and Loeb, L. A. (2001) The contribution of endogenous sources of DNA damage to the multiple mutations in cancer. *Mutat Res* **477:** 7-21.

Jacobs-Helber, S. M., Wickrema, A., Birrer, M. J., and Sawyer, S. T. (1998) AP1 regulation of proliferation and initiation of apoptosis in erythropoietin-dependent erythroid cells. *Mol Cell Biol* **18:** 3699-3707.

Jain, J., Loh, C., and Rao, A. (1995) Transcriptional regulation of the IL-2 gene. *Curr Opin Immunol* **7:** 333-342.

Jain, J., McCaffrey, P. G., Valge-Archer, V. E., and Rao, A. (1992) Nuclear factor of activated T cells contains Fos and Jun. *Nature* **356:** 801-804.

Jarrett, W. F., Crighton, G. W., and Pirie, H. M. (1969) *Theileria parva*: kinetics of replication. *Exp Parasitol* **24:** 9-25.

Jensen, K., Makins, G. D., Kaliszewska, A., Hulme, M. J., Paxton, E., and Glass, E. J. (2009) The protozoan parasite *Theileria annulata* alters the differentiation state of the infected macrophage and suppresses musculoaponeurotic fibrosarcoma oncogene (MAF) transcription factors. *Int J Parasitol* **39:** 1099-1108.

Jensen, K., Paxton, E., Waddington, D., Talbot, R., Darghouth, M. A., and Glass, E. J. (2008) Differences in the transcriptional responses induced by *Theileria annulata* infection in bovine monocytes derived from resistant and susceptible cattle breeds. *Int J Parasitol* **38:** 313-325.

Jensen, K., Speed, D., Paxton, E., Williams, J. L., and Glass, E. J. (2006a) Construction of a normalized Bos taurus and Bos indicus macrophage-specific cDNA library. *Anim Genet* **37:** 75-77.

Jensen, K., Talbot, R., Paxton, E., Waddington, D., and Glass, E. J. (2006b) Development and validation of a bovine macrophage specific cDNA microarray. *BMC Genomics* **7:** 224.

Jiang, K., Shen, Z., Ye, Y., Yang, X., and Wang, S. (2010) A novel molecular marker for early detection and evaluating prognosis of gastric cancer: N-myc downstream regulated gene-1 (NDRG1). *Scand J Gastroenterol* **45:** 898-908.

Jin, H. K., Takada, A., Kon, Y., Haller, O., and Watanabe, T. (1999) Identification of the murine Mx2 gene: interferon-induced expression of the Mx2 protein from the feral mouse gene confers resistance to vesicular stomatitis virus. *J Virol* **73:** 4925-4930.

Jochum, W., Passegue, E., and Wagner, E. F. (2001) AP-1 in mouse development and tumorigenesis. *Oncogene* **20:** 2401-2412.

Johar, D., Roth, J. C., Bay, G. H., Walker, J. N., Kroczak, T. J., and Los, M. (2004) Inflammatory response, reactive oxygen species, programmed (necrotic-like and apoptotic) cell death and cancer. *Rocz Akad Med Bialymst* **49:** 31-39.

John, S., Reeves, R. B., Lin, J. X., Child, R., Leiden, J. M., Thompson, C. B. *et al.* (1995) Regulation of cell-type-specific interleukin-2 receptor alpha-chain gene expression: potential role of physical interactions between Elf-1, HMG-I(Y), and NF-kappa B family proteins. *Mol Cell Biol* **15:** 1786-1796.

Jones, B. W., Heldwein, K. A., Means, T. K., Saukkonen, J. J., and Fenton, M. J. (2001) Differential roles of Toll-like receptors in the elicitation of proinflammatory responses by macrophages. *Ann Rheum Dis* **60 Suppl 3:** iii6-12.

Julkunen, I., Sareneva, T., Pirhonen, J., Ronni, T., Melen, K., and Matikainen, S. (2001) Molecular pathogenesis of influenza A virus infection and virus-induced regulation of cytokine gene expression. *Cytokine Growth Factor Rev* **12:** 171-180.

Jungi, T. W., Thony, M., Brcic, M., Adler, B., Pauli, U., and Peterhans, E. (1996) Induction of nitric oxide synthase in bovine mononuclear phagocytes is differentiation stage-dependent. *Immunobiology* **195:** 385-400.

Kabakchiev, B., Turner, D., Hyams, J., Mack, D., Leleiko, N., Crandall, W. *et al.* (2010) Gene expression changes associated with resistance to intravenous corticosteroid therapy in children with severe ulcerative colitis. *PLoS One* **5**.

Kalis, C., Kanzler, B., Lembo, A., Poltorak, A., Galanos, C., and Freudenberg, M. A. (2003) Toll-like receptor 4 expression levels determine the degree of LPS-susceptibility in mice. *Eur J Immunol* **33:** 798-805.

Kamau, J., de Vos, A. J., Playford, M., Salim, B., Kinyanjui, P., and Sugimoto, C. (2011) Emergence of new types of *Theileria orientalis* in Australian cattle and possible cause of theileriosis outbreaks. *Parasit Vectors* **4:** 22.

Kaminska, B., Pyrzynska, B., Ciechomska, I., and Wisniewska, M. (2000) Modulation of the composition of AP-1 complex and its impact on transcriptional activity. *Acta Neurobiol Exp (Wars)* **60:** 395-402.

Kanarek, N., London, N., Schueler-Furman, O., and Ben-Neriah, Y. (2010) Ubiquitination and degradation of the inhibitors of NF-kappaB. *Cold Spring Harb Perspect Biol* **2:** a000166.

Karin, M., Cao, Y., Greten, F. R., and Li, Z. W. (2002) NF-kappaB in cancer: from innocent bystander to major culprit. *Nat Rev Cancer* **2:** 301-310.

Karin, M. and Lin, A. (2002) NF-kappaB at the crossroads of life and death. *Nat Immunol* **3:** 221-227.

Kasibhatla, S., Genestier, L., and Green, D. R. (1999) Regulation of fas-ligand expression during activation-induced cell death in T lymphocytes via nuclear factor kappaB. *J Biol Chem* **274:** 987-992.

Kataoka, K., Nishizawa, M., and Kawai, S. (1993) Structure-function analysis of the maf oncogene product, a member of the b-Zip protein family. *J Virol* **67:** 2133-2141.

Kataoka, T., Budd, R. C., Holler, N., Thome, M., Martinon, F., Irmler, M. *et al.* (2000) The caspase-8 inhibitor FLIP promotes activation of NF-kappaB and Erk signaling pathways. *Curr Biol* **10:** 640-648.

Kawai, T. and Akira, S. (2007) Signaling to NF-kappaB by Toll-like receptors. *Trends Mol Med* **13:** 460-469.

Kawai, T., Takeuchi, O., Fujita, T., Inoue, J., Muhlradt, P. F., Sato, S. *et al.* (2001) Lipopolysaccharide stimulates the MyD88-independent pathway and results in activation of IFN-regulatory factor 3 and the expression of a subset of lipopolysaccharide-inducible genes. *J Immunol* **167:** 5887-5894.

Kel, A. E., Gossling, E., Reuter, I., Cheremushkin, E., Kel-Margoulis, O. V., and Wingender, E. (2003) MATCH: A tool for searching transcription factor binding sites in DNA sequences. *Nucleic Acids Res* **31:** 3576-3579.

Kim, H. G., Kim, J. Y., Han, E. H., Hwang, Y. P., Choi, J. H., Park, B. H. *et al.* (2011) Metallothionein-2A overexpression increases the expression of matrix metalloproteinase-9 and invasion of breast cancer cells. *FEBS Lett* **585:** 421-428.

Kim, K. I., Malakhova, O. A., Hoebe, K., Yan, M., Beutler, B., and Zhang, D. E. (2005) Enhanced antibacterial potential in UBP43-deficient mice against Salmonella typhimurium infection by up-regulating type I IFN signaling. *J Immunol* **175:** 847-854.

Kim, K. I. and Zhang, D. E. (2003) ISG15, not just another ubiquitin-like protein. *Biochem Biophys Res Commun* **307:** 431-434.

Kim, K. T., Ongusaha, P. P., Hong, Y. K., Kurdistani, S. K., Nakamura, M., Lu, K. P. *et al.* (2004a) Function of Drg1/Rit42 in p53-dependent mitotic spindle checkpoint. *J Biol Chem* **279:** 38597-38602.

Kim, L., Butcher, B. A., and Denkers, E. Y. (2004b) *Toxoplasma gondii* interferes with lipopolysaccharide-induced mitogen-activated protein kinase activation by mechanisms distinct from endotoxin tolerance. *J Immunol* **172:** 3003-3010.

Kim, S. K., Fouts, A. E., and Boothroyd, J. C. (2007) *Toxoplasma gondii* dysregulates IFN-gamma-inducible gene expression in human fibroblasts: insights from a genome-wide transcriptional profiling. *J Immunol* **178:** 5154-5165.

Kitowska, A. and Pawelczyk, T. (2010) N-myc downstream regulated 1 gene and its place in the cellular machinery. *Acta Biochim Pol* **57:** 15-21.

Kondratiev, S., Gnepp, D. R., Yakirevich, E., Sabo, E., Annino, D. J., Rebeiz, E. *et al.* (2008) Expression and prognostic role of MMP2, MMP9, MMP13, and MMP14 matrix metalloproteinases in sinonasal and oral malignant melanomas. *Hum Pathol* **39:** 337-343.

Kovary, K. and Bravo, R. (1991) The jun and fos protein families are both required for cell cycle progression in fibroblasts. *Mol Cell Biol* **11:** 4466-4472.

Kunsch, C. and Rosen, C. A. (1993) NF-kappa B subunit-specific regulation of the interleukin-8 promoter. *Mol Cell Biol* **13:** 6137-6146.

Lai, J. M., Hsieh, C. L., and Chang, Z. F. (2003) Caspase activation during phorbol ester-induced apoptosis requires ROCK-dependent myosin-mediated contraction. *J Cell Sci* **116:** 3491-3501.

Landry, J. R., Kinston, S., Knezevic, K., Donaldson, I. J., Green, A. R., and Gottgens, B. (2005) Fli1, Elf1, and Ets1 regulate the proximal promoter of the LMO2 gene in endothelial cells. *Blood* **106:** 2680-2687.

Lang, C., Algner, M., Beinert, N., Gross, U., and Luder, C. G. (2006) Diverse mechanisms employed by *Toxoplasma gondii* to inhibit IFN-gamma-induced major histocompatibility complex class II gene expression. *Microbes Infect* **8:** 1994-2005.

Lazo, J. S. and Pitt, B. R. (1995) Metallothioneins and cell death by anticancer drugs. *Annu Rev Pharmacol Toxicol* **35:** 635-653.

Le Roch, K. G., Zhou, Y., Blair, P. L., Grainger, M., Moch, J. K., Haynes, J. D. *et al.* (2003) Discovery of gene function by expression profiling of the malaria parasite life cycle. *Science* **301:** 1503-1508.

Lee, C. W., Lin, W. N., Lin, C. C., Luo, S. F., Wang, J. S., Pouyssegur, J. *et al.* (2006) Transcriptional regulation of VCAM-1 expression by tumor necrosis factor-alpha in human tracheal smooth muscle cells: involvement of MAPKs, NF-kappaB, p300, and histone acetylation. *J Cell Physiol* **207:** 174-186.

Leifso, K., Cohen-Freue, G., Dogra, N., Murray, A., and McMaster, W. R. (2007) Genomic and proteomic expression analysis of Leishmania promastigote and amastigote life stages: the Leishmania genome is constitutively expressed. *Mol Biochem Parasitol* **152:** 35-46.

Leiriao, P., Rodrigues, C. D., Albuquerque, S. S., and Mota, M. M. (2004) Survival of protozoan intracellular parasites in host cells. *EMBO Rep* **5:** 1142-1147.

Lenardo, M. J., Fan, C. M., Maniatis, T., and Baltimore, D. (1989) The involvement of NF-kappa B in beta-interferon gene regulation reveals its role as widely inducible mediator of signal transduction. *Cell* **57:** 287-294.

Leng, J., Butcher, B. A., and Denkers, E. Y. (2009) Dysregulation of macrophage signal transduction by *Toxoplasma gondii*: past progress and recent advances. *Parasite Immunol* **31:** 717-728.

Leng, J. and Denkers, E. Y. (2009) Toxoplasma gondii inhibits covalent modification of histone H3 at the IL-10 promoter in infected macrophages. *PLoS One* **4:** e7589.

Levine, N. D. (1985) Apicomplexa: The Piroplasms. *Veterinary Protozoology, The Iowa state University Press, Ames,Iowa* 291-328.

Lewis, R. T., Andreucci, A., and Nikolajczyk, B. S. (2001) PU.1-mediated transcription is enhanced by HMG-I(Y)-dependent structural mechanisms. *J Biol Chem* **276:** 9550-9557.

Li, J., Peet, G. W., Balzarano, D., Li, X., Massa, P., Barton, R. W. *et al.* (2001) Novel NEMO/IkappaB kinase and NF-kappa B target genes at the pre-B to immature B cell transition. *J Biol Chem* **276:** 18579-18590.

Li, Q. and Verma, I. M. (2002) NF-kappaB regulation in the immune system. *Nat Rev Immunol* **2:** 725-734.

Li, X., Fujikura, Y., Wang, Y. H., Sawada, T., Tokuda, N., Lovely, R. S. *et al.* (1997) Expression of ICAM-1 in implanted primary and metastatic squamous cell carcinomas in rats. *J Oral Pathol Med* **26:** 371-376.

Lin, S. C. (2006) Identification of an NF-Y/HMG-I(Y)-binding site in the human IL-10 promoter. *Mol Immunol* **43:** 1325-1331.

Lin, Y. C., Shun, C. T., Wu, M. S., and Chen, C. C. (2006) A novel anticancer effect of thalidomide: inhibition of intercellular adhesion molecule-1-mediated cell invasion and metastasis through suppression of nuclear factor-kappaB. *Clin Cancer Res* **12:** 7165-7173.

Lindner, V. and Collins, T. (1996) Expression of NF-kappa B and I kappa B-alpha by aortic endothelium in an arterial injury model. *Am J Pathol* **148:** 427-438.

Lindwall, C. and Kanje, M. (2005) The Janus role of c-Jun: cell death versus survival and regeneration of neonatal sympathetic and sensory neurons. *Exp Neurol* **196:** 184-194.

Liu, H., Shi, B., Huang, C. C., Eksarko, P., and Pope, R. M. (2008) Transcriptional diversity during monocyte to macrophage differentiation. *Immunol Lett* **117:** 70-80.

Liu, Y. L., Bai, W. T., Luo, W., Zhang, D. X., Yan, Y., Xu, Z. K. *et al.* (2011) Downregulation of NDRG1 promotes invasion of human gastric cancer AGS cells through MMP-2. *Tumour Biol* **32:** 99-105.

Livak, K. J. and Schmittgen, T. D. (2001) Analysis of relative gene expression data using real-time quantitative PCR and the 2(-Delta Delta C(T)) Method. *Methods* **25:** 402-408.

Lizundia, R., Chaussepied, M., Huerre, M., Werling, D., Di Santo, J. P., and Langsley, G. (2006) c-Jun NH2-terminal kinase/c-Jun signaling promotes survival

and metastasis of B lymphocytes transformed by *Theileria*. *Cancer Res* **66:** 6105-6110.

Longley, R. L., Woods, A., Fleetwood, A., Cowling, G. J., Gallagher, J. T., and Couchman, J. R. (1999) Control of morphology, cytoskeleton and migration by syndecan-4. *J Cell Sci* **112 (Pt 20):** 3421-3431.

Lu, G., Reinert, J. T., Pitha-Rowe, I., Okumura, A., Kellum, M., Knobeloch, K. P. *et al.* (2006) ISG15 enhances the innate antiviral response by inhibition of IRF-3 degradation. *Cell Mol Biol (Noisy -le-grand)* **52:** 29-41.

Luder, C. G., Stanway, R. R., Chaussepied, M., Langsley, G., and Heussler, V. T. (2009) Intracellular survival of apicomplexan parasites and host cell modification. *Int J Parasitol* **39:** 163-173.

Luster, A. D., Greenberg, S. M., and Leder, P. (1995) The IP-10 chemokine binds to a specific cell surface heparan sulfate site shared with platelet factor 4 and inhibits endothelial cell proliferation. *J Exp Med* **182:** 219-231.

Lynn, W. A., Liu, Y., and Golenbock, D. T. (1993) Neither CD14 nor serum is absolutely necessary for activation of mononuclear phagocytes by bacterial lipopolysaccharide. *Infect Immun* **61:** 4452-4461.

MacHugh, N. D., Weir, W., Burrells, A., Lizundia, R., Graham, S. P., Taracha, E. L. *et al.* (2011) Extensive polymorphism and evidence of immune selection in a highly dominant antigen recognized by bovine CD8 T cells specific for *Theileria annulata*. *Infect Immun* **79:** 2059-2069.

Magee, J. A., Araki, T., Patil, S., Ehrig, T., True, L., Humphrey, P. A. *et al.* (2001) Expression profiling reveals hepsin overexpression in prostate cancer. *Cancer Res* **61:** 5692-5696.

Makarov, S. S., Johnston, W. N., Olsen, J. C., Watson, J. M., Mondal, K., Rinehart, C. *et al.* (1997) NF-kappa B as a target for anti-inflammatory gene therapy: suppression of inflammatory responses in monocytic and stromal cells by stable gene transfer of I kappa B alpha cDNA. *Gene Ther* **4:** 846-852.

Malakhova, O., Malakhov, M., Hetherington, C., and Zhang, D. E. (2002) Lipopolysaccharide activates the expression of ISG15-specific protease UBP43 via interferon regulatory factor 3. *J Biol Chem* **277:** 14703-14711.

Maldonado, C., Trejo, W., Ramirez, A., Carrera, M., Sanchez, J., Lopez-Macias, C. *et al.* (2000) Lipophosphopeptidoglycan of Entamoeba histolytica induces an antiinflammatory innate immune response and downregulation of toll-like receptor 2 (TLR-2) gene expression in human monocytes. *Arch Med Res* **31:** S71-S73.

Malhotra, R. and Bird, M. I. (1997a) L-Selectin--a signalling receptor for lipopolysaccharide. *Chem Biol* **4:** 543-547.

Malhotra, R. and Bird, M. I. (1997b) L-selectin: a novel receptor for lipopolysaccharide and its potential role in bacterial sepsis. *Bioessays* **19:** 919-923.

Malhotra, R., Priest, R., Foster, M. R., and Bird, M. I. (1998) P-selectin binds to bacterial lipopolysaccharide. *Eur J Immunol* **28:** 983-988.

Malide, D., Davies-Hill, T. M., Levine, M., and Simpson, I. A. (1998) Distinct localization of GLUT-1, -3, and -5 in human monocyte-derived macrophages: effects of cell activation. *Am J Physiol* **274:** E516-E526.

Mallick, K. P., Dhar, S., Malhotra, D. V., Bhushan, C., and Gautam, O. P. (1987) Immunization of neonatal bovines against *Theileria annulata* by an infection and treatment method. *Vet Parasitol* **24:** 169-173.

Manger, I. D. and Relman, D. A. (2000) How the host 'sees' pathogens: global gene expression responses to infection. *Curr Opin Immunol* **12:** 215-218.

Mannori, G., Crottet, P., Cecconi, O., Hanasaki, K., Aruffo, A., Nelson, R. M. *et al.* (1995) Differential colon cancer cell adhesion to E-, P-, and L-selectin: role of mucin-type glycoproteins. *Cancer Res* **55:** 4425-4431.

Mantovani, F., Covaceuszach, S., Rustighi, A., Sgarra, R., Heath, C., Goodwin, G. H. *et al.* (1998) NF-kappaB mediated transcriptional activation is enhanced by the architectural factor HMGI-C. *Nucleic Acids Res* **26:** 1433-1439.

Mao, Z. G., Jiang, C. C., Yang, F., Thorne, R. F., Hersey, P., and Zhang, X. D. (2010) TRAIL-induced apoptosis of human melanoma cells involves activation of caspase-4. *Apoptosis* **15:** 1211-1222.

Martin-Sanchez, J., Viseras, J., Adroher, F. J., and Garcia-Fernandez, P. (1999) Nested polymerase chain reaction for detection of *Theileria annulata* and comparison with conventional diagnostic techniques: its use in epidemiology studies. *Parasitol Res* **85:** 243-245.

Martinez, H. J., Fedele, M., Battista, S., Pentimalli, F., Kruhoffer, M., Arra, C. *et al.* (2004) Identification of the genes up- and down-regulated by the high mobility group A1 (HMGA1) proteins: tissue specificity of the HMGA1-dependent gene regulation. *Cancer Res* **64:** 5728-5735.

Marui, N., Offermann, M. K., Swerlick, R., Kunsch, C., Rosen, C. A., Ahmad, M. *et al.* (1993) Vascular cell adhesion molecule-1 (VCAM-1) gene transcription and expression are regulated through an antioxidant-sensitive mechanism in human vascular endothelial cells
1. *J Clin Invest* **92:** 1866-1874.

Massi, D., Franchi, A., Borgognoni, L., Reali, U. M., and Santucci, M. (1999) Osteonectin expression correlates with clinical outcome in thin cutaneous malignant melanomas. *Hum Pathol* **30:** 339-344.

Matys, V., Kel-Margoulis, O. V., Fricke, E., Liebich, I., Land, S., Barre-Dirrie, A. *et al.* (2006) TRANSFAC and its module TRANSCompel: transcriptional gene regulation in eukaryotes. *Nucleic Acids Res* **34:** D108-D110.

Mbassa, G. K., Kweka, L. E., and Dulla, P. N. (1998) Immunization against East Coast Fever in field cattle with low infectivity *Theileria parva* stabilate--preliminary assessment. *Vet Parasitol* **77:** 41-48.

Mbwambo, H. A., Mkonyi, P. A., Sondi, J., and Lekaki, K. A. (1986) Chemotherapy of field cases of East Coast fever using halofuginone lactate. *Acta Trop* **43:** 401-406.

McCall, M. B., Netea, M. G., Hermsen, C. C., Jansen, T., Jacobs, L., Golenbock, D. *et al.* (2007) *Plasmodium falciparum* infection causes proinflammatory priming of human TLR responses. *J Immunol* **179:** 162-171.

McGuire, E. A., Hockett, R. D., Pollock, K. M., Bartholdi, M. F., O'Brien, S. J., and Korsmeyer, S. J. (1989) The t(11;14)(p15;q11) in a T-cell acute lymphoblastic leukemia cell line activates multiple transcripts, including Ttg-1, a gene encoding a potential zinc finger protein. *Mol Cell Biol* **9:** 2124-2132.

McHardy, N., Wekesa, L. S., Hudson, A. T., and Randall, A. W. (1985) Antitheilerial activity of BW720C (buparvaquone): a comparison with parvaquone. *Res Vet Sci* **39:** 29-33.

McKeever, D. J., Nyanjui, J. K., and Ballingall, K. T. (1997) In vitro infection with *Theileria parva* is associated with IL10 expression in all bovine lymphocyte lineages. *Parasite Immunol* **19:** 319-324.

McKeever, D. J., Taracha, E. L., Morrison, W. I., Musoke, A. J., and Morzaria, S. P. (1999) Protective immune mechanisms against *Theileria parva*: evolution of vaccine development strategies. *Parasitol Today* **15:** 263-267.

McKinsey, T. A., Brockman, J. A., Scherer, D. C., Al-Murrani, S. W., Green, P. L., and Ballard, D. W. (1996) Inactivation of IkappaBbeta by the tax protein of human T-cell leukemia virus type 1: a potential mechanism for constitutive induction of NF-kappaB. *Mol Cell Biol* **16:** 2083-2090.

Megyeri, K., Au, W. C., Rosztoczy, I., Raj, N. B., Miller, R. L., Tomai, M. A. *et al.* (1995) Stimulation of interferon and cytokine gene expression by imiquimod and stimulation by Sendai virus utilize similar signal transduction pathways. *Mol Cell Biol* **15:** 2207-2218.

Mehlhorn, H. and Shein, E. (1984) The piroplasms: life cycle and sexual stages. *Adv Parasitol* **23:** 37-103.

Melo, M. B., Jensen, K. D., and Saeij, J. P. (2011) *Toxoplasma gondii* effectors are master regulators of the inflammatory response. *Trends Parasitol* **27:** 487-495.

METROPOLIS, N. and ULAM, S. (1949) The Monte Carlo method. *J Am Stat Assoc* **44:** 335-341.

Mhadhbi, M., Naouach, A., Boumiza, A., Chaabani, M. F., BenAbderazzak, S., and Darghouth, M. A. (2010) In vivo evidence for the resistance of *Theileria annulata* to buparvaquone. *Vet Parasitol* **169:** 241-247.

Minjauw, B. and McLeod, A. (2003) Control methods and Costs of tick-borne diseases.(in Tick borne diseases and poverty). *Research report, DFID Animal Health Programme* 59-74. (http://www.dfid.gov.uk/r4d/PDF/Outputs/RLAHTickBorn_Book.pdf).

Minning, T. A., Bua, J., Garcia, G. A., McGraw, R. A., and Tarleton, R. L. (2003) Microarray profiling of gene expression during trypomastigote to amastigote transition in *Trypanosoma cruzi*. *Mol Biochem Parasitol* **131:** 55-64.

Mocellin, S., Marincola, F. M., and Young, H. A. (2005) Interleukin-10 and the immune response against cancer: a counterpoint. *J Leukoc Biol* **78:** 1043-1051.

Mogensen, T. H. (2009) Pathogen recognition and inflammatory signaling in innate immune defenses. *Clin Microbiol Rev* **22:** 240-73, Table.

Molestina, R. E., Payne, T. M., Coppens, I., and Sinai, A. P. (2003) Activation of NF-kappaB by *Toxoplasma gondii* correlates with increased expression of antiapoptotic genes and localization of phosphorylated IkappaB to the parasitophorous vacuole membrane. *J Cell Sci* **116:** 4359-4371.

Molestina, R. E. and Sinai, A. P. (2005) Host and parasite-derived IKK activities direct distinct temporal phases of NF-kappaB activation and target gene expression following Toxoplasma gondii infection. *J Cell Sci* **118:** 5785-5796.

Morrison, L. J., McLellan, S., Sweeney, L., Chan, C. N., MacLeod, A., Tait, A. *et al.* (2010) Role for parasite genetic diversity in differential host responses to Trypanosoma brucei infection
1. *Infect Immun* **78:** 1096-1108.

Morrison, W. I. and McKeever, D. J. (2006) Current status of vaccine development against *Theileria* parasites. *Parasitology* **133 Suppl:** S169-S187.

Morzaria, S. P., Irvin, A. D., Voigt, W. P., and Taracha, E. L. (1987) Effect of timing and intensity of challenge following immunization against East Coast fever. *Vet Parasitol* **26:** 29-41.

Morzaria, S. P., Roeder, P. L., Roberts, D. H., Chasey, D., and Drew, T. W. (1982) Characteristics of a continuous suspension cell line derived from a calf with sporadic bovine leukosis. *In Fifth International Symposium on Bovine Leukosis* **(ed. O. C. Straub):** 519-528.

Musoke, A., Nene, V., and Morzaria, S. P. (1993) A Sporozoite-based vaccine for *Theileria parva*. *Parasitol Today* **9:** 385-388.

Mutugi, J. J., Young, A. S., Maritim, A. C., Ndungu, S. G., Stagg, D. A., Grootenhuis, J. G. *et al.* (1988) Immunization of cattle against theileriosis using varying doses of *Theileria parva* lawrencei and *T. parva* parva sporozoites and oxytetracycline treatments. *Int J Parasitol* **18:** 453-461.

Nagpal, M. L., Chen, Y., and Lin, T. (2004) Effects of overexpression of CXCL10 (cytokine-responsive gene-2) on MA-10 mouse Leydig tumor cell steroidogenesis and proliferation. *J Endocrinol* **183:** 585-594.

Nash, P. B., Purner, M. B., Leon, R. P., Clarke, P., Duke, R. C., and Curiel, T. J. (1998) *Toxoplasma gondii*-infected cells are resistant to multiple inducers of apoptosis. *J Immunol* **160:** 1824-1830.

Neish, A. S., Read, M. A., Thanos, D., Pine, R., Maniatis, T., and Collins, T. (1995) Endothelial interferon regulatory factor 1 cooperates with NF-kappa B as

a transcriptional activator of vascular cell adhesion molecule. *Mol Cell Biol* **15:** 2558-2569.

Neumann, M., Foryst-Ludwig, A., Klar, S., Schweitzer, K., and Naumann, M. (2006) The PAK1 autoregulatory domain is required for interaction with NIK in Helicobacter pylori-induced NF-kappaB activation. *Biol Chem* **387:** 79-86.

Newson, J., Naessens, J., Stagg, D. A., and Black, S. J. (1986) A cell surface antigen associated with Theileria parva lawrencei-infected bovine lymphoid cells. *Parasite Immunol* **8:** 149-158.

Ngumi, P. N., Young, A. S., Lampard, D., Mining, S. K., Ndungu, S. G., Lesan, A. C. *et al.* (1992) Further evaluation of the use of buparvaquone in the infection and treatment method of immunizing cattle against *Theileria parva* derived from African buffalo (Syncerus caffer). *Vet Parasitol* **43:** 15-24.

Nishie, A., Masuda, K., Otsubo, M., Migita, T., Tsuneyoshi, M., Kohno, K. *et al.* (2001) High expression of the Cap43 gene in infiltrating macrophages of human renal cell carcinomas. *Clin Cancer Res* **7:** 2145-2151.

Noble, E. R., Noble, G. A., Schad, G., and Maclnnis, A. (1989) **Parasitology.** The Biology of Animal Parasites. *Sixth ed* .Lea & Fibigcr, Philadelphia, Pennsylvania. 79 p.

Norval, R. A. I., Perry, B. D., and Young, A. S. (1992) The Epidemiology of Theileriosis in Africa. *London: Academic Press*.

Oeckinghaus, A., Hayden, M. S., and Ghosh, S. (2011) Crosstalk in NF-kappaB signaling pathways. *Nat Immunol* **12:** 695-708.

Ogram, S. A. and Reeves, R. (1995) Differential regulation of a multipromoter gene. Selective 12-O-tetradecanoylphorbol-13-acetate induction of a single transcription start site in the HMG-I/Y gene. *J Biol Chem* **270:** 14235-14242.

Ohmori, Y. and Hamilton, T. A. (1990) A macrophage LPS-inducible early gene encodes the murine homologue of IP-10. *Biochem Biophys Res Commun* **168:** 1261-1267.

Ohmori, Y. and Hamilton, T. A. (1995) The interferon-stimulated response element and a kappa B site mediate synergistic induction of murine IP-10 gene transcription by IFN-gamma and TNF-alpha. *J Immunol* **154:** 5235-5244.

Olobo, J. O. and Black, S. J. (1989) Selected phenotypic and cloning properties of a bovine lymphoblastoid cell line, BL20. *Vet Immunol Immunopathol* **20:** 165-172.

Omer, O. H., El-Malik, K. H., Mahmoud, O. M., Haroun, E. M., Hawas, A., Sweeney, D. *et al.* (2002) Haematological profiles in pure bred cattle naturally infected with *Theileria annulata* in Saudi Arabia. *Vet Parasitol* **107:** 161-168.

Ong, Y. C., Reese, M. L., and Boothroyd, J. C. (2010) Toxoplasma rhoptry protein 16 (ROP16) subverts host function by direct tyrosine phosphorylation of STAT6. *J Biol Chem* **285:** 28731-28740.

Osaki, M., Oshimura, M., and Ito, H. (2004) PI3K-Akt pathway: its functions and alterations in human cancer. *Apoptosis* **9:** 667-676.

Osman, S. A. and Al-Gaabary, M. H. (2007) Clinical, haematological and therapeutic studies on tropical theileriosis in water buffaloes (Bubalus bubalis) in Egypt. *Vet Parasitol* **146:** 337-340.

Ou, R., Zhang, M., Huang, L., Flavell, R. A., Koni, P. A., and Moskophidis, D. (2008) Regulation of immune response and inflammatory reactions against viral infection by VCAM-1. *J Virol* **82:** 2952-2965.

Oura, C. A., McKellar, S., Swan, D. G., Okan, E., and Shiels, B. R. (2006) Infection of bovine cells by the protozoan parasite *Theileria annulata* modulates expression of the ISGylation system. *Cell Microbiol* **8:** 276-288.

Pain, A., Renauld, H., Berriman, M., Murphy, L., Yeats, C. A., Weir, W. *et al.* (2005) Genome of the host-cell transforming parasite *Theileria annulata* compared with T. parva. *Science* **309:** 131-133.

Palmer, G. H., Machado, J., Jr., Fernandez, P., Heussler, V., Perinat, T., and Dobbelaere, D. A. (1997) Parasite-mediated nuclear factor kappaB regulation in lymphoproliferation caused by *Theileria parva* infection. *Proc Natl Acad Sci U S A* **94:** 12527-12532.

Panne, D., Maniatis, T., and Harrison, S. C. (2004) Crystal structure of ATF-2/c-Jun and IRF-3 bound to the interferon-beta enhancer. *EMBO J* **23:** 4384-4393.

Papakonstanti, E. A. and Stournaras, C. (2002) Association of PI-3 kinase with PAK1 leads to actin phosphorylation and cytoskeletal reorganization. *Mol Biol Cell* **13:** 2946-2962.

Paramio, J. M., Casanova, M. L., Segrelles, C., Mittnacht, S., Lane, E. B., and Jorcano, J. L. (1999) Modulation of cell proliferation by cytokeratins K10 and K16. *Mol Cell Biol* **19:** 3086-3094.

Park, M. T. and Lee, S. J. (2003) Cell cycle and cancer. *J Biochem Mol Biol* **36:** 60-65.

Payne, T. M., Molestina, R. E., and Sinai, A. P. (2003) Inhibition of caspase activation and a requirement for NF-kappaB function in the *Toxoplasma gondii*-mediated blockade of host apoptosis. *J Cell Sci* **116:** 4345-4358.

Pearson, A. M. (1996) Scavenger receptors in innate immunity. *Curr Opin Immunol* **8:** 20-28.

Perkins, N. D. (2012) The diverse and complex roles of NF-kappaB subunits in cancer. *Nat Rev Cancer* **12:** 121-132.

Perkins, N. D. and Gilmore, T. D. (2006) Good cop, bad cop: the different faces of NF-kappaB. *Cell Death Differ* **13:** 759-772.

Peter, M. E. (2004) The flip side of FLIP. *Biochem J* **382:** e1-e3.

Pierantoni, G. M., Agosti, V., Fedele, M., Bond, H., Caliendo, I., Chiappetta, G. *et al.* (2003) High-mobility group A1 proteins are overexpressed in human leukaemias. *Biochem J* **372:** 145-150.

Pipano, E. and Shkap, V. (2006) *Theileria annulata* infection, in infectious diseases of livestock. *2nd edition, vol 1, J A W Coetzer & R C Tustin, Oxford University Press* 486-497.

Pitha-Rowe, I. F. and Pitha, P. M. (2007) Viral defense, carcinogenesis and ISG15: novel roles for an old ISG. *Cytokine Growth Factor Rev* **18:** 409-417.

Plattner, F. and Soldati-Favre, D. (2008) Hijacking of host cellular functions by the Apicomplexa. *Annu Rev Microbiol* **62:** 471-487.

Podhajcer, O. L., Benedetti, L. G., Girotti, M. R., Prada, F., Salvatierra, E., and Llera, A. S. (2008) The role of the matricellular protein SPARC in the dynamic interaction between the tumor and the host. *Cancer Metastasis Rev* **27:** 691-705.

Ponchel, F., Toomes, C., Bransfield, K., Leong, F. T., Douglas, S. H., Field, S. L. *et al.* (2003) Real-time PCR based on SYBR-Green I fluorescence: an alternative to the TaqMan assay for a relative quantification of gene rearrangements, gene amplifications and micro gene deletions. *BMC Biotechnol* **3:** 18.

Porter, A. G. and Janicke, R. U. (1999) Emerging roles of caspase-3 in apoptosis. *Cell Death Differ* **6:** 99-104.

Preston, P. M., Brown, C. G., Bell-Sakyi, L., Richardson, W., and Sanderson, A. (1992) Tropical theileriosis in *Bos taurus* and *Bos taurus* cross *Bos indicus* calves: response to infection with graded doses of sporozoites of *Theileria annulata*. *Res Vet Sci* **53:** 230-243.

Preston, P. M., Brown, C. G., Entrican, G., Richardson, W., and Boid, R. (1993) Synthesis of tumour necrosis factor-alpha and interferons by mononuclear cells from *Theileria annulata*-infected cattle. *Parasite Immunol* **15:** 525-534.

Preston, P. M., Hall, F. R., Glass, E. J., Campbell, J. D., Darghouth, M. A., Ahmed, J. S. *et al.* (1999) Innate and adaptive immune responses co-operate to protect cattle against *Theileria annulata*. *Parasitol Today* **15:** 268-274.

Radley, D. E., Brown, C. G. D., Cunningham, M. P., Kimber, C. D., Musisi, F., Payne, R. C. *et al.* (1975) East Coast fever : 3. Chemoprophylactic immunization of cattle using oxytetracycline and a combination of Theilerial strains. *Vet Parasitol* **1:** 51-60.

Radley, D. E., Brown, C. G., Burridge, M. J., Cunningham, M. P., Peirce, M. A., and Purnell, R. E. (1974) East Coast fever: quantitative studies of *Theileria parva* in cattle. *Exp Parasitol* **36:** 278-287.

Rao, A., Luo, C., and Hogan, P. G. (1997) Transcription factors of the NFAT family: regulation and function. *Annu Rev Immunol* **15:** 707-747.

Ravindran, S. and Boothroyd, J. C. (2008) Secretion of proteins into host cells by Apicomplexan parasites. *Traffic* **9:** 647-656.

Read, M. A., Neish, A. S., Luscinskas, F. W., Palombella, V. J., Maniatis, T., and Collins, T. (1995) The proteasome pathway is required for cytokine-induced endothelial-leukocyte adhesion molecule expression. *Immunity* **2:** 493-506.

Reeves, R. (2001) Molecular biology of HMGA proteins: hubs of nuclear function. *Gene* **277:** 63-81.

Reeves, R. (2010) Nuclear functions of the HMG proteins. *Biochim Biophys Acta* **1799:** 3-14.

Reeves, R. and Beckerbauer, L. (2001) HMGI/Y proteins: flexible regulators of transcription and chromatin structure. *Biochim Biophys Acta* **1519:** 13-29.

Reinecke, F., Levanets, O., Olivier, Y., Louw, R., Semete, B., Grobler, A. *et al.* (2006) Metallothionein isoform 2A expression is inducible and protects against ROS-mediated cell death in rotenone-treated HeLa cells. *Biochem J* **395:** 405-415.

Rempel, S. A., Golembieski, W. A., Fisher, J. L., Maile, M., and Nakeff, A. (2001) SPARC modulates cell growth, attachment and migration of U87 glioma cells on brain extracellular matrix proteins. *J Neurooncol* **53:** 149-160.

Ren, G., Zhao, X., Zhang, L., Zhang, J., L'Huillier, A., Ling, W. *et al.* (2010) Inflammatory cytokine-induced intercellular adhesion molecule-1 and vascular cell adhesion molecule-1 in mesenchymal stem cells are critical for immunosuppression. *J Immunol* **184:** 2321-2328.

Resar, L. M. (2010) The high mobility group A1 gene: transforming inflammatory signals into cancer? *Cancer Res* **70:** 436-439.

Rintelen, M., Schein, E., and Ahmed, J. S. (1990) Buparvaquone but not cyclosporin A prevents *Theileria annulata*-infected bovine lymphoblastoid cells from stimulating uninfected lymphocytes. *Trop Med Parasitol* **41:** 203-207.

Rittling, S. R. and Chambers, A. F. (2004) Role of osteopontin in tumour progression. *Br J Cancer* **90:** 1877-1881.

Robertson, G., Hirst, M., Bainbridge, M., Bilenky, M., Zhao, Y., Zeng, T. *et al.* (2007) Genome-wide profiles of STAT1 DNA association using chromatin immunoprecipitation and massively parallel sequencing. *Nat Methods* **4:** 651-657.

Robinet, A., Fahem, A., Cauchard, J. H., Huet, E., Vincent, L., Lorimier, S. *et al.* (2005) Elastin-derived peptides enhance angiogenesis by promoting endothelial cell migration and tubulogenesis through upregulation of MT1-MMP. *J Cell Sci* **118:** 343-356.

Robinson, P. M. (1982) *Theileriosis annulata* and its transmission-a review. *Trop Anim Health Prod* **14:** 3-12.

Rocchi, M. S., Ballingall, K. T., MacHugh, N. D., and McKeever, D. J. (2006) The kinetics of *Theileria parva* infection and lymphocyte transformation in vitro. *Int J Parasitol* **36:** 771-778.

Roebuck, K. A. and Finnegan, A. (1999) Regulation of intercellular adhesion molecule-1 (CD54) gene expression. *J Leukoc Biol* **66:** 876-888.

Romagnani, P., Beltrame, C., Annunziato, F., Lasagni, L., Luconi, M., Galli, G. *et al.* (1999) Role for interactions between IP-10/Mig and CXCR3 in proliferative glomerulonephritis. *J Am Soc Nephrol* **10:** 2518-2526.

Ropert, C. and Gazzinelli, R. T. (2004) Regulatory role of Toll-like receptor 2 during infection with *Trypanosoma cruzi*. *J Endotoxin Res* **10:** 425-430.

Rosette, C., Roth, R. B., Oeth, P., Braun, A., Kammerer, S., Ekblom, J. *et al.* (2005) Role of ICAM1 in invasion of human breast cancer cells. *Carcinogenesis* **26:** 943-950.

Rosowski, E. E., Lu, D., Julien, L., Rodda, L., Gaiser, R. A., Jensen, K. D. *et al.* (2011) Strain-specific activation of the NF-kappaB pathway by GRA15, a novel Toxoplasma gondii dense granule protein. *J Exp Med* **208:** 195-212.

Routledge, M. N., Wink, D. A., Keefer, L. K., and Dipple, A. (1994) DNA sequence changes induced by two nitric oxide donor drugs in the supF assay. *Chem Res Toxicol* **7:** 628-632.

Royer-Pokora, B., Rogers, M., Zhu, T. H., Schneider, S., Loos, U., and Bolitz, U. (1995) The TTG-2/RBTN2 T cell oncogene encodes two alternative transcripts from two promoters: the distal promoter is removed by most 11p13 translocations in acute T cell leukaemia's (T-ALL). *Oncogene* **10:** 1353-1360.

Ruckdeschel, K., Pfaffinger, G., Haase, R., Sing, A., Weighardt, H., Hacker, G. *et al.* (2004) Signaling of apoptosis through TLRs critically involves toll/IL-1 receptor domain-containing adapter inducing IFN-beta, but not MyD88, in bacteria-infected murine macrophages. *J Immunol* **173:** 3320-3328.

Saeij, J. P., Coller, S., Boyle, J. P., Jerome, M. E., White, M. W., and Boothroyd, J. C. (2007) Toxoplasma co-opts host gene expression by injection of a polymorphic kinase homologue. *Nature* **445:** 324-327.

Sager, H., Brunschwiler, C., and Jungi, T. W. (1998) Interferon production by *Theileria annulata*-transformed cell lines is restricted to the beta family. *Parasite Immunol* **20:** 175-182.

Sager, H., Davis, W. C., Dobbelaere, D. A., and Jungi, T. W. (1997) Macrophage-parasite relationship in theileriosis. Reversible phenotypic and functional dedifferentiation of macrophages infected with *Theileria annulata*. *J Leukoc Biol* **61:** 459-468.

Sager, H., Davis, W. C., and Jungi, T. W. (1999) Bovine monocytoid cells transformed to proliferate cease to exhibit lineage-specific functions. *Vet Immunol Immunopathol* **68:** 113-130.

Salih, D. A., Hassan, S. M., and El Hussein, A. M. (2007) Comparisons among two serological tests and microscopic examination for the detection of *Theileria annulata* in cattle in northern Sudan. *Prev Vet Med* **81:** 323-326.

Salih, D. E., Ahmed, J. S., Bakheit, M. A., Ali, E. B., El Hussein, A. M., Hassan, S. M. *et al.* (2005) Validation of the indirect TaSP enzyme-linked immunosorbent assay for diagnosis of *Theileria annulata* infection in cattle. *Parasitol Res* **97:** 302-308.

Samantaray, S. N., Bhattacharyulu, Y., and Gill, B. S. (1980) Immunisation of calves against bovine tropical theileriosis (*Theileria annulata*) with graded doses of sporozoites and irradiated sporozoites. *Int J Parasitol* **10:** 355-358.

Sanceau, J., Beranger, F., Gaudelet, C., and Wietzerbin, J. (1989) IFN-gamma is an essential cosignal for triggering IFN-beta 2/BSF-2/IL-6 gene expression in human monocytic cell lines. *Ann N Y Acad Sci* **557:** 130-41, discussion.

Sandhu, G. S., Grewal, A. S., Singh, A., Kondal, J. K., Singh, J., and Brar, R. S. (1998) Haematological and biochemical studies on experimental *Theileria annulata* infection in crossbred calves. *Vet Res Commun* **22:** 347-354.

Saraste, A. and Pulkki, K. (2000) Morphologic and biochemical hallmarks of apoptosis. *Cardiovasc Res* **45:** 528-537.

Sarhadi, V. K., Wikman, H., Salmenkivi, K., Kuosma, E., Sioris, T., Salo, J. *et al.* (2006) Increased expression of high mobility group A proteins in lung cancer. *J Pathol* **209:** 206-212.

Satyanarayana, A., Hilton, M. B., and Kaldis, P. (2008) p21 Inhibits Cdk1 in the absence of Cdk2 to maintain the G1/S phase DNA damage checkpoint. *Mol Biol Cell* **19:** 65-77.

Sauter, K. S., Brcic, M., Franchini, M., and Jungi, T. W. (2007) Stable transduction of bovine TLR4 and bovine MD-2 into LPS-nonresponsive cells and soluble CD14 promote the ability to respond to LPS. *Vet Immunol Immunopathol* **118:** 92-104.

Schein, E., Buscher, G., and Friedhoff, K. T. (1975) [Light microscopic studies on the development of *Theileria annulata* (Dschunkowsky and Luhs, 1904) in *Hyalomma anatolicum* excavatum (Koch, 1844). I. The development in the gut of engorged nymphs (author's transl)]. *Z Parasitenkd* **48:** 123-136.

Schein, E. and Friedhoff, K. T. (1978) [Light microscopic studies on the development of *Theileria annulata* (Dschunkowsky and Luhs, 1904) in *Hyalomma anatolicum* excavatum (Koch, 1844). II. The development in haemolymph and salivary glands (author's transl)]. *Z Parasitenkd* **56:** 287-303.

Schein, E. and Voigt, W. P. (1979) Chemotherapy of bovine theileriosis with Halofuginone. Short communication. *Acta Trop* **36:** 391-394.

Schimmer, A. D. and Dalili, S. (2005) Targeting the IAP family of caspase inhibitors as an emerging therapeutic strategy. *Hematology Am Soc Hematol Educ Program* 215-219.

Schmittgen, T. D. and Zakrajsek, B. A. (2000) Effect of experimental treatment on housekeeping gene expression: validation by real-time, quantitative RT-PCR. *J Biochem Biophys Methods* **46:** 69-81.

Schmuckli-Maurer, J., Casanova, C., Schmied, S., Affentranger, S., Parvanova, I., Kang'a, S. *et al.* (2009) Expression analysis of the *Theileria parva* subtelomere-encoded variable secreted protein gene family. *PLoS One* **4:** e4839.

Schmuckli-Maurer, J., Kinnaird, J., Pillai, S., Hermann, P., McKellar, S., Weir, W. *et al.* (2010) Modulation of NF-kappaB activation in *Theileria annulata*-infected cloned cell lines is associated with detection of parasite-dependent IKK signalosomes and disruption of the actin cytoskeleton. *Cell Microbiol* **12:** 158-173.

Schneider, I., Haller, D., Kullmann, B., Beyer, D., Ahmed, J. S., and Seitzer, U. (2007) Identification, molecular characterization and subcellular localization of a *Theileria annulata* parasite protein secreted into the host cell cytoplasm. *Parasitol Res* **101:** 1471-1482.

Schnittger, L., Hollmann, C., Diemer, U., Boguslawski, K., and Ahmed, J. S. (2000) Proliferation and cytokine profile of *T. annulata*-infected ovine, caprine, and bovine lymphoblastoid cells. *Ann N Y Acad Sci* **916:** 676-680.

Schwartz, S. A., Hernandez, A., and Mark, E. B. (1999) The role of NF-kappaB/IkappaB proteins in cancer: implications for novel treatment strategies. *Surg Oncol* **8:** 143-153.

Seitzer, U., Gerber, S., Beyer, D., Dobschanski, J., Kullmann, B., Haller, D. *et al.* (2010) Schizonts of *Theileria annulata* interact with the microtubuli network of their host cell via the membrane protein TaSP. *Parasitol Res* **106:** 1085-1102.

Selvey, S., Thompson, E. W., Matthaei, K., Lea, R. A., Irving, M. G., and Griffiths, L. R. (2001) Beta-actin--an unsuitable internal control for RT-PCR. *Mol Cell Probes* **15:** 307-311.

Sen, R. and Baltimore, D. (1986) Multiple nuclear factors interact with the immunoglobulin enhancer sequences. *Cell* **46:** 705-716.

Seux, M., Peuget, S., Montero, M. P., Siret, C., Rigot, V., Clerc, P. *et al.* (2011) TP53INP1 decreases pancreatic cancer cell migration by regulating SPARC expression. *Oncogene* **30:** 3049-3061.

Sgadari, C., Angiolillo, A. L., Cherney, B. W., Pike, S. E., Farber, J. M., Koniaris, L. G. *et al.* (1996) Interferon-inducible protein-10 identified as a mediator of tumor necrosis in vivo. *Proc Natl Acad Sci U S A* **93:** 13791-13796.

Sgarra, R., Tessari, M. A., Di, B. J., Rustighi, A., Zago, P., Liberatori, S. *et al.* (2005) Discovering high mobility group A molecular partners in tumour cells. *Proteomics* **5:** 1494-1506.

Shang, C., Attema, J., Cakouros, D., Cockerill, P. N., and Shannon, M. F. (1999) Nuclear factor of activated T cells contributes to the function of the CD28 response region of the granulocyte macrophage-colony stimulating factor promoter. *Int Immunol* **11:** 1945-1956.

Shannon, M. F., Himes, S. R., and Attema, J. (1998) A role for the architectural transcription factors HMGI(Y) in cytokine gene transcription in T cells. *Immunol Cell Biol* **76:** 461-466.

Sharpless, N. E. and Depinho, R. A. (2002) p53: good cop/bad cop. *Cell* **110:** 9-12.

Shaulian, E. and Karin, M. (2002) AP-1 as a regulator of cell life and death. *Nat Cell Biol* **4:** E131-E136.

Shaw, M. K. (1997) The same but different: the biology of Theileria sporozoite entry into bovine cells. *Int J Parasitol* **27:** 457-474.

Shaw, M. K. (2003) Cell invasion by Theileria sporozoites. *Trends Parasitol* **19:** 2-6.

Shaw, M. K. and Tilney, L. G. (1995) The entry of *Theileria parva* merozoites into bovine erythrocytes occurs by a process similar to sporozoite invasion of lymphocytes. *Parasitology* **111 (Pt 4):** 455-461.

Shaw, M. K., Tilney, L. G., and Musoke, A. J. (1991) The entry of *Theileria parva* sporozoites into bovine lymphocytes: evidence for MHC class I involvement. *J Cell Biol* **113:** 87-101.

Shi, Q., Bao, S., Maxwell, J. A., Reese, E. D., Friedman, H. S., Bigner, D. D. *et al.* (2004) Secreted protein acidic, rich in cysteine (SPARC), mediates cellular survival of gliomas through AKT activation. *J Biol Chem* **279:** 52200-52209.

Shiels, B., Hall, R., Glascodine, J., McDougall, C., Harrison, C., Taracha, E. *et al.* (1989) Characterization of surface polypeptides on different life-cycle stages of *Theileria annulata*. *Mol Biochem Parasitol* **34:** 209-220.

Shiels, B., Kinnaird, J., McKellar, S., Dickson, J., Miled, L. B., Melrose, R. *et al.* (1992) Disruption of synchrony between parasite growth and host cell division is a determinant of differentiation to the merozoite in *Theileria annulata*. *J Cell Sci* **101 (Pt 1):** 99-107.

Shiels, B., Langsley, G., Weir, W., Pain, A., McKellar, S., and Dobbelaere, D. (2006) Alteration of host cell phenotype by *Theileria annulata* and *Theileria parva*: mining for manipulators in the parasite genomes. *Int J Parasitol* **36:** 9-21.

Shiels, B. R., McDougall, C., Tait, A., and Brown, C. G. (1986) Identification of infection-associated antigens in *Theileria annulata* transformed cells. *Parasite Immunol* **8:** 69-77.

Shiels, B. R., McKellar, S., Katzer, F., Lyons, K., Kinnaird, J., Ward, C. *et al.* (2004) A Theileria annulata DNA binding protein localized to the host cell nucleus alters the phenotype of a bovine macrophage cell line. *Eukaryot Cell* **3:** 495-505.

Shishodia, S. and Aggarwal, B. B. (2004) Nuclear factor-kappaB: a friend or a foe in cancer? *Biochem Pharmacol* **68:** 1071-1080.

Shu, H. B., Agranoff, A. B., Nabel, E. G., Leung, K., Duckett, C. S., Neish, A. S. *et al.* (1993) Differential regulation of vascular cell adhesion molecule 1 gene expression by specific NF-kappa B subunits in endothelial and epithelial cells. *Mol Cell Biol* **13:** 6283-6289.

Sieling, P. A., Sakimura, L., Uyemura, K., Yamamura, M., Oliveros, J., Nickoloff, B. J. *et al.* (1995) IL-7 in the cell-mediated immune response to a human pathogen. *J Immunol* **154:** 2775-2783.

Singh, A., Singh, J., Grewal, A. S., and Brar, R. S. (2001) Studies on some blood parameters of crossbred calves with experimental Theileria annulata infections. *Vet Res Commun* **25:** 289-300.

Singh, D. K., Jagdish, S., Gautam, O. P., and Dhar, S. (1979) Infectivity of ground-up tick supernates prepared from *Theilerai annulata* infected Hyalomma anatolicum anatolicum. *Trop Anim Health Prod* **11:** 87-90.

Singh, J., Gill, J. S., Kwatra, M. S., and Sharma, K. K. (1993) Treatment of theileriosis in crossbred cattle in the Punjab. *Trop Anim Health Prod* **25:** 75-78.

Smith, A. E. and Buchmueller, K. L. (2011) Molecular basis for the inhibition of HMGA1 proteins by distamycin A. *Biochemistry* **50:** 8107-8116.

Smith, J. A. (1994) Neutrophils, host defense, and inflammation: a double-edged sword. *J Leukoc Biol* **56:** 672-686.

Somerville, R. P., Adamson, R. E., Brown, C. G., and Hall, F. R. (1998a) Metastasis of *Theileria annulata* macroschizont-infected cells in scid mice is mediated by matrix metalloproteinases. *Parasitology* **116 (Pt 3):** 223-228.

Somerville, R. P., Littlebury, P., Pipano, E., Brown, C. G., Shkap, V., Adamson, R. E. *et al.* (1998b) Phenotypic and genotypic alterations associated with the attenuation of a *Theileria annulata* vaccine cell line from Turkey. *Vaccine* **16:** 569-575.

Son, Y. O., Heo, J. S., Kim, T. G., Jeon, Y. M., Kim, J. G., and Lee, J. C. (2010) Over-expression of JunB inhibits mitochondrial stress and cytotoxicity in human lymphoma cells exposed to chronic oxidative stress. *BMB Rep* **43:** 57-61.

Song, P. I., Abraham, T. A., Park, Y., Zivony, A. S., Harten, B., Edelhauser, H. F. *et al.* (2001) The expression of functional LPS receptor proteins CD14 and toll-like receptor 4 in human corneal cells. *Invest Ophthalmol Vis Sci* **42:** 2867-2877.

Sounni, N. E. and Noel, A. (2005) Membrane type-matrix metalloproteinases and tumor progression. *Biochimie* **87:** 329-342.

Speiser, D. E., Lee, S. Y., Wong, B., Arron, J., Santana, A., Kong, Y. Y. *et al.* (1997) A regulatory role for TRAF1 in antigen-induced apoptosis of T cells. *J Exp Med* **185:** 1777-1783.

Spooner, R. L., Innes, E. A., Glass, E. J., and Brown, C. G. (1989) *Theileria annulata* and T. parva infect and transform different bovine mononuclear cells. *Immunology* **66:** 284-288.

Sredni, B., Weil, M., Khomenok, G., Lebenthal, I., Teitz, S., Mardor, Y. *et al.* (2004) Ammonium trichloro(dioxoethylene-o,o')tellurate (AS101) sensitizes tumors to chemotherapy by inhibiting the tumor interleukin 10 autocrine loop. *Cancer Res* **64:** 1843-1852.

Stabel, J. R. and Stabel, T. J. (1995) Immortalization and characterization of bovine peritoneal macrophages transfected with SV40 plasmid DNA. *Vet Immunol Immunopathol* **45:** 211-220.

Steigerwald, M. and Moll, H. (2005) Leishmania major modulates chemokine and chemokine receptor expression by dendritic cells and affects their migratory capacity. *Infect Immun* **73:** 2564-2567.

Steinemann, S., Ulevitch, R. J., and Mackman, N. (1994) Role of the lipopolysaccharide (LPS)-binding protein/CD14 pathway in LPS induction of tissue factor expression in monocytic cells. *Arterioscler Thromb* **14:** 1202-1209.

Stiewe, T. and Putzer, B. M. (2002) Role of p73 in malignancy: tumor suppressor or oncogene? *Cell Death Differ* **9:** 237-245.

Swan, D. G., Phillips, K., Tait, A., and Shiels, B. R. (1999) Evidence for localisation of a Theileria parasite AT hook DNA-binding protein to the nucleus of immortalised bovine host cells. *Mol Biochem Parasitol* **101:** 117-129.

Swan, D. G., Stadler, L., Okan, E., Hoffs, M., Katzer, F., Kinnaird, J. *et al.* (2003) TashHN, a *Theileria annulata* encoded protein transported to the host nucleus displays an association with attenuation of parasite differentiation. *Cell Microbiol* **5:** 947-956.

Swan, D. G., Stern, R., McKellar, S., Phillips, K., Oura, C. A., Karagenc, T. I. *et al.* (2001) Characterisation of a cluster of genes encoding *Theileria annulata* AT hook DNA-binding proteins and evidence for localisation to the host cell nucleus. *J Cell Sci* **114:** 2747-2754.

Tai, I. T. and Tang, M. J. (2008) SPARC in cancer biology: its role in cancer progression and potential for therapy. *Drug Resist Updat* **11:** 231-246.

Tait, A. and Hall, F. R. (1990) *Theileria annulata*: control measures, diagnosis and the potential use of subunit vaccines. *Rev Sci Tech* **9:** 387-403.

Takamiya, R., Baron, R. M., Yet, S. F., Layne, M. D., and Perrella, M. A. (2008) High mobility group A1 protein mediates human nitric oxide synthase 2 gene expression. *FEBS Lett* **582:** 810-814.

Takeda, K. and Akira, S. (2005) Toll-like receptors in innate immunity. *Int Immunol* **17:** 1-14.

Taylor, M. A., Coop, R. L., and Wall, R. L. (2007) Parasites of cattle. *in Veterinary Parasitology, 3rd ed Blackwell, Oxford,* 93-151.

Thanos, D., Du, W., and Maniatis, T. (1993) The high mobility group protein HMG I(Y) is an essential structural component of a virus-inducible enhancer complex. *Cold Spring Harb Symp Quant Biol* **58:** 73-81.

Thanos, D. and Maniatis, T. (1995) NF-kappa B: a lesson in family values. *Cell* **80:** 529-532.

Thomas, J. O. and Travers, A. A. (2001) HMG1 and 2, and related 'architectural' DNA-binding proteins. *Trends Biochem Sci* **26:** 167-174.

Thompson, J. E., Phillips, R. J., Erdjument-Bromage, H., Tempst, P., and Ghosh, S. (1995) I kappa B-beta regulates the persistent response in a biphasic activation of NF-kappa B. *Cell* **80:** 573-582.

Tilghman, R. W. and Hoover, R. L. (2002) The Src-cortactin pathway is required for clustering of E-selectin and ICAM-1 in endothelial cells. *FASEB J* **16:** 1257-1259.

Tindih, H. S., Marcotty, T., Naessens, J., Goddeeris, B. M., and Geysen, D. (2010) Demonstration of differences in virulence between two *Theileria parva* isolates. *Vet Parasitol* **168:** 223-230.

Toshchakov, V., Jones, B. W., Perera, P. Y., Thomas, K., Cody, M. J., Zhang, S. *et al.* (2002) TLR4, but not TLR2, mediates IFN-beta-induced STAT1alpha/beta-dependent gene expression in macrophages. *Nat Immunol* **3:** 392-398.

Triantafilou, M. and Triantafilou, K. (2004) Heat-shock protein 70 and heat-shock protein 90 associate with Toll-like receptor 4 in response to bacterial lipopolysaccharide. *Biochem Soc Trans* **32:** 636-639.

Tripathi, A. K., Sullivan, D. J., and Stins, M. F. (2006) *Plasmodium falciparum*-infected erythrocytes increase intercellular adhesion molecule 1 expression on brain endothelium through NF-kappaB. *Infect Immun* **74:** 3262-3270.

Tschopp, J., Irmler, M., and Thome, M. (1998) Inhibition of fas death signals by FLIPs. *Curr Opin Immunol* **10:** 552-558.

Tsunoda, T., Takashima, Y., Tanaka, Y., Fujimoto, T., Doi, K., Hirose, Y. *et al.* (2010) Immune-related zinc finger gene ZFAT is an essential transcriptional regulator for hematopoietic differentiation in blood islands. *Proc Natl Acad Sci U S A* **107:** 14199-14204.

Tuon, F. F., Amato, V. S., Bacha, H. A., Almusawi, T., Duarte, M. I., and Amato, N., V (2008) Toll-like receptors and leishmaniasis. *Infect Immun* **76:** 866-872.

Uilenberg, G. (1981) Theileria species of domestic livestock. In: Irvin, A.D., Cunningham, M.P., Young, A.S.(Eds.), Advances in Control of Theileriosis. Nijhoff (Martinus). *The Hague* 4-37.

Ulevitch, R. J. and Tobias, P. S. (1995) Receptor-dependent mechanisms of cell stimulation by bacterial endotoxin. *Annu Rev Immunol* **13:** 437-457.

Valentin, H., Lemasson, I., Hamaia, S., Casse, H., Konig, S., Devaux, C. *et al.* (1997) Transcriptional activation of the vascular cell adhesion molecule-1 gene in T lymphocytes expressing human T-cell leukemia virus type 1 Tax protein. *J Virol* **71:** 8522-8530.

Vallone, D., Battista, S., Pierantoni, G. M., Fedele, M., Casalino, L., Santoro, M. *et al.* (1997) Neoplastic transformation of rat thyroid cells requires the junB and fra-1 gene induction which is dependent on the HMGI-C gene product. *EMBO J* **16:** 5310-5321.

Van, K. C. and Mallard, B. A. (2001) Regulation of bovine intercellular adhesion molecule 1 (ICAM-1) and vascular cell adhesion molecule 1 (VCAM-1) on cultured aortic endothelial cells
2. *Vet Immunol Immunopathol* **79:** 129-138.

Vandesompele, J., De, P. K., Pattyn, F., Poppe, B., Van, R. N., De, P. A. *et al.* (2002) Accurate normalization of real-time quantitative RT-PCR data by geometric averaging of multiple internal control genes. *Genome Biol* **3:** RESEARCH0034.

Varghese, J., Khandre, N. S., and Sarin, A. (2003) Caspase-3 activation is an early event and initiates apoptotic damage in a human leukemia cell line. *Apoptosis* **8:** 363-370.

Veitch, N. J., Johnson, P. C., Trivedi, U., Terry, S., Wildridge, D., and MacLeod, A. (2010) Digital gene expression analysis of two life cycle stages of the human-infective parasite, *Trypanosoma brucei* gambiense reveals differentially expressed clusters of co-regulated genes. *BMC Genomics* **11:** 124.

Verjovski-Almeida, S., DeMarco, R., Martins, E. A., Guimaraes, P. E., Ojopi, E. P., Paquola, A. C. *et al.* (2003) Transcriptome analysis of the acoelomate human parasite *Schistosoma mansoni*. *Nat Genet* **35:** 148-157.

von, S. C., Xue, G., Schmuckli-Maurer, J., Woods, K. L., Nigg, E. A., and Dobbelaere, D. A. (2010) The transforming parasite *Theileria* co-opts host cell mitotic and central spindles to persist in continuously dividing cells. *PLoS Biol* **8**.

Voraberger, G., Schafer, R., and Stratowa, C. (1991) Cloning of the human gene for intercellular adhesion molecule 1 and analysis of its 5'-regulatory region. Induction by cytokines and phorbol ester. *J Immunol* **147:** 2777-2786.

Wang, J., Xu, L., Wang, E., and Huang, S. (2010) The potential landscape of genetic circuits imposes the arrow of time in stem cell differentiation. *Biophys J* **99:** 29-39.

Waris, G. and Ahsan, H. (2006) Reactive oxygen species: role in the development of cancer and various chronic conditions. *J Carcinog* **5:** 14.

Webb, B. A., Eves, R., Crawley, S. W., Zhou, S., Cote, G. P., and Mak, A. S. (2005) PAK1 induces podosome formation in A7r5 vascular smooth muscle cells in a PAK-interacting exchange factor-dependent manner. *Am J Physiol Cell Physiol* **289:** C898-C907.

Webb, B. A., Zhou, S., Eves, R., Shen, L., Jia, L., and Mak, A. S. (2006) Phosphorylation of cortactin by p21-activated kinase. *Arch Biochem Biophys* **456:** 183-193.

Weil, R., Whiteside, S. T., and Israel, A. (1997) Control of NF-kappa B activity by the I kappa B beta inhibitor. *Immunobiology* **198:** 14-23.

Weir, W., Karagenc, T., Baird, M., Tait, A., and Shiels, B. R. (2010) Evolution and diversity of secretome genes in the apicomplexan parasite *Theileria annulata*. *BMC Genomics* **11:** 42.

Weir, W., Sunter, J., Chaussepied, M., Skilton, R., Tait, A., de Villiers, E. P. *et al.* (2009) Highly syntenic and yet divergent: a tale of two Theilerias. *Infect Genet Evol* **9:** 453-461.

Whiteside, S. T. and Israel, A. (1997) I kappa B proteins: structure, function and regulation. *Semin Cancer Biol* **8:** 75-82.

Wilkie, G. M., Brown, C. G., Kirvar, B. E., Thomas, M., Williamson, S. M., Bell-Sakyi, L. J. *et al.* (1998) Chemoprophylaxis of *Theileria annulata* and *Theileria parva* infections of calves with buparvaquone. *Vet Parasitol* **78:** 1-12.

Wolle, J., Hill, R. R., Ferguson, E., Devall, L. J., Trivedi, B. K., Newton, R. S. *et al.* (1996) Selective inhibition of tumor necrosis factor-induced vascular cell adhesion molecule-1 gene expression by a novel flavonoid. Lack of effect on transcription factor NF-kappa B. *Arterioscler Thromb Vasc Biol* **16:** 1501-1508.

Wong, K. F., Luk, J. M., Cheng, R. H., Klickstein, L. B., and Fan, S. T. (2007) Characterization of two novel LPS-binding sites in leukocyte integrin betaA domain. *FASEB J* **21:** 3231-3239.

Wong, M. L. and Medrano, J. F. (2005) Real-time PCR for mRNA quantitation. *Biotechniques* **39:** 75-85.

Wood, L. J., Maher, J. F., Bunton, T. E., and Resar, L. M. (2000) The oncogenic properties of the HMG-I gene family. *Cancer Res* **60:** 4256-4261.

Wunderlich, V. and Bottger, M. (1997) High-mobility-group proteins and cancer--an emerging link. *J Cancer Res Clin Oncol* **123:** 133-140.

Xie, Q. W., Kashiwabara, Y., and Nathan, C. (1994) Role of transcription factor NF-kappa B/Rel in induction of nitric oxide synthase. *J Biol Chem* **269:** 4705-4708.

Xue, G., von, S. C., Hermann, P., Peyer, M., Maushagen, R., Schmuckli-Maurer, J. *et al.* (2010) Characterisation of gp34, a GPI-anchored protein expressed by schizonts of *Theileria parva* and *T. annulata*. *Mol Biochem Parasitol* **172:** 113-120.

Yamada, Y., Warren, A. J., Dobson, C., Forster, A., Pannell, R., and Rabbitts, T. H. (1998) The T cell leukemia LIM protein Lmo2 is necessary for adult mouse hematopoiesis. *Proc Natl Acad Sci U S A* **95:** 3890-3895.

Yamaguchi, H. and Condeelis, J. (2007) Regulation of the actin cytoskeleton in cancer cell migration and invasion. *Biochim Biophys Acta* **1773:** 642-652.

Yamaguchi, H., Wyckoff, J., and Condeelis, J. (2005) Cell migration in tumors. *Curr Opin Cell Biol* **17:** 559-564.

Yamamoto, M., Sato, S., Hemmi, H., Hoshino, K., Kaisho, T., Sanjo, H. *et al.* (2003) Role of adaptor TRIF in the MyD88-independent toll-like receptor signaling pathway. *Science* **301:** 640-643.

Yamasaki, M., Nomura, T., Sato, F., and Mimata, H. (2007) Metallothionein is up-regulated under hypoxia and promotes the survival of human prostate cancer cells. *Oncol Rep* **18:** 1145-1153.

Yamashita, K., Upadhay, S., Mimori, K., Inoue, H., and Mori, M. (2003) Clinical significance of secreted protein acidic and rich in cystein in esophageal carcinoma and its relation to carcinoma progression. *Cancer* **97:** 2412-2419.

Yang, J., Liu, X., Bhalla, K., Kim, C. N., Ibrado, A. M., Cai, J. *et al.* (1997) Prevention of apoptosis by Bcl-2: release of cytochrome c from mitochondria blocked. *Science* **275:** 1129-1132.

Yang, L., Kowalski, J. R., Yacono, P., Bajmoczi, M., Shaw, S. K., Froio, R. M. *et al.* (2006) Endothelial cell cortactin coordinates intercellular adhesion molecule-1 clustering and actin cytoskeleton remodeling during polymorphonuclear leukocyte adhesion and transmigration. *J Immunol* **177:** 6440-6449.

Yang, Z., Carter, C. D., Miller, M. S., and Bochsler, P. N. (1995) CD14 and tissue factor expression by bacterial lipopolysaccharide-stimulated bovine alveolar macrophages in vitro. *Infect Immun* **63:** 51-56.

Yie, J., Liang, S., Merika, M., and Thanos, D. (1997) Intra- and intermolecular cooperative binding of high-mobility-group protein I(Y) to the beta-interferon promoter
1. *Mol Cell Biol* **17:** 3649-3662.

Yockell-Lelievre, J., Spriet, C., Cantin, P., Malenfant, P., Heliot, L., de, L. Y. *et al.* (2009) Functional cooperation between Stat-1 and ets-1 to optimize icam-1 gene transcription. *Biochem Cell Biol* **87:** 905-918.

Yoshida, A., Yoshida, S., Khalil, A. K., Ishibashi, T., and Inomata, H. (1998) Role of NF-kappaB-mediated interleukin-8 expression in intraocular neovascularization. *Invest Ophthalmol Vis Sci* **39:** 1097-1106.

Yoshikawa, H., Matsubara, K., Zhou, X., Okamura, S., Kubo, T., Murase, Y. *et al.* (2007) WNT10B functional dualism: beta-catenin/Tcf-dependent growth promotion or independent suppression with deregulated expression in cancer. *Mol Biol Cell* **18:** 4292-4303.

Young, A. S., Burridge, M. J., and Payne, R. C. (1977) Transmission of a *Theileria* species to cattle by the ixodid tick, Amblyomma cohaerens Donitz 1909. *Trop Anim Health Prod* **9:** 37-45.

Young, A. S., Shaw, M. K., Ochanda, H., Morzaria, S. P., Dolan, T. T., and . (1992) Factors affecting the transmission of African *Theileria* species of cattle by ixodid ticks (conference proceedings). *Saint Paul, Minnesota* 15-18.

Youssef, S. and Steinman, L. (2006) At once harmful and beneficial: the dual properties of NF-kappaB. *Nat Immunol* **7:** 901-902.

Zaitseva, L., Rushworth, S. A., and MacEwan, D. J. (2011) Silencing FLIP(L) modifies TNF-induced apoptotic protein expression. *Cell Cycle* **10:** 1067-1072.

Zhang, X., Shin, J., Molitor, T. W., Schook, L. B., and Rutherford, M. S. (1999) Molecular responses of macrophages to porcine reproductive and respiratory syndrome virus infection. *Virology* **262:** 152-162.

Appendices

Appendix 1:

1.1 Table showing important microarray terminologies

Array	Refers to the physical substrate to which bio-sequence reporters are attached to create **features**.
Array Design	An **array design** is conceptual it is the layout or blueprint of one or more **arrays.**
Background/ Background noise	**Background** is the measured signal outside of a **feature** on an **array**. In many gene expression analysis methods, **background** subtraction is performed to correct measured signals for observed local and/or global **background.**
Channel	A **channel** is an intensity-based portion of an **expression** dataset that consists of the set of signal measurements across all features on an **array** for a particular labelled preparation used in **hybridization**. In some cases, such as Cy3/Cy5 array **hybridizations**, **multiple channels** (one for each label used) may be combined in a **single expression** profile to create **ratios**.
Chip	The physical medium of many **arrays** used in **gene expression.**
contig	A **contig,** an abbreviation for "contiguous sequence" is a group of clones representing overlapping regions of a genome.
Control	The reference for comparison when determining the effect of some procedure or treatment. (Deletion, mismatch, positive, negative).
Error Model	An **error model** is an algorithm that computes quality statistics such as p-values and error bars for each gene **expression** measurement.
Expression	The conversion of the genetic instructions present in a DNA sequence into a unit of biological function in a living cell. Typically involves the process of transcription of a DNA sequence into an RNA sequence followed by translation of the mRNA into protein
Feature	A **feature** refers to a specific instance of a position upon an array. Commonly referred to as a spot in a microarray experiment.
Feature Extraction	Quantitative analysis of an **array** image or scan to measure the **expression** values.
Filter/ed	A mathematical algorithm applied to image/array data for the purpose of enhancing image quality/defining expression analysis
Fluor/ Fluorophore/ Fluorescent label	A fluorescent tag bound to mRNA or cDNA extracted from a sample. When properly excited the fluor gives off measurable fluorescence which is the observable in an experiment.
Hybridization	Treating an **array** with one or more **labelled** preparations under a specified set of conditions.
Label	**Label** refers to fluorescent **labels**, for example, Cy3 and Cy5, commonly used to distinguish baseline and experimental preparations in gene **expression** microarray **hybridizations.**
Normalisation	**Normalisation** is the procedure by which signal intensities from two or more **expression** profiles (or **channels**) are made directly comparable through application of an appropriate algorithm.
Oligo / Oligonucleotide	Usually short strings of DNA or RNA to be used as **probes** (**features**) or spots. These short stretches of sequence are often chemically synthesised.
Probe	In some organisations, probe is used as a synonym for **feature.**
Ratio	Also referred to as "fold change". A **ratio** refers to a normalised signal intensity generated in a feature given **channel** divided by a normalised **signal intensity** generated by the same feature in another channel. The channels compared are typically baseline versus experimental, for example normal versus diseased or untreated vs. treated.
Target	Material that may **hybridize** to the **probe**, usually containing all of the mRNA (cDNA or cRNA) or gDNA of the subject organism.

Adapted from Rosetta BioSoftWare:
http://www.rosettabio.com/tech/geml/omg/lsr_ge_glossary.doc'.

1.2 Table showing details of raw data file types obtained from Roche NimbleGen

Directory	Subdirectory	File	Description
Design_Files		design.ndf1	Contained the complete information about the probes, including sequences, target genes, and location in the array.
		design.ngd1	Contained information on the target genes, including database source, gene name, gene accession number, and gene ID.
		DesignNotes.txt1	Contained information about the design of the array, including the number of target genes, number of probes, and number of probe replicates.
Documentation		NimbleGen_data_formats.pdf2	Contained detailed information on various data formats provided by Roche NimbleGen.
Processed_Data_Files			Contained subdirectories whose files list probe level and gene level expression values. Expression values are generated using quantile normalization (Bolstad et al., 2003, Bioinformatics, 19:185), and Robust Multichip Average (RMA) algorithm (Irizarry et al., 2003, Nucleic Acids Res. 31: e15 and Irizarry et al., 2003, Biostatistics 4:249).
	Normalized_Calls_Files	arrayID_532_RMA_calls.txt1	Contained normalized gene expression summary value for each gene in each array.
		All_norm_calls.txt1	Contained normalized gene expression summary value and information for each gene in all arrays in this order.
	Normalized_Pair_Files	arrayID_532_norm_RMA_ pair.txt1	Contained normalized gene expression value for each probe in each array.
		All_norm_pair.txt1	Contained normalized gene expression value for each probe in all arrays in this order.
Raw_Data_Files			Contained subdirectories whose files list un-normalized probe level and gene level expression values. For best results, use normalized data provided in the Normalized_Calls_Files directory, described above.
	Calls_Files	arrayID_532 _calls.txt1	Contained un-normalized gene expression summary value for each gene in each array.
		All_ calls.txt1	Contained un-normalized gene expression value and information for each gene in all arrays in this order
	Pair_Files arrayI	D_532 _pair.txt1	Contained un-normalized gene expression value for each probe in each array.
		All_ pair.txt1	Contained un-normalized gene expression value and target gene information for each probe in all arrays in this order.
root directory		SampleKey.txt1	Contained information about the samples and arrays used in this order.

1 Open with a text editor, such as Microsoft WordPad, or spreadsheet software, such as Microsoft Excel.
2 Open with Adobe Acrobat Reader.

1.3 Table showing details of primers used for semi-quantitative RT-PCR and real-time quantitative RT-PCR

Gene symbol	GenBank accession number	F/R	Primer sequences (5' → 3')	Length (bp)	Product length (bp)	Tm (°C)	Gene name
ACTB	NM_173979	F	CTCTCTTCCAGCCTTCCTTCCTGG	24	240	58.21	Actin, beta
		R	ACACGGAGTACTTGCGCTCAGG	22		58.92	
ALDH1A1	NM_174239	F	TGCTGTTGAATTTGCACACCAAGGAG	26	334	58.71	Aldehyde dehydrogenase 1 family, member A1
		R	GGCAATGCGCATATCATCAGTAACATC	27		57.24	
ANGPT4	NM_001076483	F	ACAATGACAACTGCCTCTGCAAGTGC	26	214	60.39	Angiopoietin 4
		R	GCTGCCCCTTAGATGCCCGAG	21		59.31	
AQP3	NM_001079794	F	TACCCCTCTGGACACTTGGACATGG	25	242	59.42	Aquaporin 3 (Gill blood groUp)
		R	CCGGCGATGGCGGTGAAAAGG	21		60.96	
BCL9	XR_028680	F	TACCCCTAAAGCACTCCCTGGCC	23	214	59.67	B-cell CLL/lymphoma 9
		R	CGAGTGTGGTGTGTGCTGGGAATC	24		60	
BCOR	NM_001191544	F	AGGTGTGCAAATTCAGCCCCACTG	24	244	59.88	Similar to BCL-6 corepressor
		R	ATGTCTGGGGTGACCTGGTCGG	22		59.92	
BIRC3	NM_001035293	F	GGATGATGCTATGTCAGAACACCTGAG	27	255	57.24	Baculoviral IAP repeat-containing 3
		R	TCCCAACACCTCAGTCCACCATC	23		58	
BOLA-DYA	NM_001012678	F	CTTGGGTGCTGCCTCCAGACGT	22		61.01	BOLA-DYA major histocompatibility complex, class II, DY alpha
		R	TGGAAGGAGCTCTGTGATGAAGTGG	25	248	58.23	
CALD1	NM_174258	F	CCTACCAGCGGAATGACGATGACG	24	230	59.49	Caldesmon 1
		R	CCGAGCCAGTCGCTCCAGG	19		59.17	
CCL4	NM_001075147	F	CCTTCTGTTCTCCAGCGCTCTCAG	24	192	59.08	Chemokine (C-C motif) ligand 4
		R	GCTCACTGGGGTTGGCGCAG	20		60.59	
CCL3	NM_174511	F	AGCAAGCACCGAGTCCCACCTC	22	244	60.75	chemokine (C-C motif) ligand 3
		R	CTTGGAGCACTGGCTGCTGGTC	22		59.99	
CD36	NM_174010	F	TGTGCAGAATCCAGATGAAGTGACAG	26	225	57.18	CD36 molecule (thrombospondin receptor)
		R	GCTGCTACAGCCAGGTTGAGAATG	24		58.08	
CD69	NM_174014	F	ACTGTAGGTTGGCTCCACGTGG	22	288	58.51	CD69 molecule
		R	TGGTGGCGCTGATGATGCATATTG	24		58.19	
CEACAM8	NM_205788	F	TCACAGAGGGACACAGCAGACAGC	24	203	60.41	Carcinoembryonic antigen-related cell adhesion molecule 8
		R	CGTTGTGGGCAAGCAGAAGAACATC	25		59.07	
CFLAR	NM_001012281	F	CTGTCTTCTGTGAGCTTGGCTGAGC	25	237	59.78	CASP8 and FADD-like apoptosis regulator
		R	ATCCTTGGCTATCTTGCTTCGACCCG	26		60.61	
C1QTNF1	NM_001083409	F	CTGCTTCTCGGTGCCTCCGCTG	22	273	61.98	C1q and tumor necrosis factor related protein 1
		R	CGTTGCTGTGCAGGGGCTTCTTCC	24		62.48	
CLU	NM_173902	F	CTCCAGTCCTACCAGCAGAAGATGC	25	279	58.65	Clusterin
		R	CAGTGCTTTCTCTGCCACATTCTCC	25		58.1	
COL8A1	NM_001101176	F	AAGTGGAGCAGCATCTGAAGAGACG	25	217	58.83	Collagen, type VIII, alpha 1
		R	GGTAGCGGCTTGATCCCATAGTAG	24		56.48	
CTTN	NM_001075287	F	TTGTGAGCGTCTCGCATCTGCACG	24	224	62.04	Cortactin
		R	AACACATTCTCCCGCAGCTTGTGG	24		59.94	

CXCL10	NM_001046551	F	TGCAAGTCAATCCTGCCCACGTG	23	203	59.93	Chemokine (C-X-C motif) ligand 10
		R	GAGGTAGCTTCTCTCTGGTCCATCC	25		57.67	
CX3CR1	NM_001102558	F	AGGAAGACTGACGGGCACATCG	22	243	58.66	Chemokine (C-X3-C motif) receptor 1
		R	TTGATGAGGGCAAACACCACCAGC	24		59.88	
CYP4F3	NM_001046391	F	AGCACTCGTCTGGACATGTTTGAAC	25	202	57.77	Cytochrome P450, family 4, subfamily F, polypeptide 3
		R	CATCGCGGGTGAGGTAGTACAGG	23		58.61	
DTX4	XM_606934	F	GCAGTGTCCGACCTGTAAGACC	22	216	57.03	Deltex homolog 2
		R	AGGTAACAATGTCGAGGGAAGCCAC	25		58.76	
GAPDH	NM_001034034	F	CAGCGACACTCACTCTTCTACCTTC	25	194	56.95	Glyceraldehyde-3-phosphate dehydrogenase
		R	GAACTCTTCCTCTCGTGCTCCTG	23		56.67	
ICAM1	NM_174348	F	TGGCCCTGCTCGGGACTCTG	20	191	60.25	ICAM1 intercellular adhesion molecule 1
		R	AACCTTCCAGTTGTCCCCACGG	22		58.69	
IFIT3	NM_001075414	F	GGCAGGCAAACAGCCATCATGAG	23	239	58.78	Interferon-induced protein with tetratricopeptide repeats 3
		R	CGCAAGCATTCCAGGGCTGC	20		59.22	
IGJ	NM_175773	F	TCCTAGTCAAGACATTGTGGAGAG	24	227	53.57	Iimmunoglobulin J chain
		R	TGTCATAGGTGTAACAGGTCTCAG	24		53.58	
IL2RB	XM_587301	F	ACTCACTCCAGGTCGTCCGCATAG	24	217	59.82	Interleukin 2 receptor, beta
		R	ACCTGAAGCTCATATTCCGTGCCTG	25		58.87	
IL15	NM_174090	F	GAGAAGTACTTCCATCCAGTGCTAC	25	255	54.76	Interleukin 15
		R	AGGAGAAAGCACTGCATCGCTG	22		57.59	
IL18	NM_174091	F	GGAATCAGATCACTTTGGCAAACTTGAACC	30	202	58.99	Interleukin 18
		R	GATGGTTACGGCCAGACCTCTAGTG	25		58.43	
ISG15	NM_174366	F	TGCAGAGAGCCTGGCACCAGAAC	23	268	60.97	ISG15 ubiquitin-like modifier
		R	GATGCAGTTCTGCACCACCAGC	22		58.67	
LMO2	NM_001076352	F	CTACTACAAGCTGGGCCGGAAGC	23	217	59.33	LIM domain only 2 (rhombotin-like 1)
		R	CACGATGTCGGAGTTGATGAGGAGG	25		58.95	
MFAP2	NM_174388	F	TGGGAGCAGAAGCGGCCGTG	20	221	61.77	Microfibrillar-associated protein 2
		R	CTGCTCGCTGTAGTGGGTATACTGC	25		59.01	
MFAP2**	NM_174388	F	CCGCGTCTACGTCGTCAATAAGG	23	169	57.71	Microfibrillar-associated protein 2
		R	GCAGCCCCCACAGCTCCTG	19		59.67	
MEIS3	NM_001193152	F	CGCTGCTAGCCCTGGTCTTTGAG	23	232	59.57	MEIS3 similar to Meis1, myeloid ecotropic viral integration site 1 homolog 3
		R	AGGTGGAAGCGGAGCACTTGAATG	24		59.47	
MMP13	NM_174389	F	TGGTGACTTCTACCCATTTGATGG	24	275	54.56	Matrix metallopeptidase 13 (collagenase 3)
		R	ACTGAATCCCTTGGACATCATCATC	25		54.66	
MPEG1	NM_001046464	F	AAGGATCAAGCTGTAACTACCCAGG	25	243	56.03	Macrophage expressed gene 1
		R	CCTGATGTGGTCCTCCTGAATGAG	24		56.5	
MUM1L1	XM_586767	F	CTAGCCACACAGTCAGAGGTCAG	23	228	56.34	Hypothetical LOC539380 (MUM1L1)
		R	CTTTGGTAAGTCTCCTTCTCCTTCGTG	27		57.1	
MX2	NM_173941	F	CAAGAGGCACACTCAGACTTCCACT	25	256	58.42	Myxovirus (influenza virus) resistance 2 (mouse)
		R	CCGCACCTTCTCCTCATACTTTCTG	25		57.2	
MYL4	NM_001075149	F	ATGCCGAGGTGCTGCGTGTCC	21	208	62.01	Myosin, light chain 4, alkali;
		R	GCAAGGACGTGGCGAAGCTCAG	22		60.61	
NDRG1	NM_001035009	F	AGCAGGACATTGAGACTTTGCATGGC	26	222	60.01	N-myc downstream regulated 1
		R	TGGGGAAGGACGCAGCGCC	19		61.85	
NID2	NM_001102065	F	CACTCCCACCCACGCCTTTCTG	22	261	59.67	Nidogen 2 (osteonidogen)
		R	CTATTCAGGTCATCAACCTCTCCTCGG	27		58.12	

PAK1	NM_001076898	F	CGACAGAAACCGCAGGCAGAGATG	24	249	60.12	p21 protein (Cdc42/Rac)-activated kinase 1
		R	CAGGTAAGATGGCTCGGTAAAATCGG	26		57.64	
PGM5	NM_001102335	F	TGCCCAACTTCATCCAGAGCGTGC	24	295	61.75	Phosphoglucomutase 5
		R	GCAACATTAAACTTCACTCCAAACTCTCC	29		57.07	
PIK3R6	NM_001102028	F	ACTCTAATGTACGTGCTCACTAAGGC	26	205	56.6	phosphoinositide-3-kinase, regulatory subunit 6
		R	CACTCGTCAGGTTCTGCTCGG	21		57.25	
RAB15	NM_001046538	F	AGCAGAAACGGCAGGTGGGAAGAG	24	214	60.94	RAB15,member RAS onocogene family
		R	TCATCCTCCTCCAGCTCTGCCAAG	24		59.76	
RGS1	NM_001199063	F	GTGAGGAGAATATTGAGTTCTGGCTGG	27	321	57.18	Similar to regulator of G-protein signalling 1,
		R	AGCCAGGAGCCAGTCACTTTAGAC	24		58.16	
RNASEL	NM_001098165	F	GACTGAGGACGAGGCATCTACG	22	243	56.42	Ribonuclease L
		R	GGGTTGTTATGGCTCTCAGTCTCC	24		56.75	
Runx-2	XM_002684501	F	GACAGAAGCTTGATGACTCTAAACCTAG	28	224	55.33	Runt-related transcription factor 2
		R	CGAGGGATAGGACTGGTCATAGG	23		55.17	
RYK	XM_001249766	F	CCAGACACCCTACGTGGACATCG	23	238	58.79	Similar to receptor-like tyrosine kinase
		R	TCCTGACGCTGTGAGACTGTGAC	23		58.36	
SELL	NM_174182	F	ATGCAGCGGCCATGGACAATGTG	23	211	60.6	Selectin L
		R	AATCATGTCTGTTCCCTTGGAGCAG	25		57.03	
SEPP1	NM_174459.3	F	CCGCCTTGTATATCATCTTGGTTTGCC	27	331	58.4	Selenoprotein P, plasma, 1
		R	AGGGGTATCTGGTGTGTCTGGTTTTG	26		58.46	
SERPINE1	NM_174137	F	ATGTCTCCGGTCTTTGCCTGCCTC	24	346	60.76	Serpin peptidase inhibitor, clade E member 1
		R	CGGCTGTGCTGATCTCATCCTTGTTC	26		59.91	
SLC6A6	NM_174610	F	CGTACCCCTGACCTACAACAAAGTCTAC	28	266	58.51	Solute carrier family 6 (neurotransmitter transporter, taurine),
		R	CAATGATGTGCGTGGGTTTCCTGAG	25		58.62	member 6
STAP1	NM_001077868	F	ACTGCTCTACCCTTGTACTTTGAAG	25	177	54.53	Signal transducing adaptor family member 1
		R	CTGATCAGTAAGGCATGTAAGGTC	24		53.07	
TLR4	NM_174198	F	TGGACCTGAGCTTTAACTACCTG	23	159	59.39	Toll-like receptor 4
		R	TTCCCGTCAGTATCAAGGTG	20		58.8	
TRAF1	XM_002689959	F	AGAGGGGAGTATGATGCTCTGCTGC	25	251	59.89	TNF receptor-associated factor 1
		R	TCCACGACGCACTTGACGAACATG	24		60	
TP63	NM_001191337	F	CTCGATGCAGTCTCAGTCTTCCTACG	26	258	58.58	Tumor protein p63
		R	CAGTGGGAGGTGGATGGCATGG	22		59.21	
VCAM1	NM_174484	F	CAGGCACCTTCAGGAGGGACAG	22	226	58.57	Vascular cell adhesion molecule 1
		R	CAGCCTGTTGTGCTGCAAGTCAGTG	25		60.89	
VWA5A	XM_002699100	F	GTTAGCATGGAGTGTGGAGTCATAAGC	27	248	57.67	Von Willebrand factor A domain containing 5A
		R	GGCTTCTCAAGACGGGCCTCTG	22		59.23	
XCL1	NM_175716	F	TCAGCCTCTTACTGCACAGCTCAG	24	264	58.48	Chemokine (C motif) ligand 1
		R	CAGGCAGCTTGAGGATCAGCACAG	24		59.83	

Appendix 2: Microarray results of chapter 4

2.1 Complete lists of infection associated modulated 1959 genes

2.1.1 Full list of genes in profile 1(n = 44)

S.No	SEQ. ID	Acc. No. (RefSeq)	Putative Gene symbol	Gene Name	BL20 LPS Vs BL20 FDR (4h/or18)	BL20 LPS Vs BL20 Abs: FC (4h/or18)	TBL20 Vs BL20 Abs: FC	TBL20 Vs BL20 LPS Abs: FC (4h/or18)	BW720c Response
						↑	↑ ↑	↑	
1	gi_119889107	XM_001256711	SLAMF7	Slam family member 7	0.00	2.8	415.4	148.0	---
2	gi_119903692	XM_871827	LRRTM4	Leucine rich repeat transmembrane neuronal 4	0.00	3.6	242.6	67.9	---
3	gi_51806603	---	---	Co876689 bovgen_05014 normal cattle brain cDNA clone rzpdp1056k1259q 5'	0.01	2.0	114.2	55.8	---
4	gi_31342133	NM_174389	MMP13	Matrix metallopeptidase 13 (collagenase 3)	0.00	3.1	168.2	54.2	↓
5	gi_31342239	NM_175716	XCL2	Chemokine (c motif) ligand 1 (xcl1)	0.00	8.5	356.6	42.0	↓
6	gi_119891855	XM_001250312	LOC783109	Similar to bowc1.1	0.00	2.4	93.9	39.6	---
7	gi_119927959	XM_593064	TP73	Tumor protein p73	0.00	2.7	53.6	20.0	---
8	gi_119915824	XM_001255734	LOC788785	Similar to atxn1 protein	0.00	2.9	43.0	15.0	---
9	gi_139948768	NM_001083791	SH3BGRL2	Sh3 domain binding glutamic acid-rich protein like 2	0.00	3.2	45.0	14.0	---
10	gi_119894051	XM_587301	IL2RB	Interleukin 2 receptor, beta	0.00	8.3	93.1	11.2	---
11	gi_119892822	XM_001250337	CD122	Interleukin-2 receptor subunit beta precursor (IL-2 receptor) (p70-75)	0.00	4.5	45.5	10.0	---
12	gi_27901800	NM_174182	SELL	Selectin l	0.01	2.2	21.4	9.6	↑
13	gi_119911540	XM_001253061	CCL1	Chemokine (c-c motif) ligand 1	0.00	3.0	27.1	9.2	↓
14	gi_119910732	XM_869544	MEIS3	Meis homeobox 3	0.00	8.3	71.0	8.5	↓
15	gi_119893066	XM_001252456	LOC785733	Similar to bowc1.1	0.02	2.1	16.4	7.8	---
16	gi_119896248	XM_001254114	LOC786443	Hypothetical protein (LOC786443)	0.00	14.4	92.3	6.4	---
17	gi_31342240	NM_174348	ICAM1	Intercellular adhesion molecule 1	0.00	3.8	22.8	6.0	---
18	gi_119913829	XR_028628	LOC788239	Similar to regulator of g-protein signaling 16/-r	0.02	2.0	9.6	4.7	---
19	gi_158341675	NM_001109983	PGPEP1	Pyroglutamyl-peptidase i	0.00	4.8	22.4	4.7	---
20	gi_119908880	XM_001253453	LOC785427	Similar to epidermis-specific serine protease-like protein	0.00	4.7	22.1	4.7	↑
21	gi_119900312	XM_612930	BNC2	Basonuclin 2	0.00	4.9	22.6	4.6	---
22	gi_114051048	NM_001046491	MOBKL2B	Mob1, mps one binder kinase activator-like 2b (yeast)	0.01	2.1	8.6	4.1	---
23	gi_31341516	NM_174619	STXBP1	Syntaxin binding protein 1	0.00	2.9	11.2	3.9	---
24	gi_119916814	XR_028239	LOC785278	Similar to regulator of g-protein signaling 16/-r	0.00	2.6	9.8	3.7	---
25	gi_119891399	XM_599768	JHDM1D	Jumonji c domain containing histone demethylase 1 homolog d (s. Cerevisiae)	0.00	2.7	9.9	3.7	---
26	gi_119915826	XM_868412	ATXN1	Ataxin 1	0.00	3.5	12.8	3.6	---
27	gi_119891397	XM_001249623	LOC781418	Hypothetical protein (LOC781418)	0.01	2.1	7.4	3.5	---
28	gi_119903194	XM_001255518	IL18RAP	Interleukin 18 receptor accessory protein	0.00	4.1	14.3	3.5	↓
29	gi_119914616	XM_597868	LOC519644	Similar to voltage-gated calcium channel alpha(2)delta-3 subunit	0.01	2.1	7.3	3.4	↓
30*	gi_115495042	NM_001075961	RTP4	Receptor (chemosensory) transporter protein 4	0.00	4.5	14.9	3.3	↑
31	gi_31341539	NM_174610	SLC6A6	Solute carrier family 6 (neurotransmitter transporter, taurine), member 6	0.00	17.0	55.6	3.3	↓
32	gi_28461172	NM_175772	ELN	Elastin	0.00	3.2	10.2	3.2	↓
33	gi_119887104	XM_587930	ABCG1	Atp-binding cassette, sub-family g (white), member 1	0.00	3.5	9.6	2.7	↓
34	gi_31341556	NM_174602	SLC2A1	Solute carrier family 2 (facilitated glucose transporter), member 1	0.00	2.3	6.2	2.7	↓
35	gi_77735634	NM_001034341	---	Four and a half lim domains 1 (FHL1), transcript variant 3	0.00	2.8	7.7	2.7	↑
36	gi_119906041	XM_584869	SDC4	Syndecan 4	0.00	5.6	14.9	2.7	---
37	gi_60722467	---	---	Dn512277 1248296 marc 7bov cDNA 3'	0.00	4.4	11.4	2.6	---
38	gi_119890101	XM_616138	CACHD1	Cache domain containing 1	0.00	2.3	5.7	2.5	---
39*	gi_119932755	XR_028507	RTP4	Receptor (chemosensory) transporter protein 4	0.00	4.4	11.0	2.5	↑
40	gi_114051635	NM_001046438	NRN1	Neuritin 1	0.00	12.3	29.4	2.4	---
41	gi_78369225	NM_001035273	SSBP4	Single stranded dna binding protein 4	0.00	5.6	13.3	2.4	---
42	gi_115497085	NM_001075287	CTTN	Cortactin	0.00	11.0	25.0	2.3	↓
43	gi_155372054	NM_001101164	EGLN3	Egl nine homolog 3 (c. Elegans)	0.00	2.6	5.8	2.2	---
44	gi_119919443	XM_588001	TNFRSF26	Tumor necrosis factor receptor serfamily, member 26	0.01	2.2	4.8	2.2	---

Asterisk (*) beside the serial no indicates duplicate probe present in the modulated dataset

2.1.2 Full list of genes in profile 2 (n = 254)

S.No	SEQ. ID	Acc. No. (RefSeq)	Putative Gene symbol	Gene Name	BL20 LPS Vs BL20 FDR (4h/or18)	BL20 LPS Vs BL20 Abs: FC (4h/or18)	TBL20 Vs BL20 Abs: FC	TBL20 Vs BL20 LPS Abs: FC (4h/or18)	BW720c Response
						↑	↓	↓	
1	gi_114050822	NM_001046464	MPEG1	Macrophage expressed 1	0.00	79.8	-5.6	-449.4	↑
2	gi_31343308	NM_173902	CLU	Clusterin	0.00	8.9	-31.7	-280.7	---
3	gi_51812080	---	---	Co882151 bovgen_10476 normal cattle brain cDNA clone rzpdp1056f0925q 5'	0.00	46.8	-4.0	-186.2	---
4	gi_91982958	---	---	Clone tghc9907 immunoglobulin gamma 1 heavy chain constant region, mRNA	0.00	49.0	-3.6	-177.4	---
5*	gi_119879490	XR_027375	CD200R1	Cd200 receptor 1	0.00	5.2	-25.4	-132.8	↑
6	gi_60592981	NM_001012678	BOLA-DYA	Major histocompatibility complex, class ii, dy alpha (bola-dya)	0.00	27.4	-4.8	-132.1	↑
7	gi_119901378	XM_611161	EPHA7	Eph receptor a7	0.00	4.6	-26.0	-120.1	---
8	gi_119909596	XM_001255981	LOC789139	Similar to iglv3s1 (LOC789139)	0.00	7.4	-16.3	-119.8	↑
9	gi_119919728	XR_028639	LOC535439	Hypothetical (LOC535439)	0.00	3.4	-33.9	-115.3	↑
10	gi_41386773	NM_174090	IL15	Interleukin 15	0.00	5.7	-18.9	-107.3	---
11	gi_119904381	XM_001256288	ABO	Abo blood group (transferase a, alpha 1-3-n-acetylgalactosaminyltransferase)	0.00	2.8	-35.5	-100.0	---

12	gi_51824544	---	---	Co894237 bovgen_22562 normal cattle brain cDNA clone rzpdp1056o1038q 5'	0.00	21.4	-4.6	-98.7	---
13	gi_51804673	---	---	Co874773 bovgen_03098 normal cattle brain cDNA clone rzpdp1056c1255q 3'	0.00	8.2	-11.5	-94.2	---
14	gi_51824705	---	---	Co894397 bovgen_22722 normal cattle brain cDNA clone rzpdp1056h2051q 5'	0.00	6.7	-12.7	-85.3	↑
15	gi_119915695	XR_028435	LOC786760	Similar to BTN3A2 (LOC786760)	0.00	6.5	-12.8	-82.8	↑
16	gi_31340694	NM_174703	TNXB	Tenascin Xb	0.00	6.6	-11.8	-78.0	---
17	gi_119896111	XM_593744	C8orf80	Chromosome 8 open reading frame 80	0.02	2.0	-32.4	-65.1	↑
18	gi_41386684	NM_174196	THBS1	Thrombospondin 1	0.00	2.5	-25.7	-65.0	---
19*	gi_119908116	XM_864590	RGS18	Regulator of g-protein signaling 18	0.00	29.2	-2.2	-63.3	---
20	gi_75832075	NM_175773	IGJ	Immunoglobulin j polypeptide	0.00	2.9	-20.3	-58.1	↑
21	gi_119891985	XM_596354	PLXNC1	Plexin C1	0.00	2.6	-19.4	-50.5	↑
22	gi_112210002	---	---	Ee349629 lb02756.cr_b03 gc_bgc-27 cDNA clone image:8630885	0.00	11.8	-4.1	-47.9	↓
23	gi_78369299	NM_001035404	SAMSN1	Sam domain, sh3 domain and nuclear localization signals 1	0.00	4.5	-10.2	-46.2	↑
24	gi_119910850	XM_869691	RASIP1	Ras interacting protein 1	0.00	5.4	-8.5	-46.0	↑
25	gi_115497721	NM_001075231	PDGFA	Platelet-derived growth factor alpha polypeptide	0.00	18.0	-2.5	-44.7	---
26	gi_118150845	NM_001077868	STAP1	Signal transducing adaptor family member 1	0.02	2.1	-21.2	-43.8	↑
27	gi_76628966	XM_588243	CD207	CD207 molecule, Langerin	0.00	3.8	-11.3	-42.9	↑
28	gi_45469784	---	---	Ck955404 4095662 barc 10bov cDNA clone 10bov34_k13 5'	0.00	16.5	-2.6	-42.8	↑
29	gi_119892202	XM_586498	WNT10B	Similar to wingless-type mmtv integration site family, member 10b, transcript variant 1 (LOC539337)	0.00	10.3	-4.2	-42.6	↑
30	gi_119905622	XM_001256257	LOC789517	Similar to neurotensin receptor (LOC789517)	0.00	10.5	-4.0	-42.3	---
31	gi_62751708	NM_001015520	LASS4	Lag1 homolog, ceramide synthase 4	0.00	9.2	-4.3	-39.9	↑
32*	gi_68319996	AM018804.1	EPAS1	Endothelial pas domain protein 1	0.00	12.3	-3.3	-39.9	↑
33	gi_51827054	---	---	Co896734 bovgen_25059 normal cattle brain cDNA clone rzpdp1056g181q 5'	0.00	16.3	-2.3	-38.1	---
34	gi_119879508	XM_617543	CD80	Cd80 molecule	0.00	13.4	-2.8	-37.9	↑
35	gi_51809329	---	---	Co879405 bovgen_07732 normal cattle brain cDNA clone rzpdp1056g089q 5'	0.00	3.3	-10.9	-36.2	↑
36*	gi_31340626	NM_174725	EPAS1	Endothelial pas domain protein 1	0.00	12.0	-2.9	-35.2	↑
37	gi_119930249	XM_001251416	LOC782773	Hypothetical protein (LOC782773)	0.00	4.1	-8.4	-34.8	↑
38*	gi_150247135	NM_001099374	CD200R1	Cd200 receptor 1	0.00	8.3	-4.2	-34.6	---
39	gi_76668819	XM_864611	SIM1	Single-minded homolog 1 (drosophila)	0.00	6.7	-4.9	-33.2	↑
40	gi_115494923	NM_001075952	ASGR2	Asialoglycoprotein receptor 2	0.00	3.4	-9.7	-32.7	↑
41	gi_119894218	XM_608086	LOC529634	Similar to mist (LOC529634)	0.00	3.4	-9.5	-32.2	↑
42*	gi_119914332	XM_001250255	MOBP	Myelin-associated oligodendrocyte basic protein	0.00	14.3	-2.2	-32.0	---
43	gi_119904441	XM_580490	KBTBD6	Kelch repeat and btb (poz) domain containing 6	0.00	10.3	-3.0	-30.4	---
44	gi_119930251	XM_001251461	LOC782810	Hypothetical protein (LOC782810)	0.00	3.4	-8.5	-28.9	↑
45	gi_119916402	XM_580886	CCDC68	Coiled-coil domain containing 68	0.00	5.7	-5.0	-28.1	↑
46	gi_94966920	NM_001040563	HTATIP2	Hiv-1 tat interactive protein 2, 30kda	0.00	6.5	-4.3	-27.9	---
47	gi_149642680	NM_001098991	FGR	Gardner-rasheed feline sarcoma viral (v-fgr) oncogene homolog	0.00	3.9	-7.1	-27.6	↑
48*	gi_119889877	XM_591946	GBP2	Guanylate binding protein 2, interferon-inducible	0.00	3.8	-7.3	-27.4	↑
49	gi_78369443	NM_001035293	BIRC3	Baculoviral iap repeat containing 3	0.00	5.8	-4.5	-26.1	---
50	gi_119910918	XM_869891	SIGLEC10	Sialic acid binding ig-like lectin 10	0.00	2.7	-9.4	-25.4	---
51	gi_51813369	---	---	Co883435 bovgen_11760 normal cattle brain cDNA clone rzpdp1056h1817q 5'	0.00	4.2	-5.9	-24.9	↑
52	gi_77736010	NM_001034532	PYROXD2	Pyridine nucleotide-disulphide oxidoreductase domain 2	0.00	7.2	-3.2	-23.4	---
53*	gi_119915684	XM_863936	UBD	Ubiquitin d	0.00	9.6	-2.4	-22.8	↑
54	gi_51811530	---	---	Co881601 bovgen_09926 normal cattle brain cDNA clone rzpdp1056j0915q 5'	0.00	2.3	-9.8	-22.7	↑
55	gi_89886136	NM_001014870	TMEM106A	Transmembrane protein 106a	0.00	2.1	-10.5	-22.2	↑
56	gi_119934649	XM_001256269	LOC789535	Similar to vasoactive intestinal peptide receptor 2	0.00	2.4	-8.9	-21.5	---
57	gi_119901653	XM_604128	PLEKHG1	Pleckstrin homology domain containing, family g (with RHOGEF domain) member 1	0.00	2.1	-10.3	-21.5	---
58	gi_41386777	NM_174115	MUC1	Mucin 1, cell surface associated	0.00	10.2	-2.1	-21.2	---
59	gi_119922733	XM_001249941	LOC781780	Hypothetical protein (LOC781780)	0.00	4.1	-5.1	-21.0	↑
60	gi_119903737	XM_596854	PLEK	Pleckstrin	0.00	5.6	-3.7	-20.3	↑
61	gi_51887667	---	---	Aj820191 aj820191 kn206 bos sp. CDNA clone c0006017l10	0.00	4.4	-4.6	-20.2	---
62	gi_162287249	NM_001075475	ADAM19	Adam metallopeptidase domain 19	0.00	3.0	-6.6	-19.8	---
63	gi_119890722	XM_592017	SAMD9	Sterile alpha motif domain containing 9	0.00	7.2	-2.8	-19.8	↑
64	gi_119904782	XM_868438	KCTD12	Potassium channel tetramerisation domain containing 12	0.00	5.7	-3.4	-19.5	↑
65	gi_119927147	XM_001253465	LOC785445	Similar to guanylate binding protein 4 (LOC785445)	0.00	5.5	-3.5	-19.2	↑
66	gi_119906769	XM_001250623	TP53INP1	Tumor protein p53 inducible nuclear protein 1	0.00	2.3	-8.3	-18.9	↑
67	gi_119887080	XM_584543	ICOSLG	Inducible t-cell co-stimulator ligand	0.00	3.8	-4.9	-18.9	↑
68	gi_119905627	XM_606839	NTSR1	Neurotensin receptor 1 (high affinity)	0.00	6.6	-2.8	-18.1	---
69	gi_29184272	---	---	Cb419326 592181 marc 6bov cDNA 5'	0.00	3.8	-4.7	-17.9	↑
70	gi_156120748	NM_001102051	TXLNB	Taxilin beta	0.00	8.5	-2.0	-17.3	---
71	gi_119906824	XM_001251675	LOC784120	Hypothetical protein, transcript variant 1 (LOC784120)	0.00	3.5	-4.9	-17.3	↑
72	gi_119920140	XM_001251153	LOC782514	Hypothetical protein (LOC782514)	0.00	8.3	-2.1	-17.1	---
73	gi_119918514	XM_001250260	LOC781983	Similar to proteoglycan 1 precursor-like (LOC781983)	0.00	5.6	-3.0	-16.8	↑
74	gi_77735736	NM_001034391	LRRC33	Leucine rich repeat containing 33	0.00	2.2	-7.7	-16.7	↑
75	gi_119906373	XM_594631	KLHL38	Kelch-like 38 (drosophila)	0.00	4.5	-3.7	-16.7	↑
76	gi_139948810	NM_001083735	TRIM2	Tripartite motif containing 2	0.00	5.6	-3.0	-16.6	---
77	gi_119909414	XM_590469	RASAL1	Ras protein activator like 1 (gap1 like)	0.00	8.1	-2.0	-16.5	---
78	gi_119918508	XR_027379	MYPN	Myopalladin	0.00	3.5	-4.7	-16.4	---
79	gi_119887502	XR_027685	LOC540561	Similar to titin (connectin)	0.02	2.1	-7.6	-16.2	
80	gi_119893129	XM_867752	PRMT8	Protein arginine methyltransferase 8	0.00	6.7	-2.4	-16.1	---
81	gi_119887408	XR_028509	LOC787276	Hypothetical protein (LOC787276)	0.00	2.4	-6.6	-15.9	---
82	gi_60592983	NM_001012679	BOLA-DYB	Major histocompatibility complex, class ii, dy beta (bola-dyb)	0.00	5.9	-2.7	-15.7	---
83	gi_51815496	---	---	Co885211 bovgen_13536 normal cattle brain cDNA clone rzpdp1056j083q 5'	0.00	4.1	-3.8	-15.6	---
84	gi_116004198	NM_001076987	PLAC8	Placenta-specific 8	0.00	3.4	-4.5	-15.3	↑
85	gi_51811539	---	---	Co881610 bovgen_09935 normal cattle brain cDNA clone rzpdp1056k0421q 5'	0.01	2.1	-7.1	-14.8	↑
86	gi_119900630	XM_001249758	LOC781261	Similar to clusterin precursor (Glycoprotein iii) (GPIII)	0.00	4.1	-3.6	-14.7	---
87*	gi_119879546	XM_001251104	PARP14	Poly (adp-ribose) polymerase family, member 14	0.00	3.2	-4.6	-14.6	↑
88	gi_148236122	NM_001098043	CLMP	Cxadr-like membrane protein	0.00	4.5	-3.2	-14.5	---
89	gi_119922735	XM_001251182	LOC782552	Hypothetical protein (LOC782552)	0.00	3.4	-4.1	-14.2	↑
90	gi_114050810	NM_001046507	EAF2	Ell associated factor 2	0.00	3.7	-3.8	-14.1	---
91	gi_51808399	CO878479.1	CEBPA	CCAAT/enhancer binding protein (c/ebp), alpha	0.00	2.7	-5.2	-14.0	↑
92	gi_51885959	---	---	Aj818483 kn206 bos sp. CDNA clone c0006012g21	0.00	6.0	-2.3	-13.9	---
93	gi_119936478	XM_001257128	LOC790729	Similar to osbp-related protein 6; orp6 (LOC790729)	0.01	2.3	-6.0	-13.8	---
94*	gi_119914330	XM_001250204	MOBP	Myelin-associated oligodendrocyte basic protein	0.00	6.0	-2.3	-13.8	---
95	gi_119927163	XM_001249585	LOC783074	Hypothetical protein (LOC783074)	0.00	3.8	-3.6	-13.7	↑
96*	gi_156121166	NM_001102261	GBP4	Guanylate binding protein 4	0.00	2.8	-4.8	-13.5	↑
97	gi_125991949	NM_001081581	ABAT	4-aminobutyrate aminotransferase	0.00	6.3	-2.1	-13.5	---
98	gi_119904527	XM_597949	CAB39L	Calcium binding protein 39-like	0.00	4.0	-3.2	-13.0	↑
99*	gi_119879548	XM_613140	PARP14	Poly (adp-ribose) polymerase family, member 14	0.00	3.2	-3.9	-12.6	↑
100*	gi_119923113	XM_001250460	FRMD6	Ferm domain containing 6	0.00	6.1	-2.0	-12.4	---

101	gi_114052742	NM_001045877	BMP4	Bone morphogenetic protein 4	0.00	3.0	-4.2	-12.4	---
102*	gi_119927149	XM_872465	GBP4	Guanylate binding protein 4	0.01	2.3	-5.4	-12.3	↑
103	gi_119910364	XM_583222	KIRREL2	Kin of irre like 2 (drosophila)	0.00	3.4	-3.4	-11.9	---
104	gi_119907584	XM_867197	FCHSD2	Fch and double sh3 domains 2	0.00	2.9	-4.1	-11.8	↑
105	gi_51885704	---	---	Aj818228 kn206 bos sp. CDNA clone c0006011j16	0.00	2.3	-5.1	-11.8	---
106	gi_84370132	NM_001038554	ADPRH	Adp-ribosylarginine hydrolase	0.00	2.1	-5.6	-11.8	↑
107	gi_76642926	XM_600064	SLFN11	Schlafen family member 11	0.00	2.9	-4.0	-11.8	↑
108	gi_51883657	---	---	Aj816181 kn206 bos sp. CDNA clone c0005210o22	0.00	3.7	-3.2	-11.7	↑
109	gi_156121204	NM_001102280	GAS7	Growth arrest-specific 7	0.00	2.1	-5.6	-11.6	---
110	gi_15776290	---	---	Bi775313 467737 marc 2bov cDNA 5'	0.00	2.7	-4.3	-11.6	↑
111	gi_157279976	NM_001105034	GIMAP7	Gtpase, imap family member 7	0.00	4.4	-2.6	-11.4	---
112	gi_119913163	XM_001253420	LOC785366	Similar to embigin homolog (mouse) (LOC785366)	0.01	2.2	-5.2	-11.3	↑
113	gi_51887200	---	---	Aj819724 kn206 bos sp. CDNA clone c0006016e15	0.00	4.0	-2.8	-11.2	---
114	gi_119917968	XM_866446	JAKMIP3	Janus kinase and microtubule interacting protein 3	0.02	2.1	-5.3	-10.8	↑
115	gi_62751902	NM_001015610	PLA1A	Phospholipase a1 member a	0.00	5.1	-2.1	-10.7	---
116	gi_75832127	NM_001025326	SRGN	Serglycin (srgn)	0.00	4.6	-2.3	-10.6	---
117	gi_45430044	NM_205812	PKIG	Protein kinase (camp-dependent, catalytic) inhibitor gamma	0.00	4.2	-2.5	-10.6	---
118*	gi_115496411	NM_001075349	CHN1	Chimerin (chimaerin) 1	0.00	3.2	-3.3	-10.6	↑
119	gi_119923438	XM_615898	VAV3	Vav 3 protein, transcript variant 1 (LOC521961)	0.02	2.0	-5.2	-10.5	---
120	gi_155371902	NM_001101086	CPD	Carboxypeptidase d	0.00	3.8	-2.8	-10.5	---
121*	gi_119921604	XM_001250189	GBP2	Guanylate binding protein 2, interferon-inducible	0.01	2.1	-5.1	-10.5	↑
122	gi_31341685	NM_174553	IFNAR2	Interferon (alpha, beta and omega) receptor 2	0.00	4.6	-2.3	-10.5	---
123	gi_114050846	NM_001046461	TRIM34	Trim6-trim34 readthrough (TRIM6-TRIM34)	0.00	2.1	-4.9	-10.4	↑
124	gi_119911048	XM_602125	PRKCG	Protein kinase c, gamma	0.00	2.9	-3.6	-10.4	---
125	gi_114050784	NM_001046002	CD48	CD48 molecule	0.00	4.2	-2.5	-10.3	↑
126	gi_51880943	---	---	Aj813467 kn206 bos sp. CDNA clone c0005207e23	0.02	2.0	-5.1	-10.3	↑
127	gi_156523137	NM_001102513	PCDHGB4	Protocadherin gamma subfamily b, 4	0.03	2.0	-5.1	-10.2	↑
128	gi_61870087	XM_588576	PCDHGA5	Protocadherin gamma subfamily a, 5	0.01	2.2	-4.7	-10.1	↑
129	gi_156120712	NM_001102033	SGK1	Serum/glucocorticoid regulated kinase 1	0.00	4.3	-2.3	-9.9	---
130	gi_115496777	NM_001076371	SEPT5	Septin 5	0.00	2.6	-3.9	-9.9	↑
131	gi_119911648	XM_001251943	LOC783305	Similar to tnf receptor-associated factor 4 (LOC783305)	0.00	3.7	-2.6	-9.8	---
132	gi_119922622	XM_001255033	LOC787761	Similar to g protein coupled receptor 133 (LOC787761)	0.00	2.3	-4.2	-9.8	---
133	gi_119894894	XM_600015	TNFSF9	Tumor necrosis factor (ligand) superfamily, member 9	0.00	2.3	-4.1	-9.7	---
134	gi_119888895	XM_581276	UBXN10	Ubx domain protein 10	0.00	2.5	-3.9	-9.6	---
135	gi_156120916	NM_001102135	LAMP3	Lysosomal-associated membrane protein 3	0.00	2.8	-3.4	-9.4	↑
136	gi_119914719	XM_001254179	CDHR4	Cadherin-related family member 4	0.00	2.4	-3.8	-9.3	---
137	gi_51812298	---	---	Co882366 bovgen_10691 normal cattle brain cDNA clone rzpdp1056h213q 5'	0.00	2.7	-3.4	-9.2	---
138	gi_31342628	NM_174190	SVIL	Supervillin	0.00	4.1	-2.3	-9.2	---
139	gi_29234175	---	---	Cb444296 695445 marc 6bov cDNA 3'	0.01	2.3	-3.9	-8.8	↑
140	gi_9600749	---	---	Be481216 166577 barc 5bov cDNA 5'	0.00	3.5	-2.5	-8.8	---
141	gi_139949110	NM_001083769	IRF8	Interferon regulatory factor 8	0.00	2.4	-3.7	-8.8	↓
142	gi_119925221	XM_001254480		Similar to zinc finger protein 75 (LOC614260)	0.00	3.1	-2.8	-8.7	---
143	gi_119889702	XM_001254448	LOC786893	Similar to vav 3 oncogene (LOC786893)	0.01	2.1	-4.2	-8.7	---
144	gi_31343026	NM_174020	LYST	Lysosomal trafficking regulator	0.00	2.2	-3.8	-8.6	---
145	gi_164450480	NM_001113277	KNG1	Kininogen 1	0.01	2.1	-4.1	-8.4	↑
146	gi_115495496	NM_001076276	MARCKS	Myristoylated alanine-rich protein kinase c substrate	0.00	3.8	-2.2	-8.3	---
147	gi_119889728	XM_001254754	LOC787315	Similar to vav 3 oncogene (LOC787315)	0.00	2.3	-3.6	-8.3	---
148	gi_119915696	XM_870260	BTN2A2	Butyrophilin, subfamily 2, member a2	0.00	3.2	-2.5	-8.2	---
149	gi_156120442	NM_001101897	KIAA0226	Kiaa0226	0.00	3.0	-2.7	-8.2	---
150	gi_49409176	---	---	Aj676886 kn224 cDNA clone kn224-022_e21	0.01	2.0	-4.1	-8.2	↑
151	gi_10025444	BE665170.1	PNRC1	Proline-rich nuclear receptor coactivator 1	0.00	3.4	-2.4	-8.1	↑
152	gi_51823891	---	---	Co893586 bovgen_21911 normal cattle brain cDNA clone rzpdp1056p2234q 5'	0.00	2.9	-2.8	-8.1	---
153	gi_119909598	XM_001256017	LOC789191	Similar to mgc127066 protein (LOC789191)	0.00	3.6	-2.2	-8.0	---
154	gi_116004060	NM_001076918	TLR10	Toll-like receptor 10	0.00	3.5	-2.3	-8.0	---
155	gi_119891152	XM_594668	MYO1G	Myosin ig	0.00	2.6	-3.0	-8.0	---
156	gi_51820108	---	---	Co889821 bovgen_18146 normal cattle brain cDNA clone rzpdp1056o0331q 5'	0.00	3.5	-2.2	-7.9	---
157	gi_119895312	XM_866364	OR2G3	Olfactory receptor, family 2, subfamily g, member 3	0.00	3.5	-2.2	-7.8	---
158	gi_119921600	XM_001249998	LOC781557	Hypothetical protein (LOC781557)	0.00	2.3	-3.3	-7.7	---
159	gi_119907376	XM_001255273	LOC788122	Similar to tripartite motif protein trim5 (LOC788122)	0.00	3.2	-2.4	-7.7	---
160	gi_76678805	XM_586049	LOC509148	Similar to clll7 protein (LOC509148)	0.00	3.1	-2.5	-7.7	---
161	gi_115496207	NM_001075746	GBP5	Guanylate binding protein 5	0.00	3.4	-2.2	-7.6	---
162	gi_119910891	XM_870599	LOC618268	Similar to CD33L1 (LOC618268)	0.00	2.3	-3.3	-7.5	---
163*	gi_62751495	NM_001015680	NAPEPLD	N-acyl phosphatidylethanolamine phospholipase d	0.00	2.6	-2.9	-7.5	↑
164	gi_115495090	NM_001075392	ANKRD37	Ankyrin repeat domain 37	0.00	2.5	-3.0	-7.5	---
165	gi_119923988	XR_028027	LOC784083	Similar to lar-interacting protein 1a (LOC784083)	0.01	2.4	-3.1	-7.5	---
166	gi_58765354	---	---	Cx951827 umc-bemiv_0a02-017-h02 nuclear-transfer derived blastocysts d8 bemiv cDNA 3'	0.00	3.1	-2.4	-7.5	↑
167	gi_119922554	XM_001254319	LOC786718	Hypothetical protein loc786718 (LOC786718)	0.01	2.3	-3.2	-7.4	↑
168	gi_51827041	---	---	Co896721 bovgen_25046 normal cattle brain cDNA clone rzpdp1056i111q 5'	0.01	2.2	-3.4	-7.4	↑
169	gi_6955562_	---	---	Aw427615 63840 marc 3bov cDNA 5'	0.00	2.8	-2.6	-7.4	---
170	gi_51881820	---	---	Aj814344 aj814344 kn206 bos sp. CDNA clone c0005200k24	0.00	3.0	-2.4	-7.3	↑
171	gi_114052650	NM_001046309	BAMBI	Bmp and activin membrane-bound inhibitor homolog (xenopus laevis)	0.00	3.5	-2.1	-7.2	---
172	gi_51883270	---	---	Aj815794 kn206 bos sp. cDNA clone c0005198a15	0.02	2.1	-3.4	-7.2	---
173	gi_119912293	XM_586229	GSDMB	Gasdermin b	0.00	2.7	-2.6	-7.1	---
174	gi_119907378	XM_864679	LOC516599	Similar to tripartite motif protein trim5, transcript variant 2	0.01	2.2	-3.2	-7.1	↑
175	gi_51887143	---	---	Aj819667 kn206 bos sp. cDNA clone c0006016b24	0.00	3.2	-2.2	-7.0	---
176	gi_51887526	---	---	Aj820050 kn206 bos sp. cDNA clone c0006017e07	0.00	2.9	-2.4	-7.0	↑
177*	gi_61011750	DN547960.1	AP1M2	Adaptor-related protein complex 1, mu 2 subunit	0.02	2.1	-3.3	-7.0	↑
178	gi_119919105	XM_001254753	GPR44	G protein-coupled receptor 44	0.02	2.0	-3.4	-6.9	---
179*	gi_51824596		AP1M2	Adaptor-related protein complex 1, mu 2 subunit	0.00	2.4	-2.9	-6.9	↑
180	gi_115496154	NM_001075480	C11H2orf50	Chromosome 2 open reading frame 50 ortholog	0.00	2.6	-2.6	-6.9	---
181	gi_119888565	XM_001252890	LOC785844	Hypothetical protein (LOC785844)	0.00	2.5	-2.7	-6.8	↑
182	gi_155371870	NM_001101070	FAM117A	Family with sequence similarity 117, member a	0.00	2.2	-3.1	-6.8	---
183	gi_31343630	NM_177523	SOCS2	Suppressor of cytokine signaling 2	0.00	2.5	-2.7	-6.8	---
184	gi_116003948	NM_001076862	SNX29	Sorting nexin 29	0.00	3.3	-2.1	-6.7	---
185	gi_156121170	NM_001102263	GRAMD4	Gram domain containing 4 (gramd4)	0.00	3.2	-2.1	-6.7	---
186	gi_119924029	XM_618019	LOC537832	Similar to IL1RAPL1 protein (LOC537832)	0.00	2.6	-2.6	-6.7	↑
187	gi_71034621	DR749281.1	---	Dr749281 ng010006a12h05 ng01 rearrayed soares normalized bovine placenta cDNA clone bp230018a10b10 3'	0.00	2.2	-3.0	-6.6	↑
188	gi_51809011	CO879087.1	---	Co879087 bovgen_07412 normal cattle brain cDNA clone rzpdp1056e1615q 5'	0.01	2.0	-3.3	-6.6	↑
189	gi_118150825	NM_001077856	LY6G6C	Lymphocyte antigen 6 complex, locus g6c	0.01	2.1	-3.2	-6.6	---
190	gi_51884088	AJ816612.1	---	Aj816612 kn206 bos sp. cDNA clone c0005209j9	0.01	2.1	-3.1	-6.6	↑
191	gi_51887654	AJ820178.1	---	Aj820178 kn206 bos sp. cDNA clone c0006017k17	0.00	3.2	-2.0	-6.5	---
192	gi_114052363	NM_001046345	IKBKE	Inhibitor of kappa light polypeptide gene enhancer in b-cells, kinase epsilon	0.01	2.1	-3.1	-6.5	---

193	gi_164518975	NM_001113301	SERF1B	Small edrk-rich factor 1b (centromeric) (serf1b)	0.00	2.5	-2.6	-6.5	---
194	gi_126722664	NM_001082452	PARP11	Poly (adp-ribose) polymerase family, member 11	0.00	2.5	-2.6	-6.4	↑
195	gi_119879516	XM_593520	ARHGAP31	Rho gtpase activating protein 31	0.00	2.3	-2.8	-6.4	---
196	gi_51883432	Aj815956		Aj815956 kn206 bos sp. cDNA clone c0005202f3	0.02	2.0	-3.2	-6.4	↑
197	gi_119927292	XM_001255388	SPRR4	Small proline-rich protein 4	0.00	3.0	-2.1	-6.4	---
198	gi_115496919	NM_001075675	FABP6	Fatty acid binding protein 6, ileal	0.00	2.5	-2.6	-6.4	---
199	gi_119893047	XM_613380	CD163	CD163 molecule	0.01	2.1	-3.0	-6.4	↑
200	gi_114053094	NM_001046256	MTMR9	Myotubularin related protein 9 (mtmr9)	0.00	2.4	-2.7	-6.3	↑
201	gi_119912528	XM_616376	ITGB3	Integrin, beta 3 (platelet glycoprotein iiia, antigen CD61)	0.00	2.6	-2.5	-6.3	↑
202	gi_119937182	XM_001255975	LOC789130	Similar to zinc finger protein 567 (LOC789130)	0.00	2.3	-2.7	-6.2	---
203	gi_51824234	Co893927	---	Co893927 bovgen_22252 normal cattle brain cDNA clone rzpdp1056j2443q 5'	0.00	2.4	-2.6	-6.2	↑
204	gi_51826163	Co895846	---	Co895846 bovgen_24171 normal cattle brain cDNA clone rzpdp1056n1538q 5'	0.00	2.5	-2.5	-6.2	↑
205	gi_119889555	XM_001250648	LOC782071	Similar to LFA-3 (LOC782071)	0.00	2.8	-2.2	-6.1	---
206	gi_119908832	XR_027675	LOC531974	Similar to mkiaa1151 protein (LOC531974)	0.01	2.2	-2.8	-6.1	---
207	gi_76659540	XM_864058	LOC613370	Similar to hmgb3 protein (LOC613370)	0.00	3.0	-2.0	-6.0	---
208	gi_115495920	NM_001075138	RTN4	Reticulon 4 (RTN4), transcript variant 1	0.00	3.0	-2.0	-6.0	↑
209	gi_119934667	XM_001256326	LOC789628	Hypothetical protein (LOC789628)	0.00	2.8	-2.1	-6.0	---
210	gi_119915594	XM_606763	LOC528343	Similar to olfactory receptor mor256-5 (LOC528343)	0.00	2.5	-2.4	-6.0	↑
211	gi_111087524	EE226389.1	---	Ee226389 lb0188.cr_p05 gc_bgc-18 cDNA clone image:8288503	0.01	2.0	-2.9	-6.0	---
212	gi_155722980	NM_001101042	SLC2A5	Solute carrier family 2 (facilitated glucose/fructose transporter), member 5	0.00	2.2	-2.7	-5.9	↑
213	gi_166159169	NM_001114080	---	Protocadherin gamma subfamily c, 3 (pcdhgc3), transcript variant 1	0.02	2.0	-2.9	-5.9	↑
214	gi_46418898	Cn439634	---	Cn439634 be04020a1c06 be04 normalized and subtracted bovine embryonic and extraembryonic tissue cDNA clone be04020a1c06 5'	0.00	2.4	-2.4	-5.8	---
215	gi_119901056	XM_610591	LOC532081	Hypothetical (LOC532081)	0.00	2.4	-2.4	-5.8	↑
216	gi_119915604	XM_589001	LOC511626	Similar to olfactory receptor, family 2, subfamily j, member 3	0.00	2.5	-2.3	-5.8	↑
217	gi_77735772	NM_001034409	EEPD1	Endonuclease/exonuclease/phosphatase family domain containing 1	0.00	2.3	-2.5	-5.8	---
218	gi_119924891	XM_001254602	LOC787107	Similar to steerin3 protein (LOC787107)	0.01	2.2	-2.6	-5.8	---
219*	gi_119915602	XM_001253092	Olfr129	Olfactory receptor 129	0.01	2.4	-2.4	-5.7	↑
220	gi_119895959	XM_613847	RGMB	Rgm domain family, member b	0.00	2.1	-2.7	-5.6	---
221	gi_119889872	XM_591383	GBP7	Guanylate binding protein 7	0.00	2.7	-2.1	-5.6	---
222	gi_119905278	XM_601498	CUBN	Cubilin (intrinsic factor-cobalamin receptor)	0.00	2.7	-2.0	-5.5	---
223	gi_51826533	Co896216	---	Co896216 bovgen_24541 normal cattle brain cDNA clone rzpdp1056c0748q 5'	0.00	2.7	-2.0	-5.5	---
224	gi_61946435	DN641034	---	Dn641034 umc-bend_0b02-031-a05 day 16 uterus from a non-pregnant animal bend cDNA 3'	0.01	2.1	-2.7	-5.5	---
225	gi_125991875	NM_001081602	STK38	Serine/threonine kinase 38	0.02	2.0	-2.7	-5.5	---
226	gi_119889385	XM_590074	RFX5	Regulatory factor x, 5 (influences hla class ii expression)	0.00	2.1	-2.5	-5.4	---
227*	gi_51811774		NAPEPLD	N-acyl phosphatidylethanolamine phospholipase d	0.02	2.0	-2.6	-5.3	↑
228	gi_119895611	XM_870459	LOC618132	Similar to protocadherin gamma a9 short form protein	0.01	2.3	-2.3	-5.3	↑
229	gi_119909826	XM_869529	LOC617296	Similar to plcg2 protein (LOC617296)	0.00	2.4	-2.2	-5.3	---
230	gi_51887569	Aj820093	---	Aj820093 kn206 bos sp. cDNA clone c0006017g15	0.00	2.4	-2.2	-5.3	---
231	gi_119879413	XM_001251003	LOC782355	Hypothetical protein (LOC782355)	0.01	2.3	-2.3	-5.3	---
232	gi_77736300	NM_001034678	HES1	Hairy and enhancer of split 1, (drosophila)	0.00	2.1	-2.5	-5.2	↑
233	gi_166157485	NM_001113762	ICAM5	Intercellular adhesion molecule 5, telencephalin	0.00	2.5	-2.1	-5.2	---
234	gi_119933354	XM_001256838	LOC790336	Hypothetical protein (LOC790336)	0.00	2.6	-2.0	-5.2	↑
235	gi_51886086	Aj818610	---	Aj818610 kn206 bos sp. cDNA clone c0006012n11	0.01	2.2	-2.4	-5.2	---
236	gi_119903011	XM_580522	RPS6KA5	Ribosomal protein s6 kinase, 90kda, polypeptide 5	0.01	2.0	-2.6	-5.2	---
237*	gi_119902242	XM_001253748	Olfr49	Olfactory receptor 49	0.02	2.1	-2.5	-5.2	---
238	gi_49354162	Aj669708	---	Aj669708 kn224 cDNA clone kn224-001_h03	0.01	2.2	-2.4	-5.1	---
239	gi_119910901	XM_870570	LOC618240	Hypothetical (LOC618240)	0.02	2.1	-2.4	-5.1	↑
240	gi_51887345	Aj819869	---	Aj819869 kn206 bos sp. cDNA clone c0006016l19	0.03	2.0	-2.5	-5.1	↑
241	gi_51881051	Aj813575	---	Aj813575 kn206 bos sp. cDNA clone c0005207e7	0.00	2.4	-2.1	-5.1	↑
242	gi_60443178	DN274568	---	Dn274568 1153592 marc 7bov cDNA 3'	0.00	2.5	-2.1	-5.1	---
243	gi_119934357	XM_001254441	LOC786885	Similar to glucose transporter 5 (LOC786885)	0.00	2.3	-2.2	-5.1	↑
244	gi_119934023	XM_001257056	LOC790637	Hypothetical protein (LOC790637)	0.00	2.3	-2.2	-5.1	---
245	gi_156121152	NM_001102254	NCOA7	Nuclear receptor coactivator 7	0.00	2.1	-2.4	-5.0	---
246	gi_157073983	NM_001103231	MEF2B	Myocyte enhancer factor 2b	0.01	2.0	-2.5	-5.0	---
247	gi_115497499	NM_001075894	CDKN2B	Cyclin-dependent kinase inhibitor 2b (p15, inhibits cdk4)	0.01	2.1	-2.3	-4.9	---
248	gi_119893623	XM_595689	LOC517517	Hypothetical protein (LOC517517)	0.01	2.3	-2.1	-4.7	---
249	gi_119902502	XM_601785	MYO1E	Myosin 1E	0.01	2.1	-2.2	-4.7	---
250	gi_119911605	XM_610844	NEK8	Nima (never in mitosis gene a)- related kinase 8	0.01	2.1	-2.1	-4.5	---
251	gi_119930554	XR_028682	LOC788758	Hypothetical protein (LOC788758)	0.02	2.1	-2.2	-4.5	---
252	gi_78369187	NM_001035478	SSBP2	Single-stranded dna binding protein 2	0.01	2.1	-2.2	-4.5	---
253	gi_119915568	XM_607721	LOC529277	Similar to homeostatic thymus hormone alpha (LOC529277)	0.03	2.1	-2.1	-4.4	↑
254	gi_51881606	Aj814130	---	Aj814130 kn206 bos sp. cDNA clone c0005198k15	0.02	2.0	-2.1	-4.2	↑

Asterisk (*) beside the serial no indicates duplicate probe present in the modulated dataset

2.1.3 Full list of genes in profile 3 (n = 55)

S.No	SEQ. ID	Acc. No. (RefSeq)	Putative Gene symbol	Gene Name	BL20 LPS Vs BL20 FDR (4h/or18)	BL20 LPS Vs BL20 Abs: FC (4h/or18)	TBL20 Vs BL20 Abs: FC	TBL20 Vs BL20 LPS Abs: FC (4h/or18)	BW720c Response
						↑↑	↑	↓	
1	gi_66792905	NM_001024557	OAS2	2'-5'-oligoadenylate synthetase 2, 69/71kda	0.00	125.9	3.9	-32.1	↑
2	gi_114051539	NM_001046590	CD83	CD83 molecule	0.00	57.1	2.1	-27.5	---
3	gi_114052748	NM_001046551	CXCL10	Chemokine (c-x-c motif) ligand 10	0.00	272.5	11.2	-24.3	↓
4	gi_119910571	XM_001256399	LOC789736	Hypothetical protein (LOC789736)	0.00	38.2	2.9	-13.3	↑
5	gi_29263643	Cb457261	---	Cb457261 714599 marc 6bov cDNA 5'	0.00	37.1	3.4	-11.1	↑
6	gi_119910676	XM_600955	RELB	V-rel reticuloendotheliosis viral oncogene homolog b	0.00	27.2	2.5	-10.7	---
7	gi_119910534	XM_001254854	LOC788393	Hypothetical protein (LOC788393)	0.00	36.9	3.7	-10.0	↑
8	gi_119901537	XM_584832	TNFAIP3	Tumor necrosis factor, alpha-induced protein 3	0.00	57.1	6.6	-8.6	---
9	gi_119889854	XM_001253071	TGFBR3	Transforming growth factor, beta receptor iii	0.00	37.0	4.5	-8.3	↑
10	gi_156523227	NM_001102558	CX3CR1	Chemokine (C-x3-C motif) receptor 1	0.00	48.5	5.9	-8.2	↑
11	gi_119893517	XM_001252348	LOC783896	Similar to TRAF-interacting protein with a forkhead-associated domain (LOC783896)	0.00	31.9	4.1	-7.8	---
12	gi_119910569	XM_001256395	LOC789731	Hypothetical protein (LOC789731)	0.00	29.1	3.9	-7.4	↑

13	gi_125991933	NM_001081621	TIFA	Traf-interacting protein with forkhead-associated domain	0.00	34.8	5.0	-7.0	---
14	gi_31343037	NM_174014	CD69	CD69 molecule	0.00	37.7	5.7	-6.6	↓
15	gi_119905687	XM_585095	ZBP1	Similar to putative tumor stroma and activated macrophage protein dlm-1 (LOC508333)	0.00	46.3	7.4	-6.3	↑
16	gi_119896106	XM_580928	DDX58	Dead (asp-glu-ala-asp) box polypeptide 58	0.00	13.9	2.2	-6.2	---
17	gi_62988293	NM_001017940	USP18	Ubiquitin specific peptidase 18 (usp18)	0.00	21.5	3.7	-5.7	---
18	gi_51887332	Aj819856	---	Aj819856 kn206 bos sp. cDNA clone c0006016l04	0.00	13.9	2.5	-5.7	---
19	gi_82991961	DV934772	---	Dv934772 lb0308.cr_e16 gc_bgc-30 cDNA clone image:8135034 5'	0.00	39.3	7.1	-5.5	---
20	gi_115496813	NM_001075310	BCL2L11	BCL2-like 11 (apoptosis facilitator) (BCL2L11)	0.00	14.7	2.8	-5.2	↓
21	gi_31343249	NM_173924	IL7	Interleukin 7	0.00	10.3	2.1	-5.0	↓
22	gi_27805954	NM_174366	ISG15	ISG15 ubiquitin-like modifier	0.00	120.9	25.8	-4.7	---
23*	gi_71067099	NM_001029846	OAS1	2',5'-oligoadenylate synthetase 1, 40/46kda	0.00	13.1	2.9	-4.5	↑
24*	gi_94967003	NM_001040606	OAS1	2',5'-oligoadenylate synthetase 1, 40/46kda	0.00	34.5	8.1	-4.3	↑
25	gi_62751388	NM_001015545	LGP2	Rna helicase LGP2	0.00	20.0	4.8	-4.2	↑
26	gi_156120848	NM_001102101	NFKB2	Nuclear factor of kappa light polypeptide gene enhancer in b-cells 2 (p49/p100)	0.00	28.3	7.1	-4.0	---
27	gi_115494987	NM_001075771	PARM1	Prostate androgen-regulated mucin-like protein 1	0.00	8.5	2.3	-3.7	---
28	gi_119894560	XM_584000	BST2	Bone marrow stromal cell antigen 2	0.00	17.6	4.8	-3.7	---
29	gi_119917771	XM_583612	LOC507061	Similar to dual specificity phosphatase 5 (LOC507061)	0.00	11.9	3.3	-3.6	---
30	gi_158341671	NM_001109981	ITGA6	Integrin, alpha 6	0.00	43.2	11.9	-3.6	---
31	gi_41386700	NM_174726	NFKBIZ	Nuclear factor of kappa light polypeptide gene enhancer in b-cells inhibitor, zeta	0.00	14.3	4.0	-3.6	---
32	gi_119913076	XM_587229	PLK2	Polo-like kinase 2	0.00	7.4	2.2	-3.4	---
33	gi_118150773	NM_001077827	JUN	Jun proto-oncogene	0.00	7.0	2.2	-3.1	---
34*	gi_31342215	NM_174364	INPP1	Inositol polyphosphate-1-phosphatase	0.00	6.0	2.0	-3.0	---
35	gi_119923683	XR_027350	LOC781857	Similar to interferon-induced protein 44 (antigen p44) (non-a non-b hepatitis-associated microtubular aggregates protein)	0.00	9.0	3.1	-2.8	↑
36	gi_119908035	XM_589248	LOC511831	Similar to renin (LOC511831)	0.00	9.4	3.3	-2.8	↑
37	gi_51814407	Co884407	---	Co884407 bovgen_12732 normal cattle brain cDNA clone rzpdp1056m1612q 5'	0.00	26.0	9.2	-2.8	↑
38	gi_78365288	NM_001035465	IRF5	Interferon regulatory factor 5	0.00	5.9	2.1	-2.8	↑
39	gi_119901919	XM_593090	SMAD3	Smad family member 3	0.00	10.7	4.0	-2.7	---
40	gi_157074115	NM_001103300	MAFF	V-maf musculoaponeurotic fibrosarcoma oncogene homolog f (avian)	0.00	6.7	2.6	-2.6	↓
41	gi_119879663	XR_027887	LOC525407	Hypothetical loc525407 (LOC525407)	0.00	10.9	4.3	-2.6	↑
42	gi_31343213	NM_173941	MX2	Myxovirus (influenza virus) resistance 2 (mouse)	0.00	100.5	39.9	-2.5	↑
43	gi_119925448	XM_001251333	MYO10	Myosin x	0.00	5.4	2.2	-2.4	---
44	gi_119889992	XM_872122	IFI44	Interferon-induced protein 44	0.00	7.4	3.1	-2.4	↑
45*	gi_118601803	NM_001079603	CBLN3	Cerebellin 3 precursor	0.00	9.3	3.9	-2.4	↑
46	gi_51826112	Co895796	---	Co895796 bovgen_24121 normal cattle brain cDNA clone rzpdp1056b1744q 5'	0.00	15.3	6.6	-2.3	↑
47	gi_119927124	XM_001252928	LOC784693	Similar to dipeptidyl peptidase iv (LOC784693)	0.00	5.1	2.3	-2.2	---
48	gi_147902261	NM_001098095	EXT1	Exostosin 1	0.00	4.5	2.1	-2.2	---
49	gi_119922761	XM_001252258	LOC783754	Similar to mkiaa1108 protein (LOC783754)	0.00	4.4	2.0	-2.2	---
50*	gi_62988287	NM_001017937	BAIAP2	Bai1-associated protein 2	0.00	16.4	7.6	-2.2	---
51	gi_51821917	Co891619	---	Co891619 bovgen_19944 normal cattle brain cDNA clone rzpdp1056b0838q 5'	0.00	4.3	2.0	-2.1	---
52	gi_58764282	Cx950755	---	Cx950755 umc-bcl_0b02-030-d06 day 14 cl from a pregnant animal bcl cDNA 3'	0.00	5.1	2.4	-2.1	---
53	gi_112219499	EE358869	---	Ee358869 lb02964.cr_k02 gc_bgc-29 cDNA clone image:8476732	0.00	4.7	2.2	-2.1	---
54	gi_78045237	NM_001034502	ACTA2	Actin, alpha 2, smooth muscle, aorta	0.00	11.8	5.7	-2.1	---
55	gi_51818119	Co887834	---	Co887834 bovgen_16159 normal cattle brain cDNA clone rzpdp1056p0114q 5'	0.00	4.9	2.4	-2.0	---

Asterisk (*) beside the serial no indicates duplicate probe present in the modulated dataset

2.1.4 Full list of genes in profile 4 (n = 1093)

S.No	SEQ. ID	Acc. No. (RefSeq)	Putative Gene symbol	Gene Name	BL20 LPS Vs BL20 FDR (4h/or18)	BL20 LPS Vs BL20 Abs: FC (4h/or18)	TBL20 Vs BL20 Abs: FC	TBL20 Vs BL20 LPS Abs: FC (4h/or18)	BW720c Response
						↑	No Change	↑	
1*	gi_41386706	NM_174484	VCAM1	Vascular cell adhesion molecule 1 (VCAM1)	0.00	183.1	1.0	-184.6	---
2	gi_139947562	NM_001083739	TFEC	Transcription factor ec	0.00	34.2	-1.4	-47.1	---
3	gi_119913384	XM_596594	ANKRD33B	Ankyrin repeat domain 33b	0.00	30.5	-1.5	-45.1	---
4*	gi_119908118	XM_001252844	RGS18	Regulator of g-protein signaling 18	0.00	27.5	-1.5	-42.3	---
5	gi_119924697	XM_589150	LOC511753	Similar to seven transmembrane helix receptor (LOC511753)	0.00	35.2	-1.1	-39.7	---
6	gi_119906810	XM_001254274	OSGIN2	Oxidative stress induced growth inhibitor family member 2	0.00	26.9	-1.2	-33.5	---
7	gi_119922152	XM_001252866	LOC784595	Similar to olfactory receptor olfr1174 (LOC784595)	0.00	16.1	-1.7	-26.8	---
8	gi_119930245	XM_868109	ADAMTSL5	Adamts-like 5	0.00	15.6	-1.7	-26.6	---
9	gi_119902166	XM_001251339	LOC783981	Similar to ribonuclease 12 (LOC783981)	0.00	14.4	-1.8	-26.5	---
10	gi_119911031	XM_581045	AU018091	Expressed sequence AU018091	0.00	13.5	-1.8	-24.2	---
11	gi_157427901	NM_001105388	ITK	Il2-inducible t-cell kinase	0.00	16.2	-1.4	-22.6	---
12	gi_119925538	XM_586833	LOC509794	Similar to tesc protein, transcript variant 1 (LOC509794)	0.00	16.5	-1.4	-22.5	---
13	gi_119892989	XM_591681	STYK1	Serine/threonine/tyrosine kinase 1	0.00	23.1	1.1	-21.4	---
14*	gi_155372040	NM_001101158	VCAM1	Vascular cell adhesion molecule 1	0.00	14.4	-1.5	-20.9	---
15	gi_119892383	XM_587244	SRGAP1	Slit-robo rho gtpase activating protein 1	0.00	27.7	1.3	-20.9	---
16	gi_51882056	Aj814580	---	Aj814580 kn206 bos sp. CDNA clone c0005204g20	0.00	10.4	-2.0	-20.6	↑
17	gi_119879695	XM_867115	TP63	Tumor protein p63	0.00	36.2	1.9	-19.1	---
18	gi_115496711	NM_001075696	IRAK2	Interleukin-1 receptor-associated kinase 2	0.00	9.4	-2.0	-18.5	---
19	gi_84579864	NM_001038682	AICDA	Activation-induced cytidine deaminase	0.00	16.0	-1.1	-18.3	---
20	gi_119914336	XM_871109	CCR8	Chemokine (c-c motif) receptor 8	0.00	18.2	1.0	-17.7	---
21	gi_119934789	XM_001256599	LOC790001	Similar to transmembrane protein 17 (LOC790001)	0.00	11.0	-1.6	-17.3	---
22	gi_115496259	NM_001075147	CCL4	Chemokine (c-c motif) ligand 4	0.00	13.4	-1.3	-17.3	---
23	gi_119901659	XM_001253771	LOC785913	Hypothetical protein (LOC785913)	0.00	10.8	-1.6	-16.9	---
24	gi_114052247	NM_001045923	PLS3	Plastin 3	0.00	23.5	1.4	-16.5	---
25	gi_84000076	NM_001038050	IFI27	Interferon, alpha-inducible protein 27	0.00	14.2	-1.2	-16.5	---
26	gi_51808298	---	---	Co878378 bovgen_06703 normal cattle brain cDNA clone rzpdp1056o0112q 5'	0.00	12.3	-1.3	-16.1	---
27	gi_119927221	XM_586292	FAM111B	Family with sequence similarity 111, member b	0.00	9.8	-1.6	-15.4	---
28	gi_119906812	XM_001254290	LOC786676	Hypothetical protein (LOC786676)	0.00	13.2	-1.2	-15.2	---

29	gi_115495364	NM_001075414	IFIT3	Interferon-induced protein with tetratricopeptide repeats 3	0.00	10.4	-1.4	-14.7	---
30	gi_149944702	NM_001099086	BLOC1S3	Biogenesis of lysosomal organelles complex-1, subunit 3	0.00	8.2	-1.7	-14.3	---
31	gi_149642684	NM_001098935	OSTN	Osteocrin	0.00	10.5	-1.4	-14.2	---
32	gi_51802498	---	---	Co872658 bovgen_00983 normal cattle brain cDNA clone rzpdp1056g1055q 3'	0.00	10.5	-1.3	-14.1	↑
33	gi_119906018	XM_581509	CD40	CD40 molecule, tnf receptor superfamily member 5	0.00	10.7	-1.3	-13.8	---
34	gi_115497163	NM_001075120	LPL	Lipoprotein lipase	0.00	7.2	-1.9	-13.8	---
35	gi_31343065	NM_174002	CASR	Calcium-sensing receptor	0.00	7.8	-1.7	-13.2	---
36	gi_114052816	NM_001045868	NFKBIA	Nuclear factor of kappa light polypeptide gene enhancer in b-cells inhibitor, alpha	0.00	6.6	-2.0	-13.0	---
37	gi_119927839	XM_001250816	LOC785902	Hypothetical protein (LOC785902)	0.00	8.8	-1.4	-12.7	↑
38*	gi_118150869	NM_001077879	MOBP	Myelin-associated oligodendrocyte basic protein	0.00	8.4	-1.5	-12.5	---
39	gi_119908270	XR_027843	LOC515996	Similar to kynurenine 3-monooxygenase (LOC515996)	0.00	9.8	-1.3	-12.3	---
40	gi_119921259	XR_027535	LOC781932	Similar to seven transmembrane helix receptor (LOC781932)	0.00	7.9	-1.5	-12.2	---
41	gi_119918849	XM_586751	ODZ4	Odz, odd oz/ten-m homolog 4 (drosophila)	0.00	6.9	-1.8	-12.1	---
42	gi_116004430	NM_001077106	MGC140080	Hypothetical protein mgc140080 (MGC140080)	0.00	8.0	-1.5	-12.0	---
43*	gi_28151981	---	CDK5R1	Cyclin-dependent kinase 5, regulatory subunit 1 (p35)	0.00	6.4	-1.8	-11.6	---
44	gi_68317327	---	---	Am016135 kn-252-liver, cDNA clone c0007420b02 5'	0.00	8.1	-1.4	-11.4	---
45	gi_119939076	XM_001257154	LOC790762	Similar to trace amine associated receptor 7a (LOC790762)	0.00	7.8	-1.5	-11.4	---
46	gi_119890779	XM_864659	AGMO	Alkylglycerol monooxygenase	0.00	5.9	-1.9	-11.2	---
47	gi_119907990	XM_606934	LOC528508	Similar to DTX4 protein (LOC528508)	0.00	9.2	-1.2	-11.0	---
48	gi_119927812	XM_001255631	LOC788631	Similar to t-cell receptor delta chain trdv2-2 (LOC788631)	0.00	6.2	-1.7	-10.9	---
49	gi_78045490	NM_001035045	FSCN1	Fascin homolog 1, actin-bundling protein (strongylocentrotus purpuratus)	0.00	5.5	-2.0	-10.9	---
50	gi_84000092	NM_001038063	TMCC3	Transmembrane and coiled-coil domain family 3	0.00	16.0	1.5	-10.8	---
51	gi_119895319	XM_001254960	LOC787618	Similar to olfactory receptor mor104-2 (LOC787618)	0.00	8.0	-1.4	-10.8	---
52	gi_119921165	XM_001254986	LOC787665	Similar to cfolf4 (LOC787665)	0.00	5.6	-1.9	-10.7	---
53	gi_119932608	XM_001252260	LOC783756	Similar to olfactory receptor olr1533 (LOC783756)	0.00	8.8	-1.2	-10.6	---
54	gi_119926791	XM_001250097	LOC781642	Similar to olfactory receptor mor8-2 (LOC781642)	0.00	8.7	-1.2	-10.6	---
55	gi_156120634	NM_001101994	SLC6A12	Solute carrier family 6 (neurotransmitter transporter, betaine/gaba), member 12 (SLC6A12)	0.00	9.2	-1.1	-10.4	---
56	gi_119648604	---	---	Eh177212 lb01742.cr_c23 gc_bgc-17 cDNA clone image:8565649 5'	0.00	5.2	-2.0	-10.4	---
57	gi_51813662	---	---	Co883718 bovgen_12043 normal cattle brain cDNA clone rzpdp1056f2013q 5'	0.00	6.6	-1.6	-10.3	---
58	gi_119935010	XM_001256813	LOC790300	Similar to deltex1 (LOC790300)	0.00	9.8	-1.0	-10.2	---
59*	gi_119924440	XM_868840	TAAR6	Trace amine associated receptor 6	0.00	7.3	-1.4	-10.1	---
60*	gi_119922656	XM_001256081	OR5W2	Olfactory receptor, family 5, subfamily w, member 2	0.00	7.4	-1.4	-10.1	---
61	gi_119910036	XR_027515	LOC539231	Hypothetical loc539231 (LOC539231)	0.00	11.1	1.1	-9.9	---
62	gi_119903170	XM_864858	TBC1D8	Tbc1 domain family, member 8 (with gram domain)	0.00	6.2	-1.6	-9.9	---
63	gi_31340697	NM_178572	CA2	Carbonic anhydrase ii	0.00	6.6	-1.5	-9.8	---
64*	gi_31342632	NM_174187	SPP1	Secreted phosphoprotein 1	0.00	12.0	1.2	-9.7	---
65	gi_139948963	NM_001083752	C3AR1	Complement component 3a receptor 1	0.00	19.4	2.0	-9.7	---
66	gi_119311853	---	---	Ee975255 q56911a fnm cDNA clone q5691 3'	0.00	14.2	1.5	-9.7	---
67*	gi_156120912	NM_001102133	FRMD6	Ferm domain containing 6	0.00	5.3	-1.8	-9.6	---
68	gi_119939697	XM_582730	LOC506303	Similar to h factor 1 (complement) (loc506303)	0.00	9.0	-1.1	-9.5	---
69	gi_59676571	NM_001012284	UBA7	Ubiquitin-like modifier activating enzyme 7	0.00	6.3	-1.5	-9.4	---
70	gi_29258721	---	---	Cb452339 707195 marc 6bov cDNA 3'	0.00	12.3	1.3	-9.2	---
71	gi_119933162	XM_001256684	LOC790127	Similar to killer cell immunoglobulin-like receptor kir3dl1	0.00	4.9	-1.8	-9.0	↑
72	gi_119926098	XM_001254787	LOC787369	Similar to olfactory receptor Olfr1174 (LOC787369)	0.00	7.4	-1.2	-8.9	---
73	gi_119902553	XR_027333	LOC781271	Similar to gag-pro-pol-env protein (LOC781271)	0.00	5.5	-1.6	-8.7	---
74	gi_115496899	NM_001075588	IFI6	Interferon, alpha-inducible protein 6	0.00	10.5	1.2	-8.7	---
75	gi_119928263	XM_001250225	LOC783841	Hypothetical protein loc783841 (LOC783841)	0.00	8.1	-1.1	-8.7	---
76	gi_61827360	XM_586955	OR5M9	Olfactory receptor, family 5, subfamily m, member 9	0.00	8.1	-1.1	-8.7	---
77	gi_61826046	XM_610803	Olfr1390	Olfactory receptor 1390	0.00	6.4	-1.4	-8.6	---
78	gi_76686226	XM_866296	LOC614709	Similar to protein alo17 (alk lymphoma oligomerization partner on chromosome 17)	0.00	7.0	-1.2	-8.6	---
79	gi_30794323	NM_181017	TAC3	Tachykinin 3	0.00	4.8	-1.8	-8.6	---
80	gi_59676558	NM_001012281	CFLAR	Casp8 and fadd-like apoptosis regulator	0.00	5.5	-1.6	-8.6	---
81	gi_119902180	XM_001252672	LOC784332	Similar to olfactory receptor, family 11, subfamily h, member 1	0.00	7.2	-1.2	-8.5	---
82	gi_119922313	XM_601384	Olr53	Olfactory receptor 53	0.00	7.2	-1.2	-8.5	---
83	gi_76681522	XM_593553	OR5D18	Olfactory receptor, family 5, subfamily d, member 18	0.00	6.3	-1.4	-8.5	---
84	gi_119903950	XM_866254	Adam1a	A disintegrin and metallopeptidase domain 1a	0.00	5.5	-1.5	-8.4	---
85*	gi_119892557	XM_001255374	Olr1012	Olfactory receptor 1012	0.00	8.5	1.0	-8.3	---
86	gi_157427871	NM_001105373	TMEM140	Transmembrane protein 140	0.00	5.3	-1.6	-8.3	---
87	gi_10029506			Be668915 159342 marc 4bov cDNA 5'	0.00	5.1	-1.6	-8.3	---
88	gi_119895328	XM_001255032	LOC787758	Similar to olfactory receptor mor277-1 (LOC787758)	0.00	7.8	-1.0	-8.2	---
89	gi_119920466	XM_001249777	LOC781369	Hypothetical protein (LOC781369)	0.00	5.3	-1.6	-8.2	---
90	gi_51882465			Aj814989 kn206 bos sp. CDNA clone c0005203m2	0.00	4.4	-1.9	-8.1	---
91	gi_119927666	XM_587987	LOC510786	Similar to olfactory receptor olfr1034 (LOC510786)	0.00	6.9	-1.2	-8.1	---
92	gi_155372274	NM_001101280	TRAF4	TNF receptor-associated factor 4	0.00	4.3	-1.9	-8.1	---
93	gi_47950914	---	---	Cn822845 oa_splbn_02g02_m13reverse sheep spleen\brain psport1 library ovis aries cDNA clone oa_splbn_02g02 5'	0.00	4.1	-1.9	-8.0	---
94	gi_119914298	XR_028825	LOC509859	Similar to kiaa0342 protein (LOC509859)	0.00	4.8	-1.7	-8.0	---
95	gi_76718610	XM_871454	LOC619135	Hypothetical (LOC619135)	0.00	6.8	-1.2	-8.0	---
96	gi_76686224	XM_608422	LOC529960	Similar to KIAA1618 protein (LOC529960)	0.00	6.6	-1.2	-7.9	---
97	gi_31341586	NM_174593	RASSF2	Ras association (ralgds/af-6) domain family member 2	0.00	4.7	-1.7	-7.9	---
98	gi_119892545	XM_001255291	OR6C3	Olfactory receptor, family 6, subfamily c, member 3	0.00	6.3	-1.2	-7.8	---
99	gi_119921041	XM_001252382	LOC783934	Similar to olfactory receptor mor17-2 (LOC783934)	0.00	6.3	-1.2	-7.8	---
100	gi_119931104	XM_001256850	LOC790355	Similar to olfactory receptor mor17-2 (LOC790355)	0.00	6.8	-1.1	-7.6	---
101	gi_119901479	XM_001250862	LOC783380	Similar to trace amine receptor 8 (LOC783380)	0.00	6.9	-1.1	-7.5	---
102	gi_119927907	XM_001256066	LOC789270	Similar to t-cell receptor delta chain trdv2-2 (LOC789270)	0.00	5.6	-1.3	-7.5	---
103	gi_119924695	XM_605606	Olfr827	Olfactory receptor 827	0.00	5.7	-1.3	-7.5	---
104	gi_119921949	XM_001252233	LOC783706	Similar to t-cell receptor delta chain trdv2 (LOC783706)	0.00	5.6	-1.3	-7.5	---
105	gi_119879545	XM_592997	DTX3L	Deltex 3-like (drosophila)	0.00	4.4	-1.7	-7.5	---
106	gi_119923001	XM_001252136	LOC783560	Similar to estrogen receptor-beta (LOC783560)	0.00	3.7	-2.0	-7.4	---
107	gi_56136763	---	---	Cv976042 umc-bcl_0b01-015-f02 day 14 cl +8h prostaglandin f2-alpha bcl cDNA 3'	0.00	8.3	1.1	-7.4	---
108	gi_76688849	XM_589845	LOC512340	Similar to olfactory receptor mor210-5 (LOC512340)	0.00	4.7	-1.5	-7.3	---
109	gi_166157489	NM_001113764	TYK2	Tyrosine kinase 2	0.00	3.8	-1.9	-7.3	---
110*	gi_119921250	XM_587900	OR4A47	Olfactory receptor, family 4, subfamily a, member 47	0.00	7.3	1.0	-7.3	---
111	gi_119921722	XM_001255525	LOC788476	Similar to olfactory receptor olfr1174 (LOC788476)	0.00	6.4	-1.1	-7.3	---
112	gi_162951886	NM_001112708	SNAI1	Snail homolog 1 (drosophila)	0.00	3.8	-1.9	-7.3	---
113	gi_114051256	NM_001046193	ATF3	Activating transcription factor 3	0.00	3.7	-2.0	-7.3	---
114	gi_119887633	XM_615590	IFIH1	Interferon induced with helicase c domain 1	0.00	11.4	1.6	-7.3	---
115	gi_119910857	XM_587935	PLEKHA4	Pleckstrin homology domain containing, family a (phosphoinositide binding specific) member 4	0.00	7.4	1.0	-7.3	---
116	gi_31341381	NM_176668	AOX1	Aldehyde oxidase 1	0.00	4.1	-1.7	-7.2	---
117	gi_119901000	XM_613776	TRAF1	Tnf receptor-associated factor 1	0.00	3.9	-1.8	-7.2	---
118	gi_119918771	XM_001254971	LOC787636	Hypothetical protein (LOC787636)	0.00	6.6	-1.1	-7.2	---
119	gi_119914622	XM_876930	CACNA1D	Calcium channel, voltage-dependent, l type, alpha 1d subunit	0.00	5.0	-1.5	-7.2	---

120	gi_114051859	NM_001045963	Chn2	Chimerin (chimaerin) 2	0.00	5.3	-1.4	-7.2	---
121	gi_119928126	XM_001249637	LOC782278	Hypothetical protein loc782278 (LOC782278)	0.00	6.3	-1.1	-7.1	---
122	gi_78369427	NM_001035317	MVP	Major vault protein	0.00	3.6	-2.0	-7.1	---
123	gi_76633796	XM_585978	C20orf123	Chromosome 20 open reading frame 123	0.00	3.8	-1.9	-7.1	---
124*	gi_119910956	XM_001254693	Vmn1r233	Similar to pheromone receptor (LOC787233)	0.00	5.3	-1.3	-7.0	---
125*	gi_119895348	XM_001255168	OR2L3	Olfactory receptor, family 2, subfamily l, member 3	0.00	6.6	-1.1	-7.0	---
126	gi_119930502	XM_001255446	LOC788363	Hypothetical protein (LOC788363)	0.00	5.8	-1.2	-7.0	---
127*	gi_76670425	XM_588413	TAAR6	Trace amine associated receptor 6	0.00	6.0	-1.2	-7.0	---
128*	gi_31342492	NM_178108	OAS1	2',5'-oligoadenylate synthetase 1, 40/46kda	0.00	11.2	1.6	-6.9	---
129*	gi_119922211	XM_611011	Olfr1199	Olfactory receptor 1199	0.00	5.2	-1.3	-6.9	---
130	gi_119891154	XM_863839	ZMIZ2	Similar to zmiz2 protein, transcript variant 2 (LOC537266)	0.00	5.2	-1.3	-6.8	---
131	gi_119905685	XM_001252041	LOC783430	Hypothetical protein loc783430 (LOC783430)	0.00	10.3	1.5	-6.8	---
132	gi_76619274	XM_597187	OVCH1	Ovochymase 1	0.00	5.2	-1.3	-6.8	---
133	gi_76670295	XM_865067	RNF213	Ring finger protein 213	0.00	6.8	1.0	-6.8	---
134	gi_29257333	CB450951	---	Cb450951 705652 marc 6bov cDNA 5'	0.00	7.2	1.1	-6.7	---
135	gi_51884136	Aj816660	---	Aj816660 kn206 bos sp. CDNA clone c0005209h3	0.00	10.3	1.5	-6.7	---
136	gi_119926169	XM_001255294	LOC788146	Similar to olfactory receptor olfr723 (LOC788146)	0.00	6.2	-1.1	-6.7	---
137	gi_119904826	XM_001249505	SLITRK6	Slit and ntrk-like family, member 6	0.00	6.1	-1.1	-6.6	---
138	gi_119879459	XM_865244	C3orf52	Chromosome 3 open reading frame 52	0.00	6.6	1.0	-6.6	---
139	gi_118150959	NM_001077930	ERRFI1	Erbb receptor feedback inhibitor 1	0.00	6.3	1.0	-6.6	---
140	gi_119906065	XM_589621	ZNFX1	Similar to kiaa1404 protein (LOC539807)	0.00	5.0	-1.3	-6.5	---
141	gi_114051699	NM_001046522	TMEM100	Transmembrane protein 100	0.00	7.5	1.1	-6.5	---
142	gi_87196509	NM_001010995	TPM2	Tropomyosin 2 (Beta)	0.00	4.1	-1.6	-6.5	---
143	gi_115497773	NM_001075226	RILPL1	Rab interacting lysosomal protein-like 1	0.00	4.1	-1.6	-6.4	---
144	gi_68321769	---	---	Am020577 kn-252-liver, cDNA clone c0007416o07 5'	0.00	4.5	-1.4	-6.4	---
145	gi_119894058	XM_605463	ENAM	Enamelin	0.00	4.5	-1.4	-6.4	---
146	gi_119894556	XM_593682	LOC515629	Similar to b-cell novel protein isoform 1; bcnp1 (LOC515629)	0.00	3.9	-1.7	-6.4	---
147	gi_119921254	XM_609448	OR9G1	Olfactory receptor, family 9, subfamily g, member 1	0.00	5.4	-1.2	-6.4	---
148	gi_119925075	XM_001249670	LOC781503	Similar to trace amine receptor 8 (LOC781503)	0.00	5.5	-1.2	-6.4	---
149	gi_119908943	XM_001255263	LOC788108	Similar to interspersed repeat antigen, putative (LOC788108)	0.00	5.2	-1.2	-6.3	---
150*	gi_119902162	XM_001252369	OR11G2	Olfactory receptor, family 11, subfamily g, member 2	0.00	5.2	-1.2	-6.3	---
151	gi_118151335	NM_001078135	LOC768323	Hypothetical protein (LOC768323)	0.00	6.7	1.1	-6.2	---
152*	gi_119930898	XM_001256701	OR4A47	Olfactory receptor, family 4, subfamily a, member 47	0.00	6.2	1.0	-6.2	---
153*	gi_119889733	XM_001253222	COL11A1	Collagen, type xi, alpha 1	0.00	5.2	-1.2	-6.2	---
154*	gi_119924512	XM_001253583	Olfr1303	Olfactory receptor 1303	0.00	4.5	-1.4	-6.1	↑
155	gi_51886798	AJ819322	---	Aj819322 kn206 bos sp. CDNA clone c0006015a02	0.00	4.8	-1.3	-6.1	---
156	gi_31342122	NM_174395	MYO1A	Myosin 1A	0.00	3.5	-1.8	-6.1	---
157	gi_119925028	XM_001251240	LOC786308	Hypothetical protein (LOC786308)	0.00	5.5	-1.1	-6.1	---
158	gi_76683585	XM_592773	Olr1159	Olfactory receptor 1159	0.00	4.2	-1.4	-6.0	---
159	gi_164451473	NM_001024530	SIDT2	Sid1 transmembrane family, member 2	0.00	5.6	-1.1	-6.0	---
160	gi_119924832	XM_001253774	LOC785917	Similar to olfactory receptor olr87 (LOC785917)	0.00	4.9	-1.2	-6.0	---
161	gi_119923684	XR_027801	LOC782879	Similar to interferon-induced protein 44-like (LOC782879)	0.00	6.0	1.0	-6.0	---
162	gi_119875306	XM_877339	LOC614436	Hypothetical (LOC614436)	0.00	4.6	-1.3	-6.0	---
163	gi_51803217	---	---	Co873377 bovgen_01702 normal cattle brain cDNA clone rzpdp1056j1858q 3'	0.00	6.3	1.0	-6.0	---
164	gi_119889924	XM_001252509	LOC785006	Similar to spi-c transcription factor (spi-1/pu.1 related)	0.00	5.9	1.0	-6.0	---
165	gi_70778941	NM_001025332	FABP2	Fatty acid binding protein 2, intestinal	0.00	3.2	-1.9	-5.9	↑
166	gi_119932901	XM_001255986	LOC789146	Hypothetical protein (LOC789146)	0.00	3.8	-1.6	-5.9	---
167	gi_119915708	XM_870237	LOC617905	Similar to histone h4 (LOC617905)	0.00	4.0	-1.5	-5.9	---
168*	gi_119922797	XM_001253297	Olfr591	Olfactory receptor 591	0.00	5.2	-1.1	-5.9	---
169	gi_119915700	XM_592049	OR2M2	Olfactory receptor, family 2, subfamily m, member 2	0.00	4.6	-1.3	-5.9	---
170*	gi_119923762	XM_001253761	OR5AN1	Olfactory receptor, family 5, subfamily an, member 1	0.00	3.7	-1.6	-5.9	---
171	gi_119917459	XM_580537	SLC16A12	Solute carrier family 16, member 12 (monocarboxylic acid transporter 12)	0.00	4.3	-1.4	-5.8	---
172	gi_119921747	XM_001255714	LOC788750	Similar to olfr586 protein (LOC788750)	0.00	5.7	1.0	-5.8	---
173*	gi_119923766	XM_580276	OR5AN1	Olfactory receptor, family 5, subfamily an, member 1	0.00	3.9	-1.5	-5.8	---
174	gi_51823012	---	---	Co892712 bovgen_21037 normal cattle brain cDNA clone rzpdp1056a2248q 5'	0.00	3.8	-1.5	-5.7	---
175	gi_119887639	XM_587821	TANK	Traf family member-associated nfkb activator	0.00	4.5	-1.3	-5.7	---
176	gi_76688756	XM_587788	LOC510625	Similar to olf4 (LOC510625)	0.00	4.9	-1.2	-5.7	---
177	gi_115497925	NM_001076102	EPS8	Epidermal growth factor receptor pathway substrate 8	0.00	6.0	1.1	-5.7	---
178	gi_119910567	XM_001256373	LOC789703	Hypothetical protein (LOC789703)	0.00	6.0	1.1	-5.7	---
179*	gi_119907935	XM_001253806	OR4A47	Olfactory receptor, family 4, subfamily a, member 47	0.00	4.8	-1.2	-5.7	---
180	gi_119914992	XM_583261	TXNRD3	Thioredoxin reductase 3	0.00	3.0	-1.9	-5.7	---
181	gi_119924693	XM_001255886	LOC788998	Similar to olfactory receptor mor210-5 (LOC788998)	0.00	4.8	-1.2	-5.7	---
182*	gi_119892513	XM_001254983	Olfr802	Olfactory receptor 802	0.00	4.3	-1.3	-5.7	---
183	gi_10026167	---	---	Be665576 154662 marc 4bov cDNA 5'	0.00	3.1	-1.8	-5.7	---
184	gi_119903539	XM_607432	LOC528994	Hypothetical loc528994 (LOC528994)	0.00	4.8	-1.2	-5.7	---
185	gi_119889996	XR_028184	LOC508347	Similar to interferon-induced protein 44-like (LOC508347)	0.00	5.5	1.0	-5.6	---
186	gi_119921019	XM_001251884	LOC783244	Similar to olfactory receptor mor17-2 (LOC783244)	0.00	4.7	-1.2	-5.6	---
187	gi_119901657	XM_595033	IPCEF1	Interaction protein for cytohesin exchange factors 1	0.00	5.0	-1.1	-5.6	---
188	gi_82617557	NM_205774	LOC404073	Riken cDNA 1700024p04 gene	0.00	5.0	-1.1	-5.6	---
189*	gi_119892567	XM_001255454	OR6C74	Olfactory receptor, family 6, subfamily c, member 74	0.00	5.2	-1.1	-5.6	---
190	gi_31442874	NM_174655	SLC24A1	Solute carrier family 24 (Na/K/Ca exchanger), member 1	0.00	3.6	-1.5	-5.6	---
191	gi_119922456	XM_868862	OR8G1	Olfactory receptor, family 8, subfamily g, member 1	0.00	4.0	-1.4	-5.5	---
192	gi_28311321	---	---	Bp109033 orcs bovine utero-placenta cDNA cDNA clone orcs12720 3'	0.00	3.5	-1.6	-5.5	---
193	gi_51881771	---	---	Aj814295 kn206 bos sp. CDNA clone c0005204n18	0.00	2.9	-1.9	-5.5	---
194	gi_119922789	XM_001253117	LOC784956	Hypothetical protein (LOC784956)	0.00	5.3	1.0	-5.5	---
195	gi_119938335	XM_001257058	LOC790639	Similar to pol; truncated polymerase (LOC790639)	0.00	4.3	-1.3	-5.5	---
196	gi_119644144	---	---	Eh173005 lb01647.cr_h07 gc_bgc-16 cDNA clone image:8383353 5'	0.00	7.7	1.4	-5.4	---
197	gi_119937909	XM_001256935	LOC790478	Hypothetical protein (LOC790478)	0.00	5.3	1.0	-5.4	---
198	gi_119903166	XM_001254926	LOC787570	Hypothetical protein (LOC787570)	0.00	2.9	-1.9	-5.4	---
199	gi_119927273	XM_001255295	LOC788147	Similar to atp-binding cassette protein c4 splice (LOC788147)	0.00	3.7	-1.5	-5.4	---
200*	gi_119892561	XM_001255399	OR6C74	Olfactory receptor, family 6, subfamily c, member 74	0.00	5.3	1.0	-5.4	---
201	gi_51826239	---	---	Co895922 bovgen_24247 normal cattle brain cDNA clone rzpdp1056i2437q 5'	0.00	3.0	-1.8	-5.4	---
202	gi_76685850	XM_599512	Olfr1178	Olfactory receptor 1178	0.00	5.1	-1.1	-5.4	---
203	gi_119926161	XM_589549	OR4L1	Olfactory receptor, family 4, subfamily l, member 1	0.00	4.6	-1.2	-5.4	---
204	gi_51881604	---	---	Aj814128 kn206 bos sp. cDNA clone c0005205b18	0.00	2.8	-1.9	-5.4	↑
205	gi_61877384	XM_591641	LOC513884	Similar to seven transmembrane helix receptor (LOC513884)	0.00	3.9	-1.4	-5.4	---
206	gi_119908105	XM_001256258	LOC789518	Hypothetical protein (LOC789518)	0.00	2.8	-1.9	-5.4	---
207	gi_119893024	XM_001253563	LOC785584	Similar to natural killer cell receptor protein 1 (LOC785584)	0.00	6.9	1.3	-5.4	---
208	gi_148233351	NM_001098001	FAP	Fibroblast activation protein, alpha	0.00	4.8	-1.1	-5.4	---
209	gi_119915305	XR_028046	RUNX2	Similar to runt-related transcription factor 2 (LOC536911)	0.00	6.3	1.2	-5.4	---
210	gi_31340693	NM_174701	HSD17B14	Hydroxysteroid (17-beta) dehydrogenase 14	0.00	3.0	-1.8	-5.3	---
211	gi_119917348	XM_583388	GPR146	G protein-coupled receptor 146	0.00	2.9	-1.9	-5.3	---
212*	gi_119913160	XM_001251499	PARP8	Poly (adp-ribose) polymerase family, member 8	0.00	4.7	-1.1	-5.3	---
213	gi_118151305	NM_001078119	FBXO16	F-box protein 16 (FBXO16)	0.00	3.2	-1.6	-5.3	---

214	gi_119895380	XM_001255445	OR2T4	Olfactory receptor, family 2, subfamily t, member 4	0.00	4.5	-1.2	-5.3	---
215	gi_149642672	NM_001099071	MAP3K8	Mitogen-activated protein kinase kinase kinase 8	0.00	5.5	1.0	-5.3	---
216	gi_76657295	XM_869298	Olfr890	Olfactory receptor 890	0.00	4.1	-1.3	-5.3	↑
217	gi_51824369	---	LCAT	Lecithin-cholesterol acyltransferase	0.00	5.0	-1.0	-5.3	---
218	gi_119907451	XM_868602	LOC616556	Similar to npas3 protein (LOC616556)	0.00	3.4	-1.5	-5.2	---
219	gi_119918950	XM_865914	LOC614419	Similar to odorant receptor k13 (LOC614419)	0.00	4.5	-1.2	-5.2	---
220	gi_51819191	---	---	Co888906 bovgen_17231 normal cattle brain cDNA clone rzpdp1056e2246q 5'	0.00	4.8	-1.1	-5.2	---
221	gi_157279948	NM_001105020	KRTAP9L3	Keratin associated protein 9-1	0.00	3.6	-1.5	-5.2	---
222	gi_51881277	---	---	Aj813801 kn206 bos sp. CDNA clone c0005205i9	0.00	6.1	1.2	-5.2	---
223	gi_76678008	XM_584199	OR10A3	Olfactory receptor, family 10, subfamily a, member 3	0.00	4.8	-1.1	-5.2	---
224	gi_119910279	XM_600249	DPY19L3	Dpy-19-like 3 (c. Elegans)	0.00	3.8	-1.4	-5.2	---
225	gi_46417924	---	---	Cn438660 be04 normalized and subtracted bovine embryonic and extraembryonic tissue cDNA clone be04016b2f01 5'	0.00	2.9	-1.8	-5.2	---
226	gi_119879609	XM_606096	LOC527699	Similar to Kalirin, RHOGEF kinase (LOC527699)	0.00	2.7	-1.9	-5.2	---
227	gi_119922019	XM_868429	OR8U8	Olfactory receptor, family 8, subfamily u, member 8	0.00	4.5	-1.1	-5.2	---
228	gi_119906638	XM_001251005	LOC782357	Similar to inositol polyphosphate 1-phosphatase (LOC782357)	0.00	5.9	1.1	-5.2	---
229	gi_119902030	XR_028230	REC8	REC8 homolog (yeast)	0.00	3.5	-1.5	-5.2	---
230*	gi_119931138	XM_597087	OR8G2	Olfactory receptor, family 8, subfamily g, member 2	0.00	4.9	-1.0	-5.2	---
231	gi_119889564	XM_001250774	CD58	CD58 molecule	0.00	2.6	-2.0	-5.2	---
232	gi_47686978	---	---	Cn790998 4125657 barc 8bov cDNA clone 8bov_38b16 5'	0.00	10.2	2.0	-5.1	---
233	gi_119892967	XM_870975	DUSP16	Dual specificity phosphatase 16	0.00	6.0	1.2	-5.1	---
234	gi_27806678	NM_174026	CSF1	Colony stimulating factor 1 (macrophage)	0.00	5.0	1.0	-5.1	---
235	gi_119915547	XM_601579	LOC523283	Similar to olfactory receptor olfr1365 (LOC523283)	0.00	4.2	-1.2	-5.1	---
236	gi_68425684	---	---	Am026861 kn-252-lymph, cDNA clone c0007393i02 3'	0.00	3.2	-1.6	-5.1	---
237	gi_119937889	XM_001256927	LOC790466	Similar to endothelial pas domain protein 1/hypoxia-inducible factor-2 alpha (LOC790466)	0.00	3.0	-1.7	-5.1	---
238	gi_119918606	XM_868011	Dusp13 (rat)	Dual specificity phosphatase 13	0.00	3.8	-1.3	-5.1	---
239	gi_119925451	XM_001251376	LOC782733	Hypothetical protein (LOC782733)	0.00	3.7	-1.4	-5.1	---
240	gi_119927681	XM_001254405	LOC786840	Similar to cfolf4 (LOC786840)	0.00	4.7	-1.1	-5.1	---
241	gi_119906190	XM_588232	PARP10	Poly (adp-ribose) polymerase family, member 10	0.00	2.9	-1.7	-5.0	---
242*	gi_119892577	XM_001255552	Olr1070	Olfactory receptor 1070	0.00	4.9	1.0	-5.0	---
243	gi_119892500	XM_001254798	LOC787380	Similar to integrin alpha-7 (LOC787380)	0.00	2.5	-2.0	-5.0	---
244*	gi_119915596	XM_001253001	Olfr129	Olfactory receptor 129	0.00	3.1	-1.6	-5.0	---
245	gi_149642646	NM_001099168	RBM43	Rna binding motif protein 43	0.00	3.8	-1.3	-5.0	---
246*	gi_51821409	---	OAS1	2',5'-oligoadenylate synthetase 1, 40/46kda	0.00	9.1	1.8	-5.0	---
247	gi_119905168	XM_001253613	LOC785665	Hypothetical protein (LOC785665)	0.00	3.0	-1.7	-5.0	---
248	gi_119923556	XM_001254131	LOC786468	Hypothetical protein (LOC786468)	0.00	5.0	1.0	-5.0	---
249	gi_119235075	---	---	Ee898501 b14051a ffb cDNA clone b1405 3'	0.00	3.5	-1.4	-5.0	---
250	gi_119928883	XM_581609	LOC505334	Hypothetical (LOC505334)	0.00	2.5	-2.0	-5.0	↑
251	gi_166157493	NM_001113766	TMC2	Transmembrane channel-like 2	0.00	3.2	-1.6	-5.0	---
252	gi_119915598	XM_588373	LOC511103	Similar to olfactory receptor, family 2, subfamily j, member 3	0.00	2.9	-1.7	-4.9	---
253	gi_51808686	---	---	Co878762 bovgen_07087 normal cattle brain cDNA clone rzpdp1056k234q 5'	0.00	2.8	-1.8	-4.9	---
254	gi_119891937	XM_588753	ALX1	Alx homeobox 1	0.00	5.1	1.0	-4.9	---
255	gi_156120432	NM_001101892	C1orf109	Chromosome 1 open reading frame 109	0.00	4.3	-1.1	-4.9	---
256	gi_157427785	NM_001105329	CSNK1G3	Casein kinase 1, gamma 3 (CSNK1G3)	0.00	3.6	-1.4	-4.9	---
257	gi_51811834	---	---	Co881905 bovgen_10230 normal cattle brain cDNA clone rzpdp1056k2414q 5'	0.00	3.3	-1.5	-4.9	---
258	gi_119893524	XM_001250407		Similar to n-deacetylase/n-sulfotransferase (heparan glucosaminyl) 3 (MGC142329)	0.00	2.9	-1.7	-4.9	---
259	gi_76670917	XM_605163	LOC526789	Similar to histone h4 (LOC526789)	0.00	3.1	-1.6	-4.8	---
260	gi_119901513	XM_001253901	LOC786117	Hypothetical protein (LOC786117)	0.00	2.5	-1.9	-4.8	---
261	gi_162287311	NM_001080908	CA5B	Carbonic anhydrase vb, mitochondrial	0.00	4.1	-1.2	-4.8	---
262	gi_119901493	XR_028228	LOC785236	Hypothetical protein (LOC785236)	0.00	4.6	-1.1	-4.8	---
263	gi_160707930	NM_001110785	IL6R	Interleukin 6 receptor	0.00	2.9	-1.7	-4.8	---
264	gi_51886630	---	---	Aj819154 kn206 bos sp. CDNA clone c0006014h18	0.00	3.6	-1.3	-4.8	---
265	gi_119889431	XM_585905	C1orf51	Chromosome 1 open reading frame 51	0.00	3.4	-1.4	-4.8	---
266	gi_119923401	XM_001249461	SHISA3	Shisa homolog 3 (xenopus laevis)	0.00	4.4	-1.1	-4.8	---
267	gi_119892314	XM_582025	PTPRB	Protein tyrosine phosphatase, receptor type, b	0.00	4.6	-1.0	-4.8	---
268	gi_119912777	XM_586217	LOC509283	Similar to chromosome 17 open reading frame 27	0.00	6.4	1.3	-4.8	---
269	gi_119909812	XM_582583	LOC506171	Similar to phospholipase c, gamma 2 (LOC506171)	0.00	2.8	-1.7	-4.8	---
270	gi_119915205	XM_001250256	KCNK5	Potassium channel, subfamily k, member 5	0.00	3.1	-1.5	-4.8	---
271	gi_119917845	XR_027657	LOC539889	Hypothetical (LOC539889)	0.00	3.4	-1.4	-4.8	---
272*	gi_119929609	XM_611004	OR4A47	Olfactory receptor, family 4, subfamily a, member 47	0.00	4.8	1.0	-4.8	---
273	gi_51801949	---	---	Co872113 bovgen_00438 normal cattle brain cDNA clone rzpdp1056e1858q 3'	0.00	2.5	-1.9	-4.8	---
274	gi_119879472	XM_589632	ZDHHC23	Similar to membrane-associated dhhc23 zinc finger protein (LOC512177)	0.00	5.5	1.2	-4.7	---
275	gi_139948994	NM_001083697	MGC157405	Pregnancy-associated glycoprotein (MGC157405)	0.00	4.0	-1.2	-4.7	---
276	gi_51885893	---	---	Aj818417 kn206 bos sp. CDNA clone c0006012d21	0.00	2.7	-1.7	-4.7	---
277	gi_51809527	---	---	Co879603 bovgen_07930 normal cattle brain cDNA clone rzpdp1056b2216q 5'	0.00	2.5	-1.9	-4.7	---
278	gi_119926223	XM_588414	OR2J2	Olfactory receptor, family 2, subfamily j, member 2	0.00	2.9	-1.6	-4.7	↑
279*	gi_148539985	NM_174512	CDK5R1	Cyclin-dependent kinase 5, regulatory subunit 1 (p35)	0.00	2.6	-1.8	-4.7	---
280	gi_116003876	NM_001076828	PARP9	Poly (adp-ribose) polymerase family, member 9	0.00	4.2	-1.1	-4.7	---
281	gi_119920747	XM_001251180	LOC782548	Similar to was protein family, member 1 (LOC782548)	0.00	4.3	-1.1	-4.7	---
282	gi_157427889	NM_001105382	Prune2 (rat)	Prune homolog 2 (drosophila)	0.00	7.8	1.7	-4.7	---
283	gi_76662019	XM_877625	LOC614527	Hypothetical (LOC614527)	0.00	3.1	-1.5	-4.7	---
284*	gi_119930582	XM_001255843	Olfr591	Olfactory receptor 591	0.00	4.5	1.0	-4.7	---
285*	gi_119925715	XM_001255793	OR5F1	Olfactory receptor, family 5, subfamily f, member 1	0.00	3.7	-1.3	-4.6	---
286	gi_118151377	NM_001077829	LYZ1	Lysozyme 1	0.00	5.0	1.1	-4.6	---
287*	gi_119892521	XM_001255098	Olr1012	Olfactory receptor 1012	0.00	4.5	1.0	-4.6	---
288	gi_119909824	XM_608473	LOC530011	Similar to plcg2 protein (LOC530011)	0.00	2.6	-1.8	-4.6	---
289	gi_51819056	---	---	Co888771 bovgen_17096 normal cattle brain cDNA clone rzpdp1056e1232q 5'	0.00	2.7	-1.7	-4.6	---
290	gi_119924090	XM_001251040	SERPINB4	Serpin peptidase inhibitor, clade b (ovalbumin), member 4	0.00	2.9	-1.6	-4.6	---
291	gi_119916743	XM_864316	SOCS1	Suppressor of cytokine signaling 1	0.00	8.9	2.0	-4.6	↑
292*	gi_119922658	XM_001256086	OR5W2	Olfactory receptor, family 5, subfamily w, member 2	0.00	3.6	-1.3	-4.6	---
293	gi_119923483	XM_001252794	LOC784514	Similar to olfr586 protein (LOC784514)	0.00	4.7	1.0	-4.5	---
294	gi_114051785	NM_001046630	Tas2r122	Taste receptor, type 2, member 122	0.00	4.5	1.0	-4.5	---
295	gi_119925570	XM_001254515	CXorf66	Chromosome x open reading frame 66	0.00	4.1	-1.1	-4.5	---
296	gi_119895839	XR_028142	LOC535967	Similar to kiaa0715 protein (LOC535967)	0.00	4.3	-1.0	-4.5	---
297	gi_119909965	XM_589041	LOC511659	Similar to phospholipase c, gamma 2 (LOC511659)	0.00	2.8	-1.6	-4.5	---
298	gi_119931741	XR_028812	LOC789877	Similar to pol protein (LOC789877)	0.00	2.8	-1.6	-4.5	---
299	gi_119892689	XM_001251716	LOC783379	Similar to kiaa1033 protein (LOC783379)	0.00	2.3	-2.0	-4.5	---
300	gi_115496313	NM_001075738	Gstt3	Glutathione s-transferase, theta 3	0.00	3.7	-1.2	-4.5	---
301*	gi_119915666	XM_580689	UBD	Ubiquitin D	0.00	3.3	-1.4	-4.5	---
302	gi_119895897	XM_001249627	LOC781380	Hypothetical protein (LOC781380)	0.00	2.4	-1.8	-4.5	↑
303	gi_119892596	XM_867721	ITGA7	Integrin, alpha 7	0.00	3.8	-1.2	-4.5	---
304	gi_119900588	XM_588491	LZTS1	Leucine zipper, putative tumor suppressor 1	0.00	2.9	-1.5	-4.5	---

305	gi_51815582	---	---	Co885297 bovgen_13622 normal cattle brain cDNA clone rzpdp1056d0515q 5'	0.00	3.7	-1.2	-4.4	---
306	gi_31343556	NM_177510	GCNT1	Glucosaminyl (n-acetyl) transferase 1, core 2	0.00	5.1	1.1	-4.4	---
307	gi_51808339	---	---	Co878419 bovgen_06744 normal cattle brain cDNA clone rzpdp1056f1228q 5'	0.00	5.1	1.1	-4.4	---
308	gi_119901485	XM_001253189	LOC785047	Similar to trace amine receptor 8 (LOC785047)	0.00	3.7	-1.2	-4.4	---
309	gi_119902191	XM_609796	Olfr731	Olfactory receptor 731	0.00	4.5	1.0	-4.4	---
310	gi_119901577	XM_614057	GPR126	G protein-coupled receptor 126	0.00	3.3	-1.3	-4.4	---
311	gi_119931076	XM_001256837	LOC790332	Similar to enterocytin (LOC790332)	0.00	4.3	1.0	-4.4	---
312*	gi_119932269	XM_001256929	NXF3	Nuclear rna export factor 3	0.00	2.4	-1.8	-4.4	---
313	gi_119924949	XM_001255225	LOC788043	Similar to kiaa0966 protein (LOC788043)	0.00	3.0	-1.5	-4.4	---
314	gi_119924379	XM_001254841	OR5T1	Olfactory receptor, family 5, subfamily t, member 1	0.00	4.0	-1.1	-4.4	---
315*	gi_119922460	XM_001250569	OR8G2	Olfactory receptor, family 8, subfamily g, member 2	0.00	3.9	-1.1	-4.4	---
316	gi_122692322	NM_001080336	LOC781146	Lysozyme (LOC781146)	0.00	3.5	-1.3	-4.4	---
317	gi_76679710	XM_606544	PRAMEF12	Prame family member 12	0.00	3.9	-1.1	-4.4	---
318	gi_119904820	XM_001250391	LOC782559	Hypothetical protein (LOC782559)	0.00	3.2	-1.4	-4.4	---
319	gi_119922154	XM_001252905	LOC784661	Hypothetical protein (LOC784661)	0.01	2.3	-1.9	-4.4	---
320	gi_119926726	XM_599805	NUP210	Nucleoporin 210kda	0.00	4.3	1.0	-4.4	---
321	gi_119921161	XM_001254952	LOC787604	Similar to olfactory receptor olr1075 (LOC787604)	0.00	2.8	-1.5	-4.4	---
322	gi_119874947	XM_604589	LOC526226	Similar to histone h4 (LOC526226)	0.00	2.8	-1.5	-4.4	---
323*	gi_119895356	XM_001255247	OR2L3	Olfactory receptor, family 2, subfamily l, member 3	0.00	3.8	-1.2	-4.4	---
324	gi_51815204	---	---	Co884919 bovgen_13244 normal cattle brain cDNA clone rzpdp1056k2317q 5'	0.00	3.0	-1.5	-4.4	---
325*	gi_76716222	XM_871383	Olfr49	Olfactory receptor 49	0.00	3.0	-1.4	-4.4	---
326	gi_116003864	NM_001076823	TAGAP	T-cell activation rhogtpase activating protein	0.00	7.0	1.6	-4.3	---
327	gi_119918717	XM_599400	Olfr214	Olfactory receptor 214	0.00	3.4	-1.3	-4.3	---
328	gi_51888157	---	---	Aj820681 kn206 bos sp. cDNA clone c0006020e19	0.01	2.3	-1.9	-4.3	↑
329*	gi_119895410	XM_001255686	Olfr30	Olfactory receptor 30	0.00	3.7	-1.2	-4.3	---
330	gi_119923773	XM_001250268		Hypothetical protein, transcript variant 2 (LOC783422)	0.00	3.2	-1.4	-4.3	---
331	gi_119922799	XM_001253315	LOC785238	Similar to olfactory receptor olr87 (LOC785238)	0.00	4.5	1.0	-4.3	---
332	gi_114050926	NM_001046126	ELL3	Elongation factor rna polymerase ii-like 3	0.00	5.8	1.3	-4.3	---
333*	gi_119933344	XM_001256835	Olr94	Olfactory receptor 94	0.00	3.7	-1.2	-4.3	---
334	gi_119879605	XM_865427	OSBPL11	Oxysterol binding protein-like 11	0.00	3.1	-1.4	-4.3	---
335	gi_119930790	XM_001256547	LOC789934	Similar to LOC407199 protein (LOC789934)	0.00	2.5	-1.7	-4.3	---
336	gi_119921720	XM_001255420	LOC788326	Similar to protein tyrosine phosphatase, receptor type, f polypeptide (ptprf), interacting protein (liprin), alpha 1	0.01	2.4	-1.8	-4.3	---
337	gi_115497767	NM_001075224	PPP1R13L	Protein phosphatase 1, regulatory (inhibitor) subunit 13 like	0.00	2.3	-1.9	-4.3	---
338	gi_51816596	---	---	Co886311 bovgen_14636 normal cattle brain cDNA clone rzpdp1056i2111q 5'	0.01	2.3	-1.9	-4.3	---
339	gi_51821587	---	---	Co891292 bovgen_19617 normal cattle brain cDNA clone rzpdp1056g1039q 5'	0.01	2.2	-1.9	-4.3	---
340	gi_66792729	NM_001024506	IRF9	Interferon regulatory factor 9	0.00	4.0	-1.1	-4.3	---
341	gi_119894006	XM_612336	UGT2B4	Udp glucuronosyltransferase 2 family, polypeptide b4	0.00	2.8	-1.5	-4.3	---
342	gi_119895080	XM_001256277	LOC789548	Hypothetical protein (LOC789548)	0.00	2.9	-1.5	-4.3	---
343	gi_119902087	XM_605073	LOC526700	Similar to olfactory receptor mor118-1 (LOC526700)	0.00	3.1	-1.4	-4.3	---
344	gi_119917902	XM_614294	LOC534506	Similar to kiaa0598 protein, transcript variant 1 (LOC534506)	0.00	2.9	-1.5	-4.3	---
345	gi_119929450	XM_001256653	LOC790079	Hypothetical protein (LOC790079)	0.00	2.9	-1.5	-4.3	---
346	gi_119902917	XM_869926	BATF	Basic leucine zipper transcription factor, atf-like	0.00	3.3	-1.3	-4.3	---
347	gi_115497501	NM_001075911	NR4A1	Nuclear receptor subfamily 4, group a, member 1	0.00	2.7	-1.6	-4.3	---
348	gi_51817299	---	---	Co887014 bovgen_15339 normal cattle brain cDNA clone rzpdp1056h1010q 5'	0.00	3.2	-1.3	-4.3	---
349	gi_114052379	NM_001046538	RAB15	Rab15, member ras onocogene family	0.00	2.5	-1.7	-4.3	---
350	gi_139949042	NM_001083711	TNFAIP8	Tumor necrosis factor, alpha-induced protein 8	0.00	2.4	-1.7	-4.2	---
351	gi_119923777	XM_001250364	LOC783509	Similar to l antigen family, member 3 (LOC783509)	0.00	2.5	-1.7	-4.2	---
352	gi_119911353	XR_028864	LOC790331	Similar to eukaryotic translation initiation factor 4b	0.00	3.2	-1.3	-4.2	---
353*	gi_119924442	XM_001251569	TAAR8	Trace amine associated receptor 8	0.00	3.9	-1.1	-4.2	---
354	gi_51804806	---	---	Co874906 bovgen_03231 normal cattle brain cDNA clone rzpdp1056k0255q 3'	0.00	2.4	-1.7	-4.2	---
355	gi_119935266	XM_001256915	LOC790450	Similar to rna helicase ii/gu protein (LOC790450)	0.00	2.7	-1.6	-4.2	---
356	gi_119894724	XM_599736	ANGPTL6	Angiopoietin-like 6	0.00	2.7	-1.5	-4.2	---
357	gi_51880934	---	---	Aj813458 kn206 bos sp. cDNA clone c0005201m9	0.00	2.4	-1.7	-4.2	---
358	gi_51887964	---	---	Aj820488 kn206 bos sp. cDNA clone c0006020o03	0.00	3.4	-1.2	-4.2	---
359*	gi_76657212	XM_610318	Olfr921	Olfactory receptor 921	0.00	3.5	-1.2	-4.2	---
360	gi_119904452	XM_617702	DGKH	Diacylglycerol kinase, eta	0.01	2.3	-1.9	-4.2	---
361	gi_119879589	XM_590786	MYLK	Myosin, light polypeptide kinase (mylk)	0.00	2.6	-1.6	-4.2	---
362*	gi_119920960	XM_001249726	OR52A5	Olfactory receptor, family 52, subfamily a, member 5	0.00	4.2	1.0	-4.2	---
363	gi_119894644	XM_001256245	LOC789504	Similar to bc85395_3 (LOC789504)	0.00	3.7	-1.1	-4.2	---
364	gi_51885341	---	---	Aj817865 kn206 bos sp. cDNA clone c0006005b13	0.00	3.5	-1.2	-4.2	---
365	gi_164518983	NM_001113297	ACBD7	Acyl-coa binding domain containing 7	0.00	2.5	-1.7	-4.2	---
366	gi_119900621	XM_607313	LOC528877	Similar to neuron-derived orphan receptor-1 alfa (LOC528877)	0.00	6.4	1.5	-4.2	---
367	gi_119931764	XM_001256548	LOC789935	Similar to mkiaa1301 protein (LOC789935)	0.00	2.6	-1.6	-4.2	---
368	gi_119902066	XM_589218	ZFHX2	Zinc finger homeobox 2 (LOC100505)	0.00	2.4	-1.7	-4.2	---
369	gi_119925108	XM_590561	LOC512948	Similar to olf4 (LOC512948)	0.00	4.0	-1.0	-4.2	---
370	gi_51822356	---	---	Co892055 bovgen_20380 normal cattle brain cDNA clone rzpdp1056j1631q 5'	0.00	2.3	-1.8	-4.2	---
371	gi_51882334	---	---	Aj814858 kn206 bos sp. cDNA clone c0005200e16	0.01	2.1	-2.0	-4.2	---
372	gi_119935945	XM_001257083	LOC790672	Hypothetical protein (LOC790672)	0.00	2.7	-1.5	-4.2	---
373*	gi_119902240	XM_605072	Olfr49	Olfactory receptor 49	0.01	2.3	-1.8	-4.2	---
374	gi_56145168	---	---	Cv984447 umc-bov_0b01-006-f09 day 0 oviduct post-lh surge bov cDNA 3'	0.00	2.5	-1.6	-4.2	---
375	gi_119922646	XM_867468	LOC615605	Similar to olfactory receptor mor231-1 (LOC615605)	0.00	3.5	-1.2	-4.1	---
376	gi_119921941	XM_871152	LOC618831	Similar to t cell receptor delta chain (LOC618831)	0.00	3.2	-1.3	-4.1	---
377*	gi_119895407	XM_001253323	Olfr30	Olfactory receptor 30	0.00	2.7	-1.5	-4.1	---
378	gi_115497413	NM_001076421	SPIC	Spi-c transcription factor (Spi-1/pu.1 related)	0.00	4.5	1.1	-4.1	---
379	gi_119921939	XM_001251837	LOC783209	Hypothetical protein loc783209 (LOC783209)	0.00	2.5	-1.6	-4.1	---
380	gi_119920986	XM_591949	LOC514146	Similar to olfactory receptor mor30-1 (LOC514146)	0.00	3.0	-1.4	-4.1	---
381	gi_156121338	NM_001102348	ARL4C	Adp-ribosylation factor-like 4c	0.00	5.6	1.4	-4.1	---
382	gi_119922122	XM_584568	Olfr513	Olfactory receptor 513	0.00	4.0	1.0	-4.1	---
383*	gi_119921755	XM_001255762	OR51T1	Olfactory receptor, family 51, subfamily t, member 1	0.00	2.9	-1.4	-4.1	---
384	gi_119901491	XM_865063	LOC613867	Similar to trace amine receptor 8 (LOC613867)	0.00	3.7	-1.1	-4.1	---
385	gi_119914770	XM_001255129	LOC787910	Hypothetical protein (LOC787910)	0.01	2.1	-2.0	-4.1	---
386	gi_51832764	---	---	Co875536 bovgen_03861 normal cattle brain cDNA clone rzpdp1056k0353q 3'	0.00	3.3	-1.3	-4.1	---
387	gi_29229162	---	---	Cb441787 692297 marc 6bov cDNA 3'	0.00	3.3	-1.2	-4.1	---
388	gi_119889614	XM_001251548	CTTNBP2NL	Cttnbp2 n-terminal like	0.00	2.3	-1.8	-4.1	---
389	gi_119889139	XM_592982	OR10K1	Olfactory receptor, family 10, subfamily k, member 1	0.00	3.4	-1.2	-4.1	---
390	gi_119921658	XM_001254417	LOC786859	Similar to trav20 protein (LOC786859)	0.01	2.1	-1.9	-4.1	---
391	gi_119919114	XM_870538	LOC618211	Similar to histone H4 (LOC618211)	0.00	2.6	-1.6	-4.1	---
392	gi_51818847	---	---	Co888562 bovgen_16887 normal cattle brain cDNA clone rzpdp1056i1050q 5'	0.00	4.3	1.1	-4.0	---
393	gi_119919246	XM_001254190	LOC788447	Hypothetical protein (LOC788447)	0.00	3.6	-1.1	-4.0	---

394	gi_48374082	NM_001001440	ANXA4	Annexin a4	0.00	2.4	-1.7	-4.0	---
395	gi_119924438	XM_001251459	LOC782807	Similar to trace amine receptor 8 (LOC782807)	0.00	3.2	-1.3	-4.0	---
396	gi_119890020	XM_606535	WLS	Hypothetical (LOC528123)	0.00	3.4	-1.2	-4.0	---
397	gi_139948327	NM_001083728	MAPK10	Mitogen-activated protein kinase 10	0.00	3.1	-1.3	-4.0	---
398	gi_119929037	XM_001250178	LOC783299	Similar to b7 olfactory receptor (LOC783299)	0.00	4.6	1.1	-4.0	---
399	gi_119892563	XM_001255417	OR6C70	Olfactory receptor, family 6, subfamily c, member 70	0.00	3.7	-1.1	-4.0	---
400	gi_119907486	XM_580632	OR2D2	Olfactory receptor, family 2, subfamily d, member 2	0.01	2.3	-1.8	-4.0	---
401	gi_119935923	XM_001257082	LOC790671	Similar to interphotoreceptor matrix proteoglycan 200	0.02	2.1	-1.9	-4.0	---
402	gi_51827229	---	---	Co896907 bovgen_25232 normal cattle brain cDNA clone rzpdp1056k201q 5'	0.00	2.1	-1.9	-4.0	---
403	gi_119912471	XM_584593	LOC539069	Similar to copper amine oxidase (LOC539069)	0.00	3.9	1.0	-4.0	---
404	gi_119907337	XM_001254939	Olfr676	Olfactory receptor 676	0.00	3.0	-1.3	-4.0	---
405	gi_119924385	XM_583364	OR5I1	Olfactory receptor, family 5, subfamily i, member 1	0.00	4.3	1.1	-4.0	---
406	gi_119901487	XM_001253215	LOC785080	Similar to trace amine associated receptor 6 (loc785080)	0.00	3.2	-1.2	-4.0	---
407	gi_119926100	XR_028522	LOC787388	Similar to olfactory receptor olfr1174 (LOC787388)	0.00	3.1	-1.3	-4.0	---
408	gi_76662924	XM_882063	LOC616766	Hypothetical (LOC616766)	0.01	2.4	-1.7	-4.0	---
409	gi_10870122	BF076357	---	BF076357 225899 marc 2bov cDNA 5'	0.00	3.4	-1.2	-4.0	---
410	gi_119875275	XM_609842	BACH1	Btb and cnc homology 1, basic leucine zipper transcription factor 1	0.00	2.3	-1.7	-4.0	---
411	gi_119914325	XM_616073	SCN11A	Sodium channel, voltage-gated, type xi, alpha subunit	0.00	3.7	-1.1	-4.0	---
412	gi_51812273	---	---	Co882341 bovgen_10666 normal cattle brain cDNA clone rzpdp1056l1824q 5'	0.00	2.6	-1.5	-4.0	---
413	gi_119916460	XM_001250160	LOC782394	Hypothetical protein (LOC782394)	0.00	2.4	-1.6	-4.0	---
414	gi_119902193	XM_001252966	OR4K2	Olfactory receptor, family 4, subfamily k, member 2	0.00	4.3	1.1	-4.0	---
415*	gi_119923020	XM_001253097	Olfr1303	Olfactory receptor 1303	0.00	4.1	1.0	-4.0	---
416	gi_119926936	XM_001251377	Olfr630	Olfactory receptor 630	0.00	3.7	-1.1	-4.0	---
417	gi_115496034	NM_001076311	SNX24	Sorting nexin 24	0.00	6.4	1.6	-4.0	---
418	gi_119923523	XM_001253504	LOC785507	Similar to sp alpha (LOC785507)	0.00	2.9	-1.4	-3.9	---
419	gi_119907606	XM_590174	Olr36	Olfactory receptor 36	0.00	3.2	-1.2	-3.9	---
420	gi_119901591	XM_590527	STX11	Syntaxin 11	0.00	4.5	1.1	-3.9	---
421	gi_51888463	AJ820987	---	Aj820987 kn206 bos sp. CDNA clone c0006019g01	0.01	2.3	-1.7	-3.9	---
422	gi_119894463	XM_597995	PBX4	Pre-b-cell leukemia homeobox 4	0.00	2.7	-1.4	-3.9	---
423	gi_51881154	AJ813678	---	Aj813678 kn206 bos sp. CDNA clone c0005205l4	0.01	2.3	-1.7	-3.9	---
424	gi_119890208	XM_588670	CC2D1B	Coiled-coil and c2 domain containing 1b	0.00	2.9	-1.3	-3.9	---
425	gi_51883784	AJ816308	---	Aj816308 kn206 bos sp. CDNA clone c0005210i19	0.00	2.5	-1.6	-3.9	---
426	gi_119921000	XM_001251294	LOC782658	Similar to olfr586 protein (LOC782658)	0.00	3.9	1.0	-3.9	---
427	gi_119896062	XR_027676	LOC782371	Hypothetical protein (LOC782371)	0.00	3.5	-1.1	-3.9	---
428	gi_119922219	XM_585077	LOC508315	Similar to olfactory receptor mor232-3 (LOC508315)	0.00	3.0	-1.3	-3.9	---
429*	gi_119921045	XM_593866	OR52A1	Olfactory receptor, family 52, subfamily a, member 1	0.00	3.4	-1.1	-3.9	---
430	gi_32189319	NM_181033	LPHN3	Latrophilin 3	0.00	3.6	-1.1	-3.9	---
431	gi_119921882	XM_001256453	LOC789812	Similar to olfactory receptor mor262-6 (LOC789812)	0.00	3.9	1.0	-3.9	---
432	gi_119909828	XM_586270	LOC509331	Similar to plcg2 protein (LOC509331)	0.00	2.6	-1.5	-3.9	---
433	gi_136256478	NM_001077899	NFE2L3	Nuclear factor (erythroid-derived 2)-like 3	0.00	4.8	1.2	-3.9	---
434	gi_119889279	XM_001253716	NUP210L	Nucleoporin 210kda-like	0.00	2.6	-1.5	-3.9	---
435	gi_51814505	---	---	Co884486 bovgen_12811 normal cattle brain cDNA clone rzpdp1056b079q 5'	0.00	2.9	-1.3	-3.9	---
436	gi_119921953	XM_001252278	LOC783789	Similar to t-cell receptor alpha chain (LOC783789)	0.00	3.1	-1.2	-3.9	---
437	gi_51815687	---	---	Co885402 bovgen_13727 normal cattle brain cDNA clone rzpdp1056l1615q 5'	0.00	3.3	-1.2	-3.9	---
438	gi_119892579	XM_001255560	LOC788524	Similar to cor9k3 olfactory receptor family 9 subfamily k-like	0.00	4.1	1.1	-3.9	---
439	gi_119906802	XM_869405	SLC26A7	Solute carrier family 26, member 7	0.01	2.1	-1.8	-3.9	---
440	gi_51809307	---	---	Co879383 bovgen_07710 normal cattle brain cDNA clone rzpdp1056c1320q 5'	0.00	3.3	-1.2	-3.9	---
441	gi_119892535	XM_001255202	OR6C1	Olfactory receptor, family 6, subfamily c, member 1	0.00	3.7	-1.1	-3.9	---
442	gi_119877636	XM_001252430	LOC783994	Hypothetical protein loc783994 (LOC783994)	0.00	2.4	-1.6	-3.9	---
443	gi_119903343	XM_609234	SULT6B1	Sulfotransferase family, cytosolic, 6b, member 1	0.00	3.1	-1.3	-3.9	---
444	gi_76690438	XM_583591	LOC538910	Similar to protocadherin gamma a4 (LOC538910)	0.01	2.2	-1.8	-3.9	---
445*	gi_119910954	XM_001254677	Vmn1r233	Similar to pheromone receptor (LOC787211)	0.00	3.0	-1.3	-3.9	---
446	gi_119931962	XM_587211	GPCRLTM7	Putative olfactory receptor GPCRLTM7	0.00	4.2	1.1	-3.9	---
447	gi_119905969	XM_604955	TTPAL	Tocopherol (alpha) transfer protein-like	0.00	2.3	-1.7	-3.8	---
448	gi_119907359	XM_001255071	Olfr661	Olfactory receptor 661	0.00	3.9	1.0	-3.8	---
449	gi_118151441	NM_001078159	LYZ	Lysozyme	0.01	2.2	-1.7	-3.8	---
450	gi_119922109	XM_001250343	LOC781841	Hypothetical protein (LOC781841)	0.00	2.4	-1.6	-3.8	---
451	gi_77736454	NM_001034755	MOBKL2C	Mob1, mps one binder kinase activator-like 2c (yeast)	0.00	2.6	-1.5	-3.8	---
452	gi_126723003	NM_001082454	CCRN4L	Ccr4 carbon catabolite repression 4-like (s. Cerevisiae)	0.00	4.6	1.2	-3.8	---
453	gi_67691040	---	---	Dr116230 1431370 marc 7bov cDNA 3'	0.02	2.0	-1.9	-3.8	---
454*	gi_76670422	XM_581219	TAAR8	Trace amine associated receptor 8	0.00	3.8	1.0	-3.8	---
455	gi_119906354	XM_001254631	LOC787152	Hypothetical protein (LOC787152)	0.01	2.2	-1.8	-3.8	---
456	gi_119923783	XM_001250507	LOC783650	Hypothetical protein (LOC783650)	0.00	2.6	-1.5	-3.8	---
457	gi_119930466	XM_001255198	LOC788004	Similar to f-box only protein 16 (LOC788004)	0.00	3.3	-1.2	-3.8	---
458	gi_119921039	XM_001252349	LOC783898	Similar to mor 3beta4 (LOC783898)	0.00	3.7	1.0	-3.8	---
459	gi_119923151	XM_001255840	LOC788936	Hypothetical protein loc788936 (LOC788936)	0.01	2.1	-1.8	-3.8	↑
460	gi_119925825	XM_001251152	Olfr1351	Olfactory receptor 1351	0.00	2.7	-1.4	-3.8	---
461	gi_119895944	XM_001250359	ELL2	Elongation factor, rna polymerase ii, 2	0.00	3.9	1.0	-3.8	---
462	gi_119887309	XM_585327	NIPA1	Non imprinted in prader-willi/angelman syndrome 1	0.00	2.4	-1.6	-3.8	---
463	gi_119901496	XM_001253352	LOC785282	Similar to trace amine receptor 8 (LOC785282)	0.00	3.0	-1.2	-3.8	---
464	gi_119915592	XM_001252942	OR2J3	Olfactory receptor, family 2, subfamily j, member 3	0.00	2.9	-1.3	-3.8	---
465	gi_119916182	XM_866291	PSMA8	Proteasome (prosome, macropain) subunit, alpha type, 8	0.00	3.4	-1.1	-3.8	---
466*	gi_76674338	XM_865987	OR7D4	Olfactory receptor, family 7, subfamily d, member 4	0.00	3.3	-1.1	-3.8	---
467*	gi_119925321	XM_001255568	Olfr921	Olfactory receptor 921	0.00	3.0	-1.3	-3.8	---
468	gi_114052944	NM_001046095	CXCL16	Chemokine (c-x-c motif) ligand 16	0.00	2.3	-1.6	-3.8	---
469	gi_70829482	---	---	Dr713179 lb0054.cr_n13 gc_bgc-05 cDNA clone image:7963695	0.00	2.5	-1.5	-3.7	---
470	gi_119925385	XM_866146	LOC614592	Similar to olfactory receptor olr1414 (LOC614592)	0.00	2.7	-1.4	-3.7	---
471	gi_119922177	XM_001253330	LOC785259	Hypothetical protein (LOC785259)	0.00	3.0	-1.3	-3.7	---
472	gi_51826609	---	---	Co896292 bovgen_24617 normal cattle brain cDNA clone rzpdp1056l1135q 5'	0.00	2.4	-1.6	-3.7	---
473	gi_119907937	XM_591624	OR4C13	Olfactory receptor, family 4, subfamily c, member 13	0.00	3.6	-1.1	-3.7	---
474	gi_119902201	XM_001253086	OR4K14	Olfactory receptor, family 4, subfamily k, member 14	0.00	3.3	-1.1	-3.7	---
475	gi_77404220	NM_001034056	MS4A8B	Membrane-spanning 4-domains, subfamily a, member 8b	0.00	2.3	-1.6	-3.7	---
476	gi_68427075	---	---	Am027990 am027990 kn-252-lymph, bos indicus bos indicus cDNA clone c0007394c04 3'	0.00	2.6	-1.4	-3.7	---
477	gi_29262527	---	---	Cb456145 713366 marc 6bov cDNA 3'	0.01	2.3	-1.6	-3.7	---
478	gi_119931163	XM_001256873	LOC790391	Hypothetical protein (LOC790391)	0.00	4.5	1.2	-3.7	---
479	gi_119925806	XM_001250000	LOC781561	Hypothetical protein (LOC781561)	0.02	2.2	-1.7	-3.7	---
480	gi_119888322	XM_001253419	LOC785365	Hypothetical protein (LOC785365)	0.01	2.3	-1.6	-3.7	---
481	gi_119884978	XM_001253176	GPR87	G protein-coupled receptor 87	0.00	3.6	1.0	-3.7	---
482	gi_119890516	XM_868290	KCNJ13	Potassium inwardly-rectifying channel, subfamily j, member 13	0.02	2.1	-1.8	-3.7	---
483	gi_119926154	XM_001255113	LOC787886	Hypothetical protein (LOC787886)	0.02	2.1	-1.8	-3.7	---
484	gi_119894665	XM_583975	LOC507378	Similar to Cfolf4 (LOC507378)	0.00	3.1	-1.2	-3.7	---
485	gi_119922149	XM_870554	LOC618225	Similar to olfactory receptor olfr1177 (LOC618225)	0.00	2.9	-1.3	-3.7	---
486	gi_119923034	XM_001253258	LOC785145	Similar to seven transmembrane helix receptor (LOC785145)	0.00	2.3	-1.6	-3.7	---

487	gi_119901527	XR_028449	EYA4	Eyes absent homolog 4 (drosophila)	0.00	2.6	-1.4	-3.7	---
488	gi_51822791	---	---	Co892491 bovgen_20816 normal cattle brain cDNA clone rzpdp1056i2133q 5'	0.00	2.6	-1.4	-3.7	---
489*	gi_119895352	XM_591451	OR2T8	Olfactory receptor, family 2, subfamily t, member 8	0.00	3.5	-1.1	-3.7	---
490	gi_119908082	XM_001256153	OR5L1	Olfactory receptor, family 5, subfamily l, member 1	0.00	2.6	-1.4	-3.7	---
491	gi_45498818	---	---	Ck980838 4112836 barc 9bov cDNA clone 9bov42_g03 3'	0.01	2.5	-1.5	-3.7	---
492	gi_119915994	XM_001256549	LOC789936	Similar to olfactory receptor 1160 (LOC789936)	0.00	2.5	-1.5	-3.7	---
493	gi_51824423	---	---	Co894116 bovgen_22441 normal cattle brain cDNA clone rzpdp1056h2334q 5'	0.00	3.5	-1.0	-3.7	---
494	gi_119907040	XM_590126	ZC3H12C	Similar to kiaa1726 protein, transcript variant 1 (LOC512586)	0.00	5.1	1.4	-3.6	---
495	gi_119910056	XM_001250846	NLRC5	Nlr family, card domain containing 5	0.00	4.3	1.2	-3.6	---
496	gi_119902654	XR_028233	LOC785249	Similar to loc767881 protein (LOC785249)	0.00	3.2	-1.1	-3.6	---
497	gi_119910346	XM_001253667	ZBTB32	Similar to testis zinc finger protein (LOC785741)	0.00	2.3	-1.6	-3.6	---
498	gi_45060035	---	---	Ck832605 4056810 barc 8bov cDNA clone 8bov_17p20 5'	0.01	2.4	-1.5	-3.6	---
499	gi_119924558	XM_867000	LOC615243	Similar to t-cell receptor delta (LOC615243)	0.01	2.3	-1.6	-3.6	---
500	gi_76674021	XM_604240	LOC525881	Similar to EPA6 (LOC525881)	0.00	2.9	-1.3	-3.6	---
501	gi_51888300	AJ820824	---	Aj820824 kn206 bos sp. CDNA clone c0006019n24	0.00	2.4	-1.5	-3.6	---
502	gi_119929386	XM_001256545	LOC789931	Hypothetical protein (LOC789931)	0.00	2.6	-1.4	-3.6	---
503	gi_119893667	XM_001249425	NAP1L5	Nucleosome assembly protein 1-like 5	0.01	2.3	-1.6	-3.6	---
504	gi_114703724	NM_174509	CACNB3	Calcium channel, voltage-dependent, beta 3 subunit	0.00	2.7	-1.3	-3.6	---
505	gi_156121078	NM_001102216	ZNF565	Zinc finger protein 565	0.00	2.4	-1.5	-3.6	---
506	gi_51820694	---	---	Co890406 bovgen_18731 normal cattle brain cDNA clone rzpdp1056g0160q 5'	0.00	2.9	-1.2	-3.6	---
507	gi_119924710	XM_001249554	LOC781173	Similar to guanine nucleotide release/exchange factor	0.00	2.5	-1.4	-3.6	---
508*	gi_119924436	XM_001251414	TAAR8	Trace amine associated receptor 8	0.00	3.4	-1.1	-3.6	---
509	gi_119924775	XM_587889	LOC510712	Similar to olf4 (LOC510712)	0.00	3.4	-1.1	-3.6	---
510	gi_51824784	---	---	Co894476 bovgen_22801 normal cattle brain cDNA clone rzpdp1056e0641q 5'	0.00	3.0	-1.2	-3.6	---
511	gi_119903689	XM_872068	LOC613399	Similar to kiaa0903-like protein, transcript variant 2	0.00	2.5	-1.4	-3.6	---
512	gi_31342998	NM_174030	CTGF	Connective tissue growth factor	0.00	2.6	-1.4	-3.6	---
513	gi_87278868	---	---	Dy465743 1606324 marc 11bov cDNA 3'	0.00	2.9	-1.2	-3.6	---
514	gi_27881411	NM_174294	CSN3	Casein kappa	0.00	2.5	-1.4	-3.6	---
515	gi_119921576	XM_583518	KIAA1147	KIAA1147	0.00	4.8	1.3	-3.6	---
516	gi_119921932	XM_871139	Olfr768	Olfactory receptor 768	0.00	2.9	-1.2	-3.6	---
517	gi_119936421	XM_001257122	LOC790723	Similar to connector enhancer of KSR2A (LOC790723)	0.00	3.2	-1.1	-3.6	---
518	gi_119934261	XM_001252663	LOC784317	Similar to wd repeat endosomal protein (LOC784317)	0.01	2.2	-1.6	-3.6	---
519	gi_134085668	NM_001083451	RORC	Rar-related orphan receptor c	0.02	2.0	-1.8	-3.6	---
520	gi_51886917	AJ819441	---	Aj819441 kn206 bos sp. CDNA clone c0006015g04	0.02	2.1	-1.7	-3.6	---
521	gi_21681585	AU278275	---	Au278275 cloned bovine placenta cDNA cDNA clone placenta0318 3'	0.00	4.2	1.2	-3.6	---
522	gi_119923914	XM_001255594	OR4A5	Olfactory receptor, family 4, subfamily a, member 5	0.00	3.1	-1.2	-3.6	---
523	gi_119934405	XM_001254935	LOC787580	Similar to chain a, structure of human neutral endopeptidase complexed with phosphoramidon (LOC787580)	0.02	2.0	-1.7	-3.6	---
524	gi_119912384	XM_586375	CCDC103	Coiled-coil domain containing 103	0.01	2.0	-1.8	-3.6	---
525	gi_119922290	XR_027641	LOC522586	Hypothetical (LOC522586)	0.00	2.5	-1.4	-3.6	---
526	gi_156120686	NM_001102020	CLIP4	Cap-gly domain containing linker protein family, member 4	0.00	2.4	-1.5	-3.6	---
527	gi_119905750	XM_001253180	C20orf112	Chromosome 20 open reading frame 112	0.00	2.7	-1.3	-3.6	---
528	gi_119935000	XM_001256810	LOC790297	Similar to protein kinase (LOC790297)	0.01	2.0	-1.8	-3.6	---
529	gi_119892451	XM_588270	STAT2	Signal transducer and activator of transcription 2, 113kda	0.00	2.9	-1.2	-3.5	---
530	gi_119925143	XM_001252882	LOC784626	Similar to neuron-derived orphan receptor-1 alfa (LOC784626)	0.00	3.6	1.0	-3.5	---
531	gi_119889480	XM_868112	LOC616149	Hypothetical (LOC616149)	0.01	2.3	-1.6	-3.5	---
532	gi_119936114	XM_001257101	LOC790695	Similar to t-cell receptor alpha chain (LOC790695)	0.00	2.6	-1.3	-3.5	---
533	gi_51802822	---	---	Co872982 bovgen_01307 normal cattle brain cDNA clone rzpdp1056m2256q 3'	0.00	2.4	-1.5	-3.5	---
534*	gi_119925918	XM_609712	Olfr921	Olfactory receptor 921	0.00	3.4	1.0	-3.5	---
535	gi_119921163	XM_869117	LOC616964	Similar to cfolf4 (LOC616964)	0.00	2.6	-1.4	-3.5	---
536	gi_119906071	XM_586129	B4GALT5	Udp-gal:betaglcnac beta 1,4- galactosyltransferase, polypeptide 5	0.00	6.8	1.9	-3.5	---
537	gi_60958168	---	---	Dn519419 1260254 marc 7bov cDNA 3'	0.00	2.4	-1.5	-3.5	---
538	gi_110347578	NM_174257	S100G	S100 calcium binding protein g	0.01	2.1	-1.7	-3.5	---
539	gi_115496050	NM_001076208	NR4A2	Nuclear receptor subfamily 4, group a, member 2	0.00	3.4	1.0	-3.5	---
540	gi_119921695	XM_001254784	CFH	Complement factor h	0.00	3.1	-1.1	-3.5	---
541	gi_119927361	XM_589643	CDADC1	Cytidine and dcmp deaminase domain containing 1	0.00	2.1	-1.6	-3.5	---
542	gi_119906900	XM_001254050		Glutamate receptor, ionotrophic, ampa 4 (gria4)	0.00	2.9	-1.2	-3.5	---
543	gi_156071442	NM_001101661	DEFB119	Defensin, beta 119	0.00	3.0	-1.1	-3.5	---
544	gi_119914146	XM_868259	RAGE	Renal tumor antigen	0.00	2.6	-1.3	-3.5	---
545	gi_119918504	XM_001250186	LOC781705	Hypothetical protein (LOC781705)	0.01	2.3	-1.5	-3.5	---
546	gi_76679265	XM_591472	OR7A10	Olfactory receptor, family 7, subfamily a, member 10	0.00	2.9	-1.2	-3.5	---
547	gi_119877840	XM_616959	ROBO1	Roundabout, axon guidance receptor, homolog 1 (drosophila)	0.00	2.9	-1.2	-3.5	---
548	gi_119877632	XM_603300	NRIP1	Nuclear receptor interacting protein 1	0.00	2.1	-1.7	-3.5	---
549*	gi_119920994	XM_001251099	OR51T1	Olfactory receptor, family 51, subfamily t, member 1	0.00	3.5	1.0	-3.5	---
550	gi_51812540	---	---	Co882608 bovgen_10933 normal cattle brain cDNA clone rzpdp1056l087q 5'	0.00	3.7	1.1	-3.5	---
551	gi_158819086	NM_001110183	MGC134232	Hypothetical loc618600 (MGC134232)	0.03	2.0	-1.7	-3.5	---
552	gi_164448591	NM_001113258	FHL1	Four and a half lim domains 1 (fhl1), transcript variant 1	0.00	2.5	-1.4	-3.5	---
553	gi_119910391	XM_001254872	LOC787495	Hypothetical protein loc787495 (LOC787495)	0.00	2.9	-1.2	-3.5	---
554	gi_119913871	XM_617995	AKAP6	A kinase (prka) anchor protein 6	0.00	2.9	-1.2	-3.5	---
555	gi_119902298	XM_601356	LOC523062	Similar to seven transmembrane helix receptor (LOC523062)	0.00	3.3	-1.1	-3.5	---
556	gi_119556585	---	---	Eh157580 lb01364.cr_c04 gc_bgc-13 cDNA clone image:8441982 5'	0.00	2.5	-1.4	-3.5	---
557	gi_119910344	XM_001253642	LOC785707	Hypothetical protein (LOC785707)	0.00	2.5	-1.4	-3.5	---
558	gi_76683775	XM_586650	LOC509641	Similar to olf4 (LOC509641)	0.01	2.2	-1.6	-3.5	---
559	gi_68422126	---	---	Am023811 kn-252-lymph, cDNA clone c0007400i17 5'	0.00	3.2	-1.1	-3.5	---
560	gi_119919833	XM_001254041	LOC786332	Similar to transmembrane protein with egf-like and two follistatin-like domains 1 (LOC786332)	0.00	2.8	-1.3	-3.5	---
561	gi_119929117	XM_589033	OR4A15	Olfactory receptor, family 4, subfamily a, member 15	0.00	4.0	1.2	-3.5	---
562	gi_115496747	NM_001075692	MTUS1	Mitochondrial tumor suppressor 1 (mtus1), nuclear gene encoding mitochondrial protein	0.00	2.3	-1.5	-3.4	---
563	gi_51816378	---	---	Co886093 bovgen_14418 normal cattle brain cDNA clone rzpdp1056o0525q 5'	0.00	3.8	1.1	-3.4	---
564*	gi_118151067	NM_001077987	SNX13	Sorting nexin 13	0.00	3.6	1.0	-3.4	---
565	gi_119927808	XM_001255617	LOC788608	Similar to t-cell receptor alpha chain (LOC788608)	0.00	2.4	-1.4	-3.4	---
566	gi_119918970	XM_581982	OR8G5	Olfactory receptor, family 8, subfamily g, member 5	0.01	2.4	-1.5	-3.4	---
567*	gi_119891767	XM_001249363	INSIG1	Insulin induced gene 1	0.00	2.3	-1.5	-3.4	---
568	gi_119920756	XM_001251412	LOC782764	Similar to mitochondrial cytochrome c oxidase subunit vb	0.00	2.6	-1.3	-3.4	---
569	gi_119892519	XM_001255059	OR6C76	Olfactory receptor, family 6, subfamily c, member 76	0.00	3.2	-1.1	-3.4	---
570	gi_51810873	---	---	Co880944 bovgen_09269 normal cattle brain cDNA clone rzpdp1056b0414q 5'	0.00	2.5	-1.4	-3.4	---
571	gi_51808688	---	---	Co878764 bovgen_07089 normal cattle brain cDNA clone rzpdp1056h0526q 5'	0.00	2.6	-1.3	-3.4	---
572	gi_119939528	XM_001257172	LOC790784	Similar to p63 (processed form) (LOC790784)	0.01	2.0	-1.7	-3.4	---

573	gi_51883450	AJ815974	---	Aj815974 kn206 bos sp. cDNA clone c0005202f17	0.01	2.1	-1.6	-3.4	---
574*	gi_119892525	XM_001255131	Olfr802	Olfactory receptor 802	0.00	3.2	-1.1	-3.4	---
575	gi_119918285	XM_001253310	LOC785230	Hypothetical protein (LOC785230)	0.01	2.0	-1.7	-3.4	---
576	gi_119923452	XM_001249761	LOC781734	Similar to g antigen, family d, 1 (LOC781734)	0.00	2.9	-1.2	-3.4	---
577	gi_119889486	XM_867242	NOTCH2	NOTCH 2	0.00	2.2	-1.5	-3.4	---
578*	gi_119892978	XM_001251585	KLRC1	Killer cell lectin-like receptor subfamily c, member 1	0.00	3.6	1.1	-3.4	---
579	gi_119922699	XM_868317	LOC616322	Hypothetical (LOC616322)	0.00	2.8	-1.2	-3.4	---
580	gi_119915359	XM_583214	NFKBIE	Nuclear factor of kappa light polypeptide gene enhancer in b-cells inhibitor, epsilon	0.00	3.9	1.2	-3.4	---
581	gi_119920307	XR_028058	LOC785658	Similar to spi-c transcription factor (spi-1/pu.1 related)	0.00	4.0	1.2	-3.4	---
582	gi_119910944	XM_001254581	Vmn1r67	Similar to pheromone receptor (LOC787075)	0.00	2.8	-1.2	-3.4	---
583	gi_119901769	XM_581038	MLLT4	Myeloid/lymphoid or mixed-lineage leukemia (trithorax homolog, drosophila); translocated to, 4	0.00	2.9	-1.2	-3.4	---
584	gi_119915909	XM_865312	IRF4	Interferon regulatory factor 4	0.00	4.7	1.4	-3.4	---
585	gi_51880653	AJ813177	---	Aj813177 kn206 bos sp. CDNA clone c0005207e19	0.01	2.3	-1.5	-3.4	---
586	gi_119921525	XM_001254038	LOC786324	Similar to enterocytin (LOC786324)	0.00	3.2	-1.1	-3.4	---
587	gi_119915588	XM_001252901	OR2B3	Olfactory receptor, family 2, subfamily b, member 3	0.02	2.1	-1.6	-3.4	---
588	gi_51815409	---	---	Co885124 bovgen_13449 normal cattle brain cDNA clone rzpdp1056c1211q 5'	0.00	2.9	-1.2	-3.3	---
589*	gi_119902016	XM_001252771	CBLN3	Cerebellin 3 precursor	0.00	5.2	1.5	-3.3	↑
590*	gi_119920962	XM_581965	OR52A1	Olfactory receptor, family 52, subfamily a, member 1	0.00	3.3	1.0	-3.3	---
591	gi_119903302	XM_588244	CLEC4F	C-type lectin domain family 4, member f	0.01	2.1	-1.6	-3.3	---
592*	gi_119892583	XM_001255583	Olr1070	Olfactory receptor 1070	0.00	2.6	-1.3	-3.3	---
593	gi_119938116	XM_599621	LOC521360	Hypothetical (LOC521360)	0.00	2.6	-1.3	-3.3	---
594	gi_116004282	NM_001077032	CXorf65	Chromosome x open reading frame 65	0.01	2.2	-1.5	-3.3	---
595*	gi_119887366	XM_001254094	INPP1	Inositol polyphosphate-1-phosphatase	0.00	5.9	1.8	-3.3	---
596	gi_31343166	NM_173964	TEK	Tek tyrosine kinase, endothelial	0.00	2.3	-1.4	-3.3	---
597	gi_51882655	AJ815179	---	Aj815179 kn206 bos sp. CDNA clone c0005203i11	0.01	2.1	-1.6	-3.3	---
598	gi_119940726	XM_001257205	LOC790830	Hypothetical protein (LOC790830)	0.00	2.6	-1.3	-3.3	---
599	gi_119908232	XM_618596	CDC42BPA	Cdc42 binding protein kinase alpha (dmpk-like)	0.00	2.4	-1.4	-3.3	---
600	gi_115496687	NM_001075698	IFIT5	Interferon-induced protein with tetratricopeptide repeats 5	0.00	4.1	1.2	-3.3	---
601	gi_66792745	NM_001024493	TRPV2	Transient receptor potential cation channel, subfamily v, member 2	0.01	2.2	-1.5	-3.3	---
602	gi_119910478	XM_580597	RINL	Ras and rab interactor-like	0.00	3.2	1.0	-3.3	---
603	gi_119912581	XR_027582	PITPNC1	Phosphatidylinositol transfer protein, cytoplasmic 1	0.00	2.3	-1.4	-3.3	---
604	gi_51882625	---	---	Aj815149 kn206 bos sp. cDNA clone c0005200a24	0.01	2.1	-1.6	-3.3	---
605	gi_119922265	XM_001254653	LOC787179	Similar to t cell receptor alpha chain (LOC787179)	0.00	3.4	1.0	-3.3	---
606	gi_78369353	NM_001035367	LOC527068	Aldo-keto reductase family 1 member c3 -like (LOC527068)	0.01	2.2	-1.5	-3.3	---
607	gi_119932114	XM_001256880	LOC790399	Similar to seven transmembrane helix receptor (LOC790399)	0.00	2.7	-1.2	-3.3	---
608*	gi_119928286	XM_001255475	OR13F1	Olfactory receptor, family 13, subfamily f, member 1	0.00	3.3	1.0	-3.3	---
609	gi_119913798	XM_588916	SNX33	Sorting nexin 33	0.00	2.2	-1.5	-3.3	---
610	gi_84000234	NM_001038135	REEP6	Receptor accessory protein 6	0.00	3.3	1.0	-3.3	---
611	gi_119889482	XM_611707	LOC532585	Hypothetical (LOC532585)	0.01	2.3	-1.4	-3.3	↑
612	gi_16186852	---	---	Bi898780 480531 marc 2bov cDNA 5'	0.02	2.1	-1.6	-3.3	---
613	gi_76625185	XM_603327	LOC524985	Similar to olfactory receptor mor222-1 (LOC524985)	0.00	3.0	-1.1	-3.3	---
614	gi_119920877	XM_001257254	NOVA1	Neuro-oncological ventral antigen 1	0.00	2.8	-1.2	-3.3	---
615	gi_119889147	XM_585637	LOC508806	Similar to seven transmembrane helix receptor (LOC508806)	0.00	2.5	-1.3	-3.3	---
616	gi_51884171	Aj816695	---	Aj816695 kn206 bos sp. cDNA clone c0005209g15	0.00	2.5	-1.3	-3.3	---
617	gi_119916331	XM_608193	TNIP2	Tnfaip3 interacting protein 2	0.00	2.9	-1.1	-3.3	---
618	gi_114051342	NM_001046143	CDKN2AIP	Cdkn2a interacting protein)	0.00	2.1	-1.5	-3.3	---
619*	gi_119925417	XM_613566	NUB1	Negative regulator of ubiquitin-like proteins 1	0.00	4.9	1.5	-3.3	---
620	gi_76670427	XM_604131	LOC525775	Similar to trace amine receptor 8 (LOC525775)	0.01	2.3	-1.4	-3.3	---
621*	gi_124249271	NM_001080906	NUB1	Negative regulator of ubiquitin-like proteins 1	0.00	5.7	1.7	-3.3	---
622	gi_119925658	XM_001255387	LOC788279	Similar to olf4 (LOC788279)	0.00	3.3	1.0	-3.3	---
623	gi_119926964	XM_594793	Olfr6	Olfactory receptor 6	0.00	3.4	1.0	-3.3	---
624	gi_119893520	XM_001249301	LOC780970	Hypothetical protein (LOC780970)	0.00	2.7	-1.2	-3.3	---
625	gi_110626110	NM_001013593	BCAT2	Branched chain amino-acid transaminase 2, mitochondrial	0.00	2.3	-1.4	-3.3	---
626	gi_119934846	XM_001250325	LOC785695	Hypothetical protein (LOC785695)	0.00	3.8	1.2	-3.3	---
627	gi_62116764	---	---	Dn740589 1403150 marc 7bov cDNA 3'	0.00	3.2	1.0	-3.3	---
628	gi_51826686	---	---	Co896369 bovgen_24694 normal cattle brain cDNA clone rzpdp1056d0543q 5'	0.03	2.0	-1.6	-3.3	---
629	gi_119915432	XM_869123	MUC21	Mucin 21, cell surface associated	0.01	2.1	-1.5	-3.2	---
630	gi_119892555	XM_001255364	Olfr820	Olfactory receptor 820	0.00	2.7	-1.2	-3.2	---
631	gi_119908569	XR_028737	LOC789222	Similar to zinc finger protein riz (LOC789222)	0.00	2.3	-1.4	-3.2	---
632	gi_51815757	---	---	Co885472 bovgen_13797 normal cattle brain cDNA clone rzpdp1056c199q 5'	0.00	2.9	-1.1	-3.2	---
633	gi_119914504	XM_001251656	LOC783001	Similar to chromosome 12 open reading frame 2 (LOC783001)	0.00	2.4	-1.4	-3.2	---
634*	gi_119923954	XM_595420	Olfr1276	Olfactory receptor 1276	0.00	3.1	-1.1	-3.2	---
635	gi_119314652	---	---	Ee978054 p34501a fnm cDNA clone p3450 3'	0.01	2.1	-1.5	-3.2	---
636*	gi_119919022	XM_001251836	OR8A1	Olfactory receptor, family 8, subfamily a, member 1	0.00	2.4	-1.3	-3.2	---
637	gi_119892575	XM_001255503	LOC788438	Similar to olfactory receptor mor210-4 (LOC788438)	0.00	3.0	-1.1	-3.2	---
638	gi_51881897	---	---	Aj814421 aj814421 kn206 bos sp. CDNA clone c0005204k1	0.00	2.6	-1.3	-3.2	---
639	gi_119875296	XM_001252915	LOC784671	Hypothetical protein (LOC784671)	0.01	2.3	-1.4	-3.2	---
640	gi_156120584	NM_001101968	STYXL1	Serine/threonine/tyrosine interacting-like 1	0.01	2.2	-1.4	-3.2	---
641	gi_119922882	XM_600016	LOC521749	Similar to olfactory receptor mor245-4 (LOC521749)	0.00	3.5	1.1	-3.2	---
642	gi_51815212	---	---	Co884927 bovgen_13252 normal cattle brain cDNA clone rzpdp1056i0316q 5'	0.00	2.8	-1.2	-3.2	---
643	gi_51821644	---	---	Co891349 bovgen_19674 normal cattle brain cDNA clone rzpdp1056p0648q 5'	0.00	2.6	-1.2	-3.2	---
644*	gi_119913158	XM_588962	PARP8	Poly (adp-ribose) polymerase family, member 8	0.00	3.2	1.0	-3.2	---
645	gi_51811180	---	---	Co881251 bovgen_09576 normal cattle brain cDNA clone rzpdp1056i093q 5'	0.00	2.3	-1.4	-3.2	---
646	gi_114050764	NM_001046472	GPR183	G protein-coupled receptor 183	0.01	2.2	-1.4	-3.2	---
647	gi_77736288	NM_001034672	TSPAN33	Tetraspanin 33	0.00	4.4	1.4	-3.2	---
648	gi_76686154	XM_590795	OR4C12	Olfactory receptor, family 4, subfamily c, member 12	0.00	3.0	-1.1	-3.2	---
649	gi_119921693	XM_587804	LOC510640	Similar to h factor 1 (complement), transcript variant 2	0.00	2.6	-1.2	-3.2	---
650	gi_27807288	NM_174716	ANXA2	Annexin a2	0.00	3.2	1.0	-3.2	---
651	gi_119921731	XM_001255638	LOC788640	Similar to olfactory receptor olr87 (LOC788640)	0.00	3.3	1.0	-3.2	---
652	gi_51884776	---	---	Aj817300 kn206 bos sp. CDNA clone c0006006n10	0.00	2.3	-1.4	-3.2	---
653*	gi_119921037	XM_604679	Olfr622	Olfactory receptor 622	0.00	2.5	-1.3	-3.2	---
654	gi_51818716	---	---	Co888431 bovgen_16756 normal cattle brain cDNA clone rzpdp1056n1319q 5'	0.00	3.1	1.0	-3.2	---
655	gi_119902174	XM_605040	LOC526667	Similar to olfactory receptor mor106-5 (LOC526667)	0.01	2.3	-1.4	-3.2	---
656	gi_119902413	XM_617674	MDGA2	Mam domain containing glycosylphosphatidylinositol anchor 2	0.00	2.9	-1.1	-3.2	---
657	gi_119895360	XM_586131	LOC509217	Similar to seven transmembrane helix receptor (LOC509217)	0.00	2.7	-1.2	-3.2	---
658	gi_119893497	XM_607704	NDST4	N-deacetylase/n-sulfotransferase (heparan glucosaminyl) 4	0.00	2.7	-1.2	-3.2	---
659	gi_156121044	NM_001102199	MYO1B	Myosin ib	0.00	2.4	-1.3	-3.2	---
660*	gi_134085656	NM_001083422	STK17A	Serine/threonine kinase 17a	0.00	2.3	-1.4	-3.2	---
661	gi_119915895	XM_001250447	LOC782393	Similar to eukaryotic translation elongation factor 1 epsilon 1	0.00	2.1	-1.5	-3.2	---
662	gi_119909922	XM_001256073	LOC789278	Hypothetical protein (LOC789278)	0.01	2.2	-1.4	-3.2	---
663	gi_119888596	XR_028504	SP110	Sp110 nuclear body protein	0.00	2.3	-1.4	-3.2	---

664	gi_119901002	XM_589483	C5	Complement component 5	0.00	2.4	-1.3	-3.2	---
665	gi_51808026	---	---	Co878110 bovgen_06435 normal cattle brain cDNA clone rzpdp1056a1417q 5'	0.00	4.4	1.4	-3.2	---
666	gi_119886996	XM_001249828	LCA5L	Leber congenital amaurosis 5-like	0.00	2.6	-1.2	-3.1	---
667	gi_119892507	XM_001254890	Olfr770	Olfactory receptor 770	0.00	2.9	-1.1	-3.1	---
668	gi_119924514	XM_001253602	Olfr1293	Olfactory receptor 1293	0.00	3.0	-1.1	-3.1	---
669	gi_134085676	NM_001083530	S100A3	S100 calcium binding protein a3 (s100a3)	0.00	4.0	1.3	-3.1	---
670	gi_119926165	XM_001255258	LOC788100	Similar to seven transmembrane helix receptor (LOC788100)	0.01	2.2	-1.4	-3.1	---
671	gi_68312483	---	---	Am011292 am011292 kn-252-bone-marrow, cDNA clone c0007384f18 5'	0.00	2.5	-1.3	-3.1	---
672	gi_157279990	NM_001105041	RUSC1	Run and sh3 domain containing 1	0.00	4.2	1.3	-3.1	---
673*	gi_61812675	XM_598133	Olfr622	Olfactory receptor 622	0.00	2.5	-1.3	-3.1	---
674*	gi_119929138	XM_001255607	OR51T1	Olfactory receptor, family 51, subfamily t, member 1	0.00	3.1	1.0	-3.1	---
675	gi_119937175	XM_001255947	LOC789094	Similar to ampa type glutamate receptor (LOC789094)	0.01	2.2	-1.4	-3.1	---
676	gi_116734828	NM_001075320	TIMD4	T-cell immunoglobulin and mucin domain containing 4	0.00	2.5	-1.2	-3.1	---
677	gi_51880414	---	---	Aj812938 kn206 bos sp. CDNA clone c0005208a14	0.01	2.2	-1.4	-3.1	---
678	gi_119892607	XM_001249868	LOC781440	Similar to olfactory receptor mor114-1 (LOC781440)	0.00	3.0	1.0	-3.1	---
679*	gi_119895405	XM_001253303	Olfr30	Olfactory receptor 30	0.00	2.5	-1.3	-3.1	---
680	gi_31341720	NM_174541	GABRA2	Gamma-aminobutyric acid (gaba) a receptor, alpha 2	0.00	2.5	-1.3	-3.1	---
681	gi_119892357	XM_592833	DYRK2	Dual-specificity tyrosine-(y)-phosphorylation regulated kinase 2	0.01	2.2	-1.4	-3.1	---
682	gi_119926000	XM_001250683	CA1	Carbonic anhydrase i	0.00	2.9	-1.1	-3.1	---
683	gi_119926757	XM_001256213	LOC789465	Hypothetical protein (LOC789465)	0.00	4.1	1.3	-3.1	---
684	gi_119923232	XM_612459	LOC533149	Hypothetical (LOC533149)	0.00	2.3	-1.4	-3.1	---
685	gi_119910251	XM_001250104	FTSJD1	Ftsj methyltransferase domain containing 1	0.00	5.1	1.6	-3.1	---
686	gi_119920696	XM_608251	CRLF2	Cytokine receptor-like factor 2	0.00	4.0	1.3	-3.1	---
687	gi_51809237	---	---	Co879313 bovgen_07640 normal cattle brain cDNA clone rzpdp1056d0127q 5'	0.00	2.5	-1.2	-3.1	---
688	gi_119893783	XM_001250975	LOC782331	Hypothetical protein (LOC782331)	0.00	3.0	1.0	-3.1	---
689*	gi_119907426	XM_001255664	OR52A1	Olfactory receptor, family 52, subfamily a, member 1	0.00	3.4	1.1	-3.1	---
690	gi_119902080	XM_588656	BVd1.18	T cell receptor delta chain variable region (bvd1.18)	0.00	2.6	-1.2	-3.1	---
691	gi_119888478	XM_587645	CPS1	Carbamoyl-phosphate synthase 1, mitochondrial	0.02	2.0	-1.5	-3.1	---
692*	gi_119892543	XM_001255277	Olfr802	Olfactory receptor 802	0.00	2.9	-1.1	-3.1	---
693	gi_60453989	---	---	Dn285379 1235238 marc 7bov cDNA 3'	0.00	4.6	1.5	-3.1	---
694*	gi_119920966	XM_001249871	OR52A1	Olfactory receptor, family 52, subfamily a, member 1	0.00	3.4	1.1	-3.1	---
695	gi_119884953	XM_591264	PLCH1	Phospholipase c, eta 1	0.00	5.0	1.6	-3.1	---
696	gi_51809759	---	---	Co879836 bovgen_08161 normal cattle brain cDNA clone rzpdp1056d159q 5'	0.01	2.2	-1.4	-3.1	---
697	gi_51882102	---	---	Aj814626 kn206 bos sp. CDNA clone c0005200h11	0.00	2.9	-1.1	-3.1	---
698	gi_119924516	XM_001253624	LOC785683	Similar to olfactory receptor olr758 (LOC785683)	0.00	2.5	-1.2	-3.1	---
699	gi_119927331	XM_586485	LOC509509	Similar to t-cell receptor alpha chain (LOC509509)	0.01	2.2	-1.4	-3.1	---
700	gi_119889928	XM_609742	COL24A1	Collagen, type xxiv, alpha 1	0.00	3.1	1.0	-3.1	---
701	gi_119889322	XM_001254388	LOC786817	Hypothetical protein (LOC786817)	0.01	2.2	-1.4	-3.1	---
702	gi_51887120	---	---	Aj819644 aj819644 kn206 bos sp. CDNA clone c0006016a22	0.01	2.3	-1.3	-3.1	---
703	gi_119921654	XM_870882	LOC618552	Similar to t-cell receptor alpha chain (LOC618552)	0.00	2.7	-1.1	-3.1	---
704	gi_115497951	NM_001075871	IER2	Immediate early response 2	0.00	4.0	1.3	-3.1	---
705	gi_119915866	XM_607555	HIVEP1	Human immunodeficiency virus type i enhancer binding protein 1	0.00	3.8	1.2	-3.1	---
706	gi_51817518	---	---	Co887233 bovgen_15558 normal cattle brain cDNA clone rzpdp1056j1016q 5'	0.00	2.6	-1.2	-3.1	---
707	gi_119911171	XM_609549	ZNF584	Similar to zinc finger protein 420 (LOC531064)	0.01	2.1	-1.5	-3.1	---
708	gi_119920543	XM_868002	MAP7D2	Map7 domain containing 2	0.00	3.1	1.0	-3.1	---
709	gi_119893022	XM_587046	Clec2e	C-type lectin domain family 2, member e	0.00	2.5	-1.2	-3.1	---
710	gi_119921415	XM_001249872	LOC781446	Similar to olfactory receptor olr1108 (LOC781446)	0.00	2.9	-1.0	-3.0	---
711	gi_119929786	XM_001255691	LOC788715	Similar to low-density lipoprotein receptor-related protein 1b precursor lrp-dit) (LOC788715)	0.00	2.6	-1.2	-3.0	---
712	gi_51814035	---	---	Co884088 bovgen_12413 normal cattle brain cDNA clone rzpdp1056m0216q 5'	0.00	2.3	-1.3	-3.0	---
713	gi_119901510	XM_001253691	TAAR1	Trace amine associated receptor 1	0.00	3.0	1.0	-3.0	---
714	gi_119923060	XM_001253760	LOC785898	Similar to olfactory receptor (LOC785898)	0.00	2.7	-1.1	-3.0	---
715	gi_119891945	XM_001249702	MGAT4C	Mannosyl (alpha-1,3-)-glycoprotein beta-1,4-n-acetylglucosaminyltransferase, isozyme c (putative)	0.00	3.1	1.0	-3.0	---
716	gi_119923045	XM_001253400	LOC785338	Hypothetical protein (LOC785338)	0.00	2.4	-1.2	-3.0	---
717	gi_119938379	XM_001257069	LOC790653	Similar to mll5 (LOC790653)	0.01	2.3	-1.3	-3.0	---
718	gi_156120930	NM_001102142	SP7	Sp7 transcription factor	0.00	2.5	-1.2	-3.0	---
719	gi_164448597	NM_001035271	KLF6	Kruppel-like factor 6	0.00	2.1	-1.4	-3.0	---
720*	gi_51815648	---	BAIAP2	Bai1-associated protein 2	0.00	4.1	1.4	-3.0	---
721	gi_119901506	XM_001253621	Taar3	Trace amine-associated receptor 3	0.00	2.4	-1.2	-3.0	---
722	gi_119895362	XM_868904	OR2M4	Olfactory receptor, family 2, subfamily m, member 4	0.00	2.8	-1.1	-3.0	---
723	gi_119929817	XM_593643	Olfr1086	Olfactory receptor 1086	0.00	2.5	-1.2	-3.0	---
724	gi_51820553	---	---	Co890265 bovgen_18590 normal cattle brain cDNA clone rzpdp1056j0134q 5'	0.00	2.2	-1.4	-3.0	---
725	gi_119889478	XM_608618	Olfr1402	Olfactory receptor 1402	0.00	2.8	-1.1	-3.0	---
726	gi_119915614	XM_001253184	LOC785040	Similar to seven transmembrane helix receptor (LOC785040)	0.00	2.9	-1.1	-3.0	---
727	gi_119902205	XM_001253130	LOC784974	Similar to olfactory receptor MOR242-1 (LOC784974)	0.00	3.1	1.0	-3.0	---
728	gi_119894688	XM_001249956	ZSWIM4	Similar to flj00044 protein (LOC781514)	0.00	2.5	-1.2	-3.0	---
729	gi_51884045	---	---	Aj816569 aj816569 kn206 bos sp. CDNA clone c0005209l7	0.00	2.4	-1.3	-3.0	---
730	gi_119877213	XM_614756	ROBO2	Roundabout, axon guidance receptor, homolog 2 (drosophila)	0.01	2.2	-1.4	-3.0	---
731	gi_119916408	XM_616601	WDR7	Similar to rabconnectin-3 beta (loc536469)	0.00	2.2	-1.4	-3.0	---
732	gi_119906499	XM_588521	VCPIP1	Similar to kiaa1850 protein, transcript variant 1 (LOC539643)	0.01	2.0	-1.5	-3.0	---
733	gi_51884568	---	---	Aj817092 kn206 bos sp. cDNA clone c0006007h13	0.00	2.9	-1.0	-3.0	---
734	gi_119922419	XM_001254973	Olfr1132	Olfactory receptor 1132	0.00	2.8	-1.1	-3.0	---
735	gi_119930323	XM_001253262	LOC785149	Similar to olfactory receptor olr1414 (LOC785149)	0.01	2.2	-1.4	-3.0	---
736	gi_119928129	XM_001253316	LOC785240	Hypothetical protein (LOC785240)	0.00	2.3	-1.3	-3.0	---
737	gi_119916443	XM_881561	LOC616344	Hypothetical loc616344 (LOC616344)	0.00	3.5	1.2	-3.0	---
738	gi_119920998	XM_001251219	LOC782589	Similar to seven transmembrane helix receptor (LOC782589)	0.00	2.6	-1.1	-3.0	---
739	gi_119923950	XM_001250244	LOC781758	Similar to olfactory receptor olr753 (LOC781758)	0.02	2.2	-1.4	-3.0	---
740	gi_119889472	XM_001255499	LOC788724	Similar to hist2h2aa1 protein (LOC788724)	0.00	2.5	-1.2	-3.0	---
741	gi_76662928	XM_588102	OR2M3	Olfactory receptor, family 2, subfamily m, member 3	0.00	2.9	1.0	-3.0	---
742*	gi_119902300	XM_001254661	Olfr1276	Olfactory receptor 1276	0.00	3.0	1.0	-3.0	---
743	gi_119924838	XM_001253851	LOC786035	Similar to seven transmembrane helix receptor (LOC786035)	0.00	2.7	-1.1	-3.0	---
744*	gi_119895332	XM_001255076	OR2T8	Olfactory receptor, family 2, subfamily t, member 8	0.00	2.8	-1.1	-3.0	---
745	gi_116003900	NM_001076841	H2-T24	Histocompatibility 2, t region locus 24	0.00	3.1	1.0	-3.0	---
746	gi_51824355	---	---	Co894048 bovgen_22373 normal cattle brain cDNA clone rzpdp1056j0944q 5'	0.00	2.5	-1.2	-3.0	---
747	gi_51822391	---	---	Co892090 bovgen_20415 normal cattle brain cDNA clone rzpdp1056l2144q 5'	0.00	2.5	-1.2	-3.0	---
748	gi_119924939	XM_001255062	LOC787802	Similar to t cell receptor alpha chain (LOC787802)	0.01	2.2	-1.4	-3.0	---
749	gi_77735876	NM_001034463	C21orf33	Chromosome 21 open reading frame 33	0.00	2.6	-1.1	-3.0	---
750	gi_51884353	---	---	Aj816877 kn206 bos sp. CDNA clone c0005208n17	0.00	4.5	1.5	-3.0	---
751	gi_119923948	XM_001250190	Olfr1280	Olfactory receptor 1280	0.00	2.7	-1.1	-3.0	---
752	gi_119921644	XM_001254228	LOC786593	Similar to t-cell receptor alpha chain (LOC786593)	0.00	3.0	1.0	-3.0	---

753	gi_119881228	XM_001251762	DVL3	Dishevelled, dsh homolog 3 (drosophila)	0.00	2.3	-1.3	-3.0	---
754	gi_119895593	XR_028187	LOC510849	Similar to protocadherin gamma b6 (LOC510849)	0.01	2.2	-1.3	-3.0	---
755	gi_119894394	XM_585315	BOD1L	Biorientation of chromosomes in cell division 1-like	0.00	2.1	-1.4	-3.0	---
756	gi_51882386	---	---	Aj814910 kn206 bos sp. cDNA clone c0005203o21	0.01	2.3	-1.3	-3.0	---
757	gi_51812990	---	---	Co883056 bovgen_11381 normal cattle brain cDNA clone rzpdp1056b034q 5'	0.00	2.4	-1.2	-3.0	---
758	gi_119935071	XM_001256856	LOC790362	Similar to myst histone acetyltransferase (monocytic leukemia) 4 (LOC790362)	0.01	2.2	-1.3	-3.0	---
759	gi_51883172	---	---	Aj815696 kn206 bos sp. cDNA clone c0005202l4	0.00	2.2	-1.3	-3.0	---
760	gi_119915680	XM_001253103	LOC786846	Similar to olfactory receptor 9, rat orthologue of mouse mor156-2a, transcript variant 1 (LOC786846)	0.01	2.2	-1.3	-3.0	---
761	gi_119907926	XM_869607	OR8H3	Olfactory receptor, family 8, subfamily h, member 3	0.00	2.6	-1.1	-3.0	---
762	gi_119922650	XM_601354	Olfr1239	Olfactory receptor 1239	0.01	2.3	-1.3	-3.0	---
763	gi_51807744	---	---	Co877828 bovgen_06153 normal cattle brain cDNA clone rzpdp1056a1220q 5'	0.00	2.5	-1.2	-3.0	---
764	gi_119895350	XM_001255203	LOC788011	Similar to olfactory receptor olr1566 (LOC788011)	0.00	2.4	-1.2	-3.0	---
765	gi_119923779	XM_001250462	LOC783543	Similar to l antigen family, member 3, transcript variant 2	0.00	2.4	-1.2	-3.0	---
766	gi_119879601	XM_612607	KALRN	Kalirin, rhogef kinase	0.01	2.2	-1.4	-3.0	---
767	gi_51827036	---	---	Co896716 bovgen_25041 normal cattle brain cDNA clone rzpdp1056c101q 5'	0.01	2.2	-1.3	-2.9	---
768	gi_119922048	XM_001254493	NCKAP5	Nck-associated protein 5	0.01	2.1	-1.4	-2.9	---
769	gi_31341372	NM_176674	COX7A1	Cytochrome c oxidase subunit viia polypeptide 1 (muscle)	0.01	2.0	-1.4	-2.9	---
770	gi_75864894	---	---	Dt884531 1437726 marc 7bov cDNA 5'	0.00	2.8	-1.0	-2.9	---
771	gi_117935050	NM_178109	EIF2AK2	Eukaryotic translation initiation factor 2-alpha kinase 2	0.00	2.9	1.0	-2.9	---
772	gi_119921111	XM_001253992	LOC786246	Similar to t-cell receptor alpha chain (LOC786246)	0.00	2.9	1.0	-2.9	---
773*	gi_119921043	XM_001252468	OR52A5	Olfactory receptor, family 52, subfamily a, member 5	0.00	2.8	-1.0	-2.9	---
774	gi_51881271			Aj813795 kn206 bos sp. CDNA clone c0005205j12	0.00	2.7	-1.1	-2.9	---
775	gi_139949155	NM_001083740	GPT	Glutamic-pyruvate transaminase (alanine aminotransferase)	0.00	2.4	-1.2	-2.9	---
776	gi_119929446	XM_001256647	LOC790072	Hypothetical protein (LOC790072)	0.00	3.4	1.2	-2.9	---
777	gi_148226500	NM_001098047	GPR21	G protein-coupled receptor 21	0.01	2.4	-1.2	-2.9	---
778	gi_119925030	XM_001251274	LOC786338	Hypothetical protein (LOC786338)	0.00	2.9	1.0	-2.9	---
779	gi_77736166	NM_001034610	RIPK2	Receptor-interacting serine-threonine kinase 2	0.00	2.6	-1.1	-2.9	---
780	gi_51818876	---	---	Co888591 bovgen_16916 normal cattle brain cDNA clone rzpdp1056l0443q 5'	0.01	2.2	-1.3	-2.9	---
781	gi_51818604	---	---	Co888319 bovgen_16644 normal cattle brain cDNA clone rzpdp1056e045q 5'	0.01	2.2	-1.3	-2.9	---
782	gi_119924682	XM_581926	LOC538674	Similar to protocadherin (LOC538674)	0.01	2.2	-1.3	-2.9	---
783	gi_68427045	---	---	Am027970 am027970 kn-252-lymph, bos indicus bos indicus cDNA clone c0007393m15 3'	0.00	3.2	1.1	-2.9	---
784	gi_119892509	XM_001254905	Olfr794	Olfactory receptor 794	0.01	2.2	-1.3	-2.9	---
785	gi_119895309	XM_601243	OR2C3	Olfactory receptor, family 2, subfamily c, member 3	0.00	2.7	-1.1	-2.9	---
786*	gi_119920034	XM_001251323	LOC784096	Riken cDNA 1700014n06 gene	0.00	2.5	-1.2	-2.9	---
787*	gi_119928444	XM_001256165	OR52A1	Olfactory receptor, family 52, subfamily a, member 1	0.00	2.8	-1.0	-2.9	---
788	gi_51819323	---	---	Co889038 bovgen_17363 normal cattle brain cDNA clone rzpdp1056g0341q 5'	0.00	2.1	-1.4	-2.9	---
789	gi_119902109	XM_001251139	LOC782490	Hypothetical protein (LOC782490)	0.01	2.3	-1.2	-2.9	---
790*	gi_119892559	XM_001255392	OR6C6	Olfactory receptor, family 6, subfamily c, member 6	0.00	2.7	-1.1	-2.9	---
791	gi_119924200	XM_614803	GLRA3	Glycine receptor, alpha 3	0.00	2.7	-1.0	-2.9	---
792	gi_119921093	XM_869126	LOC616970	Similar to t-cell receptor delta (LOC616970)	0.00	2.6	-1.1	-2.9	---
793*	gi_119931641	XM_613045	STK17A	Serine/threonine kinase 17a	0.00	2.5	-1.1	-2.9	---
794	gi_119934383	XM_001254673	LOC787205	Hypothetical protein (LOC787205)	0.01	2.1	-1.4	-2.9	---
795	gi_76662918	XM_868812	OR2L2	Olfactory receptor, family 2, subfamily l, member 2	0.01	2.3	-1.3	-2.9	---
796	gi_50872142	NM_001002890	KLRD1	Killer cell lectin-like receptor subfamily d, member 1	0.01	2.2	-1.3	-2.9	---
797	gi_51813436	---	---	Co883502 bovgen_11827 normal cattle brain cDNA clone rzpdp1056i048q 5'	0.02	2.1	-1.3	-2.9	---
798	gi_119925323	XM_001255584	Olfr905	Olfactory receptor 905	0.00	2.5	-1.2	-2.9	---
799	gi_119927767	XM_868179	OR5M3	Olfactory receptor, family 5, subfamily m, member 3	0.00	2.6	-1.1	-2.9	---
800	gi_51813625	---	---	Co883682 bovgen_12007 normal cattle brain cDNA clone rzpdp1056b1620q 5'	0.01	2.3	-1.2	-2.9	---
801	gi_139947537	NM_001083736	JAM2	Junctional adhesion molecule 2	0.00	4.4	1.5	-2.9	---
802	gi_116004236	NM_001077009	P2RY14	Purinergic receptor p2y, g-protein coupled, 14	0.00	2.7	-1.1	-2.9	---
803	gi_119915421	XM_584616	LOC507917	MHC class i heavy chain (LOC507917)	0.00	2.6	-1.1	-2.9	---
804*	gi_76677494	XM_587133	OR6C4	Olfactory receptor, family 6, subfamily c, member 4	0.01	2.2	-1.3	-2.9	---
805	gi_51820271	---	---	Co889984 bovgen_18309 normal cattle brain cDNA clone rzpdp1056c0838q 5'	0.00	2.9	1.0	-2.9	---
806	gi_119916333	XM_001250672	LOC782780	Hypothetical protein (LOC782780)	0.00	2.6	-1.1	-2.9	---
807	gi_119894667	XM_001256348	LOC789667	Similar to olf4 (LOC789667)	0.00	3.1	1.1	-2.9	---
808	gi_157427975	NM_001105426	RNASE13	Ribonuclease, rnase a family, 13 (non-active)	0.00	3.5	1.2	-2.9	---
809*	gi_76635921	XM_596754	Olfr561	Olfactory receptor 561	0.01	2.3	-1.3	-2.9	---
810	gi_119906418	XM_001250149	LOC782051	Similar to alpha 2 actin (LOC782051)	0.00	2.7	-1.0	-2.9	---
811	gi_119892569	XM_001255472	LOC788396	Similar to olfactory receptor mor265-1 (LOC788396)	0.00	3.1	1.1	-2.8	---
812	gi_51809379	---	---	Co879455 bovgen_07782 normal cattle brain cDNA clone rzpdp1056l0127q 5'	0.03	2.0	-1.4	-2.8	---
813	gi_119918790	XM_001255453	LOC788371	Hypothetical protein (LOC788371)	0.02	2.0	-1.4	-2.8	---
814	gi_51885865	---	---	Aj818389 kn206 bos sp. CDNA clone c0006012c16	0.01	2.2	-1.3	-2.8	---
815	gi_119921256	XM_001249957	OR5M10	Olfactory receptor, family 5, subfamily m, member 10	0.02	2.0	-1.4	-2.8	---
816	gi_119922015	XM_001253993	OR8J1	Olfactory receptor, family 8, subfamily j, member 1	0.01	2.5	-1.2	-2.8	---
817	gi_31341996	NM_174439	TMPRSS15	Transmembrane protease, serine 15	0.01	2.3	-1.2	-2.8	---
818	gi_51821972	---	---	Co891674 bovgen_19999 normal cattle brain cDNA clone rzpdp1056a0534q 5'	0.00	2.5	-1.1	-2.8	---
819	gi_118151099	NM_001078004	PELI1	Pellino homolog 1 (drosophila)	0.00	3.8	1.3	-2.8	---
820	gi_119902376	XM_001253943	VPS39	Similar to vps39/vam6-like protein (LOC520990)	0.01	2.2	-1.3	-2.8	---
821	gi_119920980	XM_001250243	OR51F2	Olfactory receptor, family 51, subfamily f, member 2	0.00	2.4	-1.2	-2.8	---
822	gi_119917386	XM_001253094	LOC784919	Similar to olfactory receptor olr507 (LOC784919)	0.01	2.4	-1.2	-2.8	---
823	gi_119921914	XM_001250926	LOC782296	Similar to olfactory receptor mor114-3 (LOC782296)	0.00	2.7	-1.0	-2.8	---
824	gi_51817560	---	---	Co887275 bovgen_15600 normal cattle brain cDNA clone rzpdp1056k1923q 5'	0.00	2.5	-1.1	-2.8	---
825	gi_119909160	XR_028423	LOC615031	Hypothetical (LOC615031)	0.00	2.6	-1.1	-2.8	---
826	gi_149642782	NM_001098895	SLC25A30	Solute carrier family 25, member 30	0.00	2.2	-1.3	-2.8	---
827*	gi_119902302	XM_001254703	Olfr1276	Olfactory receptor 1276	0.01	2.2	-1.3	-2.8	---
828*	gi_119895412	XM_600845	Olfr30	Olfactory receptor 30	0.00	2.5	-1.1	-2.8	---
829	gi_119903309	XM_605410	SRD5A2	Steroid-5-alpha-reductase, alpha polypeptide 2 (3-oxo-5 alpha-steroid delta 4-dehydrogenase alpha 2)	0.01	2.1	-1.3	-2.8	---
830	gi_51886476	---	---	Aj819000 kn206 bos sp. cDNA clone c0006014a01	0.00	2.3	-1.2	-2.8	---
831	gi_119922890	XM_001255730	Olfr1316	Olfactory receptor 1316	0.00	2.5	-1.1	-2.8	---
832	gi_76684604	XM_870419	Olr468	Olfactory receptor 468	0.01	2.3	-1.2	-2.8	---
833	gi_119907381	XM_593669	OR52H1	Olfactory receptor, family 52, subfamily h, member 1	0.01	2.3	-1.2	-2.8	---
834	gi_119911558	XM_588697	TNFAIP1	Tumor necrosis factor, alpha-induced protein 1 (endothelial)	0.00	2.7	-1.0	-2.8	---
835	gi_119892515	XM_584195	LOC507560	Similar to olfactory receptor olr920 (LOC507560)	0.01	2.4	-1.2	-2.8	---
836	gi_119910989	XR_028595	LOC788051	Similar to zinc finger protein 616 (LOC788051)	0.03	2.0	-1.4	-2.8	---
837	gi_119908142	XM_001249329	LOC780987	Hypothetical protein (LOC780987)	0.00	2.2	-1.3	-2.8	---

838	gi_119926167	XM_001255280	LOC788129	Similar to seven transmembrane helix receptor (LOC788129)	0.01	2.3	-1.2	-2.8	---
839	gi_27805856	NM_174285	CREB1	Camp responsive element binding protein 1	0.00	2.1	-1.3	-2.8	---
840	gi_119920625	XM_001250573	LOC782015	Similar to melanoma antigen family b, 4 (LOC782015)	0.00	2.4	-1.2	-2.8	---
841	gi_119887404	XM_589101	FSIP2	Fibrous sheath interacting protein 2	0.00	2.4	-1.2	-2.8	---
842	gi_119931421	XM_001254549	LOC787028	Similar to olfactory receptor mor111-1 (LOC787028)	0.00	2.8	1.0	-2.8	---
843	gi_119893030	XM_584745	LOC508026	Similar to pregnancy-zone protein (LOC508026)	0.03	2.0	-1.4	-2.8	---
844	gi_119894646	XM_590569	LOC512956	Similar to olfactory receptor (LOC512956)	0.00	2.6	-1.1	-2.8	---
845	gi_119921997	XM_001253442	LOC785406	Similar to olfactory receptor mor185-5 (LOC785406)	0.00	2.8	1.0	-2.8	---
846*	gi_119892531	XM_001255188	Olr1012	Olfactory receptor 1012	0.01	2.3	-1.2	-2.8	---
847	gi_119903385	XM_599529	Ttc39d	Tetratricopeptide repeat domain 39d	0.00	2.5	-1.1	-2.8	---
848	gi_119922520	XM_001252579	LOC784191	Similar to seven transmembrane helix receptor (LOC784191)	0.00	2.5	-1.1	-2.8	---
849	gi_149643056	NM_001099198	MGC165685	Hypothetical protein loc786491 (MGC165685)	0.01	2.2	-1.3	-2.8	---
850	gi_119892549	XM_001255334	LOC788199	Similar to olfactory receptor mor113-4 (LOC788199)	0.01	2.2	-1.2	-2.8	---
851*	gi_119922221	XM_001254166	Olfr1199	Olfactory receptor 1199	0.00	2.7	1.0	-2.8	---
852	gi_119892152	XM_001250287	LOC781800	Similar to ubie-yghl1 fusion protein (LOC781800)	0.02	2.1	-1.3	-2.8	---
853	gi_119912466	XM_001255693	LOC789252	Similar to copper containing amine oxidase 3 (LOC789252)	0.01	2.2	-1.3	-2.8	---
854	gi_51882753	---	---	Aj815277 aj815277 kn206 bos sp. CDNA clone c0005203f3	0.01	2.2	-1.2	-2.8	---
855	gi_119909126	XM_001252899	LOC784650	Similar to guanylate cyclase 70 kda subunit (LOC784650)	0.01	2.3	-1.2	-2.8	---
856	gi_119925348	XM_001250814	LOC785762	Similar to prostaglandin f synthase-like1 protein (LOC785762)	0.00	2.7	1.0	-2.8	---
857	gi_119922591	XM_001254813	LOC787405	Similar to t cell receptor delta chain (LOC787405)	0.00	3.4	1.2	-2.8	---
858	gi_51809994	---	---	Co880069 bovgen_08394 normal cattle brain cDNA clone rzpdp1056f1825q 5'	0.00	2.4	-1.2	-2.8	---
859	gi_119922293	XM_610277	Gm4911	Predicted pseudogene 4911	0.00	2.6	-1.1	-2.8	---
860	gi_119902304	XM_001254746	Olfr1277	Olfactory receptor 1277	0.00	2.5	-1.1	-2.8	---
861	gi_119910745	XM_870804	GNG8	Guanine nucleotide binding protein (G protein), gamma 8	0.00	2.4	-1.1	-2.8	---
862	gi_116004418	NM_001077100	MGC137454	Hypothetical protein (MGC137454)	0.00	2.5	-1.1	-2.7	---
863	gi_119921172	XM_001255156	LOC787947	Similar to Cfolf4 (LOC787947)	0.01	2.3	-1.2	-2.7	---
864	gi_119924969	XM_590908	OR52N5	Olfactory receptor, family 52, subfamily n, member 5	0.00	2.5	-1.1	-2.7	---
865	gi_119924106	XM_001254827	LOC787427	Similar to serpinb3 (LOC787427)	0.01	2.4	-1.2	-2.7	---
866	gi_119903698	XM_001253179	LOC785033	Similar to olfactory receptor mor245-12 (LOC785033)	0.01	2.3	-1.2	-2.7	---
867	gi_88319945	NM_176638	CASP4	Caspase 4, apoptosis-related cysteine peptidase	0.00	3.2	1.2	-2.7	---
868	gi_119894615	XM_868476	OR10H3	Olfactory receptor, family 10, subfamily h, member 3	0.00	2.5	-1.1	-2.7	---
869	gi_163915356	NM_001113173	CXCL11	Chemokine (c-x-c motif) ligand 11 (CXCL11)	0.01	2.4	-1.1	-2.7	---
870	gi_119645494	---	---	Eh174267 lb01651.cr_a21 gc_bgc-16 cDNA clone image:8384735 5'	0.00	4.9	1.8	-2.7	---
871	gi_119914158	XM_001255194	LOC787999	Hypothetical protein (LOC787999)	0.00	2.6	-1.0	-2.7	---
872	gi_119907422	XM_592902	LOC514976	Similar to olfactory receptor hpfh1or (LOC514976)	0.02	2.1	-1.3	-2.7	---
873	gi_119935565	XM_001257018	LOC790589	Similar to olfactory receptor olr726 (LOC790589)	0.00	2.5	-1.1	-2.7	---
874	gi_119893818	XM_612659	LOC533295	Similar to y53f4b.4a (LOC533295)	0.01	2.4	-1.1	-2.7	---
875	gi_115497081	NM_001075656	JUNB	Jun b proto-oncogene	0.00	3.9	1.4	-2.7	---
876	gi_116003880	NM_001076831	COL3A1	Collagen, type iii, alpha 1	0.00	2.7	1.0	-2.7	---
877	gi_119929284	XM_001250912	LOC785874	Hypothetical protein (LOC785874)	0.01	2.4	-1.2	-2.7	---
878	gi_119927416	XM_001256048	LOC789240	Similar to testis derived transcript (LOC789240)	0.01	2.2	-1.2	-2.7	---
879	gi_119902188	XM_586246	OR4M1	Olfactory receptor, family 4, subfamily m, member 1	0.02	2.1	-1.3	-2.7	---
880	gi_51822925	---	---	Co892625 bovgen_20950 normal cattle brain cDNA clone rzpdp1056k1533q 5'	0.00	2.2	-1.2	-2.7	---
881	gi_119902105	XM_001250965	LOC782316	Similar to t cell receptor alpha chain (LOC782316)	0.00	3.3	1.2	-2.7	---
882	gi_29394713	---	---	Cb531727 754593 marc 6bov cDNA 3'	0.00	2.4	-1.1	-2.7	---
883	gi_76686152	XM_593724	OR4C46	Olfactory receptor, family 4, subfamily c, member 46	0.00	2.3	-1.2	-2.7	---
884*	gi_119920037	XR_027774	LOC784212	Riken cDNA 1700014n06 gene	0.02	2.0	-1.3	-2.7	---
885	gi_76677166	XM_598492	OR6Y1	Olfactory receptor, family 6, subfamily y, member 1	0.00	2.4	-1.1	-2.7	---
886*	gi_119902168	XM_001252434	OR11G2	Olfactory receptor, family 11, subfamily g, member 2	0.00	2.5	-1.1	-2.7	---
887	gi_31342172	NM_174376	KLRA1	Killer cell lectin-like receptor subfamily a pseudogene 1	0.00	3.2	1.2	-2.7	---
888	gi_119901504	XM_600290	Taar4	Trace amine-associated receptor 4	0.00	2.5	-1.1	-2.7	---
889	gi_119887587	XM_001252615	SCN9A	Sodium channel, voltage-gated, type ix, alpha subunit	0.01	2.2	-1.2	-2.7	---
890	gi_41386789	NM_174356	IL12B	Interleukin 12b (natural killer cell stimulatory factor 2, cytotoxic lymphocyte maturation factor 2, p40)	0.00	2.3	-1.2	-2.7	---
891	gi_119916421	XM_001249415	LOC781345	Hypothetical protein (LOC781345)	0.01	2.1	-1.3	-2.7	---
892	gi_119884883	XM_606901	PRKCI	Protein kinase c, iota	0.00	2.6	-1.0	-2.7	---
893	gi_119928081	XM_001251993	LOC783368	Similar to Attractin (LOC783368)	0.01	2.2	-1.2	-2.7	---
894	gi_7056080_	---	---	Aw485974 69107 marc 4bov cDNA 5'	0.01	2.1	-1.3	-2.7	---
895	gi_115497291	NM_001075634	TCIRG1	T-cell, immune regulator 1, atpase, h+ transporting, lysosomal v0 subunit a3	0.00	2.1	-1.3	-2.7	---
896	gi_31341616	NM_174579	POU1F1	Pou class 1 homeobox 1	0.01	2.2	-1.2	-2.7	---
897	gi_119925795	XM_586018	OR9G4	Olfactory receptor, family 9, subfamily g, member 4	0.01	2.4	-1.1	-2.7	---
898	gi_119928284	XM_580340	OR13C9	Olfactory receptor, family 13, subfamily c, member 9	0.00	2.6	1.0	-2.7	---
899	gi_119915640	XM_592285	Olr1768	Olfactory receptor 1768	0.01	2.4	-1.1	-2.7	---
900	gi_119926136	XM_599438	PM20D2	Peptidase m20 domain containing 2	0.00	4.2	1.6	-2.7	---
901	gi_134085852	NM_001083407	SPATA20	Spermatogenesis associated 20	0.00	2.4	-1.1	-2.7	---
902	gi_119901508	XM_001253652	TAAR2	Trace amine associated receptor 2	0.00	2.4	-1.1	-2.7	---
903	gi_61808422	XM_586491	OR4C6	Olfactory receptor, family 4, subfamily c, member 6	0.01	2.2	-1.2	-2.7	---
904	gi_51883358	---	---	Aj815882 kn206 bos sp. CDNA clone c0005202h22	0.02	2.1	-1.3	-2.7	---
905	gi_76680252	XM_870182	LOC521256	Similar to olfactory receptor olfr566 (LOC521256)	0.01	2.2	-1.2	-2.7	---
906	gi_119906377	XR_028594	LOC515601	Similar to hyaluronan synthase type 2 (LOC515601)	0.01	2.3	-1.2	-2.7	---
907	gi_51809708	---	---	Co879785 bovgen_08110 normal cattle brain cDNA clone rzpdp1056k1413q 5'	0.00	2.5	-1.1	-2.7	---
908	gi_119908080	XM_001256129	LOC789351	Hypothetical protein (LOC789351)	0.00	2.4	-1.1	-2.7	---
909	gi_77404247	NM_001034041	SNCA	Synuclein, alpha (non a4 component of amyloid precursor)	0.00	2.5	-1.1	-2.7	---
910	gi_119903002	XM_867514	TTC8	Tetratricopeptide repeat domain 8	0.00	2.3	-1.2	-2.7	---
911	gi_119909243	XM_614458	CLIP1	Cap-gly domain containing linker protein 1	0.00	2.2	-1.2	-2.6	---
912	gi_119924434	XM_001251222	LOC782594	Similar to trace amine receptor 4 (LOC782594)	0.01	2.2	-1.2	-2.6	---
913	gi_119926744	XM_001251442	LOC787053	Hypothetical protein (LOC787053)	0.00	3.7	1.4	-2.6	---
914	gi_119907881	XM_001251517	LOC782866	Similar to olfactory receptor olfr987 (LOC782866)	0.01	2.3	-1.2	-2.6	---
915	gi_119913890	XM_001249357	LOC781017	Hypothetical protein (LOC781017)	0.01	2.2	-1.2	-2.6	---
916	gi_119924826	XM_001253694	LOC785794	Similar to g antigen, family d, 1 (LOC785794)	0.03	2.0	-1.3	-2.6	---
917	gi_149643100	NM_001098958	CDKN1A	Cyclin-dependent kinase inhibitor 1a (p21, cip1)	0.00	2.2	-1.2	-2.6	---
918	gi_51824812	---	---	Co894504 bovgen_22829 normal cattle brain cDNA clone rzpdp1056i0644q 5'	0.01	2.2	-1.2	-2.6	---
919	gi_119924383	XM_001254912	Olfr1124	Olfactory receptor 1124	0.00	2.5	-1.1	-2.6	---
920	gi_51888409	---	---	Aj820933 kn206 bos sp. CDNA clone c0006019i15	0.01	2.3	-1.2	-2.6	---
921	gi_51880814	---	---	Aj813338 kn206 bos sp. CDNA clone c0005206l14	0.01	2.2	-1.2	-2.6	---
922	gi_119920952	XM_870254	LOC617921	Similar to olfactory receptor mor14-2 (LOC617921)	0.01	2.2	-1.2	-2.6	---
923	gi_119907885	XM_001251593	LOC782933	Similar to olfactory receptor olfr987 (LOC782933)	0.03	2.0	-1.3	-2.6	---
924	gi_31342685	NM_174169	RGS7	Regulator of g-protein signaling 7	0.01	2.3	-1.2	-2.6	---
925	gi_31342076	NM_174411	PAG1B	Pregnancy-associated glycoprotein 1 (pag1b)	0.02	2.1	-1.3	-2.6	---
926	gi_119917416	XM_001250496	LOC782888	Hypothetical protein (LOC782888)	0.00	2.6	1.0	-2.6	---
927	gi_119902589	XR_027721	DMXL2	Dmx-like 2	0.00	2.4	-1.1	-2.6	---
928	gi_78050076	NM_001035055	CLDN11	Claudin 11	0.01	2.4	-1.1	-2.6	---
929	gi_158519826	NM_001110096	BEX4	Brain expressed, x-linked 4	0.02	2.2	-1.2	-2.6	---
930	gi_119931487	XM_001255207	LOC788017	Similar to Ser/Thr protein kinase par-1balpha (LOC788017)	0.01	2.1	-1.2	-2.6	---
931	gi_119921691	XM_001249303	LOC781004	Hypothetical protein (LOC781004)	0.00	2.5	1.0	-2.6	---

932*	gi_119921055	XM_001252743	Olr94	Olfactory receptor 94	0.01	2.3	-1.2	-2.6	---
933	gi_75832085	NM_177432	IRF1	Interferon regulatory factor 1 (irf1)	0.00	4.4	1.7	-2.6	---
934	gi_119889562	XM_001250696	LOC782107	Similar to kiaa0466 protein (LOC782107)	0.00	2.1	-1.2	-2.6	---
935	gi_119911429	XR_027573	LOC783256	Similar to brca1-binding helicase-like protein bach1	0.00	2.5	-1.1	-2.6	---
936	gi_119890257	XR_027905	LOC784417	Similar to cytochrome p450, family 4,subfamily a,polypeptide 11	0.02	2.0	-1.3	-2.6	---
937	gi_119915977	XM_588519	NFATC1	Nuclear factor of activated t-cells, cytoplasmic, calcineurin-dependent 1	0.00	2.5	1.0	-2.6	---
938	gi_119922217	XM_593873	Olfr1257	Olfactory receptor 1257	0.00	2.5	1.0	-2.6	---
939*	gi_119925767	XM_868453	LOC616431	Riken cDNA 1700014n06 gene	0.00	2.4	-1.1	-2.6	---
940	gi_119923068	XM_001253958	LOC786202	Similar to olfactory receptor (LOC786202)	0.02	2.2	-1.2	-2.6	---
941	gi_115495730	NM_001076164	PPP1R3C	Protein phosphatase 1, regulatory (inhibitor) subunit 3c	0.03	2.0	-1.3	-2.6	---
942	gi_164452934	NM_001080297	SWAP70	Swap-70 protein (swap70)	0.00	2.1	-1.2	-2.6	---
943	gi_51885968	---	---	Aj818492 kn206 bos sp. cDNA clone c0006012h09	0.01	2.3	-1.1	-2.6	---
944	gi_51885590	---	---	Aj818114 kn206 bos sp. cDNA clone c0006011d09	0.00	3.4	1.3	-2.6	---
945*	gi_119929994	XM_001256551	OR13F1	Olfactory receptor, family 13, subfamily f, member 1	0.00	2.6	1.0	-2.6	---
946	gi_119905975	XM_602010	NCOA3	Nuclear receptor coactivator 3	0.01	2.2	-1.2	-2.6	---
947	gi_116004376	NM_001077079	C1orf185	Chromosome 1 open reading frame 185	0.02	2.1	-1.2	-2.6	---
948	gi_27806988	NM_174545	GABRG2	Gamma-aminobutyric acid (gaba) a receptor, gamma 2	0.00	2.4	-1.1	-2.6	---
949	gi_119910565	XM_001256367	LOC789693	Hypothetical protein (LOC789693)	0.00	2.2	-1.2	-2.6	---
950	gi_119887145	XR_028592	SIK1	Salt-inducible kinase 1	0.00	2.1	-1.2	-2.6	---
951	gi_157428069	NM_001105473	STOM	Stomatin	0.00	4.0	1.6	-2.6	---
952	gi_116004410	NM_001077096	TNFRSF19	Tumor necrosis factor receptor superfamily, member 19	0.00	2.2	-1.1	-2.6	---
953	gi_119902141	XM_001252038	RNASE11	Ribonuclease, rnase a family, 11 (non-active)	0.02	2.1	-1.2	-2.5	---
954	gi_119905174	XR_028303	LOC505099	Hypothetical (LOC505099)	0.01	2.2	-1.2	-2.5	---
955	gi_68425682	---	---	Am026859 kn-252-lymph, cDNA clone c0007393h11 3'	0.01	2.3	-1.1	-2.5	---
956	gi_119922207	XM_001253994	LOC786248	Similar to c4bp alpha chain (LOC786248)	0.03	2.0	-1.3	-2.5	---
957	gi_28603729	NM_176626	PAG18	Pregnancy-associated glycoprotein 18 (PAG18)	0.00	2.4	-1.0	-2.5	---
958	gi_119912262	XM_001254120	KRTAP4-6	Keratin associated protein 4-6	0.02	2.1	-1.2	-2.5	---
959	gi_51814500	---	---	Co884481 bovgen_12806 normal cattle brain cDNA clone rzpdp1056g0217q 5'	0.01	2.2	-1.1	-2.5	---
960	gi_115497393	NM_001076097	SULT1C4	Sulfotransferase family, cytosolic, 1c, member 4 (SULT1C4)	0.03	2.0	-1.3	-2.5	---
961	gi_119927333	XM_001255661	LOC788676	Similar to t-cell receptor alpha chain (LOC788676)	0.01	2.2	-1.1	-2.5	---
962	gi_94966908	NM_001040554	HLA-A	Major histocompatibility complex, class i, a	0.00	4.0	1.6	-2.5	---
963*	gi_119929795	XM_581848	OR8A1	Olfactory receptor, family 8, subfamily a, member 1	0.01	2.2	-1.2	-2.5	---
964	gi_119928966	XM_001253584	LOC785624	Similar to olf4 (LOC785624)	0.01	2.2	-1.1	-2.5	---
965	gi_119922291	XM_001251181	MAGEB17	Melanoma antigen family b, 17	0.02	2.0	-1.2	-2.5	---
966	gi_51887303	---	---	Aj819827 aj819827 kn206 bos sp. CDNA clone c0006016j19	0.01	2.1	-1.2	-2.5	---
967*	gi_119907553	XM_870343	Olfr561	Olfactory receptor 561	0.01	2.2	-1.1	-2.5	---
968	gi_119901893	XM_001251257	DENND4A	Denn/madd domain containing 4a	0.00	2.1	-1.2	-2.5	---
969	gi_119922801	XM_589238	Olfr594	Olfactory receptor 594	0.01	2.3	-1.1	-2.5	---
970*	gi_119924375	XM_001254801	OR5F1	Olfactory receptor, family 5, subfamily f, member 1	0.01	2.3	-1.1	-2.5	---
971	gi_76651124	XM_870382	Olfr124	Olfactory receptor 124	0.01	2.2	-1.2	-2.5	---
972	gi_119927729	XM_001254998	Olfr143	Olfactory receptor 143	0.01	2.2	-1.1	-2.5	---
973	gi_134085628	NM_001083391	ELMO2	Engulfment and cell motility 2	0.00	2.3	-1.1	-2.5	---
974	gi_115496269	NM_001075993	ODF2L	Outer dense fiber of sperm tails 2-like	0.02	2.0	-1.2	-2.5	---
975	gi_119903020	XM_001251107	B2M	Beta-2-microglobulin	0.00	2.2	-1.2	-2.5	---
976	gi_119920001	XM_001250962	LOC783475	Hypothetical protein (LOC783475)	0.01	2.3	-1.1	-2.5	---
977	gi_119888344	XM_001252286	LOC784637	Similar to bicaudal d homolog 1 (drosophila) (LOC784637)	0.02	2.0	-1.2	-2.5	---
978	gi_119930598	XM_001255904	LOC789026	Hypothetical protein (LOC789026)	0.01	2.4	1.0	-2.5	---
979*	gi_119891769	XM_001249423	INSIG1	Insulin induced gene 1	0.00	2.4	1.0	-2.5	---
980	gi_119937584	XM_871051	LOC618728	Similar to neural cell adhesion protein (LOC618728)	0.02	2.1	-1.2	-2.5	---
981	gi_119915423	XR_028666	LOC788634	Similar to non-classical mhc class i antigen (LOC788634)	0.01	2.1	-1.2	-2.5	---
982	gi_119889249	XM_581374	ADAR	Adenosine deaminase, RNA-specific	0.00	4.0	1.6	-2.5	---
983	gi_119921920	XM_001251100	LOC782474	Similar to olfactory receptor mor112-1 (LOC782474)	0.02	2.2	-1.1	-2.5	---
984*	gi_119892609	XM_867045	OR6C4	Olfactory receptor, family 6, subfamily c, member 4	0.01	2.2	-1.1	-2.5	---
985	gi_76616267	XM_870706	TRIM69	Tripartite motif containing 69	0.01	2.2	-1.1	-2.5	---
986*	gi_119889739	XM_001253287	COL11A1	Collagen, type xi, alpha 1	0.00	2.4	1.0	-2.4	---
987	gi_118151015	NM_001077961	NDST3	N-deacetylase/n-sulfotransferase (heparan glucosaminyl) 3	0.00	2.3	-1.1	-2.4	---
988	gi_119915551	XM_871334	Olfr1535	Olfactory receptor 1535	0.01	2.2	-1.1	-2.4	---
989	gi_154152200	NM_001100309	TDRD7	Tudor domain containing 7	0.00	4.4	1.8	-2.4	---
990	gi_119921007	XM_001251527	LOC782875	Similar to olfactory receptor olr88 (LOC782875)	0.01	2.2	-1.1	-2.4	---
991	gi_119933559	XM_001256916	LOC790451	Hypothetical protein (LOC790451)	0.00	2.4	1.0	-2.4	---
992	gi_119904810	XM_001253713	LOC785828	Similar to replication protein a2, 32kda (LOC785828)	0.03	2.1	-1.2	-2.4	---
993*	gi_119894398	XM_001253396	OR5W2	Olfactory receptor, family 5, subfamily w, member 2	0.01	2.4	1.0	-2.4	---
994	gi_149643024	NM_001099037	ABCD2	ATP-binding cassette, sub-family d (ald), member 2 (ABCD2)	0.02	2.1	-1.2	-2.4	---
995	gi_119895358	XM_582424	OR2L13	Olfactory receptor, family 2, subfamily l, member 13	0.01	2.2	-1.1	-2.4	---
996	gi_119912322	XM_618105	KRT39	Keratin 39	0.01	2.3	-1.0	-2.4	---
997*	gi_119927679	XM_001254322	OR7D4	Olfactory receptor, family 7, subfamily d, member 4	0.01	2.3	-1.1	-2.4	---
998	gi_119879617	XM_001254174	LOC786513	Similar to leishmanolysin-like (metallopeptidase m8 family)	0.02	2.0	-1.2	-2.4	---
999	gi_119922011	XM_001253957	OR8K1	Olfactory receptor, family 8, subfamily k, member 1	0.02	2.1	-1.2	-2.4	---
1000	gi_76253719	NM_001002892	ST3GAL2	ST3 beta-galactoside alpha-2,3-sialyltransferase 2	0.00	2.4	1.0	-2.4	---
1001	gi_149642586	NM_001098900	SLC44A3	Solute carrier family 44, member 3	0.01	2.2	-1.1	-2.4	---
1002	gi_157074077	NM_001103280	TRDN	Triadin	0.01	2.2	-1.1	-2.4	---
1003	gi_119912444	XM_001255546	LOC789125	Similar to alpha-n-acetylglucosaminidase (LOC789125)	0.00	2.2	-1.1	-2.4	---
1004	gi_119921413	XM_583529	LOC506992	Similar to olfactory receptor mor160-5 (LOC506992)	0.01	2.3	-1.0	-2.4	---
1005	gi_119908975	XM_594035	SETD7	Set domain containing (lysine methyltransferase) 7	0.00	2.1	-1.1	-2.4	---
1006	gi_51883259	---	---	Aj815783 kn206 bos sp. CDNA clone c0005202j4	0.02	2.1	-1.1	-2.4	---
1007	gi_56119115	NM_001007819	DDX4	Dead (asp-glu-ala-asp) box polypeptide 4	0.00	2.4	1.0	-2.4	---
1008	gi_115495458	NM_001075504	NLGN3	Neuroligin 3	0.01	2.1	-1.1	-2.4	---
1009	gi_45469018	---	---	Ck954638 4094593 barc 10bov cDNA clone 10bov33_n24 3'	0.00	2.4	1.0	-2.4	---
1010	gi_155372024	NM_001101150	NOVA1	Neuro-oncological ventral antigen 1 (nova1)	0.01	2.1	-1.1	-2.4	---
1011	gi_119895374	XM_001255418	LOC788323	Similar to olfactory receptor 2t29 (LOC788323)	0.00	2.4	1.0	-2.4	---
1012	gi_119921664	XM_587190	LOC616123	Similar to t cell receptor delta (LOC616123)	0.02	2.0	-1.2	-2.4	---
1013	gi_119902186	XM_869270	LOC617084	Similar to seven transmembrane helix receptor (LOC617084)	0.01	2.3	1.0	-2.4	---
1014	gi_119893491	XM_614586	LOC541108	Similar to hist2h2aa1 protein (LOC541108)	0.01	2.0	-1.2	-2.4	---
1015	gi_119930158	XM_869637	Olfr284	Olfactory receptor 284	0.01	2.3	1.0	-2.4	---
1016	gi_51818470	---	HEY1	Hairy/enhancer-of-split related with yrpw motif 1	0.02	2.1	-1.1	-2.4	---
1017	gi_84000380	NM_001038200	PRP8	Prolactin-related protein viii (PRP8)	0.01	2.2	-1.1	-2.4	---
1018	gi_31341292	NM_176643	DDHD1	Ddhd domain containing 1	0.00	2.2	-1.1	-2.4	---
1019	gi_119921234	XM_597790	RAPGEF5	Rap guanine nucleotide exchange factor (GEF) 5	0.02	2.0	-1.2	-2.4	---
1020	gi_119892869	XM_871851	CAPRIN2	Caprin family member 2	0.00	2.3	-1.0	-2.4	---
1021	gi_51880611	---	---	Aj813135 aj813135 kn206 bos sp. cDNA clone c0005206g15	0.01	2.0	-1.2	-2.3	---
1022	gi_115496829	NM_001075309	GPM6A	Glycoprotein m6a	0.01	2.3	1.0	-2.3	---
1023	gi_119895074	XM_001255309	LOC789216	Similar to interferon regulatory factor 1 (LOC789216)	0.00	4.5	1.9	-2.3	---
1024	gi_51817930	---	---	Co887645 bovgen_15970 normal cattle brain cDNA clone rzpdp1056l1213q 5'	0.03	2.1	-1.1	-2.3	---
1025	gi_149642938	NM_001098988	NEK6	Nima (never in mitosis gene a)-related kinase 6	0.00	3.5	1.5	-2.3	---
1026	gi_119893961	XM_598333	RASSF6	Ras association (ralgds/af-6) domain family member 6	0.02	2.1	-1.1	-2.3	---
1027	gi_31341715	NM_174543	GABRA4	Gamma-aminobutyric acid (gaba) a receptor, alpha 4	0.01	2.3	1.0	-2.3	---
1028	gi_119923620	XM_609508	LOC531024	Similar to olfactory receptor olfr1197 (LOC531024)	0.01	2.3	1.0	-2.3	---
1029	gi_154385465	---	---	Ev628744 lb02244.cr_a21 gc_bgc-22 cDNA clone	0.01	2.1	-1.1	-2.3	---

				image:8596319 5'					
1030	gi_51884285	---	---	Aj816809 kn206 bos sp. CDNA clone c0005209a1	0.01	2.1	-1.1	-2.3	---
1031	gi_119908469	XM_001252162	DVL1	Dishevelled, dsh homolog 1 (drosophila)	0.01	2.0	-1.1	-2.3	---
1032	gi_62751672	NM_001015586	DSTN	Destrin (actin depolymerizing factor)	0.01	2.2	-1.1	-2.3	---
1033	gi_119914058	XM_001249413	C14orf129	Chromosome 14 open reading frame 129	0.01	2.2	1.0	-2.3	---
1034	gi_147900717	NM_001098141	GYPA	Glycophorin a	0.01	2.2	-1.0	-2.3	---
1035	gi_119912260	XM_001254106	LOC787090	Similar to hair keratin cysteine rich protein (LOC787090)	0.02	2.1	-1.1	-2.3	---
1036	gi_119875947	XM_615721	NCAM2	Neural cell adhesion molecule 2	0.02	2.1	-1.1	-2.3	---
1037	gi_119924389	XR_027626	LOC784129	Hypothetical protein (LOC784129)	0.03	2.0	-1.1	-2.3	---
1038	gi_119879088	XM_001252292	OR5H1	Olfactory receptor, family 5, subfamily h, member 1	0.01	2.1	-1.1	-2.3	---
1039	gi_119894037	XM_001251291	LOC782655	Hypothetical protein (LOC782655)	0.01	2.3	1.0	-2.3	---
1040	gi_29263084	---	---	Cb456702 713982 marc 6bov cDNA 3'	0.01	2.1	-1.1	-2.3	---
1041	gi_119924185	XM_001255673	OR4D1	Olfactory receptor, family 4, subfamily d, member 1	0.01	2.1	-1.1	-2.3	---
1042*	gi_119892551	XM_001255346	OR6C74	Olfactory receptor, family 6, subfamily c, member 74	0.01	2.2	-1.0	-2.3	---
1043	gi_114053296	NM_001046390	TES	Testis derived transcript (3 lim domains)	0.01	2.1	-1.1	-2.3	---
1044*	gi_119892565	XM_001255442	OR6C6	Olfactory receptor, family 6, subfamily c, member 6	0.01	2.2	1.0	-2.3	---
1045*	gi_119890804	XM_001252604	SNX13	Sorting nexin 13	0.01	2.1	-1.1	-2.3	---
1046	gi_119892287	XM_001252824	LOC785803	Similar to lysozyme (LOC785803)	0.01	2.3	1.0	-2.3	---
1047	gi_76627174	XM_867591	LOC615713	Hypothetical (LOC615713)	0.01	2.2	-1.1	-2.3	---
1048	gi_119878574	XM_595936	CADM2	Cell adhesion molecule 2	0.01	2.1	-1.1	-2.3	---
1049	gi_51810612	---	---	Co880683 bovgen_09008 normal cattle brain cDNA clone rzpdp1056e1113q 5'	0.01	2.1	-1.1	-2.3	---
1050	gi_119921417	XM_586484	Olfr282	Olfactory receptor 282	0.01	2.1	-1.1	-2.3	---
1051	gi_157279882	NM_001104987	MCTP1	Multiple c2 domains, transmembrane 1	0.01	2.2	-1.0	-2.3	---
1052	gi_51810298	---	---	Co880369 bovgen_08694 normal cattle brain cDNA clone rzpdp1056f177q 5'	0.01	2.2	1.0	-2.3	---
1053	gi_51887857	---	---	Aj820381 kn206 bos sp. CDNA clone c0006018e07	0.01	2.2	1.0	-2.3	---
1054	gi_76623803	XM_586022	LOC509128	Similar to olfactory receptor, family 11, subfamily h, member 1	0.01	2.2	1.0	-2.3	---
1055	gi_119928697	XM_593499	OR4K15	Olfactory receptor, family 4, subfamily k, member 15	0.01	2.1	-1.1	-2.3	---
1056	gi_75832089	NM_181012	IDH1	Isocitrate dehydrogenase 1 (nadp+), soluble	0.02	2.0	-1.1	-2.3	---
1057	gi_119306996	---	---	Ee970422 q25371a FNM cDNA clone q2537 3'	0.01	2.1	-1.1	-2.3	---
1058	gi_119902074	XM_593013	LOC515064	Similar to TCR delta (LOC515064)	0.01	2.2	1.0	-2.3	---
1059*	gi_119895354	XM_001255231	OR2L3	Olfactory receptor, family 2, subfamily l, member 3	0.01	2.1	-1.1	-2.3	---
1060	gi_119887420	XM_001254873	NCKAP1	Nck-associated protein 1	0.01	2.2	-1.0	-2.3	---
1061	gi_119922263	XM_001254600	LOC787105	Similar to t-cell receptor alpha chain (LOC787105)	0.01	2.1	-1.1	-2.2	---
1062	gi_119921087	XM_001253675	LOC785752	Hypothetical protein (LOC785752)	0.02	2.2	1.0	-2.2	---
1063	gi_119906534	XM_612068	PI15	Peptidase inhibitor 15	0.01	2.1	-1.0	-2.2	---
1064	gi_51887457	---	---	Aj819981 kn206 bos sp. CDNA clone c0006017a22	0.03	2.0	-1.1	-2.2	---
1065*	gi_119892977	XM_591626	KLRC1	Killer cell lectin-like receptor subfamily c, member 1	0.01	2.2	1.0	-2.2	---
1066	gi_90991697	NM_001012285	LEPR	Leptin receptor	0.03	2.0	-1.1	-2.2	---
1067	gi_119914208	XM_580659	LOC538493	Similar to chromosome 14 open reading frame 173	0.00	2.2	1.0	-2.2	---
1068	gi_119922421	XM_602604	Olfr1134	Olfactory receptor 1134	0.02	2.1	-1.1	-2.2	---
1069	gi_31342589	NM_174209	UACA	Uveal autoantigen with coiled-coil domains and ankyrin repeats	0.01	2.2	1.0	-2.2	---
1070	gi_119892851	XM_608933	METTL20	Methyltransferase like 20	0.01	2.2	1.0	-2.2	---
1071	gi_119901594	XM_600433	PHACTR2	Phosphatase and actin regulator 2	0.01	2.2	1.0	-2.2	---
1072	gi_119891943	XM_001249912	LRRIQ1	Leucine-rich repeats and iq motif containing 1	0.01	2.1	-1.0	-2.2	---
1073	gi_119922783	XM_001252792	SLC30A9	Solute carrier family 30 (zinc transporter), member 9	0.01	2.0	-1.1	-2.2	---
1074	gi_119918958	XM_583490	LOC506960	Similar to seven transmembrane helix receptor (LOC506960)	0.02	2.1	1.0	-2.2	---
1075	gi_119902535	XM_613448	PRTG	Protogenin	0.02	2.1	-1.0	-2.2	---
1076	gi_119902733	XM_617753	LOC537580	Hypothetical (LOC537580)	0.02	2.1	1.0	-2.2	---
1077	gi_119921109	XM_001253971	LOC786219	Similar to t-cell receptor alpha chain (LOC786219)	0.01	2.2	1.0	-2.2	---
1078	gi_119921057	XM_001252809	LOC784539	Similar to olfactory receptor olfr598 (LOC784539)	0.03	2.0	-1.1	-2.2	---
1079	gi_119928796	XR_028820	LOC789937	Similar to wd and tetratricopeptide repeats protein 1	0.00	2.1	1.0	-2.1	---
1080	gi_119907383	XM_610954	LOC532436	Similar to olfactory receptor mor31-7 (LOC532436)	0.02	2.0	-1.0	-2.1	---
1081	gi_157074135	NM_001103310	LOC789977	Hypothetical (LOC789977)	0.02	2.1	1.0	-2.1	---
1082	gi_51808439	---	---	Co878519 bovgen_06844 normal cattle brain cDNA clone rzpdp1056n0811q 5'	0.02	2.1	1.0	-2.1	---
1083	gi_119913333	XM_614947	CDH9	Cadherin 9, type 2 (T1-cadherin)	0.02	2.1	-1.0	-2.1	---
1084	gi_119892713	XR_028263	LOC505479	Similar to grp94 neighboring nucleotidase (LOC505479)	0.02	2.1	1.0	-2.1	---
1085	gi_76669664	XM_864501	OR6C75	Olfactory receptor, family 6, subfamily c, member 75	0.02	2.1	1.0	-2.1	---
1086*	gi_164420765	NM_001113247	CHN1	Chimerin (chimaerin) 1	0.03	2.0	-1.1	-2.1	---
1087	gi_119915801	XM_001254745	LOC788718	Hypothetical protein (LOC788718)	0.00	3.9	1.8	-2.1	---
1088	gi_148229657	NM_181002	AOC3	Amine oxidase,copper containing 3(vascular adhesion protein 1)	0.02	2.0	-1.0	-2.1	---
1089	gi_119919308	XM_600752	BATF2	Basic leucine zipper transcription factor, atf-like 2	0.01	2.0	1.0	-2.1	---
1090	gi_51820855	---	---	Co890567 bovgen_18892 normal cattle brain cDNA clone rzpdp1056j1149q 5'	0.01	2.0	1.0	-2.1	---
1091	gi_119889551	XM_001250479	LOC781930	Hypothetical protein (LOC781930)	0.01	2.0	-1.0	-2.1	---
1092	gi_119900577	XM_617223	LOC537068	Similar to piwi-like 2 (drosophila) (LOC537068)	0.02	2.1	1.0	-2.1	---
1093	gi_77735964	NM_001034509	LOC515736	Caspase-15 (LOC515736)	0.02	2.0	1.0	-2.1	---

Asterisk (*) beside the serial no indicates duplicate probe present in the modulated dataset

2.1.5 Full list of genes in profile 5 (n = 288)

S.No	SEQ. ID	Acc. No. (RefSeq)	Putative Gene symbol	Gene Name	BL20 LPS Vs BL20 FDR (4h/or18)	BL20 LPS Vs BL20 Abs: FC (4h/or18)	TBL20 Vs BL20 Abs: FC	TBL20 Vs BL20 LPS Abs: FC (4h/or18)	BW720c Response
						↓	↓ ↓	↓	
1	gi_29273881	---	---	Cb467496 733248 marc 6bov cDNA 5'	0.00	-2.8	-367.6	-132.5	---
2	gi_119922045	XM_001254453	LOC786899	Hypothetical protein (LOC786899)	0.01	-2.1	-220.9	-106.5	↑
3	gi_119930329	XM_001253356	LOC785289	Hypothetical protein (LOC785289)	0.00	-2.2	-203.6	-93.3	↑
4	gi_119902260	XM_603355	LOC404176	T-cell receptor delta chain (LOC404176)	0.00	-2.7	-238.3	-88.0	↑
5	gi_119913552	XM_606794	IGF1R	Insulin-like growth factor 1 receptor	0.01	-2.0	-171.5	-85.2	---
6	gi_119925613	XM_583887	GXYLT2	Glucoside xylosyltransferase 2	0.00	-2.7	-222.3	-83.3	---
7	gi_119915839	XM_588122	F13A1	Coagulation factor xiii, a1 polypeptide	0.00	-2.3	-165.6	-71.2	---
8	gi_119917736	XM_609898	SORCS3	Sortilin-related vps10 domain containing receptor 3	0.00	-5.4	-364.8	-67.3	---
9	gi_119919107	XM_591760	SLC15A3	Solute carrier family 15, member 3	0.00	-2.4	-158.8	-66.7	↑
10	gi_119911249	XM_867060	LAIR1	Leukocyte-associated immunoglobulin-like receptor 1	0.00	-3.3	-174.7	-52.8	---
11	gi_119922043	XM_001254436	LOC786880	Hypothetical protein (LOC786880)	0.00	-2.4	-114.4	-47.4	↑
12	gi_119923075	XM_001254039	LOC786327	Hypothetical protein (LOC786327)	0.00	-2.5	-96.9	-39.1	↑
13*	gi_118151215	NM_001078068	PPP1R14C	Protein phosphatase 1, regulatory (inhibitor) subunit 14c	0.00	-6.0	-219.0	-36.3	---
14	gi_119918053	XM_001256302	LOC789595	Hypothetical protein (LOC789595)	0.00	-4.2	-148.2	-35.5	↑
15	gi_119891326	XM_590508	CPA4	Carboxypeptidase a4	0.00	-3.4	-119.2	-35.2	↑
16	gi_119910462	XM_592455	LOC514582	Similar to b-cell receptor CD22-b (LOC514582)	0.00	-2.4	-82.1	-34.8	↑

17	gi_119911490	XM_001252357	LOC785058	Hypothetical protein (LOC785058)	0.00	-7.3	-243.5	-33.5	↑
18	gi_117377406	---	---	Eg706640 nbm28c02.y1 cow lens. Unnormalized (NBM) cDNA clone nbm28c02 5'	0.00	-3.0	-90.8	-30.1	↑
19	gi_75872327	---	---	Dt891920 1473102 marc 7bov cDNA 5'	0.00	-2.2	-62.9	-28.3	---
20	gi_119889163	XM_001251523	FCRLA	Fc receptor-like a	0.00	-2.8	-80.3	-28.2	↑
21	gi_134085858	NM_001083409	C1QTNF1	C1q and tumor necrosis factor related protein 1	0.00	-5.4	-150.3	-27.7	↑
22	gi_119922040	XR_028437	LOC786767	Hypothetical protein (LOC786767)	0.01	-2.1	-50.0	-23.8	↑
23	gi_7055130_	---	---	Aw485024 63440 marc 3bov cDNA 5'	0.00	-3.1	-71.7	-23.3	↑
24	gi_76660614	XM_597941	CCR6	Chemokine (c-c motif) receptor 6	0.00	-3.1	-71.6	-23.2	↑
25	gi_126723186	NM_174198	TLR4	Toll-like receptor 4	0.00	-2.9	-61.4	-21.4	↑
26	gi_134085612	NM_001083388	COL18A1	Collagen, type xviii, alpha 1	0.00	-3.7	-72.5	-19.6	---
27*	gi_119895038	XM_001256059	ZNF77	Similar to zinc finger protein 77 (LOC789258)	0.00	-2.3	-42.3	-18.2	---
28*	gi_119914433	XM_585399	ZNF77	Similar to zinc finger protein 77 (LOC508603)	0.00	-2.3	-39.6	-17.2	---
29	gi_68422364	---	---	Am024035 kn-252-lymph, cDNA clone c0007392c13 3'	0.00	-3.8	-60.5	-16.0	↑
30	gi_119893570	XM_615475	LEF1	Lymphoid enhancer-binding factor 1	0.00	-3.5	-52.4	-15.0	↑
31*	gi_119906950	XM_001251159	PPP1R14C	Protein phosphatase 1, regulatory (inhibitor) subunit 14c	0.00	-6.3	-92.1	-14.7	---
32	gi_119900339	XM_614789	KANK1	Kn motif and ankyrin repeat domains 1	0.00	-3.0	-43.9	-14.6	↑
33	gi_119895702	XM_616288	SH3TC2	Sh3 domain and tetratricopeptide repeats 2	0.01	-2.0	-26.6	-13.1	↑
34	gi_119925247	XM_001254851	LOC787461	Similar to retina-derived pou-domain factor-1 (LOC787461)	0.00	-3.5	-45.4	-13.1	---
35	gi_119909284	XM_868620	HVCN1	Hydrogen voltage-gated channel 1	0.00	-2.3	-30.4	-13.0	↑
36	gi_149642838	NM_001099200	PNPLA1	Patatin-like phospholipase domain containing 1	0.00	-7.5	-93.7	-12.5	---
37	gi_119910899	XM_001254077	LOC786386	Hypothetical protein (LOC786386)	0.00	-2.4	-28.7	-12.0	---
38	gi_119911051	XM_599883	CACNG6	Calcium channel, voltage-dependent, gamma subunit 6	0.00	-2.6	-27.8	-10.6	---
39	gi_119912992	XM_001252543	LOC784141	Hypothetical protein (LOC784141)	0.00	-3.4	-35.1	-10.2	↑
40	gi_119904678	XM_869633	LOC617384	Similar to atpase, aminophospholipid transporter-like, class i, type 8a, member 2 (LOC617384)	0.00	-7.8	-77.8	-10.0	---
41	gi_51822678	---	---	Co892378 bovgen_20703 normal cattle brain cDNA clone rzpdp1056m2034q 5'	0.00	-3.6	-36.1	-9.9	---
42	gi_51809258	---	---	Co879334 bovgen_07661 normal cattle brain cDNA clone rzpdp1056j1530q 5'	0.01	-2.1	-20.5	-9.7	---
43	gi_119919031	XM_869090	VSIG2	Similar to v-set and immunoglobulin domain containing 2	0.00	-2.3	-21.9	-9.3	---
44	gi_51812473	---	---	Co882541 bovgen_10866 normal cattle brain cDNA clone rzpdp1056j2225q 5'	0.00	-2.3	-21.3	-9.3	---
45	gi_119916419	XM_587341	ALPK2	Alpha-kinase 2	0.00	-11.3	-104.0	-9.2	---
46	gi_119920608	XM_001249720	LOC781352	Hypothetical protein (LOC781352)	0.01	-2.1	-19.1	-9.2	---
47	gi_51826329	---	---	Co896012 bovgen_24337 normal cattle brain cDNA clone rzpdp1056e0933q 5'	0.00	-3.0	-26.4	-8.9	↑
48	gi_119911988	XM_582998	SPECC1	Sperm antigen with calponin homology and coiled-coil domains1	0.00	-2.8	-24.4	-8.8	↑
49	gi_119920594	XM_001249399	LOC781057	Hypothetical protein (LOC781057)	0.01	-2.1	-18.2	-8.7	---
50	gi_51821293	---	---	Co891000 bovgen_19325 normal cattle brain cDNA clone rzpdp1056e0735q 5'	0.00	-2.2	-19.5	-8.7	---
51	gi_119920600	XM_001249543	LOC781191	Hypothetical protein (LOC781191)	0.01	-2.0	-17.7	-8.7	↑
52*	gi_119902292	XM_001253121	RASGRP1	Ras guanyl releasing protein 1 (calcium and dag-regulated)	0.00	-2.8	-23.8	-8.6	↑
53	gi_115496172	NM_001075149	MYL4	Myosin, light chain 4, alkali; atrial, embryonic	0.00	-6.9	-58.7	-8.6	↑
54	gi_156120728	NM_001102041	C13orf18	Chromosome 13 open reading frame 18	0.01	-2.1	-17.8	-8.6	↑
55	gi_119913257	XM_616682	SPEF2	Sperm flagellar 2	0.00	-2.5	-20.8	-8.2	---
56	gi_119920598	XM_001249501	LOC781114	Hypothetical protein (LOC781114)	0.02	-2.0	-16.3	-8.2	---
57	gi_119933176	XM_001256699	LOC790148	Similar to mgc127009 protein (LOC790148)	0.01	-2.0	-15.8	-7.9	↑
58	gi_31341796	NM_174511	CCL3	Chemokine (c-c motif) ligand 3	0.00	-3.7	-29.2	-7.8	↑
59	gi_119889183	XR_028030	LOC517126	Similar to fc receptor-like 5 (LOC517126)	0.00	-3.9	-30.0	-7.8	---
60	gi_76672950	XM_607792	GAB2	Grb2-associated binding protein 2	0.00	-2.6	-20.1	-7.8	↑
61	gi_119906188	XM_001253797	LOC786946	Hypothetical protein loc786946 (LOC786946)	0.00	-2.3	-18.1	-7.7	---
62	gi_115496605	NM_001076352	LMO2	Lim domain only 2 (rhombotin-like 1)	0.01	-2.0	-15.7	-7.7	↑
63	gi_119912910	XM_599356	FAM20A	Family with sequence similarity 20, member a	0.00	-2.8	-21.3	-7.7	---
64*	gi_156120738	NM_001102046	POU6F2	Pou class 6 homeobox 2	0.00	-2.9	-22.4	-7.7	---
65	gi_119918583	XR_027958	LOC531034	Similar to synaptopodin 2-like (LOC531034)	0.00	-2.3	-17.6	-7.6	↑
66	gi_119905537	XM_001253283	LOC785870	Similar to prodynorphin (LOC785870)	0.00	-2.8	-20.3	-7.3	---
67*	gi_119902290	XM_612430	RASGRP1	RAS guanyl releasing protein 1 (calcium and dag-regulated)	0.00	-2.8	-20.3	-7.3	↑
68	gi_51810356	---	---	Co880427 bovgen_08752 normal cattle brain cDNA clone rzpdp1056k019q 5'	0.00	-2.4	-17.0	-7.1	↑
69	gi_156523111	NM_001102500	MMRN1	Multimerin 1	0.00	-3.1	-21.8	-7.0	↑
70	gi_31342484	NM_174258	Cald1	Caldesmon 1	0.00	-4.6	-31.7	-6.9	---
71	gi_119910079	XM_592529	LPCAT2	Lysophosphatidylcholine acyltransferase 2	0.01	-2.2	-14.7	-6.8	↑
72	gi_78050050	NM_001035070	ASB14	Ankyrin repeat and socs box-containing 14	0.00	-2.2	-14.8	-6.8	↑
73	gi_119924763	XM_601339	PSD2	Pleckstrin and sec7 domain containing 2	0.00	-5.6	-37.8	-6.8	---
74	gi_119891244	XR_028414	C7orf58	Chromosome 7 open reading frame 58	0.00	-3.2	-21.5	-6.8	↑
75	gi_119919341	XR_027385	LOC520070	Similar to tumor endothelial marker 1, (LOC520070)	0.00	-3.2	-22.0	-6.8	---
76	gi_119893188	XM_608437	LOC529975	Hypothetical (LOC529975)	0.00	-2.6	-17.0	-6.6	---
77	gi_115495262	NM_001075943	PEX5L	Peroxisomal biogenesis factor 5-like	0.00	-2.3	-15.2	-6.5	---
78	gi_119909623	XM_871314	LOC404062	Immunoglobin light chain vj region (LOC404062)	0.00	-4.8	-30.8	-6.4	---
79	gi_118150919	NM_001077905	CPA5	Carboxypeptidase a5	0.00	-4.6	-28.2	-6.1	---
80*	gi_119920009	XM_601830	NXF3	Nuclear rna export factor 3	0.00	-27.3	-166.5	-6.1	---
81	gi_156121314	NM_001102335	PGM5	Phosphoglucomutase 5	0.00	-8.5	-50.8	-6.0	↑
82	gi_115496048	NM_001075977	GMPR	Guanosine monophosphate reductase	0.00	-3.0	-17.7	-6.0	---
83	gi_49411022	---	---	Aj678437 kn224 cDNA clone kn224-026_h03	0.00	-2.7	-16.0	-6.0	---
84	gi_32189337	NM_174143	PIGR	Polymeric immunoglobulin receptor	0.00	-6.4	-38.3	-5.9	↑
85*	gi_119902288	XM_001253077	RASGRP1	Ras guanyl releasing protein 1 (calcium and dag-regulated)	0.00	-2.4	-14.3	-5.9	↑
86	gi_119900832	XM_001249686	LOC781282	Similar to polydom (LOC781282)	0.00	-3.2	-19.1	-5.9	---
87	gi_148238272	NM_001098016	ITIH2	Inter-alpha (globulin) inhibitor h2	0.00	-5.3	-30.8	-5.9	↑
88	gi_89886135	NM_001013585	S1PR1	Sphingosine-1-phosphate receptor 1	0.00	-9.4	-54.6	-5.8	↑
89	gi_51826409	---	---	Co896092 bovgen_24417 normal cattle brain cDNA clone rzpdp1056a0831q 5'	0.00	-11.9	-67.5	-5.7	---
90*	gi_119889658	XM_001252361	KIAA1324	Kiaa1324	0.00	-3.3	-18.6	-5.6	---
91	gi_77404230	NM_001034043	Gulo	Gulonolactone (l-) oxidase	0.00	-4.9	-27.5	-5.6	---
92	gi_51887072	---	---	Aj819596 kn206 bos sp. CDNA clone c0006015o15	0.01	-2.1	-11.4	-5.3	---
93	gi_122692374	NM_001080353	MGC148792	Similar to elafin (mgc148792)	0.00	-3.6	-19.0	-5.3	---
94	gi_31341725	NM_174538	FCGR1A	Fc fragment of igg, high affinity ia, receptor (CD64)	0.00	-2.5	-12.8	-5.2	↑
95	gi_155372098	NM_001101188	ASB16	Ankyrin repeat and socs box containing 16	0.00	-5.1	-25.2	-5.0	---
96	gi_156523197	NM_001102543	DUSP27	Dual specificity phosphatase 27 (putative)	0.00	-4.6	-22.7	-5.0	↑
97	gi_119940186	XM_607283	LOC528849	Similar to mer receptor tyrosine kinase (LOC528849)	0.00	-3.7	-18.1	-4.9	---
98	gi_119927744	XM_869472	bTrappin-5	Trappin 5 (btrappin-5)	0.00	-5.5	-26.9	-4.9	---
99	gi_158519866	NM_001110070	CTSW	Cathepsin W	0.00	-9.0	-43.6	-4.8	---
100	gi_156120752	NM_001102053	KANK4	Kn motif and ankyrin repeat domains 4	0.00	-2.8	-13.6	-4.8	---
101	gi_119910848	XM_581838	LOC505540	Hypothetical (LOC505540)	0.00	-5.7	-27.2	-4.8	---
102	gi_164414434	NM_001113227	ELMO1	Engulfment and cell motility 1 (elmo1), transcript variant 1	0.00	-2.3	-10.8	-4.8	↑
103	gi_119894347	XM_602917	DOK7	Docking protein 7	0.00	-2.6	-12.6	-4.8	---
104	gi_119891299	XM_607870	LOC529423	Similar to family with sequence similarity 40, member b	0.00	-4.4	-21.0	-4.7	↑
105	gi_118151371	NM_001078149	GSTA3	Glutathione s-transferase alpha 3	0.00	-10.0	-46.9	-4.7	---
106	gi_119891361	XM_001251678	LOC784524	Similar to cytosolic carboxypeptidase 3 (LOC784524)	0.00	-2.5	-11.5	-4.7	↑
107	gi_150247093	NM_001099397	GAPT	Grb2-binding adaptor protein, transmembrane	0.00	-2.5	-11.5	-4.7	↑
108	gi_31343049	NM_174010	CD36	CD36 molecule (thrombospondin receptor)	0.00	-24.3	-111.0	-4.6	↑

109	gi_76674996	XM_603316	XKRX	Similar to membrane protein xplac (LOC524975)	0.00	-5.9	-26.7	-4.6	---
110	gi_119941394	XM_001257213	LOC790840	Hypothetical protein (LOC790840)	0.00	-2.8	-12.8	-4.6	---
111	gi_155372256	NM_001101271	FAM176B	Family with sequence similarity 176, member b	0.00	-6.6	-30.0	-4.5	↑
112	gi_115495674	NM_001076228	PTPRG	Protein tyrosine phosphatase, receptor type, g	0.00	-2.5	-11.4	-4.5	↑
113	gi_51816005	---	---	Co885720 bovgen_14045 normal cattle brain cDNA clone rzpdp1056m074q 5'	0.00	-4.9	-22.5	-4.5	↑
114	gi_51809242	---	---	Co879318 bovgen_07645 normal cattle brain cDNA clone rzpdp1056g2111q 5'	0.00	-2.6	-11.5	-4.5	↑
115	gi_84370178	NM_001038568	GPR84	G protein-coupled receptor 84	0.00	-4.1	-18.1	-4.5	↑
116	gi_119903128	XM_580552	MERTK	C-mer proto-oncogene tyrosine kinase	0.00	-4.5	-20.0	-4.4	---
117	gi_119888204	XM_595958	DNAH7	Dynein, axonemal, heavy chain 7	0.00	-2.8	-11.9	-4.3	---
118	gi_156120860	NM_001102107	CALCRL	Calcitonin receptor-like	0.00	-5.4	-23.2	-4.3	---
119	gi_115496321	NM_001075915	POU2AF1	Pou class 2 associating factor 1	0.00	-2.4	-10.1	-4.3	---
120	gi_119927740	XM_001250419	PI3	Protease inhibitor 3, skin-derived (skalp) (pi3)	0.00	-4.2	-17.8	-4.2	---
121	gi_119904117	XM_605012	LCN2	Lipocalin 2	0.00	-6.1	-25.6	-4.2	---
122	gi_51823209	---	---	Co892909 bovgen_21234 normal cattle brain cDNA clone rzpdp1056d1644q 5'	0.01	-2.2	-8.8	-4.1	---
123	gi_119895212	XM_001251719	LOC783028	Similar to prr16 protein (LOC783028)	0.01	-2.1	-8.4	-4.0	---
124	gi_119904406	XR_028798	LOC536255	Hypothetical (LOC536255)	0.00	-2.5	-10.1	-4.0	↑
125	gi_70793607	---	---	Am038299 kn-252-spleen, cDNA clone c0007409k18 3'	0.00	-2.8	-11.2	-4.0	↑
126	gi_119920899	XM_001253921	LOC786146	Hypothetical protein loc786146 (LOC786146)	0.00	-2.9	-11.5	-3.9	---
127	gi_119904676	XM_594814	LOC516657	Similar to atpase, aminophospholipid transporter-like, class i, type 8a, member 2 (LOC516657)	0.00	-3.1	-12.2	-3.9	---
128	gi_148540299	NM_001098474	EG667604	Predicted gene 8721	0.01	-2.2	-8.7	-3.9	↑
129	gi_119887556	XM_001254330	LOC786733	Hypothetical protein (LOC786733)	0.01	-2.1	-7.7	-3.8	---
130	gi_51811404	---	---	Co881475 bovgen_09800 normal cattle brain cDNA clone rzpdp1056h1915q 5'	0.00	-2.2	-8.4	-3.7	↑
131	gi_126723450	NM_001082467	C6orf26	Chromosome 6 open reading frame 26	0.00	-2.7	-9.9	-3.7	---
132	gi_139948854	NM_001083706	PDGFD	Platelet derived growth factor d	0.00	-2.6	-9.5	-3.7	↑
133*	gi_51827365	---	RPSA	Ribosomal protein sa	0.00	-2.6	-9.6	-3.7	↑
134	gi_114050912	NM_001046512	TSPAN12	Tetraspanin 12	0.00	-8.2	-29.9	-3.6	↑
135	gi_119918570	XM_001252944	CDH23	Cadherin-related 23	0.00	-7.8	-28.3	-3.6	---
136	gi_115494983	NM_001076301	APOD	Apolipoprotein d	0.00	-2.8	-10.1	-3.6	↑
137	gi_119902084	XR_027480	LOC613744	Hypothetical (LOC613744)	0.01	-2.0	-7.3	-3.6	↑
138	gi_119894846	XM_611456	ARHGEF18	Rho/rac guanine nucleotide exchange factor (GEF) 18	0.00	-3.1	-11.2	-3.6	↑
139	gi_119925656	XM_001255377	LOC788264	Similar to rap guanine nucleotide exchange factor (LOC788264)	0.00	-2.7	-9.5	-3.5	---
140	gi_157428139	NM_001105511	RNASE2	Ribonuclease, rnase a family, 2 (liver, eosinophil-derived neurotoxin) (RNase2)	0.00	-10.0	-34.8	-3.5	---
141	gi_157074113	NM_001103299	PLS1	Plastin 1	0.00	-2.8	-9.9	-3.5	---
142	gi_118151317	NM_001078121	LOC768255	Hypothetical protein (LOC768255)	0.00	-2.2	-7.7	-3.4	↑
143*	gi_119925245	XM_618000	POU6F2	Pou class 6 homeobox 2	0.00	-2.8	-9.7	-3.4	---
144	gi_114051470	NM_001046060	GIMAP4	GTPase, imap family member 4	0.00	-2.7	-9.2	-3.3	↑
145	gi_119904673	XM_869410	LOC617199	Similar to atpase, aminophospholipid transporter-like, class i, type 8a, member 2 (LOC617199)	0.00	-10.3	-34.1	-3.3	---
146	gi_119904699	XM_872272	LOC505426	Similar to mflj00298 protein, transcript variant 2 (LOC505426)	0.00	-2.9	-9.8	-3.3	---
147	gi_119893582	XM_599206	SGMS2	Sphingomyelin synthase 2	0.00	-2.9	-9.7	-3.3	↑
148	gi_119920329	XM_586812	CACNA1F	Calcium channel, voltage-dependent, l type, alpha 1f subunit	0.00	-3.2	-10.4	-3.3	↑
149	gi_61888881	NM_001013600	BOLA-DOB	Major histocompatibility complex, class ii, do beta	0.00	-3.5	-11.6	-3.3	↑
150	gi_149642786	NM_001099152	LBH	Limb bud and heart development homolog (mouse)	0.00	-2.9	-9.6	-3.3	↑
151	gi_119240719	---	---	Ee904145 b46270a ffb cDNA clone b4627 5'	0.00	-3.2	-10.3	-3.3	---
152*	gi_51810577	---	RPSA	Ribosomal protein sa	0.00	-2.8	-9.1	-3.3	↑
153	gi_156120434	NM_001101893	ZNF423	Zinc finger protein 423	0.01	-2.2	-7.0	-3.2	---
154	gi_61946762	---	---	Dn641361 umc-bof_0a01-016-a04 ovarian follicle bof cDNA 3'	0.00	-3.0	-9.7	-3.2	↑
155	gi_119934258	XM_001252637	LOC784284	Similar to receptor-like protein tyrosine phosphatase gamma a-type	0.01	-2.0	-6.5	-3.2	---
156	gi_119906110	XM_001252909	LOC785384	Hypothetical protein (LOC785384)	0.01	-2.1	-6.6	-3.2	---
157	gi_110347592	NM_001024505	---	Engulfment and cell motility 1 (ELMO1), transcript variant 2	0.01	-2.1	-6.9	-3.2	---
158	gi_119912932	XM_001249520	LOC781143	Hypothetical protein (LOC781143)	0.00	-2.7	-8.5	-3.2	↑
159	gi_119917116	XM_870165	SH2B2	Sh2b adaptor protein 2	0.01	-2.0	-6.5	-3.2	---
160	gi_31342006	NM_174436	Prkg1	Protein kinase, cgmp-dependent, type 1	0.00	-4.3	-13.7	-3.2	---
161	gi_119927948	XM_001256226	LOC789480	Similar to breast cancer antiestrogen resistance 3 (LOC789480)	0.00	-5.7	-17.8	-3.1	↑
162	gi_119917849	XM_607507	PPAPDC1A	Phosphatidic acid phosphatase type 2 domain containing 1a	0.00	-2.9	-9.1	-3.1	↑
163	gi_119907018	XM_866023	C11orf52	Chromosome 11 open reading frame 52	0.00	-11.5	-35.9	-3.1	↑
164	gi_115496130	NM_001076499	LOC390213	Double c2-like domains, gamma, pseudogene	0.01	-2.1	-6.6	-3.1	↑
165	gi_119912938	XR_028796	LOC615883	Similar to slit3 (LOC615883)	0.00	-4.8	-14.9	-3.1	---
166	gi_51815966	---	---	Co885681 bovgen_14006 normal cattle brain cDNA clone rzpdp1056g0625q 5'	0.01	-2.2	-6.6	-3.1	---
167	gi_119912710	XR_028608	LOC788092	Similar to beta heavy chain of outer-arm axonemal dynein atpase (LOC788092)	0.00	-2.4	-7.3	-3.1	---
168	gi_118151127	NM_001078018	SEZ6	Seizure related 6 homolog (mouse)	0.00	-3.1	-9.5	-3.0	---
169	gi_119895258	XR_028366	LOC514894	Hypothetical (LOC514894)	0.01	-2.0	-6.1	-3.0	↑
170	gi_156121258	NM_001102307	RGNEF	190 kda guanine nucleotide exchange factor	0.00	-5.9	-17.5	-2.9	---
171	gi_119932453	XM_001256991	LOC790552	Similar to multidrug resistance-associated protein	0.00	-2.6	-7.6	-2.9	---
172	gi_31342140	NM_174388	MFAP2	Microfibrillar-associated protein 2	0.00	-7.7	-22.5	-2.9	↑
173	gi_62751568	NM_001015669	DBC1	Deleted in bladder cancer 1	0.00	-2.2	-6.4	-2.9	↑
174*	gi_78370166	NM_001035285	SERINC2	Serine incorporator 2	0.00	-2.5	-7.2	-2.9	↑
175	gi_119924426	XR_027552	LOC782012	Similar to deubiquitinating enzyme dub2 (LOC782012)	0.01	-2.5	-7.3	-2.9	↑
176	gi_119912178	XM_612461	ABCC3	Atp-binding cassette, sub-family c (cftr/mrp), member 3	0.00	-2.3	-6.8	-2.9	↑
177	gi_9751160	---	---	Av615490 adipocyte cell line cDNA clone e1ad012c06 5'	0.00	-2.5	-7.2	-2.9	↑
178	gi_119895794	XM_001253881	LOC786092	Hypothetical protein (LOC786092)	0.00	-4.7	-13.6	-2.9	---
179	gi_119924746	XM_001251460	LOC782808	Similar to rap guanine nucleotide exchange factor (LOC782808)	0.00	-2.4	-6.9	-2.9	---
180	gi_51817133	---	---	Co886848 bovgen_15173 normal cattle brain cDNA clone rzpdp1056k2113q 5'	0.00	-2.3	-6.5	-2.9	---
181	gi_76638859	XM_582510	GPR81	G protein-coupled receptor 81	0.00	-9.5	-27.3	-2.9	---
182	gi_119909533	XM_001254956	LOC787612	Hypothetical protein loc787612 (LOC787612)	0.00	-2.8	-7.9	-2.9	↑
183	gi_110347586	NM_001014879	PPP2R2B	Protein phosphatase 2, regulatory subunit b, beta	0.00	-5.2	-14.9	-2.8	---
184	gi_60972164	---	---	Dn526932 1271740 marc 7bov cDNA 5'	0.00	-2.4	-6.9	-2.8	↑
185	gi_119895769	XM_617891	EBF1	Early b-cell factor 1	0.00	-3.4	-9.5	-2.8	---
186	gi_51810857	---	---	Co880928 bovgen_09253 normal cattle brain cDNA clone rzpdp1056n2313q 5'	0.00	-8.2	-23.1	-2.8	---
187	gi_119893677	XM_001249755	LOC781459	Hypothetical protein (LOC781459)	0.01	-2.1	-5.7	-2.8	↑
188	gi_119894965	XM_870596	GIPC3	Gipc pdz domain containing family, member 3	0.00	-5.0	-14.1	-2.8	---
189	gi_119913498	XM_582218	ZO1	Tight junction protein 1	0.00	-4.2	-11.6	-2.8	---
190	gi_51818387	---	---	Co888102 bovgen_16427 normal cattle brain cDNA clone rzpdp1056g1725q 5'	0.01	-2.0	-5.5	-2.8	↑
191	gi_51822808	---	---	Co892508 bovgen_20833 normal cattle brain cDNA clone rzpdp1056n1649q 5'	0.00	-3.4	-9.3	-2.8	↑
192	gi_51823236	---	---	Co892936 bovgen_21261 normal cattle brain cDNA clone rzpdp1056h0445q 5'	0.00	-2.4	-6.7	-2.8	---
193	gi_119915518	XM_608214	LOC529757	Similar to lymphotoxin-beta, transcript variant 1 (LOC529757)	0.00	-6.8	-18.6	-2.7	Down
194	gi_111104592	---	---	Ee243456 lb02230.cr_g22 gc_bgc-22 cDNA clone	0.01	-2.0	-5.5	-2.7	↑

				image:8261424					
195	gi_76638411	XM_612023	MBNL3	Muscleblind-like 3 (drosophila)	0.01	-2.1	-5.6	-2.7	↑
196	gi_119908015	XM_604649	IL24	Interleukin 24	0.00	-2.4	-6.6	-2.7	---
197	gi_156121118	NM_001102237	TMEM132A	Transmembrane protein 132a	0.00	-2.2	-5.9	-2.7	---
198	gi_119910909	XM_870781	KLK12	Kallikrein-related peptidase 12	0.00	-2.7	-7.2	-2.7	---
199	gi_119895214	XM_867687	PRR16	Proline rich 16	0.00	-2.6	-6.9	-2.7	---
200	gi_51817522	---	---	Co887237 bovgen_15562 normal cattle brain cDNA clone rzpdp1056a203q 5'	0.00	-2.4	-6.2	-2.6	---
201	gi_66792889	NM_001024553	KCND1	Potassium voltage-gated channel, shal-related subfamily, member 1	0.00	-2.3	-6.1	-2.6	↑
202	gi_51886061	---	---	Aj818585 kn206 bos sp. cDNA clone c0006012m03	0.00	-2.9	-7.6	-2.6	↑
203	gi_119890531	XM_001254797	LOC787378	Similar to iq motif containing with aaa domain (LOC787378)	0.00	-3.5	-9.1	-2.6	---
204*	gi_119889656	XM_001252338	KIAA1324	Kiaa1324	0.00	-2.3	-5.9	-2.6	---
205	gi_119893792	XM_001251250	LOC782618	Hypothetical protein (LOC782618)	0.01	-2.0	-5.3	-2.6	---
206	gi_31342494	NM_174254	CABP1	Calcium binding protein 1	0.00	-2.3	-6.0	-2.6	---
207	gi_51885046	---	---	Aj817570 kn206 bos sp. cDNA clone c0006006a15	0.00	-2.7	-7.0	-2.6	↑
208	gi_62460475	NM_001014892	C16orf5	Chromosome 16 open reading frame 5	0.01	-2.1	-5.4	-2.5	---
209	gi_119891365	XM_605871	AGBL3	Atp/gtp binding protein-like 3	0.01	-2.2	-5.5	-2.5	↑
210	gi_119914793	XM_001255342	NBEAL2	Neurobeachin-like 2	0.01	-2.1	-5.3	-2.5	---
211*	gi_119931673	XM_001249309	SERINC2	Serine incorporator 2	0.00	-2.2	-5.5	-2.5	↑
212	gi_70788841	---	---	Am033533 am033533 kn-252-spleen, cDNA clone c0007407m24 3'	0.00	-2.8	-7.1	-2.5	↑
213	gi_119895089	XM_001256303	RAPGEF6	Rap guanine nucleotide exchange factor (GEF) 6	0.00	-3.2	-7.9	-2.5	---
214	gi_51810688	---	RPS3A	Ribosomal protein s3a	0.00	-3.2	-8.0	-2.5	↑
215	gi_51810363	---	---	Co880434 bovgen_08759 normal cattle brain cDNA clone rzpdp1056d0510q 5'	0.00	-19.2	-47.8	-2.5	---
216	gi_119917978	XM_591917	C10orf92	Chromosome 10 open reading frame 92	0.00	-2.5	-6.2	-2.5	---
217	gi_119893204	XM_001255230	LOC788054	Similar to bcl-rambo (LOC788054)	0.00	-2.4	-5.9	-2.5	↑
218	gi_51888365	---	---	Aj820889 kn206 bos sp. cDNA clone c0006019k19	0.00	-5.0	-12.2	-2.5	---
219	gi_119903859	XM_613774	DTNB	Dystrobrevin, beta	0.01	-2.1	-5.2	-2.5	↑
220	gi_119906935	XM_586071	TRPC6	Transient receptor potential cation channel, subfamily c, member 6	0.00	-2.9	-7.0	-2.5	---
221	gi_119891011	XM_588627	LRRN3	Leucine rich repeat neuronal 3	0.00	-4.3	-10.7	-2.5	---
222	gi_119913675	XM_864691	CPEB1	Cytoplasmic polyadenylation element binding protein 1	0.00	-2.2	-5.5	-2.4	---
223	gi_51821936	---	---	Co891638 bovgen_19963 normal cattle brain cDNA clone rzpdp1056h0138q 5'	0.01	-2.2	-5.3	-2.4	---
224	gi_31342868	NM_174091	IL18	Interleukin 18 (interferon-gamma-inducing factor)	0.00	-4.3	-10.4	-2.4	↑
225	gi_119927615	XM_001253466	LOC785446	Similar to ob-cadherin-1 (LOC785446)	0.00	-23.5	-57.1	-2.4	---
226	gi_61675701	NM_001013402	SGCA	Sarcoglycan, alpha (50kda dystrophin-associated glycoprotein)	0.00	-3.1	-7.4	-2.4	↑
227	gi_51826740	---	---	Co896423 bovgen_24748 normal cattle brain cDNA clone rzpdp1056o0232q 5'	0.01	-2.0	-4.9	-2.4	↑
228	gi_119908963	XM_866831	RNF150	Ring finger protein 150	0.00	-2.9	-7.0	-2.4	↑
229	gi_156121234	NM_001102295	TM6SF1	Transmembrane 6 superfamily member 1	0.00	-2.2	-5.3	-2.4	---
230	gi_119894870	XM_612193	MYO1F	Myosin if	0.00	-3.6	-8.5	-2.4	↑
231	gi_77736358	NM_001034707	RGS5	Regulator of g-protein signaling 5	0.00	-3.6	-8.5	-2.4	---
232	gi_119894939	XM_582663	TBXA2R	Thromboxane a2 receptor	0.00	-5.8	-13.7	-2.4	↑
233	gi_156120626	NM_001101989	TMEM144	Transmembrane protein 144	0.00	-5.7	-13.5	-2.4	↑
234	gi_156120736	NM_001102045	FCRL1	Fc receptor-like 1	0.00	-2.4	-5.5	-2.3	↑
235	gi_119912092	XM_595012	IGF2BP1	Insulin-like growth factor 2 mrna binding protein 1	0.01	-2.1	-5.0	-2.3	---
236	gi_119914721	XM_601010	LOC522724	Similar to bassoon protein (LOC522724)	0.01	-2.1	-4.9	-2.3	↑
237	gi_115495806	NM_001076172	MARCKSL1	Marcks-like 1	0.00	-3.3	-7.5	-2.3	---
238	gi_119935543	XM_001257014	LOC790584	Hypothetical protein (LOC790584)	0.01	-2.1	-4.8	-2.3	↑
239	gi_119917956	XR_028155	LOC616097	Hypothetical loc616097 (LOC616097)	0.00	-2.4	-5.5	-2.3	---
240*	gi_119932781	XM_581475	ABCG2	Atp-binding cassette, sub-family g (white), member 2	0.00	-2.8	-6.4	-2.3	↑
241	gi_119893202	XM_870126	CECR1	Cat eye syndrome chromosome region, candidate 1	0.00	-2.7	-6.2	-2.3	↑
242	gi_119920461	XM_615546	LOC541298	Similar to interleukin 1 receptor accessory protein-like 1	0.01	-2.0	-4.7	-2.3	↑
243	gi_119886199	XM_590382	DZIP1L	Daz interacting protein 1-like	0.00	-3.9	-8.9	-2.3	---
244	gi_119934220	XM_001251698	LOC783056	Hypothetical protein (LOC783056)	0.00	-2.5	-5.7	-2.3	---
245	gi_76681354	XM_876891	LOC510087	Similar to loc508140, transcript variant 2 (LOC510087)	0.01	-2.1	-4.7	-2.2	---
246	gi_119912116	XM_584605	NGFR	Nerve growth factor receptor	0.00	-25.0	-55.6	-2.2	---
247	gi_119891420	XM_597033	SVOPL	Svop-like	0.00	-9.8	-21.7	-2.2	---
248	gi_119901319	XM_001254544	LOC787023	Hypothetical protein (LOC787023)	0.00	-3.2	-7.0	-2.2	---
249	gi_119909629	XM_867430	GGT1	Gamma-glutamyltransferase 1	0.00	-2.8	-6.1	-2.2	---
250	gi_156120476	NM_001101914	NINJ2	Ninjurin 2	0.00	-4.0	-8.7	-2.2	---
251	gi_119912285	XM_870899	RAPGEFL1	Rap guanine nucleotide exchange factor (gef)-like 1	0.00	-2.4	-5.2	-2.2	---
252	gi_51819194	---	---	Co888909 bovgen_17234 normal cattle brain cDNA clone rzpdp1056g0746q 5'	0.00	-2.2	-4.7	-2.2	---
253	gi_51816309	---	---	Co886024 bovgen_14349 normal cattle brain cDNA clone rzpdp1056p1219q 5'	0.00	-4.4	-9.6	-2.2	---
254	gi_119890374	XM_594566	KLF17	Kruppel-like factor 17	0.00	-2.9	-6.4	-2.2	---
255	gi_51884658	---	---	Aj817182 aj817182 kn206 bos sp. cDNA clone c0006007d06	0.00	-3.1	-6.7	-2.2	↑
256	gi_99028972	NM_174195	TCN2	Transcobalamin ii	0.01	-2.1	-4.6	-2.2	↑
257	gi_62460541	NM_001014923	NFE2	Nuclear factor (erythroid-derived 2), 45kda	0.00	-20.7	-44.5	-2.2	---
258	gi_118150847	NM_001077867	OSTBETA	Organic solute transporter beta	0.00	-6.9	-14.8	-2.1	↑
259	gi_51816466	---	MRPL49	Mitochondrial ribosomal protein l49	0.01	-2.0	-4.4	-2.1	---
260	gi_110626118	NM_001040495	IGFBP6	Insulin-like growth factor binding protein 6	0.00	-2.9	-6.2	-2.1	---
261	gi_77735824	NM_001034435	CTSK	Cathepsin k	0.00	-3.7	-7.9	-2.1	↑
262	gi_119889381	XM_001254920	LOC787557	Hypothetical protein (LOC787557)	0.00	-2.6	-5.5	-2.1	↑
263	gi_115495086	NM_001075767	ATP2A1	Atpase, ca++ transporting, cardiac muscle, fast twitch 1	0.00	-2.4	-5.1	-2.1	---
264	gi_119888991	XM_001249302	LOC780966	Hypothetical protein (LOC780966)	0.01	-2.1	-4.4	-2.1	---
265	gi_122692514	NM_001080250	AMICA1	Adhesion molecule, interacts with cxadr antigen 1	0.00	-2.2	-4.7	-2.1	↑
266	gi_119919496	XM_001256184	LOC789424	Hypothetical protein (LOC789424)	0.00	-2.4	-5.1	-2.1	↑
267	gi_119904297	XM_001255213	LOC788022	Hypothetical protein (LOC788022)	0.00	-3.1	-6.4	-2.1	↑
268	gi_164448627	NM_001015642	CPXM	Carboxypeptidase x (CPXM)	0.00	-4.8	-10.1	-2.1	---
269	gi_154152128	NM_001100334	AFAP1L1	Actin filament associated protein 1-like 1	0.00	-3.0	-6.3	-2.1	---
270	gi_115496685	NM_001075325	FOLR2	Folate receptor 2 (fetal)	0.00	-2.9	-6.1	-2.1	↑
271	gi_155371954	NM_001101113	GPX7	Glutathione peroxidase 7	0.01	-2.1	-4.4	-2.1	---
272	gi_149642888	NM_001099151	LHFPL2	Lipoma hmgic fusion partner-like 2	0.00	-2.5	-5.1	-2.0	↑
273*	gi_112817614	NM_001037478	ABCG2	ATP-binding cassette, sub-family g (white), member 2	0.00	-2.9	-6.0	-2.0	↑
274	gi_119910592	XM_583110	LOC506634	Hypothetical (LOC506634)	0.00	-2.7	-5.5	-2.0	↑
275	gi_115495372	NM_001076284	PCBP3	Poly(rc) binding protein 3	0.00	-2.7	-5.4	-2.0	---
276	gi_119891765	XR_028844	LOC790134	Similar to deubiquitinating enzyme dub1 (LOC790134)	0.00	-2.5	-5.1	-2.0	↑
277	gi_119895827	XM_001250068	ADRA1B	Adrenergic, alpha-1b-, receptor	0.00	-2.6	-5.4	-2.0	↑
278	gi_134085895	NM_001083469	TMEM156	Transmembrane protein 156	0.00	-4.5	-9.2	-2.0	↑
279	gi_119912559	XM_586841	LOC509801	Similar to ig-beta, (LOC509801)	0.00	-2.3	-4.6	-2.0	---
280	gi_119916122	XM_001249390	LOC781041	Hypothetical protein (LOC781041)	0.00	-26.5	-53.9	-2.0	---
281	gi_119915523	XM_868666	LOC615744	Similar to lst-1 gene product, transcript variant 1 (LOC615744)	0.00	-4.9	-9.8	-2.0	↑
282	gi_155371996	NM_001101135	PAQR8	Progestin and adipoq receptor family member viii	0.00	-2.5	-5.1	-2.0	---
283	gi_28849942	NM_174776	TAP	Tracheal antimicrobial peptide	0.01	-2.0	-4.1	-2.0	---
284	gi_86204308	---	---	Dy059203 001016bemn049454ht bemn cDNA	0.00	-9.1	-18.2	-2.0	---
285	gi_148356245	NM_001098380	HSPB2	Heat shock 27kda protein 2	0.01	-2.1	-4.2	-2.0	---

286	gi_119922978	XM_001251667	LOC783012	Hypothetical protein (LOC783012)	0.00	-2.7	-5.4	-2.0	↑
287	gi_157279838	NM_001104964	ART5	Adp-ribosyltransferase 5	0.00	-7.6	-15.2	-2.0	↑
288	gi_10169687	---	---	Be755695 209602 marc 2bov cDNA 5'	0.00	-2.3	-4.5	-2.0	↑

Asterisk (*) beside the serial no indicates duplicate probe present in the modulated dataset

2.1.6 Full list of genes in profile 6 (n = 71)

S.No	SEQ. ID	Acc. No. (RefSeq)	Putative Gene symbol	Gene Name	BL20 LPS Vs BL20 FDR (4h/or18)	BL20 LPS Vs BL20 Abs: FC (4h/or18)	TBL20 Vs BL20 Abs: FC	TBL20 Vs BL20 LPS Abs: FC (4h/or18)	BW720c Response
						↓	↑	↑	
1	gi_119919150	XM_587468	AHNAK	AHNAK nucleoprotein	0.01	-2.1	112.4	235.4	---
2	gi_119907136	XM_592427	OAF	Oaf homolog (drosophila)	0.00	-23.4	5.7	134.1	↓
3	gi_119920686	XM_586146	LOC509230	Hypothetical (LOC509230)	0.00	-5.1	22.3	113.1	---
4	gi_119895006	XM_590414	LOC512831	Similar to heterogeneous nuclear ribonucleoproteins a2/b1 (HNRNP a2 / HNRNP b1) (LOC512831)	0.00	-2.4	44.5	106.1	↓
5	gi_122692346	NM_001080368	THEM4	Thioesterase superfamily member 4	0.00	-19.4	5.4	104.2	---
6	gi_119912853	XM_604523	LOC526163	Similar to cmrf-35 antigen (LOC526163)	0.01	-2.1	47.4	99.0	---
7	gi_119902404	XM_869291	TMEM62	Transmembrane protein 62	0.00	-3.3	22.8	75.4	---
8*	gi_148233315	NM_001098165	RNASEL	Ribonuclease l (2',5'-oligoisoadenylate synthetase-dependent)	0.00	-3.3	18.6	60.6	---
9	gi_49409620	---	---	Aj677254 kn224 cDNA clone kn224-023_e12	0.00	-7.6	7.7	58.6	---
10	gi_31341924	NM_174464	SPARC	Secreted protein, acidic, cysteine-rich (osteonectin)	0.00	-14.0	3.8	53.4	---
11	gi_164451483	NM_001024533	SLA	Src-like-adaptor	0.00	-2.5	18.4	45.5	---
12	gi_78042479	NM_001035009	NDRG1	N-myc downstream regulated 1	0.00	-7.9	5.5	43.4	---
13	gi_119894531	XM_602953	PDE4C	Phosphodiesterase 4c, camp-specific	0.00	-2.4	17.1	41.5	↑
14	gi_115497115	NM_001076483	ANGPT4	Angiopoietin 4	0.00	-7.5	4.9	36.5	↓
15	gi_119937227	XM_001256143	LOC789368	Similar to solute carrier family 38, member 5 (LOC789368)	0.00	-9.8	3.7	36.4	---
16	gi_62751481	NM_001015534	GALNT6	Udp-n-acetyl-alpha-d-galactosamine:polypeptide n-acetylgalactosaminyltransferase 6 (galnac-t6)	0.00	-2.6	12.4	32.8	---
17	gi_115495710	NM_001075904	LRRC6	Leucine rich repeat containing 6	0.00	-6.0	5.3	31.9	---
18*	gi_119908657	XR_027398	RNASEL	Ribonuclease l (2',5'-oligoisoadenylate synthetase-dependent)	0.00	-2.4	12.9	31.2	---
19	gi_119879461	XM_001253104	GCET2	Germinal center expressed transcript 2	0.00	-8.1	3.7	30.1	↑
20	gi_119933556	XM_001256914	LOC790449	Similar to PCDH19 protein (LOC790449)	0.00	-5.2	5.6	29.4	↓
21	gi_119915783	XM_617171	CMAH	Cytidine monophosphate-n-acetylneuraminic acid hydroxylase (cmp-n-acetylneuraminate monooxygenase) pseudogene	0.00	-11.0	2.5	27.7	---
22	gi_51809852	---	---	Co879927 bovgen_08252 normal cattle brain cDNA clone rzpdp1056n145q 5'	0.00	-3.5	7.6	26.3	---
23	gi_157279936	NM_001105014	TRIM44	Tripartite motif containing 44	0.00	-4.1	6.1	25.1	↑
24	gi_154707907	NM_001099095	GZMA	Granzyme a (granzyme 1, cytotoxic t-lymphocyte-associated serine esterase 3)	0.00	-4.1	6.1	24.8	---
25	gi_116004014	NM_001076898	PAK1	P21 protein (cdc42/rac)-activated kinase 1	0.00	-3.7	6.1	22.3	↑
26	gi_119888157	XM_580320	STEAP3	STEAP family member 3	0.01	-2.0	10.9	21.9	---
27	gi_119889474	XR_028680	LOC788729	Similar to B-cell cll/Lymphoma 9 (LOC788729)	0.00	-3.2	6.6	21.1	---
28	gi_119913792	XM_866155	PSTPIP1	Proline-serine-threonine phosphatase interacting protein 1	0.00	-6.4	3.2	20.7	---
29	gi_119889467	XM_871861	LOC613322	Hypothetical (LOC613322)	0.00	-3.0	6.9	20.6	↑
30	gi_61316456	NM_001013003	NEIL2	Nei endonuclease viii-like 2 (e. Coli)	0.00	-2.8	7.1	20.1	---
31	gi_119913787	XM_616041	TBC1D2B	Tbc1 domain family, member 2b	0.00	-2.7	7.4	19.6	---
32	gi_119901593	XM_593801	FUCA2	Fucosidase, alpha-l- 2, plasma	0.00	-2.9	6.4	18.5	↑
33	gi_119910039	XM_587049	GPR114	G protein-coupled receptor 114	0.01	-2.1	8.5	18.2	---
34	gi_117935052	NM_001024930	CCR7	Chemokine (c-c motif) receptor 7	0.00	-8.9	2.0	17.9	---
35	gi_31341731	NM_174536	ENTPD1	Ectonucleoside triphosphate diphosphohydrolase 1	0.00	-2.3	7.6	17.1	---
36	gi_62751350	NM_001015580	SLC38A5	Solute carrier family 38, member 5	0.00	-5.1	3.2	16.1	---
37	gi_119879477	XM_585702	ZBTB20	Similar to btb/poz zinc finger protein DPZF (LOC508864)	0.00	-2.3	6.7	15.1	---
38	gi_119896213	XM_600235	MLLT3	Myeloid/lymphoid or mixed-lineage leukemia (trithorax homolog, drosophila); translocated to, 3	0.00	-3.3	4.2	13.9	---
39	gi_77736587	NM_001034795	GALM	Galactose mutarotase (aldose 1-epimerase)	0.00	-6.9	2.0	13.9	---
40	gi_119911895	XM_866482	PIK3R5	Phosphoinositide-3-kinase, regulatory subunit 5	0.00	-2.3	6.0	13.5	---
41	gi_51822883	---	---	Co892583 bovgen_20908 normal cattle brain cDNA clone rzpdp1056b0260q 5'	0.00	-5.6	2.4	13.5	---
42	gi_51802721	---	---	Co872881 bovgen_01206 normal cattle brain cDNA clone rzpdp1056n0454q 3'	0.00	-2.3	4.9	11.2	---
43	gi_95147677	NM_001033119	FOXA3	Forkhead box a3	0.00	-2.5	4.3	10.8	---
44	gi_119930210	XM_001249776	LOC781367	Similar to ep2 receptor (LOC781367)	0.01	-2.1	5.0	10.7	---
45	gi_119918268	XM_877825	AP3M2	Adaptor-related protein complex 3, mu 2 subunit	0.00	-2.5	4.1	10.4	---
46	gi_77736204	NM_001034629	EPHX1	Epoxide hydrolase 1, microsomal (xenobiotic)	0.00	-2.3	4.4	10.3	↑
47	gi_122692482	NM_001080293	ENPP2	Ectonucleotide pyrophosphatase/phosphodiesterase 2	0.00	-3.4	3.0	10.0	---
48	gi_119906384	XM_601798	MTSS1	Metastasis suppressor 1	0.00	-2.5	3.8	9.3	↑
49	gi_119928343	XM_001255819	LOC788911	Similar to ectonucleotide pyrophosphatase/phosphodiesterase 2 (autotaxin) (LOC788911)	0.00	-3.2	2.8	9.1	↓
50	gi_119918529	XM_585583	PRF1	Perforin 1 (pore forming protein)	0.01	-2.0	4.4	8.9	---
51	gi_115496985	NM_001076382	MGST2	Microsomal glutathione s-transferase 2	0.00	-3.1	2.7	8.2	---
52	gi_119879750	XM_596716	DGKG	Diacylglycerol kinase, gamma 90kda	0.00	-3.4	2.4	8.1	---
53	gi_51817761	---	---	Co887476 bovgen_15801 normal cattle brain cDNA clone rzpdp1056l1719q 5'	0.00	-2.3	3.5	8.1	---
54	gi_29398540	---	---	Cb533633 761630 marc 6bov cDNA 3'	0.00	-3.8	2.1	8.0	---
55	gi_156120702	NM_001102028	PIK3R6	Phosphoinositide-3-kinase, regulatory subunit 6	0.01	-2.0	3.8	7.8	↓
56	gi_134085680	NM_001083454	ABI3	ABI family, member 3	0.00	-3.0	2.5	7.6	---
57	gi_156121270	NM_001102313	HRC	Histidine rich calcium binding protein	0.01	-2.2	3.3	7.1	---
58	gi_154152162	NM_001100375	BBS12	Bardet-biedl syndrome 12	0.01	-2.1	3.3	7.0	---
59	gi_158937245	NM_001110194	HCK	Hemopoietic cell kinase	0.00	-2.7	2.3	6.3	---
60*	gi_119907280	XM_001252306	SUMO3	SMT3 suppressor of mif two 3 homolog 3 (s. Cerevisiae)	0.00	-2.6	2.3	6.0	---
61*	gi_115497781	NM_001076449	SUMO3	SMT3 suppressor of mif two 3 homolog 3 (s. Cerevisiae)	0.01	-2.1	2.8	5.9	---
62	gi_94966784	NM_001040490	TNFRSF1B	Tumor necrosis factor receptor superfamily, member 1b	0.01	-2.1	2.8	5.9	---
63	gi_155372272	NM_001101279	LOC781494	Similar to myeloid-associated differentiation marker	0.01	-2.1	2.7	5.7	↑
64	gi_119893596	XM_584935	SLC39A8	Solute carrier family 39 (zinc transporter), member 8	0.01	-2.1	2.6	5.5	---
65	gi_119915318	XR_028520	LOC512304	Similar to enpp5 (LOC512304)	0.00	-2.5	2.2	5.5	---
66	gi_125991861	NM_001081619	MGC151839	Similar to calpain (MGC151839)	0.01	-2.0	2.7	5.4	---
67	gi_116003874	NM_001076826	ANTXR2	Anthrax toxin receptor 2	0.01	-2.1	2.6	5.4	---
68	gi_119914706	XM_609627	SEMA3F	SEMA domain, immunoglobulin domain (ig), short basic domain, secreted, (semaphorin) 3f	0.00	-2.5	2.0	5.1	---
69	gi_119913706	XM_001250647	LOC782068	Hypothetical protein (LOC782068)	0.01	-2.1	2.2	4.6	---
70	gi_49357521	---	---	Aj671973 kn224 cDNA clone kn224-007_o17	0.01	-2.0	2.2	4.4	---
71	gi_119908660	XM_611689	LAMC1	Laminin, gamma 1 (formerly lamb2)	0.01	-2.0	2.1	4.2	---

Asterisk (*) beside the serial no indicates duplicate probe present in the modulated dataset

2.1.7 Full list of genes in profile 8 (n = 132)

S.No	SEQ. ID	Acc. No. (RefSeq)	Putative Gene symbol	Gene Name	BL20 LPS Vs BL20 FDR (4h/or18)	BL20 LPS Vs BL20 Abs: FC (4h/or18) ↓	TBL20 Vs BL20 Abs: FC No change	TBL20 Vs BL20 LPS Abs: FC (4h/or18) ↑	BW720c Response
1	gi_116004314	NM_001077046	PLIN3	Perilipin 3	0.00	-9.5	1.8	17.2	---
2	gi_119920411	XM_001252291	BCOR	Bcl6 corepressor	0.00	-21.0	-1.4	15.2	---
3	gi_31340780	NM_174669	SERPINE2	Serpin peptidase inhibitor, clade e (nexin, plasminogen activator inhibitor type 1), member 2	0.00	-9.2	1.6	15.0	---
4	gi_119892844	XM_581489	FGD4	Fyve, rhogef and ph domain containing 4	0.00	-9.4	1.6	14.9	---
5	gi_116004122	NM_001076954	GOLGA7B	Golgin a7 family, member b	0.00	-5.7	1.9	10.8	---
6	gi_115495426	NM_001075876	CAMKV	Cam kinase-like vesicle-associated	0.00	-15.7	-1.5	10.6	---
7*	gi_118151321	NM_001078125	ARMCX6	Armadillo repeat containing, x-linked 6	0.00	-15.5	-1.5	10.2	---
8	gi_119913698	XM_868029	LOC616063	Similar to myeloid-associated differentiation marker	0.00	-8.3	1.2	9.7	---
9	gi_51822234	---	---	Co891936 bovgen_20261 normal cattle brain cdna clone rzpdp1056m1641q 5'	0.00	-13.1	-1.4	9.6	---
10	gi_156120776	NM_001102065	NID2	Nidogen 2 (osteonidogen)	0.00	-8.7	1.0	9.0	---
11	gi_119908995	XM_602397	SLC7A11	Solute carrier family 7, (cationic amino acid transporter, y+ system) member 11	0.00	-9.3	-1.1	8.8	---
12	gi_119888246	XR_027752	PLCL1	Phospholipase c-like 1	0.00	-12.5	-1.4	8.8	---
13*	gi_119922570	XM_001254638	ARMCX6	Armadillo repeat containing, x-linked 6	0.00	-12.3	-1.5	8.5	---
14	gi_119893809	XM_613340	RBM47	Rna binding motif protein 47	0.00	-4.5	1.8	8.1	---
15	gi_148230339	NM_174557	IGFBP4	Insulin-like growth factor binding protein 4	0.00	-4.4	1.8	7.9	---
16	gi_51801726	---	---	Co871894 bovgen_00219 normal cattle brain cdna clone rzpdp1056i1952q 3'	0.00	-5.4	1.2	6.8	---
17	gi_31340894	NM_174766	TNS1	Tensin 1	0.00	-10.8	-1.6	6.6	---
18*	gi_119908122	XM_001252887	RGS1	Regulator of g-protein signaling 1	0.00	-5.6	1.2	6.6	---
19	gi_31341563	NM_174601	SLC1A5	Solute carrier family 1 (neutral amino acid transporter), member 5	0.00	-3.6	1.8	6.5	---
20	gi_78369387	NM_001035353	PLVAP	Plasmalemma vesicle associated protein	0.00	-4.3	1.5	6.5	---
21	gi_150247056	NM_001099366	SPRY1	Sprouty homolog 1, antagonist of FGF signaling (drosophila)	0.00	-5.0	1.3	6.5	---
22	gi_154152126	NM_001100354	OLFML2B	Olfactomedin-like 2b	0.00	-3.9	1.6	6.4	---
23	gi_156120814	NM_001102084	NELL2	Nel-like 2 (chicken)	0.00	-4.9	1.3	6.4	---
24	gi_51826539			Co896222 bovgen_24547 normal cattle brain cdna clone rzpdp1056g0845q 5'	0.00	-4.8	1.3	6.3	---
25	gi_115497431	NM_001075560	NUDT16	Nudix (nucleoside diphosphate linked moiety x)-type motif 16	0.00	-6.2	1.0	6.3	---
26	gi_119879733	XM_614853	ETV5	ETS variant 5	0.00	-4.4	1.4	6.2	---
27	gi_119230367	---	---	Ee893793 a88211a ffb cdna clone a8821 3'	0.00	-4.8	1.3	6.2	---
28	gi_156718123	NM_001103097	F2R	Coagulation factor ii (thrombin) receptor	0.00	-4.8	1.2	6.0	---
29*	gi_119908120	XM_613370	RGS1	Regulator of g-protein signaling 1	0.00	-4.5	1.3	5.8	---
30	gi_115494955	NM_001075853	PDK2	Pyruvate dehydrogenase kinase, isozyme 2	0.00	-4.4	1.3	5.8	---
31	gi_112218025			Ee357395 lb02958.cr_p24 gc_bgc-29 cdna clone image:8474570	0.00	-3.5	1.6	5.7	---
32	gi_119918344	XM_001256392	LOC789727	Hypothetical protein (LOC789727)	0.00	-2.8	2.0	5.6	↑
33	gi_157954058	NM_001109806	FCGR2B	Fc fragment of igg, low affinity iib, receptor (CD32)	0.00	-5.1	1.1	5.4	---
34	gi_134085719	NM_001083488	FAM107A	Family with sequence similarity 107, member a	0.00	-2.9	1.8	5.2	---
35	gi_157074119	NM_001103302	LOC618633	Similar to myeloid-associated differentiation marker	0.00	-2.8	1.8	5.1	---
36	gi_116004140	NM_001076960	ARMCX2	Armadillo repeat containing, x-linked 2	0.00	-3.5	1.5	5.1	---
37	gi_51812106	---	---	Co882174 bovgen_10499 normal cattle brain cdna clone rzpdp1056d2128q 5'	0.00	-4.3	1.2	5.0	---
38	gi_77736420	NM_001034738	LTB4R	Leukotriene b4 receptor	0.00	-3.2	1.6	5.0	---
39	gi_31343314	NM_173899	CD5	CD5 molecule	0.00	-4.9	1.0	4.8	---
40	gi_148237174	NM_001098148	KIAA1383	KIAA1383	0.00	-2.6	1.8	4.8	---
41	gi_119930243	XM_585571	PCSK4	Proprotein convertase subtilisin/kexin type 4	0.00	-2.9	1.6	4.7	---
42	gi_76657936	XM_597134	LGALS12	Lectin, galactoside-binding, soluble, 12	0.00	-5.5	-1.2	4.6	---
43	gi_51820532	---	---	Co890244 bovgen_18569 normal cattle brain cdna clone rzpdp1056p2248q 5'	0.00	-3.3	1.4	4.6	---
44	gi_119906547	XR_027912	LOC535166	Similar to sulfatase 1 (LOC535166)	0.00	-2.6	1.7	4.6	---
45	gi_119903494	XM_595079	EML6	Echinoderm microtubule associated protein like 6	0.00	-6.3	-1.4	4.5	---
46	gi_150247133	NM_001099371	HPDL	4-hydroxyphenylpyruvate dioxygenase-like	0.00	-3.2	1.4	4.5	---
47	gi_119887452	XM_874476	GPR155	G protein-coupled receptor 155	0.00	-4.0	1.1	4.5	---
48	gi_119904602	XM_582091	STARD13	Star-related lipid transfer (start) domain containing 13	0.00	-4.5	-1.0	4.4	---
49	gi_119913769	XM_612854	ARNT2	Aryl-hydrocarbon receptor nuclear translocator 2	0.00	-2.3	1.8	4.3	---
50	gi_51819829	---	---	Co889544 bovgen_17869 normal cattle brain cdna clone rzpdp1056p2346q 5'	0.00	-3.4	1.2	4.2	---
51	gi_114052243	NM_001046358	CMTM8	Cklf-like marvel transmembrane domain containing 8	0.01	-2.1	2.0	4.2	↓
52	gi_31343172	NM_173962	SV2A	Synaptic vesicle glycoprotein 2a	0.00	-5.5	-1.3	4.2	---
53	gi_126158902	NM_001081577	SLC1A4	Solute carrier family 1 (glutamate/neutral amino acid transporter), member 4	0.00	-3.2	1.3	4.2	---
54	gi_119910001	XR_028045	LOC786252	Similar to armadillo repeat containing 2 (LOC786252)	0.00	-3.6	1.1	4.1	---
55	gi_119912114	XM_614523	NXPH3	Neurexophilin 3	0.00	-3.3	1.2	4.1	---
56	gi_148238184	NM_001098020	TLE1	Transducin-like enhancer of split 1 (e(sp1) homolog, drosophila) (tle1)	0.00	-2.2	1.9	4.1	---
57	gi_61016342	---	---	DN550204 1408544 marc 7bov cdna 5'	0.00	-5.0	-1.2	4.1	---
58	gi_119901706	XM_596626	SYNJ2	Synaptojanin 2	0.01	-2.1	1.9	4.0	---
59	gi_119913067	XM_001252617	PDE4D	Phosphodiesterase 4d, camp-specific	0.00	-5.2	-1.3	3.9	---
60	gi_156121146	NM_001102251	Jakmip1	Janus kinase and microtubule interacting protein 1	0.00	-3.2	1.2	3.8	---
61	gi_119891341	XM_868371	PODXL	Podocalyxin-like	0.00	-4.7	-1.3	3.8	---
62	gi_149642966	NM_001099031	POC1B	Poc1 centriolar protein homolog b (chlamydomonas)	0.00	-5.2	-1.4	3.8	---
63	gi_51803202	---	---	Co873362 bovgen_01687 normal cattle brain cdna clone rzpdp1056h1957q 3'	0.00	-4.2	-1.1	3.7	---
64*	gi_51804582	---	SPP1	Secreted phosphoprotein 1	0.00	-4.1	-1.1	3.7	---
65	gi_156120560	NM_001101956	MGC152278	Similar to myeloid-associated differentiation marker	0.00	-3.3	1.1	3.7	---
66	gi_119895490	XM_601210	HBEGF	Heparin-binding egf-like growth factor	0.00	-2.6	1.4	3.6	---
67	gi_119892809	XM_615197	CARD10	Caspase recruitment domain family, member 10	0.00	-4.2	-1.2	3.6	---
68	gi_114051791	NM_001045971	SPINT2	Serine peptidase inhibitor, kunitz type, 2	0.00	-2.5	1.4	3.6	---
69	gi_114051388	NM_001046175	MAP1LC3A	Microtubule-associated protein 1 light chain 3 alpha	0.01	-2.1	1.7	3.5	---
70	gi_119887600	XM_615555	GALNT3	Udp-n-acetyl-alpha-d-galactosamine:polypeptide n-acetylgalactosaminyltransferase 3 (GALNAC-t3)	0.01	-2.2	1.6	3.5	---
71	gi_119927446	XM_868985	LOC616864	Similar to proton/amino acid transporter 4 (LOC616864)	0.01	-2.1	1.7	3.5	---

72	gi_119920662	XM_586585	FRMPD4	Ferm and pdz domain containing 4	0.00	-2.6	1.3	3.5	---
73	gi_82675971	---	---	Dv815778 lb01717.cr_l17 gc_bgc-17 cdna clone image:8094211 5'	0.01	-2.0	1.7	3.5	---
74	gi_114050922	NM_001046448	TSPAN14	Tetraspanin 14	0.00	-2.9	1.2	3.5	---
75	gi_31342305	NM_174331	GRK5	G protein-coupled receptor kinase 5	0.00	-3.4	1.0	3.5	---
76	gi_15378372	---	---	Bi537262 396963 marc 4bov cdna 5'	0.00	-2.2	1.6	3.4	---
77	gi_62460585	NM_001014947	MAPK13	Mitogen-activated protein kinase 13	0.00	-4.5	-1.3	3.4	---
78	gi_76665844	XM_609088	AADACL3	Arylacetamide deacetylase-like 3	0.00	-5.7	-1.7	3.4	---
79	gi_115497717	NM_001075593	PLEKHA1	Pleckstrin homology domain containing, family a (phosphoinositide binding specific) member 1 (plekha1)	0.01	-2.1	1.6	3.4	---
80	gi_116004188	NM_001076984	GLIPR1	Gli pathogenesis-related 1	0.00	-4.3	-1.3	3.4	---
81	gi_51803037	---	---	Co873197 bovgen_01522 normal cattle brain cdna clone rzpdp1056e1355q 3'	0.00	-2.3	1.4	3.4	---
82	gi_51814093	---	---	Co884145 bovgen_12470 normal cattle brain cdna clone rzpdp1056m1024q 5'	0.00	-2.5	1.4	3.4	---
83	gi_115495864	NM_001075533	ST6GALNAC2	ST6 (alpha-n-acetyl-neuraminyl-2,3-beta-galactosyl-1,3)-n-acetylgalactosaminide alpha-2,6-sialyltransferase 2	0.00	-3.3	1.0	3.4	---
84	gi_115495270	NM_001075169	SORBS1	Sorbin and sh3 domain containing 1	0.00	-2.8	1.2	3.4	---
85	gi_51818199	---	---	Co887914 bovgen_16239 normal cattle brain cdna clone rzpdp1056i127q 5'	0.00	-2.8	1.2	3.3	---
86	gi_119932478	XM_001256999	LOC790565	Similar to KIAA0882 protein (LOC790565)	0.00	-5.7	-1.7	3.3	---
87	gi_126723520	NM_001082439	IGSF8	Immunoglobulin superfamily, member 8	0.02	-2.0	1.6	3.3	---
88	gi_31342040	NM_174422	PDE6H	Phosphodiesterase 6h, cgmp-specific, cone, gamma	0.01	-2.2	1.5	3.2	---
89	gi_119929752	XM_872864	ARRB2	Arrestin, beta 2	0.00	-3.4	-1.1	3.2	---
90*	gi_116686101	NM_001077402	FCGR3A	Fc fragment of igg, low affinity iiia, receptor (CD16A)	0.00	-2.7	1.2	3.2	---
91	gi_51814346	---	DNAJC6	DNAj (hsp40) homolog, subfamily c, member 6	0.01	-2.2	1.5	3.2	---
92	gi_119930626	XM_870478	TLE2	Transducin-like enhancer of split 2 (e(sp1) homolog, drosophila)	0.00	-3.1	1.0	3.2	---
93	gi_31342110	NM_174398	NCALD	Neurocalcin delta	0.00	-3.1	1.0	3.2	---
94	gi_157785606	NM_001105637	MAF	V-maf musculoaponeurotic fibrosarcoma oncogene homolog (avian)	0.00	-2.4	1.3	3.1	---
95	gi_76611568	XM_869196	E2F2	E2f transcription factor 2	0.01	-2.1	1.5	3.1	---
96	gi_115495180	NM_001076537	TRIM9	Tripartite motif containing 9	0.00	-3.2	1.0	3.1	---
97	gi_78365245	NM_001035418	ARHGEF9	Cdc42 guanine nucleotide exchange factor (Gef) 9	0.00	-3.0	1.0	3.1	---
98	gi_156121042	NM_001102198	SLC19A3	Solute carrier family 19 (sodium/hydrogen exchanger), member 3	0.01	-2.1	1.5	3.1	---
99	gi_51810610	---	---	Co880681 bovgen_09006 normal cattle brain cdna clone rzpdp1056l159q 5'	0.00	-3.0	1.0	3.1	---
100	gi_119909968	XM_870732	GPT2	Glutamic pyruvate transaminase (alanine aminotransferase) 2	0.00	-2.8	1.1	3.0	---
101	gi_119909938	XR_028750	SPIRE2	Spire homolog 2 (drosophila)	0.00	-2.4	1.2	3.0	---
102	gi_51814374	---	---	Co884380 bovgen_12705 normal cattle brain cdna clone rzpdp1056f1329q 5'	0.00	-2.4	1.3	3.0	---
103	gi_115497811	NM_001076453	SLC19A1	Solute carrier family 19 (folate transporter), member 1	0.00	-2.4	1.2	3.0	---
104	gi_154152082	NM_001100341	C1orf74	Chromosome 1 open reading frame 74	0.00	-4.4	-1.5	3.0	---
105	gi_155371832	NM_001101051	MFNG	Mfng o-fucosylpeptide 3-beta-n-acetylglucosaminyltransferase	0.00	-3.1	-1.1	2.9	---
106	gi_51812300	---	---	Co882368 bovgen_10693 normal cattle brain cdna clone rzpdp1056o0813q 5'	0.00	-2.2	1.3	2.9	---
107	gi_115496721	NM_001075152	TMC4	Transmembrane channel-like 4	0.01	-2.2	1.3	2.9	---
108	gi_82812588	---	---	Dv878359 lb0261.cr_k19 gc_bgc-26 cdna clone image:8279949 5'	0.01	-2.0	1.4	2.9	---
109	gi_123858767	NM_001080366	PJA1	Praja ring finger 1	0.00	-2.7	1.1	2.9	---
110	gi_119911133	XM_001256455	C19orf51	Chromosome 19 open reading frame 51	0.00	-2.6	1.1	2.9	---
111	gi_156523107	NM_001102498	NKAPL	NFkB activating protein-like	0.00	-2.5	1.1	2.9	---
112*	gi_31342344	NM_174317	FCGR3A	Fc fragment of igg, low affinity iiia, receptor (CD16A)	0.00	-2.4	1.2	2.8	---
113	gi_41386781	NM_174231	ADRB2	Adrenergic, beta-2-, receptor, surface	0.00	-2.5	1.1	2.8	---
114	gi_119915572	XM_588389	ZKSCAN4	Similar to zinc finger protein 307, transcript variant 1 (LOC539620)	0.00	-3.2	-1.1	2.8	---
115	gi_119912967	XM_596546	SH3PXD2B	Sh3 and px domains 2b	0.00	-2.8	1.0	2.8	---
116*	gi_164420752	NM_001113245	TRAF3IP3	TRAF3 interacting protein 3	0.00	-4.6	-1.7	2.8	---
117	gi_94966796	NM_001040496	ART3	Adp-ribosyltransferase 3	0.01	-2.1	1.3	2.8	---
118	gi_119896289	XM_867351	KIAA1797	Kiaa1797	0.00	-2.4	1.1	2.7	---
119	gi_51804553	---	ANKRD1	Ankyrin repeat domain 1 (cardiac muscle)	0.00	-2.4	1.1	2.7	---
120	gi_51816423	---	---	Co886138 bovgen_14463 normal cattle brain cDNA clone rzpdp1056k1213q 5'	0.00	-2.5	1.1	2.6	---
121	gi_51823084	---	---	Co892784 bovgen_21109 normal cattle brain cDNA clone rzpdp1056l2445q 5'	0.00	-2.3	1.1	2.6	---
122	gi_119914579	XM_001250879	ARHGEF3	Rho guanine nucleotide exchange factor (GEF) 3	0.00	-4.7	-1.8	2.6	---
123	gi_119912784	XM_001253301	MXRA7	Matrix-remodelling associated 7	0.00	-2.2	1.2	2.6	---
124	gi_115496251	NM_001075741	GPRC5B	G protein-coupled receptor, family c, group 5, member b	0.00	-2.4	1.0	2.5	---
125	gi_82691756	---	---	Dv831563 lb01919.cr_p18 gc_bgc-19 cdna clone image:8116580 5'	0.00	-2.3	1.1	2.5	---
126	gi_56710322	NM_001008664	TLR3	Toll-like receptor 3	0.00	-4.8	-2.0	2.4	---
127	gi_118150831	NM_001077858	CTPS	CTP synthase	0.00	-2.2	1.1	2.4	---
128	gi_119887519	XM_607085	PDK1	Pyruvate dehydrogenase kinase, isozyme 1	0.01	-2.1	1.1	2.4	---
129	gi_78042497	NM_001035017	PHGDH	Phosphoglycerate dehydrogenase	0.00	-2.3	1.0	2.3	---
130	gi_119918586	XM_586457	FUT11	Fucosyltransferase 11 (alpha (1,3) fucosyltransferase)	0.01	-2.0	1.1	2.2	---
131	gi_119907072	XR_028456	LOC614237	Similar to apolipoprotein c-iii (LOC614237)	0.00	-4.0	-1.9	2.1	---
132	gi_157954050	NM_001109796	CARD11	Caspase recruitment domain family, member 11	0.01	-2.0	1.0	2.1	---

Asterisk (*) beside the serial no indicates duplicate probe present in the modulated dataset

2.2 Complete list of 'biological function and disease' categories identified by IPA in modulated gene list (1959 genes)

	Category	p-value
1	Inflammatory Response	8.22E-17-8.68E-04
2	Hematological System Development and Function	1.46E-12-7.67E-04
3	Tissue Morphology	1.46E-12-4.88E-04
4	Cellular Development	6.01E-12-6.08E-04
5	Hematopoiesis	6.01E-12-7.39E-04
6	Nervous System Development and Function	6.74E-12-6.74E-12
7	Cell-To-Cell Signaling and Interaction	7.36E-12-8.63E-04
8	Cellular Movement	1E-11-7.87E-04
9	Cell Death	4.79E-11-7.39E-04
10	Inflammatory Disease	4.99E-11-7.75E-04
11	Cancer	1.08E-10-6.92E-04
12	Cell-mediated Immune Response	1.11E-10-7.39E-04
13	Cellular Function and Maintenance	1.11E-10-6.93E-04
14	Renal and Urological Disease	6.21E-10-9.19E-05
15	Dermatological Diseases and Conditions	9.06E-10-8.03E-04
16	Immune Cell Trafficking	1.11E-09-7.39E-04
17	Immunological Disease	1.39E-09-7.66E-04
18	Infectious Disease	1.52E-09-6.93E-04
19	Cellular Growth and Proliferation	2.48E-09-8.39E-04
20	Tissue Development	7.22E-09-5.07E-04
21	Respiratory Disease	3.79E-08-6.93E-04
22	Gastrointestinal Disease	4.86E-08-5.07E-04
23	Hepatic System Disease	1.94E-07-5.07E-04
24	Antimicrobial Response	2.33E-07-6.33E-04
25	Organismal Survival	3.14E-07-2.07E-06
26	Reproductive System Disease	5.54E-07-6E-05
27	Connective Tissue Disorders	6.16E-07-7.75E-04
28	Skeletal and Muscular Disorders	6.16E-07-7.75E-04
29	Organismal Injury and Abnormalities	1.2E-06-8E-04
30	Humoral Immune Response	2.03E-06-4.43E-04
31	Antigen Presentation	5.62E-06-6.48E-04
32	Cell Signaling	5.72E-06-2.56E-04
33	Molecular Transport	5.72E-06-3.7E-04
34	Vitamin and Mineral Metabolism	5.72E-06-1.24E-04
35	Hematological Disease	7.29E-06-7.69E-04
36	Neurological Disease	7.9E-06-7.97E-04
37	Gene Expression	7.99E-06-2.72E-04
38	Genetic Disorder	8.81E-06-7.75E-04
39	Infection Mechanism	1.16E-05-4.76E-04
40	Metabolic Disease	1.27E-05-6.2E-04
41	Cardiovascular System Development and Function	1.32E-05-5.18E-04
42	Organismal Development	1.32E-05-5.18E-04
43	Cell Morphology	1.85E-05-6.93E-04
44	Lymphoid Tissue Structure and Development	1.89E-05-8.39E-04
45	Endocrine System Disorders	2.1E-05-6.07E-04
46	Small Molecule Biochemistry	2.12E-05-3.7E-04
47	DNA Replication, Recombination, and Repair	2.42E-05-2.42E-05
48	Embryonic Development	5.1E-05-1.58E-04
49	Organismal Functions	5.35E-05-5.35E-05
50	Cellular Assembly and Organization	1.39E-04-8.63E-04
51	Cardiovascular Disease	1.42E-04-6.25E-04
52	Skeletal and Muscular System Development and Function	1.43E-04-4.69E-04
53	Hair and Skin Development and Function	1.58E-04-5.69E-04
54	Renal and Urological System Development and Function	1.58E-04-1.58E-04
55	Cellular Compromise	1.74E-04-3.29E-04
56	Tumor Morphology	1.74E-04-3.67E-04
57	Post-Translational Modification	2.14E-04-2.14E-04
58	Connective Tissue Development and Function	2.2E-04-2.2E-04
59	Amino Acid Metabolism	3.7E-04-3.7E-04
60	Carbohydrate Metabolism	4.27E-04-4.27E-04
61	Free Radical Scavenging	4.67E-04-4.67E-04

2.3 Full list of 'canonical pathways' identified by IPA in modulated gene list (1959 genes)

	Ingenuity Canonical Pathways	-log(p-value)	Ratio
1	Dendritic Cell Maturation	1.27E+01	1.81E-01
2	Role of Macrophages, Fibroblasts and Endothelial Cells in Rheumatoid Arthritis	7.19E+00	1.14E-01
3	Activation of IRF by Cytosolic Pattern Recognition Receptors	6.63E+00	2.08E-01
4	Hepatic Fibrosis / Hepatic Stellate Cell Activation	6.59E+00	1.56E-01
5	Crosstalk between Dendritic Cells and Natural Killer Cells	6.52E+00	1.86E-01
6	TNFR2 Signaling	6.23E+00	2.94E-01
7	Role of Pattern Recognition Receptors in Recognition of Bacteria and Viruses	6.09E+00	1.84E-01
8	CD40 Signaling	5.84E+00	2.00E-01
9	NF-kB Signaling	5.23E+00	1.31E-01
10	LPS-stimulated MAPK Signaling	5.04E+00	1.71E-01
11	G-Protein Coupled Receptor Signaling	4.38E+00	8.70E-02
12	4-1BB Signaling in T Lymphocytes	4.29E+00	2.35E-01
13	Production of Nitric Oxide and Reactive Oxygen Species in Macrophages	4.25E+00	1.07E-01
14	April Mediated Signaling	4.19E+00	2.09E-01
15	IL-12 Signaling and Production in Macrophages	4.15E+00	1.21E-01
16	B Cell Activating Factor Signaling	4.00E+00	2.00E-01
17	Communication between Innate and Adaptive Immune Cells	3.93E+00	1.28E-01
18	Atherosclerosis Signaling	3.83E+00	1.31E-01
19	PI3K Signaling in B Lymphocytes	3.70E+00	1.19E-01
20	IL-17A Signaling in Fibroblasts	3.67E+00	2.00E-01
21	VDR/RXR Activation	3.45E+00	1.48E-01
22	Role of Osteoblasts, Osteoclasts and Chondrocytes in Rheumatoid Arthritis	3.38E+00	9.58E-02
23	TNFR1 Signaling	3.36E+00	1.70E-01
24	Type II Diabetes Mellitus Signaling	3.36E+00	9.38E-02
25	Toll-like Receptor Signaling	3.29E+00	1.64E-01
26	Role of PKR in Interferon Induction and Antiviral Response	3.24E+00	1.74E-01
27	IL-6 Signaling	3.23E+00	1.30E-01
28	iCOS-iCOSL Signaling in T Helper Cells	3.23E+00	1.15E-01
29	NF-kB Activation by Viruses	3.13E+00	1.34E-01
30	Type I Diabetes Mellitus Signaling	3.10E+00	1.16E-01
31	Role of Tissue Factor in Cancer	3.10E+00	1.23E-01
32	Altered T Cell and B Cell Signaling in Rheumatoid Arthritis	3.06E+00	1.30E-01
33	RANK Signaling in Osteoclasts	3.01E+00	1.26E-01
34	Interferon Signaling	2.98E+00	1.94E-01
35	TREM1 Signaling	2.98E+00	1.36E-01
36	Lymphotoxin Î² Receptor Signaling	2.98E+00	1.48E-01
37	Regulation of IL-2 Expression in Activated and Anergic T Lymphocytes	2.84E+00	1.24E-01
38	B Cell Receptor Signaling	2.78E+00	1.03E-01
39	GÎ±12/13 Signaling	2.73E+00	1.09E-01
40	Death Receptor Signaling	2.70E+00	1.38E-01
41	Induction of Apoptosis by HIV1	2.64E+00	1.36E-01
42	Hepatic Cholestasis	2.57E+00	8.67E-02
43	IL-17A Signaling in Airway Cells	2.50E+00	1.25E-01
44	LXR/RXR Activation	2.45E+00	1.08E-01
45	Angiopoietin Signaling	2.40E+00	1.22E-01
46	CD28 Signaling in T Helper Cells	2.39E+00	9.85E-02
47	Role of IL-17A in Arthritis	2.37E+00	1.27E-01
48	Role of IL-17F in Allergic Inflammatory Airway Diseases	2.37E+00	1.52E-01
49	Reelin Signaling in Neurons	2.32E+00	1.22E-01
50	Erythropoietin Signaling	2.31E+00	1.15E-01
51	Role of RIG1-like Receptors in Antiviral Innate Immunity	2.31E+00	1.43E-01
52	Role of JAK1, JAK2 and TYK2 in Interferon Signaling	2.28E+00	1.85E-01
53	FcÎ³ Receptor-mediated Phagocytosis in Macrophages and Monocytes	2.28E+00	1.08E-01
54	TWEAK Signaling	2.27E+00	1.54E-01
55	IL-10 Signaling	2.27E+00	1.15E-01
56	Agrin Interactions at Neuromuscular Junction	2.27E+00	1.30E-01
57	Growth Hormone Signaling	2.27E+00	1.20E-01
58	Macropinocytosis Signaling	2.27E+00	1.18E-01
59	HMGB1 Signaling	2.24E+00	1.10E-01
60	T Helper Cell Differentiation	2.23E+00	1.25E-01
61	PPAR Signaling	2.21E+00	1.04E-01
62	Role of JAK family kinases in IL-6-type Cytokine Signaling	2.20E+00	1.85E-01
63	Small Cell Lung Cancer Signaling	2.15E+00	1.01E-01
64	Systemic Lupus Erythematosus Signaling	2.15E+00	8.48E-02
65	T Cell Receptor Signaling	2.14E+00	1.01E-01
66	PKCÎ¸ Signaling in T Lymphocytes	2.00E+00	8.45E-02
67	O-Glycan Biosynthesis	1.99E+00	1.16E-01

68	CD27 Signaling in Lymphocytes	1.96E+00	1.23E-01
69	Natural Killer Cell Signaling	1.95E+00	1.00E-01
70	Role of JAK1 and JAK3 in Î³c Cytokine Signaling	1.93E+00	1.16E-01
71	ATM Signaling	1.91E+00	1.30E-01
72	MIF Regulation of Innate Immunity	1.87E+00	1.20E-01
73	Pancreatic Adenocarcinoma Signaling	1.86E+00	9.24E-02
74	Molecular Mechanisms of Cancer	1.86E+00	6.90E-02
75	Glioma Signaling	1.78E+00	8.93E-02
76	Glucocorticoid Receptor Signaling	1.77E+00	7.12E-02
77	ILK Signaling	1.74E+00	8.29E-02
78	Role of NFAT in Regulation of the Immune Response	1.67E+00	7.50E-02
79	IGF-1 Signaling	1.66E+00	9.35E-02
80	Leukocyte Extravasation Signaling	1.64E+00	8.04E-02
81	MSP-RON Signaling Pathway	1.64E+00	1.18E-01
82	Inhibition of Angiogenesis by TSP1	1.64E+00	1.28E-01
83	Estrogen-Dependent Breast Cancer Signaling	1.59E+00	1.00E-01
84	JAK/Stat Signaling	1.56E+00	1.09E-01
85	Nitrogen Metabolism	1.54E+00	4.13E-02
86	PI3K/AKT Signaling	1.53E+00	7.86E-02
87	IL-15 Signaling	1.52E+00	1.03E-01
88	Virus Entry via Endocytic Pathways	1.52E+00	9.00E-02
89	NRF2-mediated Oxidative Stress Response	1.52E+00	7.77E-02
90	IL-17A Signaling in Gastric Cells	1.51E+00	1.60E-01
91	Acute Phase Response Signaling	1.49E+00	7.87E-02
92	Ceramide Signaling	1.46E+00	9.20E-02
93	p53 Signaling	1.44E+00	9.38E-02
94	Cdc42 Signaling	1.38E+00	7.47E-02
95	Prostate Cancer Signaling	1.37E+00	8.25E-02
96	OX40 Signaling Pathway	1.37E+00	8.89E-02
97	IL-15 Production	1.35E+00	1.25E-01
98	Thrombopoietin Signaling	1.31E+00	9.52E-02
99	HGF Signaling	1.29E+00	8.57E-02
100	Nicotinate and Nicotinamide Metabolism	1.29E+00	6.67E-02
101	Renal Cell Carcinoma Signaling	1.28E+00	9.46E-02
102	Parkinson's Signaling	1.27E+00	1.67E-01
103	14-3-3-mediated Signaling	1.26E+00	8.33E-02
104	Intrinsic Prothrombin Activation Pathway	1.26E+00	1.18E-01
105	IL-3 Signaling	1.25E+00	9.46E-02
106	PDGF Signaling	1.25E+00	8.86E-02
107	Human Embryonic Stem Cell Pluripotency	1.25E+00	7.14E-02

2.4 Full list of important biological functions identified by Ingenuity associated with genes modulated by *Theileria* infection relative to BL20-LPS

	Important functions	Repressed by parasite no. Genes (Pro/anti)	*p*-value	Enhanced by parasite no. Genes (Pro/anti)	*p*-value
1	**Inflammatory Response**	**111**		**34**	
	Immune response	100 (43,27)	2.12E-09	27 (15,7)	4.51E-04
	Activation of leukocyte	46 (27,9)	2.67E-06	13 (9,1)	3.76E-03
	Antimicrobial response	19 (3,1)	4.88E-05	_	_
	Activation of lymphocyte	31 (19,7)	9.48E-05	9 (5,1)	1.20E-02
	Antiviral response	13 (3,1)	9.60E-05	2 (0,0)	1.17E-02
	Inflammation	30 (12,3)	7.22E-04	12 (3,2)	6.49E-04
	Inflamatory response	41 (17,10)	3.34E-04	16 (7,3)	2.30E-04
2	**Cellular Development**	**146**		**31**	
	Development of cells	84 (34,21)	3.74E-04	30 (14,4)	8.94E-05
	Development of leukocytes	54 (20,14)	4.18E-07	18 (9,2)	2.54E-03
	Differentiation of cancer cells	7 (3,1)	1.68E-04	_	_
	Differentiation of cells	94 (45,32)	6.55E-04	_	_
3	**Hematological System Development and Function**	**120**		**40**	
	Activation of leukocyte	46 (27,9)	2.67E-06	13 (9,1)	3.76E-03
	Adhesion of leukocyte	21 (10,1)	2.78E-04	7 (3,1)	7.24E-03
	Cell movement of leukocyte	37 (16,10)	1.15E-03	20(6,7)	4.46E-07
	Development of leukocytes	54 (20,14)	4.18E-07	_	_
	Development of lymphocytes	51 (19,12)	1.74E-06	17(7,2)	1.97E-04
	Proliferation of lymphocytes	49 (24,16)	7.80E-07	14 (7,3)	2.07E-03
	Differentiation of leukocytes	36 (20,10)	1.65E-03	_	_
	Hematological process	72 (31,18)	1.37E-07	20 (8,4)	1.26E-03
4	**Cell-To-Cell Signaling and Interaction**	**126**		**38**	
	Activation of leukocyte	46 (27,9)	2.67E-06	13 (9,1)	3.76E-03
	Adhesion of cells	59 (23,11)	2.75E-06	10 (5,2)	3.20E-03
	Response of cell	36 (9,8)	4.32E-05	_	_
	Binding of eukaryotic cell	36 (14,10)	1.08E-04	12(5,2)	2.25E-03
	Stimulation of eukaryotic cells	15 (12,1)	2.83E-03	7 (3,0)	1.38E-03
5	**Tissue Morphology**	**77**		**26**	
	Quantity of leukocyte	47 (11,8)	7.47E-07	15 (1,0)	3.79E-04
	Quantity of antigen presenting cell	14 (5,0)	3.46E-03	_	_
	Quantity of phagocytes	20 (5,1)	1.02E-03	7 (1,0)	8.40E-03
6	**Cellular Growth and Proliferation**	**140**		**45**	
	Proliferation of cells	124 (72,51	3.13E-03	40 (18,13)	8.48E-04
	Proliferation of leukocyte	50 (25,17)	1.75E-06	6 (4,0)	7.66E-03
	Induction of leukocyte	9 (7,3)	2.23E-04	_	_
	Stimulation of leukocytes	11 (9,3)	2.87E-03	_	_
7	**Immunological Disease**	**150**		**52**	
	Immunological disorder	150 (6,5)	1.37E-03	52 (0,2)	1.50E-05
8	**Cell Death**	**170**		**52**	
	Cell death of cancer cells	20 (6,4)	1.15E-05	_	_
	Apoptosis of tumor cell line	72 (34,22)	2.34E-06	20 (12,7)	3.07E-03
	Apoptosis	134 (70,53)	2.10E-05	42 (24,19)	1.13E-04
	Cell death of tumor cell line	78 (38,28)	2.10E-05	24 (13,9)	9.39E-04
	Cell death	151 (75,62)	6.59E-05	49 (26,22)	3.22E-05
	Cytotoxicity of lymphocytes	15 (8,6)	1.65E-04	_	_
	Cell death of normal cell	_	_	23 (8,9)	6.77E-03
9	**Cell-mediated Immune Response**	**57**		**18**	
	Adhesion of T lymphocytes	10 (5,0)	8.50E-04	_	_
	Differentiation of T lymphocytes	24 (9,1)	1.45E-03	_	_
	Induction of T lymphocytes	6 (3,0)	2.50E-03	_	_
	T cell development	_	_	16 (7,2)	2.60E-04

10	**Cellular Function and Maintenance**	**67**		**28**	
	Differentiation of T lymphocytes	24 (9,1)	1.45E-03	_	_
11	**Tissue Development**	**74**		**29**	
	Adhesion of cells	59 (23,11)	2.75E-06	10 (5,2)	2.30E-03
	Generation of lymphocytes	11 (5,2)	5.69E-04	_	_
12	**Cellular Movement**	**100**		**46**	
	Movement of cells	82 (42,29)	1.67E-04	38 (19,12)	4.47E-09
	Migration of leukocytes	36 (22,9)	1.75E-03	17(6,3)	2.49E-05
	Invasion of eukaryotic cells	_	_	14(10,3)	5.92E-04
	Infiltration of leukocytes	25 (8,6)	3.30E-04	14 (2,3)	1.41E-06
	Migration of antigen presenting cells	14 (7,1)	1.65E-04	_	_
	Influx of leukocytes	7 (4,1)	2.02E-03	_	_
	Chemoattraction of leukocytes	6 (6,0)	4.19E-03	_	_
13	**Antimicrobial Response**	**19**		**19**	
	Antimicrobial Response	19 (3,1)	4.88E-05	_	_
	Antiviral response	13 (3,1)	9.60E-05	2 (0,0)	1.17E-02
14	**Cancer**	**189**		**60**	
	Metastasis of cells	10 (2,6)	3.23E-03	13 (3,1)	2.29E-03
	Tumourigenesis	179 (26,25)	1.73E-03	60 (6,2)	1.74E-05
	Cancer	173 (16,13)	7.55E-05	56 (3,1)	1.58E-05
	Disease of tumor	18 (2,4)	7.29E-04	_	_
	Growth of tumor	20 (2,9)	1.18E-03	_	_
	Tumor	_	_	43 (4,2)	1.11E-04
15	**Antigen Presentation**	**45**		**16**	
	Differentiation of macrophages	10 (7,2)	4.76E-03	_	_
	Chemoattraction of antigen presenting cells	4(4,1)	3.73E-03	_	_
	Activation of monocytes	8(7,1)	2.37E-03	_	_
16	**Cell Signaling**	**46**		**35**	
	Activation of cells	61 (35,15)	2.85E-06	20 (12,2)	6.10E-05
	Activation of leukocytes	46 (27,9)	2.67E-06	13 (9,1)	3.76E-03
	Adhesion of cells	59 (23,11)	2.75E-06	10 (5,2)	3.20E-03
	Activation of lymphocyte	31 (19,17)	9.48E-05	9 (5,1)	1.20E-02
	Production of nitric oxide	17(8,2)	1.65E-04	_	_
	Binding of eukaryotic cell	36 (14,10)	1.08E-04	12 (5,2)	2.25E-03
17	**Cellular Assembly and Organization**	**21**		**19**	
	Formation of actin filaments	_	_	8 (3,1)	1.30E-03
	Formation of cellular protrusions	_	_	10 (4,0)	2.71E-03
	Formation of actin cytoskeleton	4 (0,0)	1.01E-03	4 (2,0)	1.10E-02
	Formation of filaments	_	_	9 (5,1)	4.06E-03
	Formation of cytoskeleton	5 (0,0)	2.11E-04	_	_
	Elongation of plasma membrane projection	7 (4,0)	3.95E-03	_	_
18	**Organismal Injury and Abnormalities**	**29**		**20**	
	Angiogenesis	32 (13,8)	2.64E-04	_	_
19	**Cell Morphology**	**53**		**17**	
	Shape changes of eukaryotic cells	_	_	11 (6,3)	6.12E-04
	Shape changes	_	_	13 (7,4)	3.65E-03
20	**DNA Replication, Recombination, and Repair**	**26**		**13**	
	Synthesis of DNA	26 (9,13)	3.67E-03	10 (4,3)	3.77E-03
21	**Gene expression**	**61**		**1**	
	Expression of synthetic promotor	31 (23,9)	1.00E-03	_	_
	Transcription of synthetic promotor	28 (21,8)	1.38E-03	_	_
	Activation of NF-kB binding site	10 (6,2)	2.08E-03	_	_
	Transactivation	41 (27,14)	2.15E-03	_	_

The criteria applied for the selection of major biological function categories were maximum number of genes and the P-value of significance. P-values in the range of 2.12E-09 to 1.10E-02 indicated statistical significance

Appendix 3: Microarray results of chapter 5

3.1 Complete lists of TashAT2 modulated 466 genes showing similar response in parasite infection

3.1.1 Full list of TashAT2 modulated repressed genes (n = 353) showing similar response in parasite infection

S.No	SEQ. ID	Acc. No. (RefSeq)	Putative Gene symbol	Gene Name	TashAT2 transfected BoMac array results: TashAT2 vs PCAGGS control FDR	TashAT2 vs PCAGGS control abs: FC	TahAT2 PMA vs control PMA abs: FC	Infection associated TBL20 array results: TBL20 vs BL20 abs: FC	TBL20 LPS vs BL20 LPS abs:FC (4h/or18)	BW720c Response
						↓	↓ /--	↓ /--	↓ /--	
1	gi_119904441	XM_580490	KBTBD6	Kelch repeat and btb (poz) domain containing 6	0.000	-193.13	-23.66	-3.0	-26.96	--
2	gi_51827054	CO896734	---	Co896734 bovgen_25059 normal cattle brain cDNA clone rzpdp1056g181q 5' sequence	0.000	-148.50	-10.67	-2.3	-39.82	--
3	gi_119893539	XM_597721	C4orf31	Chromosome 4 open reading frame 31	0.000	-95.97	-161.26	-4.2	-2.21	--
4 *	gi_118601863	NM_001079634	S100A14	S100 calcium binding protein a14	0.000	-73.91	-81.80	-2.8	-4.04	--
5 *	gi_113204619	NM_001015570	LGALS9	Lectin, galactoside-binding, soluble, 9	0.000	-55.55	-146.46	-4.0	-2.42	↑
6	gi_31342140	NM_174388	MFAP2	Microfibrillar-associated protein 2	0.000	-52.90	-68.35	-22.5	-8.57	↑
7	gi_155372278	NM_001101282	PTER	Phosphotriesterase related	0.000	-46.06	-13.84	-3.0	-2.29	--
8 *	gi_115496411	NM_001075349	CHN1	Chimerin 1	0.000	-35.99	-22.44	-3.3	-11.21	↑
9	gi_156631000	NM_174459	SEPP1	Selenoprotein p, plasma, 1	0.000	-31.85	-20.75	-18.1	-32.12	↑
10	gi_119912910	XM_599356	FAM20A	Family with sequence similarity 20, member a	0.000	-31.30	-18.06	-21.3	-18.36	--
11	gi_119917968	XM_866446	JAKMIP3	Janus kinase and microtubule interacting protein 3	0.000	-29.29	-5.88	-5.3	-16.13	↑
12	gi_119891852	XM_001253861	LOC786058	Similar to neuron navigator 3 (LOC786058)	0.000	-23.15	-1.76	-3.7	-2.99	↑
13	gi_119647255	EH175940	---	Eh175940 lb01656.cr_a03 gc_bgc-16cDNA clone image:8386637 5' sequence	0.000	-22.95	-20.23	-3.3	-3.40	--
14	gi_51809236	CO879312	---	Co879312 bovgen_07639 normal cattle brain cDNA clone rzpdp1056h0111q 5' sequence	0.000	-22.50	-1.90	-3.3	-2.50	↑
15	gi_51887303	AJ819827	---	Aj819827 kn206 bos sp. cDNA clone c0006016j19 Seq	0.000	-19.98	-7.75	-1.2	-2.25	--
16	gi_148236122	NM_001098043	CLMP	CXADR-like membrane protein	0.000	-19.47	-33.85	-3.2	-12.63	--
17	gi_112203941	EE344148	---	Ee344148 lb02547.cr_a22 gc_bgc-25cDNA clone image:8617440 sequence	0.000	-18.59	-1.78	-3.4	-3.07	↑
18	gi_49410464	AJ677881	---	Aj677881 kn224cDNA clone kn224-024_p02 sequence	0.000	-18.55	-29.00	-5.4	-3.52	--
19	gi_89886135	NM_001013585	S1PR1	Sphingosine-1-phosphate receptor 1	0.000	-17.70	-64.46	-54.6	-15.19	↑
20	gi_119891847	XM_607306	NAV3	Neuron navigator 3	0.000	-17.61	-1.57	-3.7	-2.72	↑
21	gi_114052379	NM_001046538	RAB15	Rab15, member ras onocogene family	0.000	-17.52	-7.59	-1.7	-4.76	--
22	gi_78369427	NM_001035317	MVP	Major vault protein	0.000	-17.27	-23.91	-2.0	-9.94	--
23	gi_45430004	NM_205788	CEACAM8	Carcinoembryonic antigen-related cell adhesion molecule 8	0.000	-17.26	-39.63	-6.0	-9.41	↑
24	gi_119916193	XM_612197	LOC532965	Similar to alpha3a chain laminin (LOC532965)	0.000	-16.92	-25.49	-4.2	-2.41	--
25	gi_119887265	XM_587548	PLCL2	Phospholipase c-like 2	0.000	-15.51	-10.53	-5.0	-4.30	↑
26	gi_119909284	XM_868620	HVCN1	Hydrogen voltage-gated channel 1	0.000	-15.22	-8.63	-30.4	-24.83	↑
27	gi_51880943	AJ813467	---	Aj813467 kn206 bos sp. cDNA clone c0005207e23 seq	0.000	-15.12	-14.90	-5.1	-10.63	↑
28	gi_119935010	XM_001256813	LOC790300	Similar to deltex1 (loc790300)	0.000	-14.61	-12.26	-1.0	-12.21	--
29	gi_10870122	BF076357	---	BF076357 225899 marc 2bov cDNA 5' seq	0.000	-13.97	-4.30	-1.2	-3.33	--
30	gi_119888854	XM_866713	MAN1C1	Mannosidase, alpha, class 1c, member 1	0.000	-13.33	-8.32	-4.3	-3.83	--
31	gi_119940186	XM_607283	LOC528849	Similar to mer receptor tyrosine kinase (LOC528849)	0.000	-12.50	-13.10	-18.1	-11.92	--
32	gi_115496605	NM_001076352	LMO2	Lim domain only 2 (rhombotin-like 1)	0.000	-12.25	-30.10	-15.7	-10.54	↑
33	gi_119919045	XM_869718	PKNOX2	Pbx/knotted 1 homeobox 2	0.000	-12.02	-7.59	-3.7	-4.63	--
34	gi_119890631	XM_606290	KIF1A	Kinesin family member 1A	0.000	-11.86	-14.21	-23.7	-18.01	↑
35	gi_119925613	XM_583887	GXYLT2	Glucoside xylosyltransferase 2	0.000	-11.69	-9.28	-222.3	-87.74	--
36	gi_51809634	CO879711	---	Co879711 bovgen_08036 normal cattle brain cDNA clone rzpdp1056j1411q 5' sequence	0.000	-11.62	-9.69	-2.7	-2.85	↑
37	gi_119915305	XR_028046	RUNX2	Similar to runt-related transcription factor 2 (LOC536911)	0.000	-11.58	-2.93	1.2	-5.73	--
38	gi_119879695	XM_867115	TP63	Tumor protein p63	0.000	-11.42	-3.62	1.9	-36.69	--
39	gi_157279834	NM_001104962	ANK1	Ankyrin 1, erythrocytic	0.000	-11.29	-10.10	-93.6	-82.95	↑
40	gi_61870087	XM_588576	PCDHGA5	Protocadherin gamma subfamily A, 5	0.000	-10.70	-10.47	-4.7	-7.65	↑
41	gi_156120752	NM_001102053	KANK4	KN motif and ankyrin repeat domains 4	0.000	-10.50	-2.65	-13.6	-9.45	--
42	gi_119893961	XM_598333	RASSF6	Ras association (ralgds/af-6) domain family member 6	0.000	-9.90	-8.91	-1.1	-1.97	--
43	gi_51825172	CO894862	---	Co894862 bovgen_23187 normal cattle brain cDNA clone rzpdp1056i0635q 5' sequence	0.000	-9.87	-1.73	-3.2	1.07	↑
44	gi_156120844	NM_001102099	FRMD4B	Ferm domain containing 4b	0.000	-9.67	-14.93	-4.3	-7.29	↑
45	gi_115495518	NM_001075426	ANGPTL1	Angiopoietin-like 1	0.000	-9.59	-3.79	-8.7	-10.42	↑
46	gi_119909544	XM_865632	NEFH	Neurofilament, heavy polypeptide	0.000	-9.57	-9.91	-3.5	-1.46	--
47	gi_119916232	XM_618609	MYOM1	Myomesin 1, 185kda	0.000	-9.28	-2.87	-9.7	-8.35	↑
48	gi_157427975	NM_001105426	RNASE13	Ribonuclease, rnase a family, 13 (non-active)	0.000	-9.12	-2.90	1.2	-2.22	--
49	gi_119906362	XM_605757	FER1L6	Fer-1-like 6 (c. Elegans)	0.000	-8.87	-10.14	-2.8	-1.73	--
50	gi_119916293	XM_588401	IMPA2	Inositol(myo)-1(or 4)-monophosphatase 2	0.000	-8.46	-8.13	-4.9	-6.05	--
51	gi_116003880	NM_001076831	COL3A1	Collagen, type iii, alpha 1	0.000	-8.46	-9.27	1.0	-2.22	--
52	gi_157427889	NM_001105382	Prune2 (rat)	Prune homolog 2 (drosophila)	0.000	-8.44	-7.17	1.7	-3.85	--
53	gi_119905157	XM_866719	IL15RA	Interleukin 15 receptor, alpha	0.000	-8.16	-7.24	-2.7	2.17	--
54	gi_119908399	XM_580673	PIK3CD	Phosphoinositide-3-kinase, catalytic, delta polypeptide	0.000	-7.75	-5.62	-2.7	-1.44	--
55	gi_31342993	NM_174034	CYBA	Cytochrome b-245, alpha polypeptide	0.000	-7.73	-8.56	-5.5	-4.84	↑
56	gi_115494923	NM_001075952	ASGR2	Asialoglycoprotein receptor 2	0.000	-7.62	-20.22	-9.7	-27.15	↑
57	gi_51815966	CO885681	---	Co885681 bovgen_14006 normal cattle brain cDNA clone rzpdp1056g0625q 5' sequence	0.000	-7.54	-4.59	-6.6	-6.60	--
58	gi_134085858	NM_001083409	C1QTNF1	C1q and tumor necrosis factor related protein 1	0.000	-7.41	-8.49	-150.3	-69.48	↑
59	gi_62751653	NM_001015673	MPZL2	Myelin protein zero-like 2	0.000	-7.38	-4.54	-3.0	-2.41	--
60	gi_51818194	CO887909	---	Co887909 bovgen_16234 normal cattle brain cDNA clone rzpdp1056n1629q 5' sequence	0.000	-7.32	-3.87	-3.1	-3.33	↑
61	gi_119895036	XM_588822	LOC511478	Hypothetical loc511478 (loc511478)	0.000	-7.29	-5.85	-3.2	-2.57	--
62	gi_119910630	XM_001256469	LOC789828	Similar to carcinoembryonic antigen-related cell adhesion molecule 1 isoform 3l	0.000	-7.14	-21.31	-5.9	-9.42	↑

63 *	gi_119892099	XM_585454	KRT6A	Keratin 6a	0.000	-7.06	-5.20	-3.2	-2.28	--
64	gi_60979607	DN532330	– – -	Dn532330 1360359 marc 7bovcDNA 5' sequence	0.000	-6.88	-3.93	-2.7	-2.91	--
65	gi_119919341	XR_027385	LOC520070	Similar to tumor endothelial marker 1, (LOC520070)	0.000	-6.87	-6.02	-22.0	-13.88	--
66	gi_156120782	NM_001102068	PDE7B	Phosphodiesterase 7b	0.000	-6.78	-2.66	-3.3	-4.79	--
67	gi_31342868	NM_174091	IL18	Interleukin 18 (interferon-gamma-inducing factor)	0.000	-6.66	-3.73	-10.4	-4.28	↑
68	gi_110626118	NM_001040495	IGFBP6	Insulin-like growth factor binding protein 6	0.000	-6.65	-6.28	-6.2	-3.20	--
69	gi_119895570	XM_581784	SLC23A1	Solute carrier family 23(nucleobase transporters), member1	0.000	-6.52	-3.92	-3.6	-1.89	--
70	gi_149642786	NM_001099152	LBH	Limb bud and heart development homolog (mouse)	0.000	-6.31	-1.87	-9.6	-6.51	↑
71	gi_119916443	XM_881561	LOC616344	Hypothetical (LOC616344)	0.000	-6.29	-9.13	1.2	-3.03	--
72	gi_156120706	NM_001102030	LOC515697	Apolipoprotein l, 3-like (LOC515697)	0.000	-6.18	-9.42	-15.0	-11.85	↑
73	gi_122692576	NM_001080280	SLC20A2	Solute carrier family 20 (phosphate transporter), member 2	0.000	-6.11	-5.14	-2.7	-2.03	↑
74	gi_78042515	NM_001035027	PLTP	Phospholipid transfer protein	0.000	-6.10	-4.00	-3.1	-2.23	--
75	gi_119916419	XM_587341	ALPK2	Alpha-kinase 2	0.000	-6.01	-1.56	-104.0	-12.42	--
76 *	gi_119907773	XM_001251746	CD82	CD82 molecule	0.000	-5.94	-4.62	-2.7	-4.47	--
77 *	gi_119874935	XM_001249464	ITSN1	Intersectin 1 (SH3 domain protein)	0.000	-5.77	-3.43	-3.7	-3.80	--
78	gi_125991897	NM_001081594	RASD2	Rasd family, member 2	0.000	-5.72	-8.14	-4.3	-1.59	--
79	gi_119937889	XM_001256927	LOC790466	Similar to endothelial pas domain protein 1/hypoxia-inducible factor-2 alpha (LOC790466)	0.000	-5.70	-3.57	-1.7	-4.16	--
80	gi_119905554	XR_028664	SLC4A11	Solute carrier family 4, sodium borate transporter, member 11	0.000	-5.67	-6.08	-3.0	1.37	--
81	gi_119895756	XM_580665	GM2A	GM2 ganglioside activator	0.000	-5.64	-3.16	-2.8	-2.77	--
82	gi_51822678	CO892378	– – -	Co892378 bovgen_20703 normal cattle brain cDNA clone rzpdp1056m2034q 5' sequence	0.000	-5.59	-3.66	-36.1	-24.70	--
83 *	gi_62752830	NM_001015601	RASGEF1A	Rasgef domain family, member 1a	0.000	-5.53	-5.41	-6.2	-11.68	↑
84 *	gi_119932781	XM_581475	ABCG2	ATP-binding cassette, sub-family g (white), member 2	0.000	-5.51	-4.51	-6.4	-2.77	↑
85	gi_119892308	XM_598691	KCNMB4	Potassium large conductance calcium-activated channel, subfamily m, beta member 4	0.000	-5.51	-4.06	-3.9	-5.18	--
86 *	gi_119915471	XM_001249886	LY6G6C	Lymphocyte antigen 6 complex, locus g6c	0.000	-5.44	-5.58	-3.6	-6.94	--
87 *	gi_51826800	CO896484	RASGEF1A	Rasgef domain family, member 1a	0.000	-5.43	-5.32	-6.5	-11.91	↑
88	gi_31341755	NM_174526	CRYBB1	Crystallin, beta b1	0.000	-5.37	-9.49	-4.6	-11.41	--
89 *	gi_118150825	NM_001077856	LY6G6C	Lymphocyte antigen 6 complex, locus g6c	0.000	-5.28	-5.32	-3.2	-6.81	--
90 *	gi_118151127	NM_001078018	SEZ6	Seizure related 6 homolog (mouse)	0.000	-5.27	-3.22	-9.5	-3.96	--
91	gi_119910121	XM_615431	LOC535363	Similar to ob-cadherin-1, transcript variant 1 (LOC535363)	0.000	-5.18	-4.49	-41.6	-2.94	--
92	gi_119915324	XM_590184	GPR110	G protein-coupled receptor 110	0.000	-5.18	-13.45	-10.4	-5.72	--
93	gi_139948280	NM_001083751	SYNPO2	Synaptopodin 2	0.000	-5.12	-1.33	-17.0	-9.86	--
94 *	gi_51818470	CO888185	HEY1	Hairy/enhancer-of-split related with yrpw motif 1	0.000	-5.07	-3.96	-1.1	-2.53	--
95	gi_119909414	XM_590469	RASAL1	Ras protein activator like 1 (GAP1 like)	0.000	-4.98	-5.99	-2.0	-19.73	--
96	gi_155371958	NM_001101115	SPOCK2	Sparc/osteonectin, cwcv and kazal-like domains proteoglycan (testican) 2	0.000	-4.97	-3.93	-5.4	-8.79	↑
97	gi_119927615	XM_001253466	LOC785446	Similar to ob-cadherin-1 (LOC785446)	0.000	-4.94	-4.08	-57.1	-4.09	--
98	gi_119892785	XM_610055	LOC531557	Similar to apolipoprotein l, 3 (LOC531557)	0.000	-4.91	-3.87	-4.2	-4.11	↑
99	gi_51812540	CO882608	– – -	Co882608 bovgen_10933 normal cattle brain cDNA clone rzpdp1056l087q 5' sequence	0.000	-4.88	-4.30	1.1	-3.21	--
100	gi_51811539	CO881610	– – -	Co881610 bovgen_09935 normal cattle brain cDNA clone rzpdp1056k0421q 5' sequence	0.000	-4.78	-18.80	-7.1	-17.89	↑
101	gi_51808554	CO878630	– – -	Co878630 bovgen_06955 normal cattle brain cDNA clone rzpdp1056e225q 5' sequence	0.000	-4.75	-2.23	-9.6	-9.78	↑
102	gi_156120634	NM_001101994	SLC6A12	Solute carrier family 6 (neurotransmitter transporter, betaine/gaba), member 12	0.000	-4.74	-12.11	-1.1	-12.83	--
103	gi_119904529	XM_590570	EBPL	Emopamil binding protein-like	0.000	-4.71	-4.82	-3.0	-3.40	--
104 *	gi_119895038	XM_001256059	ZNF77	Zinc finger protein 77	0.000	-4.70	-3.57	-42.3	-21.36	--
105	gi_119891326	XM_590508	CPA4	Carboxypeptidase a4	0.000	-4.70	-2.26	-119.2	-114.07	↑
106 *	gi_119914433	XM_585399	ZNF77	Zinc finger protein 77	0.000	-4.65	-3.56	-39.6	-20.92	--
107	gi_49411022	AJ678437	– – -	Aj678437 kn224cDNA clone kn224-026_h03 sequence	0.000	-4.60	-3.22	-16.0	-9.53	--
108	gi_115497925	NM_001076102	EPS8	Epidermal growth factor receptor pathway substrate 8	0.000	-4.59	-4.37	1.1	-4.81	--
109	gi_51824780	CO894472	– – -	Co894472 bovgen_22797 normal cattle brain cDNA clone rzpdp1056c2346q 5' sequence	0.000	-4.57	-2.78	-3.0	-3.06	--
110	gi_119903128	XM_580552	MERTK	C-mer proto-oncogene tyrosine kinase	0.000	-4.55	-8.57	-20.0	-13.51	--
111 *	gi_112817614	NM_001037478	ABCG2	ATP-binding cassette, sub-family g (white), member 2	0.000	-4.52	-4.78	-6.0	-2.33	↑
112 *	gi_31340626	NM_174725	EPAS1	Endothelial pas domain protein 1	0.000	-4.46	-3.45	-2.9	-33.05	↑
113 *	gi_88319943	NM_001001172	HEY1	Hairy/enhancer-of-split related with yrpw motif 1	0.000	-4.44	-3.60	-3.1	-2.01	--
114	gi_149642784	NM_001099025	NTNG2	Netrin g2	0.000	-4.44	-4.89	-3.3	-4.01	--
115	gi_61888881	NM_001013600	BOLA-DOB	Major histocompatibility complex, class ii, do beta	0.000	-4.43	-3.68	-11.6	-27.61	↑
116	gi_119895617	XM_588575	LOC539652	Similar to protocadherin gamma b3 short form protein	0.000	-4.38	-5.49	-3.9	-7.41	↑
117	gi_119919496	XM_001256184	LOC789424	Hypothetical protein (LOC789424)	0.000	-4.37	-4.53	-5.1	-2.41	↑
118	gi_51820161	CO889874	– – -	Co889874 bovgen_18199 normal cattle brain cDNA clone rzpdp1056c0845q 5' sequence	0.000	-4.22	-2.49	-8.4	-6.70	↑
119	gi_119933246	XM_001256766	LOC790239	Hypothetical protein (LOC790239)	0.000	-4.06	-3.66	-2.8	-2.84	--
120	gi_119908049	XM_611589	LOC515828	Hypothetical (LOC515828)	0.000	-3.98	-3.07	-236.9	-222.75	--
121	gi_119912389	XM_597900	C1QL1	Complement component 1, q subcomponent-like 1	0.000	-3.91	-3.53	-3.2	1.29	--
122	gi_77735752	NM_001034399	FXYD6	Fxyd domain containing ion transport regulator 6	0.000	-3.86	-2.90	-3.6	1.24	↑
123 *	gi_68319996	AM018804	EPAS1	Endothelial pas domain protein 1	0.000	-3.85	-2.89	-3.3	-47.56	↑
124	gi_122692514	NM_001080250	AMICA1	Adhesion molecule, interacts with cxadr antigen 1	0.000	-3.83	-2.79	-4.7	-2.58	↑
125	gi_51807407	CO877491	– – -	Co877491 bovgen_05816 normal cattle brain cDNA clone rzpdp1056a2459q 3' sequence	0.000	-3.83	-2.91	-3.3	-3.09	↑
126	gi_139949110	NM_001083769	IRF8	Interferon regulatory factor 8	0.000	-3.82	-2.43	-3.7	-7.05	↓
127	gi_31343103	NM_173985	AIF1	Allograft inflammatory factor 1	0.000	-3.81	-2.65	-3.6	-2.13	↑
128	gi_29257333	CB450951	– – -	Cb450951 705652 marc 6bovcDNA 5' sequence	0.000	-3.78	-2.28	1.1	-6.82	--
129	gi_118150959	NM_001077930	ERRFI1	ERBB receptor feedback inhibitor 1	0.000	-3.75	-2.64	1.0	-7.81	--
130	gi_84000076	NM_001038050	IFI27	Interferon, alpha-inducible protein 27	0.000	-3.72	-3.80	-1.2	-20.13	--
131	gi_51825034	CO894726	– – -	Co894726 bovgen_23051 normal cattle brain cDNA clone rzpdp1056a0148q 5' sequence	0.000	-3.71	-3.42	-4.7	-8.54	↑
132	gi_51821293	CO891000	– – -	Co891000 bovgen_19325 normal cattle brain cDNA clone rzpdp1056e0735q 5' sequence	0.000	-3.70	-1.32	-19.5	-8.66	--
133 *	gi_156121314	NM_001102335	PGM5	Phosphoglucomutase 5	0.000	-3.70	-2.36	-50.8	-14.70	↑
134	gi_119932747	XM_001254656	LOC787184	Similar to interleukin 7 receptor (LOC787184)	0.000	-3.67	-2.77	-7.1	-12.58	--
135	gi_119915240	XM_865759	TRERF1	Transcriptional regulating factor 1	0.000	-3.66	-3.25	-2.7	-2.53	--
136	gi_115495364	NM_001075414	IFIT3	Interferon-induced protein with tetratricopeptide repeats 3	0.000	-3.66	-5.57	-1.4	-11.41	--
137 *	gi_119918758	XM_865363	C11orf75	Chromosome 11 open reading frame 75	0.000	-3.66	-3.72	-2.7	-2.14	--
138	gi_76690438	XM_583591	LOC538910	Similar to protocadherin gamma a4 (LOC538910)	0.000	-3.63	-3.97	-1.8	-4.15	--
139	gi_51813585	CO883646	– – -	Co883646 bovgen_11971 normal cattle brain cDNA clone rzpdp1056m0315q 5' sequence	0.000	-3.61	-3.97	-3.2	-2.86	--
140	gi_158519860	NM_001110076	C8G	Complement component 8, gamma polypeptide	0.000	-3.60	-2.15	-3.0	-3.57	--
141	gi_156120978	NM_001102166	RAB40B	Rab40b, member ras oncogene family	0.000	-3.58	-3.25	-3.5	-2.59	--
142	gi_51819167	CO888882	– – -	Co888882 bovgen_17207 normal cattle brain cDNA clone rzpdp1056k0539q 5' sequence	0.000	-3.56	-7.41	-6.0	-4.62	--
143	gi_114051615	NM_001045985	SORBS3	Sorbin and SH3 domain containing 3	0.000	-3.54	-3.49	-3.1	-5.72	↑
144	gi_31341685	NM_174553	IFNAR2	Interferon (alpha, beta and omega) receptor 2	0.000	-3.52	-2.88	-2.3	-10.28	--
145	gi_31342479	NM_174260	CAPN3	Calpain 3, (p94)	0.000	-3.51	-2.37	-3.9	-2.28	↑
146	gi_119913259	XM_599818	IL7R	Interleukin 7 receptor	0.000	-3.51	-2.53	-4.9	-9.02	--
147	gi_119907033	XM_615064	DIXDC1	DIX domain containing 1	0.000	-3.50	-3.13	-3.1	-1.95	--

148	gi_119925538	XM_586833	LOC509794	Similar to tesc protein, transcript variant 1 (LOC509794)	0.001	-3.44	-5.25	-1.4	-23.27	--
149	gi_95147663	NM_001040472	CD3G	CD3G molecule, gamma (CD3-TCR complex)	0.000	-3.43	-3.92	-5.7	-7.19	↑
150	gi_119919833	XM_001254041	LOC786332	Similar to transmembrane protein with egf-like and two follistatin-like domains 1	0.000	-3.42	-3.44	-1.3	-2.30	--
151	gi_119905465	XM_867900	AKR1E2	Aldo-keto reductase family 1, member e2	0.001	-3.41	-3.28	-3.1	-3.97	↑
152	gi_119922048	XM_001254493	NCKAP5	NCK-associated protein 5	0.000	-3.40	-2.08	-1.4	-2.32	--
153	gi_6955562b	AW427615	– – -	Aw427615 63840 marc 3bovcDNA 5' sequence	0.000	-3.39	-1.89	-2.6	-12.17	--
154 *	gi_164420765	NM_001113247	CHN1	Chimerin 1	0.000	-3.35	-3.10	-1.1	-1.60	--
155	gi_51813747	CO883803	– – -	Co883803 bovgen_12128 normal cattle brain cDNA clone rzpdp1056e214q 5' sequence	0.000	-3.35	-4.70	-3.2	-2.30	--
156	gi_119920038	XM_001254134	LOC786473	Similar to zinc finger, cchc domain containing 12	0.000	-3.35	-1.99	-2.9	-5.37	--
157	gi_31343627	NM_177520	MGAT4A	Mannosyl (alpha-1,3-)-glycoprotein beta-1,4-n-acetylglucosaminyltransferase, isozyme a	0.000	-3.34	-3.15	-3.4	-4.99	--
158	gi_119907990	XM_606934	LOC528508	Similar to DTX4 protein (LOC528508)	0.001	-3.34	-8.47	-1.2	-13.20	--
159	gi_51825868	CO895554	– – -	Co895554 bovgen_23879 normal cattle brain cDNA clone rzpdp1056f1749q 5' sequence	0.000	-3.33	-3.59	-3.7	-6.70	--
160	gi_89886136	NM_001014870	TMEM106A	Transmembrane protein 106a	0.000	-3.32	-1.99	-10.5	-15.32	↑
161	gi_114050810	NM_001046507	EAF2	Ell associated factor 2	0.001	-3.30	-3.24	-3.8	-17.34	--
162	gi_51886086	AJ818610	– – -	Aj818610 kn206 bos sp. cDNA clone c0006012n11 seq	0.001	-3.27	-1.74	-2.4	-9.43	--
163 *	gi_122692344	NM_001080363	PNPLA4	Patatin-like phospholipase domain containing 4	0.001	-3.23	-3.77	-2.6	-3.24	--
164	gi_119905276	XM_865369	C1QL3	Complement component 1, q subcomponent-like 3	0.001	-3.22	-1.45	-5.3	-4.44	--
165 *	gi_119918577	XM_001252006	VCL	Vinculin	0.001	-3.21	-2.53	-3.7	-3.84	--
166	gi_51807418	CO877502	– – -	Co877502 bovgen_05827 normal cattle brain cDNA clone rzpdp1056a1958q 3' sequence	0.001	-3.20	-4.42	-7.2	-17.10	↑
167	gi_166159169	NM_001114080	– – -	Protocadherin gamma subfamily c, 3 (PCDHGC3), transcript variant 1	0.001	-3.19	-2.84	-2.9	-6.35	↑
168	gi_119925772	XM_001256054	LOC789248	Similar to zinc finger, cchc domain containing 12	0.001	-3.18	-2.20	-3.0	-6.11	--
169	gi_119919463	XM_001252801	LOC785604	Hypothetical protein (LOC785604), transcript variant 1	0.001	-3.18	-3.69	-4.3	-2.12	↑
170	gi_119891871	XM_591008	GNB3	Guanine nucleotide binding protein (g protein), beta polypeptide 3	0.001	-3.11	-1.87	-2.7	-1.68	--
171	gi_119894463	XM_597995	PBX4	Pre-b-cell leukemia homeobox 4	0.001	-3.11	-2.97	-1.4	-3.64	--
172	gi_119909727	XR_028833	LOC526847	Hypothetical (LOC526847)	0.001	-3.09	-3.71	-3.3	-6.29	--
173	gi_125991759	NM_173976	TPPP	Tubulin polymerization promoting protein	0.001	-3.09	-2.29	-5.0	-4.29	--
174	gi_119895615	XM_588574	LOC511274	Similar to protocadherin gamma a6 (LOC511274)	0.001	-3.09	-5.03	-3.9	-7.02	↑
175	gi_119907265	XR_027897	AMPD3	Adenosine monophosphate deaminase 3	0.001	-3.07	-1.79	-40.4	-42.52	↑
176	gi_157427855	NM_001105365	ITGB7	Integrin, beta 7	0.001	-3.06	-2.81	-12.3	-2.49	↑
177	gi_114052363	NM_001046345	IKBKE	Inhibitor of kappa light polypeptide gene enhancer in b-cells, kinase epsilon	0.001	-3.05	-4.14	-3.1	-5.55	--
178	gi_155371838	NM_001101054	CDKN2C	Cyclin-dependent kinase inhibitor 2c (p18, inhibits cdk4)	0.001	-3.04	-1.65	-2.7	-3.08	--
179	gi_119925997	XM_869237	LOC617055	Similar to bank (LOC617055)	0.001	-3.04	-1.28	-10.5	-18.34	--
180	gi_119895636	XM_596806	PCDHB13	Protocadherin beta 13	0.001	-3.03	-2.66	-5.3	-5.61	↑
181	gi_76253719	NM_001002892	ST3GAL2	ST3 beta-galactoside alpha-2,3-sialyltransferase 2	0.001	-3.03	-1.75	1.0	-2.30	--
182	gi_31340697	NM_178572	CA2	Carbonic anhydrase ii	0.001	-3.02	-7.35	-1.5	-11.30	--
183	gi_119916460	XM_001250160	LOC782394	Hypothetical protein (LOC782394)	0.001	-3.00	-4.12	-1.6	-4.13	--
184	gi_148237208	NM_001098017	PTPN6	Protein tyrosine phosphatase, non-receptor type 6	0.001	-3.00	-2.21	-31.9	-43.83	↑
185	gi_148229657	NM_181002	AOC3	Amine oxidase, copper containing 3 (vascular adhesion protein 1)	0.001	-2.99	-1.90	-1.0	-2.31	--
186	gi_114052323	NM_001046535	Rbpms	Rna binding protein gene with multiple splicing	0.001	-2.97	-2.05	-6.4	-4.90	↑
187	gi_119894365	XM_870556	LOC618227	Hypothetical (LOC618227)	0.001	-2.97	-2.33	-5.6	-5.28	--
188 *	gi_139948327	NM_001083728	MAPK10	Mitogen-activated protein kinase 10	0.001	-2.96	-2.82	-1.3	-3.39	--
189	gi_77404220	NM_001034056	MS4A8B	Membrane-spanning 4-domains, subfamily a, member 8b	0.001	-2.96	-3.05	-1.6	-3.94	--
190	gi_119904873	XM_864748	LOC613706	Similar to atp-binding cassette protein c4 splice	0.001	-2.92	-5.02	-2.9	-3.09	--
191	gi_119909946	XM_593446	CPNE7	Copine 7	0.001	-2.90	-1.54	-2.8	-2.04	--
192	gi_51884658	AJ817182	– – -	Aj817182 kn206 bos sp. cDNA clone c0006007d06 sequence	0.001	-2.89	-2.57	-6.7	-5.89	↑
193	gi_156120860	NM_001102107	CALCRL	Calcitonin receptor-like	0.001	-2.89	-2.36	-23.2	-4.80	--
194	gi_115494983	NM_001076301	APOD	Apolipoprotein d	0.001	-2.89	-1.07	-10.1	-11.85	↑
195	gi_30794323	NM_181017	TAC3	Tachykinin 3	0.001	-2.89	-2.36	-1.8	-7.66	--
196	gi_51886061	AJ818585	– – -	Aj818585 kn206 bos sp. cDNA clone c0006012m03 sequence	0.001	-2.88	-2.70	-7.6	-5.34	↑
197	gi_114053244	NM_001046251	VRK3	Vaccinia related kinase 3	0.001	-2.88	-2.41	-2.8	-2.68	--
198	gi_51885046	AJ817570	– – -	Aj817570 kn206 bos sp. cDNA clone c0006006a15 seq	0.001	-2.88	-2.56	-7.0	-4.93	↑
199	gi_115495650	NM_001075552	PIK3IP1	Phosphoinositide-3-kinase interacting protein 1	0.001	-2.87	-2.07	-2.8	-3.61	--
200	gi_119895619	XM_870861	LOC618528	Similar to protocadherin gamma b2 short form protein	0.001	-2.87	-2.80	-4.3	-5.71	↑
201 *	gi_119920668	XM_590366	PNPLA4	Patatin-like phospholipase domain containing 4	0.001	-2.85	-2.81	-2.8	-2.92	--
202	gi_155371902	NM_001101086	CPD	Carboxypeptidase d	0.001	-2.85	-1.54	-2.8	-16.69	--
203	gi_119912361	XM_875498	LOC514744	Hypothetical loc514744, transcript variant 4 (LOC514744)	0.001	-2.84	-5.52	-8.3	1.42	↑
204	gi_119921169	XR_028574	LOC787851	Similar to RBP-Ms/type 3 (LOC787851)	0.001	-2.84	-2.42	-5.2	-4.34	--
205	gi_139948709	NM_001083767	C12orf53	Chromosome 12 open reading frame 53	0.001	-2.81	-2.28	-6.2	-6.22	↑
206	gi_119892759	XR_028120	LOC518495	Hypothetical loc518495 (LOC518495)	0.001	-2.81	-4.53	-13.7	-10.35	↑
207	gi_157074179	NM_001103334	PCDHGC3	Protocadherin gamma subfamily c, 3, transcript variant 2	0.001	-2.79	-2.45	-4.3	-3.45	↑
208	gi_164448611	NM_001075425	CLSTN3	Calsyntenin 3	0.001	-2.78	-2.52	-6.0	-1.62	--
209	gi_51814009	CO884065	– – -	Co884065 bovgen_12390 normal cattle brain cDNA clone rzpdp1056o085q 5' sequence	0.001	-2.76	-2.84	-3.0	-3.55	--
210 *	gi_119919887	XM_580464	ATP2B3	ATPase, ca++ transporting, plasma membrane 3	0.001	-2.75	-1.41	-3.1	-1.64	--
211	gi_119894347	XM_602917	DOK7	Docking protein 7	0.001	-2.74	-2.28	-12.6	-5.94	--
212	gi_31341586	NM_174593	RASSF2	Ras association (RALGDS/Af-6) domain family member 2	0.001	-2.71	-1.82	-1.7	-5.53	--
213	gi_119919492	XM_001256176	LOC789415	Hypothetical protein (LOC789415)	0.001	-2.71	-3.41	-4.0	-2.65	↑
214	gi_115497713	NM_001076440	SPA17	Sperm autoantigenic protein 17	0.001	-2.71	-2.39	-2.8	-5.99	--
215	gi_119889938	XM_001250562	LOC781999	Similar to amp deaminase (LOC781999)	0.001	-2.70	-1.45	-12.1	-17.45	--
216	gi_115497719	NM_001076119	TSPAN5	Tetraspanin 5	0.001	-2.67	-1.87	-4.0	-3.76	--
217	gi_77736300	NM_001034678	HES1	Hairy and enhancer of split 1, (drosophila)	0.001	-2.66	-2.30	-2.5	-6.72	↑
218	gi_51825504	CO895190	– – -	Co895190 bovgen_23515 normal cattle brain cDNA clone rzpdp1056a1147q 5' sequence	0.001	-2.65	-2.20	-7.7	-6.00	↑
219	gi_119908832	XR_027675	LOC531974	Similar to mkiaa1151 protein (LOC531974)	0.001	-2.64	-2.83	-2.8	-6.34	--
220	gi_51887072	AJ819596	– – -	Aj819596 kn206 bos sp. cDNA clone c0006015o15 seq	0.001	-2.63	-2.44	-11.4	-8.00	--
221	gi_45465357	CK950977	– – -	Ck950977 4090253 barc 10bovcDNA clone 10bov27_j04 5' sequence	0.001	-2.63	-1.80	-4.2	-3.99	--
222	gi_114050926	NM_001046126	ELL3	Elongation factor rna polymerase ii-like 3	0.002	-2.62	-2.43	1.3	-3.73	--
223	gi_148540319	NM_001098473	B3GNT3	Udp-glcnac:betagal beta-1,3-n-acetylglucosaminyltransferase 3	0.002	-2.62	-1.54	-4.3	-4.33	↑
224	gi_70778797	NM_001025333	OSTalpha	Organic solute transporter alpha	0.001	-2.62	-3.69	-3.6	-2.27	--
225 *	gi_119904381	XM_001256288	ABO	Abo blood group (transferase a, alpha 1-3-n-acetylgalactosaminyltransferase; transferase b, alpha 1-3-galactosyltransferase)	0.002	-2.62	-2.66	-35.5	-77.46	--
226	gi_119893382	XM_603482	WNT7B	Wingless-type mmtv integration site family, member 7b	0.001	-2.61	-2.87	-3.0	-2.30	--
227	gi_157074155	NM_001103321	GALNT4	Udp-n-acetyl-alpha-d-galactosamine:polypeptide n-acetylgalactosaminyltransferase 4 (GALNAC-t4)	0.001	-2.61	-2.24	-3.2	5.27	↑
228	gi_119895759	XM_608339	CCDC69	Coiled-coil domain containing 69	0.002	-2.60	-2.19	-2.8	-2.06	--
229	gi_51813662	CO883718	– – -	Co883718 bovgen_12043 normal cattle brain cDNA clone rzpdp1056f2013q 5' sequence	0.003	-2.60	-8.06	-1.6	-12.94	--

230	gi_119921194	XR_028648	LOC788414	Hypothetical protein (LOC788414)	0.002	-2.60	-1.61	-2.7	-4.16	↑
231	gi_51880396	AJ812920	– – -	AJ812920 kn206 bos sp. cDNA clone c0005201f5 seq	0.002	-2.60	-2.91	-3.4	-2.69	↑
232	gi_111104592	EE243456	– – -	Ee243456 lb02230.cr_g22 gc_bgc-22cDNA clone image:8261424 sequence	0.001	-2.59	-2.06	-5.5	-5.33	↑
233	gi_115496313	NM_001075738	Gstt3	Glutathione s-transferase, theta 3	0.002	-2.58	-2.59	-1.2	-5.55	--
234	gi_31342246	NM_175717	CA11	Carbonic anhydrase xi	0.001	-2.58	-2.01	-8.7	-9.73	↑
235	gi_119927167	XM_868813	LOC616717	Hypothetical (LOC616717)	0.001	-2.57	-1.98	-4.0	-4.02	↑
236	gi_157279990	NM_001105041	RUSC1	Run and SH3 domain containing 1	0.001	-2.57	-2.39	1.3	-2.53	--
237	gi_119913108	XM_600430	IL6ST	Interleukin 6 signal transducer(gp130,oncostatin m receptor)	0.001	-2.56	-2.47	-3.1	-2.55	--
238 *	gi_118150779	NM_001077833	PRKCZ	Protein kinase c, zeta	0.002	-2.53	-2.54	-3.9	-2.00	--
239	gi_31341450	NM_174647	PPP1R1B	Protein phosphatase 1, regulatory (inhibitor) subunit 1b	0.002	-2.52	-2.11	-3.1	-3.71	--
240	gi_119892433	XM_584663	ARHGAP9	Rho gtpase activating protein 9	0.002	-2.51	-3.01	-4.0	-2.79	↑
241	gi_119895613	XM_001254336	LOC786740	Similar to protocadherin gamma a7 precursor (pcdh-gamma-a7)	0.003	-2.51	-2.59	-2.9	-5.97	↑
242	gi_164518983	NM_001113297	ACBD7	Acyl-coa binding domain containing 7	0.003	-2.50	-1.84	-1.7	-4.97	--
243	gi_31342621	NM_174191	SYN1	Synapsin i	0.003	-2.50	-2.91	-2.8	-3.30	--
244	gi_148229444	NM_001098093	ST5	Suppression of tumorigenicity 5	0.002	-2.49	-3.76	-13.4	-1.66	--
245	gi_48374082	NM_001001440	ANXA4	Annexin a4	0.002	-2.49	-2.33	-1.7	-3.79	--
246	gi_119934023	XM_001257056	LOC790637	Hypothetical protein (LOC790637)	0.002	-2.49	-2.67	-2.2	-5.29	--
247	gi_115495730	NM_001076164	PPP1R3C	Protein phosphatase 1, regulatory (inhibitor) subunit 3c	0.002	-2.49	-1.59	-1.3	-2.69	--
248 *	gi_51808399	CO878479	CEBPA	CCAAT/enhancer binding protein (c/ebp), alpha	0.002	-2.48	-2.47	-5.2	-13.96	↑
249	gi_62460541	NM_001014923	NFE2	Nuclear factor (erythroid-derived 2), 45kda	0.003	-2.47	-2.04	-44.5	-6.40	--
250	gi_119936811	XM_001250386	LOC781880	Similar to multidrug resistance-associated protein(mrp)-like protein-2 (mlp-2)	0.003	-2.46	-2.53	-3.7	-3.86	↑
251	gi_157427775	NM_001105322	KRT17	Keratin 17	0.003	-2.45	-5.07	-3.6	1.23	--
252	gi_51823975	CO893670	– – -	Co893670 bovgen_21995 normal cattle brain cDNA clone rzpdp1056i0938q 5' sequence	0.003	-2.44	-2.42	-3.4	-4.02	↑
253	gi_76678805	XM_586049	LOC509148	Similar to CLLL7 protein (LOC509148)	0.004	-2.43	-2.20	-2.5	-7.51	--
254	gi_119919548	XM_879446	LOC540854	Hypothetical, transcript variant 3 (LOC540854)	0.003	-2.42	-3.38	-3.5	-2.48	↑
255	gi_119902226	XR_027935	LOC535046	Similar to cadherin-24 (LOC535046)	0.003	-2.42	-1.35	-3.6	-6.10	↑
256	gi_119901197	XM_608490	MAN1A1	Mannosidase, alpha, class 1a, member 1	0.003	-2.42	-1.77	-3.5	-1.50	--
257	gi_51888625	AJ821149	– – -	Aj821149 aj821149 kn206 bos sp. cDNA clone c0006018o05 sequence	0.004	-2.42	-1.96	-2.7	-3.29	↑
258	gi_119900520	XM_589465	SIT1	Signaling threshold regulating transmembrane adaptor 1	0.005	-2.40	-2.38	-8.2	-8.12	↑
259	gi_31342739	NM_174147	PLAU	Plasminogen activator, urokinase	0.003	-2.40	-3.87	-5.5	2.39	--
260	gi_119895598	XM_865017	PCDHB14	Protocadherin beta 14	0.004	-2.40	-1.94	-3.0	-4.42	↑
261	gi_29267700	CB461316	– – -	Cb461316 721270 marc 6bovcDNA 3' sequence	0.006	-2.38	-1.82	-27.9	-21.64	↑
262 *	gi_119908469	XM_001252162	DVL1	Dishevelled, dsh homolog 1 (drosophila)	0.005	-2.38	-3.73	-1.1	-2.64	--
263 *	gi_119907771	XM_001251709	CD82	CD82 molecule	0.005	-2.37	-3.13	-3.4	-3.36	↑
264	gi_122692362	NM_001080360	KCTD1	Potassium channel tetramerisation domain containing 1	0.004	-2.36	-2.82	-4.3	-6.98	↑
265 *	gi_41386706	NM_174484	VCAM1	Vascular cell adhesion molecule 1	0.005	-2.36	-24.67	1.0	-224.00	--
266	gi_148236812	NM_001098118	MRAS	Muscle ras oncogene homolog	0.004	-2.36	-3.66	-5.2	-6.05	↑
267 *	gi_51815648	CO885363	BAIAP2	Bai1-associated protein 2	0.005	-2.36	-2.01	1.4	-2.45	--
268	gi_68422588	AM024227	– – -	Am024227 kn-252-lymph,bos taurus cDNA clone c0007396p19 3' sequence	0.005	-2.35	-2.52	-4.7	-5.23	↑
269	gi_119912178	XM_612461	ABCC3	ATP-binding cassette, sub-family c (cftr/mrp), member 3	0.004	-2.35	-2.26	-6.8	-5.76	↑
270	gi_51591896	NM_001004024	JUP	Junction plakoglobin	0.005	-2.34	-2.39	-3.3	-4.58	--
271	gi_51885704	AJ818228	– – -	Aj818228 kn206 bos sp. cDNA clone c0006011j16 sequence	0.005	-2.32	-2.00	-5.1	-13.50	--
272	gi_115495988	NM_001075518	ALDH3B1	Aldehyde dehydrogenase 3 family, member b1	0.005	-2.32	-2.63	-2.9	1.20	--
273	gi_115496555	NM_001075713	MYL6B	Myosin, light chain 6b, alkali, smooth muscle and non-muscle	0.005	-2.31	-2.41	-2.6	-3.85	--
274	gi_119930931	XM_001256733	LOC790194	Similar to cgmp-specific phosphodiesterase (LOC790194)	0.005	-2.31	-1.65	-3.2	-4.27	↑
275	gi_119919465	XM_001252823	– – -	Hypothetical protein, transcript variant 2 (LOC785604)	0.005	-2.30	-2.63	-4.0	-3.12	↑
276	gi_51816295	CO886010	– – -	Co886010 bovgen_14335 normal cattle brain cDNA clone rzpdp1056c249q 5' sequence	0.007	-2.30	-1.51	-2.8	-2.18	--
277	gi_51823984	CO893679	– – -	Co893679 bovgen_22004 normal cattle brain cDNA clone rzpdp1056b1442q 5' sequence	0.005	-2.30	-4.28	-3.6	-3.06	↑
278	gi_119919467	XM_001257253	LOC790877	Hypothetical protein, transcript variant 3 (LOC790877)	0.005	-2.30	-3.09	-4.4	-2.84	↑
279	gi_76638883	XM_591410	P2RX7	Purinergic receptor p2x, ligand-gated ion channel, 7	0.006	-2.29	-4.20	-3.2	-2.70	--
280	gi_119908015	XM_604649	IL24	Interleukin 24	0.007	-2.29	2.41	-6.6	-4.40	--
281	gi_119915955	XM_001256057	LOC789256	Hypothetical protein (LOC789256)	0.007	-2.29	-1.77	-3.1	-1.89	--
282	gi_51818847	CO888562	– – -	Co888562 bovgen_16887 normal cattle brain cDNA clone rzpdp1056i1050q 5' sequence	0.005	-2.28	-2.20	1.1	-4.20	--
283	gi_119903838	XM_582962	PLB1	Phospholipase b1	0.010	-2.26	-1.79	-3.7	-4.85	↑
284	gi_119910850	XM_869691	RASIP1	Ras interacting protein 1	0.006	-2.26	-2.24	-8.5	-47.33	↑
285	gi_87196509	NM_001010995	TPM2	Tropomyosin 2 (beta)	0.007	-2.26	-1.55	-1.6	-5.04	--
286	gi_119901064	XM_597850	OGFRL1	Opioid growth factor receptor-like 1	0.006	-2.25	-1.65	-4.2	-5.90	--
287	gi_118151237	NM_001078081	C6orf25	Chromosome 6 open reading frame 25 (c6orf25)	0.007	-2.24	-2.21	-3.8	-4.49	--
288	gi_119925143	XM_001252882	LOC784626	Similar to neuron-derived orphan receptor-1 alfa	0.007	-2.24	-1.40	1.0	-5.41	--
289	gi_119930624	XM_001249903	LOC783914	Hypothetical protein (LOC783914)	0.007	-2.23	-2.07	-2.7	-3.51	--
290	gi_125991949	NM_001081581	ABAT	4-aminobutyrate aminotransferase	0.007	-2.23	-1.78	-2.1	-20.75	--
291 *	gi_119909004	XM_870711	MDK	Midkine (neurite growth-promoting factor 2)	0.007	-2.22	-2.11	-4.2	-8.20	--
292	gi_87271067	DY457942	– – -	Dy457942 1585752 marc 11bovcDNA 3' sequence	0.007	-2.22	-1.82	-2.9	-1.87	--
293	gi_119907581	XM_592504	STARD10	Star-related lipid transfer (start) domain containing 10	0.007	-2.22	-1.89	-5.8	-3.88	--
294	gi_119927352	XM_001250999	LOC785349	Similar to DTFT5783 (LOC785349)	0.009	-2.21	-3.25	-4.4	-6.84	↑
295	gi_41386767	NM_174009	CD34	CD34 molecule	0.008	-2.21	-2.07	-12.6	-18.20	--
296	gi_51816347	CO886062	– – -	Co886062 bovgen_14387 normal cattle brain cDNA clone rzpdp1056i1418q 5' sequence	0.008	-2.20	-2.26	-4.3	-1.48	↑
297	gi_51884851	AJ817375	– – -	Aj817375 kn206 bos sp. cDNA clone c0006006j21 seq	0.007	-2.20	-1.46	-3.6	-4.24	↑
298	gi_119901000	XM_613776	TRAF1	TNF receptor-associated factor 1	0.009	-2.20	-5.87	-1.8	-10.95	--
299	gi_119923417	XM_001250290	LOC781803	Similar to osbp related protein 10 (LOC781803)	0.009	-2.20	-2.17	-4.9	-4.54	↑
300	gi_61888849	NM_001013582	AK1	Adenylate kinase 1	0.007	-2.19	-1.83	-2.9	-1.81	↑
301	gi_119909629	XM_867430	GGT1	Gamma-glutamyltransferase 1	0.009	-2.19	-1.93	-6.1	-3.96	--
302	gi_119909828	XM_586270	LOC509331	Similar to plcg2 protein (LOC509331)	0.008	-2.19	-2.31	-1.5	-3.95	--
303	gi_51818911	CO888626	– – -	Co888626 bovgen_16951 normal cattle brain cDNA clone rzpdp1056m2243q 5' sequence	0.010	-2.18	-1.53	-3.3	-3.73	↑
304	gi_7055130b	AW485024	– – -	Aw485024 63440 marc 3bovcDNA 5' sequence	0.008	-2.18	-4.18	-71.7	-33.36	↑
305	gi_119937909	XM_001256935	LOC790478	Hypothetical protein (LOC790478)	0.009	-2.18	-2.12	1.0	-4.13	--
306	gi_119901882	XM_580814	SERINC5	Serine incorporator 5	0.008	-2.18	-1.37	-2.8	-1.52	--
307	gi_119909826	XM_869529	LOC617296	Similar to PLCG2 protein (LOC617296)	0.008	-2.18	-2.82	-2.2	-4.69	--
308	gi_60453989	DN285379	– – -	DN285379 1235238 marc 7bov cDNA 3' sequence	0.008	-2.17	-1.66	1.5	-3.10	--
309	gi_114053334	NM_001046099	ECSCR	Endothelial cell-specific chemotaxis regulator	0.013	-2.17	-1.91	-2.6	-3.21	--
310	gi_119904995	XM_581907	MCF2L	Mcf.2 cell line derived transforming sequence-like	0.010	-2.16	-1.05	-25.0	-32.70	↑
311	gi_115496553	NM_001076491	ATP8B3	Atpase, class i, type 8b, member 3	0.012	-2.15	-1.63	-2.9	-1.97	--
312	gi_51811313	CO881384	– – -	Co881384 bovgen_09709 normal cattle brain cDNA clone rzpdp1056o179q 5' sequence	0.010	-2.15	-4.92	-26.4	-33.63	--
313	gi_119930598	XM_001255904	LOC789026	Hypothetical protein (LOC789026)	0.010	-2.15	1.30	1.0	-2.38	--
314	gi_156121054	NM_001102204	RIN2	Ras and rab interactor 2	0.009	-2.15	-2.48	-7.4	-3.55	↑
315	gi_51884304	AJ816828	– – -	Aj816828 kn206 bos sp. cDNA clone c0005208p21 seq	0.010	-2.13	-1.69	-3.1	-2.88	↑
316	gi_47952192	CN824123	– – -	Cn824123 oa_splbn_07g03_m13reverse sheep spleen\brain psport1 library ovis aries cDNA clone	0.013	-2.13	-1.62	-2.7	-3.34	↑

				oa_splbn_07g03 5' sequence						
317	gi_119913104	XM_602275	MAP3K1	Mitogen-activated protein kinase kinase kinase 1	0.010	-2.12	-1.72	-6.2	-3.92	--
318	gi_119901259	XM_001253056	LOC784866	Hypothetical protein (LOC784866)	0.012	-2.12	-2.02	-3.1	-2.98	--
319	gi_51824423	CO894116	– – -	Co894116 bovgen_22441 normal cattle brain cDNA clone rzpdp1056h2334q 5' sequence	0.011	-2.12	-1.88	-1.0	-3.45	--
320	gi_119929731	XM_869028	LOC616895	Retinoic acid receptor beta (LOC616895)	0.017	-2.11	-1.23	-3.7	-1.50	--
321	gi_51821577	CO891282	– – -	Co891282 bovgen_19607 normal cattle brain cDNA clone rzpdp1056m1045q 5' sequence	0.013	-2.11	-1.39	-12.9	-33.01	↑
322	gi_119911632	XM_604237	EFCAB5	EF-hand calcium binding domain 5	0.016	-2.11	-2.57	-4.6	-2.78	--
323	gi_76668819	XM_864611	SIM1	Single-minded homolog 1 (drosophila)	0.015	-2.10	-1.83	-4.9	-19.31	↑
324 *	gi_119892012	XM_611497	ZNF385A	Zinc finger protein 385A	0.012	-2.10	-1.38	-7.0	-2.24	↑
325 *	gi_75832046	NM_173935	MDK	Midkine (neurite growth-promoting factor 2)	0.013	-2.09	-2.23	-4.0	-7.18	--
326	gi_156121204	NM_001102280	GAS7	Growth arrest-specific 7	0.013	-2.09	-1.75	-5.6	-13.79	--
327 *	gi_119890150	XM_867937	FAM151A	Family with sequence similarity 151, member a	0.018	-2.09	-2.41	-3.2	1.25	↑
328	gi_51801600	CO871768	– – -	Co871768 bovgen_00093 normal cattle brain cDNA clone rzpdp1056l1557q 3' sequence	0.013	-2.08	-4.32	-2.8	-2.45	--
329 *	gi_119909631	XM_001253630	GGT5	Gamma-glutamyltransferase 5	0.017	-2.08	-1.97	-9.1	-8.98	↑
330	gi_51815582	CO885297	– – -	Co885297 bovgen_13622 normal cattle brain cDNA clone rzpdp1056d0515q 5' sequence	0.013	-2.08	-2.30	-1.2	-3.85	--
331	gi_119907061	XM_582232	SCN2B	Sodium channel, voltage-gated, type ii, beta	0.015	-2.08	-1.24	-2.9	-1.59	--
332	gi_119894838	XM_592551	FCER2	Fc fragment of ige, low affinity ii, receptor for (CD23)	0.014	-2.08	-2.30	-3.0	-3.37	--
333	gi_160333826	NM_001110441	TMEM145	Transmembrane protein 145	0.014	-2.07	-2.12	-4.6	-5.69	--
334	gi_51812559	CO882627	– – -	Co882627 bovgen_10952 normal cattle brain cDNA clone rzpdp1056b2211q 5' sequence	0.015	-2.07	-2.40	-3.0	-3.41	--
335	gi_119912471	XM_584593	LOC539069	Similar to copper amine oxidase (LOC539069)	0.017	-2.07	-1.32	1.0	-3.09	--
336	gi_119891937	XM_588753	ALX1	ALX homeobox 1	0.014	-2.06	-1.38	1.0	-3.44	--
337	gi_116003924	NM_001076850	UGCG	Udp-glucose ceramide glucosyltransferase	0.014	-2.06	-2.02	-8.9	-8.94	--
338	gi_155722980	NM_001101042	SLC2A5	Solute carrier family 2 (facilitated glucose/fructose transporter), member 5	0.021	-2.06	-1.48	-2.7	-7.55	↑
339	gi_119919471	XM_001257252	– – -	Hypothetical protein, transcript variant 2 (LOC790877)	0.015	-2.04	-2.28	-4.4	-2.78	--
340	gi_29275040	CB468655	– – -	Cb468655 734502 marc 6bovcDNA 5' sequence	0.015	-2.04	-1.40	-3.4	-4.55	↑
341	gi_71034621	DR749281	– – -	Dr749281 ng010006a12h05 ng01 rearrayed soares normalized bovine placenta cDNA clone bp230018a10b10 3' sequence	0.017	-2.04	-3.25	-3.0	-7.10	↑
342	gi_82660204	DV800011	– – -	Dv800011 lb01310.cr_o08 gc_bgc-13cDNA clone image:8183650 5' sequence	0.015	-2.04	-2.04	-10.6	-9.77	--
343	gi_77736348	NM_001034702	ENO3	Enolase 3 (beta, muscle)	0.017	-2.03	-2.19	-6.5	-8.31	↑
344	gi_119895593	XR_028187	LOC510849	Similar to protocadherin gamma b6 (LOC510849)	0.018	-2.03	-1.89	-1.3	-2.48	
345	gi_119908895	XM_616231	DCLK2	Doublecortin-like kinase 2	0.019	-2.03	-2.07	-3.1	-3.37	--
346	gi_119934004	XM_586352	LOC509406	Hypothetical (LOC509406)	0.018	-2.03	-4.27	-5.4	-7.41	↑
347	gi_134085863	NM_001083514	LASS1	Lag1 homolog, ceramide synthase 1	0.018	-2.03	-1.59	-3.8	-4.48	--
348	gi_119892869	XM_871851	CAPRIN2	Caprin family member 2	0.018	-2.02	-1.71	-1.0	-1.58	--
349 *	gi_119892014	XM_872514	ZNF385A	Zinc finger protein 385a	0.018	-2.02	-1.20	-6.2	-2.05	↑
350 *	gi_78369652	NM_001035494	RPH3AL	Rabphilin 3a-like (without c2 domains)	0.019	-2.02	-2.46	-6.9	1.24	--
351	gi_119901199	XM_001250567	LOC782005	Similar to man9-mannosidase (LOC782005)	0.018	-2.01	-1.54	-3.0	1.02	--
352	gi_119912116	XM_584605	NGFR	Nerve growth factor receptor	0.021	-2.01	-1.71	-55.6	-2.40	--
353 *	gi_119908232	XM_618596	CDC42BPA	Cdc42 binding protein kinase alpha (DMPK-like)	0.019	-2.00	-2.02	-1.4	-1.83	--

3.1.2 Full list of TashAT2 modulated up-regulated genes (n = 113) showing similar response in parasite infection

S.No	SEQ. ID	Acc. No. (RefSeq)	Putative Gene symbol	Gene Name	TashAT2 transfected BoMac array results: TashAT2 vs PCAGGS control FDR	TashAT2 vs PCAGGS control abs: FC	TahAT2 PMA vs control PMA abs: FC	Infection associated TBL20 array results: TBL20 vs BL20 abs: FC	TBL20 LPS vs BL20 LPS abs:FC (4h/or18)	BW720c Response
						↑	↑/--	↑/--	↑/--	
1	gi_61016342	DN550204	– – -	DN550204 1408544 marc 7bovcDNA 5' sequence	0.000	397.2	417.78	-1.2	5.37	--
2	gi_156120814	NM_001102084	NELL2	Nel-like 2 (chicken)	0.000	265.1	322.08	1.3	7.53	--
3	gi_60997329	DN540953	– – -	Dn540953 marc 7bov cDNA 3' sequence	0.000	144.3	198.00	45.9	33.94	--
4	gi_119918977	XM_600048	VWA5A	Von willebrand factor a domain containing 5a	0.000	116.3	199.83	31.5	33.23	--
5	gi_119923735	XM_586767	MUM1L1	Melanoma associated antigen (mutated) 1-like 1	0.000	91.4	85.15	28.8	25.85	--
6	gi_155372078	NM_001101176	COL8A1	Collagen, type viii, alpha 1	0.000	74.9	100.62	5.0	3.23	↓
7	gi_156120838	NM_001102096	TOX	Thymocyte selection-associated high mobility group box	0.000	64.2	32.82	8.1	3.54	--
8	gi_119902404	XM_869291	TMEM62	Transmembrane protein 62	0.000	61.8	50.92	22.8	65.56	--
9	gi_119889179	XM_001252441	LOC784007	Similar to LOC496253 protein	0.000	46.3	56.68	96.3	74.79	--
10	gi_115494987	NM_001075771	PARM1	Prostate androgen-regulated mucin-like protein 1	0.000	44.3	45.93	2.3	-3.47	--
11*	gi_78365245	NM_001035418	ARHGEF9	Cdc42 guanine nucleotide exchange factor (GEF) 9	0.000	42.2	44.42	1.0	1.84	--
12	gi_51827110	CO896790	– – -	Co896790 bovgen_25115 normal cattle brain cDNA clone rzpdp1056m161q 5' sequence	0.000	34.4	22.39	6.7	5.39	--
13	gi_114051791	NM_001045971	SPINT2	Serine peptidase inhibitor, kunitz type, 2	0.000	33.9	41.81	1.4	3.19	--
14	gi_119918691	XM_001252439	C10orf72	Chromosome 10 open reading frame 72	0.000	18.4	7.76	2.0	3.36	--
15	gi_122692456	NM_001080306	PRSS23	Protease, serine, 23	0.000	16.7	31.18	23.3	30.66	--
16	gi_119908954	XM_614680	INPP4B	Inositol polyphosphate-4-phosphatase, type ii, 105kda	0.000	14.8	23.19	4.0	2.15	↑
17	gi_68427085	AM027998	– – -	Am027998 kn-252-lymph, bos indicus bos indicus cDNA clone c0007394g06 3' sequence	0.000	11.6	2.69	2.8	1.92	--
18	gi_31342530	NM_174239	ALDH1A1	Aldehyde dehydrogenase 1 family, member a1	0.000	10.5	112.82	14.0	64.46	↓
19	gi_41386781	NM_174231	ADRB2	Adrenergic, beta-2-, receptor, surface	0.000	10.0	15.62	1.1	3.94	--
20	gi_119907228	XM_618666	PDE3B	Phosphodiesterase 3b, cgmp-inhibited	0.000	9.1	11.73	3.0	2.34	--
21	gi_119903692	XM_871827	LRRTM4	Leucine rich repeat transmembrane neuronal 4	0.000	9.0	47.50	242.6	219.67	--
22	gi_119907150	XM_612483	SORL1	Sortilin-related receptor, l(dlr class) a repeats containing	0.000	8.9	6.49	4.1	18.50	↑
23	gi_112219499	EE358869	– – -	EE358869 lb02964.cr_k02 gc_bgc-29 cDNA clone image:8476732 sequence	0.000	8.5	11.63	2.2	-2.79	--
24	gi_78042501	NM_001035019	SMPDL3A	Sphingomyelin phosphodiesterase, acid-like 3a	0.000	7.4	6.70	2.2	-2.03	--
25	gi_119879477	XM_585702	ZBTB20	Zinc finger and btb domain containing 20	0.000	7.0	5.73	6.7	16.12	--
26*	gi_119923900	XM_001251680	Gm41	Melanoma antigen, family b, 4 pseudogene	0.000	6.9	5.63	2.2	3.62	↓
27	gi_119910070	XM_586929	MT2A	Metallothionein 2a	0.000	6.1	3.30	4.5	4.87	--
28	gi_119900406	XR_028276	LOC785532	Similar to dap-1 alpha (LOC785532)	0.000	6.1	6.44	4.4	4.80	--
29	gi_139948748	NM_001083764	MYL12B	Myosin, light chain 12b, regulatory	0.000	6.0	8.63	3.6	6.81	--

30*	gi_158937245	NM_001110194	HCK	Hemopoietic cell kinase	0.000	5.9	6.11	2.3	6.33	--
31	gi_31341534	NM_174613	SLC7A5	Solute carrier family 7 (cationic amino acid transporter, y+ system), member 5	0.000	5.9	-1.42	2.9	4.61	↓
32	gi_119901194	XM_001250525	LOC781963	Similar to sphingomyelin phosphodiesterase, acid-like 3a	0.000	5.8	6.35	2.0	-2.21	--
33	gi_139948480	NM_001083649	RASGEF1B	RASGEF domain family, member 1b	0.000	5.8	9.35	32.9	-2.15	--
34	gi_51802721	CO872881	– – -	Co872881 bovgen_01206 normal cattle brain cDNA clone rzpdp1056n0454q 3' sequence	0.000	5.4	4.41	4.9	10.22	--
35*	gi_119935095	XM_585695	Gm41	Melanoma antigen, family b, 4 pseudogene	0.000	5.4	4.60	3.0	4.14	↓
36	gi_136256366	NM_174035	CYBB	Cytochrome b-245, beta polypeptide	0.000	5.2	4.20	2.2	2.13	--
37	gi_119908995	XM_602397	SLC7A11	Solute carrier family 7, (cationic amino acid transporter, y+ system) member 11	0.000	5.2	-2.31	-1.1	17.30	--
38*	gi_119905669	XM_001249927	PMEPA1	Prostate transmembrane protein, androgen induced 1	0.000	5.0	4.94	2.7	2.07	--
39*	gi_118150817	NM_001077850	BCAS1	Breast carcinoma amplified sequence 1	0.000	5.0	5.69	2.2	3.36	--
40*	gi_119927606	XM_001253379	CYP3A4	Cytochrome p450, family 3, subfamily a, polypeptide 4	0.000	4.9	-2.21	-2.6	1.91	--
41	gi_156718111	NM_001103091	LTBP1	Latent transforming growth factor beta binding protein 1	0.000	4.8	9.68	2.4	1.74	↓
42	gi_119889181	XM_001252489	LOC784072	Similar to cd84-h1 (loc784072)	0.000	4.4	2.93	13.1	13.31	--
43	gi_119884823	XM_587050	SERPINI1	Serpin peptidase inhibitor, clade i (neuroserpin), member 1	0.000	4.4	4.31	9.2	5.38	--
44	gi_51822234	CO891936	– – -	Co891936 bovgen_20261 normal cattle brain cDNA clone rzpdp1056m1641q 5' sequence	0.000	4.3	-2.07	-1.4	10.39	--
45	gi_31342766	NM_174137	SERPINE1	Serpin peptidase inhibitor, clade e (nexin, plasminogen activator inhibitor type 1), member 1	0.000	4.3	3.17	67.6	43.63	↓
46*	gi_150247128	NM_001099368	PCDHGA2	Protocadherin gamma subfamily a, 2	0.000	4.2	6.58	2.4	1.69	--
47	gi_119933556	XM_001256914	LOC790449	Similar to PCDH19 protein (LOC790449)	0.000	3.9	3.57	5.6	38.82	↓
48	gi_119879733	XM_614853	ETV5	ETS variant 5	0.000	3.9	1.55	1.4	5.52	--
49*	gi_190360732	NM_001128499	TGIF1	TGFB-induced factor homeobox 1	0.000	3.9	2.31	2.0	2.09	--
50	gi_119916372	XM_616030	SMAD7	Smad family member 7	0.000	3.8	3.43	2.1	1.11	--
51*	gi_119895626	XR_028461	PCDHGA2	Protocadherin gamma subfamily a, 2	0.000	3.8	5.05	2.1	3.04	--
52	gi_119890101	XM_616138	CACHD1	Cache domain containing 1	0.000	3.7	3.77	5.7	3.27	--
53	gi_31342041	NM_174423	PLAUR	Plasminogen activator, urokinase receptor	0.000	3.7	1.15	3.6	2.10	--
54	gi_77735810	NM_001034432	CREB3L3	Camp responsive element binding protein 3-like 3	0.000	3.7	3.44	5.7	6.69	↓
55*	gi_119923957	XM_001250482	Gm41	Melanoma antigen, family b, 4 pseudogene	0.000	3.6	2.47	2.2	3.40	↓
56	gi_115496251	NM_001075741	GPRC5B	G protein-coupled receptor, family c, group 5, member b	0.000	3.5	4.65	1.0	1.72	--
57	gi_119891399	XM_599768	JHDM1D	Jumonji c domain containing histone demethylase 1 homolog d (s. Cerevisiae)	0.000	3.5	2.62	9.9	9.27	--
58	gi_51815450	CO885165	– – -	Co885165 bovgen_13490 normal cattle brain cDNA clone rzpdp1056e197q 5' sequence	0.000	3.5	3.02	14.9	12.66	--
59	gi_139948893	NM_001083648	CHST1	Carbohydrate (keratan sulfate gal-6) sulfotransferase 1	0.000	3.4	2.31	4.9	-1.68	--
60	gi_60722467	DN512277	– – -	Dn512277 1248296 marc 7bov cDNA 3' sequence	0.000	3.3	3.38	11.4	3.90	--
61	gi_119906547	XR_027912	LOC535166	Similar to sulfatase 1 (LOC535166)	0.001	3.1	1.76	1.7	4.37	--
62	gi_119923683	XR_027350	LOC781857	Similar to interferon-induced protein 44 (antigen p44)	0.001	3.1	1.48	3.1	-4.30	↑
63*	gi_119894560	XM_584000	BST2	Bone marrow stromal cell antigen 2	0.001	3.0	3.41	4.8	-4.02	--
64	gi_119889540	XM_596143	LOC517961	Hypothetical (LOC517961)	0.001	3.0	3.15	2.5	1.39	↓
65*	gi_119922382	XM_001254377	Gm41	Melanoma antigen, family b, 4 pseudogene	0.001	2.9	2.10	3.2	5.13	↓
66	gi_84000564	NM_001034457	WBSCR22	Williams beuren syndrome chromosome region 22	0.001	2.9	2.48	2.9	2.76	--
67	gi_119917674	XM_589432	ELOVL3	Elongation of very long chain fatty acids (fen1/elo2, sur4/elo3, yeast)-like 3	0.001	2.8	3.58	3.6	3.65	↓
68	gi_119901328	XM_618588	PRDM1	Pr domain containing 1, with znf domain	0.001	2.8	2.41	3.9	10.91	--
69	gi_115495710	NM_001075904	LRRC6	Leucine rich repeat containing 6	0.001	2.7	3.37	5.3	21.15	--
70	gi_149643068	NM_001098866	ACPP	Acid phosphatase, prostate	0.001	2.7	3.65	4.5	3.36	--
71	gi_110347584	NM_182786	FOS	FBJ murine osteosarcoma viral oncogene homolog	0.001	2.7	-1.85	3.8	4.48	--
72	gi_119889992	XM_872122	IFI44	Interferon-induced protein 44	0.001	2.7	2.39	3.1	-4.50	↑
73	gi_46559375	NM_206971	SEC16B	Sec16 homolog b (s. Cerevisiae)	0.001	2.7	1.86	4.2	4.63	--
74*	gi_51814346	CO884356	DNAJC6	DNAj (hsp40) homolog, subfamily c, member 6	0.002	2.6	7.23	1.5	-3.30	--
75*	gi_148233315	NM_001098165	RNASEL	Ribonuclease l (2',5'-oligoisoadenylate synthetase-dependent)	0.001	2.6	3.07	18.6	72.89	--
76*	gi_118150929	NM_001077912	TPST1	Tyrosylprotein sulfotransferase 1	0.001	2.6	3.07	2.7	1.60	--
77	gi_119917796	XM_604643	CASP7	Caspase 7, apoptosis-related cysteine peptidase	0.001	2.6	3.26	6.2	5.40	--
78	gi_116004140	NM_001076960	ARMCX2	Armadillo repeat containing, x-linked 2	0.001	2.6	3.84	1.5	3.27	--
79	gi_157074115	NM_001103300	MAFF	V-maf musculoaponeurotic fibrosarcoma oncogene homolog f (avian)	0.002	2.5	1.43	2.6	-4.11	↓
80	gi_119917033	XM_001250581	LOC782311	Similar to tyrosylprotein sulfotransferase 1, transcript variant 2 (LOC782311)	0.002	2.4	2.81	2.1	1.73	--
81	gi_119910001	XR_028045	LOC786252	Similar to armadillo repeat containing 2 (LOC786252)	0.003	2.4	2.73	1.1	3.05	--
82	gi_155372230	NM_001101257	FAM89A	Family with sequence similarity 89, member a	0.003	2.4	2.92	4.5	2.67	--
83*	gi_119929648	XM_864342	Gm41	Melanoma antigen, family b, 4 pseudogene	0.003	2.4	2.19	3.1	4.29	↓
84	gi_31341539	NM_174610	SLC6A6	Solute carrier family 6 (neurotransmitter transporter, taurine), member 6	0.003	2.4	2.31	55.6	8.36	↓
85	gi_150247056	NM_001099366	SPRY1	Sprouty homolog 1, antagonist of fgf signaling (drosophila)	0.003	2.4	2.38	1.3	5.40	--
86	gi_58764282	CX950755	– – -	Cx950755 umc-bcl_0b02-030-d06 day 14 cl from a pregnant animal bclcDNA 3' sequence	0.005	2.4	2.52	2.4	-3.36	--
87	gi_147899351	NM_001098072	NRAP	Nebulin-related anchoring protein	0.005	2.4	3.01	8.4	3.06	--
88	gi_119889474	XR_028680	LOC788729	Similar to b-cell cll/lymphoma 9 (LOC788729)	0.003	2.4	1.75	6.6	22.61	--
89	gi_125991933	NM_001081621	TIFA	TRAF-interacting protein with forkhead-associated domain	0.004	2.3	3.33	5.0	-10.34	--
90	gi_119916277	XM_616212	PTPRM	Protein tyrosine phosphatase, receptor type, m	0.004	2.3	2.17	6.8	10.65	--
91*	gi_115495042	NM_001075961	RTP4	Receptor (chemosensory) transporter protein 4	0.004	2.3	1.86	14.9	4.69	↑
92	gi_119915345	XM_001255058	LOC787796	Hypothetical protein (LOC787796)	0.006	2.3	1.24	8.4	7.17	--
93*	gi_119888383	XM_586318	NINJ1	Ninjurin 1	0.005	2.3	1.77	3.0	4.29	--
94	gi_119903215	XM_865470	LOC614107	Similar to hexokinase ii (loc614107)	0.005	2.3	1.58	2.3	3.33	--
95	gi_119889467	XM_871861	LOC613322	Hypothetical loc613322 (loc613322)	0.005	2.2	2.44	6.9	27.21	↑
96*	gi_119901428	XM_001251458	Gm41	Melanoma antigen, family b, 4 pseudogene	0.006	2.2	1.41	2.5	5.16	↓
97	gi_119893596	XM_584935	SLC39A8	Solute carrier family 39 (zinc transporter), member 8	0.007	2.2	2.72	2.6	4.23	--
98	gi_119888157	XM_580320	STEAP3	Steap family member 3	0.006	2.2	1.88	10.9	21.37	--
99	gi_119910534	XM_001254854	LOC788393	Hypothetical protein loc788393 (loc788393)	0.006	2.2	-1.36	3.7	-7.87	↑
100	gi_119893517	XM_001252348	LOC783896	Similar to TRAF-interacting protein with a forkhead-associated domain (LOC783896)	0.007	2.2	2.86	4.1	-11.74	--
101	gi_119903224	XM_001255831	HK2	Hexokinase 2	0.007	2.2	1.53	2.0	2.81	--
102*	gi_118150987	NM_001077947	GPR77	G protein-coupled receptor 77	0.009	2.2	1.98	2.3	5.57	--
103	gi_51816841	CO886556	– – -	Co886556 bovgen_14881 normal cattle brain cDNA clone rzpdp1056n2423q 5' sequence	0.008	2.1	2.01	2.3	2.46	--
104	gi_115497873	NM_001075202	IER3	Immediate early response 3	0.008	2.1	1.11	14.3	20.10	--
105	gi_31340867	NM_174758	NPC1	Niemann-pick disease, type c1	0.009	2.1	1.10	2.8	2.25	--
106	gi_164420718	NM_001075214	GSTO1	Glutathione s-transferase omega 1	0.011	2.1	1.94	3.3	2.63	--
107	gi_78045548	NM_001035075	XAF1	Xiap associated factor 1	0.014	2.1	2.24	3.0	-1.61	↑
108	gi_119915318	XR_028520	LOC512304	Similar to enpp5 (LOC512304)	0.011	2.1	3.31	2.2	5.57	--
109	gi_31343172	NM_173962	SV2A	Synaptic vesicle glycoprotein 2a	0.011	2.1	2.88	-1.3	2.31	--
110	gi_134085833	NM_001083490	HOXC13	Homeobox c13	0.012	2.1	1.39	10.1	11.48	↑
111	gi_31340793	NM_174662	FAS	Fas (TNF receptor superfamily, member 6)	0.012	2.1	1.04	4.0	1.52	--
112	gi_84000334	NM_001038183	CSRP2	Cysteine and glycine-rich protein 2	0.013	2.0	2.23	2.2	3.06	--
113*	gi_167583505	NM_001114515	NUPR1	Nuclear protein, transcriptional regulator, 1	0.013	2.0	-1.64	4.3	3.69	↑

3.2 List of PMA induced up-regulated genes (n = 342) showing modulated expression profiles in TashAT2

Profile 1 n = 52

S.No	SEQ. ID	Acc. No. (RefSeq)	Putative Gene symbol	Gene Name	BoMac PMA vs BoMac Abs FC:	TashAT2 PMA vs PCAGGS PMA Abs: FC
					↑	↑ ↑
1	gi_136256085	NM_001038533	F2RL2	Coagulation factor II (thrombin) receptor-like 2	2.54	16.52
2	gi_58332431	NM_178317	TRIB2	Tribbles homolog 2 (Drosophila)	2.68	13.30
3	gi_31342775	NM_174132	OLR1	Oxidized low density lipoprotein (lectin-like) receptor 1	8.42	11.36
4	gi_119901828	XM_604049	AQPEP	Laeverin	4.97	9.51
5	gi_76642509	XM_871034	LOC618709	Hypothetical (LOC618709)	2.53	8.26
6	gi_155371894	NM_001101082	SEMA3C	Sema domain, immunoglobulin domain (Ig), short basic domain, secreted, (semaphorin) 3C	2.36	6.32
7	gi_119893972	XM_596732	LOC518539	Similar to epiregulin (LOC518539)	5.40	6.18
8	gi_119889047	XM_592485	SLAMF8	SLAM family member 8	2.34	6.09
9	gi_58764139	CX950612	– – -	CX950612 UMC-bcl_0B02-028-b07 Day 14 CL from a pregnant animal bclcdna 3' sequence	3.89	6.01
10	gi_119901966	XM_605853	PAQR5	Progestin and adipoq receptor family member V	2.98	5.88
11	gi_76642926	XM_600064	SLFN11	Schlafen family member 11	2.14	5.57
12	gi_51815461	CO885176	– – -	CO885176 bovgen_13501 normal cattle brain cdna clone rzpdp1056b2017q 5' sequence	2.50	5.39
13	gi_31341636	NM_174571	PECAM1	Platelet/endothelial cell adhesion molecule	2.37	4.99
14	gi_119928196	XM_001254362	LOC786779	Similar to retinoic acid inducible in neuroblastoma cells RAINB1 (LOC786779)	4.28	4.46
15	gi_139949115	NM_001083796	VASN	Vasorin	2.38	3.97
16	gi_119908002	XM_588921	FAIM3	Fas apoptotic inhibitory molecule 3	2.07	3.62
17	gi_119916372	XM_616030	SMAD7	SMAD family member 7	2.48	3.43
18*	gi_119906905	XM_001250441	MMP1	Matrix metallopeptidase 1 (interstitial collagenase)	2.45	3.41
19	gi_119888296	XM_866583	FAM117B	Family with sequence similarity 117, member B	2.04	3.35
20	gi_119910070	XM_586929	MT2A	Metallothionein 2A	4.50	3.30
21	gi_77735772	NM_001034409	EEPD1	Endonuclease/exonuclease/phosphatase family domain containing 1	2.26	3.23
22*	gi_119919612	XM_584932	LONRF3	LON peptidase N-terminal domain and ring finger 3	2.32	3.17
23	gi_119879453	XM_616928	PLCXD2	Phosphatidylinositol-specific phospholipase C, X domain containing 2	2.07	3.16
24*	gi_119919610	XM_001249810	LONRF3	LON peptidase N-terminal domain and ring finger 3	2.08	3.13
25	gi_60993766	DN539166	– – -	DN539166 1384921 MARC 7bovcdna 5' sequence	2.24	3.10
26*	gi_27806540	NM_174112	MMP1	Matrix metallopeptidase 1 (interstitial collagenase)	2.84	3.07
27	gi_82809590	DV875361	– – -	DV875361 LB02527.CR_C12 GC_BGC-25 cdna clone IMAGE:8209862 5' sequence	2.15	2.82
28	gi_115496543	NM_001076011	ITPKC	Inositol 1,4,5-trisphosphate 3-kinase C	2.46	2.82
29*	gi_119916246	XM_587139	TGIF1	TGFB-induced factor homeobox 1	5.31	2.80
30	gi_119891800	XR_027344	LOC781850	Hypothetical protein (LOC781850)	2.42	2.75
31	gi_61946697	DN641296	– – -	DN641296 UMC-bof_0A01-015-b03 Ovarian follicle recruited bofcdna 3' sequence	7.44	2.68
32	gi_119891399	XM_599768	JHDM1D	Jumonji C domain containing histone demethylase 1 homolog D (S. Cerevisiae)	4.33	2.62
33	gi_155372082	NM_001101178	ITPRIP	Inositol 1,4,5-triphosphate receptor interacting protein	2.18	2.60
34	gi_119912488	XM_001256211	LOC789463	Similar to retina copper-containing monoamine oxidase (LOC789463)	2.77	2.56
35	gi_119916129	XM_597764	RNF125	Ring finger protein 125	6.32	2.50
36	gi_122692454	NM_001080309	YOD1	YOD1 OTU deubiquinating enzyme 1 homolog (S. Cerevisiae)	2.15	2.43
37	gi_119908015	XM_604649	IL24	Interleukin 24	37.63	2.41
38*	gi_190360732	NM_001128499	TGIF1	TGFB-induced factor homeobox 1	4.16	2.31
39	gi_119900349	XM_613366	CD274	CD274 molecule	2.07	2.29
40	gi_111103930	EE242794	– – -	EE242794 LB02227.CR_O10 GC_BGC-22cdna clone IMAGE:8260452 sequence	2.23	2.28
41	gi_119912455	XR_028746	KCNH4	Potassium voltage-gated channel, subfamily H (eag-related), member 4	2.08	2.27
42	gi_60456158	DN287548	– – -	DN287548 1241808 MARC 7bovcdna 3' sequence	2.18	2.22
43	gi_51807744	CO877828	– – -	CO877828 bovgen_06153 normal cattle brain cdna clone rzpdp1056a1220q 5' sequence	3.81	2.21
44	gi_148747149	NM_174363	INHBA	Inhibin, beta A	3.05	2.17
45	gi_119910262	XM_612960	CCNE1	Cyclin E1	2.13	2.15
46	gi_31341980	NM_174445	PTGS2	Prostaglandin-endoperoxide synthase 2 (prostaglandin G/H synthase and cyclooxygenase)	20.46	2.12
47	gi_51823760	CO893455	– – -	CO893455 bovgen_21780 normal cattle brain cdna clone rzpdp1056k1350q 5' sequence	2.18	2.11
48	gi_83035104	NM_001037617	C21orf91	Chromosome 21 open reading frame 91	2.55	2.10
49	gi_119890536	XM_583937	GBX2	Gastrulation brain homeobox 2	2.24	2.08
50	gi_115497081	NM_001075656	JUNB	Jun B proto-oncogene	2.06	2.05
51	gi_119894688	XM_001249956	ZSWIM4	Zinc finger, SWIM-type containing 4	4.09	2.03
52	gi_118151325	NM_001078128	SOX4	SRY (sex determining region Y)-box 4	2.60	2.02

Profile 2 n = 220

S.No	SEQ. ID	Acc. No. (RefSeq)	Putative Gene symbol	Gene name	BoMac PMA vs BoMac Abs FC:	TashAT2 PMA vs PCAGGS PMA Abs: FC
					↑	↓
1*	gi_28849922	NM_175700	CXCL2	Chemokine (C-X-C motif) ligand 2	12.41	-22.83
2	gi_148223508	NM_001098056	TNFRSF11B	Tumor necrosis factor receptor superfamily, member 11b	9.96	-16.34
3	gi_119894606	XM_588006	PGLYRP2	Peptidoglycan recognition protein 2	9.73	-10.80
4	gi_119910051	XM_595523	– – -	Similar to fractalkine (LOC517354)	108.81	-10.46
5	gi_31343250	NM_173925	IL8	Interleukin 8	12.97	-9.13
6	gi_119912966	XM_612159	STC2	Stanniocalcin 2	6.08	-8.63
7	gi_31342642	NM_174183	IL8	Selectin P (SELP)	5.51	-7.92
8	gi_83721976	NM_001003904	FANK1	Fibronectin type III and ankyrin repeat domains 1	6.14	-7.91
9	gi_119892044	XM_582930	KRT18	Keratin 18	13.61	-7.82
10	gi_51884334	AJ816858	– – -	AJ816858 AJ816858 KN206 Bos sp. cDNA clone C0005208o15 sequence	8.92	-7.67
11	gi_31343615	NM_175827	CCL5	Chemokine (C-C motif) ligand 5	5.49	-7.53
12	gi_119905157	XM_866719	IL15RA	Interleukin 15 receptor, alpha	4.23	-7.24
13	gi_164448607	NM_001076870	IHH	Indian hedgehog	4.07	-7.09
14	gi_119888971	XM_868383	CDA	Cytidine deaminase	7.18	-7.04
15	gi_77736420	NM_001034738	LTB4R	Leukotriene B4 receptor	5.20	-6.80
16	gi_119911895	XM_866482	PIK3R5	Phosphoinositide-3-kinase, regulatory subunit 5	3.57	-6.45
17	gi_115496489	NM_001075341	CDC42EP2	CDC42 effector protein (Rho GTPase binding) 2	7.75	-6.17
18	gi_119919428	XM_599739	FGF19	Fibroblast growth factor 19	5.51	-6.11
19	gi_119908509	XM_607245	SCNN1D	Sodium channel, nonvoltage-gated 1, delta	6.32	-6.01
20	gi_125630654	NM_001081512	SPRY4	Sprouty homolog 4 (Drosophila)	15.66	-5.86
21	gi_115497399	NM_001075256	KLK7	Kallikrein-related peptidase 7	5.48	-5.67
22	gi_119912361	XM_875498	LOC514744	Hypothetical LOC514744, transcript variant 4 (LOC514744)	2.91	-5.52
23	gi_31341396	NM_181022	GNAT1	Guanine nucleotide binding protein (G protein), alpha transducing activity polypeptide1	4.52	-5.42
24	gi_164452922	NM_001040512	LIMD2	LIM domain containing 2 (LIMD2)	2.83	-5.29
25	gi_119874949	XR_027735	LOC510140	Hypothetical protein (LOC515053)	2.84	-5.07
26	gi_157427775	NM_001105322	KRT17	Keratin 17	2.96	-5.07

27	gi_31342285	NM_174337	LOC281812	Fibroblast growth factor-binding protein (FGF-BP) (LOC281812)	8.23	-5.00
28*	gi_155372040	NM_001101158	VCAM1	Vascular cell adhesion molecule 1	3.45	-4.93
29	gi_45430044	NM_205812	PKIG	Protein kinase (camp-dependent, catalytic) inhibitor gamma	3.14	-4.76
30	gi_119908887	XM_587667	TMEM154	Transmembrane protein 154	4.31	-4.65
31	gi_115497953	NM_001076103	TRIB3	Tribbles homolog 3 (Drosophila)	7.30	-4.58
32	gi_119894242	XM_001250804	LOC783341	Similar to fibroblast growth factor-binding protein (LOC783341)	7.47	-4.43
33	gi_112210002	EE349629	SELP	EE349629 LB02756.CR_B03 GC_BGC-27cdna clone IMAGE:8630885 sequence	6.14	-4.32
34	gi_76636135	XM_865027	OMP	Olfactory marker protein	2.94	-4.32
35	gi_51801600	CO871768	– – -	CO871768 bovgen_00093 normal cattle braincdna clone rzpdp1056l1557q 3' sequence	2.88	-4.32
36	gi_119923241	XM_001252681	CCL5	Similar to multidrug resistance-associated protein (LOC784347)	2.26	-4.23
37	gi_7055130	AW485024	– – -	AW485024 63440 MARC 3bovcdna 5' sequence	2.37	-4.18
38	gi_76620857	XM_871003	GDF15	Growth differentiation factor 15	3.43	-4.07
39	gi_119905633	XM_611249	SLCO4A1	Solute carrier organic anion transporter family, member 4A1	4.93	-4.03
40	gi_119938175	XM_001257028	LTB4R	Similar to dual specificity phosphatase (EC 3.1.3.-) HVH2 - rat (LOC790602)	8.83	-4.02
41	gi_94966792	NM_001040497	EGR4	Early growth response 4	2.93	-4.01
42	gi_139948867	NM_001083732	GEM	GTP binding protein overexpressed in skeletal muscle	3.80	-4.00
43	gi_125630668	NM_001081520	LY6G6E	Lymphocyte antigen 6 complex, locus G6E	2.43	-3.99
44	gi_119913026	XM_589415	LOC507969	Similar to neuronal apoptosis inhibitory protein (LOC539780)	3.51	-3.95
45	gi_76655846	XM_593654	BIRC3	Similar to dual specificity phosphatase (EC 3.1.3.-) HVH2 - rat (LOC540380)	2.76	-3.94
46	gi_119892163	XM_591526	FMNL3	Formin-like 3	2.28	-3.89
47	gi_31342739	NM_174147	PLAU	Plasminogen activator, urokinase	6.38	-3.87
48	gi_31342652	NM_174181	BDKRB2	Selectin E (SELE)	6.92	-3.85
49	gi_119903277	XM_613518	CYP26B1	Cytochrome P450, family 26, subfamily B, polypeptide 1	8.31	-3.83
50	gi_51883613	AJ816137	– – -	AJ816137 AJ816137 KN206 Bos sp. Cdna clone C0005199e18 sequence	2.34	-3.80
51	gi_119902263	XM_001253931	FMN1	Formin 1	2.83	-3.80
52	gi_119901909	XM_608288	IGDCC3	Immunoglobulin superfamily, DCC subclass, member 3	2.04	-3.79
53	gi_114052738	NM_001046298	FLI1	Friend leukemia virus integration 1	2.06	-3.79
54	gi_119914056	XM_583508	BDKRB2	Bradykinin receptor B2	4.46	-3.77
55*	gi_49428238	AJ694819	LYST	Lysosomal trafficking regulator	2.09	-3.76
56	gi_157785620	NM_001105626	TTYH2	Tweety homolog 2 (Drosophila)	2.77	-3.73
57	gi_27819627	NM_174359	IL2RG	Interleukin 2 receptor, gamma	3.57	-3.71
58	gi_119892376	XM_001251597	LOC781063	Hypothetical protein (LOC782937)	3.10	-3.71
59*	gi_119905155	XM_001252652	PFKFB3	6-phosphofructo-2-kinase/fructose-2,6-biphosphatase 3	2.73	-3.69
60	gi_119928947	XM_001253195	LOC537304	Hypothetical protein (LOC785053)	2.56	-3.68
61	gi_156120610	NM_001101981	TBC1D2	TBC1 domain family, member 2	2.20	-3.68
62	gi_117935052	NM_001024930	CCR7	Chemokine (C-C motif) receptor 7	5.43	-3.66
63	gi_119920689	XM_581517	GYG2	Glycogenin 2	2.05	-3.66
64	gi_119922372	XM_610090	LOC538598	Similar to FMN1 protein (LOC531592)	3.06	-3.64
65	gi_119904445	XM_593034	OLFM4	Olfactomedin 4	2.52	-3.61
66	gi_119904862	XM_593336	ABCC4	ATP-binding cassette, sub-family C (CFTR/MRP), member 4	2.99	-3.61
67	gi_115432044	NM_173888	ADM	Adrenomedullin	2.13	-3.56
68	gi_119936795	XM_001249731	– – -	Similar to multidrug resistance-associated protein (LOC781332)	2.91	-3.54
69	gi_119914998	XM_581556	MGLL	Monoglyceride lipase	2.32	-3.53
70*	gi_119908050	XM_001252091	5430435G22Rik	RIKEN cdna 5430435G22 gene	3.81	-3.51
71	gi_119893320	XM_870947	CEBPB	Similar to BIK1 (LOC618614)	7.37	-3.49
72	gi_119892705	XM_607295	CHST11	Carbohydrate (chondroitin 4) sulfotransferase 11	6.48	-3.43
73	gi_147906802	NM_001098101	ESM1	Endothelial cell-specific molecule 1	10.06	-3.40
74	gi_119935945	XM_001257083	LOC614838	Hypothetical protein (LOC790672)	2.95	-3.40
75	gi_51810587	CO880658	– – -	CO880658 bovgen_08983 normal cattle braincdna clone rzpdp1056e2228q 5' sequence	2.03	-3.39
76*	gi_118150789	NM_001077837	PFKFB3	6-phosphofructo-2-kinase/fructose-2,6-biphosphatase 3	3.85	-3.39
77	gi_157427895	NM_001105385	KLF4	Kruppel-like factor 4 (gut)	5.20	-3.35
78	gi_115432056	NM_001037100	BCL2A1	BCL2-related protein A1	3.60	-3.33
79	gi_155371934	NM_001101102	MDFIC	Myod family inhibitor domain containing	3.14	-3.31
80	gi_119930084	XM_595414	LOC517246	Similar to cytochrome P450 CYP3A24 (LOC517246)	5.83	-3.30
81	gi_119932216	XM_001256909	LOC511224	Hypothetical protein LOC790441 (LOC790441)	2.48	-3.28
82	gi_126722714	NM_001082456	WNT11	Wingless-type MMTV integration site family, member 11	2.54	-3.23
83	gi_119903421	XM_001251996	F2R	Butyrate response factor 2 (ZFP36L2)	3.62	-3.22
84	gi_119935611	XM_001257030	LOC790607	Similar to membrane cofactor protein (LOC790607)	2.30	-3.21
85	gi_119892165	XM_001251013	AQP5	Aquaporin 5	2.39	-3.21
86	gi_119890874	XM_617961	– – -	Similar to semaphorin III/collapsin-1 (LOC537777)	2.11	-3.20
87	gi_31342177	NM_174373	KCNJ2	Potassium inwardly-rectifying channel, subfamily J, member 2	2.54	-3.13
88	gi_82651886	DV798971	FLT3LG	DV798971 Hw_loin_61_050825_A06CF-24-HW loin cdna librarycdna sequence	3.08	-3.13
89	gi_119900643	XM_604596	EGR3	Early growth response 3	3.76	-3.10
90*	gi_119910855	XM_001253556	FGF21	Fibroblast growth factor 21	3.11	-3.05
91	gi_119908394	XM_580530	GPR157	G protein-coupled receptor 157	3.10	-3.04
92	gi_45430034	NM_205806	ST3GAL4	ST3 beta-galactoside alpha-2,3-sialyltransferase 4	2.56	-3.04
93	gi_68433683	AM031784	LOC784977	AM031784 AM031784 KN-252-spleen, Bos sp. Bos sp. Cdna clone C0007402j18 3' sequence	2.44	-3.03
94	gi_156718123	NM_001103097	F2R	Coagulation factor II (thrombin) receptor	3.43	-3.02
95	gi_119915977	XM_588519	NFATC1	Nuclear factor of activated T-cells, cytoplasmic, calcineurin-dependent 1	3.45	-2.99
96	gi_114051875	NM_001046118	LAPTM5	Lysosomal protein transmembrane 5	3.17	-2.98
97*	gi_119925448	XM_001251333	MYO10	Myosin X	2.73	-2.96
98	gi_78369443	NM_001035293	BIRC3	Baculoviral IAP repeat containing 3	4.47	-2.95
99	gi_119906122	XR_028705	LOC507766	Similar to breast cancer putative transcription factor (LOC507766)	2.66	-2.95
100	gi_119913384	XM_596594	ANKRD33B	Ankyrin repeat domain 33B	8.47	-2.95
101	gi_119913029	XR_027889	LOC529061	Similar to Microtubule-associated serine/threonine-protein kinase 4 (LOC529061)	3.82	-2.95
102	gi_156523181	NM_001102535	HR	Hairless homolog (mouse)	2.22	-2.93
103	gi_149642660	NM_001099057	LOC515333	Ankyrin repeat domain 55 (ANKRD55)	2.86	-2.91
104	gi_60729463	DN519273	LOC781928	DN519273 1260085 MARC 7bovcdna 3' sequence	4.42	-2.90
105*	gi_119911031	XM_581045	AU018091	Expressed sequence AU018091	2.89	-2.90
106	gi_126158902	NM_001081577	SLC1A4	Solute carrier family 1 (glutamate/neutral amino acid transporter), member 4	2.39	-2.89
107	gi_119925198	XM_001254231	EGR4	Hypothetical protein (LOC786597)	2.30	-2.87
108	gi_61752704	CR451798	LOC781332	CR451798 CR451798 Normalized and Subtracted bovine embryonic and extraembryonic tissues (bcaz/BE03) cdna clone bcaz0015.n.11 5' sequence	2.21	-2.86
109	gi_119907746	XM_001253132	LOC504861	Similar to LOC387763 protein (LOC784977)	3.16	-2.86
110	gi_114051987	NM_001046392	ARHGAP25	Rho gtpase activating protein 25	2.59	-2.85
111	gi_119913658	XM_587247	SLC2A6	Similar to KIAA1745 protein, transcript variant 1 (LOC510140)	6.76	-2.85
112	gi_119904470	XM_001250967	ANKRD55	Hypothetical protein (LOC782318)	2.13	-2.81
113	gi_115496423	NM_001075725	TP53I11	Tumor protein p53 inducible protein 11	3.10	-2.81
114	gi_119925527	XM_595233	LOC515053	Similar to ABCC4 protein (LOC517069)	2.53	-2.80
115	gi_119935431	XM_001256981	LOC785195	Similar to alpha2,3-sialyltransferase (LOC790542)	2.43	-2.79
116	gi_29255914	CB449532	– – -	CB449532 703738 MARC 6bovcdna 5' sequence	8.64	-2.78
117	gi_119909395	XR_027267	TBX3	T-box 3	4.03	-2.77
118	gi_28603825	NM_176788	LPO	CCAAT/enhancer binding protein (C/EBP), beta (CEBPB)	3.58	-2.77
119	gi_51808063	CO878147	– – -	CO878147 bovgen_06472 normal cattle braincdna clone rzpdp1056k0128q 5' sequence	10.85	-2.76
120	gi_125991751	NM_174603	SLC2A3	Solute carrier family 2 (facilitated glucose transporter), member 3	2.71	-2.76
121	gi_119909447	XM_595626	PXN	Paxillin	2.31	-2.75
122	gi_51887696	AJ820220	LOC790269	AJ820220 AJ820220 KN206 Bos sp. Cdna clone C0006017m22 sequence	3.21	-2.73
123	gi_119913525	XM_583647	ALDH1A3	Aldehyde dehydrogenase 1 family, member A3	4.15	-2.72
124	gi_48675380	NM_001001601	CDH5	Cadherin 5, type 2 (vascular endothelium)	3.66	-2.72
125	gi_156121346	NM_001102352	LOC540380	Rho gtpase activating protein 27 (ARHGAP27)	2.69	-2.72

126	gi_31342036	NM_174426	PLUNC	Palate, lung and nasal epithelium associated	2.25	-2.71
127	gi_51816867	CO886582	– – -	CO886582 bovgen_14907 normal cattle brain cdna clone rzpdp1056h0512q 5' sequence	2.22	-2.70
128	gi_149642860	NM_001099141	BMP2	Bone morphogenetic protein 2	3.33	-2.66
129	gi_119904923	XM_001254844	– – -	Similar to OPR (LOC787451)	2.35	-2.66
130	gi_77735472	NM_001034259	DUSP18	Dual specificity phosphatase 18	2.59	-2.65
131	gi_119907177	XM_864208	UBASH3B	Ubiquitin associated and SH3 domain containing B	2.23	-2.64
132	gi_119894051	XM_587301	IL2RB	Interleukin 2 receptor, beta	2.66	-2.64
133	gi_118150959	NM_001077930	ERRFI1	ERBB receptor feedback inhibitor 1	3.64	-2.64
134	gi_148229402	NM_001098111	PCDH12	Protocadherin 12	2.13	-2.63
135	gi_119904637	XM_001250734	– – -	Hypothetical protein (LOC782141)	2.97	-2.61
136	gi_51819617	CO889332	ARHGAP25	CO889332 bovgen_17657 normal cattle brain cdna clone rzpdp1056a0441q 5' sequence	2.16	-2.60
137	gi_119908069	XM_610795	KLHDC8A	Kelch domain containing 8A	3.51	-2.58
138	gi_119901706	XM_596626	SYNJ2	Synaptojanin 2	2.28	-2.58
139	gi_112244680	EE384448	LOC531141	EE384448 LB03075.CR_P10 GC_BGC-30cdna clone IMAGE:8512956 sequence	2.59	-2.57
140	gi_51816802	CO886517	ST3GAL4	CO886517 bovgen_14842 normal cattle brain cdna clone rzpdp1056k249q 5' sequence	2.38	-2.56
141	gi_119912895	XM_001256686	LOC790129	Similar to SOX9 (LOC790129)	9.07	-2.56
142	gi_119912909	XM_607611	SLC16A6	Solute carrier family 16, member 6 (monocarboxylic acid transporter 7)	2.48	-2.55
143	gi_119914706	XM_609627	SEMA3F	Sema domain, immunoglobulin domain (Ig), short basic domain, secreted, (semaphorin) 3F	2.58	-2.54
144	gi_119916743	XM_864316	SOCS1	Suppressor of cytokine signaling 1	2.85	-2.53
145	gi_51805159	CO875259	KCNJ2	CO875259 bovgen_03584 normal cattle brain cdna clone rzpdp1056d1057q 3' sequence	2.05	-2.49
146	gi_51803597	CO873754	– – -	CO873754 bovgen_02079 normal cattle brain cdna clone rzpdp1056b2154q 3' sequence	2.23	-2.48
147	gi_156121054	NM_001102204	RIN2	Ras and Rab interactor 2	2.60	-2.48
148	gi_164452932	NM_001035421	KCTD11	Potassium channel tetramerisation domain containing 11	2.07	-2.47
149	gi_68427075	AM027990	LOC517069	AM027990 KN-252-lymph, Bos indicus Bos indicus cdna clone C0007394c04 3' sequence	4.33	-2.47
150	gi_119903174	XR_028610	LOC515082	Similar to mitogen-activated protein kinase kinase kinase kinase 4 (LOC509109)	2.30	-2.46
151*	gi_82632008	gb_DV779132	GNG2	Guanine nucleotide binding protein (G protein), gamma 2	2.03	-2.44
152	gi_139949110	NM_001083769	IRF8	Interferon regulatory factor 8	3.95	-2.43
153*	gi_115497587	NM_001075888	CYP3A4	Cytochrome P450, family 3, subfamily A, polypeptide 4	8.12	-2.43
154	gi_31342230	NM_174358	IL2RA	Interleukin 2 receptor, alpha	2.35	-2.39
155	gi_119909134	XR_028220	LOC790441	Similar to cytosolic branched-chain amino acid aminotransferase (LOC785193)	2.24	-2.39
156	gi_119914094	XM_869719	CCDC85C	Coiled-coil domain containing 85C	2.21	-2.38
157	gi_119894841	XM_584508	LRRC8E	Leucine rich repeat containing 8 family, member E	2.52	-2.38
158	gi_157074163	NM_001103326	BCAT1	Mucin-like protocadherin (MUPCDH)	2.35	-2.37
159*	gi_150247091	NM_001099367	CYP3A4	Cytochrome P450, family 3, subfamily A, polypeptide 4	14.16	-2.37
160	gi_119901537	XM_584832	TNFAIP3	Tumor necrosis factor, alpha-induced protein 3	22.30	-2.36
161	gi_15378656	BI537546	LOC529030	BI537546 416108 MARC 4bovcdna 5' sequence	2.24	-2.35
162	gi_119926074	XM_001254560	LOC790542	Similar to AKNA protein (LOC787047)	2.35	-2.35
163	gi_31340830	NM_174744	MMP9	Matrix metallopeptidase 9 (gelatinase B, 92kda gelatinase, 92kda type IV collagenase)	2.53	-2.35
164	gi_77735806	NM_001034430	PDLIM2	PDZ and LIM domain 2 (mystique)	2.01	-2.35
165*	gi_119918132	XM_001250478	DPPA2	Developmental pluripotency associated 2	2.99	-2.35
166	gi_119913047	XM_865521	ADAMTS6	ADAM metallopeptidase with thrombospondin type 1 motif, 6	7.27	-2.32
167*	gi_31342121	NM_174394	MYO10	Myosin X	2.36	-2.32
168	gi_119908995	XM_602397	SLC7A11	Solute carrier family 7, (cationic amino acid transporter, y+ system) member 11	5.78	-2.31
169	gi_119905496	XM_866049	FERMT1	Fermitin family member 1	2.95	-2.31
170	gi_154707907	NM_001099095	GZMA	Granzyme A (granzyme 1, cytotoxic T-lymphocyte-associated serine esterase 3)	2.81	-2.29
171*	gi_119903752	XM_001252683	MXD1	MAX dimerization protein 1	2.17	-2.28
172	gi_119906930	XM_001254662	LOC787451	Hypothetical protein (LOC787190)	2.07	-2.28
173	gi_119903689	XM_872068	MUpCDH	Similar to KIAA0903-like protein, transcript variant 2 (LOC613399)	2.05	-2.28
174	gi_76631782	XM_583252	CHST3	Carbohydrate (chondroitin 6) sulfotransferase 3	2.81	-2.27
175	gi_119888514	XM_581382	IRS1	Insulin receptor substrate 1	3.67	-2.26
176	gi_119893184	XM_584724	WNT5B	Wingless-type MMTV integration site family, member 5B	2.65	-2.26
177	gi_10026167	BE665576	– – -	BE665576 154662 MARC 4bovcdna 5' sequence	2.31	-2.24
178	gi_122692524	NM_001080256	SLC2A6	Solute carrier family 2 (facilitated glucose transporter), member 6	2.86	-2.23
179	gi_119916536	XM_870860	LOC786597	Similar to Kremen2 protein (LOC618527)	2.18	-2.22
180	gi_119902633	XM_617463	OSBPL3	Oxysterol binding protein-like 3	3.90	-2.22
181	gi_119892435	XM_595759	INHBE	Inhibin, beta E	5.57	-2.22
182*	gi_119927606	XM_001253379	CYP3A4	Cytochrome P450, family 3, subfamily A, polypeptide 4	11.27	-2.21
183	gi_51881771	AJ814295	LOC518435	AJ814295 AJ814295 KN206 Bos sp. cDNA clone C0005204n18 sequence	2.87	-2.21
184	gi_15379008	BI537898	– – -	BI537898 428179 MARC 4bovcdna 5' sequence	4.83	-2.21
185	gi_119895714	XR_027478	– – -	Similar to PGC-1-related estrogen receptor alpha coactivator (LOC514750)	4.34	-2.21
186	gi_41386686	NM_173931	LIF	Leukemia inhibitory factor (cholinergic differentiation factor)	10.23	-2.21
187	gi_119915466	XM_001249749	LOC784347	Chromosome 6 open reading frame 25 (c6orf25)	2.61	-2.20
188	gi_149642596	NM_001098868	BOK	BCL2-related ovarian killer	2.27	-2.18
189	gi_119912654	XM_001253289	LOC785193	Hypothetical protein (LOC785195)	2.83	-2.18
190	gi_119930998	XM_001256787	– – -	Similar to multidrug resistance-associated protein (LOC790269)	2.81	-2.17
191	gi_31341809	NM_181030	FLT3LG	Fms-related tyrosine kinase 3 ligand	3.25	-2.16
192	gi_157074011	NM_001103245	EFHD2	EF-hand domain family, member D2	2.15	-2.15
193	gi_51887526	AJ820050	LOC617455	AJ820050 KN206 Bos sp. cDNA clone C0006017e07 sequence	3.37	-2.13
194	gi_31343234	NM_173933	LPO	Lactoperoxidase	2.82	-2.13
195	gi_29263643	CB457261	LOC618527	CB457261 714599 MARC 6bovcdna 5' sequence	14.95	-2.12
196	gi_51821600	CO891305	LOC514626	CO891305 bovgen_19630 normal cattle brain cdna clone rzpdp1056a0847q 5' seq	3.62	-2.11
197	gi_160333614	NM_001110532	BAG4	BCL2-associated athanogene 4	2.36	-2.11
198	gi_115496062	NM_001075755	MTHFD2	Methylenetetrahydrofolate dehydrogenase (NADP+ dependent) 2, methenyltetrahydrofolate cyclohydrolase	2.55	-2.11
199	gi_51817723	CO887438	RILPL1	CO887438 bovgen_15763 normal cattle brain cdna clone rzpdp1056c0813q 5' sequence	2.36	-2.10
200	gi_51819799	CO889514	PCDH12	CO889514 bovgen_17839 normal cattle brain cdna clone rzpdp1056l0438q 5' sequence	2.28	-2.09
201	gi_51817431	CO887146	– – -	CO887146 bovgen_15471 normal cattle brain cdna clone rzpdp1056a2317q 5' sequence	2.16	-2.09
202	gi_119901959	XM_872521	TLE3	Transducin-like enhancer of split 3 (E(sp1) homolog, Drosophila)	3.81	-2.09
203	gi_119912792	XM_596084	RHBDF2	Rhomboid 5 homolog 2 (Drosophila)	3.39	-2.08
204	gi_51887200	AJ819724	LOC537777	AJ819724 KN206 Bos sp. Cdna clone C0006016e15 sequence	2.47	-2.08
205	gi_115497773	NM_001075226	RILPL1	Rab interacting lysosomal protein-like 1	2.15	-2.08
206	gi_51824812	CO894504	– – -	CO894504 bovgen_22829 normal cattle braincdna clone rzpdp1056i0644q 5' sequence	2.10	-2.08
207	gi_51822234	CO891936	– – -	CO891936 bovgen_20261 normal cattle braincdna clone rzpdp1056m1641q 5' sequence	4.56	-2.07
208	gi_119904633	XM_587329	SLC7A1	Solute carrier family 7 (cationic amino acid transporter, y+ system), member 1	2.40	-2.07
209	gi_119907587	XM_612432	P2RY2	Purinergic receptor P2Y, G-protein coupled, 2	2.03	-2.07
210	gi_119905914	XM_614691	TOP1	Topoisomerase (DNA) I	2.58	-2.06
211	gi_119879641	XM_589607	MFI2	Antigen p97 (melanoma associated) identified by monoclonal antibodies 133.2 and 96.5	2.01	-2.06
212	gi_139948300	NM_001083644	BCAT1	Branched chain amino-acid transaminase 1, cytosolic	2.45	-2.05
213*	gi_119885538	XM_865626	RASA2	RAS p21 protein activator 2	3.99	-2.04
214	gi_119931602	XM_001256019	FAM107B	Similar to HPCL1 (LOC789196)	2.04	-2.04
215	gi_126723073	NM_175801	FST	Follistatin	3.26	-2.04
216	gi_51808839	CO878915	P2RY2	CO878915 bovgen_07240 normal cattle brain cdna clone rzpdp1056d054q 5' sequence	2.31	-2.03
217	gi_156121148	NM_001102252	PTK2B	PTK2B protein tyrosine kinase 2 beta	2.07	-2.03
218	gi_119900885	XM_592054	TNFSF15	Tumor necrosis factor (ligand) superfamily, member 15	2.08	-2.01
219	gi_60456280	DN287670	LOC539803	DN287670 1241977 MARC 7bov cdna 3' sequence	2.11	-2.01
220	gi_66792735	NM_001024507	SESN2	Sestrin 2	2.90	-2.00

Profile 3 n = 70

S.No	SEQ. ID	Acc. No. (RefSeq)	Putative Gene symbol	Gene Name	BoMac PMA vs BoMac Abs FC:	TashAT2 PMA vs PCAGGS PMA Abs: FC
					↑	↓↓
1	gi_156121012	NM_001102183	ERG	V-ets erythroblastosis virus E26 oncogene homolog (avian)	2.81	-511.27
2	gi_119907136	XM_592427	OAF	OAF homolog (Drosophila)	2.46	-223.43
3*	gi_113204619	NM_001015570	LGALS9	Lectin, galactoside-binding, soluble, 9	2.03	-146.46
4	gi_114053308	NM_001046283	F2RL1	Coagulation factor II (thrombin) receptor-like 1	4.37	-119.55
5	gi_31342788	NM_174128	NRG1	Neuregulin 1 (NRG1)	2.06	-110.75
6	gi_31343056	NM_174006	CCL2	Chemokine (C-C motif) ligand 2	40.23	-104.77
7	gi_31342385	NM_174300	CXCL5	Chemokine (C-X-C motif) ligand 5	10.66	-102.90
8	gi_119913746	XM_602502	BNC1	Basonuclin 1	2.38	-64.63
9	gi_89886135	NM_001013585	S1PR1	Sphingosine-1-phosphate receptor 1	12.56	-64.46
10	gi_45430004	NM_205788	CEACAM8	Carcinoembryonic antigen-related cell adhesion molecule 8 (CEACAM8)	2.72	-39.63
11	gi_119902549	XM_603066	SHC4	SHC (Src homology 2 domain containing) family, member 4	3.96	-38.93
12	gi_119941886	XM_001257225	LOC790854	Similar to oxysterol 7alpha-hydroxylase (LOC790854)	5.39	-36.95
13	gi_148237696	NM_174083	HRH1	Histamine receptor H1	3.31	-34.42
14	gi_148236122	NM_001098043	CLMP	CXADR-like membrane protein	2.76	-33.85
15	gi_83035050	NM_001037590	ASGR1	Asialoglycoprotein receptor 1	2.26	-31.39
16*	gi_114326490	NM_001048165	CXCL2	Chemokine (C-X-C motif) ligand 2	9.23	-30.31
17	gi_115496605	NM_001076352	LMO2	LIM domain only 2 (rhombotin-like 1)	3.25	-30.10
18	gi_49410464	AJ677881	– – -	AJ677881 KN224cDNA clone KN224-024_P02 sequence	4.49	-29.00
19	gi_84000286	NM_001038155	TNS4	Tensin 4	3.67	-27.85
20*	gi_114050914	NM_001046513	CXCL2	Chemokine (C-X-C motif) ligand 2	4.35	-27.60
21	gi_115497387	NM_001076095	RAB39B	RAB39B, member RAS oncogene family	3.61	-26.64
22	gi_119916193	XM_612197	LOC532965	Similar to alpha3a chain laminin (LOC532965)	4.02	-25.49
23*	gi_41386706	NM_174484	VCAM1	Vascular cell adhesion molecule 1	11.81	-24.67
24	gi_119894821	XM_607258	LOC528826	Similar to mucin 16 (LOC528826)	2.12	-24.09
25	gi_119917473	XM_599002	LOC520752	Hypothetical (LOC520752)	2.13	-24.06
26	gi_119906495	XM_608003	CYP7B1	Cytochrome P450, family 7, subfamily B, polypeptide 1	4.04	-23.27
27	gi_119910630	XM_001256469	LOC789828	Similar to carcinoembryonic antigen-related cell adhesion molecule 1 isoform 3L	2.75	-21.31
28	gi_158262744	NM_001109962	DCLK1	Doublecortin-like kinase 1 (DCLK1)	9.63	-21.00
29	gi_119889464	XM_863903	TCHH	Trichohyalin	10.34	-20.94
30	gi_119902622	XM_869016	FGF7	Fibroblast growth factor 7	5.44	-20.68
31	gi_115494923	NM_001075952	ASGR2	Asialoglycoprotein receptor 2	2.76	-20.22
32	gi_51811539	gb_CO881610	– – -	CO881610 bovgen_09935 normal cattle braincdna clone rzpdp1056k0421q 5' sequence	3.30	-18.80
33	gi_42730748	CK778435	– – -	CK778435 965595 MARC 3bovcdna 3' sequence	2.70	-17.65
34	gi_51812192	CO882260	– – -	CO882260 bovgen_10585 normal cattle braincdna clone rzpdp1056d208q 5' sequence	2.26	-15.74
35	gi_119889196	XM_001251267	LOC783721	Hypothetical protein (LOC783721)	3.17	-14.39
36	gi_119894823	XM_001254224	LOC786588	Similar to mucin 16 (LOC786588)	2.04	-14.29
37	gi_115497119	NM_001075890	KLK10	Kallikrein-related peptidase 10	3.25	-13.83
38	gi_119915324	XM_590184	GPR110	G protein-coupled receptor 110	3.32	-13.45
39	gi_119940186	XM_607283	LOC528849	Similar to MER receptor tyrosine kinase (LOC528849)	3.11	-13.10
40	gi_156120634	NM_001101994	SLC6A12	Solute carrier family 6 (neurotransmitter transporter, betaine/GABA), member 12	2.35	-12.11
41*	gi_119923630	XM_591244	RAET1E	Retinoic acid early transcript 1E	2.65	-10.37
42	gi_119906362	XM_605757	FER1L6	Fer-1-like 6 (C. Elegans)	2.23	-10.14
43	gi_119902777	XR_027766	LOC533088	Similar to glutathione peroxidase 2 (LOC533088)	3.90	-9.73
44	gi_119903128	XM_580552	MERTK	C-mer proto-oncogene tyrosine kinase	3.75	-8.57
45	gi_119907990	XM_606934	LOC528508	Similar to DTX4 protein (LOC528508)	2.13	-8.47
46	gi_51813662	CO883718	– – -	CO883718 bovgen_12043 normal cattle braincdna clone rzpdp1056f2013q 5' sequence	2.52	-8.06
47*	gi_119908717	XM_877066	BATF3	Basic leucine zipper transcription factor, ATF-like 3	2.97	-7.89
48	gi_119913440	XR_028647	SLC6A3	Solute carrier family 6 (neurotransmitter transporter, dopamine), member 3	3.08	-7.81
49	gi_119918141	XM_865568	SLC7A2	Solute carrier family 7 (cationic amino acid transporter, y+ system), member 2	2.00	-7.44
50	gi_31340697	NM_178572	CA2	Carbonic anhydrase II	2.62	-7.35
51	gi_119908662	XM_588297	LAMC2	Laminin, gamma 2	3.06	-7.20
52	gi_119915151	XM_001256822	LOC790310	Hypothetical protein (LOC790310)	3.54	-7.14
53	gi_119904218	XM_870651	PRDM12	PR domain containing 12	3.52	-7.09
54	gi_115495492	NM_001075925	ADORA2B	Adenosine A2b receptor	3.22	-6.76
55	gi_119901000	XM_613776	TRAF1	TNF receptor-associated factor 1	2.38	-5.87
56	gi_119909626	XM_870153	ADORA2A	Adenosine A2a receptor	2.22	-5.81
57	gi_157074015	NM_001103247	PPP1R3B	Protein phosphatase 1, regulatory (inhibitor) subunit 3B	2.00	-5.68
58	gi_77735388	NM_001034215	DIRAS3	DIRAS family, GTP-binding RAS-like 3	2.78	-5.40
59	gi_119909181	XR_027532	LOC540363	Similar to transmembrane protein 132B (LOC540363)	2.38	-5.30
60	gi_158341669	NM_001109980	SLC16A3	Solute carrier family 16, member 3 (monocarboxylic acid transporter 4)	2.17	-5.18
61	gi_122692576	NM_001080280	SLC20A2	Solute carrier family 20 (phosphate transporter), member 2	2.01	-5.14
62	gi_119296266	EE959692	– – -	EE959692 K29921A fnm cDNA clone K2992 3' sequence	2.08	-5.13
63	gi_119907907	XM_607470	RTN4RL2	Reticulon 4 receptor-like 2	2.44	-4.92
64	gi_51813747	CO883803	– – -	CO883803 bovgen_12128 normal cattle brain cdna clone rzpdp1056e214q 5' sequence	2.11	-4.70
65	gi_119911699	XR_028261	DOC2B	Double C2-like domains, beta	2.12	-4.54
66	gi_10870122	BF076357	– – -	BF076357 225899 MARC 2bovcdna 5' sequence	2.02	-4.30
67	gi_114051971	NM_001046393	FAM107B	Family with sequence similarity 107, member B	2.05	-4.30
68	gi_51823984	CO893679	– – -	CO893679 bovgen_22004 normal cattle brain cdna clone rzpdp1056b1442q 5' sequence	2.06	-4.28
69	gi_119910538	XM_598392	HIPK4	Homeodomain interacting protein kinase 4	2.12	-4.24
70	gi_119905261	XM_587891	FRMD4A	FERM domain containing 4A	2.09	-4.06

3.3 List of PMA induced down-regulated genes (n = 211) showing modulated expression profiles in TashAT2

Profile 4 n=91

S.No	SEQ. ID	Acc. No. (RefSeq)	Putative Gene symbol	Gene Name	BoMac PMA vs BoMac Abs FC:	TashAT2 PMA vs PCAGGS PMA Abs: FC
					↓	↓↓
1	gi_77735740	NM_001034393	SFRP2	Secreted frizzled-related protein 2	-2.21	-150.59
2	gi_51814063	CO884115	– – -	Co884115 bovgen_12440 normal cattle brain cDNA clone rzpdp1056h2429q 5' sequence	-2.46	-48.53
3	gi_119904441	XM_580490	KBTBD6	Kelch repeat and BTB (poz) domain containing 6	-9.03	-23.66
4	gi_119920522	XM_001252954	LOC784734	Hypothetical protein (LOC784734)	-2.04	-22.36
5	gi_51819965	CO889677	– – -	Co889677 bovgen_18002 normal cattle brain cDNAclone rzpdp1056a1334q 5' sequence	-2.71	-21.82
6	gi_156631000	NM_174459	SEPP1	Selenoprotein p, plasma, 1	-2.11	-20.75

7	gi_119920520	XM_601227	LOC522938	Hypothetical protein (LOC522938)	-2.30	-17.94
8	gi_155372278	NM_001101282	PTER	Phosphotriesterase related	-2.80	-13.84
9	gi_51817307	CO887022	– – -	Co887022 bovgen_15347 normal cattle braincDNA clone rzpdp1056p1323q 5' sequence	-2.27	-12.92
10	gi_119911365	XM_594205	HLF	Hepatic leukemia factor	-2.18	-12.13
11	gi_116004188	NM_001076984	GLIPR1	Gli pathogenesis-related 1	-2.85	-11.68
12	gi_51827054	CO896734	– – -	Co896734 bovgen_25059 normal cattle brain cDNAclone rzpdp1056g181q 5' sequence	-11.84	-10.67
13	gi_119934268	XM_001252747	CGNL1	Cingulin-like 1	-3.82	-10.32
14	gi_119921717	XM_606666	TLN2	Talin 2	-2.90	-10.11
15	gi_119909284	XM_868620	HVCN1	Hydrogen voltage-gated channel 1	-2.09	-8.63
16	gi_119919045	XM_869718	PKNOX2	PBX/knotted 1 homeobox 2	-2.87	-7.59
17	gi_119893558	XM_001251198	LOC783187	Hypothetical protein (LOC783187)	-2.95	-6.80
18	gi_119891548	XM_593382	TMEM139	Transmembrane protein 139	-2.44	-5.97
19*	gi_51808233	gb_CO878313	RPS8	Ribosomal protein s8	-2.64	-5.97
20	gi_119901355	XM_595871	GPR63	G Protein-coupled receptor 63	-4.94	-5.92
21	gi_119917968	XM_866446	JAKMIP3	Janus kinase and microtubule interacting protein 3	-3.21	-5.88
22	gi_126723194	NM_001082453	RHOBTB1	Rho-related btb domain containing 1	-2.02	-5.88
23	gi_139948606	NM_001083721	FAM70A	Family with sequence similarity 70, member a	-2.38	-5.78
24	gi_89191836	NM_174702	AQP1	Aquaporin 1 (colton blood group)	-2.95	-5.38
25	gi_119912745	XM_587641	EVPL	Envoplakin	-2.66	-5.35
26	gi_119893332	XM_001253780	PNPLA3	Patatin-like phospholipase domain containing 3	-2.04	-4.76
27	gi_51815966	CO885681	– – -	Co885681 bovgen_14006 normal cattle brain cDNAclone rzpdp1056g0625q 5' sequence	-2.46	-4.59
28	gi_75870703	DT890296	– – -	Dt890296 1471293 marc 7bovcDNA3' sequence	-2.45	-4.56
29	gi_139948704	NM_001083715	LMOD1	Leiomodin 1 (smooth muscle)	-5.94	-4.51
30	gi_51810144	CO880219	– – -	Co880219 bovgen_08544 normal cattle brain cDNAclone rzpdp1056l2216q 5' sequence	-2.04	-4.51
31	gi_51816156	CO885871	– – -	Co885871 bovgen_14196 normal cattle brain cDNAclone rzpdp1056m022q 5' sequence	-5.31	-4.45
32	gi_119911058	XM_001254384	LOC788991	Hypothetical protein (LOC788991)	-2.08	-4.41
33	gi_77736204	NM_001034629	EPHX1	Epoxide hydrolase 1, microsomal (xenobiotic)	-2.09	-4.32
34	gi_155372204	NM_001101243	CCDC92	Coiled-coil domain containing 92	-2.92	-4.03
35	gi_111084835	EE223727	– – -	EE223727 lb01821.cr_j13 gc_bgc-18 cDNAclone image:8293359 sequence	-2.10	-4.03
36	gi_51801578	CO871746	– – -	Co871746 bovgen_00071 normal cattle brain cDNAclone rzpdp1056g2254q 3' sequence	-6.71	-3.93
37	gi_119895570	XM_581784	SLC23A1	Solute carrier family 23 (Nucleobase transporters), member 1	-2.35	-3.92
38	gi_51804999	CO875099	– – -	Co875099 bovgen_03424 normal cattle brain cDNAclone rzpdp1056i1557q 5' sequence	-2.03	-3.82
39	gi_119914113	XM_872590	LOC509824	Similar to os08g0528700, transcript variant 4 (loc509824)	-2.43	-3.80
40	gi_51804084	CO874235	– – -	Co874235 bovgen_02560 normal cattle brain cDNAclone rzpdp1056j0258q 3' sequence	-2.42	-3.74
41	gi_119938792	XM_865450	LOC614607	Similar to 214k23.2.2 (novel protein, isoform 2), transcript variant 1 (LOC614607)	-3.62	-3.69
42	gi_119908450	XM_592463	PLCH2	Phospholipase c, eta 2	-2.47	-3.61
43	gi_51821340	CO891047	– – -	Co891047 bovgen_19372 normal cattle braincDNAclone rzpdp1056m0937q 5' sequence	-2.93	-3.41
44	gi_75748738	DT816862 CN436163	– – -	Dt816862 lb0165.cr_h07 gc_bgc-16cDNAclone image:8079513 5' sequence cn436163 be04008b1g04 be04 normalized and subtracted bovine embryonic and	-2.35	-3.39
45	gi_46415427		– – -	extraembryonic tissuecDNAclone be04008b1g04 5' sequence	-2.38	-3.29
46	gi_114051010	NM_001046474	PPM1K	Protein phosphatase, mg2+/mn2+ dependent, 1k	-5.47	-3.27
47	gi_119915240	XM_865759	TRERF1	Transcriptional regulating factor 1	-2.72	-3.25
48	gi_157427807	NM_001105340	TRAF5	TNF receptor-associated factor 5	-3.14	-3.09
49	gi_119895746	XM_601340	FAT2	Fat tumor suppressor homolog 2 (drosophila)	-2.61	-3.08
50	gi_51814379	CO884385	– – -	Co884385 bovgen_12710 normal cattle braincDNAclone rzpdp1056k1011q 5' sequence	-5.23	-3.06
51	gi_51808765	CO878841	– – -	Co878841 bovgen_07166 normal cattle brain cDNAclone rzpdp1056k029q 5' sequence	-2.02	-3.05
52	gi_76656160	XM_596273	LOC518089	Hypothetical (LOC518089)	-2.07	-3.02
53	gi_119913583	XM_001253211	LOC785074	Hypothetical protein (LOC785074)	-2.42	-2.97
54	gi_119916232	XM_618609	MYOM1	Myomesin 1, 185kda	-3.37	-2.87
55	gi_51817833	CO887548	– – -	Co887548 bovgen_15873 normal cattle brain cDNAclone rzpdp1056a1011q 5' sequence	-2.05	-2.84
56	gi_149643004	NM_001099089	ZFP3	Zinc finger protein 3 homolog (mouse)	-9.04	-2.70
57	gi_51822437	CO892136	– – -	Co892136 bovgen_20461 normal cattle brain cDNAclone rzpdp1056c0239q 5' sequence	-3.93	-2.67
58	gi_156120782	NM_001102068	PDE7B	Phosphodiesterase 7b	-6.29	-2.66
59	gi_76677151	XM_586975	LOC509911	Similar to solute carrier family 16 member 1 (LOC509911)	-3.02	-2.56
60	gi_164448635	NM_001113261	PTPRR	Protein tyrosine phosphatase, receptor type, r (ptprr), transcript variant 2	-3.16	-2.53
61	gi_51820161	CO889874	– – -	Co889874 bovgen_18199 normal cattle brain cDNA clone rzpdp1056c0845q 5' sequence	-2.12	-2.49
62	gi_119909586	XM_596386	ZNF280A	Zinc finger protein 280a	-6.73	-2.45
63	gi_156120854	NM_001102104	ANKRD29	Ankyrin repeat domain 29	-2.47	-2.42
64	gi_78369255	NM_001035416	LDB3	Lim domain binding 3 (ldb3)	-2.59	-2.40
65	gi_119904597	XM_584268	FRY	Furry homolog (drosophila)	-2.01	-2.37
66	gi_119914328	XM_589824	LOC615277	Similar to loc443715 protein, transcript variant 1 (LOC615277)	-2.81	-2.36
67*	gi_156121314	NM_001102335	PGM5	Phosphoglucomutase 5	-2.12	-2.36
68	gi_82617553	NM_001035457	PRSS35	Protease, serine, 35	-4.55	-2.35
69	gi_51815100	CO884817	– – -	Co884817 bovgen_13142 normal cattle brain cDNAclone rzpdp1056m0313q 5' sequence	-2.99	-2.31
70	gi_77736300	NM_001034678	HES1	Hairy and enhancer of split 1, (drosophila)	-2.27	-2.30
71*	gi_119909503	XM_867110	Inpp5j	Inositol polyphosphate 5-phosphatase j	-2.47	-2.30
72	gi_51826056	CO895740	– – -	Co895740 bovgen_24065 normal cattle brain cDNAclone rzpdp1056c1438q 5' sequence	-2.08	-2.30
73	gi_51825154	CO894844	– – -	Co894844 bovgen_23169 normal cattle brain cDNAclone rzpdp1056c0137q 5' sequence	-2.02	-2.29
74	gi_68319921	AM018729	– – -	Am018729 kn-252-liver,bos taurus cDNAclone c0007412e16 5' sequence	-2.03	-2.29
75	gi_116004120	NM_001076949	SEPT3	Septin 3	-2.38	-2.29
76	gi_51811352	CO881423	– – -	Co881423 bovgen_09748 normal cattle braincDNAclone rzpdp1056g2014q 5' sequence	-2.55	-2.26
77	gi_119911113	XM_609306	LOC530828	Hypothetical loc530828 (LOC530828)	-2.18	-2.24
78	gi_51816763	CO886478	– – -	Co886478 bovgen_14803 normal cattle brain cDNAclone rzpdp1056f186q 5' sequence	-3.64	-2.23
79	gi_51807037	CO877123	– – -	Co877123 bovgen_05448 normal cattle brain cDNAclone rzpdp1056a1952q 3' sequence	-2.29	-2.23
80	gi_51808554	CO878630	– – -	Co878630 bovgen_06955 normal cattle brain cDNAclone rzpdp1056e225q 5' sequence	-2.38	-2.23
81	gi_77735458	NM_001034252	FBXL21	F-box and leucine-rich repeat protein 21 (gene/pseudogene)	-2.07	-2.22
82	gi_148237208	NM_001098017	PTPN6	Protein tyrosine phosphatase, non-receptor type 6	-2.05	-2.21
83	gi_61889064	NM_001001854	CLDN1	Claudin 1	-2.11	-2.20
84	gi_119892874	XM_865269	SSPN	Sarcospan (kras oncogene-associated gene)	-3.18	-2.20
85	gi_51818031	CO887746	– – -	Co887746 bovgen_16071 normal cattle brain cDNAclone rzpdp1056a1216q 5' sequence	-2.07	-2.16
86	gi_51825825	CO895511	– – -	Co895511 bovgen_23836 normal cattle brain cDNAclone rzpdp1056j0947q 5' sequence	-2.83	-2.14
87	gi_119933474	XM_001256893	LOC790417	Similar to proproteinase e (LOC790417)	-6.77	-2.09
88	gi_115495650	NM_001075552	PIK3IP1	Phosphoinositide-3-kinase interacting protein 1	-2.08	-2.07
89	gi_45071668	CK837937	– – -	Ck837937 4063255 barc 8bovcDNAclone 8bov_10b21 5' sequence	-2.64	-2.06
90	gi_51808976	CO879052	– – -	Co879052 bovgen_07377 normal cattle brainc dna clone rzpdp1056o2328q 5' sequence	-2.50	-2.02
91	gi_51823406	CO893101	– – -	Co893101 bovgen_21426 normal cattle brain cDNAclone rzpdp1056m1837q 5' sequence	-2.76	-2.00

Profile 5 n = 91

S.No	SEQ. ID	Acc. No. (RefSeq)	Putative Gene symbol	gene name	BoMac PMA vs BoMac Abs FC: ↓	TashAT2 PMA vs PCAGGS PMA Abs: FC ↑
1	gi_119889379	XM_613217	CGN	Cingulin	-4.01	5.23
2	gi_119927684	XM_001254424	LOC786868	Similar to polydom protein (LOC786868)	-3.00	5.14
3	gi_119889682	XM_613047	KCNC4	Potassium voltage-gated channel, shaw-related subfamily, member 4	-2.27	4.41
4	gi_51821139	CO890846	– – -	Co890846 bovgen_19171 normal cattle brain cDNAclone rzpdp1056f1741q 5' sequence	-2.35	4.36
5	gi_119900832	XM_001249686	LOC781282	Similar to polydom (LOC781282)	-2.25	4.36
6	gi_31342442	NM_174278	CNGA1	Cyclic nucleotide gated channel alpha 1	-2.83	4.33

7	gi_94967001	NM_001040604	GADD45B	Growth arrest and dna-damage-inducible, beta	-2.54	4.30
8*	gi_119891767	XM_001249363	INSIG1	Insulin induced gene 1	-3.78	4.29
9	gi_164420790	NM_001113252	TGFB2	Transforming growth factor, beta 2	-2.91	4.28
10	gi_118151293	NM_001078111	ZC4H2	Zinc finger, c4h2 domain containing	-2.23	4.25
11*	gi_118151149	NM_001078029	FAM13C	Family with sequence similarity 13, member c	-4.52	4.02
12*	gi_62460611	NM_001014959	DNAJB5	Dnaj (HSP40) homolog, subfamily b, member 5	-2.02	3.94
13	gi_154152010	NM_001100299	CRISPLD2	Cysteine-rich secretory protein lccl domain containing 2	-2.02	3.88
14	gi_119920254	XM_001253942	AR	Androgen receptor	-5.55	3.88
15	gi_119942112	XM_001257229	LOC790860	Similar to histamine n-methyltransferase (LOC790860)	-2.88	3.87
16	gi_76666197	XM_588979	LOC539724	Similar to androgen receptor (dihydrotestosterone receptor) (LOC539724)	-5.31	3.87
17	gi_51824106	CO893799	– – -	Co893799 bovgen_22124 normal cattle brain cDNAclone rzpdp1056b0846q 5' sequence	-2.90	3.82
18	gi_27807398	NM_174796	PIK3R3	Phosphoinositide-3-kinase, regulatory subunit 3 (gamma)	-2.48	3.68
19	gi_119908963	XM_866831	RNF150	Ring finger protein 150	-3.29	3.68
20	gi_51804591	CO874691	– – -	Co874691 bovgen_03016 normal cattle braincDNAclone rzpdp1056a1457q 3' sequence	-2.79	3.65
21	gi_119890423	XM_001251596	LOC782936	Similar to phosphatidylinositol 3-kinase regulatory subunit (LOC782936)	-2.29	3.57
22*	gi_119891769	XM_001249423	INSIG1	Insulin induced gene 1	-3.83	3.52
23*	gi_77735702	NM_001034378	ANKRD1	Ankyrin repeat domain 1 (cardiac muscle)	-2.81	3.52
24*	gi_118150923	NM_001077909	INSIG1	Insulin induced gene 1	-3.67	3.51
25	gi_78365290	NM_001035434	HNMT	Histamine n-methyltransferase	-2.38	3.47
26	gi_37712997	CF763779	– – -	Cf763779 ces005100skin cDNAlibrarycDNAclone ccl005100 5' sequence	-3.92	3.41
27*	gi_119894560	XM_584000	BST2	Bone marrow stromal cell antigen 2	-2.72	3.41
28	gi_51819098	CO888813	– – -	Co888813 bovgen_17138 normal cattle brain cDNAclone rzpdp1056i0649q 5' sequence	-5.57	3.35
29	gi_119915318	XR_028520	LOC512304	Similar to enpp5 (LOC512304)	-2.09	3.31
30	gi_145562057	ES346223	– – -	Es346223 u3g19ca.r1 cattle subcutaneous adipose tissue cDNA library cDNAclone u3g19ca 5' sequence	-3.03	3.31
31	gi_119890099	XM_600332	RAVER2	Ribonucleoprotein, ptb-binding 2	-3.36	3.31
32	gi_119931385	XM_001253959	LOC786203	Similar to hiv-1 rev binding protein-like (LOC786203)	-2.09	3.28
33	gi_51883802	AJ816326	– – -	Aj816326 kn206 bos sp. cDNAclone c0005210h22 sequence	-3.47	3.25
34*	gi_94967003	NM_001040606	OAS1	2',5'-oligoadenylate synthetase 1, 40/46kda	-3.44	3.25
35	gi_51826474	CO896157	– – -	Co896157 bovgen_24482 normal cattle braincDNAclone rzpdp1056p0647q 5' sequence	-2.40	3.24
36	gi_119917854	XM_880481	FGFR2	Fibroblast growth factor receptor 2	-4.68	3.23
37	gi_51881346	AJ813870	– – -	Aj813870 kn206 bos sp. cDNAclone c0005205h15 sequence	-2.84	3.21
38	gi_119879761	XM_581912	THPO	Thrombopoietin	-2.40	3.19
39	gi_119887370	XM_001251262	LOC783219	Hypothetical protein (LOC783219)	-2.23	3.18
40	gi_157074121	NM_001103303	SLC46A3	Solute carrier family 46, member 3	-3.45	3.15
41	gi_119917192	XM_587493	AGFG2	Arfgap with fg repeats 2	-2.10	3.07
42*	gi_51821409	CO891116	OAS1	2',5'-oligoadenylate synthetase 1, 40/46kda	-3.97	3.03
43	gi_119888584	XM_584793	ZNF362	Zinc finger protein 362	-2.57	2.98
44*	gi_119905065	XM_001251706	FLRT3	Fibronectin leucine rich transmembrane protein 3	-8.26	2.96
45	gi_148277667	NM_174547	GUCY2C	Guanylate cyclase 2c (heat stable enterotoxin receptor)	-2.38	2.94
46*	gi_51825967	gb_CO895653	CHRNA3	Cholinergic receptor, nicotinic, alpha 3	-3.12	2.85
47	gi_51809329	CO879405	– – -	Co879405 bovgen_07732 normal cattle braincDNAclone rzpdp1056g089q 5' sequence	-2.03	2.85
48	gi_119878572	XM_001249734	VGLL3	Vestigial like 3 (drosophila)	-2.49	2.83
49	gi_119233167	EE896593	– – -	Ee896593 b03011a ffbcDNAclone b0301 3' sequence	-2.64	2.77
50	gi_61316453	NM_001013001	WNT2	Wingless-type mmtv integration site family member 2	-2.11	2.77
51	gi_154366939	EV610519	– – -	EV610519 lb004155.cr_p03 gc_bgc-04cDNAclone image:9065141 5' sequence	-2.20	2.76
52	gi_49423002	AJ690394	– – -	Aj690394 aj690394 kn261cDNAclone kn261-053_k04 sequence	-3.17	2.70
53	gi_119901460	XM_618496	BACH2	BTB and cnc homology 1, basic leucine zipper transcription factor 2	-2.79	2.65
54	gi_51884726	AJ817250	– – -	Aj817250 kn206 bos sp. cDNAclone c0006006p18 sequence	-2.00	2.61
55	gi_119920249	XM_590017	KIAA2022	KIAA2022	-2.40	2.54
56	gi_121583852	NM_001015635	RASL11B	Ras-like, family 11, member b	-7.62	2.54
57	gi_119893809	XM_613340	RBM47	RNA binding motif protein 47	-3.52	2.54
58	gi_119902721	XR_028578	LOC538778	Hypothetical loc538778 (loc538778)	-4.06	2.52
59	gi_51812194	CO882262	– – -	Co882262 bovgen_10587 normal cattle braincDNAclone rzpdp1056c2420q 5' sequence	-2.16	2.50
60	gi_51808026	CO878110	– – -	Co878110 bovgen_06435 normal cattle braincDNAclone rzpdp1056a1417q 5' sequence	-2.55	2.45
61*	gi_119905063	XM_607863	FLRT3	Fibronectin leucine rich transmembrane protein 3	-7.06	2.45
62	gi_62460603	NM_001014952	TRIM45	Tripartite motif containing 45	-2.38	2.45
63	gi_119895914	XM_001249756	LOC781690	Hypothetical protein (LOC781690)	-2.30	2.43
64	gi_51807654	CO877738	– – -	Co877738 bovgen_06063 normal cattle braincDNAclone rzpdp1056a0317q 5' sequence	-2.59	2.42
65	gi_119879589	XM_590786	MYLK	Myosin, light polypeptide kinase (mylk)	-2.50	2.38
66	gi_51815587	CO885302	– – -	Co885302 bovgen_13627 normal cattle braincDNAclone rzpdp1056a1213q 5' sequence	-2.17	2.35
67*	gi_118151321	NM_001078125	ARMCX6	Armadillo repeat containing, x-linked 6	-2.27	2.34
68	gi_77735632	NM_001034340	CYR61	Cysteine-rich, angiogenic inducer, 61	-2.65	2.33
69*	gi_119922570	XM_001254638	ARMCX6	Armadillo repeat containing, x-linked 6	-2.34	2.28
70	gi_119914463	XM_585971	PDZRN3	PDZ domain containing ring finger 3	-2.88	2.26
71	gi_119885610	XM_590531	SPSB4	spla/ryanodine receptor domain and socs box containing 4	-2.40	2.25
72	gi_51818557	CO888272	– – -	co888272 bovgen_16597 normal cattle brain cDNAclone rzpdp1056j1628q 5' sequence	-2.08	2.22
73*	gi_31342492	NM_178108	OAS1	2',5'-oligoadenylate synthetase 1, 40/46kda	-2.90	2.21
74	gi_125630662	NM_001081519	DDIT4L	DNA-damage-inducible transcript 4-like	-2.68	2.21
75	gi_119908935	XM_615424	ZNF827	Zinc finger protein 827	-2.27	2.20
76	gi_119922580	XM_868651	GPR137C	G protein-coupled receptor 137c	-3.20	2.20
77	gi_157073967	NM_001103222	SLC2A2	Solute carrier family 2 (facilitated glucose transporter), member 2	-4.67	2.18
78	gi_125630680	NM_001081523	HABP4	Hyaluronan binding protein 4	-2.33	2.18
79	gi_75832087	NM_177501	FUT8	Fucosyltransferase 8 (alpha (1,6) fucosyltransferase)	-2.91	2.17
80	gi_119233198	EE896624	– – -	EE896624 b03211a ffbcDNA clone b0321 3' sequence	-2.48	2.16
81	gi_114051857	NM_001045960	TCEAL1	Transcription elongation factor a (sii)-like 1	-2.30	2.14
82	gi_115497913	NM_001076462	C1orf110	Chromosome 1 open reading frame 110	-4.56	2.10
83	gi_51809241	CO879317	– – -	Co879317 bovgen_07644 normal cattle brain cDNA clone rzpdp1056c1024q 5' sequence	-3.24	2.08
84	gi_114052465	NM_001045905	NUDT13	Nudix (nucleoside diphosphate linked moiety x)-type motif 13	-2.13	2.07
85	gi_115497025	NM_001075661	ZPBP2	Zona pellucida binding protein 2	-2.07	2.07
86	gi_119930546	XM_001255692	LOC788716	Similar to fucosyltransferase 8 (alpha (1,6) fucosyltransferase) (LOC788716)	-2.66	2.05
87	gi_51802497	CO872657	– – -	Co872657 bovgen_00982 normal cattle brain cDNAclone rzpdp1056d0757q 5' sequence	-2.03	2.04
88	gi_119879570	XM_610099	C3orf15	Chromosome 3 open reading frame 15	-2.42	2.04
89	gi_77736302	NM_001034679	Rcan1	Regulator of calcineurin 1	-3.42	2.03
90	gi_115497021	NM_001076059	FBXL4	F-box and leucine-rich repeat protein 4	-2.28	2.03
91	gi_31343567	NM_175804	NR2F1	Nuclear receptor subfamily 2, group f, member 1	-2.97	2.03

Profile 6 n = 29

S.No	SEQ. ID	Acc. No. (RefSeq)	Putative Gene symbol	Gene Name	BoMac PMA vs BoMac Abs FC:	TashAT2 PMA vs PCAGGS PMA Abs: FC
					↓	↑ ↑
1	gi_119903692	XM_871827	LRRTM4	Leucine rich repeat transmembrane neuronal 4	-11.60	47.50
2	gi_126165231	NM_001081717	EFEMP1	EGF containing fibulin-like extracellular matrix protein 1	-2.18	32.81
3	gi_119920877	XM_001257254	NOVA1	Neuro-oncological ventral antigen 1	-2.60	25.39
4	gi_156523203	NM_001102546	PDE4B	Phosphodiesterase 4B, cAMP-specific	-2.06	20.13
5	gi_119892229	XM_592100	AMIGO2	Adhesion molecule with Ig-like domain 2	-2.94	14.81
6	gi_51818729	CO888444	– – -	CO888444 BovGen_16769 normal cattle brain cDNAclone RZPDp1056M0317Q 5' sequence	-2.77	13.52

7	gi_119891169	XM_592060	HECW1	HECT, C2 and WW domain containing E3 ubiquitin protein ligase 1	-2.15	12.91
8	gi_51818632	CO888347	– – -	CO888347 BovGen_16672 normal cattle brain cDNAclone RZPDp1056M2030Q 5' sequence	-2.51	10.99
9	gi_51820224	CO889937	– – -	CO889937 BovGen_18262 normal cattle brain cDNAclone RZPDp1056M1637Q 5' sequence	-4.25	10.91
10	gi_115497559	NM_001075897	JAKMIP2	Janus kinase and microtubule interacting protein 2	-2.17	10.61
11	gi_119891802	XM_598424	LGR5	Leucine-rich repeat containing G protein-coupled receptor 5	-2.85	10.43
12	gi_119885258	XM_866829	LOC615109	Similar to beta-galactoside alpha-2,6-sialyltransferase (LOC615109)	-2.52	9.55
13	gi_119929905	XM_001256313	LOC789611	Similar to membrane glycoprotein LIG-1 (LOC789611)	-2.04	9.07
14*	gi_139948585	NM_001083776	FAM155A	Family with sequence similarity 155, member A	-2.18	8.71
15	gi_119884936	XM_618021	VEPH1	Ventricular zone expressed PH domain homolog 1 (zebrafish)	-2.67	8.66
16*	gi_119907214	XM_001250844	SOX6	SRY (sex determining region Y)-box 6	-2.79	7.95
17	gi_119915236	XM_001252205	DAAM2	Dishevelled associated activator of morphogenesis 2	-2.11	7.59
18	gi_51819474	CO889189	– – -	CO889189 BovGen_17514 normal cattle brain cDNAclone RZPDp1056J1148Q 5' sequence	-2.18	6.93
19*	gi_115497983	NM_001076473	PPAP2B	Phosphatidic acid phosphatase type 2B	-2.24	6.73
20	gi_119922192	XM_616412	ITGB8	Integrin, beta 8	-2.17	6.66
21*	gi_150247128	NM_001099368	PCDHGA2	Protocadherin gamma subfamily A, 2	-2.15	6.58
22*	gi_119907210	XM_001250746	SOX6	SRY (sex determining region Y)-box 6	-2.56	6.53
23	gi_157279998	NM_001105045	C5orf13	Chromosome 5 open reading frame 13	-2.28	6.52
24	gi_51821825	CO891528	– – -	CO891528 BovGen_19853 normal cattle brain cDNAclone RZPDp1056A1732Q 5' sequence	-2.61	5.51
25	gi_76638411	XM_612023	MBNL3	Muscleblind-like 3 (Drosophila)	-2.24	5.49
26	gi_119912551	XM_607943	TANC2	Tetratricopeptide repeat, ankyrin repeat and coiled-coil containing 2	-2.09	5.41
27	gi_62117152	DN740977	– – -	DN740977 1404247 MARC 7BOVcDNA3' sequence	-2.17	5.34
28	gi_119884953	XM_591264	PLCH1	Phospholipase C, eta 1	-2.22	4.52
29	gi_115497789	NM_001075225	NTRK2	Neurotrophic tyrosine kinase, receptor, type 2	-2.02	4.41

3.4 Full list of 'biological function and disease categories' in TashAT2/Infection modulated overlapping dataset (1,206 genes)

	Category	p-value
1	Cancer	1.8E-22-1.15E-04
2	Inflammatory Disease	1.83E-18-1.1E-04
3	Cell Death	2.99E-18-1.34E-04
4	Inflammatory Response	1.08E-17-1.25E-04
5	Skeletal and Muscular Disorders	1.3E-17-1.1E-04
6	Genetic Disorder	1.4E-17-1.09E-04
7	Immunological Disease	1.98E-16-1.02E-04
8	Cellular Movement	2.44E-16-1.28E-04
9	Neurological Disease	2.66E-15-1.02E-04
10	Cellular Growth and Proliferation	1.45E-14-6.81E-05
11	Connective Tissue Disorders	8E-14-2.47E-05
12	Gastrointestinal Disease	1.09E-13-1.02E-04
13	Respiratory Disease	3.05E-13-1.03E-04
14	Gene Expression	9.12E-13-6.54E-05
15	Cell-To-Cell Signaling and Interaction	4.76E-12-1.25E-04
16	Reproductive System Disease	4.97E-12-9.83E-05
17	Cellular Development	6.46E-12-1.3E-04
18	Cellular Function and Maintenance	1.78E-11-1.28E-04
19	Dermatological Diseases and Conditions	7.93E-11-4.13E-05
20	Organismal Injury and Abnormalities	2.26E-10-1.3E-04
21	Hepatic System Disease	2.7E-10-1.02E-04
22	Hematological Disease	3.19E-10-1.3E-04
23	Free Radical Scavenging	1.09E-09-6.5E-05
24	Cardiovascular Disease	4.11E-09-1.29E-04
25	Cellular Compromise	6.37E-08-9.39E-05
26	Cell Morphology	6.89E-08-1.14E-04
27	Antigen Presentation	1.54E-07-1.25E-04
28	Infectious Disease	3.27E-07-1.28E-04
29	Lipid Metabolism	6.56E-07-1.28E-04
30	Small Molecule Biochemistry	6.56E-07-1.28E-04
31	Hypersensitivity Response	1.79E-06-1.79E-06
32	Renal and Urological Disease	2.64E-06-6.57E-05
33	Cellular Assembly and Organization	2.84E-06-1.27E-04
34	Ophthalmic Disease	1.11E-05-1.11E-05
35	Metabolic Disease	2.06E-05-1.27E-04
36	Post-Translational Modification	2.27E-05-2.27E-05
37	Cell Signaling	2.83E-05-1.12E-04
38	Molecular Transport	3.11E-05-1.29E-04
39	Vitamin and Mineral Metabolism	3.11E-05-1.12E-04
40	Psychological Disorders	3.4E-05-3.4E-05
41	DNA Replication, Recombination, and Repair	4.88E-05-4.88E-05
42	Nutritional Disease	7.75E-05-7.75E-05
43	Endocrine System Disorders	8.3E-05-1.27E-04
44	Carbohydrate Metabolism	1.28E-04-1.28E-04
45	Developmental Disorder	1.29E-04-1.29E-04

3.5 Full list of IPA Canonical and Custom Pathways identified in TashAT2 modulated overlapping dataset (1,206 genes)

	Ingenuity Canonical Pathways	-log(p-value)	Ratio
1	Production of Nitric Oxide and Reactive Oxygen Species in Macrophages	6.97E+00	1.07E-01
2	HMGB1 Signaling	5.78E+00	1.40E-01
3	IL-6 Signaling	5.04E+00	1.30E-01
4	Role of Tissue Factor in Cancer	5.00E+00	1.23E-01
5	IL-8 Signaling	4.94E+00	9.33E-02
6	G-Protein Coupled Receptor Signaling	4.65E+00	6.60E-02
7	TNFR2 Signaling	4.55E+00	2.06E-01
8	NF-κB Signaling	4.54E+00	9.66E-02
9	Role of JAK1 and JAK3 in γc Cytokine Signaling	4.54E+00	1.47E-01
10	IL-2 Signaling	4.38E+00	1.55E-01
11	Protein Kinase A Signaling	3.81E+00	7.01E-02
12	CD40 Signaling	3.77E+00	1.29E-01
13	Insulin Receptor Signaling	3.56E+00	9.29E-02
14	ERK/MAPK Signaling	3.54E+00	7.84E-02
15	PI3K Signaling in B Lymphocytes	3.53E+00	9.09E-02
16	Acute Phase Response Signaling	3.50E+00	8.43E-02
17	PKCθ Signaling in T Lymphocytes	3.50E+00	8.45E-02
18	HIF1α Signaling	3.34E+00	1.02E-01
19	Rac Signaling	3.30E+00	8.94E-02
20	LPS-stimulated MAPK Signaling	3.28E+00	1.10E-01
21	NF-κB Activation by Viruses	3.28E+00	1.10E-01
22	CXCR4 Signaling	2.89E+00	7.69E-02
23	IL-3 Signaling	2.72E+00	1.08E-01
24	Integrin Signaling	2.72E+00	7.14E-02
25	PAK Signaling	2.66E+00	8.41E-02
26	Apoptosis Signaling	2.66E+00	9.38E-02
27	Myc Mediated Apoptosis Signaling	2.57E+00	1.15E-01
28	IL-1 Signaling	2.56E+00	8.41E-02
29	JAK/Stat Signaling	2.49E+00	1.09E-01
30	Role of PRR in Recognition of Bacteria and Viruses	2.46E+00	9.20E-02
31	PPAR Signaling	2.44E+00	8.41E-02
32	TNFR1 Signaling	2.39E+00	1.13E-01
33	cAMP-mediated signaling	2.05E+00	6.39E-02
34	IL-15 Signaling	1.88E+00	8.96E-02
35	Inositol Phosphate Metabolism	1.87E+00	5.56E-02
36	TGF-β Signaling	1.77E+00	7.87E-02
37	Actin Cytoskeleton Signaling	1.70E+00	5.46E-02
38	Interferon Signaling	1.65E+00	1.11E-01
39	TREM1 Signaling	1.54E+00	7.58E-02
40	Acute Myeloid Leukemia Signaling	1.43E+00	7.32E-02
41	PI3K/AKT Signaling	1.43E+00	5.71E-02
42	Role of JAK family kinases in IL-6-type Cytokine signaling	1.35E+00	1.11E-01
	Custom Pathway analysis	**-log(p-value)**	**Ratio**
1	NF-κB response genes	8.58E+00	1.12E-01
2	NF-κB dot org derived pathway/ Targets	5.49E+00	8.01E-02
3	NF-κB Signaling	3.42E+00	5.74E-02
4	AP1targets	3.13E+00	1.76E-01
5	WNTsiganlling	2.02E+00	1.22E-01
6	Toll-like Receptor Signaling	1.66E+00	8.89E-02
7	ATF2network	1.63E+00	1.00E-01

3.6 Important genes identified in the biological function and disease categories in TashAT2/ infection modulated overlapping dataset

Important Categories	Key Molecules modulated in TashAT2 in predicted manner
Cancer (119/252) Cancer (106) Tumourigenesis (113) Neoplasia (107) Carcinoma (82) Formation of secondary tumor (4) Transformation (21)	**Cancer:** ABAT,ABCC3,ABCG2,ADRB2,ALDH1A1,ANGPTL1,ANXA4, AOC3, APOD,BCAS1,BST2,CA2,CALCRL,CAPN3,CASP7, CD34, CD3G, CD8,CDC42BPA,CDKN2C,CEBPA,COL3A1, CPA4,CREB3L3,CSRP2, CYBA,CYP3A4,DIXDC1, DVL1,EAF2, EPAS1,EPS8,ERRFI1,ETV5, FAS, FCER2,FOS, HES1 (includes EG:15205),EY1,HK2,IER3, IFI27, IFI44,IFIT3, IFNAR2, IGFBP6,IKBKE,IL15RA,IL18, IL24, IL7R,IRF8, JUP, KIF1A, KRT17, KRT6A,LMO2,LTBP1, MAP3K1, MDK,MERTK, MT2A, MUM1L1, NAV3,NFE2,NGFR,NPC1,NTNG2, P2RX7, PDE3B, PDE7B, PIK3CD, PIK3IP1,PLAU,PLAUR,PNPLA4, PPP1R3C, PRDM1,PRKCZ,PRSS23,PTPN6,RASAL1, Rbpms, RNASEL, RPH3AL,S100A14,S1PR1,SCN2B,SERPINE1,SLC2A5, SLC7A11,SLC7A5, SMAD7,SPINT2,SPOCK2,ST5,STEAP3, SYNPO2,TIFA,TP63, TPM2,UGCG,VCAM1,VWA5A, XAF1, ZBTB20
Cell Death (75/215) Cell death of cancer cells (55) Cell death of blood cells (25) Apoptosis of leukocytes (16) Cell viability (13)	**Cell Death** ABCC3,ABCG2,ALPK2,CA2,CASP7,CD82,CDC42BPA,CDKN2C,CEBPA, CYP3A4,DVL1,EPAS1,FAS,FCER2,FOS,GGT1,HCK,HES1 (includes EG:15205),IER3,IFNAR2,IGFBP6,IKBKE,IL15RA,IL18,IL24,IRF8,ITSN1, JUP,KIF1A,LASS1,LMO2,LTBP1,MAP3K1,MAPK10,MDK,MT2A,NGFR, NUPR1,PLAU,PLAUR,PMEPA1,PPP1R1B,PRDM1,PRKCZ,PTPN6,PTPRM, RNASEL,SERPINE1,SERPINI1,SLC7A11,SMAD7,TP63,TRAF1,UGCG, XAF1
Inflammatory Response (56/ 130) Immune response (50) Inflammation (19) Phagocytosis of cells (10) Respiratory burst (7) Inflammatory response (23) Adhesion of phagocytes (7)	**Inflammatory Response** DRB2,AIF1,AOC3,BST2,CA2,CALCRL,CD3G,CHN1,COL3A1,CYBA,CYBB, FAS,FCER2,FOS,GGT5,GM2A,GPR77,HCK,IER3,IFI44,IFNAR2, IKBKE, IL15RA,IL18,IL24,IL6ST,IL7R,IRF8,KRT17,LGALS9, LTBP1, MAPK10, MERTK,NPC1,NUPR1,P2RX7,PIK3CD,PLAU, PLAUR, PRDM1,PRKCZ, PTPN6,RNASEL,S100A14,S1PR1, SERPINE1,SIT1, SMAD7,TPST1, VCAM1
Cellular Movement (51/133) Cell movement (51) Migration of cells (47) Leukocyte migration (24) Cell movement of leukocytes (19) Dissemination of tumor cells (2)	**Cellular Movement** ADRB2,AIF1,ANGPTL1,AOC3,CALCRL,CD34,CD82,CHST1,CYBB,EPAS1,EPS8,ERRFI1,ETV5,FAS,FOS,GGT5,HCK,HEY1,IGFBP6,IL15RA,IL18, IL6ST,IRF8,ITGB7,JUP,KRT6A,LGALS9,MAP3K1, MCF2L,MDK,MRAS, MYL12B, NGFR,NPC1,P2RX7,PIK3CD, PIK3IP1,PLAU,PLAUR,PLTP, PRKCZ,PTPN6,PTPRM,S100A14,S1PR1, SCN2B, SERPINE1, SMAD7, TP63, VCAM1,VCL
Cell Morphology (57/84) Shape change (20) Morphology of cells (18) Outgrowth of neuritis (14) Reorganization of cytoskeleton (8) Ruffling (5)	**Cell Morphology** ARHGEF9,BAIAP2,CD3G,CHN1,FAS,FOS,GAS7,HCK,HES1 (includes EG:15205),LMO2,NGFR,P2RX7,PDE3B,PLAU, PLAUR,SERPINE1,SORBS3,TP63,VCAM1,VCL

The given table represents the most relevant biological process categories and key molecules from each category that can be linked to the phenotype of parasite infection and LPS stimulation of BL20 cells. Similarly, prediction of whether the molecules promoted (pro) or inhibited (anti) the designated functional category identified by IPA is also indicated. The absolute fold change for each molecule is given in brackets.